Acta Cryst. (1976). B32, 775

Molecular Packing Modes. Carboxylic Acids

BY L. LEISEROWITZ

Department of Structural Chemistry, Weizmann Institute of Science, Rehovot, Israel

(*Received* 29 *April* 1975; *accepted* 14 *July* 1975)

Some features of the packing modes of carboxylic acids are discussed. Monocarboxylic acids R–CO_2H, containing residues R, which are either nonchiral or racemic, almost invariably form cyclic hydrogen-bonded pairs. If the R group is small, the molecules may interlink by single O–H···O bonds to form a chain motif in which the O–H···O(carboxyl) bond is almost linear, the C=O···(H)O angle $\simeq 130°$, and the O–H proton donor lies in the plane of the carbonyl system O=C<, to which it is hydrogen-bonded. Monocarboxylic acids with chiral residues and which are enantiomeric show some tendency to form a hydrogen-bonded chain motif along a twofold screw axis. The angular geometry of this O–H···O bond shows considerable variation and seems to be dependent upon the van der Waals contacts between the R groups along the hydrogen-bonded chain. Dicarboxylic acids HO_2C–R–CO_2H form extended chains, the carboxyl groups being interlinked by O–H···O bonds into cyclic pairs. This arrangement is adopted, almost without exception, for all types of R groups. Carboxylic acids, in which the intramolecular environments of the two carboxyl O atoms are identical, may show orientational disorder of the carboxyl group in the crystal. This depends on the intermolecular environment of the carboxyl dimer. Belonging to this category are *p*-substituted benzoic acids, which almost invariably adopt the packing motif in which the carboxyl dimers lie side by side with a neighbouring phenyl ring on the same plane and are separated from each other by C–H···O contacts of $\sim 3{\cdot}5$ Å. This arrangement is conducive to disorder of the carboxyl dimer. The benzoic acids, and indeed many planar acids, form stacks in which the direction of offset between the carboxyl groups lies either along the carbonyl C=O bond or the hydroxyl C–OH bond. The carboxyl group in these two stacking types may show disorder of the carboxyl dimer, suggesting that the energy difference between the two stacking types is small. Carboxylic acids also form interplanar contact *via* an antiparallel arrangement of C–O bonds which may be either C=O or C–OH bonds or a disordered combination thereof. Intramolecular forces probably favour the synplanar C=C–C=O conformation in the α,β-unsaturated acids R–CH=CH–CO_2H. The antiplanar C=C–C=O form may be induced by intermolecular forces. Orientational disorder between the syn- and antiplanar C=C–C=O conformations may be induced by the stacking forces of the carboxyl dimers. The observed antiplanar C=C–C=O conformation in a number of acids has been associated with a motif containing a lateral C–H···O(carbonyl) contact $\simeq 3{\cdot}5$ Å. The few known crystal structures of carboxylic acids containing an acetylenic C–H proton donor have not shown acetylenic C–H···O(carbonyl) interactions which are strikingly short. Indeed, but-3-ynoic acid shows only a ≡C–H···C≡C contact. The minimum van der Waals distance between carboxyl O atoms appears to be dependent upon their direction of approach. Hydroxyl O atoms which make contact so that their C–O(H) bonds are almost collinear (C–O···O–C), may approach each other to within 2·9 Å. Carbonyl and hydroxyl O atoms which are arranged so that their electron lone-pair lobes are directed at each other do not make contact less than 3·5 Å.

1. Introduction

This work is part of a programme concerned with the systematics of packing of hydrogen-bonded groups. The scope of this paper encompasses principal features of the molecular packing modes of carboxylic acids R–CO_2H in the crystalline state. Much information of chemical interest is hidden in crystal structures because they represent minimum energy arrangements, and whereas little can be inferred from a single structure, certain trends become apparent if enough structures are available. Our precise purpose, therefore, lies in the detection of the primary molecular interactions present in carboxylic acid structures. The paper is divided into three sections. Firstly, we consider the geometry of the carboxyl group, and its conformational properties with respect to the attached residue R. Secondly, we describe the various modes of interlinking carboxylic acids by hydrogen bonds and finally we consider the packing environment about the hydrogen-bonded carboxyl dimer.

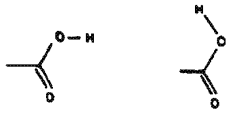
2. The carboxyl group

2.1. *Geometry of the carboxyl group*

Major geometric features of the carboxyl group in a number of crystal structures are listed in Table 1. The molecules chosen were those in which there is no ori-

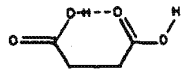
UM00013978
NOVARTIS EXHIBIT 1517
Novartis v. Regents, IPR2023-01347
Page 2724 of 4460

entational disorder of the carboxyl group in the crystal. The average bond lengths and angles are C=O 1·21, C–O(H) 1·31, O–H (neutrons) 1·00 Å, O=C–O 123°. The C–O–H angle lies between 110–114·5° (neutrons). The O–H group has been observed, in the crystalline phase, to adopt either a synplanar (1*a*) or antiplanar



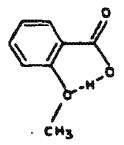
(1*a*) (1*b*)

(1*b*) O=C–O–H conformation. According to the infrared spectrum of gaseous monomeric formic acid (Miyazawa & Pitzer, 1959), the synplanar structure is the more stable conformer by 2 kcal mole^{-1}; indeed, microwave studies (Lide, 1964) have indicated this difference to be at least 4 kcal mole^{-1}. These findings are consistent with the observation that the antiplanar O=C–O–H form (1*b*) occurs only when the O–H bond participates in an intramolecular O–H···O bond, particularly in 1,2-disubstituted dicarboxylic acids as



(2)

shown in (2). The crystal structure of *o*-methoxybenzoic acid (Gopalakrishna & Cartz, 1972) is a rare exception of a monocarboxylic acid not interlinked by an O–H···O(carbonyl) bond; rather the molecule forms an intramolecular O–H···O(methoxy) hydrogen bond *via* the antiplanar O=C–OH conformer as shown in (3).

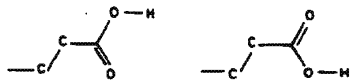


(3)

We may conclude in general that the hydroxyl group which does not participate in an intramolecular O–H···O bond lies in the synplanar O=C–O–H form.

2.2. *Conformation of the carboxyl group*

The conformational features of the carboxyl group, as well as of esters and amides, have been discussed (Leiserowitz & Schmidt, 1965; Dunitz & Strickler, 1968; Einspahr & Donohue, 1973). In the crystal structures of α,β-saturated carboxylic acids R–CH_2–CH_2–CO_2H the synplanar C^β–C^α–C=O arrangement (4*a*) is adopted without any known exceptions. It had been



(4*a*) (4*b*)

Table 1. *Bond lengths* (Å) *and angles* (°) *of carboxyl groups with no orientational disorder*

Compound	C=O	C–OH	O–H	O–C=O	C–O–H	Method*	Reference
Formic acid (formic acid: formamide)	1·202	1·320		125·4		X	Nahringbauer & Larsson (1968)
Acetic acid at −140°C	1·206	1·321	1·01	121·9	110·5	N	Jönsson (1971)
	1·226	1·319		121·3		X	Nahringbauer (1970)
Acetic acid (acetic acid: phosphoric acid)	1·230	1·302	0·99	121·5	110·0	N	Jönsson (1972)
	1·234	1·303		121·4		X	Jönsson (1972)
β-Tetrolic acid	1·204	1·310		122·9		X	Benghiat & Leiserowitz (1972*a*)
Oxalic acid dihydrate	1·212	1·291	1·03	126·6	114·4	N	Delaplane & Ibers (1969)
	1·212	1·285		126·8		X	Sabine, Cox & Craven (1969)
Oxalic acid (oxalic acid: acetamide)	1·212	1·298		126·2		X	Leiserowitz & Nader (1972)
Oxalic acid (oxalic acid: furamide)	1·201	1·301		126·2		X	Huang, Leiserowitz & Schmidt (1973)
Glycollic acid	1·203	1·312	1·00	123·2	110·2	N	Ellison, Johnson & Levy (1971)
	1·202	1·314		123·2		X	Pijper (1971)
Fumaramic acid	1·209	1·310		124·0		X	Benghiat *et al.* (1972)
D-Tartaric acid	1·200	1·317		125·7		X	Okaya, Stemple & Kay (1966)
Hippuric acid	1·196	1·328		124·1		X	Ringertz (1971)
Maleic acid	1·220	1·302		120·7		X	James & Williams (1974)
o-Chlorobenzoic acid	1·208	1·295		124·5		X	Ferguson & Sim (1961)
(−)-*o*-Carboxyphenyl methyl sulphoxide	1·214	1·318		122·0		X	Dahlén (1974)
(±)-*o*-Carboxyphenyl methyl sulphoxide	1·209	1·292		122·2		X	Dahlén (1973)
o-Ethoxybenzoic acid	1·214	1·332		118·3		X	Gopalakrishna & Cartz (1972)
2,3-Dimethylbenzoic acid	1·189	1·313		121·7		X	Smith, Florencio & García-Blanco (1971)

* X = X-ray diffraction, N = neutron diffraction.

UM00013979
NOVARTIS EXHIBIT 1517
Novartis v. Regents, IPR2023-01347
Page 2725 of 4460

assumed by Leiserowitz & Schmidt (1965) that the preferred conformation was determined by the non-bonded interactions between C^β and its attached H atoms on the one hand, and the hydroxyl or carbonyl O atoms on the other. Mainly because of the difference between the angles C^α–C=O and C^α–C–O(H) the non-bonded distances $C^\beta\cdots O$ and $H^\beta\cdots O$ are 0·1–0·2 Å larger for the usual synplanar than for the alternative antiplanar conformation (4*b*). The synplanar rule does not apply to the α,β-unsaturated acids R–CH=CH–CO_2H; there are several molecules showing the antiplanar C^β=C^α–C=O form. Dunitz & Strickler (1968) accounted for the observed antiplanar C=C–C=O conformation by regarding the double bonds as being decomposed into two bent bonds. Thus the antiplanar C=C–C=O conformation, *i.e.* the synplanar C=C–COH conformer, would correspond to the energetically favoured staggered disposition of bonds. Dunitz & Strickler concluded that these two factors, non-bonded interactions and the preference for staggered rather than eclipsed disposition of bonds, are both operating in favour of the synplanar conformation C–C–C=O in saturated systems. If C^β–C^α is a double bond, then the first factor favours synplanarity, the second antiplanarity. The correctness of this approach of taking into account interaction between bonds is borne out by a comparison of the conformational properties of β-substituted *trans*-unsaturated acids R–CX=CH–CO_2H as a function of the size of the atom substituent X on the β-carbon. In allenedicarboxylic acid HO_2C–CH=C=CH–CO_2H, where the X substituent is absent, the molecule exhibits an antiplanar C=C–C=O conformation, both in its own structure (Leiserowitz & Nader, 1973) [C=O 1·22, C–O(H) 1·29 Å] and in its complex with acetamide (Nader, 1976). Molecules containing β-substituents such as Cl, *e.g.* β-chloro-*trans*-cinnamic acid (Filippakis, Leiserowitz, Rabinovich & Schmidt, 1972), or CH_3, *e.g.* vitamin A acid (Stam, 1972), exhibit the synplanar C=C–C=O conformation.

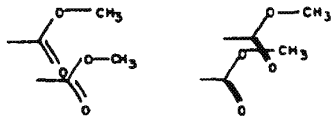
All the unsaturated carboxy-esters R–CH=CH–CO_2CH_3 listed in Table 2 exhibit the synplanar C=C–C=O arrangement. This feature must be due primarily to intramolecular forces only since the packing environments about the carboxy-ester groups in these crystal structures differ from each other. This point is highlighted by the stacking arrangements of monomethyl fumarate (Leiserowitz & Tang, 1976) and monomethyl *trans,trans*-muconate (Rabinovich & Schmidt, 1967) (Figs. 1 and 2); in the fumarate the carboxy-ester groups are stacked with an offset mainly along the carbonyl C=O bonds (5*a*) whereas in the muconate the offset is along the C–O(CH_3) bond (5*b*).

Table 2. *Conformations of α,β-trans unsubstituted carboxylic acids and esters about the carboxyl carbon–carbon bond and their* C–O *bond lengths* (Å)

Compound	Conformation	C=O	C–OH	References
Monomethyl fumarate, ester group	*syn*	1·198	1·328	Leiserowitz & Tang (1976)
acid group	*anti* + disorder	1·246	1·276	
Monomethyl *trans,trans*-muconate				
ester group	*syn*	1·17	1·38	Rabinovich & Schmidt (1967)
acid group	*anti*	1·23	1·31	
Dimethyl *trans,trans*-muconate	*syn*	1·203	1·338	Filippakis, Leiserowitz & Schmidt (1967)
Methyl *m*-bromocinnamate	*syn*	1·19	1·41	Leiserowitz & Schmidt (1965)
Methyl *p*-bromocinnamate	*syn*	1·19	1·32	Leiserowitz & Schmidt (1965)
Acrylic acid	*syn*	1·24†	1·30	Higgs & Sass (1963), Chatani, Sakata & Nitta (1963)
Crotonic acid	*syn*	1·237	1·297	Robertson & Sutherland (1964)
Sorbic acid	*syn*	1·240	1·310	Robertson & Sutherland (1964)
trans-β-2-Furylacrylic acid	*syn*	1·24	1·30	Filippakis & Schmidt (1967)
trans-β-2-Thienylacrylic acid, β-form	*syn*	1·22	1·31	Block, Filippakis & Schmidt (1967)
trans-β-2-Thienylacrylic acid, γ-form	*syn* + disorder	1·25	1·29	Block, Filippakis & Schmidt (1967)
trans-β-Ionylidene crotonic acid	*syn*	1·22	1·30	Koch (1972)
3-(1,1,5-Trimethyl-5-cyclohexen-6-yl)-pronenoic acid	*syn* + disorder	1·256	1·287	Schenk (1972)
trans,trans-Muconic acid, molecule *A*	disorder + *syn*	1·257	1·275	Bernstein & Leiserowitz (1972)
trans,trans-Muconic acid, molecule *B*	*syn*	1·236	1·294	
trans,trans-Muconamic acid*	*syn*			
Fumaramic acid	*syn*	1·209	1·310	Benghiat *et al.* (1972)
Octa-2,6-*trans,trans*-dienedioic acid	*syn* + disorder	1·245	1·283	Martuscelli (1969)
Octa-2,6-*cis,trans*-dienedioic acid	disorder	1·261	1·261	Martuscelli & Mazzarella (1969)
at the *trans* end of the molecule				
Fumaric acid, monoclinic form	*anti*	1·22	1·29	Brown (1966)
Fumaric acid, triclinic form	*anti*	1·228	1·290	Bednowitz & Post (1966)
Fumaric acid (fumaric acid:				
β-picoline *N*-oxide)	*syn*	1·19	1·33	Gorres, McAfee & Jacobson (1975)
trans-Cinnamic acid	*anti*	1·22	1·30	Ladell, McDonald & Schmidt (1956)
p-Chloro-*trans*-cinnamic acid	disorder	1·263	1·264	Glusker, Zacharias & Carrell (1975)

* The C=C–C=O conformation in *trans,trans*-muconamic acid is shown to be synplanar in §3.2.3.
† The C–O bond lengths were averaged from two crystal structure analyses.

UM00013980
NOVARTIS EXHIBIT 1517
Novartis v. Regents, IPR2023-01347
Page 2726 of 4460

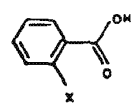


(5*a*) (5*b*)

In the α,β-unsaturated carboxylic acids R–CH=CH–CO_2H the picture does not appear to be clear-cut. Of the 21 acids listed in Table 2, 13 lie in the synplanar form, 5 in the antiplanar form, and 3 show pronounced orientational disorder of the carboxyl group. These results indicate that the conformation of the carboxyl group is determined by a combination of inter- and intramolecular forces. The questions arising from these observations are, firstly, which conformation is preferred by intramolecular forces only and secondly, what are the intermolecular forces which play a role in determining the conformation of the carboxyl group?

As regards the first question, there is little doubt that intramolecular forces lead to a preference for the synplanar conformation C=C–C=O in the esters R–CH=CH–CO_2CH_3. Let us then compare the molecular geometries of the fragment –CH=CH–CO_2 in analogous ester and acid molecules. The acid and ester fragments were chosen from fumaramic acid (Benghiat, Kaufman, Leiserowitz & Schmidt, 1972) and monomethyl fumarate (Leiserowitz & Tang, 1976), respectively. The bond lengths and angles are shown in Fig. 3(*a*) and (*b*). The average scatter from the mean of 0·005 Å in bond length and 0·7° in angle between the two fragments indicates that their intramolecular force fields are similar to each other. This similarity is consistent with the fact that most of the carboxylic acid molecules listed in Table 2 are in the synplanar C=C–C=O conformation, implying that intramolecular forces show a preference, albeit slight, for the synplanar conformer. Moreover we shall show later that all the molecules listed in Table 2 which exist in the antiplanar form have similar packing environments about their carboxyl groups and that their antiplanar C=C–C=O conformations are probably induced by intermolecular forces.

In the *o*-substituted benzoic acids (6) the *o*-substituent (=F, CH_3, Cl, Br) makes contact with the carbonyl O atom except for *o*-fluorobenzoic acid (Krausse & Dunken, 1966). Its C–O lengths of 1·255 and 1·280 Å indicate a pronounced measure of disorder of the carboxyl group. Obviously the relatively bulky substituents Br, Cl and CH_3 in (6) preclude disorder of the carboxyl groups. That this disorder in *o*-fluorobenzoic acid is enhanced by intermolecular forces will be brought out later.



(6)

X=F (Krausse & Dunken, 1966)
=CH_3 (Smith, Florencio & Garcia-Blanco, 1971)
=Cl (Ferguson & Sim, 1961)
=Br (Ferguson & Sim, 1962)

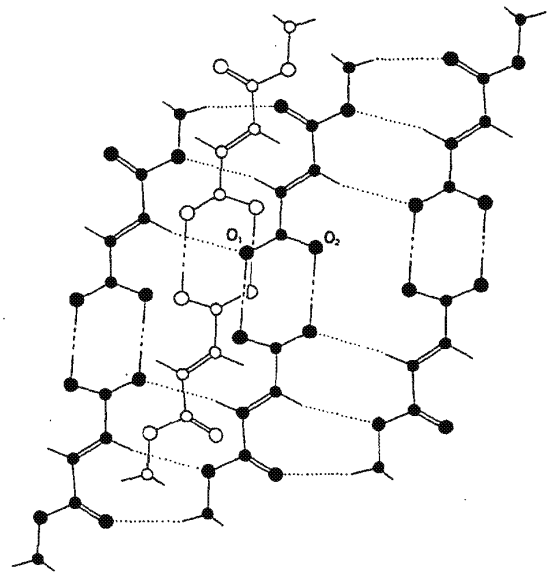


Fig. 1. Monomethyl fumarate (Leiserowitz & Tang, 1976). Intra- and interlayer packing. Distances: C–O_1 1·246, C–O_2 1·276, O–H···O 2·650, C–H···O, 3·54 Å. The layer structure is planar to within 0·1 Å.

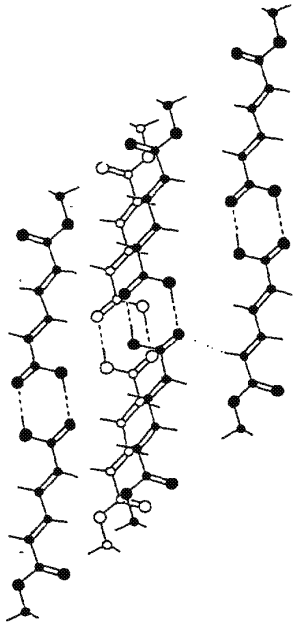
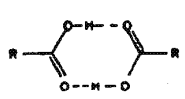


Fig. 2. Monomethyl *trans,trans*-muconate (Rabinovich & Schmidt, 1967) intra- and interlayer structure. Distances: C–O(H) 1·31, C=O 1·23, O–H···O 2·62 and C–H···O (carbonyl) 3·49 Å. Offset from coplanarity between molecules is 0·8 Å.

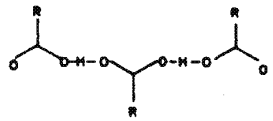
UM00013981
NOVARTIS EXHIBIT 1517
Novartis v. Regents, IPR2023-01347
Page 2727 of 4460

3. Modes of interlinking carboxyl groups *via* the O–H···O bond

Carboxylic acid molecules R–CO_2H may be interlinked to form either the cyclic hydrogen-bonded dimer (7), which is the most commonly observed motif in the solid state, or the rarely encountered *catemer** motif (8) in which each carboxyl group is linked to two neighbours *via* single O–H···O(carbonyl) bonds. We shall analyse in this section the various ways in which carboxyl groups may be linked to form the *catemer* as well as account for its rare occurrence in the solid.



(7)

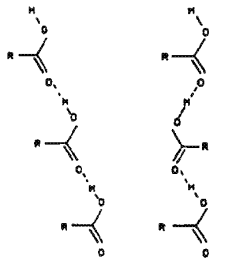


(8)

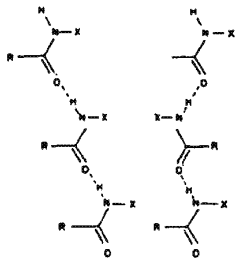
3.1. *The catemer motif*

The *catemer* motif (8) consists of carboxylic acid molecules related to each other in the crystal by space symmetry. We shall make use of only those symmetry elements which occur most frequently in molecular crystals, namely translation, the twofold screw axis, and the glide, and neglect n-fold screw axes ($n=3,4,6$) which are rarely encountered.

Catemer motifs may be constructed for both the syn- as well as the antiplanar O=C–O–H conformer. Two postulated arrangements incorporating the antiplanar O=C–OH conformer are shown in (9*a*) and (9*b*). The

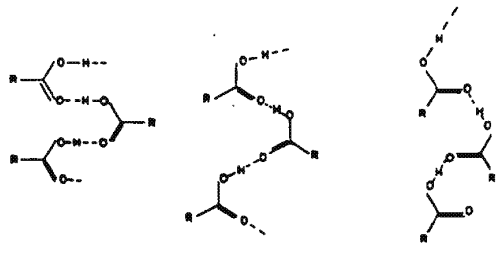


(9*a*) (9*b*)



(10*a*) (10*b*)

O–H···O=C bond in (9*a*) is approximately collinear, in (9*b*) the C=O···O angle is variable. While similar packing modes occur in the crystal structures of secondary amides, RCONHX, as shown in motifs (10*a*) and (10*b*), the *catemer* motifs (9) have not been encountered in carboxylic acid structures, presumably because of the unfavourable antiplanar O=C–OH conformer.



(11*a*) (11*b*) (11*c*)

Assuming the synplanar O=C–O–H conformer we may formulate three distinct hydrogen-bonding packing modes shown in (11*a*), (11*b*) and (11*c*). The molecules are related by 2_1 axes (or glides) in all three arrangements. Motif (11*a*) is a hydrogen-bonded coplanar system in which the O–H proton donor points almost at the carbonyl O acceptor atom with a C=O···(H)O angle close to 120° yielding a translation axis of ~5 Å. At first sight this arrangement does not appear unreasonable. Indeed amide groups in the crystal structures of adipamide (Hospital & Housty, 1966) and of the β-form of *o*-chlorobenzamide (Kato, Takaki & Sakurai, 1974) are arranged in a very similar pattern as shown in (12) with the primary difference that along the 5 Å twofold screw axis of adipamide and *o*-chloro-

* The word *catemer* has been suggested by Berney (1973) to describe an infinite chain of molecular units which are closely coupled. In this text *catemer* is used to describe a chain of carboxyl groups linked to each other by single O–H···O bonds.

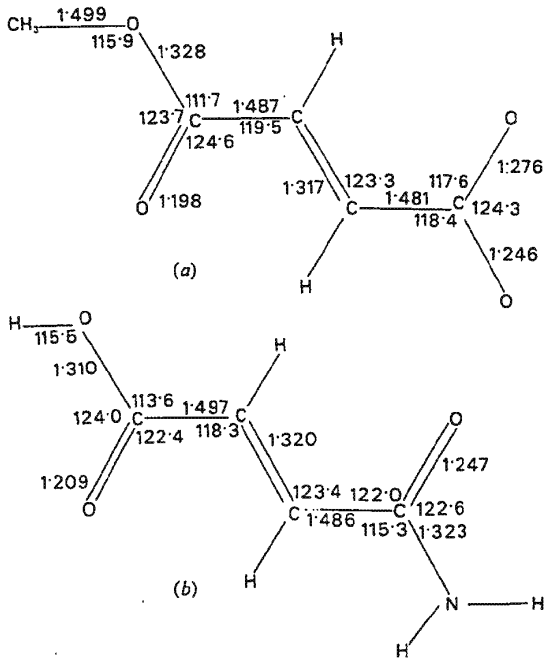
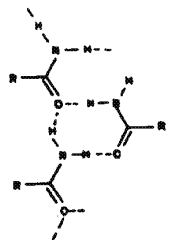


Fig. 3. Bond lengths (Å) and angles (°). (*a*) Monomethyl fumarate (Leiserowitz & Tang, 1976). (*b*) Fumaramic acid (Benghiat *et al.*, 1972).

UM00013982
NOVARTIS EXHIBIT 1517
Novartis v. Regents, IPR2023-01347
Page 2728 of 4460

benzamide the amide groups are linked by N–H···O bonds of ~2·95 Å, which are replaced in the carboxylic acid motif (11) by a van der Waals contact of similar length between the carbonyl and hydroxyl O atoms.

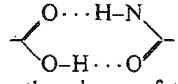


(12)

This short O···O distance of 2·95 Å would not be unusual; distances in the range 2·9–3·1 Å have been observed in the crystal structures of fumaric acid (Brown, 1966; Bednowitz & Post, 1966), furane-α,α′-dicarboxylic acid (Martuscelli & Pedone, 1968), and maleic acid (James & Williams, 1974) between hydroxyl O atoms, as shown in (13). The electron lone-pair lobes of these hydroxyl O atoms (assuming sp^3 hybridization) are not directed at each other.



(13)

However, a short contact of 3 Å between carbonyl and hydroxyl O atoms would be unfavourable in the *catemer* (11*a*). This is borne out by the crystal structure of the benzamide–succinic acid complex (Huang, Leiserowitz & Schmidt, 1973), from which it was deduced that O lone-pair···lone-pair interactions do not permit an approach less than 3·5 Å between two O atoms of neighbouring carboxyl groups arranged as in motif (11*a*), the lone-pair lobes of the carbonyl and hydroxyl O atoms being partially directed towards each other. Benzamide and succinic acid form a centrosymmetric 2:1 complex unit (Fig. 4) *via* the hydrogen-bond pairing of their carboxyl and amide groups. These complex units are interlinked, along a 5 Å axis, by N–H···O bonds of 3·0 Å between the benzamide molecules. The carboxyl-amide pair  is distorted; the twist angle between the planes of the carboxyl and amide groups is 20°. By means of this distortion a separation of 3·6 Å is achieved between the carbonyl and hydroxyl O atoms of the carboxyl groups related by the 5 Å axis. Were the carboxyl group coplanar with the amide group, then the separation between the O atoms would be 3·0 Å, *i.e.* the inter-pair N–H···O distance.

The unfavourable O···O separation of 3 Å in the planar motif (11*a*) may be increased by rotating the carboxyl group about its C–C bond by an angle of ~20° out of the hydrogen-bonding plane to achieve an arrangement of carboxyl groups as in the benzamide–succinic acid complex, as well as by changing the tilt of the carboxyl group about an axis perpendicular to its plane. However, these changes would reduce the linearity of the O–H···O bond and increase the C=O···(H)O angle. Nevertheless such a hydrogen-bond motif has been observed in the crystal structure of the enantiomeric 2-D-methyloctadecanoic acid (Abrahamsson, 1959*a*) in which the molecules are hydrogen-bonded along a 2_1 axis of 5·0 Å. Only the *xz* projection was reported, yet it clearly shows that the plane of the carboxyl group is appreciably tilted with respect to the 5 Å axis. On the other hand, the racemic 2-DL-methyloctadecanoic acid (Abrahamsson, 1959*b*) exists as hydrogen-bonded dimers (7). Its aliphatic chains are close-packed along a 5 Å axis as in the chiral structure which is indicative of the adjustment of the hydrogen bond of the enantiomeric structure to the requirements of close-packing of aliphatic chains along the 5 Å axis.

The poor contact between O atoms in motif (11*a*) may be improved while maintaining a planar hydrogen-bonded system and a linear O–H···O bond by simply increasing the C=O···O angle from the initial value, of ~130°, to 180°, yielding a collinear O–H···O=C bond shown in motif (11*b*), which has a translation axis of ~6·3 Å. Although the collinear hydrogen bond is commonly observed in amides (N–H···O=C),

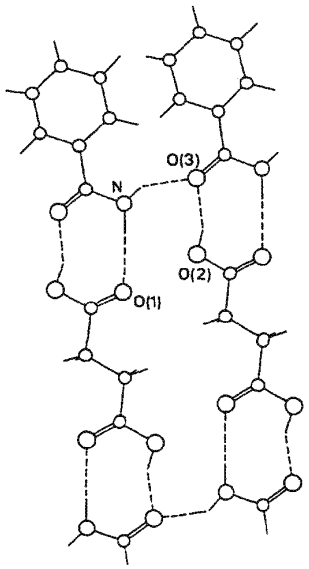
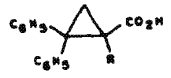


Fig. 4. 2:1 Complex of benzamide with succinic acid (Huang, Leiserowitz & Schmidt, 1973). Hydrogen-bond packing. Distances: N···O(3) 3·02, O(1)···O(2) 3·60 Å.

UM00013983
NOVARTIS EXHIBIT 1517
Novartis v. Regents, IPR2023-01347
Page 2729 of 4460

quite the opposite is true for the O–H···O=C bond, particularly in carboxylic acids. An approximately collinear O–H···O=C hydrogen bond exists in the structure of enantiomeric (*R*)-(+)-2,2-diphenyl-1-methylcyclopropane carboxylic acid (Lin, Paul & Curtin, 1974), which forms the *catemer* motif (11*b*) along a 2_1 axis of 6·3 Å. Walborsky, Barash, Young & Impastato (1961) had originally deduced from infrared measurements that these enantiomeric 2,2-diphenylcyclopropane carboxylic acids (14) exist as hydrogen-



(14)

bonded *catemers* in the crystal whereas the racemate exists as dimers. The enantiomer (−)-2-methyl-2-ethyl-

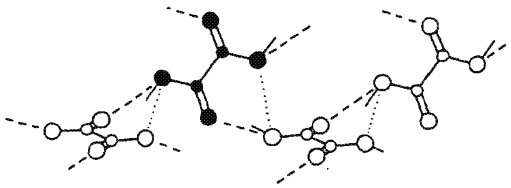


Fig. 5. α-Oxalic acid (Derissen & Smit, 1974). Hydrogen-bonding chain along the 7·85 Å glide axis.

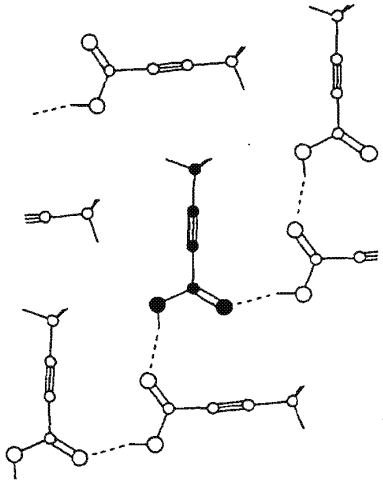
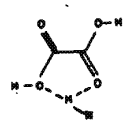


Fig. 6. β-Tetrolic acid (Benghiat & Leiserowitz, 1972*a*). Hydrogen-bonding layer.

eicosanoic acid (von Sydow, 1958) also forms a hydrogen-bonded chain along a 2_1 axis of 8·2 Å, *i.e.* 2 Å longer than the corresponding axis of the enantiomeric diphenylmethylcyclopropane carboxylic acid. This extended 8 Å axis can only permit a distorted hydrogen bond with the C=O···(H)O and C–O(H)···O(carbonyl) angles lying between 130–180°. A *catemer* motif with an axial length of 7·84 Å is observed in the crystal structure of α-oxalic acid (Derissen & Smit, 1974). The geometry of its hydrogen-bonding system is: O–H···O(carbonyl) 2·702 Å, and O–H···O(carbonyl) 146°. The C–O–H angle is 107°. The O–H bond is not directed at the carbonyl O atom; rather it straddles the carbonyl and hydroxyl O atoms as shown in Fig. 5. This O–H···O(hydroxyl) distance is 3·11 Å, and the O–H···O(hydroxyl) angle is 125°, suggesting that it represents an interaction. A somewhat similar arrangement is observed in the crystal structure of the complex of furamide with oxalic acid (Huang, Leiserowitz & Schmidt, 1973), in which an N–H bond straddles the O atoms of the oxalic acid as shown in (15) with distances N–H···O(hydroxyl) 3·10 and N–H···O(carbonyl) 2·94 Å. β-oxalic acid (Derissen & Smit, 1974)



(15)

forms cyclic hydrogen-bonded pairs with an O–H···O(carbonyl) distance of 2·674 Å. Derissen & Smit pointed out that despite the observation that the O–H···O distance is shorter in the β-modification (2·674 *vs.* 2·702 Å) and furthermore that the hydrogen-bonding angles in the β-form are more favourable, the α-form is nevertheless the more stable of the two. The reported heats of sublimation for α- and β-oxalic acid are 23·45 and 22·28 kcal mole^{-1} (Bradley & Cotson, 1953). The preferred stability of α-oxalic acid may be due in part to its O–H···O(hydroxyl) interaction.

The third *catemer* motif (11*c*) contains a linear O–H···O bond with a C=O···(H)O angle of ∼120° and a translation axis of ∼7·0 Å. This motif has been observed in a limited number of monocarboxylic acids, namely formic acid (Holtzberg, Post & Fankuchen, 1953), acetic acid (Jönsson, 1971; Nahringbauer, 1970) and β-tetrolic acid (Benghiat & Leiserowitz, 1972*a*). Both formic and acetic acids appear in planar hydrogen-bonded arrays *via* glides of axial lengths 6·5 and 7·0 Å, respectively.

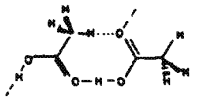
Table 3. *Hydrogen-bond distances* (Å) *and angles* (°) *in formic, acetic and β-tetrolic acids*

	O–H–O	C–O–H	C=O–(H)O	C–O(H)–O	Method*	References
Formic acid	2·58		122	114	X	Holtzberg, Post & Fankuchen (1953)
Acetic acid	2·631	110·5	133·2	119·6	N	Jønsson (1971)
β-Tetrolic acid	2·655	111	136·7	121·4	X	Benghiat & Leiserowitz (1972*a*)

* X = X-rays, N = neutrons

UM00013984
NOVARTIS EXHIBIT 1517
Novartis v. Regents, IPR2023-01347
Page 2730 of 4460

It is noteworthy that the hydrogen-bonding arrangement in acetic acid contains the cyclic 'dimer' (16).

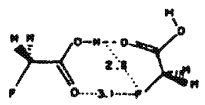


(16)

This 'dimer' is almost coplanar so that a methyl C–H bond is directed at the carbonyl O atom forming a C–H···O contact of 3·4 Å (H···O 2·4 Å). Jönsson (1971) had pointed out in a neutron diffraction study of acetic acid that this C–H···O arrangement should not be regarded as constituting a C–H···O bond without conclusive spectroscopic evidence. The methyl group of acetic acid exhibits static disorder in its crystalline 1:1 complex with phosphoric acid (Jönsson, 1972) hinting that the synplanar H–C–C=O conformer in the acetic acid crystal may be additionally stabilized by the C–H···O 'interaction'.

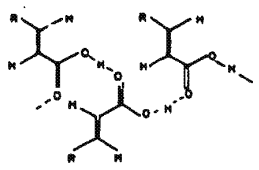
Tetrolic acid is dimorphic. The molecules in the metastable α-modification (Benghiat & Leiserowitz, 1972*a*) are linked into hydrogen-bonded pairs whereas the stable β-tetrolic acid exhibits the *catemer* motif (Fig. 6), the set of coplanar carboxyl groups being interlinked by single O–H···O bonds *via* a 2_1 axis of 7·1 Å.

There is an increasing distortion of the hydrogen bond comparing formic, acetic and β-tetrolic acid in that order (Table 3). The O–H···O bond is somewhat lengthened, and the C=O···(H)O and the C–O···O(carbonyl) angles are opened appreciably. This increasing distortion may be correlated with the relative sizes of the groups R in view of the close contact between R and the carbonyl O atom. Indeed this close R···O(carbonyl) contact severely restricts the size and nature of R and in fact rules out the *catemer* (11*c*) for the vast majority of carboxylic acids. We illustrate this by considering model compounds with progressively larger R groups.



(17)

Monofluoroacetic acid (Kanters & Kroon, 1972) with a residue CH_2F just slightly larger than the CH_3 group of acetic acid, does not appear in the *catemer* motif in the solid; it rather forms cyclic dimers. Assuming the observed synplanar F–C–C=O conformation and acceptable van der Waals contacts of F···O 3·1 and F···H 2·8 Å, the fluoro acid may be inserted into the *catemer* motif (11*c*) only with 'poor' hydrogen-bonding angles [C=O···O ~155°, C–O(H)···O ~126°] as shown in (17). This argument is applicable to molecules R–CH_2–CO_2H which exhibit a preference for the synplanar R–C–C=O conformation, *e.g.* bromoacetic acid (Vor der Bruck & Leiserowitz, 1976), trichloroacetic acid (Jönsson & Hamilton, 1972) and α,β-saturated acids R–CH_2–CH_2–CO_2H, a class which invariably appears in the synplanar C^{β}–C^{α}–C=O conformation, and which all form cyclic hydrogen-bonded dimers in the solid state.



(18)

These steric arguments are less convincing when applied to the α,β-*trans* unsaturated carboxylic acids R–CH=CH–CO_2H. The molecule may be inserted into the *catemer* (11*c*) provided the conformation of C=C–C=O is antiplanar as shown in (18). Since the less-favoured antiplanar C=C–C=O conformation does not occur infrequently (see § 2.2), the *catemer* (11*c*) cannot be discounted simply on the grounds that the synplanar C=C–C=O form is preferred.

It would seem that, by and large, better packing is achieved with cyclic hydrogen-bonded dimers than with the *catemer* (11) in view of the absence of constraints on the shape of the carboxy residue R in the formation of the cyclic dimer as compared to the *catemer*, as well as the greater degrees of freedom in the arrangement of the dimer units in the crystal to promote favourable intermolecular contacts.

These arguments promoting the cyclic hydrogen-bonded dimer (7) cannot be applied as forcefully to enantiomeric monocarboxylic acids R*–CO_2H. The chiral molecules forming the cyclic dimer would have to be related by either crystallographic or local twofold symmetry. A crystallographic twofold axis, which would have to lie perpendicular to the cyclic dimer, could impose unnecessary constraints on the overall crystal structure; twofold symmetry localized to the dimer could result in different packing environments of the two molecules of the dimer. The crystal structures of the three chiral monocarboxylic acids discussed above which form *catemer* motifs show that the O–H···O hydrogen-bond geometry is sufficiently flexible to allow the 2_1 axes about which these molecules are hydrogen-bonded to vary in length from 5–8 Å in order to accommodate suitable packing. However, it may be assumed that if molecular packing cannot be accommodated within these limits then the chiral acids must form cyclic dimers. This is probably the case for levopimaric acid, $C_{20}H_{30}O_2$ (Karle, 1972), which forms the dimer between two independent molecules in the asymmetric unit. The molecule is very bulky and probably cannot pack suitably along a *catemer* axis lying within the limits of 5–8 Å.

UM00013985
NOVARTIS EXHIBIT 1517
Novartis v. Regents, IPR2023-01347
Page 2731 of 4460

The very fact that 'distorted' O–H···O systems have been found almost only in chiral acids, and that the *catemer* (11*c*), with C=O···(H)O and C–O(H)···O(carbonyl) angles close to 120°, has been observed to date only in formic, acetic and β-tetrolic acid implies that there are preferred directional properties of the O–H···O(carbonyl) bond, namely the bond tends to be linear, the C=O···(H)O angle to be close to 120°, and the O–H bond to lie in the plane of the carbonyl system to which it is hydrogen-bonded.

3.2. *Dicarboxylic acids*

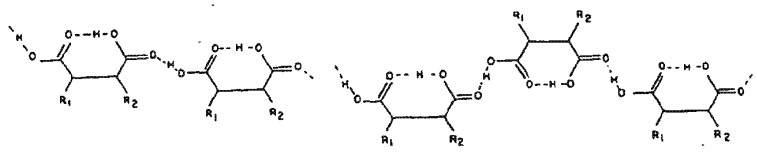
This discussion will be centred primarily on the various ways dicarboxylic acids form one-dimensional chains in which the carboxyl groups are linked to each other *via* cyclic pairs (7) of O–H···O bonds. The analysis will include 1,2-disubstituted acids which form intramolecular O–H···O bonds, chain-like dicarboxylic acids (19), followed by a detailed examination of monocarbonamide derivatives (20).



(19)

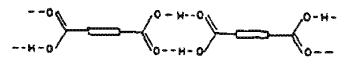
(20)

3.2.1. 1,2-*Disubstituted acids with an intramolecular* O–H···O *bond.* The 1,2-disubstituted carboxylic acids may be divided into two classes, one which contains an intramolecular O–H···O bond between the two neighbouring carboxyl groups and the other which does not. Molecules belonging to the first class may be interlinked *via* an O–H···O(carbonyl) bond between the available O–H proton donor and carbonyl O acceptor. This linkage may be achieved either by translation (21*a*), or along a 2_1 axis or glide (21*b*). The translation motif is possible if R_1 and R_2 are sufficiently small so as not to hinder each other, their intermolecular contact being governed by the length of the intermolecular O–H···O bond. Maleic acid (James & Williams, 1974) appears in this motif. The 2_1 axis (or glide) motif (21*b*) has the advantage that it does not depend on the sizes of R_1 and R_2. Furan-3,4-dicarboxylic acid (Williams & Rundle, 1964) exhibits this arrangement as well as cyclopropane-1,1-dicarboxylic acid (Meester, Schenk & MacGillavry, 1971), in which the interlinked molecules are related by a non-crystallographic glide plane. Motifs (21*a*) and (21*b*) are not the only modes in which these molecules may be interlinked, *e.g.* bicyclo[2,2,2]-octa-2,5-diene-2,3-dicarboxylic acid (Hechtfischer, Steigemann & Hoppe, 1970) does not contain the linear chains (21); rather the chains are helical with distorted fourfold screw axis symmetry.

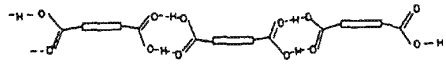


(21*a*) (21*b*)

3.2.2. *Chain-like dicarboxylic acids.* Dicarboxylic acids which contain carboxyl groups which are antiparallel to each other almost invariably achieve O–H···O hydrogen-bonded chains in which the molecules are interlinked by translation symmetry (22). The crystal structure of chiral (−)-chlorosuccinic acid (Kryger, Rasmussen & Danielsen, 1972) provides an example of this rule for, despite the asymmetric Cl substituent, the two carboxyl groups are almost antiparallel to each other, yielding the hydrogen-bonded arrangement (22).

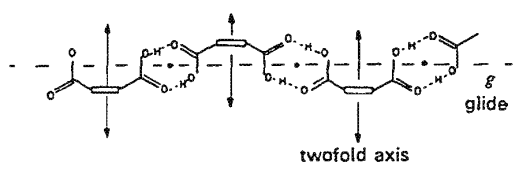


(22)



(23)

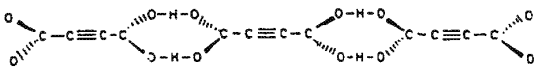
Dicarboxylic acids containing carboxyl groups which are not antiparallel to each other cannot generate hydrogen-bonded chains by translation only. Rather, these molecules form chains (23) in which each carboxyl group participates in a hydrogen-bonded cyclic dimer. There are two principal modes of generating the chains (23) depending upon the molecular symmetry. If the two carboxyl groups are not related by molecular symmetry, they may each form cyclic hydrogen-bonded dimers about centres of inversion (assuming a racemic structure) and so generate the motif (23). If the two carboxyl groups are related by molecular twofold symmetry, the hydrogen-bond motif (23) may be generated by a glide *g* (assuming a racemic structure) which is perpendicular to the molecular twofold axis and so forming a chain of (pseudo) 2/*g* symmetry, as shown in (24). The centres of the hydrogen-bonded



(24)

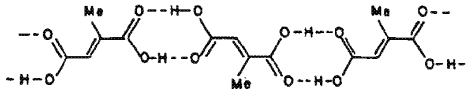
UM00013986
NOVARTIS EXHIBIT 1517
Novartis v. Regents, IPR2023-01347
Page 2732 of 4460

dimers lie on the glide plane half-way between the twofold axes. This motif encompasses a wide variety of molecules which may be subdivided into three classes. In one class the molecule itself possesses a twofold axis, which is part of the crystal symmetry. Structures belonging to this group include β-glutaric acid (Morrison & Robertson, 1949*a*) and phthalic acid (van Schalkwyk, 1954). The second set comprises crystal structures in which the twofold symmetry is localized to the molecule and the hydrogen-bonding chain (24), *i.e.* is not part of the overall crystal symmetry. Crystal structures formed in this manner are 3,3-dimethylglutaric acid (Benedetti, Claverini & Pedone, 1972) and allenedicarboxylic acid (Leiserowitz & Nader, 1973).



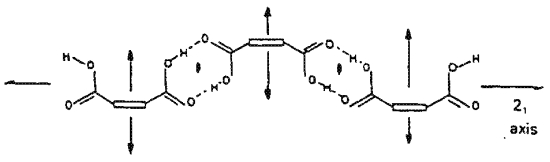
(25)

It is of interest that anhydrous acetylenedicarboxylic acid (Benghiat, Leiserowitz & Schmidt, 1972) forms this type of hydrogen-bonding chain shown in (25) by virtue of the dihedral angle of 58° between the planes of the two carboxyl groups. We are not able to state with certainty whether the non-planarity of anhydrous acetylenedicarboxylic acid is due primarily to intermolecular forces. The dihydrated form (Dunitz & Robertson, 1947), phenylpropiolic acid (Rollett, 1955), and acetylenedicarbonamide (Leiserowitz & Tang, 1976) are all planar molecules, which seems to imply that the non-planarity of acetylenedicarboxylic acid is induced by crystal forces.

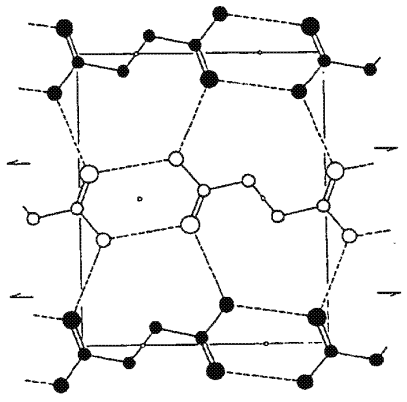


(26)

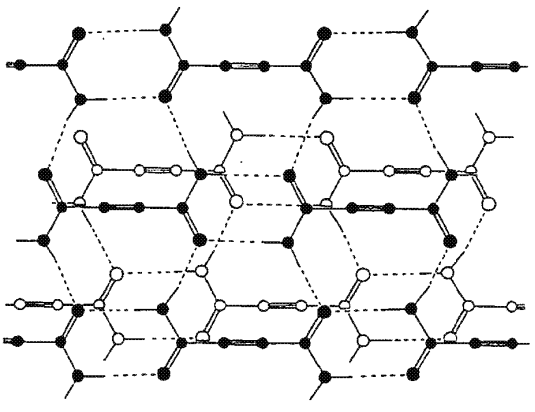
In molecules of the third class only the carboxyl groups are related by pseudo twofold symmetry, *e.g.* mesaconic acid (Gupta & Yadav, 1972). Its hydrogen-bonded chain (26) is propagated by a glide, the plane of which is almost perpendicular to that of the molecule. A chain similar to (24) may be formed *via* (pseudo) symmetry $2_1/m$. Furane-α,α'-dicarboxylic acid (Martuscelli & Pedone, 1968) and isophthalic acid (Alcala & Martínez-Carrera, 1972) fall into this class.



(27)



(*a*)



(*b*)

Fig. 7. (*a*) Succinamide (Davies & Pasternak, 1956). Hydrogen-bonding layer. (*b*) Acetylenedicarbonamide (Leiserowitz & Tang, 1976). Intra- and interlayer structure.

Table 4. *Cell constants of some acid-amide* (HO_2C–X–$CONH_2$) *crystal structures*

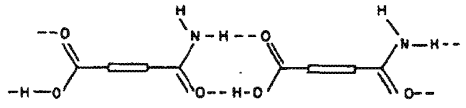
Compound	*a* (Å)	*b* (Å)	*c* (Å)	β (°)	*Z*	Space group	References
Fumaramic acid	7·367	9·041	3·742	99·39	2	$P2_1$	Benghiat, Kaufman, Leiserowitz & Schmidt (1972)
Succinamic acid	5·64	5·24	9·68	95·5	2	*Pc*	
trans,trans-Muconamic acid*	7·1	10·1	9·6	107	4	*P2/c*	
(−)-2-Bromosuccinamic acid	7·70	9·23	8·88		4	$P2_12_12_1$	Murakami & Iitaka (1969)

* The crystals of muconamic acid gave poor diffraction photographs

UM00013987
NOVARTIS EXHIBIT 1517
Novartis v. Regents, IPR2023-01347
Page 2733 of 4460

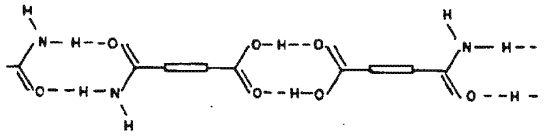
We may anticipate that, in enantiomeric dicarboxylic acids containing carboxyl groups which are related by (pseudo) molecular twofold symmetry, the hydrogen-bond chain may be formed *via* a 2_1 axis generating a chain of (pseudo) symmetry 222_1 as shown in (27). The cyclic hydrogen-bonded dimers are formed about twofold axes. These dimers are planar only if the planes of the carboxyl groups are parallel to the molecular twofold axis.

3.2.3. *Monocarbonamide derivatives of dicarboxylic acids.* Monocarbonamide derivatives of dicarboxylic acids (labelled here as carboxy-amide molecules) form hydrogen-bonded chains (28*a*) similar to (22), in which

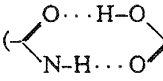


(28*a*)

the amide and carboxyl groups are interlinked, *via* a pair of O–H···O(amide) and N–H···O(carboxyl) hydrogen bonds, into a cyclic dimer.



(28*b*)

There is a second chain motif (28*b*) which comprises alternating hydrogen-bonded pairs of carboxyl groups and amide groups. Of these two chain motifs it would seem that the former is less favourable, for within the cyclic carboxy-amide pair () there is a mismatch between the lengths of the O–H···O and N–H···O bonds (O–H···O 2·6, N–H···O 2·9 Å) and the C–N–H and C–O–H bond angles (C–N–H 120°, C–O–H 112°). Yet the molecules listed in Table 4 all appear in motif (28*a*). They form two-dimensional hydrogen-bonded networks, unlike dicarboxylic acids, by virtue of the additional N–H proton donor on the amide group. It is instructive to analyse the general features of their hydrogen-bond networks to determine the interplay between hydrogen-bonding interactions and intermolecular steric forces and, as a corollary thereof, to account for the preference of the motif (28*a*) over that of (28*b*). A clearer understanding of the packing characteristics of the carboxy-amides may be achieved by first reviewing some of the principal features of primary amide packing.

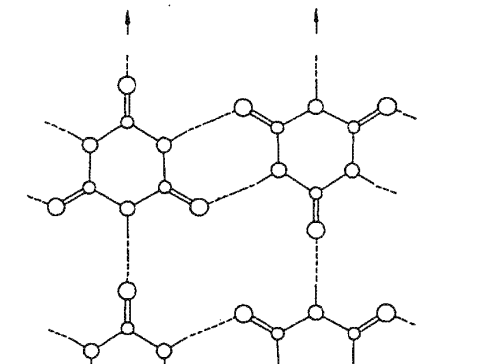
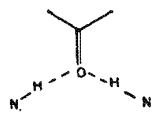


Fig. 8. Cyanuric acid (Verschoor & Keulen, 1971). Hydrogen-bonded layer.



(29)

An analysis of the molecular packing modes of primary amides $R–CONH_2$ (Leiserowitz & Schmidt, 1969) has shown that their hydrogen-bond structure tends to adopt, R permitting, the motif (29), achieved *via* interpair N–H···O bonds along a 2_1 axis (or glide) of 9·5 ± 0·3 Å. This hydrogen-bonding arrangement has been found in a number of structures including succindiamide (Davies & Pasternak, 1956) and acetylenedicarbonamide (Leiserowitz & Tang, 1976). The hydrogen-bonding arrangements of these two structures are shown in Fig. 7(*a*) and (*b*). The N–H···O motif (29) is coplanar, and contains linear N–H···O bonds symmetrically disposed about the carbonyl C=O bond with C=O···N angles ≃120°.

This motif (29) is compatible with the electron density distribution of the carbonyl O as determined from the diffraction analyses of fumaramic acid (X-ray study at 20°C) (Hirshfeld, 1971), cyanuric acid (combined X-ray and neutron study at −170°C) (Verschoor & Keulen, 1971; Coppens & Vos, 1971), diketopiperazine (X-ray study at −150°C) (Harel & Hirshfeld, 1976), allenedicarboxylic acid acetamide (X-ray study at −160°C) (Berkovitch-Yellin, Leiserowitz & Nader, 1976). The electron density maps of these molecules, in particular the latter three as their diffraction data were measured at low temperatures, displayed the lone-pair lobes of the carbonyl O; two peaks (L) in the plane of the carbonyl system with an O···L distance of ~0·6 Å and an L···O=C angle of ~110°. While these results indicate that the geometry of the N–H···O motif (29) is most favourable when the carbonyl O participates in *two* hydrogen bonds, the question arises

UM00013988
NOVARTIS EXHIBIT 1517
Novartis v. Regents, IPR2023-01347
Page 2734 of 4460

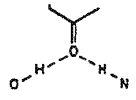
whether this N–H···O geometry is preferred if the system contains only *one* N–H···O hydrogen bond. This question is answered in part by the structural and polarized infrared results on cyanuric acid as discussed by Leiserowitz & Schmidt (1969); and Coppens & Vos (1971). Its hydrogen-bonding network (Fig. 8) consists of cyclic hydrogen-bonded N–H···O pairs with an angular geometry shown in (30*a*), and collinear N–H···O=C bonds shown in (30*b*).



(30*a*) (30*b*)

Their respective N–H···O distances (Å) and corresponding N–H stretching frequencies ν_s (cm^{-1}) are 2·805 and 3060, and 2·784 and 3210. These results seem to be in contradiction to the linear correlation between $\Delta\nu$ and N···O distance (R) given by Nakamoto, Margoshes & Rundle (1955) in which the slope, $\Delta R/\Delta\nu_s \simeq 8\times10^{-4}$ (Å cm). Clearly the difference in ν_s between the two N–H···O geometries in cyanuric acid suggests that $\Delta\nu_s$ is dependent not only on the N···O distance but also on the angular geometry of the N–H···O bond, and furthermore, that motif (30*a*) is energetically preferred over that of (30*b*).

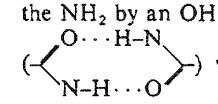
Within the crystal structure of fumaramic acid (Benghiat, Kaufman, Leiserowitz & Schmidt, 1972) the amide and carboxyl groups of molecules related by translation form hydrogen-bonded pairs (O–H···O 2·66, N–H···O 2·84 Å) generating chains (28*a*). These chains are interlinked, along a 2_1 axis of 9·04 Å (Table 4) by N–H···O bonds of 2·94 Å forming an arrangement shown in Fig. 9 similar to that of the primary amides discussed above. Naturally the hydrogen-bond motif about the carbonamide O in fumaramic acid, shown in (31), is similar to that of (29).



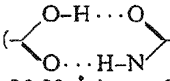
(31)

The crystal structure of succinamic acid HO_2C–$(CH_2)_2$–$CONH_2$ has not been determined. Yet its hydrogen-bond network is easily deduced from its cell constants (Table 4). The molecules are interlinked by translation *via* their amide and carboxyl groups to generate the hydrogen-bond chain (28*a*), as in fumaramic acid. This hydrogen-bond chain of succinamic acid lies along the vector $\mathbf{a}+\mathbf{b}=7{\cdot}7$ Å, which matches in length the mean of the hydrogen-bonding translation axes of succindiamide (Davies & Pasternak, 1956) = 7·99 Å, and β-succinic acid (Morrison & Robertson, 1949*b*) = 7·61 Å. The hydrogen-bond chains of succinamic acid are cross-linked *via* a c glide of 9·7 Å by N–H···O bonds between amide groups.

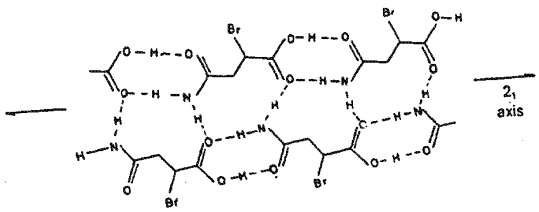
The amide group of succinamic acid makes a shallow angle of ~43° [= arcsin $(b/a+b)$] with the c glide plane in a manner similar to that observed in the crystal structures of aliphatic primary amides CH_3–$(CH_2)_n$–$CONH_2$ (Turner & Lingafelter, 1955*a*, *b*), which leads to a somewhat distorted modification of the 'ideal' N–H···O bond motif (31). If so, the obvious question arises why does succinamic acid not form a hydrogen-bond network similar to that of succindiamide (Fig. 7*a*) with its rather ideal interpair N–H···O bond arrangement. Insertion of succinamic acid into the hydrogen-bond sheet structure of succindiamide would replace the NH_2 by an OH group. Hence the amide intrapair



would be substituted by the carboxy-amide pair

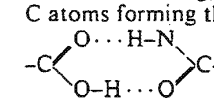


, and the interpair N–H···O bond of 2·93 Å by an O(carbonyl)···O(hydroxyl) contact of ~2·9 Å. The geometry of this contact is such that the electron lone pair lobes of the two O atoms would be directed at each other. For this type of approach a separation of 2·9 Å is too short; an acceptable distance would be 3·6 Å as discussed earlier (§ 3.1). Hence it would hardly be possible to pack succinamic acid into the more ideal hydrogen-bond network of succindiamide.



(32)

The chiral (−)-2-bromosuccinamic acid (Murakami & Iitaka, 1969) also forms the chain motif (28*a*). These chains are not interlinked into a two-dimensional hydrogen-bond network as fumaramic and succinamic acid. Rather, the chains are paired by N–H···O bonds between amide and carboxyl groups *via* a 2_1 axis parallel to the chain axis of 7·7 Å as shown in (32). The Br atoms are directed outwards from the pair of hydrogen-bonded chains and thus do not interfere sterically with the interchain N–H···O bond. Indeed were 2-bromosuccinamic acid to lie in an extended two-dimensional hydrogen-bond network similar to that of succinamic acid, the structure would incorporate short intermolecular contacts involving the Br atoms. The motif (32) is only possible if the hydrogen-bond chain axis is ~8 Å long, *i.e.* twice the distance between the C atoms forming the carboxy-amide pair

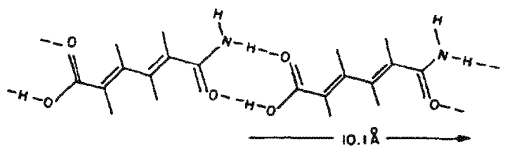


which equals 4 Å. In other words,

UM00013989
NOVARTIS EXHIBIT 1517
Novartis v. Regents, IPR2023-01347
Page 2735 of 4460

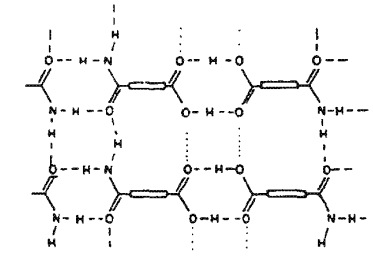
only succinamic or fumaramic acid derivatives may pack in such a manner.

trans,trans-Muconamic acid (HO_2C–CH=CH–CH=CH–CO_2H) also forms the hydrogen-bond chain motif (28*a*) along **b** since its length of 10·1 Å is the mean between the lengths of the hydrogen-bonding translation axes of mucondiamide (Leiserowitz & Schmidt, 1969) = 10·3 Å, and muconic acid (Bernstein & Leiserowitz, 1972) = 9·9 Å. These muconamic chains are interlinked *via* a *c* glide of 9·6 Å by N–H···O bonds in a manner similar to fumaramic acid. The hydrogen-bonding translation axis of 10·1 Å also indicates that the conformation of C=C–C=O at the carboxyl end of muconamic acid must be synplanar, since only a synplanar conformation can be accommodated into the hydrogen-bonding motif (33) with *b* of 10·1 Å. We naturally assume that the C=C–C=O conformation at the amide end is synplanar. We are not aware of any exceptions to this rule.

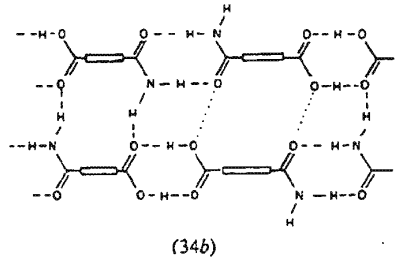


(33)

As mentioned earlier, the translation motif (28*b*) comprising hydrogen-bonded amide and carboxyl pairs has not been observed. One drawback of this motif lies in the two-dimensional hydrogen-bonded networks which may be constructed therefrom. The only possible modes of interlinking the chains (28*b*) by N–H···O bonds are by translation as shown in motifs (34*a*) and (34*b*); the interpair N–H···O bond links amide groups in motif (34*a*) and links amide and carboxyl groups in (34*b*). However, both arrangements would contain the poor O(carbonyl)···O(hydroxyl) contact of ~2·9 Å discussed earlier (§ 3.1). Therefore we tend to rule out such an arrangement.



(34*a*)

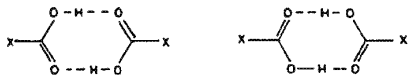


(34*b*)

4. The carboxyl dimer and its environment

4.1. *The disordered carboxyl dimer*

In this section we shall examine the systematics of packing environment about the carboxyl dimer and the effect of environment on the carboxyl group. We begin with symmetric molecules where the intramolecular environment about the carbonyl and hydroxyl O atoms are identical. In this class of molecules X–CO_2H there exist two equivalent orientations (35*a*) and (35*b*) of the carboxyl dimer mutually indistinguishable unless incorporated into the crystal.



(35*a*) (35*b*)

Therefore the observed degree of orientational disorder of the carboxyl dimer, *i.e.* the random incorporation of (35*a*) or (35*b*) at a point in the crystal, must be due to intermolecular forces. The disorder manifests itself in the observed lengths of the C–O bonds and the (disordered) locations of the hydroxyl H atom. Currie, Speakman & Curry (1967) had noted that the difference between C=O(carbonyl) and C–OH(hydroxyl) distances ranges widely from 0·04–0·12 Å, for which they accounted by assuming orientational disorder between (35*a*) and (35*b*).

Dunitz & Strickler (1968) pointed out that if the hydrogen-bonded pairs of aromatic carboxylic acids interact only weakly with one another in the solid, the arrangement in one pair must be largely independent of the arrangement in the other pairs, and so they predicted the possibility of disorder of the carboxyl group.

Recently Dieterich, Paul & Curtin (1974) pointed out a linear correlation between the difference in C–O lengths (Δr) and the difference in C–C–O angles ($\Delta\theta$) in aromatic carboxylic acids. They showed that there is a continuum of these values from completely ordered (with large values of Δr and $\Delta\theta$) to those which show disorder.

A carboxyl dimer containing C–O bonds equal in length exists in a state of disorder, either static or dynamic. Static disorder involves the existence of the two dimer orientations (35*a*) or (35*b*) and no proton transfer across the O–H···O bond. In dynamic disorder the hydroxyl proton is delocalized; either the proton is centrally situated in a symmetric O–H–O bond and the C–O bonds of the carboxyl group are in a state of resonance, or the proton undergoes rapid oscillations across the O–H···O bond accompanied by interconversion between the carbonyl C=O and hydroxyl C–O(H) bonds. As we shall observe later there

UM00013990
NOVARTIS EXHIBIT 1517
Novartis v. Regents, IPR2023-01347
Page 2736 of 4460

is no correlation between the difference in length between the C–O bonds and the length of the O–H···O hydrogen bond. This is strikingly so for identical molecules in different packing environments. This fact seems to be incompatible with dynamic disorder for we should expect a decrease in the length of the O–H···O bond with increased delocalization of the proton. Moreover, infrared spectra of carboxylic acids containing C–O bonds of equal length show the presence of the carbonyl C=O stretching mode, so we at least disqualify the symmetric O–H–O bond.

Complete static disorder implies that the crystal coordinates of the two disordered O atoms are separated by approximately 0·1 Å. Treating these two half-occupancy O atoms as a single atom should induce artificially high temperature factors in a least-squares structure-factor computation. Thus this effect should be evident in a comparison between ordered and disordered carboxyl groups which have the same thermal motion. This condition is well satisfied if the two carboxyl groups lie in the same crystal and are related by molecular symmetry. These demands are ideally fulfilled in trimesic acid, discussed below, where it is found the more equal in length the carboxyl C–O bonds, the higher the temperature factors of its O atoms.

The question then arises as to how intermolecular forces determine the degree of disorder of the carboxyl dimer. On the reasonable assumption that its orientation is determined primarily by nearest-neighbour interactions, we envisage a tendency towards disorder based on the following two criteria: (i) the neighbouring contacts of the carbonyl and hydroxyl O atoms are of a similar nature; (ii) the surroundings of the carbonyl and hydroxyl O atoms may be dissimilar, yet the lattice energy difference between the two orientations (35*a*) and (35*b*) of the carboxyl dimer is negligible. That the intermolecular environment of the carbonyl and hydroxyl O atoms may be identical is illustrated by the crystal structures of mellitic and trimesic acids, in which the two carboxyl O atoms are related to each other by crystallographic symmetry.

Mellitic acid (Darlow, 1961) contains two crystallographically independent molecules, each lying on a twofold axis (Fig. 10). Of the four independent hydrogen-bonded dimers (labelled *A*, *B*, *C*, *D*), two, *A* and *B*, lie on twofold axes while *C* and *D* have no symmetry constraints. The carboxyl dimers are not planar, the dihedral angles between the planes of the carboxyl groups of the dimers *A*, *B*, *C*, and *D* are 37°, 4°, 20° and 31°, respectively. It is unlikely that the O–H···O bonds in the dimers *A* and *B* are symmetric, since their O–H···O distances of 2·68 and 2·66 Å are no shorter than the O–H···O distances of 2·66 and 2·64 Å in dimers *C* and *D* in which the carboxyl C=O bonds are quite distinct.

The crystal structure of trimesic acid (Duchamp & Marsh, 1969) contains carboxyl dimers showing a wide spread in C–O bond length. The hydrogen-bonding motif (Fig. 11) is a two-dimensional network formed by six molecules bound together through pairs of O–H···O bonds. The networks are not planar, pleats involving dihedral angles of about 70° being formed by means of a twisting of some of the carboxyl groups out of the planes of their benzene rings. The carboxyl groups were classified by Duchamp & Marsh into three groups (Fig. 11). Group (I) comprises carboxyl groups which lie on the 70° pleat and are severely twisted out of the plane of their benzene rings (average twist 23°). Their average C=O, C–OH and O–H···O distances are 1·218, 1·319 and 2·652 Å. The second category (II) are the carboxyl groups which lie on planar sections

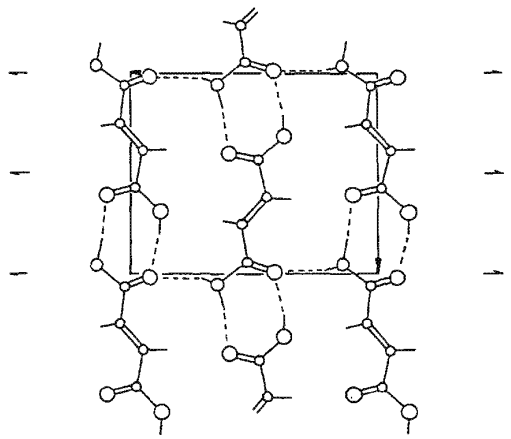


Fig. 9. Fumaramic acid (Benghiat *et al.*, 1972). Packing arrangement.

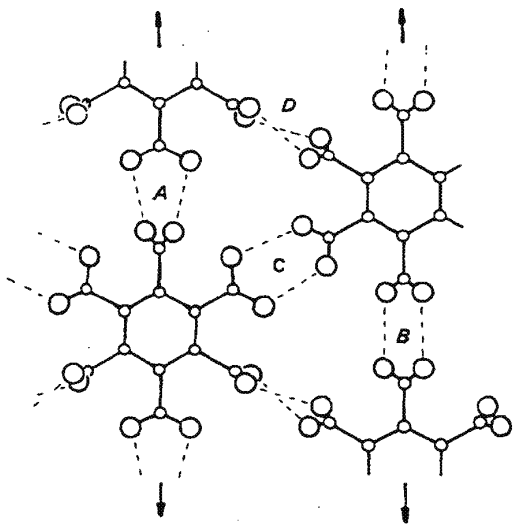


Fig. 10. Mellitic acid. Molecules linked by the four independent sets (*A*, *B*, *C*, *D*) of hydrogen bonds [reproduced from Darlow (1961)].

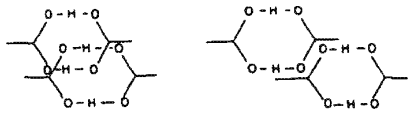
UM00013991
NOVARTIS EXHIBIT 1517
Novartis v. Regents, IPR2023-01347
Page 2737 of 4460

of the layer and are approximately coplanar with their benzene rings (average twist 3°). For these the C=O, C–OH and O–H···O distances are 1·245, 1·279 and 2·631 Å. The third category (III) comprises the carboxyl groups which form disordered O–H···O bonds about a twofold axis (C–O 1·255, O–H···O, 2·645 Å) as well as the carboxyl groups (C=O 1·244, C–OH 1·275, O···H–O 2·632 Å) in which the hydroxyl H atoms are partially disordered ($\frac{2}{3}$:$\frac{1}{3}$). Duchamp & Marsh were of the opinion that the O–H···O bond of (III) cannot be symmetric as the O–H···O distances are too long. On the other hand, they suggested that the bond lengths of the carboxyl group of (II) are indicative of considerable resonance. We could as well assume that these carboxyl groups are also disordered as in (III). Indeed the H peaks of (II) appear on the difference map (Fig. 11) to be more diffuse than those of (I); the average temperature factors U_H of these H atoms are 0·07 and 0·04 Å^2, respectively. The values of the principal magnitudes of the thermal ellipsoids $U_1 > U_2 > U_3$ (listed by Duchamp & Marsh) of the O atoms averaged for each of (I), (II), (III) [*i.e.*, $\langle U_1 \rangle$, $\langle U_2 \rangle$, $\langle U_3 \rangle$ for each category] are [0·070, 0·039, 0·030 Å^2], [0·090, 0·044, 0·032 Å^2] and [0·121, 0·062, 0·036 Å^2] respectively. These results are indicative of disorder; the more equal in length the carboxyl C–O bonds, the higher the 'thermal motion'.

We may rationalize that dimers of (I), which lie at the 70° pleat have very different force fields at their carbonyl and hydroxyl O atoms prohibiting disorder. On the other hand, the dimers of (II) lie in the planar section of the layer structure so that the force fields at their carbonyl and hydroxyl O atoms are, perhaps, more equal, resulting in partial disorder.

While it appears difficult to decipher the complex packing of trimesic acid, there are crystal structures showing order/disorder of their carboxyl dimers which lend themselves more easily to analysis by virtue of their relatively simple packing motifs. Molecules which fall into this class include benzoic and propiolic acid derivatives.

4.1.1. *Benzoic acids*. Some of the packing features of substituted benzoic acids have been discussed by Miller, Curtin & Paul (1974), in particular their stacking characteristics. They had observed that the carboxyl groups form interplanar contacts with each other, either *via* the stacking motif (36*a*) or an antiparallel arrangement of C–O bonds (36*b*).



(36*a*) (36*b*)

In this discussion we shall confine ourselves primarily to the systematics of the packing environment about the carboxyl group in the *p*-substituted benzoic acids (p = H, CH_3, Cl, Br, CO_2H, C_6H_5), *o*-halogenated acids and 2,6-disubstituted acids.

The C–O bond lengths of *p*-toluic acid (Takwale & Pant, 1971) are almost equal (1·272, 1·275 Å) indicating pronounced disorder. The molecules are interlinked by methyl–methyl contacts. These chains make lateral contact with each other, forming a layer structure (Fig. 12). This lateral contact incorporates a motif (37) in which the *m*- and *o*-substituted C–H bonds make symmetric and edge-on contacts with the O–H···O bond of the carboxyl dimer. In the interlayer contact the carboxyl dimer is sandwiched between the methyl groups which lie at almost equal distances from the two O atoms forming the O–H···O bond. As might be expected, this symmetric environment about the O atoms induces disorder.

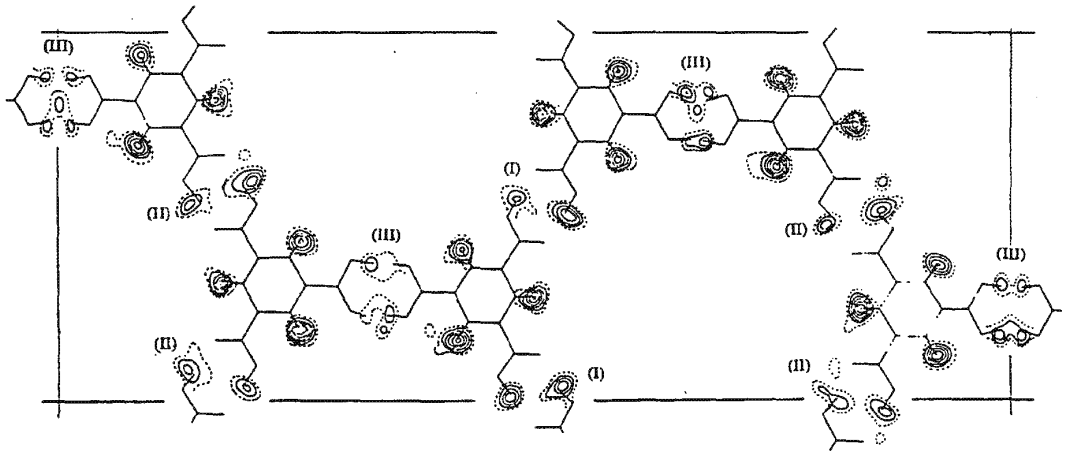
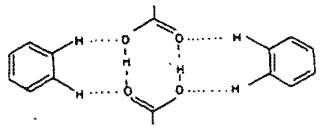


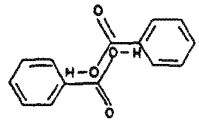
Fig. 11. 1,3,5-Trimesic acid. The hydrogen-bond motif showing hydrogen peaks. The carboxyl dimers belonging to categories (I), (II) and (III) are denoted (see §4.1) [reproduced from Duchamp & Marsh (1969)].

UM00013992
NOVARTIS EXHIBIT 1517
Novartis v. Regents, IPR2023-01347
Page 2738 of 4460



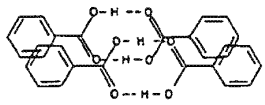
(37)

Terephthalic acid (Bailey & Brown, 1967) crystallizes in two triclinic modifications. The structure of the more stable α-form was determined with an extensive set of X-ray intensities while only partial X-ray data were collected for the less stable β-form. The C–O bond lengths were found to be almost equal in the α-form (1·262, 1·272 Å), less so in the β-form (1·25, 1·28 Å) indicating carboxyl disorder which is pronounced in the α- and partial in the β-form. In both modifications the molecules pack in chains of cyclic hydrogen-bonded dimers, which make lateral contact with each other to form layer structures [Fig. 13(*a*) and (*b*)]. These two-layer structures are identical with each other and incorporate the lateral C–H···O contacts of motif (37). The difference between the α- and β-modifications lies in their interlayer arrangements. In the α-form the carboxyl dimers are closely stacked, the carboxyl groups being offset along the direction of the shorter 'C=O' bond of 1·262 Å. In the β-form the contact between the carboxyl dimers is characterized by an antiparallel arrangement of 'C–O(H)'hydroxyl bonds of 1·28 Å as shown in (38).

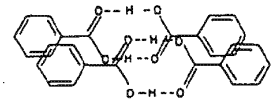


(38)

We therefore attribute the almost complete disorder of the carboxyl group of the α-form and the partial disorder of the carboxyl group of the β-form on the one hand to the similar environment of both O atoms within the layer and, on the other hand we infer, at least for the α-form, that the interlayer interactions permit pronounced disorder despite differences in interstack environment of the two carboxyl O atoms. The C–O bond lengths of the α-form do suggest a slight preference for the stacking arrangement (39*a*), where the carboxyl groups are offset along their C=O bonds, over that of (39*b*).



(39*a*)



(39*b*)

The strong disorder of the α-form seems to suggest that either the interactions between the stacked dimers

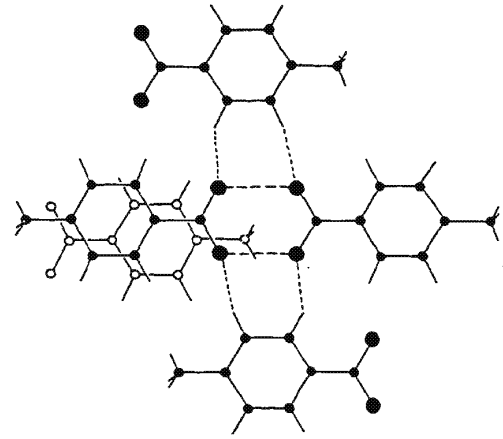
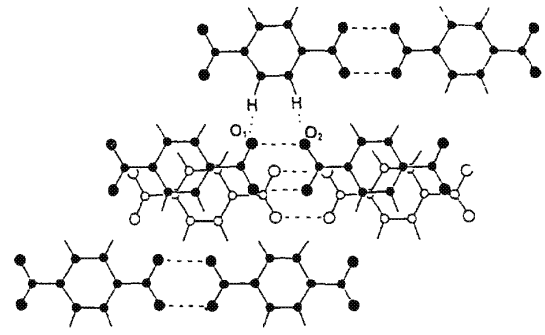
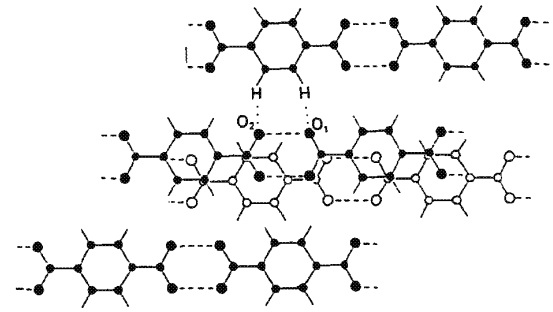


Fig. 12. *p*-Toluic acid (Takwale & Pant, 1971). Intra- and interlayer arrangement. Distances: C–O 1·272, 1·275, O–H···O 2·63, C–H···O 3·59, 3·47 Å. Offset between adjacent molecules in the layer is 1·35 Å.



(*a*)

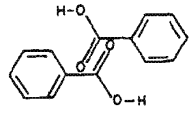


(*b*)

Fig. 13. (*a*) α-Terephthalic acid (Bailey & Brown, 1967). Intra- and interlayer packing. Distances: O–H···O 2·608, C–O_2 1·262, C–O_1 1·272, C–H···O 3·48, 3·60 Å. Offset from coplanarity between adjacent hydrogen-bonded chains is 0·6 Å. (*b*) β-Terephthalic acid (Bailey & Brown, 1967). Intra- and interlayer packing. Distances: O···O 2·58, C–O_1 1·25, C–O_2 1·28, C–H···O 3·46, 3·48 Å. Offset from coplanarity between adjacent hydrogen-bonded chains is 0·6 Å.

UM00013993
NOVARTIS EXHIBIT 1517
Novartis v. Regents, IPR2023-01347
Page 2739 of 4460

may be weak (Dunitz & Strickler, 1968) or that the energy difference between the two carboxyl dimer orientations (39*a*) and (39*b*) in their stacks is small. The first suggestion is perhaps ruled out on the basis that carboxylic acids show a tendency to crystallize in stacks.



(40)

Regarding the interlayer motif (38) of β-terephthalic acid, it is noteworthy that benzoic acid (Sim, Robertson & Goodwin, 1955), which also exhibits the intralayer arrangement (37), shows an interplanar arrangement (40) which, at first sight, is similar to that of β-terephthalic acid (38). The crystal structure of benzoic acid was determined from two-dimensional X-ray data so that the error in its C–O lengths of 1·24 and 1·29 Å must be at least 0·02Å. Comparing the interlayer motifs of β-terephthalic acid and benzoic acid shows an antiparallel pairing of 'C–OH' bonds in terephthalic acid, whereas in benzoic acid the 'C=O' bonds are paired antiparallel. It is difficult to reconcile this difference unless we assume effective long-range interactions which are different in the two structures. This point is substantiated by the crystal structures of the analogous *p*-bromobenzoic acid (Ohkura, Kashino & Haisa, 1972) and *p*-chlorobenzoic acid (Miller, Paul & Curtin, 1974). The C–O bonds of the bromo acid are distinct with lengths of 1·225 and 1·307 Å, unlike the chloro acid with lengths of 1·253 and 1·273 Å. Both acids display the intralayer motif (37) common to benzoic acids and the carboxyl-stacking motif (38*a*), yet the bromo acid shows no evidence of carboxyl disorder. We, therefore, conclude that the extent of order/disorder of the carboxyl group is also dependent on fairly long-range interactions.

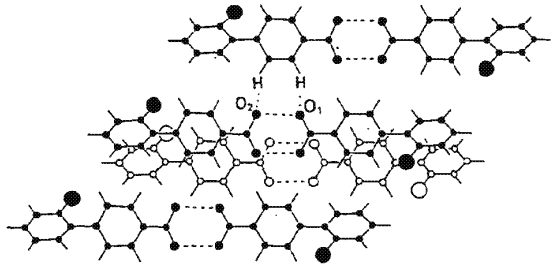


Fig. 14. 2′-Chlorobiphenyl-4-carboxylic acid (Sutherland, 1969). Intra- and interlayer packing. Distances: $O_1\cdots O_2$ 2·610, C–O_1 1·289, C–O_2 1·261, C–H···O 3·58, 3·52 Å. Offset from coplanarity between layer molecules is 0·2 Å.

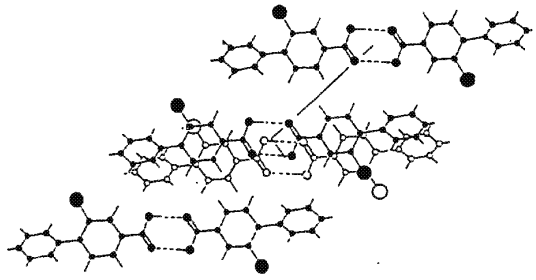


Fig. 15. 2-Chlorobiphenyl-4-carboxylic acid (Sutherland & Hoy, 1969). Packing arrangement seen normal to the plane of the carboxyl pair. Distances: C–O 1·315, C=O 1·205, and O–H···O 2·62 Å.

The crystal structures of some substituted biphenyl-4-carboxylic acids also show the packing features found in the 4-substituted benzoic acids. 2′-Chlorobiphenyl-4-carboxylic acid (Sutherland, 1969) (Fig. 14) and the iodo derivative (Sutherland, 1970) both show the layer motif (37) and the carboxyl stacking motif (39*b*). The C–O bond lengths in both structures (2′-Cl, 1·261, 1·289; 2′-I, 1·250, 1·264 Å) indicate appreciable disorder. The stacking of their carboxyl groups, which are offset along the direction of the 'C–O(H)' bonds, is unlike that of the disordered carboxyl groups of α-terephthalic acid, where the offset is along the 'C=O' bond, providing further evidence of the small energy difference between the stacks (39*a*) and (39*b*).

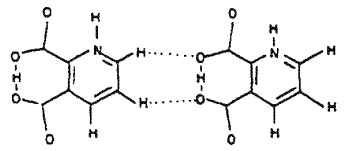
The crystal structure of 2-chlorobiphenyl-4-carboxylic acid (Sutherland & Hoy, 1969) (Fig. 15) does not contain the lateral C–H···O contacts of the layer motif (37), as such an arrangement would incur very short contacts involving the Cl atom. The carboxyl groups are stacked as in motif (39*a*), *i.e.* they are offset along the direction of the C=O bond. The C–O lengths of 1·205 and 1·315 Å indicate no disorder which may be correlated with the asymmetric lateral environment of the carboxyl dimer.

The lateral C–H···O contacts of motif (37) are also present in the *o*-halogenated benzoic acids (F, Cl, Br). The carboxyl bonds of the Cl (Ferguson & Sim, 1961) and Br (Ferguson & Sim, 1962) derivatives show distinct carbonyl and hydroxyl character in keeping with the asymmetric intramolecular environment of the carboxyl group (§ 2.2). On the other hand, the C–O lengths of 1·255 and 1·280 Å in *o*-fluorobenzoic acid (Krausse & Dunken, 1966) tend to be equal: the stacking pattern of its carboxyl groups (Fig. 16) resembles motif (39*a*). Despite the asymmetric intramolecular environment of the carboxyl group introduced by the F substituent, its relative smallness compared with CH_3, Cl and Br obviously permits some orientational disorder.

The common occurrence in benzoic acids of the intralayer motif (37) with its C–H···O contacts of ~3·5 Å raises the question whether the motif is induced by close-packing or weak C–H···O interactions, or a combination of these two effects. A similar question was recently raised by Kvick, Koetzle, Thomas & Takusagawa (1974) in their discussion of the lateral

UM00013994
NOVARTIS EXHIBIT 1517
Novartis v. Regents, IPR2023-01347
Page 2740 of 4460

C–H···O contacts (H···O 2·40, 2·30 Å) in pyridine-2,3-dicarboxylic acid shown in (41), which is similar to motif (37).



(41)

That close-packing plays a dominant role in the formation of (37) is confirmed by the crystal structure of pentafluorobenzoic acid (Benghiat & Leiserowitz, 1972*b*), which exhibits an arrangement similar to the intralayer motif (37) in which the (C)H···O contacts are replaced by (C)F···O contacts of 3·2 Å. The pentafluorobenzoic acid molecule is not planar, unlike the unsubstituted benzoic acids already described; the carboxyl group is twisted out of the plane of the ring by 30°. Its C–O lengths of 1·228 and 1·278 Å and the presence of the hydroxyl H atom on a difference map indicated that the carboxyl pair does not exhibit appreciable disorder. This lack of disorder was attributed to the packing normal to the plane of the carboxyl dimer which revealed that it is sandwiched between C–F bonds and differences in environment about the carbonyl and hydroxyl O atoms.

We conclude that benzoic acids which appear in the layer motif (37) may show disorder of their carboxyl dimers which is compatible with the lateral symmetric environment about the two O atoms of the carboxyl group. Regarding the interlayer motif, an almost symmetric environment, as observed in *p*-toluic acid, permits disorder. Stacked carboxyl dimers may be offset along the C–O bond, which may be either the C=O bond or the C–O(H) bond or a disordered combination thereof. Medium-range interactions obviously play a role in determining the extent of C–O order/disorder in this structure type, as demonstrated by the crystal structure of *p*-bromobenzoic acid. Carboxyl groups also form interplanar antiparallel arrangements of C–O bonds, either C=O or C–OH.

We now consider the symmetrically substituted benzoic acids in which the lateral C–H···O contacts of motif (37) would be precluded, *i.e.* molecules with di-*o* or di-*m*-substituted phenyl rings. Molecules belonging to this class are 3,4,5-trimethylbenzoic acid, 2,4,6-trimethylbenzoic acid (mesitoic acid) and 2,6-dimethylbenzoic acid.

In 3,4,5-trimethylbenzoic acid (Cano, Martínez-Carrera & García-Blanco, 1970) the carboxyl pair is sandwiched edge-on by the *m*-substituted methyl C atoms lying opposite the midpoints of the O–H···O bonds. The contacts above the plane of the carboxyl dimer with the Me groups are not symmetrically disposed with respect to the carboxyl group, yet the C–O lengths of 1·251 and 1·287 Å show evidence of disorder. The carboxyl pairs of mesitoic acid (Florencio & Smith, 1970; Benghiat & Leiserowitz, 1972*c*) display disorder according to their C–O lengths of 1·248 and 1·275 Å and to the fact that the difference map shows disordered hydroxyl H atoms. This effect may be due to the presence of the *o*-methyl groups which are related by molecular twofold symmetry, and which would provide similar contact geometry for the carboxyl group in its two equivalent orientations. Furthermore, the O atoms are partially shielded from intermolecular contacts by the *o*-methyl groups. The extent of shielding is dependent upon the degree of coplanarity of the carboxyl group with the benzene ring; the larger the angle of twist the more exposed are the O atoms. The angle of twist in mesitoic acid is 48·5 *versus* 53·5° in 2,6-dimethylbenzoic acid (Anca, Martínez-Carrera & García-Blanco, 1967) which has C–O lengths of 1·226 and 1·276 Å, indicating less disorder than in mesitoic acid.

4.1.2. *Propiolic acids.* In the propiolic acid series R–C≡C–CO_2H, the (room temperature) orthorhombic form of phenylpropiolic acid (Rollett, 1955) has C–O bonds which are equivalent by virtue of crystallographic symmetry. Both anhydrous acetylenedicarboxylic acid and α-tetrolic acid display pronounced disorder of their carboxyl dimers not imposed by crystallographic symmetry. The crystal structure of acet-

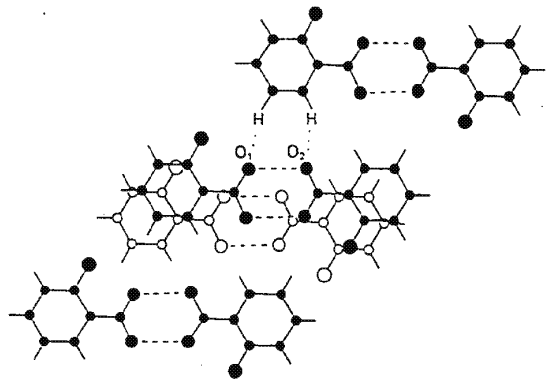


Fig. 16. *o*-Fluorobenzoic acid (Krausse & Dunken, 1966). Intra- and interlayer packing. Distances: O···O 2·642, C···O_1 1·255, C···O_2 1·280; C–H···O 3·62 and 3·89 Å. Offset from coplanarity between molecular pairs is 0·3 Å.

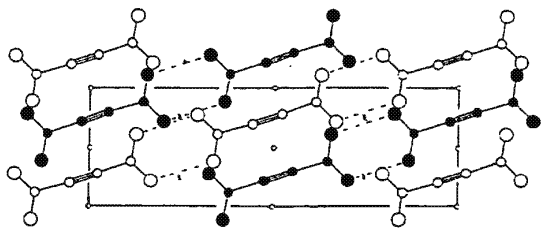
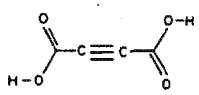


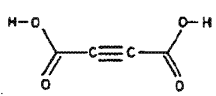
Fig. 17. Acetylenedicarboxylic acid (Benghiat, Leiserowitz & Schmidt, 1972). Packing arrangement seen along [010].

UM00013995
NOVARTIS EXHIBIT 1517
Novartis v. Regents, IPR2023-01347
Page 2741 of 4460

ylenedicarboxylic acid (Benghiat, Leiserowitz & Schmidt, 1972) (Fig. 17) does show a measure of packing symmetry about the carboxyl O atoms which perhaps accounts for the disorder as indicated by the C–O lengths (1·261, 1·248, 1·262, 1·244 Å) and the location of 'split' H atoms on a difference map. A symmetric hydrogen bond is ruled out as the O–H···O distance of 2·668 Å is 0·01 Å longer than the unsymmetric O–H···O(carbonyl) bonds of both propiolic acid (Leiserowitz & Olovsson, 1976) and β-tetrolic acid (Benghiat & Leiserowitz, 1972*a*). Furthermore, the infrared spectrum of crystalline anhydrous acetylenedicarboxylic acid (Leiserowitz, 1975, unpublished results) shows the band at 1700 cm^{-1}, due to the carbonyl stretching mode. We infer from the disorder of the carboxyl dimers that the intramolecular separation of the two carboxyl groups by the acetylene bond is sufficient to permit the existence of both conformers (42*a*) and (42*b*).



(42*a*)



(42*b*)

α-Tetrolic acid (Benghiat & Leiserowitz, 1972*a*) forms cyclic hydrogen-bonded pairs. The C–O bonds are almost equal in length (1·252, 1·265 Å) and disordered hydroxyl H atoms were located on a difference map. A symmetric O–H···O bond is incompatible with the O···O distance of 2·649 Å, being only 0·006 Å shorter than that of the unsymmetric O–H···O bonds of both propiolic acid and β-tetrolic acid. Furthermore,

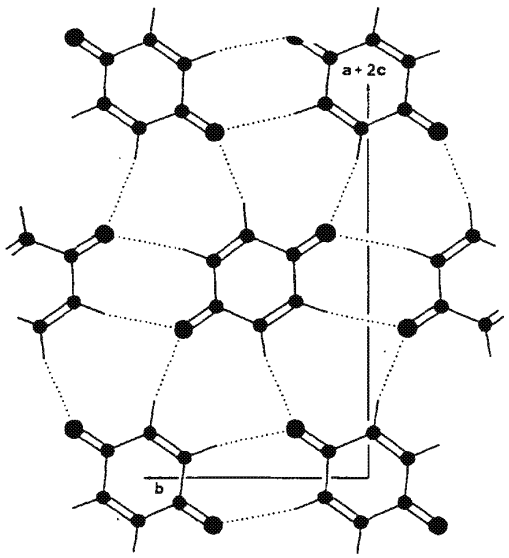


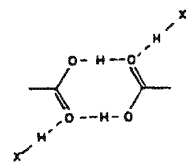
Fig. 18. Benzoquinone (Trotter, 1960*a*). Layer structure. The C–H···O contacts are marked.

the infrared spectra of both forms of tetrolic acid (Leiserowitz, 1975, unpublished results) show a band at 1690 cm^{-1} due to the carbonyl C=O stretching mode. [The spectrum of the β-form shows an additional band at 1630 cm^{-1} which may be associated with the *catemer* O–H···O bond (Walborsky *et al.*, 1961).] In α-tetrolic acid the hydrogen-bonded pairs are linked by Me···Me contacts generating linear chains. These chains are interconnected to form an approximate layer structure. Neither the intra- nor the interlayer contacts are symmetrically disposed about the disordered carboxyl group. The interlayer arrangement of α-tetrolic acid does not include closely stacked groups, as in β-tetrolic acid which exhibits the carboxyl stacking motif (39*a*). Rather, it includes an antiparallel arrangement of disordered C–O bonds similar to that observed in benzoic acid (40) and β-terephthalic acid (38).

Propiolic acid (Leiserowitz & Olovsson, 1976) H–C≡C–CO_2H, in contrast to α-tetrolic acid and acetylenedicarboxylic acid, forms hydrogen-bonded dimers, which show distinct carbonyl and hydroxyl character (C–O 1·218, 1·310 Å). As this structure will be discussed later, suffice it to say that an acetylenic C–H···O(carbonyl) contact of 3·3 Å may be responsible for stabilizing the fixed orientation of its carboxyl group.

4.2. *The carboxyl dimer and possible* C–H···O *interactions*

The carbonyl O atom, which participates in the O–H···O bond of the carboxyl dimer, is capable of accepting another acid proton donor, X–H, where X



(43)

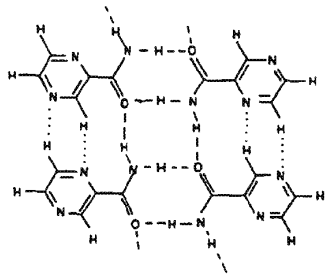
is N or O, as shown in (43). There are numerous carboxylic acid structures which demonstrate the principle that, if the molecule contains an additional proton donor, the structure adopted will satisfy the full complement of two hydrogen bonds to the carbonyl O atom. The question we wish to raise is whether a C–H bond is a proton donor sufficiently strong to form a C–H···O(carbonyl) interaction and thus induce its existence in motif (43).

Rather conclusive crystallographic and spectroscopic evidence for C–H···*A* interactions exists where *A* is a strong proton acceptor and C–H is a constituent of the halo-forms, hydrogen cyanide, and acetylene derivatives as discussed by Sim (1967). Donohue (1968) has discussed the evidence for the C–H···O interaction in the solid state, particularly those C–H groups

UM00013996
NOVARTIS EXHIBIT 1517
Novartis v. Regents, IPR2023-01347
Page 2742 of 4460

which do not appear to be under the influence of activating groups tending to promote ionization of the H atom. The existence of these C–H···O interactions has been claimed by a number of workers, notably Sutor (1963), on the basis of short C–H···O distances of approximately 3·2 Å. Donohue presented arguments that an O···H distance of 2·4 Å is not presumptive evidence of hydrogen-bond formation and doubted whether many of the short C–H···O distances (H···O 2·2 Å) can be regarded as hydrogen bonds in the same sense that the term is used for O–H···O, N–H···O and N–H···N systems.

What then is an essential yardstick for an acceptable C–H···O interaction in the solid state? It is not unreasonable to base ourselves partially on the stereochemical considerations deduced from the packing modes of O–H···O and N–H···O systems, *i.e.* that the C–H bond be directed towards the O atom, lies in the plane of the carbonyl system, makes, if possible, an angle close to 120° with the C=O bond, and last, but not least, that the C–H···O distance be short. There is a general tendency to regard a C–H···O contact as not being a significant interaction if the C–H···O distance is greater than 3·3 Å. In this context we comment on the hydrogen-bonding structure of β-pyrazincarboxamide (Rø & Sørum, 1972*a*) shown in (44*a*).



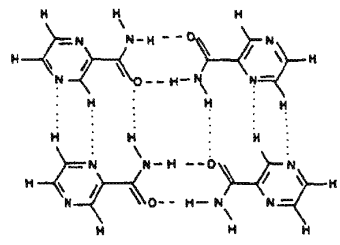
(44*a*)

The N–H···O distance in the hydrogen-bonded pair in (44*a*) is 2·92 Å, while the N–H···O distance along the 10·7 Å glide is as long as 3·24 Å. The C–H···N contacts of 3·38 Å along the glide prevent a closer approach between N and O. Thus it appears that packing forces have induced a pronounced stretch of the interpair N–H···O bond of pyrazincarboxamide. By analogy we shall not, *a priori*, regard a C–H···O interaction as insignificant if its C···O distance is 0·2–0·3 Å greater than 3·2 Å.

There remains, however, the problem of how we may be further assured whether a given C–H···O contact, which satisfies the stereochemical conditions stated above, plays a determining role in forming the crystal structure. To resolve this question we may query whether the motif involving the C–H···O contact repeats itself in a number of different structures and secondly, whether the molecule in question could not have adopted a more favourable arrangement, but for the C–H···O contact. We illustrate this approach by analysing relevant aspects of the crystal structures of pyrazincarboxamide, uracil and benzoquinone.

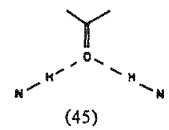
Pyrazincarboxamide crystallizes in four modifications, α,β,γ,δ (Tamura, Kuwano & Sasada, 1961), of which the α-, β-, and δ-forms have been reported. The α-form (Takaki, Sasada & Watanabe, 1960) contains two types of cyclic hydrogen-bonded pairs, N–H···O bonds of 2·90 Å and N–H···N bonds of 3·14 Å. The hydrogen-bonding structure of the β-form (44*a*), just discussed, contains N–H···O bonds of 2·92 and 3·24 Å.

The δ-form (Rø & Sørum, 1972*b*) contains only the NH···O bond of 2·90 Å involved in the cyclic amide pair. These pairs are related along a 5·73 Å axis to form an extended ribbon (44*b*) which is approximately coplanar. The contacts along the ribbon are N–H···O 3·48 Å and C–H···N 3·40 Å. These results seem to suggest that C–H···N interactions as well as weak N–H···O interactions stabilize the structure. In the β-form (44*a*) the relatively short interpair N–H···O bond (3·24 Å) is achieved since the pairs, being interlinked by a glide, do not form a coplanar set, and thus permit a closer approach between pairs.

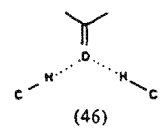


(44*b*)

In the structure of uracil (Parry, 1954; Stewart & Jensen, 1967) one carbonyl O atom participates in two N–H···O hydrogen bonds (45), and the other makes short contacts of 3·25 and 3·32 Å with two C–H bonds (46).



(45)



(46)

A more homogeneous hydrogen-bonded structure could be formed were both carbonyl O atoms to participate in N–H···O bonds, as in 5-fluorouracil (Fallon, 1973) or 6-azauracil (Singh & Hodgson, 1974) suggesting that the observed hydrogen-bond structure of uracil is compensated by the motif (46) containing the two C–H···O contacts.

Bernstein, Cohen & Leiserowitz (1974), in a review on the structural features of quinones, attributed C–H···O interactions of 3·5 Å to account for the layer structure of 1,4-benzoquinone (Trotter, 1960*a*) (Fig. 18). The argument was reinforced by the observation

UM00013997
NOVARTIS EXHIBIT 1517
Novartis v. Regents, IPR2023-01347
Page 2743 of 4460

that in the 1:1 crystal complex of thymine with benzoquinone (Sakurai & Okunuki, 1971) in which each component occupies alternate layers, the benzoquinone layer is identical with that of its mono-component structure. The different interlayer environments of benzoquinone in the two structures indicate that its layer arrangement must be primarily determined by intra- and not interlayer forces. It may, however, be argued that the layer structure of benzoquinone corresponds to a very close-packed system. It is noteworthy that tetrafluoro-*p*-benzoquinone (Meresse, Courseille & Chanh, 1974) does not form a layer motif as in benzoquinone; rather the molecules pack in such a way that a C=O bond points towards the C atom of a C=O of a neighbouring molecule inclined at a steep angle to

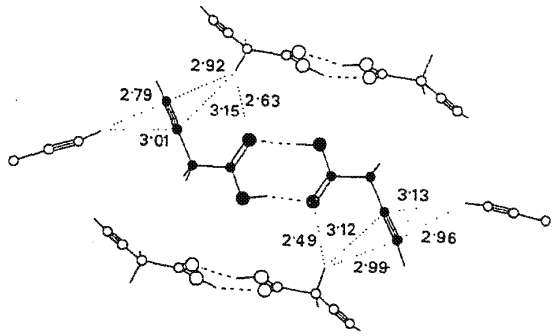


Fig. 19. Butynoic acid (Benghiat & Leiserowitz, 1972*c*). Packing arrangement showing C–H···C≡C and C–H···O contacts.

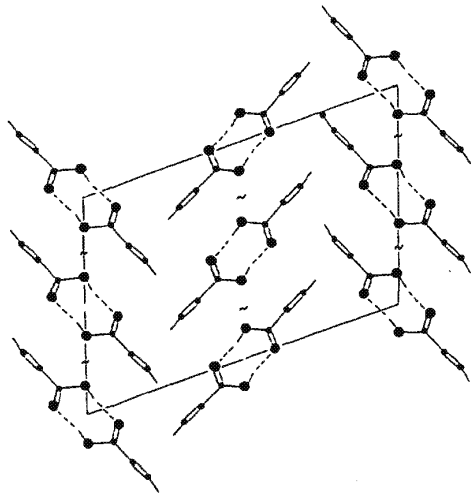


Fig. 20. Propiolic acid (Leiserowitz & Olovsson, 1976). Packing arrangement seen along the *b* axis.

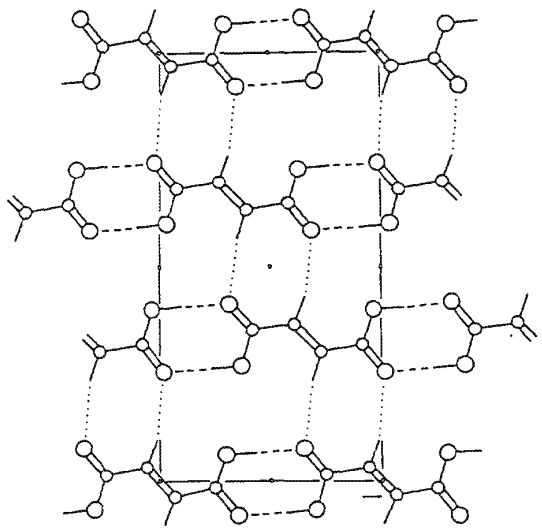


Fig. 21. Fumaric acid (Brown, 1966; Bednowitz & Post, 1966). Intralayer structure of the triclinic and monoclinic modifications. Averaged distances for these two forms are: C=O 1·225, C–OH 1·292, O–H···O 2·680, and C–H···O 3·44 Å. The layer structure is planar to within 0·2 Å.

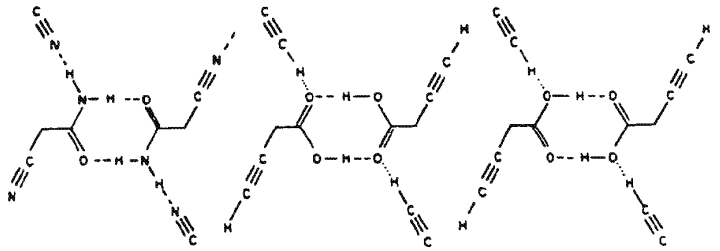
the first and with an O···C separation of 2·9 Å. This C=O···C interaction, which is not uncommon, has been discussed by Bolton (1964).

The above examples do seem to present evidence, albeit tenuous, for the existence of C–H···O and C–H···N interactions. At this point we pass on to C–H···O contacts in carboxylic acid structures considering C(*sp*)–H and C(sp^2)–H bonds in turn.

4.2.1. *The carboxyl dimer and the* C(*sp*)–H···O *contact*. The crystal structure of but-3-ynoic acid (Benghiat & Leiserowitz, 1972*c*) does not contain intermolecular ≡C–H···O contacts. Rather, the acetylenic C–H bond points at the C≡C triple bond (Fig. 19). The H···C≡C (midpoint) distance is 3·0 Å. A C(sp^3)–H bond is directed towards the carbonyl O atom (C–H···O 3·45, H···O 2·6 Å).

Benghiat & Leiserowitz (1972*c*) argued that the specific and attractive nature of this ≡C–H···C≡C interaction be gauged from the fact that the crystal structure of butynoic acid does not incorporate ≡C–H···O contacts. Whether butynoic acid can indeed form an acceptable structure with ≡C–H···O contacts was considered by examining the hydrogen-bonding structure (47) of an analogous compound, cyanoacetamide (Chieh & Trotter, 1970). The structure consists of hydrogen-bonded dimers where the available N–H bond is linked to a cyano group. Were butynoic acid to adopt either of the isostructural arrangements (48*a*) or (48*b*), the group –C≡N···H–N with an N···(H)–N distance of 3·1 Å would be replaced by a ≡C–H···O contact of 3·2–3·4 Å. The hypothetical arrangement

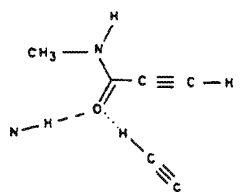
UM00013998
NOVARTIS EXHIBIT 1517
Novartis v. Regents, IPR2023-01347
Page 2744 of 4460



(47) (48*a*) (48*b*)

(48*a*) contains a C–H···O(carbonyl) interaction but requires an antiplanar conformation of the O=C–C–C group. The preferred synplanar conformation embodies a C–H···O(hydroxyl) interaction (48*b*). In the absence of either (48*a*) or (48*b*) it was concluded, tentatively, that the ≡C–H···C≡C(midpoint) and the C(sp^3)–H···O(carbonyl) interactions in the observed structure override the acetylenic C–H···O forces in the hypothetical arrangements (48).

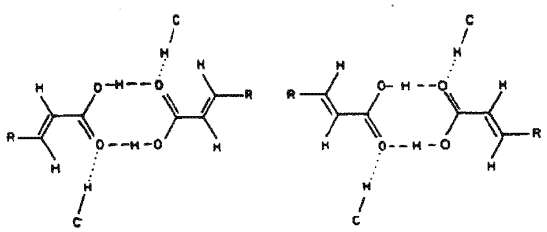
The structure of propiolic acid (Leiserowitz & Olovsson, 1976), in contrast to butynoic acid, should permit an acetylenic ≡C–H···O(carbonyl) interaction. The crystal structure (Fig. 20) shows hydrogen-bonded dimers interlinked by a ≡C(–H)···C≡C contact of 3·76 Å (H···C≡C 2·85 Å) and a non-linear ≡C–(H)···O(carbonyl) contact of 3·3 Å (H···O 2·8 Å). The C–O lengths of 1·218 and 1·310 Å are distinct indicating little or no disorder, unlike α-tetrolic acid or acetylenedicarboxylic acid. This suggests that the C–H···O(carbonyl) contact plays a role in fixing the orientation of the carboxyl group. It may be argued that but for the C–H···O(carbonyl) interaction, the molecules could have adopted a structure similar to that of β-tetrolic acid (Fig. 6), incorporating the hydrogen-bond *catemer* motif (11*c*) and an acetylenic C–H···C≡C contact but not a C–H···O(carbonyl) contact. However, it is difficult to reconcile the non-linear C–H···O contact of propiolic acid with the convincing C–H···O(carbonyl) interaction of 3·2 Å in the crystal structure of the analogous *N*-methylpropiolamide (Leiserowitz & Tuval, 1976) shown in (49). This C–H···O system is linear, the C=O···H angle is 123° and the C–H bond is almost coplanar with the carbonyl system.



(49)

Regarding the ≡C–H···C≡C motif found in butynoic and propiolic acids, it is noteworthy that a (≡C–)D···C≡C(midpoint) contact of 2·68 Å occurs in the low-temperature phase of solid acetylene-d_2 (Koski & Sandor, 1975). These contacts are analogous to the ≡C–I···C≡C (midpoint) contacts found in diiodoacetylene (Dunitz, Gehrer & Britton, 1972). These I···C≡C contacts of about 3·4 Å were interpreted by the authors as being donor···acceptor interactions.

4.2.2. *α,β-trans-Unsaturated acids and the* C(sp^2)–H···O *contact.* The packing arrangements about the carboxyl dimer of an α,β-unsaturated acid, R–CH=CH–CO_2H' participating in a lateral C(sp^2)–H···O(carbonyl) contact with a C=O···H angle of ~130° are shown in (50) and (51), for syn- and antiplanar C=C–C=O conformations, respectively. Of these two arrangements, in-



(50) (51)

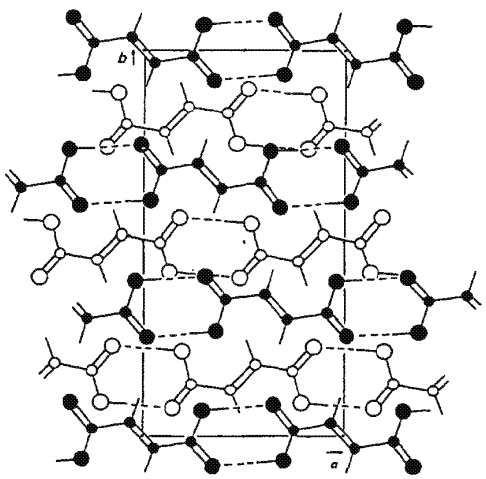


Fig. 22. Fumaric acid (Brown, 1966). Interlayer structure of the monoclinic form.

UM00013999
NOVARTIS EXHIBIT 1517
Novartis v. Regents, IPR2023-01347
Page 2745 of 4460

termolecular H···H repulsion is certainly more severe in (50); thus (51) containing the antiplanar C=C–C=O conformer should be preferred. While intramolecular forces favour the synplanar C=C–C=O conformation in α,β-unsaturated acids, the acids which exhibit the antiplanar C=C–C=O conformation, *i.e.* α- and β-fumaric acid, monomethyl muconate, monomethyl fumarate and α-*trans*-cinnamic acid, pack in the motif (51). Bernstein & Leiserowitz (1972) had pointed out that the crystal structures of fumaric acid (Brown, 1966; Bednowitz & Post, 1966), and *trans,trans*-monomethylmuconate (Rabinovich & Schmidt, 1967) involve C–H···O contacts of about 3·5 Å incorporating motif (51). Fumaric acid is dimorphic ($P\bar{1}$, $Z=1$; $P2_1/c$, $Z=6$); in both modifications the molecular structures contain carboxyl groups with distinct carbonyl and hydroxyl character (average values C=O 1·225, C–OH 1·292 Å) and exhibit the antiplanar C=C–C=O conformation. Fumaric acid lies in layers in its two crystal forms; moreover, these layers are isostructural (Fig. 21). In the monoclinic structure (Fig. 22), the layers are related by 2_1 axes; in the triclinic structure (Fig. 23) the layers are related by translation. Since intramolecular forces favour the synplanar C=C–C=O conformer, the antiplanar C=C–C=O conformation of fumaric acid must be due primarily to intralayer forces, *i.e.* C–H···O(carbonyl) forces; the interlayer interactions are probably ruled out, since the packing of the layers is different in the two structures. Indeed, the synplanar C=C–C=O conformation is adopted by fumaric acid (C–O 1·19, 1·33 Å) in the adduct β-picoline *N*-oxide:fumaric acid (Gorres, McAfee & Jacobson, 1975).

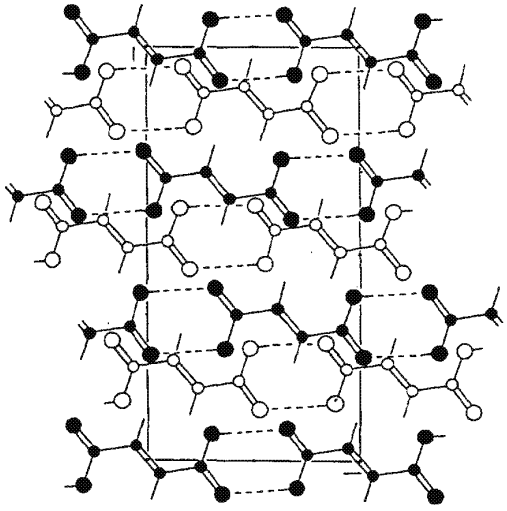


Fig. 23. Fumaric acid (Bednowitz & Post, 1966). Interlayer structure of the triclinic form.

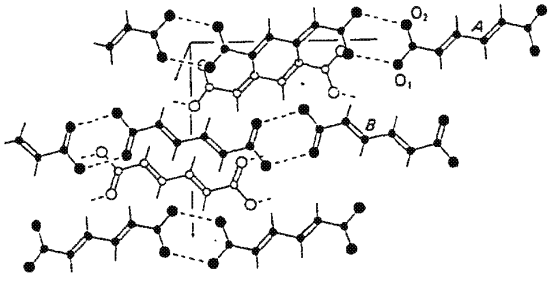
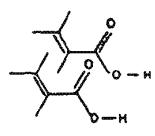


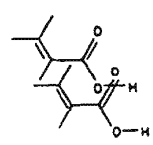
Fig. 24. *trans,trans*-Muconic acid (Bernstein & Leiserowitz, 1972). Intra- and interlayer packing. Distances are: for molecule *A*, C–O_1 1·275, C–O_2 1·257, O–H···O 2·605 Å; for molecule *B*, C–O 1·294, C=O 1·236, and O–H···2·614 Å. The layer structure is planar to within 0·15 Å.

The packing features of the higher analogue *trans,trans*-muconic acid (Bernstein & Leiserowitz, 1972) differ from those of fumaric acid in both the intra- and interlayer structures. Muconic acid is triclinic ($P\bar{1}$), containing two molecules, say *A* and *B*, per unit cell, each of which forms hydrogen-bonded chains. These chains constitute a layer structure (Fig. 24) in which the two independent molecules *A* and *B* are related to each other by a pseudo 2_1 axis. Within the layer all the C–H bonds are directed approximately at the O atoms with an average C–H···O distance of 3·5 Å. The C–O lengths of 1·257 and 1·275 Å in *A* tend to be equal while those in *B* are unlike in length (1·236, 1·294 Å), indicating specific carbonyl and hydroxyl bond character. The equal O–H···O distances of 2·605 and 2·614 Å for *A* and *B* and the infrared spectrum (Bernstein & Leiserowitz, 1972), which exhibits a carbonyl stretching band at 1680 cm^{-1}, indicate that the near equality of the C–O lengths of *A* is due to disorder of its carboxyl dimer. The conformation of C=C–C=O is synplanar in *B*, and shows a slight preference for synplanarity in *A*.

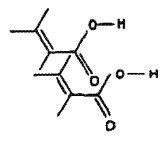
Since the intralayer environments of *A* and *B* are essentially identical, the difference in orientational order/disorder of their carboxyl groups must be associated with interlayer environment. The direction of offset between successive layers is such that the interlayer contacts of *A* and *B* are not alike; this is evident particularly along the 4 Å stack axis. The stacking of the carboxyl dimers of *B* is shown in (52). The stacking patterns of carboxyl dimers of *A* assuming synplanar and antiplanar C=C–C=O conformations, are shown in (53*a*) and (53*b*), respectively.



(52)



(53*a*)

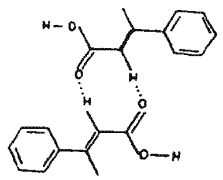


(53*b*)

UM00014000
NOVARTIS EXHIBIT 1517
Novartis v. Regents, IPR2023-01347
Page 2746 of 4460

Regarding the monomethyl derivatives of fumaric acid (Leiserowitz & Tang, 1976) and muconic acid (Rabinovich & Schmidt, 1967), both structures (Figs. 2 and 3) exhibit the motif (51) with intralayer C–H···O distances of 3·54 and 3·49 Å, respectively. The carboxyl group of the fumarate shows a measure of disorder (1·246, 1·276 Å) with a slight preference for the antiplanar C=C–C=O conformation; on the other hand, the carboxyl group of the muconate shows distinct carbonyl C=O and hydroxyl C–OH bonds (1·228, 1·308 Å), the conformation of C=C–C=O being antiplanar. This difference in carboxyl disorder between these two structures must be due primarily to differences in their stacking arrangements. The stacking geometry of the C=C–CO_2H groups of the fumarate (Fig. 2) resembles that of the *B* molecules (52) of muconic acid. However, the conformation of the C=C–C=O group is antiplanar and partially disordered in the fumarate, and is synplanar in the *B* molecules of muconic acid. Similarly, while the stacking arrangement of the C=C–CO_2H groups of the muconate resembles that of the *A* molecules of muconic acid (53), the antiplanar carboxyl group of the muconate exhibits little or no disorder while the carboxyl group of *A* shows pronounced disorder.

We may resolve this apparent incongruity as follows. The tendency towards the antiplanar C=C–C=O conformation in the fumarate is consistent with a balance between the stacking and intramolecular forces on one hand, which would favour the synplanar C=C–C=O conformation like the *B* molecules of muconic acid, and, on the other hand, the lateral C–H···O contact of the fumarate which would favour the antiplanar C=C–C=O conformation. Similarly, the antiplanar C=C–C=O conformation in the muconate is possibly stabilized by a balance between the C–H···O interaction which would favour the antiplanar C=C–C=O conformation, and the stacking arrangement which favours a disordered carboxyl group as in the *A* molecular stack in muconic acid.



(54)

α-*trans*-Cinnamic acid (Ladell, McDonald & Schmidt, 1956) exists in the antiplanar C=C–C=O conformation in the solid state. The carbonyl and hydroxyl bonds are distinct (1·22, 1·30 Å). The structure (54) shows a lateral C–H···O(carbonyl) contact of 3·66 Å. The carboxyl dimers are not stacked along a short axis, rather the molecules form plane-to-plane contact across the centre of inversion, so that the carboxyl pairs are sandwiched between benzene rings. *p*-Chloro-*trans*-cinnamic acid (Glusker, Zacharias & Carrell, 1975) also displays a motif similar to (54) with a C–H···O contact of 3·6 Å. Its carboxyl groups are disordered (1·263, 1·264 Å) and stacked along a short 3·9 Å axis, but the molecular offset is not along either of the C–O bonds, as in (36*a*), rather along the C–Cl bond.

A lateral C–H···O contact similar to that of (51) is incorporated into the packing arrangement of furane-α,α′-dicarboxylic acid (Martuscelli & Pedone, 1968). The structure consists of hydrogen-bonded rods which interlink to form a layer structure (Fig. 25). The intralayer contacts between the hydrogen-bonded rods include C–H···O(carbonyl) contacts of 3·32 Å. The interlayer arrangement comprises a 3·66 Å translation stacking of carboxyl groups offset along the direction of the carbonyl C=O bond.

Acrylic acid, the smallest of the α,β-unsaturated

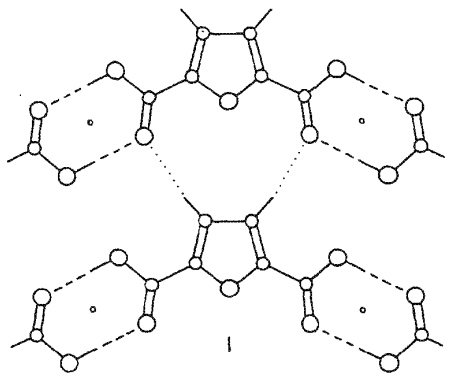


Fig. 25. Furane-α,α′-dicarboxylic acid (Martuscelli & Pedone, 1968). Intralayer packing. Distances: C–O 1·315, C=O 1·205, O–H···O 2·66 and C–H···O 3·32 Å. Adjacent molecules within the layer are offset by 0·8 Å.

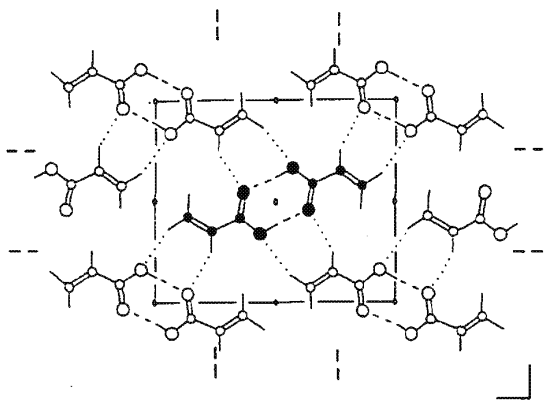
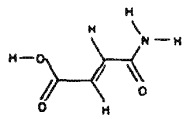


Fig. 26. Acrylic acid (Higgs & Sass, 1963; Chatani, Sakata & Nitta, 1963). Packing arrangement seen along [001]. Distances: C–H···O 3·3 and 3·6 Å.

UM00014001
NOVARTIS EXHIBIT 1517
Novartis v. Regents, IPR2023-01347
Page 2747 of 4460

acids, crystallizes in a layer structure, but does not exhibit motif (51). Nevertheless, the lateral environment (Fig. 26) about the carboxyl pairs does comprise C–H···O(carbonyl and hydroxyl) contacts of 3·32 and 3·56 Å, very similar to the intralayer motif (37) of the benzoic acid derivatives.

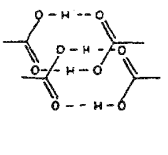
We deduce from the packing motifs of the α,β-unsaturated acids discussed above, which exist in the antiplanar C=C–C=O form, that molecules R–CH=CH–CO_2H which do not, or cannot, form C–H···O(carbonyl) contacts exist either in the synplanar C=C–C=O conformation or show some disorder of their carboxyl groups depending upon the nature of their stacking arrangements. In terms of these arguments, we may account for the conformational properties of fumaramic (Benghiat, Kaufman, Leiserowitz & Schmidt, 1972) and muconamic acids (see § 3.2.3). Fumaramic acid, an analogue of fumaric acid and monomethyl fumarate, displays a synplanar C=C–C=O conformation at the carboxyl end of the molecule; the synplanar C=C–C=O conformation at the amide end is consistent with the conformational pattern of amides. Assuming the antiplanar C=C–C=O conformation (55), it is possible to construct a hydrogen-bonding scheme similar to that of the observed crystal structure (Fig. 9). However, such a packing scheme would not include a C–H···O(carbonyl) contact; nor is it possible to devise a packing scheme from (55) containing the full complement of hydrogen bonds as well as a C–H···O(carbonyl) contact. In a similar manner we may account for the synplanar C=C–C=O conformation in muconamic acid.



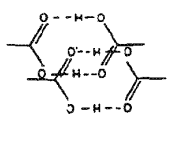
(55)

4.3. *Intralayer contacts between carboxyl dimers*

The lateral contacts between carboxyl groups observed in the layer structures of fumaric acid, monomethyl fumarate and furane-α,α′-dicarboxylic acid all include the motif (56) which incorporates the contact geometry between hydroxyl O atoms (–O···O–) dis-

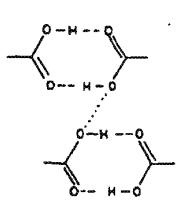


(59a)

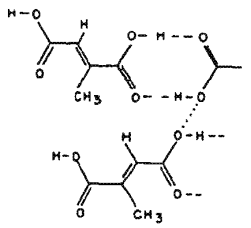


(59b)

cussed earlier (§ 3.1). The distance between the hydroxyl O atoms lies in the range 2·96–3·13 Å. This type of contact is also present in the layer structure of mesaconic acid (Gupta & Yadav, 1972) shown in (57). The distance between the hydroxyl O atoms is 2·88 Å.

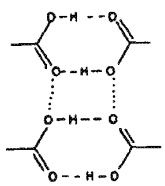


(56)



(57)

According to Gupta & Yadav, this short O···O contact represents an O–H···O hydrogen bond, *i.e.* the hydroxyl O–H bond participates in a bifurcated O–H···O hydrogen bond. While it is possible that this short contact is stabilized by an electrostatic interaction between the O–H proton donor and the lone pair lobe of the neighbouring hydroxyl O atom, it is difficult to describe it as a hydrogen bond; the O–H bond in no way points towards the hydroxyl O atom.

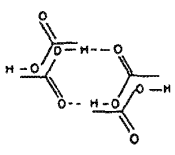


(58)

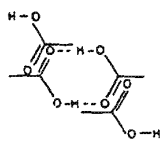
Lateral contact between carboxyl dimers as shown in (58), in which there is no offset between the two dimers parallel to the O–H···O line, *i.e.* the angle O–(H)–O···O is ~90°, has not been encountered. This arrangement is unfavourable and does not permit close intermolecular contact as demonstrated by the crystal structure of benzamide–succinic acid discussed earlier (§ 3.1).

4.4. *Interlayer contact between carboxyl dimers*

The two principal modes of interplanar contact between carboxyl dimers are shown in (59) and (60).



(60a)



(60b)

UM00014002
NOVARTIS EXHIBIT 1517
Novartis v. Regents, IPR2023-01347
Page 2748 of 4460

Molecules which pack in this manner are listed in Table 5. The dimers which appear in motif (59) may be offset along either the C=O bond (59*a*), the C–OH bond (59*b*) or a disordered combination thereof, as is evident from Table 5. Thus the energy difference between the two modes (59*a*) and (59*b*) must be small. A very similar situation arises in (60) where the carboxyl groups interact *via* an antiparallel arrangement of C–O bonds, which may have either carbonyl (60*a*) or hydroxyl character (60*b*), or a disordered combination of the two.

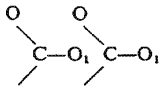
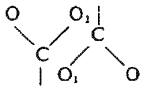
This paper has demonstrated evidence favouring the role of O–H···O lone pair geometry in the hydrogen-bonding of carboxyl groups. The hydrogen-bonding modes of carboxylic acids have been discussed, in particular monocarboxylic acids $R-CO_2H$ as a function of the size and chirality of R. The study has revealed some of the systematics of benzoic acid packing, the primary stacking features of carboxyl groups, the layer structures of some α,β-unsaturated carboxylic acids in terms of C^{α}–H···O(carbonyl) contacts and the antiplanar conformation of the $C^{\beta}=C^{\alpha}-C=O$ system. It is hoped that this paper has shown the need for further studies, *e.g.* crystal structure analyses of monocarboxylic acids containing chiral residues to correlate the hydrogen-bonding motifs and the nature of the chiral residues; a more detailed knowledge of the energy of the O–H···O(carbonyl) bond as a function of angular geometry and of the possible role played by C–H···O(carbonyl) contacts in determining overall crystal structure.

I am indebted to the late G. M. J. Schmidt for his support, advice and criticism of this work. I am grateful to V. Benghiat, J. Bernstein, C.-P. Tang and O. Vor der Bruck who were engaged in structure analyses. I wish to thank F. Nader, M. Lahav and A. Hagler for stimulating discussions, and J. D. Dunitz for various suggestions. Lastly I wish to express my sincere thanks to I. Olovsson and members of his laboratory for their kindness, assistance, and for the working facilities they placed at my disposal during my stay in Uppsala. Partial support from a MINERVA grant is acknowledged.

References

ABRAHAMSSON, S. (1959*a*). *Acta Cryst.* **12**, 301–304.
ABRAHAMSSON, S. (1959*b*). *Acta Cryst.* **12**, 304–309.
ALCALA, R. & MARTÍNEZ-CARRERA, S. (1972). *Acta Cryst.* B**28**, 1671–1677.

Table 5. *The two modes* (59) *and* (60) *of interplanar contact between carboxyl groups*

Compound	Length (Å) of C–O_1 bond in motif (59) 	Length (Å) of C–O_1 bond in motif (60) 	References
β-Tetrolic acid	1·204		Benghiat & Leiserowitz (1972*a*)
α-Tetrolic acid		1·252	Benghiat & Leiserowitz (1972*a*)
Furane-α,α′-dicarboxylic acid	1·205		Martuscelli & Pedone (1968)
Fumaramic acid	1·209		Benghiat, Kaufman, Leiserowitz & Schmidt (1972)
Triclinic fumaric acid		1·22	Bednowitz & Post (1966)
Monomethyl fumarate	1·276		Leiserowitz & Tang (1976)
trans,trans-Muconic acid, molecule *B*	1·236		Bernstein & Leiserowitz (1972)
molecule *A*	1·275		
Monomethyl *trans,trans*-muconate	1·23		Rabinovich & Schmidt (1967)
Benzoic acid		1·24	Sim, Robertson & Goodwin (1955)
β-Terephthalic acid		1·28	Bailey & Brown (1967)
α-Terephthalic acid	1·262		Bailey & Brown (1967)
p-Chlorobenzoic acid	1·253		Miller, Paul & Curtin (1974)
p-Bromobenzoic acid	1·225		Ohkura, Kashimo & Haisa (1972)
p-Nitrobenzoic acid		1·242	Tavale & Pant (1971)
2-Chlorobiphenyl-4-carboxylic acid	1·205		Sutherland & Hoy (1969)
2′-Chlorobiphenyl-4-carboxylic acid	1·289		Sutherland (1969)
2′-Iodobiphenyl-4-carboxylic acid	1·264		Sutherland (1970)
o-Fluorobenzoic acid	1·255		Krausse & Dunken (1966)
o-Chlorobenzoic acid	1·295		Ferguson & Sim (1961)
o-Bromobenzoic acid	1·346		Ferguson & Sim (1962)
1-Naphthoic acid	1·25		Trotter (1960*b*)
2-Naphthoic acid*		1·33	Trotter (1961)

* The two C–O lengths of 1·33 and 1·37 in 2-naphthoic acid are obviously unreliable

UM00014003
NOVARTIS EXHIBIT 1517
Novartis v. Regents, IPR2023-01347
Page 2749 of 4460

ANCA, R., MARTÍNEZ-CARRERA, S. & GARCÍA-BLANCO, S. (1967). *Acta Cryst.* **23**, 1010–1016.
BAILEY, M. & BROWN, C. J. (1967). *Acta Cryst.* **22**, 387–391.
BEDNOWITZ, A. L. & POST, B. (1966). *Acta Cryst.* **21**, 566–571.
BENEDETTI, E., CLAVERINI, R. & PEDONE, C. (1972). *Cryst. Struct. Commun.* **1**, 27–30.
BENGHIAT, V., KAUFMAN, H. W., LEISEROWITZ, L. & SCHMIDT, G. M. J. (1972). *J. Chem. Soc. Perkin* II, pp. 1758–1763.
BENGHIAT, V. & LEISEROWITZ, L. (1972*a*). *J. Chem. Soc. Perkin* II, pp. 1763–1768.
BENGHIAT, V. & LEISEROWITZ, L. (1972*b*). *J. Chem. Soc. Perkin* II, pp. 1778–1785.
BENGHIAT, V. & LEISEROWITZ, L. (1972*c*). *J. Chem. Soc. Perkin* II, pp. 1772–1778.
BENGHIAT, V., LEISEROWITZ, L. & SCHMIDT, G. M. J. (1972). *J. Chem. Soc. Perkin* II, pp. 1769–1772.
BERKOVITCH-YELLIN, Z., LEISEROWITZ, L. & NADER, F. (1976). To be published.
BERNEY, C. V. (1973). *J. Amer. Chem. Soc.* **95**, 708–716.
BERNSTEIN, J., COHEN, M. D. & LEISEROWITZ, L. (1974). *The Chemistry of the Quinonoid Compounds*. Part 1, edited by S. PATAI, pp. 92–101. London: John Wiley.
BERNSTEIN, J. & LEISEROWITZ, L. (1972). *Isr. J. Chem.* **10**, 601–612.
BLOCK, S., FILIPPAKIS, S. E. & SCHMIDT, G. M. J. (1967). *J. Chem. Soc.* (*B*), pp. 233–238.
BOLTON, W. (1964). *Acta Cryst.* **17**, 147–152.
BRADLEY, R. & COTSON, S. (1953). *J. Chem. Soc.* pp. 1684–1688.
BROWN, C. J. (1966). *Acta Cryst.* **21**, 1–5.
CANO, F. H., MARTÍNEZ-CARRERA, S. & GARCÍA-BLANCO, S. (1970). *Acta Cryst.* B**26**, 972–979.
CHATANI, Y., SAKATA, Y. & NITTA, I. (1963). *Polymer Lett.* **1**, 419–421.
CHIEH, P. C. & TROTTER, J. (1970). *J. Chem. Soc.* (*A*), pp. 184–187.
COPPENS, P. & VOS, A. (1971). *Acta Cryst.* B**27**, 146–158.
CURRIE, M., SPEAKMAN, J. C. & CURRY, N. A. (1967). *J. Chem. Soc.* (*A*), pp. 1862–1869.
DAHLÉN, B. (1973). *Acta Cryst.* B**29**, 595–602.
DAHLÉN, B. (1974). *Acta Cryst.* B**30**, 642–646.
DARLOW, S. F. (1961). *Acta Cryst.* **14**, 159–166.
DAVIES, D. R. & PASTERNAK, R. A. (1956). *Acta Cryst.* **9**, 334–340.
DELAPLANE, R. G. & IBERS, J. A. (1969). *Acta Cryst.* B**25**, 2423–2437.
DERISSEN, J. L. & SMIT, P. H. (1974). *Acta Cryst.* B**30**, 2240–2242.
DIETERICH, D. A., PAUL, I. C. & CURTIN, D. Y. (1974). *J. Amer. Chem. Soc.* **96**, 6372–6380.
DONOHUE, J. (1968). *Structural Chemistry and Molecular Biology*, edited by A. RICH & N. DAVIDSON, pp. 443–465. San Francisco: Freeman.
DUCHAMP, D. J. & MARSH, R. E. (1969). *Acta Cryst.* B**25**, 5–19.
DUNITZ, J. D., GEHRER, H. & BRITTON, D. (1972). *Acta Cryst.* B**28**, 1989–1994.
DUNITZ, J. D. & ROBERTSON, J. M. (1947). *J. Chem. Soc.* pp. 148–154.
DUNITZ, J. D. & STRICKLER, P. (1968). *Structural Chemistry and Molecular Biology*, edited by A. RICH & N. DAVIDSON, pp. 443–465. San Francisco: Freeman.
EINSPAHR, H. & DONOHUE, J. (1973). *Acta Cryst.* B**29**, 1875–1880.
ELLISON, R. D., JOHNSON, C. K. & LEVY, H. A. (1971). *Acta Cryst.* B**27**, 333–344.
FALLON, L. (1973). *Acta Cryst.* B**29**, 2549–2556.
FERGUSON, G. & SIM, G. A. (1961). *Acta Cryst.* **14**, 1262–1270.
FERGUSON, G. & SIM, G. A. (1962). *Acta Cryst.* **15**, 346–350.
FILIPPAKIS, S. E., LEISEROWITZ, L., RABINOVICH, D. & SCHMIDT, G. M. J. (1972). *J. Chem. Soc. Perkin* II, pp. 1750–1758.
FILIPPAKIS, S. E., LEISEROWITZ, L. & SCHMIDT, G. M. J. (1967). *J. Chem. Soc.* (*B*), pp. 290–296.
FILIPPAKIS, S. E. & SCHMIDT, G. M. J. (1967). *J. Chem. Soc.* (*B*), pp. 229–232.
FLORENCIO, F. & SMITH, P. (1970). *Acta Cryst.* B**26**, 659–666.
GLUSKER, J. P., ZACHARIAS, D. E. & CARRELL, H. L. (1975). *J. Chem. Soc. Perkin* II, 68–74.
GOPALAKRISHNA, E. M. & CARTZ, L. (1972). *Acta Cryst.* B**28**, 2917–2924.
GORRES, B. T., MCAFEE, E. R. & JACOBSON, R. A. (1975). *Acta Cryst.* B**31**, 158–161.
GUPTA, M. P. & YADAV, S. R. P. (1972). *Acta Cryst.* B**28**, 2682–2686.
HAREL, M. & HIRSHFELD, F. L. (1976). To be published.
HECHTFISCHER, S. VON, STEIGEMANN, W. & HOPPE, W. (1970). *Acta Cryst.* B**26**, 1713–1722.
HIGGS, M. A. & SASS, R. L. (1963). *Acta Cryst.* **16**, 657–661.
HIRSHFELD, F. L. (1971). *Acta Cryst.* B**27**, 769–781.
HOLTZBERG, F., POST, B. & FANKUCHEN, I. (1953). *Acta Cryst.* **6**, 127–130.
HOSPITAL, M. & HOUSTY, J. (1966). *Acta Cryst.* **20**, 626–630.
HUANG, C.-M., LEISEROWITZ, L. & SCHMIDT, G. M. J. (1973). *J. Chem. Soc. Perkin* II, pp. 503–508.
JAMES, M. N. G. & WILLIAMS, G. J. B. (1974). *Acta Cryst.* B**30**, 1249–1257.
JÖNSSON, P. -G. (1971). *Acta Cryst.* B**27**, 893–898.
JÖNSSON, P. -G. (1972). *Acta Chem. Scand.* **26**, 1599–1619.
JÖNSSON, P. -G. & HAMILTON, W. C. (1972). *J. Chem. Phys.* **56**, 4433–4439.
KANTERS, J. A. & KROON, J. (1972). *Acta Cryst.* B**28**, 1946–1949.
KARLE, I. L. (1972). *Acta Cryst.* B**28**, 2000–2007.
KATO, Y., TAKAKI, Y. & SAKURAI, K. (1974). *Acta Cryst.* B**30**, 2683–2687.
KOCH, B. (1972). *Acta Cryst.* B**28**, 1151–1159.
KOSKI, H. H. & SÁNDOR, E. (1975). *Acta Cryst.* B**31**, 350–353.
KRAUSSE, J. & DUNKEN, H. (1966). *Acta Cryst.* **20**, 67–73.
KRYGER, L., RASMUSSEN, S. E. & DANIELSEN, J. (1972). *Acta Chem. Scand.* **26**, 2339–2348.
KVICK, A., KOETZLE, T. F., THOMAS, R. & TAKUSAGAWA, F. (1974). *J. Chem. Phys.* **60**, 3866–3874.
LADELL, J., MCDONALD, T. R. R. & SCHMIDT, G. M. J. (1956). *Acta Cryst.* **9**, 195.
LEISEROWITZ, L. & NADER, F. (1972). *Angew. Chem. Int. Ed.* **11**, 514–515.
LEISEROWITZ, L. & NADER, F. (1973). *Angew. Chem. Int. Ed.* **12**, 158–159.
LEISEROWITZ, L. & OLOVSSON, I. (1976). To be published.
LEISEROWITZ, L. & SCHMIDT, G. M. J. (1965). *Acta Cryst.* **18**, 1058–1067.
LEISEROWITZ, L. & SCHMIDT, G. M. J. (1969). *J. Chem. Soc.* (*A*), pp. 2372–2382.

UM00014004
NOVARTIS EXHIBIT 1517
Novartis v. Regents, IPR2023-01347
Page 2750 of 4460

LEISEROWITZ, L. & TANG, C.-P. (1976). To be published.
LEISEROWITZ, L. & TUVAL, M. (1976). To be published.
LIDE, D. R. JR (1964). *Ann. Rev. Phys. Chem.* **15**, 225–250.
LIN, C.-T., PAUL, I. C. & CURTIN, D. Y. (1974). *J. Amer. Chem. Soc.* **96**, 3699–3701.
MARTUSCELLI, E. (1969). *Acta Cryst.* B**25**, 2540–2546.
MARTUSCELLI, E. & MAZZARELLA, L. (1969). *Acta Cryst.* B**25**, 2022–2029.
MARTUSCELLI, E. & PEDONE, C. (1968). *Acta Cryst.* B**24**, 175–179.
MEESTER, M. A. M., SCHENK, H. & MACGILLAVRY, C. H. (1971). *Acta Cryst.* B**27**, 630–634.
MERESSE, A., COURSEILLE, C. & CHANH, N. B. (1974). *Acta Cryst.* B**30**, 524–526.
MILLER, R. S., CURTIN, D. Y. & PAUL, I. C. (1974). *J. Amer. Chem. Soc.* **96**, 6340–6349.
MILLER, R. S., PAUL, I. C. & CURTIN, D. Y. (1974). *J. Amer. Chem. Soc.* **96**, 6334–6339.
MIYAZAWA, T. & PITZER, K. S. (1959). *J. Chem. Phys.* **30**, 1076–1086.
MORRISON, J. D. & ROBERTSON, J. M. (1949*a*). *J. Chem. Soc.* pp. 1001–1008.
MORRISON, J. D. & ROBERTSON, J. M. (1949*b*). *J. Chem. Soc.* pp. 980–986.
MURAKAMI, Y. & IITAKA, Y. (1969). *Chem. Pharm. Bull. Japan*, **17**, 2397–2404.
NADER, F. (1976). To be published.
NAHRINGBAUER, I. (1970). *Acta Chem. Scand* **24**, 453–462.
NAHRINGBAUER, I. & LARSSON, G. (1969). *Ark. Kem.* **30**, 91–102.
NAKAMOTO, K., MARGOSHES, M. & RUNDLE, R. E. (1965). *J. Amer. Chem. Soc.* **77**, 6480–6486.
OHKURA, K., KASHINO, S. & HAISA, M. (1972). *Bull. Chem. Soc. Japan*, **45**, 2651–2652.
OKAYA, Y., STEMPLE, N. R. & KAY, M. I. (1966). *Acta Cryst.* **21**, 237–243.
PARRY, G. S. (1954). *Acta Cryst.* **7**, 313–320.
PIJPER, W. P. (1971). *Acta Cryst.* B**27**, 344–348.
RABINOVICH, D. & SCHMIDT, G. M. J. (1967). *J. Chem. Soc.* (*B*), pp. 286–289.
RINGERTZ, H. (1971). *Acta Cryst.* B**27**, 285–291.
ROBERTSON, J. M. & SUTHERLAND, S. A. (1964). Private communication.
ROLLETT, J. S. (1955). *Acta Cryst.* **8**, 487–494.
RØ, G. & SØRUM, H. (1972*a*). *Acta Cryst.* B**28**, 991–998.
RØ, G. & SØRUM, H. (1972*b*). *Acta Cryst.* B**28**, 1677–1684.
SABINE, T. M., COX, G. W. & CRAVEN, B. M. (1969). *Acta Cryst.* B**25**, 2437–2441.
SAKURAI, T. & OKUNUKI, M. (1971). *Acta Cryst.* B**27**, 1445–1453.
SCHALKWYK, T. G. D. VAN (1954). *Acta Cryst.* **7**, 775.
SCHENK, H. (1972). *Cryst. Struct. Commun.* **1**, 143–146.
SIM, G. A. (1967). *Ann. Rev. Phys. Chem.* **18**, 57–80.
SIM, G. A., ROBERTSON, J. M. & GOODWIN, T. H. (1955). *Acta Cryst.* **8**, 157–164.
SINGH, P. & HODGSON, D. J. (1974). *Acta Cryst.* B**30**, 1430–1435.
SMITH, P., FLORENCIO, F. & GARCÍA-BLANCO, S. (1971). *Acta Cryst.* B**27**, 2255–2260.
STAM, C. H. (1972). *Acta Cryst.* B**28**, 2936–2945.
STEWART, R. F. & JENSEN, L. H. (1967). *Acta Cryst.* **23**, 1102–1105.
SUTHERLAND, H. H. (1969). *Acta Cryst.* B**25**, 171–178.
SUTHERLAND, H. H. (1970). *Acta Cryst.* B**26**, 1217–1224.
SUTHERLAND, H. H. & HOY, T. G. (1969). *Acta Cryst.* B**25**, 1013–1022.
SUTOR, D. J. (1963). *J. Chem. Soc.* pp. 1105–1110.
SYDOW, E. VON (1958). *Acta Chem. Scand.* **12**, 777–779.
TAKAKI, Y., SASADA, Y. & WATANABE, T. (1960). *Acta Cryst.* **13**, 693–702.
TAKWALE, M. G. & PANT, L. M. (1971). *Acta Cryst.* B**27**, 1152–1158.
TAMURA, C., KUWANO, H. & SASADA, Y. (1961). *Acta Cryst.* **14**, 693.
TAVALE, S. S. & PANT, L. M. (1971). *Acta Cryst.* B**27**, 1479–1481.
TROTTER, J. (1960*a*). *Acta Cryst.* **13**, 86–95.
TROTTER, J. (1960*b*). *Acta Cryst.* **13**, 732–736.
TROTTER, J. (1961). *Acta Cryst.* **14**, 101–105.
TURNER, J. D. & LINGAFELTER, E. C. (1955*a*). *Acta Cryst.* **8**, 549–550.
TURNER, J. D. & LINGAFELTER, E. C. (1955*b*). *Acta Cryst.* **8**, 551–557.
VERSCHOOR, G. C. & KEULEN, E. (1971). *Acta Cryst.* B**27**, 134–145.
VOR DER BRUCK, O. & LEISEROWITZ, L. (1976). To be published.
WALBORSKY, H. M., BARASH, L., YOUNG, A. E. & IMPASTATO, F. J. (1961). *J. Amer. Chem. Soc.* **83**, 2517–2525.
WILLIAMS, D. E. & RUNDLE, R. E. (1964). *J. Amer. Chem. Soc.* **86**, 1660–1666.

UM00014005
NOVARTIS EXHIBIT 1517
Novartis v. Regents, IPR2023-01347
Page 2751 of 4460

Aust. J. Chem., 1998, 51, 403–408

Molecular Cocrystals of Carboxylic Acids. XXXI* Adducts of 2-Aminopyrimidine and 3-Amino-1,2,4-triazole with Heterocyclic Carboxylic Acids

Daniel E. Lynch,[A,B] *Tariq Latif,*[A] *Graham Smith,*[C] *Karl A. Byriel,*[D] *Colin H. L. Kennard*[D] *and Simon Parsons*[E]

[A] School of Natural and Environmental Sciences, Coventry University, Priory Street, Coventry CV1 5FB, U.K.
[B] Author to whom correspondence should be addressed.
[C] School of Physical Sciences, Queensland University of Technology, P.O. Box 2434, Brisbane, Qld. 4001.
[D] Department of Chemistry, The University of Queensland, Brisbane, Qld. 4072.
[E] Department of Chemistry, The University of Edinburgh, West Mains Road, Edinburgh EH9 3JJ, U.K.

A series of molecular adducts of 2-aminopyrimidine and 3-amino-1,2,4-triazole with heterocyclic carboxylic acids have been prepared and characterized by using X-ray powder diffraction and in four cases by single-crystal X-ray diffraction methods. These four compounds are the (1 : 1) adducts of 2-aminopyrimidine with indole-3-acetic acid [$(C_4H_5N_3)(C_{10}H_9NO_2)$], *N*-methylpyrrole-2-carboxylic acid [$(C_4H_5N_3)(C_6H_7NO_2)$] and thiophen-2-carboxylic acid [$(C_4H_5N_3)(C_5H_4O_2S)$], and the (1 : 1) adduct of 3-amino-1,2,4-triazole with thiophen-2-carboxylic acid [$(C_2H_4N_4)(C_5H_4O_2S)$]. Other compounds described are the (1 : 1) adducts of 3-amino-1,2,4-triazole with indole-3-acetic acid and *N*-methylpyrrole-2-carboxylic acid.

Introduction

We have previously discussed the different types of secondary hydrogen-bonding interactions which have been observed in carboxylic acid adducts of 2-aminopyrimidine (2-ap),[1,2] the primary interaction being the formation of a hydrogen-bonded cyclic dimer between the acid and complementary base site on the 2-ap molecule (designated as A–P).[3,4] The intermolecular distances involved in this interaction were found to be slightly acentric with the two average distances between non-hydrogen atoms being 2·660 and 2·911 Å.[2] The majority of acid molecules studied thus far have included substituted benzoic, phenoxyacetic and aliphatic dicarboxylic acids although our last reported structure included the heterocyclic acid indole-2-carboxylic acid (ica).[2] This adduct structure still had the primary A–P interaction but the secondary interactions were unexpected. The combination of the indole N–H and the secondary 2-ap base site allowed the formation of a unique cyclic quartet, as shown in Fig. 1, and provided us with a new concept in the design of hydrogen-bonding networks. To further develop this idea we decided to prepare more 2-ap adducts with a series of heterocyclic carboxylic acids. The compounds chosen were indole-3-acetic acid (iaa) (which has a flexible acid group and a free N–H), *N*-methylpyrrole-2-carboxylic acid (mpca) (which has an identical acid substitution as ica but has a methylated nitrogen) and thiophen-2-carboxylic acid (tca) (which only possesses the carboxylic acid). In addition

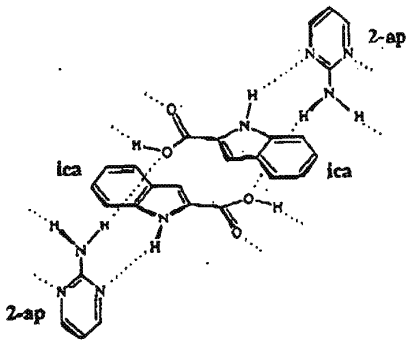


Fig. 1. Hydrogen-bonding interactions between ica and 2-ap.

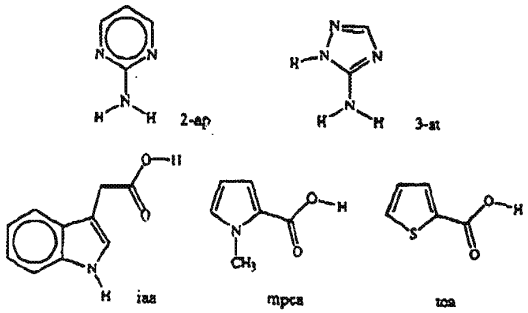
* Part XXX, *J. Chem. Crystallogr.*, 1998, in press.

Manuscript received 28 November 1997 © CSIRO Australia 1998 0004-9425/98/050403$05.00

UM00014006
NOVARTIS EXHIBIT 1517
Novartis v. Regents, IPR2023-01347
Page 2752 of 4460

05/23/2006 14:02 PRI LIBRARY → 917818637208 NO.793 D003

to these, adducts of 3-amino-1,2,4-triazole (3-at) have also been prepared to provide a complementary set of complexes. All known adducts of 3-at[5–9] display highly varied secondary hydrogen-bonding arrays, due to the availability of the additional heterocyclic nitrogen and the neighbouring N–H moiety, and could possibly supply the relevant conditions for the desired quartet. Interestingly, all except one of the previous complexes of 3-at involve nitro-substituted benzoic acids although none display any hydrogen-bonding interactions involving nitro groups. The other structure is the 1 : 1 adduct of 3-at with pyrazine-2,3-dicarboxylic acid.[7]



Reported in this paper are the (1 : 1) adducts of 2-aminopyrimidine with indole-3-acetic acid [compound (1)], *N*-methylpyrrole-2-carboxylic acid [compound (2)] and thiophen-2-carboxylic acid [compound (3)]; and 3-amino-1,2,4-triazole with indole-3-acetic acid [compound (4)], *N*-methylpyrrole-2-carboxylic acid [compound (5)] and thiophen-2-carboxylic acid [compound (6)]. The structures of complexes (1)–(3) and (6) have been determined by single-crystal X-ray diffraction. X-Ray powder diffraction techniques were used to characterize all compounds.

Experimental

Preparations

Complexes (1)–(6) were prepared by using equimolar amounts (2·2 mmol) of indole-3-acetic acid, *N*-methylpyrrole-2-carboxylic acid and thiophen-2-carboxylic acid with respectively 2-aminopyrimidine [(2-ap)(iaa)] (1), [(2-ap)(mpca)] (2) and [(2-ap)(tca)] (3); and 3-amino-1,2,4-triazole [(3-at)(iaa)] (4), [(3-at)(mpca)] (5) and [(3-at)(tca)] (6). All preparations involved refluxing for 20 min at *c.* 70°C in 40 cm^3 of absolute ethanol, the product being subsequently obtained by the total evaporation of the solvent at room temperature: for (1), light brown prisms (m.p. 102–105°C); for (2), colourless prisms (m.p. 95–98°C); for (3), colourless prisms (m.p. 107–109°C); for (4), a light brown powder (m.p. 102–104°C); for (5), a white powder (m.p. 101–103°C); and for (6), colourless prisms (m.p. 151·5–153°C). For compounds (1)–(6), microanalysis identified 1 : 1 stoichiometries. X-Ray powder diffraction data: for (1), *d* (*I*/*I*$_0$) 4·84 (100%), 4·92 (16), 9·62 (14), 14·00 (12), 4·23 (10), 7·00 (10), 3·61 (9), 4·98 Å (9); for (2), *d* (*I*/*I*$_0$) 6·01 (100%), 6·10 (59), 6·77 (41), 3·92 (39), 3·97 (38), 3·31 (37), 5·72 (24), 4·06 Å (23); for (3), *d* (*I*/*I*$_0$) 5·53 (100%), 3·40 (6), 2·77 (5), 5·67 (5), 5·93 (4), 3·43 (3), 3·34 (2), 3·72 Å (2); for (4), *d* (*I*/*I*$_0$) 20·73 (100%), 4·60 (94), 6·96 (90), 3·62 (73), 4·45 (64), 5·30 (60), 4·70 (58), 3·70 Å (40); for (5), *d* (*I*/*I*$_0$) 5·88 (100%), 5·16 (96), 5·31 (84), 4·26 (78), 3·40 (73), 3·97 (69), 3·41 (66), 3·38 Å (64); for (6), *d* (*I*/*I*$_0$) 7·28 (100%), 3·70 (91), 3·93 (59), 5·42 (45), 3·10 (44), 4·41 (17), 3·40 (16), 2·64 Å (13). Adduct formation was identified in each case by X-ray powder diffraction techniques by using a Philips PW1700 System diffractometer (Cu Kα X-radiation). For 2-ap, *d* (*I*/*I*$_0$) 3·57 (100%), 3·03 (100), 7·53 (80), 5·45 (60), 3·78 (45), 4·20 (40), 3·11 (40), 4·80 Å (25); for 3-at, *d* (*I*/*I*$_0$) 3·20 (100%), 4·24 (94), 3·37 (89), 5·31 (87), 4·60 (80), 3·05 (77), 2·91 (58), 3·36 Å (55). Infrared spectra were recorded as pressed disks in KBr on a Nicolet 205 Fourier-transform infrared spectrometer.

Crystallography

Crystal Data

(1) [$(C_4H_5N_3)(C_{10}H_9NO_2)$], mol. wt 270·3, monoclinic, space group *C* 2/*c*, *a* 29·78(2), *b* 4·6348(3), *c* 20·69(1) Å, β 109·28(2)°, *V* 2695(2) $Å^3$, *F*(000) 1136, D_c(*Z* = 8) 1·332 g cm^{-3}, μ(Mo Kα) 0·93 cm^{-1}, temperature 298(2) K.

(2) [$(C_4H_5N_3)(C_6H_7NO_2)$], mol. wt 220·2, orthorhombic, space group $P2_12_12_1$, *a* 5·7306(6), *b* 16·311(1), *c* 23·910(2) Å, *V* 2234·9(4) $Å^3$, *F*(000) 928, D_c(*Z* = 8) 1·309 g cm^{-3}, μ(Cu Kα) 7·90 cm^{-1}, temperature 220(2) K.

(3) [$(C_4H_5N_3)(C_5H_4O_2S)$], mol. wt 223·3, monoclinic, space group $P2_1/n$, *a* 12·306(2), *b* 5·4112(4), *c* 16·66(2) Å, β 105·844(5)°, *V* 1067(2) $Å^3$, *F*(000) 464, D_c(*Z* = 4) 1·390 g cm^{-3}, μ(Mo Kα) 2·87 cm^{-1}, temperature 298(2) K.

(6) [$(C_2H_4N_4)(C_5H_4O_2S)$], mol. wt 212·2, monoclinic, space group $P2_1/n$, *a* 8·392(4), *b* 11·746(4), *c* 9·927(5) Å, β 106·69(3)°, *V* 937·4(7) $Å^3$, *F*(000) 440, D_c(*Z* = 4) 1·504 g cm^{-3}, μ(Cu Kα) 29·46 cm^{-1}, temperature 220(2) K.

Data Collection, Structure Solution and Refinement

X-Ray diffraction data for compounds (1)–(3) and (6) were collected from crystals of dimensions 0·50 by 0·25 by 0·15 mm (1), 0·31 by 0·27 by 0·19 mm (2), 0·30 by 0·25 by 0·20 mm (3) and 0·42 by 0·25 by 0·15 mm (6) on an Enraf–Nonius CAD-4 diffractometer by using crystal-monochromatized Mo Kα X-radiation (λ 0·71073 Å) [compounds (1) and (3)] and on a Stoe Stadi-4 diffractometer, equipped with an Oxford Cryosystems low-temperature device operating at 220 K, by using monochromatized Cu Kα X-radiation (λ 1·54178 Å) [compounds (2) and (6)]. Negligible change in the intensities of three standards, monitored throughout the respective data collection periods for all four compounds, indicated no significant crystal decomposition. Of 2424 (2377 unique) (1), 2995 (2722-unique) (2), 1297 (1234 unique) (3) and 2461 (1653 unique) (6) reflections collected up to $2\theta_{max}$ 50° [$2\theta_{max}$ 70° for (2) and (6)], 1455 for (1), 2357 for (2), 514 for (3) and 1331 for (6) with $F_o > 4{\cdot}0\sigma(F_o)$ were considered observed and were used in the expression of conventional refinement values. Data were corrected for Lorentz and polarization effects but no absorption corrections were applied. The structures were solved by direct methods and refined by full matrix least squares (SHELX-97[10]) with anisotropic thermal parameters for all non-hydrogen atoms, giving residuals* R_1, wR_2 and *S* of respectively 0·074, 0·117 and 1·0 for (1), 0·050, 0·064 and 1·1 for (2), 0·065, 0·159 and 1·0 for (3), and 0·053, 0·148 and 1·1 for (6). The values for *A* and *B* in the weighting scheme $w = [\sigma^2(F_o^2) + (AP)^2 + BP]^{-1}$ {where $P = [(\text{max. } F_o^2, 0) + 2(F_c^2)]/3$} were 0·1526, 0·00 (1), 0·0331, 2·09 (2), 0·1155, 0·00 (3) and 0·1024, 0·31 (6). For compounds (1), (2) and (6), hydrogens were located by difference methods, and

* $R_1 = \sum ||F_o| - |F_c|| / \sum |F_o|$ and $wR_2 = [\sum w(F_o^2 - F_c^2)^2 / \sum w(F_o)^2]^{1/2}$.

Aton

N(1A)
C(2A)
N(21A
N(3A)
C(4A)
C(5A)
C(6A)
N(1B)
C(2B)
C(3B)
C(31B
C(32B
O(31B
O(32B
C(4B)
C(5B)
C(6B)
C(7B)
C(8B)
C(9B)

N(1A)
C(2A)
N(3A)
C(4A)
C(5A)
C(6A)
N(21A
S(1B)
C(2B)
C(3B)
C(4B)
C(5B)
C(21B
O(21B
O(22B

A Occu

UM00014007
NOVARTIS EXHIBIT 1517
Novartis v. Regents, IPR2023-01347
Page 2753 of 4460

05/23/2006 14:02 PRI LIBRARY → 917818637208 NO. 153 0004

Table 1. Atomic coordinates and equivalent isotropic displacement parameters for (1)-(3) and (6)
U_{eq} is defined as one-third of the trace of the orthogonalized U_{ij} tensor

Atom	10^4x	10^4y	10^4z	10^3U_{eq} (Å^2)	Atom	10^4x	10^4y	10^4z	10^3U_{eq} (Å^2)
	Compound (1)					Compound (2)			
N(1A)	4001(1)	-2607(7)	5418(2)	51(1)	N(1A)	-2036(7)	912(2)	4730(1)	43(1)
C(2A)	4383(1)	-1603(7)	5280(2)	44(1)	C(2A)	-1662(8)	1174(2)	5257(2)	38(1)
N(21A)	4308(1)	268(8)	4757(2)	60(1)	N(21A)	-3253(7)	980(2)	5846(2)	45(1)
N(3A)	4833(1)	-2278(7)	5629(2)	56(1)	N(3A)	223(7)	1619(2)	5420(1)	39(1)
C(4A)	4895(1)	-4163(9)	6141(2)	64(1)	C(4A)	1745(9)	1809(3)	5029(2)	44(1)
C(5A)	4530(1)	-5316(9)	6315(2)	64(1)	C(5A)	1464(9)	1592(3)	4479(2)	51(1)
C(6A)	4087(1)	-4471(9)	5938(2)	59(1)	C(6A)	-472(9)	1128(3)	4345(2)	49(1)
N(1B)	1941(1)	-1077(7)	2329(1)	44(1)	N(1B)	-49(7)	3560(2)	10132(1)	43(1)
C(2B)	2287(1)	-1134(7)	2959(2)	44(1)	C(11B)	850(10)	3870(3)	9604(2)	58(1)
C(3B)	2179(1)	765(7)	3386(1)	39(1)	C(2B)	-1958(9)	3851(2)	10429(2)	41(1)
C(31B)	2451(1)	1310(10)	4130(2)	51(1)	C(21B)	-3418(8)	4523(3)	10234(2)	41(1)
C(32B)	2963(1)	493(8)	4349(2)	47(1)	O(21B)	-4985(6)	4749(2)	10609(1)	51(1)
O(31B)	3100(1)	-1076(7)	4908(1)	73(1)	O(22B)	-3232(7)	4847(2)	9775(1)	50(1)
O(32B)	3237(1)	1201(7)	4055(1)	68(1)	C(3B)	-2184(10)	3368(3)	10898(2)	49(1)
C(4B)	1453(1)	4180(7)	3153(2)	45(1)	C(4B)	-429(11)	2782(3)	10892(2)	55(1)
C(5B)	1041(1)	5016(8)	2654(2)	52(1)	C(5B)	890(10)	2910(3)	10418(2)	51(1)
C(6B)	914(1)	3797(8)	1992(2)	56(1)	N(1C)	-399(7)	2428(2)	7483(1)	45(1)
C(7B)	1180(1)	1753(8)	1830(2)	50(1)	C(2C)	-752(8)	2178(3)	6951(2)	40(1)
C(8B)	1602(1)	686(6)	2338(2)	39(1)	N(21C)	796(8)	2406(2)	6560(2)	49(1)
O(9B)	1741(1)	2093(7)	3006(1)	36(1)	N(3C)	-2571(7)	1702(2)	6784(1)	42(1)
					C(4C)	-4060(9)	1476(3)	7176(2)	48(1)
					C(5C)	-3819(9)	1681(3)	7731(2)	51(1)
					C(6C)	-1948(9)	2177(3)	7862(2)	48(1)
					N(1D)	7853(7)	4640(2)	7506(1)	44(1)
					C(11D)	8350(11)	4602(3)	6910(2)	63(2)
					C(2D)	6050(9)	4273(3)	7797(2)	43(1)
					C(21D)	4322(9)	3748(2)	7535(2)	44(1)
					O(21D)	2873(6)	3425(2)	7903(1)	50(1)
					O(22D)	4207(7)	3607(2)	7037(1)	58(1)
					C(3D)	6298(9)	4486(3)	8356(2)	47(1)
					O(4D)	8266(10)	4991(3)	8399(2)	54(1)
					C(5D)	9169(10)	5071(3)	7875(2)	52(1)
	Compound (3)					Compound (6)			
N(1A)	-1300(6)	-2275(8)	1511(4)	54(2)	N(1A)	-1422(3)	13822(2)	5331(2)	42(1)
C(2A)	-843(8)	-1579(10)	927(6)	59(3)	N(2A)	-62(3)	13111(2)	5522(2)	35(1)
N(3A)	-1226(7)	604(8)	451(4)	59(2)	C(3A)	1194(3)	13460(2)	6591(3)	34(1)
C(4A)	-2118(9)	1714(12)	585(6)	66(2)	N(31A)	2638(3)	12965(2)	7023(3)	48(1)
C(5A)	-2653(9)	923(12)	1162(7)	69(3)	N(4A)	666(3)	14399(2)	7099(2)	38(1)
C(6A)	-2203(8)	-1081(11)	1609(6)	57(2)	C(5A)	-930(4)	14587(3)	6288(3)	41(1)
N(21A)	29(8)	-2667(9)	790(5)	81(3)	S(1B)^A	280(1)	9330(1)	2209(1)	46(1)
S(1B)	180(2)	396(3)	3929(2)	71(1)	C(1B)^B	280(1)	9330(1)	2209(1)	46(1)
C(2B)	791(7)	1086(10)	3155(6)	55(2)	C(2B)	1779(3)	9619(2)	3704(3)	33(1)
C(3B)	1730(6)	-404(11)	3175(6)	66(3)	C(21B)	1619(3)	10605(2)	4583(2)	29(1)
C(4B)	1886(10)	-2122(13)	3854(6)	77(3)	O(21B)	365(2)	11234(2)	4128(2)	37(1)
C(5B)	1100(12)	-1884(12)	4281(7)	82(3)	O(22B)	2741(2)	10773(2)	5714(2)	37(1)
C(21B)	358(7)	3020(11)	2523(5)	53(2)	O(3B)^A	3201(3)	8796(2)	4009(2)	46(1)
O(21B)	-529(5)	4210(7)	2626(4)	60(2)	S(3B)^B	3201(3)	8796(2)	4009(2)	46(1)
O(22B)	816(6)	3473(8)	1085(4)	78(2)	C(4B)	2757(5)	8014(3)	2802(4)	66(1)
					C(5B)	1280(6)	8211(3)	1841(4)	60(1)

^{A}Occupancy factor: 0·80. ^{B}Occupancy factor: 0·20.

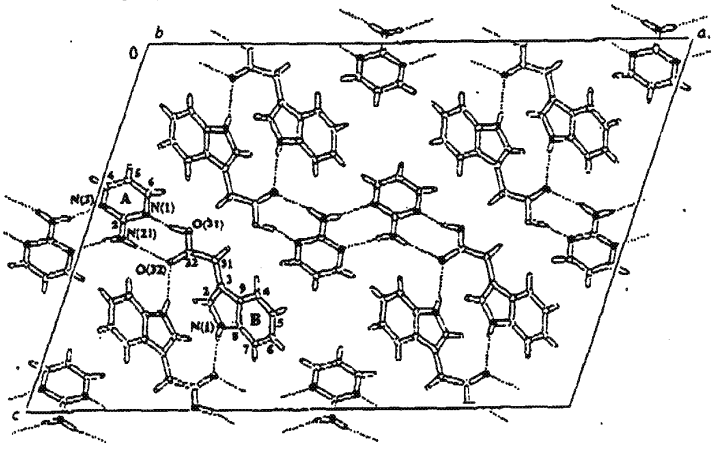


Fig. 2. Atom numbering scheme and hydrogen-bonding interactions in the unit cell for (1). Unless otherwise indicated, atoms are carbon.

UM00014008
NOVARTIS EXHIBIT 1517
Novartis v. Regents, IPR2023-01347
Page 2754 of 4460

05/23/2006 14:02 PRI LIBRARY → 917818637208 NO.793 D005

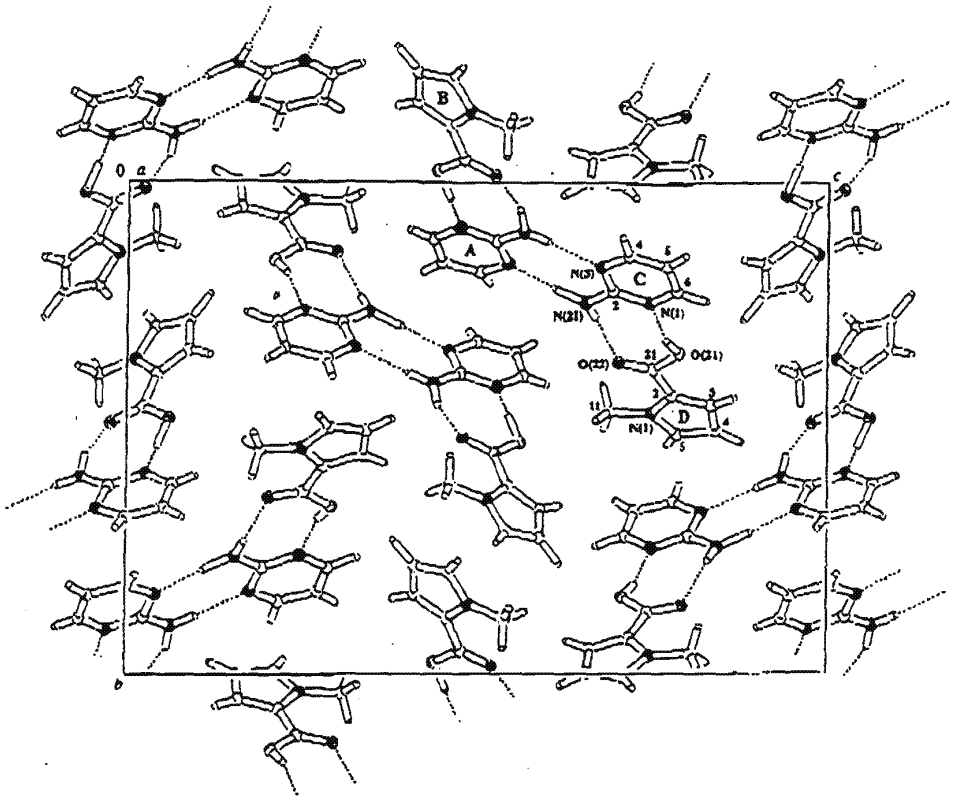


Fig. 3. Atom numbering scheme and hydrogen-bonding interactions in the unit cell for (2).

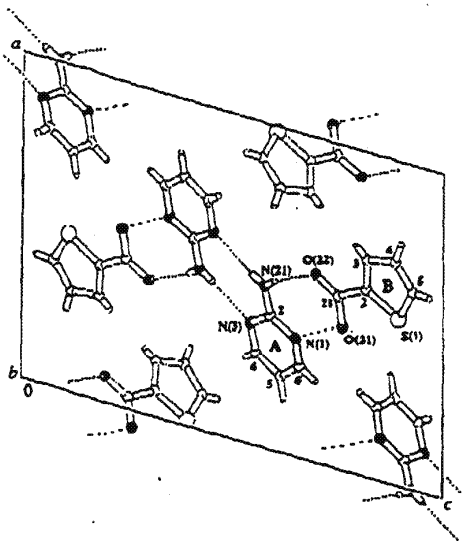


Fig. 4. Atom numbering scheme and hydrogen-bonding interactions in the unit cell for (3).

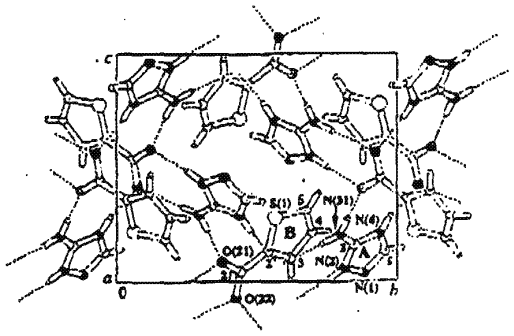


Fig. 5. Atom numbering scheme and hydrogen-bonding interactions in the unit cell for (6).

both pc
the me
at calc
cyclic a
at calc
hydroge
absolut
degree

Result

Fine
(6) are
anisotr
dinates
for com
an Acc
31 Dec
Chemis

Discuss

2-Amin

The
three 2
seen in
plexes (
geometi
Howeve
in the
interact
In cc
through
gen and
3·011(5
action
betwee
nitroge
N 155(3
nitroge
the latt
Comj
only is
2-ap st
2-amino
all four
up the
adducts
unique
creates
interacti
These a
pyrimid
--O(22I
carbon
3·591(6
Comj
complex
listed ir

* The ex

UM00014009
NOVARTIS EXHIBIT 1517
Novartis v. Regents, IPR2023-01347
Page 2755 of 4460

both positional and thermal parameters were refined although the methyl hydrogens in (2) were included in the refinement at calculated positions as riding models. For (3), all heterocyclic and amino hydrogens were included in the refinement at calculated positions as riding models. No carboxylic acid hydrogen for the tca molecule in (3) could be located. The absolute configuration of (2) could not be determined with any degree of certainty [absolute structure parameter: −0·1(5)].

Results

Final atomic coordinates for adducts (1)–(3) and (6) are given in Table 1. Bond distances and angles, anisotropic thermal parameters, hydrogen atom coordinates, and observed and calculated structure factors for compounds (1)–(3) and (6) have been deposited as an Accessory Publication (copies are available, until 31 December 2003, from the Australian Journal of Chemistry, P.O. Box 1139, Collingwood, Vic. 3066).

Discussion

2-Aminopyrimidine Series: Complexes (1)–(3)

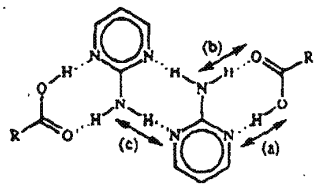
The primary molecular association observed in all three 2-ap adducts is typical of A:P:P:A packing as seen in the majority of 2-ap/carboxylic acid 1:1 complexes (Figs 2–4). Consequently, the hydrogen-bonding geometries for all three A:P:P:A sets are listed in Table 2. However, the real interest in this work can be seen in the first two structures where there are unique interactions between the A:P:P:A sets.

In complex (1) the iaa molecules form like-dimers through an interaction between the indole nitrogen and the carbonyl oxygen [N(1B)–H(1B)···O(32B) 3·011(5) Å, ∠N–H···O 154(3)°]. Within this interaction there is also a possible C–H···N association between the α-methine group and adjacent indole nitrogen [C(2B)–H(2B)···N(1B) 3·434(5) Å, ∠C–H···N 155(3)°]. As in the structure of 2-ap/ica,[2] the indole nitrogen of iaa plays an important role in determining the lattice packing.

Compound (2) is unique in two ways because not only is it noncentrosymmetric, the only other similar 2-ap structure being the 1:2 adduct of 2-ap with 2-aminobenzoic acid (2-aba) (space group *Pa*),[1] but all four molecules involved in the A:P:P:A set make up the asymmetric unit. Usually in 2-ap/acid 1:1 adducts, as for (1) and (3), only an A:P pair is unique and then inversion across a symmetry point creates the A:P:P:A set. Two further intermolecular interactions in (2) help determine the lattice packing. These are both C–H···O/N interactions between a pyrimidine carbon and carbonyl oxygen [C(6A)–H(6A)···O(22D) 3·339(6) Å, ∠C–H···O 142(3)°] and a pyrrole carbon and pyrrole nitrogen [C(5B)–H(5B)···N(1B) 3·591(6) Å, ∠C–H···O 154(3)°].

Compound (3), however, is a standard 2-ap/acid 1:1 complex with no further interactions other than those listed in Table 2. Even though the carboxylic acid proton on the tca molecule in (3) could not be located, additional infrared analysis confirmed that, like (1) and (2), compound (3) was not a proton-transfer complex.

Table 2. Hydrogen bond geometries for the A:P:P:A sets observed in adducts (1)–(3)
Features (a)–(c) are defined as follows



Adduct	Distance (Å) and ∠D–H···A (deg) (a)	(b)	(c)
(1)	2·635(5), 161(3)	3·067(5), 174(3)	3·064(5), 172(3)
(2)	2·678(6), 160(3) 2·677(6), 173(3)	2·914(6), 172(3) 2·904(6), 161(3)	2·990(6), 179(3) 3·032(6), 178(3)
(3)	2·65(1)	2·91(1), 167(3)	3·04(1), 175(3)
Average[A]	2·660 Å	2·925 Å	

[A] Taking into account the three structures.

[(3-at)(tca)] (6)

The primary hydrogen-bonding interaction in the structure of (6) is an $R_2^2(8)$ graph set cyclic dimer [N(2A)–H(2A)···O(21B) 2·681(8) Å, ∠N–H···O 171(3)°; N(31A)–H(31A)···O(21B) 2·894(8) Å, ∠N–H···O 178(3)°] (Fig. 5). This is similar to five of the six previously known adducts of 3-amino-1,2,4-triazole* and in the 2-ap structures [(1)·(3)]. However, the location of the tca acid proton as well as complementary infrared analysis of (6) shows that, like all known 3-at/acid adducts, this is a proton-transfer complex. Additional infrared analysis on compounds (4) and (5) confirms that these are also proton-transfer complexes. The two remaining N–H sites on the triazole moiety then link the essentially parallel tca molecules through interactions with both carboxylate oxygens [N(31A)–H(32A)···O(21B) 2·772(8) Å, ∠N–H···O 171(3)°; N(4A)

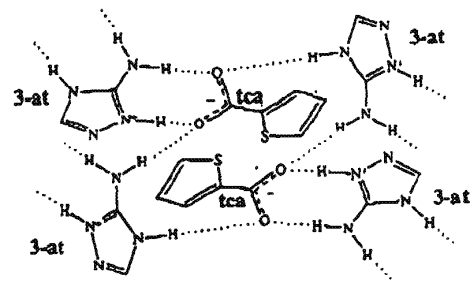


Fig. 6. Hydrogen-bonding interactions between tca and 3-at.

* The exception is the 1:1 adduct of 3-at with 3,5-dinitrosalicylic acid.[6]

UM00014010
NOVARTIS EXHIBIT 1517
Novartis v. Regents, IPR2023-01347
Page 2756 of 4460

05/23/2006 14:02 PRI LIBRARY → 917818637208 NO.793 D007

H(4A)···O(22B) 2·728(8) Å, ∠N–H···O 171(3)°] which is a formation (Fig. 6) similar to that seen in the structure of 2-ap with tca. This then leaves one triazole nitrogen and the tca sulfur free of any intermolecular associations. Furthermore, the thiophen ring is disordered with S(1B) and C(3B) interchanging. The structure was subsequently refined with both atoms occupying each site in a ratio of *c.* 80:20 for the principal atom at that site.

Acknowledgments

The authors acknowledge financial support from the School of Natural and Environmental Sciences of Coventry University, U.K., the Australian Research Council, and the University of Queensland.

References

[1] Smith, G., Gentner, J. M., Lynch, D. E., Byriel, K. A., and Kennard, C. H. L., *Aust. J. Chem.*, 1995, 48, 1151.
[2] Lynch, D. E., Latif, T., Smith, G., Byriel, K. A., and Kennard, C. H. L., *J. Chem. Crystallogr.*, 1997, in press.
[3] Etter, M. C., *J. Phys. Chem.*, 1991, 95, 4601.
[4] Etter, M. C., and Adsmond, D., *J. Chem. Soc., Chem. Commun.*, 1990, 589.
[5] Lynch, D. E., Smith, G., Byriel, K. A., and Kennard, C. H. L., *Acta Crystallogr., Sect. C*, 1991, 48, 1265.
[6] Byriel, K. A., Kennard, C. H. L., Lynch, D. E., Smith, G., and Thompson, J., *Aust. J. Chem.*, 1992, 45, 969.
[7] Lynch, D. E., Smith, G., Byriel, K. A., Kennard, C. H. L., and Whittaker, A. K., *Aust. J. Chem.*, 1994, 47, 309.
[8] Lynch, D. E., Smith, G., Byriel, K. A., and Kennard, C. H. L., *Acta Crystallogr., Sect. C*, 1994, 50, 1291.
[9] Lynch, D. E., Smith, G., Byriel, K. A., and Kennard, C. H. L., *Acta Crystallogr., Sect. C*, 1996, 52, 231.
[10] Sheldrick, G. M., SHELX-97, University of Göttingen, Federal Republic of Germany, 1997.

UM00014011
NOVARTIS EXHIBIT 1517
Novartis v. Regents, IPR2023-01347
Page 2757 of 4460

This Page is Inserted by IFW Indexing and Scanning Operations and is not part of the Official Record

BEST AVAILABLE IMAGES

Defective images within this document are accurate representations of the original documents submitted by the applicant.

Defects in the images include but are not limited to the items checked:

- ☐ BLACK BORDERS
- ☐ IMAGE CUT OFF AT TOP, BOTTOM OR SIDES
- ☐ FADED TEXT OR DRAWING
- ☐ BLURRED OR ILLEGIBLE TEXT OR DRAWING
- ☐ SKEWED/SLANTED IMAGES
- ☐ COLOR OR BLACK AND WHITE PHOTOGRAPHS
- ☐ GRAY SCALE DOCUMENTS
- ☐ LINES OR MARKS ON ORIGINAL DOCUMENT
- ☐ REFERENCE(S) OR EXHIBIT(S) SUBMITTED ARE POOR QUALITY
- ☐ OTHER: _____

IMAGES ARE BEST AVAILABLE COPY.
As rescanning these documents will not correct the image problems checked, please do not report these problems to the IFW Image Problem Mailbox.

Supramolecular Control of Reactivity in the Solid State Using Linear Molecular Templates†

Leonard R. MacGillivray,* Jennifer L. Reid, and John A. Ripmeester

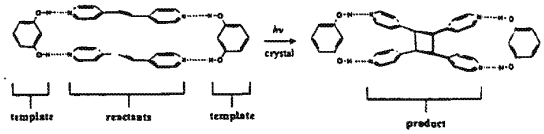
Steacie Institute for Molecular Sciences
National Research Council of Canada
Ottawa, Ontario, Canada, K1A 0R6

Received April 10, 2000

Since the work of Schmidt which delineated a "topochemical principle" for [2 + 2] photoreactions in the solid state,[1] chemists have strived to design molecules that will predictably crystallize to allow such reactions to occur. Such an approach to synthesis can lead to the formation of covalent bonds 'at will' in solids to facilitate the high yield, solvent-free synthesis[2] of molecules available either in low yields, as part of mixtures, or are not accessible in the liquid phase. Despite this realization, there remains no method to align olefins in solids that is reliable and may be used with reactants of diverse size, shape, and functionality,[3] criteria which, in principle, could offer synthetic freedoms realized in solution. The process has, moreover, largely remained one of trial and error,[4] often requiring weak intermolecular interactions between substituents[4−6] or constraining environments of cavities[7,8] to steer double bonds for reaction.

With this in mind, we describe a method involving a linear template,[9] based on 1,3-dihydroxybenzene (resorcinol),[10] to enforce topochemical alignment[1] of olefins in the solid state, by way of hydrogen bonds,[9−12] such that they undergo [2 + 2] photoreaction. We reasoned that an approach that exploits the strength and directionality of hydrogen bonds,[11,12] in the form of a molecule that enforces alignment of two sites within a discrete complex for reaction,[12] would largely eliminate consequences of intermolecular forces that have made topochemical designs unreliable.[4−6,13] Moreover, by separating the steering and reacting part supramolecularly, we reasoned that it should be possible to transfer a reaction between appropriately functionalized reactants in which the template may be used in diverse chemical environments[9] and, following reaction, recycled for further synthesis.[7] This method permits activation of molecules photostable as pure solids and we demonstrate how the method provides an entry to the regio- and stereocontrolled[12] solvent-free synthesis of cyclic molecules.[14] Whereas linear templates have been applied in solution, such an approach to engineering reactivity, where a single molecule organizes two molecules within a discrete complex for reaction, has not been realized in the solid state.[9,15]

Scheme 1



trans-1,2-Bis(4-pyridyl)ethylene (4,4′-bpe) crystallizes to form a layered structure in which olefins of neighboring layers lie orthogonal and separated by 6.52 Å.[16] 4,4′-bpe does not conform to the topochemical principle and is photostable.

To orient the olefins of 4,4′-bpe such that they are photoactive, we turned to structure studies based on resorcinol.[10] Such studies suggested that cocrystallization of 4,4′-bpe with resorcinol would yield a four-component assembly, 2(4,4′-bpe)·2(resorcinol) **1**, held together by four O−H···N hydrogen bonds, in which two pyridine units of 4,4′-bpe lie approximately orthogonal to the diol, interacting by way of $\pi-\pi$ interactions (Scheme 1). The olefins of the complex would be arranged in a parallel fashion, separated by ~4 Å. Photoreaction of the complex would give, in contrast to the liquid phase,[17] a single product, *rctt*-tetrakis(4-pyridyl) cyclobutane (tpcb).

An ORTEP perspective of **1** is shown in Figure 1.[18] As anticipated, the components assemble to form a cyclic array held together by four O−H···N hydrogen bonds.[19] In this arrangement, the olefins lie parallel and separated by 3.65 Å. Olefins of adjacent complexes pack such that they lie offset and are separated by 4.71 Å. As a result, the double bonds of the assembly are the sole olefins of the solid that conform to the topochemical principle.[1]

UV irradiation of a powdered crystalline sample of **1** placed between two glass plates (Hg lamp) produced tpcb, stereospecifically (yield: 100%), after a period of 42 h, as determined by ^{1}H NMR spectroscopy and ESI$^+$-MS.[20] As confirmed by structure analysis of a recrystallized portion of the reacted material,[21] photoreaction of **1**, as shown in Figure 2, produced tpcb. Interestingly, the template and product assemble to form a three-component array, (tpcb)·2(resorcinol) **2**, held together by four

* Author for correspondence. Steacie Institute for Molecular Sciences. Telephone: (613) 993-4406. Fax: (613) 998-7833. E-mail: lmacgil@ned1.sims.nrc.ca. New address: Department of Chemistry, University of Iowa, Iowa City, IA, 52242. Telephone: (319) 335-3504. Fax: (319)335-1270. E-mail: len-macgillivray@uiowa.edu.

† Published as NRCC No. 43845.

(1) For photodimerization to occur in the solid state, olefins should be parallel and separated by < 4.2 Å. See: Schmidt, G. M. J. *Pure Appl. Chem.* **1971**, *27*, 647.

(2) Metzger, J. O. *Angew. Chem., Int. Ed.* **1998**, *37*, 2975.

(3) Joy, A.; Ramamurthy, V. *Chem. Eur. J.* **2000**, *6*, 1287.

(4) Coates, G. W.; Dunn, A. R.; Henlink, L. M.; Ziller, J. W.; Lobkovsky, E. B.; Grubbs, R. H. *J. Am. Chem. Soc.* **1998**, *120*, 3641.

(5) Sharma, C. V. K.; Panneerselvam, K.; Shimoni, L.; Katz, H.; Carrell, H. L.; Desiraju, G. R. *Chem. Mater.* **1994**, *6*, 1282.

(6) Sarma, J. A. R. P.; Desiraju, G. R. *Acc. Chem. Res.* **1986**, *19*, 222.

(7) Tanaka, K.; Toda, F.; Mochizuki, E.; Yasui, N.; Kai, Y.; Miyahara, I.; Hirotsu, K. *Angew. Chem., Int. Ed.* **1999**, *38*, 3523.

(8) Brett, T. J.; Alexander, J. M.; Clark, J. L.; Ross, C. R., II; Harbison, G. S.; Stezowski, J. J. *Chem. Commun.* **1999**, 1275.

(9) Anderson, S.; Anderson, H. L. In *Templated Organic Synthesis*; Diederich, F., Stang, P. J., Eds.: Wiley-VCH: New York, 2000.

(10) MacGillivray, L. R.; Atwood, J. L. *J. Am. Chem. Soc.* **1997**, *119*, 6931.

(11) Desiraju, G. R. *Angew. Chem., Int. Ed. Engl.* **1995**, *34*, 2311.

(12) For a method involving a molecule that self-assembles, by way of hydrogen bonds, to form a discrete complex for [2 + 2] photoreaction in the solid state, see: Feldman, K. S.; Campbell, R. F. *J. Org. Chem.* **1995**, *60*, 1924.

(13) Ito, Y.; Borecka, B.; Trotter, J.; Scheffer, J. R. *Tetrahedron Lett.* **1995**, *36*, 6083.

(14) Prautzsch, V.; Ibach, S.; Vögtle, F. *J. Incl. Phenom. Macrocycl. Chem.* **1999**, *33*, 427.

(15) (a) Template strategies to solid-state synthesis have been described. Molecule synthesis, see: Cho, T. H.; Chaudhuri, B.; Snider, B. B.; Foxman, B. M. *Chem. Commun.* **1996**, 1337. Polymer synthesis, see: (b) Kane, J. J.; Liao, R.-F.; Lauher, J. W.; Fowler, F. W. *J. Am. Chem. Soc.* **1995**, *117*, 12003. (c) Vela, M. J.; Snider, B. B.; Foxman, B. M. *Chem. Mater.* **1998**, *10*, 3167. (d) Coa, G.; Mallouk, T. E. *J. Solid State Chem.* **1991**, *94*, 59. (e) Tieke, B.; Wegner, G. *Makromol. Chem., Rapid Commun.* **1981**, *2*, 543. (f) Chatani, Y. *Prog. Polym. Sci. Jpn* **1974**, *7*, 149. See also ref 7.

(16) Vansant, J.; Smets, G.; Declercq, J. P.; Germain, G.; Van Meerssche, M. *J. Org. Chem.* **1980**, *45*, 1557.

(17) Vansant, J.; Toppet, S.; Smets, G.; Declercq, J. P.; Germain, G.; Van Meerssche, M. *J. Org. Chem.* **1980**, *45*, 1565.

(18) Single crystals of **1** were grown by cocrystallization of 4,4-bpe with resorcinol in EtOH/MeCN (1:1). Crystal data for **1**: crystal size 0.3 × 0.3 × 0.4 mm, triclinic, space group $P\bar{1}$, a = 8.070(1) Å, b = 9.832(1) Å, c = 10.876(1) Å, α = 73.119(1)°, β = 72.563(1)°, γ = 66.184(1)°, U = 738.8(1) Å^3. 2θ = 45°, Mo Kα radiation (λ = 0.71070 Å) for Z = 2 and R = 0.054.

(19) **1** may form a divergent, polymeric assembly. Studies are underway to determine factors that contribute to formation of the convergent, discrete structure.

(20) For details, see Supporting Information.

(21) Single crystals of **2** were grown by recrystallizing a portion of reacted **1** from EtOH/toluene (10:1). Crystal data for **2**: crystal size 0.2 × 0.2 × 0.2 mm, monoclinic, space group $P2_1/n$, a = 11.367(1) Å, b = 9.749(1) Å, c = 14.273(1) Å, β = 111.668(3)°, U = 1469.7(3) Å^3. 2θ = 45°, Mo Kα radiation (λ = 0.71070 Å) for Z = 2 and R = 0.064.

10.1021/ja001239i CCC: $19.00 © 2000 American Chemical Society
Published on Web 07/29/2000

UM00014013
NOVARTIS EXHIBIT 1517
Novartis v. Regents, IPR2023-01347
Page 2759 of 4460

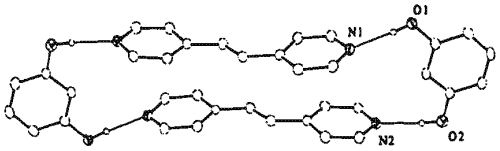


Figure 1. ORTEP perspective of **1**. Selected interatomic distances (Å): O1···N1 2.734(2), O2···N2 2.753(2).

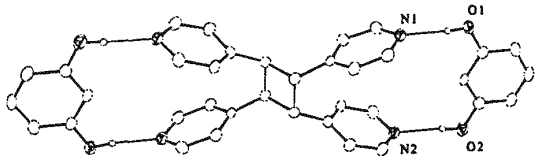
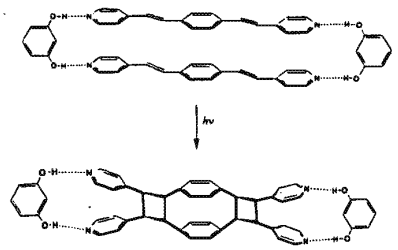


Figure 2. ORTEP perspective of the photoactivated complex **2**. Selected interatomic distances (Å): O1···N1 2.718(1), O2···N2 2.788(1).

Scheme 2



O−H···N hydrogen bonds, analogous to **1**. The structure of **2** favors the onward progress of the reaction and we suggest accounts for the quantitative conversion of 4,4′-bpe to tpcb.[12,22]

We have expanded the approach to additional reactants and templates.[20] *trans*-1,2-bis(2-pyridyl)ethylene (2,2′-bpe), upon cocrystallization with resorcinol is a suitable reactant, while 5-methoxyresorcinol (5-OMe-resorcinol), upon cocrystallization with 4,4′-bpe is a suitable template. 2,2′-bpe is photostable as a pure compound,[17] and reactivity experiments reveal that the olefins of both complexes, the sole bonds of each solid that conform to the topochemical principle, photodimerize, stereospecifically (yield: 100%), to yield *rctt*-isomers.[22]

With the realization that this approach permits reliable engineering of reactivity achieved, we set out to design a system involving two reaction centers. We anticipated that photoreaction of 1,4-bis[2-(4-pyridyl)ethenyl]benzene (1,4-bpeb)[23] would give a tricyclic [2.2]paracyclophane (Scheme 2).[24,25] If successful, the approach, in addition to displaying tolerance to lengthening of the reactant, would provide a novel entry to cyclic molecules[14] where low yields often requiring large batches of solvent are encountered in solution.

An ORTEP perspective of 2(1,4-bpeb)·2(5-OMe-resorcinol) **3** is shown in Figure 3.[26] As with **1**, the components form a four-component complex held together by four O−H···N hydrogen bonds. The olefins of 1,4-bpeb, one of which lies disordered across two positions (occupancies: 70:30), are aligned within the assembly such that the olefin of the major site meets the topochemical principle[1] with the ordered olefin, the two double bonds being separated by 3.70 Å. Two ordered olefins of two neighboring assemblies lie parallel and within 3.95 Å.

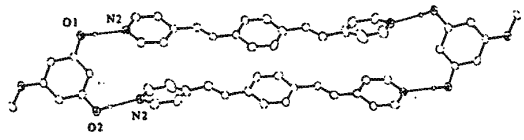


Figure 3. ORTEP perspective of **3** which leads to a [2.2]paracyclophane. Selected interatomic distances (Å): O1···N1 2.731(4), O2···N2 2.736(4).

UV irradiation of **3** produced the expected cyclophane (60%), along with a monocyclized dimer (30%) and indefinable products (10%), after 49 h. The cyclophane is characterized by pairs of doublets at 8.35 and 7.25 ppm, 7.07 and 6.78 ppm, and 4.74 and 4.61 ppm which correspond to the pyridyl, phenylene, and cyclobutane protons, respectively. The splitting pattern of the phenylene moiety is indicative of an *exo*, rather than an *endo*, isomer,[25] while the good yield of the cyclophane is consistent with a dynamic model of disorder.[27] The synthesis has, moreover, been regio- and stereoselective, proceeding by way of a monocyclized product in which the indefinable materials may be attributed to photoreactions involving nearest neighbor assemblies.[22] To our knowledge, **3** represents the first example in which a linear template has been used to organize more than one reaction center, in this case two sites for the designed synthesis of a molecule with an inner cyclic framework.[9]

We have presented a reliable method for aligning olefins in the solid state. The method utilizes linear templates[9] to organize single or multiple reaction centers to conduct regio- and stereocontrolled molecular synthesis in solids. Experiments are underway to modify the components of the system such that further analogies between solution and solid-state synthesis may be explored (e.g., functional group tolerance).[28] We are also investigating whether this approach may be applied to other reactions to devise templates that will allow the solid state to be used for the designed synthesis of molecular frameworks of increasing size and complexity.

Acknowledgment. We are grateful for funding from the Natural Sciences and Engineering Research Council of Canada for a research grant (L.R.M.) and doctoral scholarship (J.L.R.).

Supporting Information Available: Crystallographic reports and tables of positional and thermal parameters, bond lengths and angles, NMR data, and ESI$^+$-MS data (PDF). This material is available free of charge via the Internet at http://pubs.acs.org.

JA001239I

(22) Studies are underway to determine if the crystal structure involving the reactants is maintained during the reaction. See: Enkelmann, V.; Wegner, G.; Novak, K.; Wagener, K. B. *J. Am. Chem. Soc.* **1993**, *115*, 10390.

(23) Amoroso, A. J.; Thompson, A. M. W. C.; Maher, J. P.; McCleverty, J. A.; Ward, M. D. *Inorg. Chem.* **1995**, *34*, 4828.

(24) Hasegawa, H.; Mackawa, Y.; Kato, S.; Saigo, K. *Chem. Lett.* **1987**, 907.

(25) Nakamura, Y.; Hayashida, Y.; Wada, Y.; Nishimura, J. *Tetrahedron* **1997**, *53*, 4593.

(26) Single crystals of **3** were grown by cocrystallization of 1,4-bpeb with 5-OMe-resorcinol from EtOH/MeCN (8:1). Crystal data for **3**: crystal size 0.1 × 0.2 × 0.3 mm, triclinic, space group $P\bar{1}$, a = 9.460(1) Å, b = 9.470(1) Å, c = 13.744(1) Å, α = 83.164(2)°, β = 72.181(2)°, γ = 67.693(2)°, U = 1086.0(2) Å^3, 2θ = 45°, Mo Kα radiation (λ = 0.71070 Å) for Z = 2 and R = 0.059.

(27) Galli, S.; Mercandelli, P.; Sironi, A. *J. Am. Chem. Soc.* **1999**, *121*, 3767.

(28) Fu, G. C.; Nguyen, S. T.; Grubbs, R. H. *J. Am. Chem. Soc.* **1993**, *115*, 9856.

UM00014014
NOVARTIS EXHIBIT 1517
Novartis v. Regents, IPR2023-01347
Page 2760 of 4460

Structural Preferences of Hydrogen-Bonded Networks in Organic Solution—the Cyclic $CA_3 \cdot M_3$ "Rosette"

John P. Mathias, Eric E. Simanek, Jonathan A. Zerkowski, Christopher T. Seto, and George M. Whitesides*

Contribution from the Department of Chemistry, Harvard University, Cambridge, Massachusetts 02138

*Received September 29, 1993. Revised Manuscript Received February 27, 1994**

Abstract: Crystals grown from a solution containing equimolar portions of barbital (3) and *N,N'*-bis(4-*tert*-butylphenyl)-melamine (4) in toluene/isopropyl alcohol (1:1 v/v) comprise a cyclic $CA_3 \cdot M_3$ "rosette" (5). The six molecules in this supramolecular motif are held together by 18 hydrogen bonds. Characterization of *solutions* of equimolar mixtures of 3 and 4 in chloroform by ^1H NMR spectroscopy, gel permeation chromatography, and vapor pressure osmometry demonstrates that the same cyclic $CA_3 \cdot M_3$ rosette (5) is also the most probable structure, when [3] = [4] > 4 mM. ^1H NMR exchange experiments confirm that the $CA_3 \cdot M_3$ rosette (5) is qualitatively much less stable in chloroform solution than the supramolecular aggregate hub(M)$_3$:3barbital (1) that is preorganized for self-assembly by a covalent tris(melamine) derivative. Complexes formed between 4 and different isocyanurates indicate that intermolecular interactions, as a consequence of the steric bulk of the substituents on these derivatives, favor the formation of the cyclic $CA_3 \cdot M_3$ rosette over competing linear hydrogen-bonded motifs. There is inferential evidence for formation of a complex of modest stability with composition $CA \cdot M_2$ when 2[3] = [4].

Introduction

The potential of molecular self-assembly for the preparation of large supramolecular aggregates depends on the identification of noncovalently stabilized structural motifs whose enthalpic driving force for self-assembly is sufficient to overcome the unfavorable entropic consequences associated with the aggregation of several components into a single supramolecular entity.[1-3] We have chosen to use hydrogen bonds as primary elements with which to form supramolecular aggregates, in order to take advantage of the extensive body of information concerning hydrogen-bonded aggregation in solution[4,5] and in the solid state.[6,7] The hydrogen-bonded CA·M lattice[8] is the template on which we have based the design of a family of self-assembled hydrogen-bonded aggregates that are stable in organic solution.[9-11] Covalent preorganization of three melamines into a "tripod" molecule has facilitated the self-assembly of supramolecular aggregates that are stabilized by cyclic $CA_3 \cdot M_3$ rosettes, such as those represented schematically by **1** and **2** (Figure 1). We have demonstrated that these aggregates are stable in chloroform solution and have characterized their structures by ^1H and ^{13}C NMR spectroscopies, gel permeation chromatography, vapor pressure osmometry, and UV spectrophotometry.[9-13] With one exception, we have not been able to grow crystals of these aggregates and, therefore, have not been able to characterize them by X-ray crystallography.[14] We have determined the X-ray structure of a cyclic rosette of composition $CA_3 \cdot M_3$ (Figure 2).[15] This $CA_3 \cdot M_3$ rosette

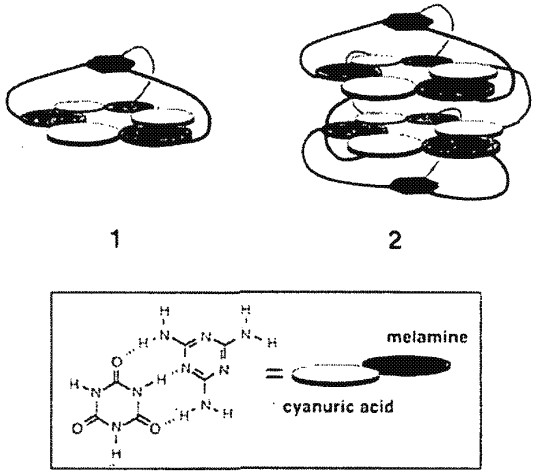


Figure 1. Schematic structures of two previously reported supramolecular aggregates based on $CA_3 \cdot M_3$ rosettes.

* Abstract published in *Advance ACS Abstracts*, April 1, 1994.

(1) Whitesides, G. M.; Mathias, J. P.; Seto, C. T. *Science* **1991**, *254*, 1312-1319.

(2) Lehn, J.-M. *Angew. Chem., Int. Ed. Engl.* **1990**, *29*, 1304-1319.

(3) Lindsey, J. S. *New J. Chem.* **1991**, *15*, 153-180. Baxter, P.; Lehn, J.-M.; DeCian, A.; Fischer, J. *Angew. Chem., Int. Ed. Engl.* **1993**, *32*, 69-72. Krämer, R.; Lehn, J.-M.; DeCian, A.; Fischer, J. *Angew. Chem., Int. Ed. Engl.* **1993**, *32*, 703-706. Copp, S. B.; Subramanian, S.; Zaworotko, M. J. *Angew. Chem., Int. Ed. Engl.* **1993**, *32*, 706-709. Ashton, P. R.; Bissel, R. A.; Spencer, N.; Stoddart, J. F.; Tolley, M. S. *Synlett.* **1992**, 914-918. Ashton, P. R.; Bissel, R. A.; Spencer, N.; Stoddart, J. F.; Tolley, M. S. *Synlett.* **1992**, 923-926. Constable, E. C. *Tetrahedron* **1992**, *48*, 10013-10059.

(4) For recent examples, see: Geib, S. J.; Vicent, C.; Fan, E.; Hamilton, A. D. *Angew. Chem., Int. Ed. Engl.* **1993**, *32*, 119-121. Fan, E.; Van Arman, S. A.; Kincaid, S.; Hamilton, A. D. *J. Am. Chem. Soc.* **1993**, *115*, 369-370. Yang, J.; Fan, E.; Geib, S. J.; Hamilton, A. D. *J. Am. Chem. Soc.* **1993**, *115*, 5314-5315. Bonazzi, S.; DeMorais, M. M.; Gottarelli, G.; Mariani, P.; Spada, G. P. *Angew. Chem., Int. Ed. Engl.* **1993**, *32*, 248-250. Boner-Law, R. P.; Sanders, J. K. M. *Tetrahedron Lett.* **1993**, *34*, 1677-1680. Mascal, M.; Moody, C. J.; Morrell, A. I.; Slawin, A. M. Z.; Williams, D. J. *J. Am. Chem. Soc.* **1993**, *115*, 813-814. Yoon, S. S.; Still, W. C. *J. Am. Chem. Soc.* **1993**, *115*, 823-824. Liang, G.-B.; Desper, J. M.; Gellman, S. H. *J. Am. Chem. Soc.* **1993**, *115*, 925-938.

(5) Zimmerman, S. C.; Duerr, B. F. *J. Org. Chem.* **1992**, *57*, 2215-2217.

(6) Desiraju, G. R. *Crystal Engineering: The Design of Organic Solids*; Elsevier: New York, 1989; pp 115-173.

(7) Etter, M. C. *Acc. Chem. Res.* **1990**, *23*, 120-126.

(8) We have illustrated the structure of the CA·M lattice in previous papers, see ref 1. This structure is a putative one, however, and has not been established unequivocally by single-crystal X-ray crystallography. The X-ray crystal structure of (CA)-(M)-3HCl has been reported, see: Wang, Y.; Wei, B.; Wang, Q. *J. Crystallogr. Spectrosc. Res.* **1990**, *20*, 79-82.

(9) Seto, C. T.; Whitesides, G. M. *J. Am. Chem. Soc.* **1993**, *115*, 905-916.

(10) Seto, C. T.; Mathias, J. P.; Whitesides, G. M. *J. Am. Chem. Soc.* **1993**, *115*, 1321-1329.

(11) Seto, C. T.; Whitesides, G. M. *J. Am. Chem. Soc.* **1993**, *115*, 1330-1340.

(12) Seto, C. T.; Whitesides, G. M. *J. Am. Chem. Soc.* **1990**, *112*, 6409-6410.

(13) Seto, C. T.; Whitesides, G. M. *J. Am. Chem. Soc.* **1991**, *113*, 712-713.

0002-7863/94/1516-4316$04.50/0 © 1994 American Chemical Society

UM00014015
NOVARTIS EXHIBIT 1517
Novartis v. Regents, IPR2023-01347
Page 2761 of 4460

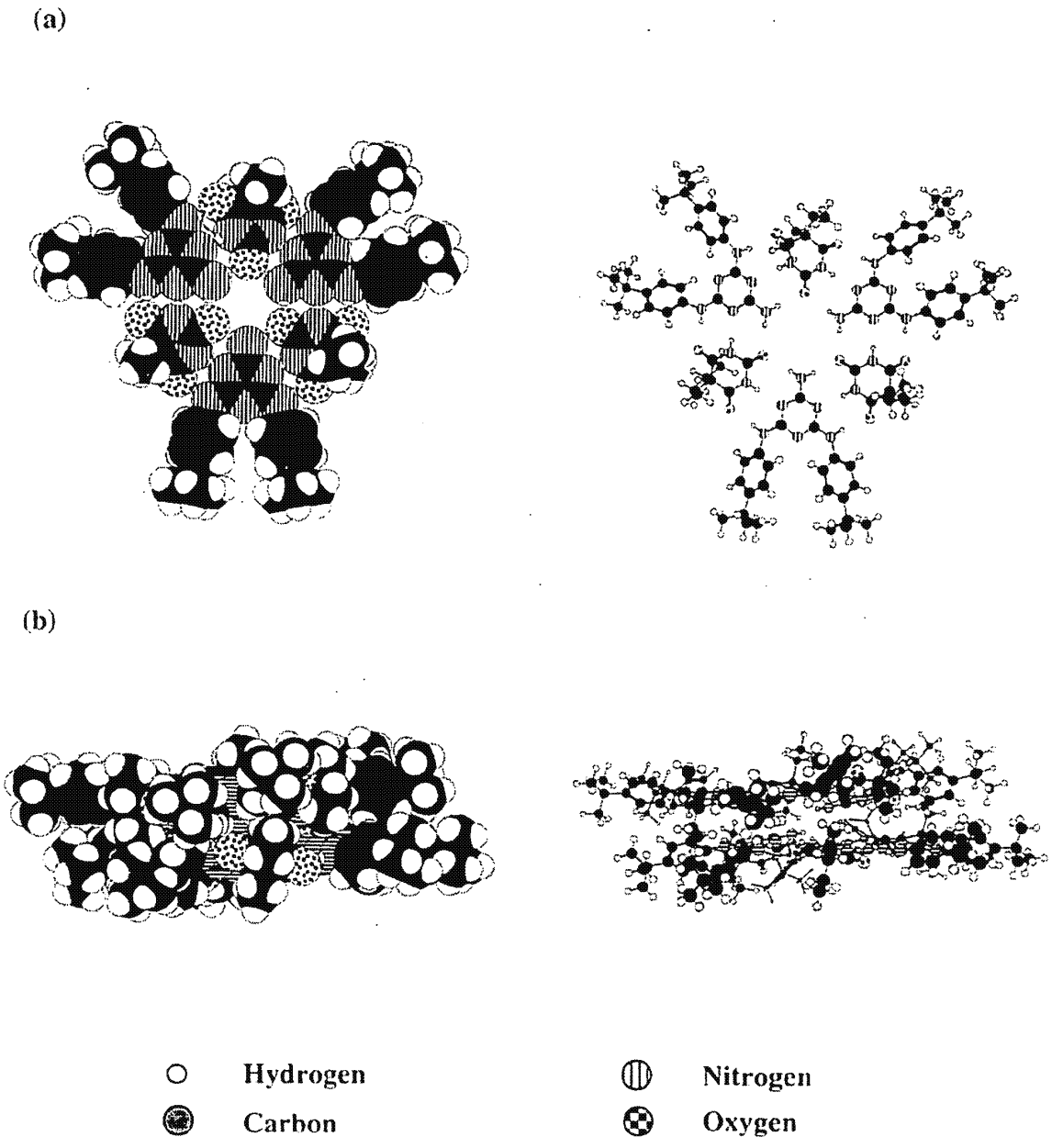


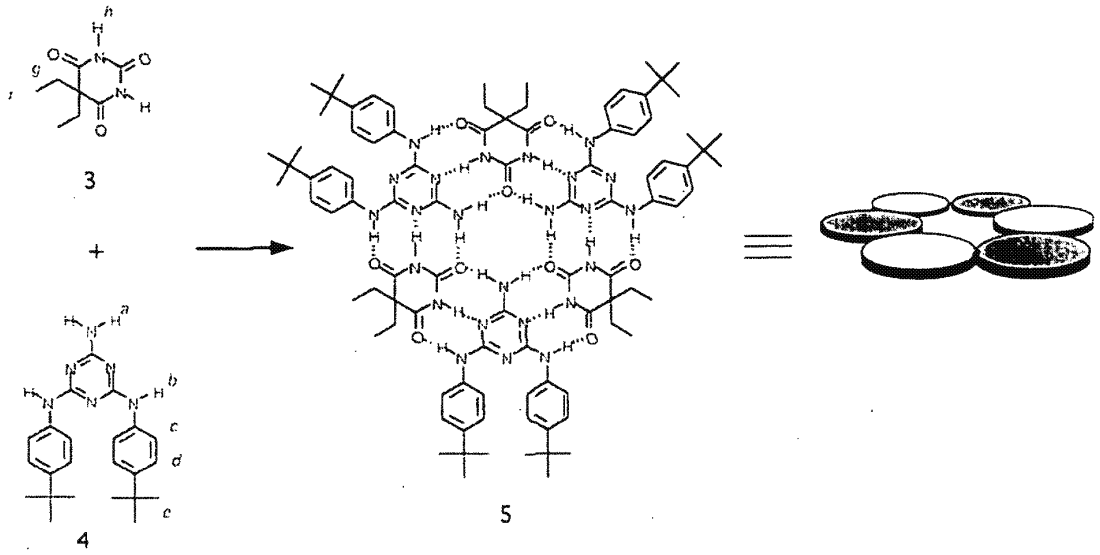
Figure 2. (a) X-ray crystal structure and (b) packing of the CA_3M_3 rosette 5 formed between equimolar portions of 3 and 4 in van der Waal's surface and ball-and-stick representations.

(5) incorporates barbital (3) and *N,N'*-bis(4-*tert*-butylphenyl)-melamine (4) (Scheme 1). The finite cyclic CA_3M_3 rosette is only one of many possible hydrogen-bonded motifs that could be adopted in the solid state by an equimolar mixture of 3 and 4. We have, for example, seen two infinite hydrogen-bonded motifs, a linear tape and a crinkled tape, in 1:1 cocrystals between barbital and a number of disubstituted melamine derivatives.[16-19] These three motifs are shown together in Figure 3. Progression from one motif to another occurs as a consequence of the intermolecular steric interactions that occur between the substituents on the melamine and barbiturate derivatives. Intermolecular steric interaction between the substituents on adjacent melamines (linear tape), and also between the substituents on proximal melamine and barbiturate molecules (crinkled tape), are greater in these tape motifs than in the cyclic rosette. The regions of potential intermolecular steric overlap between substituents in each of these motifs are indicated on Figure 3. The steric bulk of the two *p*-*tert*-butylphenyl substituents in 4 is crucial in dictating the structural motif that is adopted in the cocrystal between 3 and

(14) Attempts to grow crystals of these aggregates that are suitable for X-ray crystallography have resulted in either amorphous powders or glasses.
(15) Zerkowski, J. A.; Seto, C. T.; Whitesides, G. M. *J. Am. Chem. Soc.* 1992, *114*, 5473–5475.
(16) Zerkowski, J. A.; Seto, C. T.; Wierda, D. A.; Whitesides, G. M. *J. Am. Chem. Soc.* In press.
(17) Zerkowski, J. A.; Whitesides, G. M. *J. Am. Chem. Soc.* In press.
(18) Zerkowski, J. A.; Mathias, J. P.; Whitesides, G. M. *J. Am. Chem. Soc.* In press.
(19) Zerkowski, J. A.; Whitesides, G. M. *J. Am. Chem. Soc.* In press.

UM00014016
NOVARTIS EXHIBIT 1517
Novartis v. Regents, IPR2023-01347
Page 2762 of 4460

Scheme 1. Self-Assembly of the $CA_3 \cdot M_3$ Rosette



4. It is the $CA_3 \cdot M_3$ rosette that allows the sterically demanding groups on adjacent melamines to get as far away as possible from each other and from the ethyl substituents on the barbital ring.

In order to understand the occurrence and stability of the $CA_3 \cdot M_3$ rosette, we have examined the aggregates formed between barbital (3) and *N,N'*-bis(4-*tert*-butylphenyl)melamine (4) in both the solid state and in solution. The objectives of this study were (i) to assess whether the $CA_3 \cdot M_3$ rosette between 3 and 4 in the solid state was thermodynamically stable or kinetically determined, using X-ray powder diffraction and (ii) to determine the structural preference for the $CA_3 \cdot M_3$ rosette in solution using ^{1}H NMR spectroscopy, gel permeation chromatography, and vapor pressure osmometry. The results are beginning to define the structural preferences and stability of the $CA_3 \cdot M_3$ rosette—the basis for all of the self-assembled aggregates we have examined.

Results and Discussion

Assessing the Stability of the Cyclic $CA_3 \cdot M_3$ Rosette in the Solid-State by X-ray Powder Diffraction. Crystals of the 1:1 complex (5) formed between 3 and 4 grew on slow evaporation of a solution in isopropyl alcohol/toluene (~1:1 v/v). The structure of 5 in the solid state is shown in Figure 2.[15] The X-ray powder diffraction (XPD) pattern of 5 was calculated from this crystal structure (Figure 4a). We have used the calculated XPD pattern as the basis to search for other polymorphs of 5 in the solid state and, therefore, to infer the stability of the $CA_3 \cdot M_3$ rosette of 3 and 4, relative to tapes or other structures.[20,21]

Crystalline powders of 5 were obtained by recrystallization of an equimolar mixture of 3 and 4 from a variety of solvents. These powders were dried by evaporation at room temperature under atmospheric pressure (~2–5 days), ground, and subjected to XPD using X-rays from CuKα (λ = 1.54178 Å) with $3.6° < 2\theta < 33.6°$. XPD patterns for powders of 5 obtained from solutions in chloroform, acetone, acetonitrile, methanol/THF (1:1 v/v), and isopropyl alcohol/toluene (1:1 v/v: the solvent of crystallization) are illustrated in Figure 4b (traces i–v). The positions of the peaks in the XPD patterns from the various solvents and the calculated pattern are similar. Figure 4b (trace vi) shows the XPD pattern obtained after the powder from isopropyl alcohol/toluene (1:1 v/v) was annealed at 95 °C for 7 days. There are no significant changes in the positions of peaks or the overall pattern in the XPD picture after annealing this sample. The $CA_3 \cdot M_3$ rosette appears, therefore, to be a thermodynamically stable morphology.

From these observations by XPD, we conclude that the structure for the 1:1 complex between 3 and 4 in the solid state is independent of the solvent used for crystallization.[22] We infer that the self-assembly of the cyclic CA_3M_3 rosette reflects the formation of a stable cyclic aggregate of 3 and 4, rather than a kinetic artifact of rates of nucleation or crystal growth.

The 1:1 Complex Formed between 3 and 4 in Chloroform Is More Soluble Than 3 or 4 Alone. The solubilities of 3 and 4 in chloroform are low (<0.5 mM). Adding aliquots of 3 to 4 in chloroform, however, leads to the formation of a hydrogen-bonded supramolecular aggregate (5) that is highly soluble (>100 mM), once the relative proportions of 3 and 4 are 1:1. This significant increase in solubility of the molecules on aggregation in chloroform is also exhibited in the formation of self-assembled aggregates of types 1 and 2 (Figure 1).[9] In all of these cases, self-assembly of the $CA_3 \cdot M_3$ rosette allows the polar, hydrogen-bonding functionalities in the components to form soluble cyclic aggregates rather than extended insoluble networks. Small hydrogen-bonded linear oligomers formed between 3 and 4 would have large areas of polar functionality in contact with the solution. Indeed, the solubilities of 1:1 complexes between barbital (3) and other *N,N'*-bis(4-alkylphenyl)melamines with less bulky substituents are very low in chloroform (<2 mM). Even the 1:1 complex between barbital and *N,N'*-bis(4-isopropylphenyl)melamine has a solubility below 5 mM in chloroform. The high solubility of the 1:1 complex formed between 3 and 4 can, we believe, be interpreted as a consequence of self-assembly of the cyclic $CA_3 \cdot M_3$ rosette.

Assessing the Characteristics of the Cyclic $CA_3 \cdot M_3$ Rosette in Solution by ^{1}H NMR Spectroscopy. ^{1}H NMR spectra of solutions obtained by titration of a solid barbital (3) into a suspension of

(20) We have made many attempts to grow crystals from equimolar solutions of 3 and 4 from other solvents and to search for other polymorphs directly by X-ray crystallography, without success. In these cases, the smallest dimensions of any single crystals obtained was less than 0.05 mm.

(21) We have previously inferred the existence of different morphologies for 1:1 mixtures of melamines and barbiturates using XPD, see ref 16. Confirmation of these different morphologies was then provided by ^{13}C solid-state NMR—Wazeer, M.; McDonald, J.; Weisbecker, C.; Whitesides, G. M. Unpublished results.

(22) The positions of the major peaks in the pattern obtained from chloroform coincide with those in the calculated pattern. Although there is an absence of peaks in new positions and or shifting in the position of peaks from the calculated pattern there does, however, appear to be a broadening and loss of resolution in the pattern. We do not rule out the presence of other polymorphs or minor impurities to account for this phenomena.

UM00014017
NOVARTIS EXHIBIT 1517
Novartis v. Regents, IPR2023-01347
Page 2763 of 4460

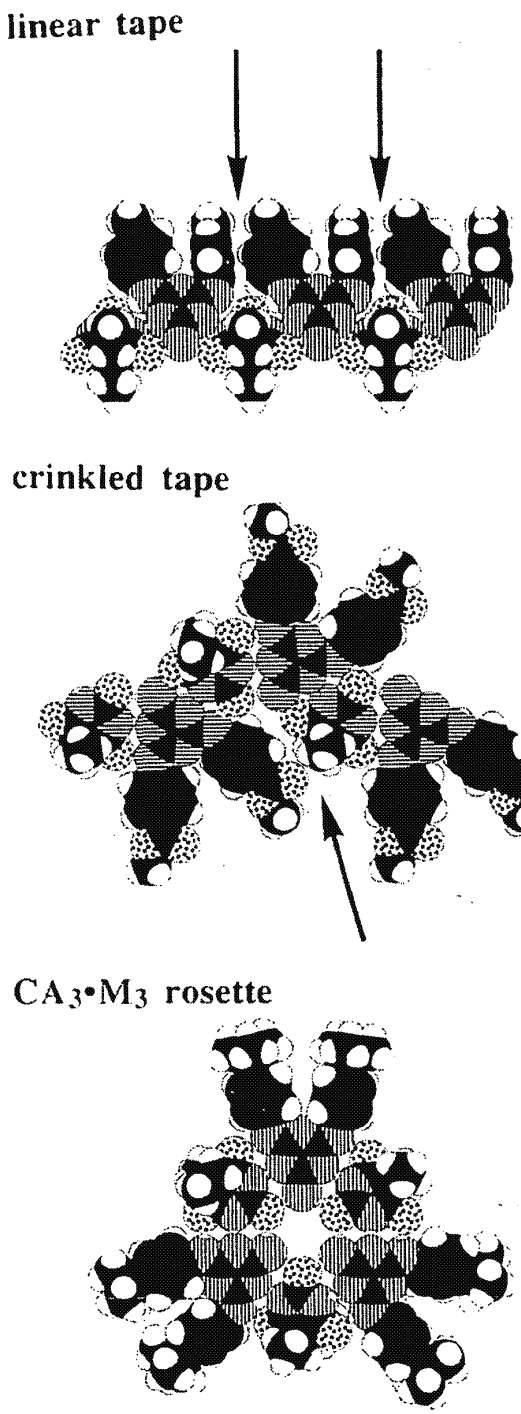


Figure 3. Crystallographic structures of the three hydrogen-bonded motifs observed in cocrystals between derivatives of barbituric acid and *N,N'*-disubstituted melamine. They are the linear tape (top), the crinkled tape (middle), and the CA_3·M_3 rosette (bottom). Regions of intermolecular steric interaction between the substituents on adjacent melamine rings in the linear tape and between the substituents on melamine rings and proximal barbiturates in the crinkled tape motifs are indicated by arrows.

N,N'-bis(4-*tert*-butylphenyl)melamine (4) in $CDCl_3$ are illustrated in Figure 5a–d (the nominal concentration of 4 was 7 mM). Annotation of these spectra refer to the labels on 3 and 4 in Scheme 1. Addition of barbital solubilizes 4 until 1:1 stoichiometry is reached. At this stoichiometry, the solution becomes homogeneous. Further aliquots of barbital remain insoluble.

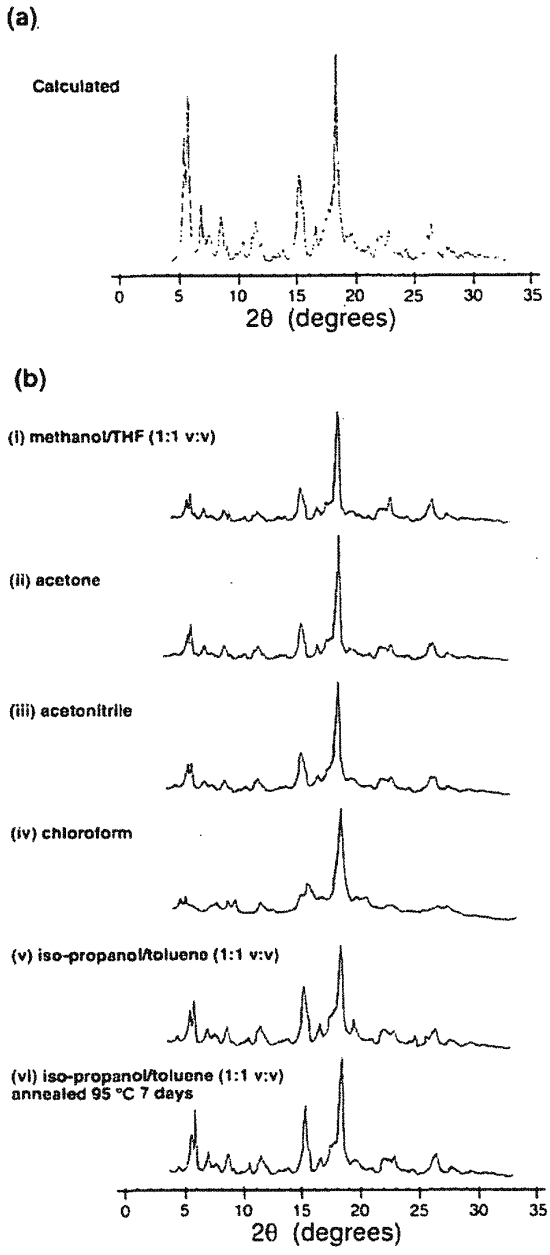


Figure 4. (a) Calculated XPD pattern for the CA_3·M_3 rosette 5. (b) Patterns obtained from XPD on samples of 5 formed by crystallization from different solvents.

During this titration, the chemical shift of the NH_2 protons (H^a) on the melamine derivative 4 moves downfield from 5.45 to 7.15 ppm. The chemical shift of the NH protons (H^b) on 4 moves downfield from 7.25 to 9.60 ppm. The changes in chemical shift for H^a and H^b on addition of barbital suggest that they are involved in strong hydrogen bonding. One set of phenyl protons (H^c) on 4 also moves downfield from 7.45 to 7.60 ppm during the titration. The hydrogen-bonded imide protons on barbital (H^b) in the 1:1 aggregate appear as a broad signal at δ 14.1 ppm.[23,24]

UM00014018
NOVARTIS EXHIBIT 1517
Novartis v. Regents, IPR2023-01347
Page 2764 of 4460

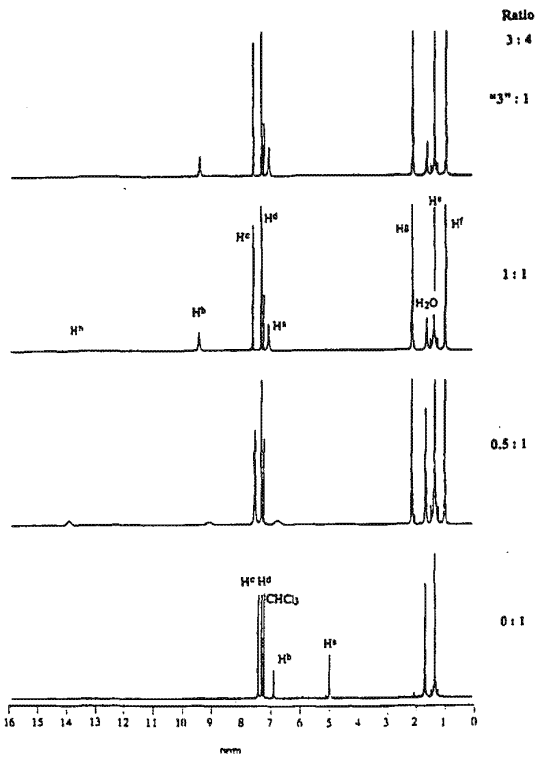


Figure 5. ^{1}H NMR spectra of a titration between 3 and 4 (500 MHz, $CDCl_3$). Solid 3 was added to a suspension of 4 and heated to reflux to afford a homogeneous solution. Annotations refer to those indicated on Scheme 1. The resonance for the isocyanurate protons H^b is broadened into the base line in the $CA_3{\cdot}M_3$ rosette.

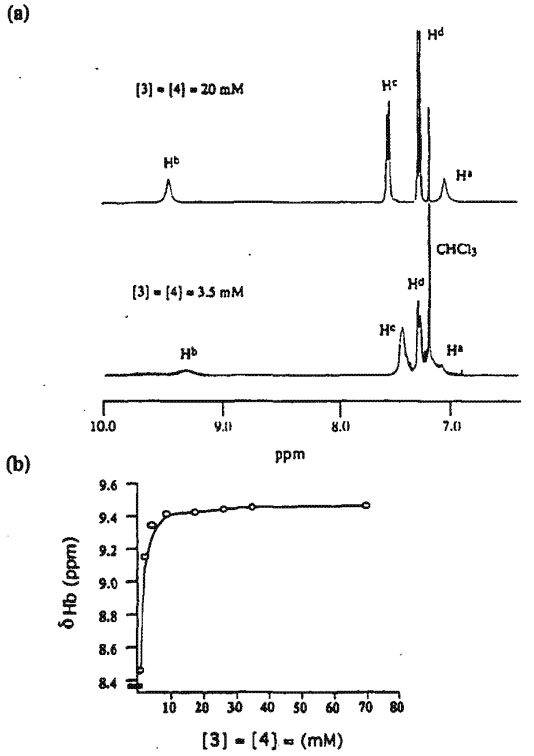


Figure 6. (a) Partial ^{1}H NMR spectra for 5 taken at [3] = [4] = 20 mM and [3] = [4] = 3.5 mM concentrations. (b) Plot of the chemical shift of H^b on the melamine derivative 4 against concentration. Annotations refer to those in Scheme 1.

The absence of separate peaks associated with "bound" and "free" components in this titration suggests that exchange between complexes and uncomplexed states is fast on the NMR time scale, at room temperature. This rapid exchange observed for 5 contrasts to that observed for aggregates of type 1 and 2 (Figure 1): exchange between bound and unbound states in these aggregates is slow on the NMR time scale; both states are clearly visible.[9-11] The aggregate 5 therefore exhibits more rapid exchange of bound and free components than does the covalently preorganized aggregates 1 and 2.

The effects of concentration on the chemical shift of the melamine NH protons (H^b) in 5 are illustrated in Figure 6. Little change occurs as a solution of 5 in chloroform is diluted from [3] = [4] = 70 to 4 mM (Figure 6a). Below [3] = [4] = 4 mM, a sharp upfield shift is seen for H^b, and the resolution of the spectra decreases sharply (Figure 6b). The curve obtained for δH^b vs [concn] from these data (Figure 6c) suggests that the degree of hydrogen bonding is insensitive to concentration when [3] = [4] > 4 mM and, therefore, that the assembly/disassembly of the complex formed between 3 and 4 displays positive cooperativity once this concentration is reached.[25] The degree of hydrogen bonding should change more steadily as a function of concentration for noncooperative association. When [3] = [4] < 4 mM, the degree of hydrogen bonding is very sensitive to changes in concentration. The concentration-dependent aggregation seen for 5 by ^{1}H NMR in $CDCl_3$ correlates strongly with that observed by VPO (see later).

Figure 7 shows the changes in the ^{1}H NMR spectrum of a solution of 5 in chloroform that occur with temperature. These variable temperature NMR experiments were performed with concentrations [3] = [4] = 3 mM in $CDCl_3$. This concentration is below that required to give a well defined aggregate, and there is, therefore, little detail in the NMR spectrum at room temperature. In this experiment, we hoped to see the transition from a poorly defined mixture of rapidly equilibrating structures at higher temperature to separate, more ordered structures as the rate of exchange was reduced at progressively lower temperatures.

Decreasing the temperature from 293 to 226 K did sharpen the resonances. At 293 K the chemical shifts of the phenyl protons (H^3/H^4, δ 7.30 and 7.45, respectively) are close to those observed for 4 in chloroform. Resonances for the melamine protons H^a and H^b also appear as broad signals that are upfield, relative to their position in 5. The barbiturate protons H^b (not shown) are broadened completely into the base line. As the temperature decreases, the progression to the fully assembled $CA_3{\cdot}M_3$ rosette is apparent, until at 226 K, H^c/H^d appear predominantly (>90%) as two sharp signals at δ 7.30 and 7.60, respectively, and the chemical shifts and peak shapes of all other protons correspond to those seen in the fully bound 1:1 complex 5 (Figure 5a). NOE effects in related systems have confirmed that the melamine protons H_c *do* correspond to the doublet that is farthest downfield, δ 7.60 ppm in 5, relative to H^d at δ 7.30 ppm. At higher temperatures the doublet for the aromatic protons H^c displays broadening, probably as a consequence of exchange between the fully-assembled state and several different partially assembled states. At 226 K, the rate of exchange between states is slow enough to see the individual components and the majority of H^c

(23) The chemical shift of the barbiturate protons (H^b) in DMSO is δ 11.2 ppm; in 5% DMSO/$CHCl_3$ (v/v) it is 10.9 ppm.

(24) The appearance of H^b as a broad signal in 5 contrasts with observations made on previously reported supramolecular aggregates such as 1 and 2, and, indeed, with many of the other $CA_3{\cdot}M_3$ rosettes reported in Scheme 4 later in this paper. In all of these cases, the hydrogen-bonded isocyanurate/barbiturate protons appear as sharp signals in the region 14–16 ppm in $CDCl_3$.

UM00014019
NOVARTIS EXHIBIT 1517
Novartis v. Regents, IPR2023-01347
Page 2765 of 4460

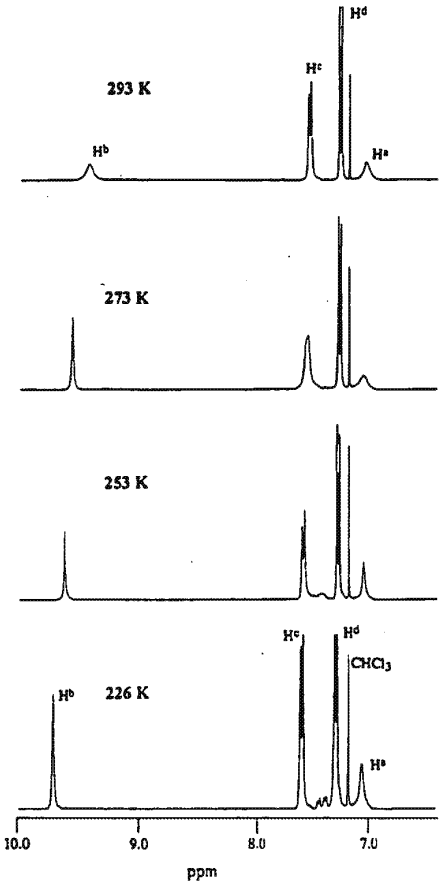


Figure 7. Spectra obtained from variable temperature ^1H NMR on the aggregate **5** at a concentration of [3] = [4] = 3 mM, with respect to the components (400 MHz, $CDCl_3$). Annotations refer to those in Scheme 1.

appears as a doublet at δ 7.60 ppm, corresponding to the fully-assembled rosette **5**. Other aggregates are visible as two small doublets at approximately δ 7.4 ppm. The differences in line broadening between H^c and H^d at 273 K suggest that both of these doublets are due to H^c and that the corresponding doublets for H^d are incorporated into the single doublet observed. The difference in the behavior of H^c and H^d during the cooling of this solution is a consequence of the closer proximity of H^c than H^d to the hydrogen bonding sites. While H^d will also undergo exchange, this position is not close enough to the hydrogen-bonded region to experience a significant change in its environment and, therefore, in its chemical shift during complexation and decomplexation.

The data from variable-temperature NMR spectroscopy suggest that the 1:1 complex formed between **3** and **4** (at 4 mM) is present predominantly (>90%) as the single hydrogen-bonded structure represented by the cyclic $CA_3{\cdot}M_3$ rosette (**5**) at 226 K. They also suggest that the remaining material is present in other hydrogen bonded forms—perhaps smaller linear oligomers?

Assessing the Characteristics of the Cyclic $CA_3{\cdot}M_3$ Rosette in Solution by Gel Permeation Chromatography (GPC). Gel permeation chromatography can be used to examine the heterogeneity and relative stabilities of hydrogen-bonded self-assembled aggregates in solution.[26,27] The kinetic stability of a complex must, however, be sufficient for it to elute intact. We have demonstrated that complexes of types **1** and **2** (Figure 1) are stable enough to be characterized by GPC.[9-11] Complexes of type **1**, however, dissociate significantly during the 7–10 min required for analysis. As a result, their peaks exhibit tailing.

Examination of the 1:1 complex formed between **3** and **4** by GPC (eluting with $CHCl_3$) shows no evidence for a supramolecular aggregate that is stable enough to pass through the GPC column without dissociation. While **3** is sufficiently insoluble that it does not elute off the column alone, **4** elutes from the column after xylenes as a broadened peak suggesting that it absorbs to the column matrix. Mixtures of [3] = [4] do not elute from the column before the xylenes marker. The low solubility of both components in chloroform precluded running an experiment in which the eluent was a solution of either component in chloroform, so that dissociation of the rosette during analysis would no longer be an irreversible process.

Characterizing the $CA_3{\cdot}M_3$ Rosette by Vapor Pressure Osmometry (VPO). The 1:1 complex formed between barbital (**3**) and *N,N'*-bis(4-*tert*-butylphenyl)melamine (**4**) was examined by VPO over the concentration range 0.5–32 mM (all concentrations refer to those of the individual components, not of the putative $CA_3{\cdot}M_3$ rosette). The plot of $\Delta V{\cdot}[3 \text{ or } 4]^{-1}$ vs [3 or 4] obtained from VPO is shown in Figure 8a. The curvature of this plot shows that **5** displays nonideal behavior in solution at concentrations below ~4 mM. Data obtained from a self-assembled aggregate of type **1**—hubM_3:3*neo*hex(CA)—and the cyclic decapeptide *N,N'*-bis(^{t}Boc)-gramicidin S are included in Figure 8a for reference.[28] Both hubM_3:3*neo*hex(CA) and *N,N'*-bis-(^{t}Boc)-gramicidin S give straight lines in the plot of $\Delta V{\cdot}[3 \text{ or } 4]^{-1}$ vs [3 or 4] that show a slight negative slope as the concentration increases. We have proposed that this feature is a result of concentration-dependent aggregation (both structures have hydrogen bond donors and acceptors on their periphery).[9] Aggregation causes the actual number of particles in solution to decrease. The *change in vapor pressure* sensed by osmometry is, therefore, smaller than would be expected under ideal conditions. Thus, the ratio of $\Delta V{\cdot}[3 \text{ or } 4]^{-1}$ vs [3 or 4] decreases, resulting in a negative slope to the plot.

At concentrations [3] = [4] > 4 mM (2.5 g/L), the behavior of **5** is similar to that of hubM_3:3*neo*hex(CA) and *N,N'*-bis-(*tBoc*)-gramicidin S. Analysis of the data from three separate experiments for **5** over the range 4–32 mM (Figure 8a; inset) gives the apparent molecular weights for the aggregate in solution shown in Figure 8b, when compared against four different standards of known molecular weight. The calculated molecular weight for the cyclic $CA_3{\cdot}M_3$ rosette **5** is 1.72 kDa. While the use of many molecular weight standards leads to a distribution of observed molecular weights for the unknown sample, it decreases the bias caused by any nonideal behavior of the standards. The agreement between the observed molecular weight and the value calculated for the cyclic $CA_3{\cdot}M_3$ rosette **5** lead us to conclude that this motif is the most probable structure for the 1:1 complex between **3** and **4** in solution, at concentrations when [3] = [4] > mM.

Data from the equimolar mixture when [3] = [4] < 4 mM exhibit a highly negative slope. This observation is consistent with an increasing degree of aggregation between the molecules as the concentration increases in this range. We believe that the components **3** and **4** are present in solution in a mixture of states including **5**, the uncomplexed components, and larger hydrogen-bonded oligomers when [3] = [4] < 4 mM. Treatment of these data suggest the average molecular weight of any aggregates in solution below 4 mM is in the range 0.5–0.8 kDa (FW_3 184, FW_4

(25) Similar observations have been made, and conclusions drawn, concerning the self-assembly of a hydrogen-bonded trimer by Zimmerman, see ref 5.

(26) Part C, Polymer Symposia 21. In *Journal of Polymer Science*; Johnson, J. F., Ed.; 1968; pp 1–344.

(27) Stevens, F. J. *Biochemistry* **1986**, *25*, 981–993. Stevens, F. J. *Biophysics J.* **1989**, *55*, 1155–1167.

(28) Original data from VPO for hubM_3:3*neo*hex(CA) and *N,N'*-bis-(^{t}Boc)-gramicidin S were reported in ref 9.

UM00014020
NOVARTIS EXHIBIT 1517
Novartis v. Regents, IPR2023-01347
Page 2766 of 4460

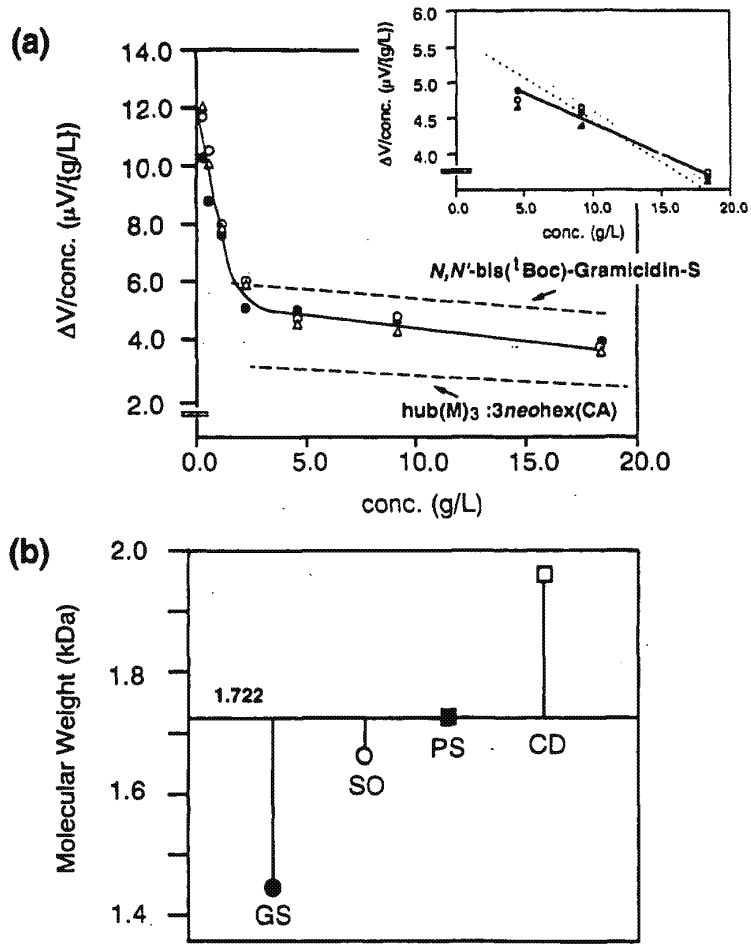


Figure 8. Estimation of the molecular weight in solution of rosette 5 by vapor pressure osmometry. (a) Concentration dependence of data from VPO for the equimolar mixture of 3 and 4 over the range [3] = [4] = 0.5–32 mM. Results from three separate experiments (○, △, and ●) are shown. The solid line joining these data is provided as a guide to the eye. The dashed lines illustrate concentration dependence of data from a self-assembled aggregate, hub(M)$_3$:*neo*hex(CA) and the cyclic decapeptide *N,N*-bis(tBoc)-gramicidin S. The inset shows a plot of the same data over the range 4–32 mM (three experiments). These data were used to calculate the molecular weight for 5 in chloroform. (b) Observed molecular weights for 5. The solid horizontal bar and associated number represent the calculated molecular weight of the cyclic CA$_3$·M$_3$ rosette. Measurements were correlated against four different molecular weight standards: *N,N'*-bis(tBoc)-gramicidin-S (FW 1342) (●), sucrose octaacetate (FW 679) (○), polystyrene (av FW 5050, polydispersity 1.05) (■), and perbenzoyl-β-cyclodextrin (FW 3321) (□). Measurements were made in chloroform at 37 °C.

390). The concentration dependent behavior when [3] = [4] < 4 mM observed for 5 in VPO correlates strongly with that witnessed by ^{1}H NMR spectroscopy.

Evidence for an Aggregate of Composition CA·M$_2$ when 2[3] = [4]. An anomaly in Figure 5 is the appearance of a signal for H^b at 2[3] = [4] and its disappearance at [3] = [4]. We have explored this feature further and believe that 2[3] = [4] probably arises from the trimer 7 with structure CA·M$_2$ (Scheme 2). The very low solubility (<0.5 mM) of 3 and the presence of hydrogen-bonded imide protons suggests that *all* 3 is in association with at least 1 equiv of 4. Three hypothetical structures result (6–8). The low solubility of 4 favors 7 over 6 and 8. Additional evidence from ^{1}H NMR that favors 7 over 6 and 8 is the absence of aromatic signals for free 4 when 2[3] = [4]. If 8 were present in the mixture, a well-resolved imide resonance H^b derived from the rosette should be equally well-resolved in [3] = [4].

VPO indicates that the average molecular weight of the species present when 2[3] = [4] is between MW 450 and 700. The MW of 7 is 964 (FW$_3$ = 184, FW$_4$ = 390). A disparity between calculated MW and that obtained through VPO measurements is not uncommon, and although the discrepancy between calculated and experimental MW is unusually large, these values for 2[3] = [4] *are* different than those calculated for [3] = [4] which varied from 1450 to 1950 (MW for 5 is 1722). The number-averaged molecular weights for 6 and 8 are calculated to be 482 and 721.

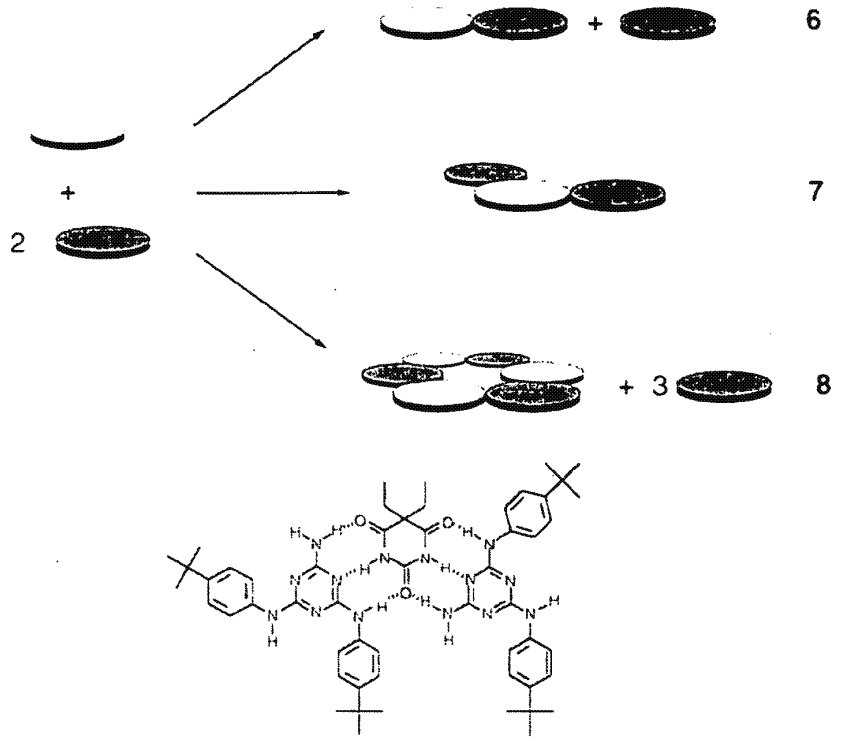
Removal of solvent by evaporation from a THF/MeOH solution with 2[3] = [4] and analysis by XPD of the resulting solid reveals a PD pattern that is the superposition of uncomplexed melamine and rosette. This observation reinforces our belief that the rosette motif is a favorable architecture in the solid state.

We believe that the appearance of a resolved H^b resonance for 7 and its absence in 5 is a result of the relative dynamic behaviors of these aggregates. One inference from these line shapes is that 7 is more slowly exchanging than 5. We cannot presently rationalize these relative stabilities.

The NH resonances (H^a and H^b) of the melamines of the rosette are better resolved than those of the trimer. This difference is in the opposite sense than what is observed for the barbiturate H^b. Two points must be considered. First, the width of the peaks due to H^a and H^b in the trimer are the average of hydrogen bonded and nonbonded protons. Second, imide protons are much

UM00014021
NOVARTIS EXHIBIT 1517
Novartis v. Regents, IPR2023-01347
Page 2767 of 4460

Scheme 2. Hypothetical Structures Resulting from 2[3] = [4][a]

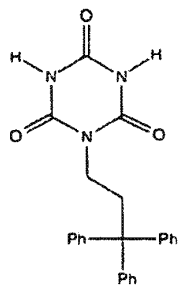


[a] One of a number of isomers of composition $CA \cdot M_2$ is indicated; the positions and relative stereochemistries of the phenyl groups in the system we have studied is not defined by the available information.

more sensitive to environment than are the NH protons of the melamines.[29]

Assessing the Relative Stabilities of the $CA_3 \cdot M_3$ Rosette and a Covalently Preorganized Aggregate Hub(M)$_3$:3barbital. The exchange experiment illustrated in Scheme 3 was performed to assess the *relative* stabilities of the $CA_3 \cdot M_3$ rosette **5** (six components, preorganized by steric interactions between substituents) and the supramolecular aggregate hub(M)$_3$:3barbital **10** (four components, preorganized by covalent bonding). The failure to observe the rosette **5** by GPC indicates that this aggregate is substantially less stable than **10**. A solution of **5** in $CDCl_3$ (10 μmol of each component, **3** and **4**, in 1 mL) was treated with uncomplexed hub(M)$_3$ (3.3 μmol) and incubated in an NMR tube at 25 °C for 7 days.[30] Exchange of the barbital from the $CA_3 \cdot M_3$ rosette to the aggregate **10** was complete, as judged by ^{1}H NMR. This observation confirms that the thermodynamic stability of **5** is lower than that of **10** but does not permit a quantitative estimate of the equilibrium constant. Incubation of a solution of **10** with 3 equiv of *N,N'*-bis(*p-tert*-butylphenyl)-melamine **4** had no effect on the ^{1}H NMR spectrum. No exchange was observed.[31]

The Generality of the $CA_3 \cdot M_3$ Rosette Motif in Solution. Scheme 4 summarizes the different combinations of components that afford a cyclic $CA_3 \cdot M_3$ rosette in solution, as judged by ^{1}H NMR.[32] These results demonstrate that the steric bulk of the *p-tert*-butylphenyl substituent on **4** is the key feature that favors formation of the $CA_3 \cdot M_3$ rosette between **3** and *N,N'*-bis(4-alkylphenyl)melamine. Formation of the cyclic $CA_3 \cdot M_3$ rosette appears to be a more general feature, however, of complexation between *N,N'*-bis(4-*tert*-butylphenyl)melamine **4** and sterically demanding isocyanurates. The steric bulk of the substituents in 3,3,3-triphenylpropylisocyanurate **12** also appears to favor formation of the $CA_3 \cdot M_3$ rosette strongly, even with less sterically hindered derivatives of melamine.[33]



12

Conclusions

The cyclic $CA_3 \cdot M_3$ rosette (**5**) appears to be the stable 1:1 complex between barbital (**3**) and *N,N'*-bis(*p-tert*-butylphenyl)-melamine (**4**) in the solid state. Indeed, the cyclic $CA_3 \cdot M_3$ motif is the only morphology observed in the solid state by XPD. Data

(29) The ^{1}H NMR spectrum at low temperatures of aggregates of structure **1** show that the chemical shifts for imide resonances occur between 13 and 16 ppm. The N–H resonances, however, often appear with very similar chemical shifts. A similar observation has been made with aggregates similar to **5** based on asymmetric melamines.

(30) Exchange is certainly complete in a much shorter interval.

(31) These indications of the relative stabilities of **5** and **10** are, therefore, in agreement with the predictions suggested by the behavior of the aggregates under analysis by GPC.

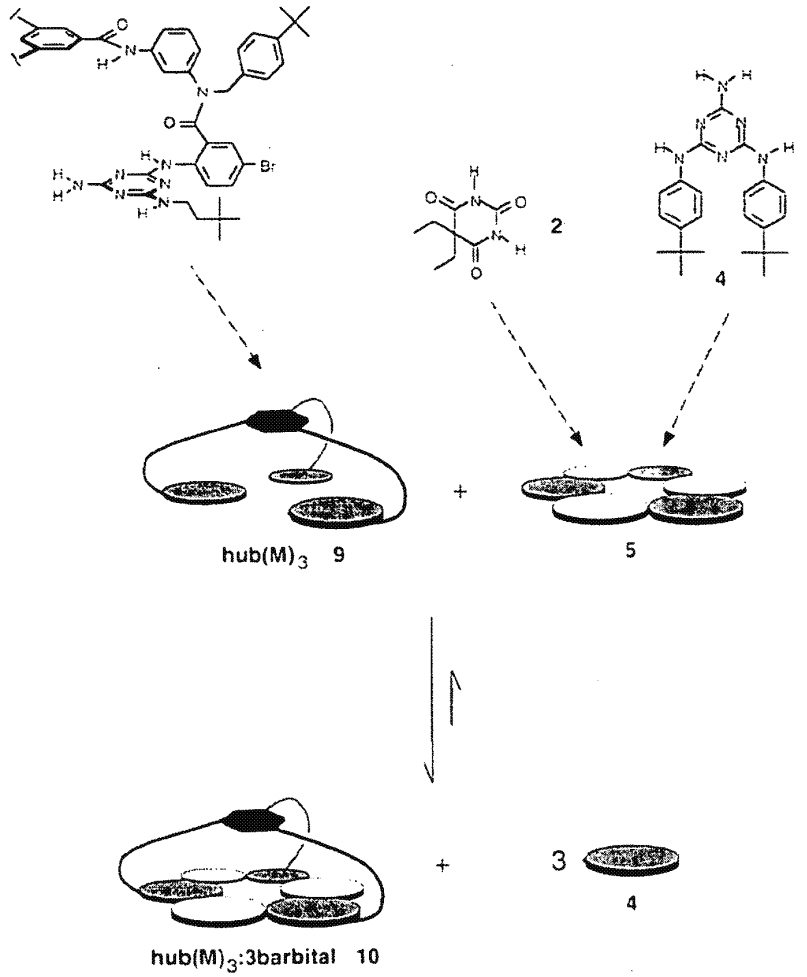
(32) The syntheses of **11** and **12** are reported in ref 9. Those for **13** and **14** are reported in ref 16, and that for **15** is reported in ref 18.

(33) The synthesis and characterization of **12** is reported in ref 9.

(34) Mathias, J. P.; Simanek, E. E.; Whitesides, G. M. *J. Am. Chem. Soc.*, following paper in this issue.

UM00014022
NOVARTIS EXHIBIT 1517
Novartis v. Regents, IPR2023-01347
Page 2768 of 4460

Scheme 3. Exchange Experiment To Assess the Relative Stabilities of the Self-Assembled Aggregates 5 and 10



from solution, when taken together, indicate that the $CA_3{\cdot}M_3$ rosette is the major species present in equimolar mixtures of 3 and 4 in chloroform solution at concentrations greater than ~4 mM.

Studies by NMR and VPO establish that the self-assembly of the $CA_3{\cdot}M_3$ rosette between 3 and 4 is concentration dependent. Below 4 mM, the components 3 and 4 are present as an equilibrating mixture of linear structures (probably containing two or three of both 3 and 4). Above this concentration, the hydrogen-bonded aggregate is insensitive to concentration.

The $CA_3{\cdot}M_3$ rosette is less stable than aggregates of type 1 and 2, as judged by GPC. This finding has been confirmed by the direct competition experiments performed between the $CA_3{\cdot}M_3$ rosette 5 and the self-assembled aggregate 10. These experiments demonstrate that 10 has greater thermodynamic stability than 5.

The stability of 5 is too low to be interesting, by itself, as a building block for supramolecular chemistry. As the common structural motif for all of the more complex structures we have generated, it is interesting as the simpliest aggregate of its class. We emphasize the $CA_3{\cdot}M_3$ rosette 5 displays a surprisingly *high* degree of stability for a supramolecular aggregate that is composed of six particles and stabilized by only 18 hydrogen bonds. Complexes of cyanuric acid and melamine with smaller substituents do *not* form well-defined rosettes, in solution or in the solid state. These observations indicate that intermolecular steric interactions around the periphery of the rosette can be used to assist self-assembly of supramolecular aggregates. The data presented in Scheme 4 reinforce the notion that steric crowding around the periphery of the self-assembled aggregates may be used to select the $CA_3{\cdot}M_3$ rosette in preference to other hydrogen bonded motifs in this series of self-assembled aggregates. Peripheral steric crowding could, therefore, represent an alternative or supplemental strategy for the preparation of self-assembled aggregates based on the $CA_3{\cdot}M_3$ rosette, without the need for covalent preorganization. The validity of this hypothesis, and the development of strategies to increase the stability of such supramolecular aggregates, are discussed in the following paper in this issue.[34]

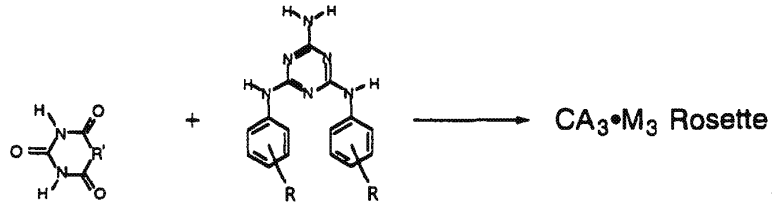
Experimental Section

X-ray Powder Diffraction. Crystals of the 1:1 complexes were obtained as the homogeneous solutions cooled to room temperature, filtered, dried, and ground with an agate mortar and pestle. The resulting powder was placed in the well of a fiberboard sample holder, and the surface of the powder was pressed flat with a spatula. Scans were performed from 3.6° to 33.6° in 2θ, counting 30 s at each step of 0.1°, on a Philips powder diffractometer.

NMR Spectroscopy. NMR experiments were performed with a Bruker AM 500 instrument. The NOE spectra of these supramolecular aggregates were recorded at 25 °C, with an evolution period of 3.0 s and

UM00014023
NOVARTIS EXHIBIT 1517
Novartis v. Regents, IPR2023-01347
Page 2769 of 4460

Scheme 4. Effect of Different Substituents on the Self-Assembly of the CA_3M_3 Rosette in Chloroform, as Judged by ^1H NMR Spectroscopy[a]



R'		R		Rosette ?
CEt_2	(3)	*p*-Me	(13)	No
CEt_2	(3)	*p*-^{i}Pr	(14)	No
$NCH_2CH_2C(Me)_3$	(11)	*p*-^{t}Bu	(4)	No
CEt_2	(3)	*p*-^{t}Bu	(4)	Yes
$NCH_2CH_2C(Ph)_3$	(12)	*p*-^{t}Bu	(4)	Yes
$NCH_2CH_2C(Ph)_3$	(12)	*p*-Me	(15)	Yes
$NCH_2CH_2C(Ph)_3$	(12)	*m*-Me	(16)	Yes

[a] "Yes" indicates formation of a rosette; "No" indicates that formation of a rosette was not observed.

a relaxation delay of 6.0 s. The complex (5.0 μmol) was dissolved in 0.7 mL of $CDCl_3$, and the sample was degassed with five freeze–pump–thaw cycles.

Gel Permeation Chromatography. Gel permeation chromatography was performed using a Waters 600E HPLC with a Waters 484 UV detector and Waters analytical gel permeation column (Ultrastyragel, 1000Å pore size). Elutions were performed at room temperature using HPLC grade CH_2Cl_2 or $CHCl_3$ as the eluent at a flow rate of 1.0 mL/min. The injection volume was 20 μL.

Molecular Weight Determinations by Vapor Pressure Osmometry. Molecular weight determinations were made with a Wescan Model 233 vapor pressure osmometer operated at 35 °C. The molecular weight of the complexes were measured in HPLC grade glass distilled chloroform at concentrations of approximately 0.5, 1, 2, 4, 8, and 16 mM. At each concentration, 3–4 measurements were taken. Calibration curves were generated using four molecular weight standards: sucrose octaacetate (MW 679), perbenzoyl β-cyclodextrin (MW 3321), polystyrene (MW 5050, polydispersity = 1.05), and a derivative of gramacidin S in which the two ornithine amino groups had been converted to their *tert*-butylcarbamates (MW 1342).

Specific Procedures. ***N,N'*-Bis(4-*tert*-butylphenyl)melamine (4).** Two equivalents of 4-*tert*-butylaniline (0.94 mL, 6.72 mmol) were added to a solution of cyanuric chloride (618 mg, 3.36 mmol) and diisopropylethylamine (DIPEA) (2.45 mL) in THF (50 mL) at 25 °C. After 2 h TLC showed complete conversion to the bis-addition product. The reaction mixture was cooled and concentrated *in vacuo*, and the residue was partitioned between EtOAc (125 mL) and brine (75 mL). The organic extract was washed with brine (70 mL), dried over $MgSO_4$, filtered, and concentrated *in vacuo* to give of the crude bis-adduct as a white solid. This bis-adduct was suspended in 1,4-dioxane (10 mL), and NH_4OH (10 mL) was added. The mixture was sealed in a Parr vessel, and the reaction stirred at 95 °C for 7 h. After cooling and depressurization, the reaction mixture was concentrated *in vacuo*, and the residue was partitioned between EtOAc (150 mL) and brine (100 mL). The organic extract was washed with brine (50 mL), dried over $MgSO_4$, filtered, and concentrated *in vacuo*. The mixture was purified by column chromatography (eluted with EtOAc) to give 1.12 g (2.89 mmol, 86%) of the product as a white solid: ^1H NMR (500 MHz, DMSO-d_6) δ 8.89 (s, 2 H), 7.60 (br s, 4 H), 7.23 (d, J_{ab} = 8 Hz, 4 H), 6.45 (br s, 2 H), 1.25 (s, 18 H); ^{13}C NMR (125 MHz, DMSO-d_6) δ 166.84, 164.47, 143.85, 137.46, 124.63, 120.15, 33.72, 31.17; HRMS–FAB calcd for $C_{23}H_{31}N_6$ 391.2609, found 391.2610 $(M + H)^+$.

Acknowledgment. This work was supported by The National Science Foundation (Grants CHE-91-22331 to G.M.W., DMR-89-20490 to the Harvard University Materials Research Laboratory, and CHE-80-00670 for the purchase of the Siemens X-ray diffractometer). NMR instrumentation was supported by the National Sience Foundation Grant CHE-88-14019 and the National Institutes of Health Grant 1 S10 RR4870. Mass spectrometry was performed by Dr. A. Tyler. The Harvard University Mass Spectrometry Facility was supported by The National Science Foundation Grant CHE-90-20043 and The National Institutes of Health Grant 1 S10 RR06716-01. We thank Professor Robert Cohen (MIT, Chemical Engineering) for the loan of his vapor pressure osmometer. J.P.M. was an SERC/NATO Postdoctoral Fellow, 1991–1993. C.T.S. was an Eli Lilly Predoctoral Fellow, 1991.

UM00014024
NOVARTIS EXHIBIT 1517
Novartis v. Regents, IPR2023-01347
Page 2770 of 4460

MOLECULAR PHARMACOLOGY, 23:273-277

SHORT COMMUNICATIONS

Hydrogen Bonding Interaction of Diphenylhydantoin and 9-Ethyladenine

Crystal Structure of a 2:1 Complex

DONALD MASTROPAOLO,[1] ARTHUR CAMERMAN,[1] AND NORMAN CAMERMAN[2]

Departments of Medicine (Neurology) and Pharmacology, University of Washington, Seattle, Washington 98195, and Department of Biochemistry, University of Toronto, Toronto, Ontario, Canada M5S1A8

Received July 12, 1982; Accepted October 12, 1982

SUMMARY

A hydrogen-bonded complex of diphenylhydantoin (DPH) and 9-ethyladenine (EtAd) crystallizes from 2,4-pentanedione with the asymmetrical unit consisting of two DPH molecules, one EtAd molecule, and one solvent molecule. The crystal structure was solved by direct methods and refined to a residual of $R = 0.054$. Structure determination reveals that one DPH hydrogen-bonds to EtAd in a Watson-Crick scheme while the second DPH N(3)—H bonds to EtAd N(3) to form a 2:1 DPH-EtAd complex. Comparisons are made with barbiturate-adenine complexes and with an earlier postulation of a 1:1 DPH-EtAd complex derived from NMR and IR data. The 2,4-pentanedione molecule adopts the keto-enol configuration with an asymmetrical intramolecular hydrogen bond.

DPH[3] and phenobarbitol are the most widely used drugs in the treatment of grand mal, psychomotor, and focal epilepsies. Although certain stereochemical similarities have been shown to exist between these and other anticonvulsants (1), molecular mechanisms of action of antiepileptic drugs are not well understood.

The similarity of barbiturates to uracil has prompted several investigations into their hydrogen-bonding capabilities with adenine molecules. Since hydrogen bonds involving nucleic acids are important components of living systems, it has been suggested that some of the biological effects of barbiturates may derive from an ability to specifically bind and inactivate adenine-containing nucleic acids or coenzymes. Indeed, selective hydrogen bond formation between barbiturates and adenine derivatives has been firmly established *in vitro* by spectroscopic methods (2) as well as by the X-ray structure analysis of several crystalline, intermolecular complexes (3–6). However, it is still not clear whether such interactions are connected with barbiturates' pharmacological actions. The reported (7) selective accumulation of 5,5-DPH in nucleic acid-rich subcellular fractions of rat brain suggested that hydantoins may also interact with adenine derivatives, and a recent IR and NMR study (8) indicated that hydrogen bond formation between various substituted hydantoins and EtAd does occur. This study concluded that EtAd forms 1:1 complexes with 1,5,5-trimethylhydantoin and 3,5,5-trimethylhydantoin, but, because of solubility problems, could not determine with certainty the kind of association occurring between EtAd and DPH. From analogy with the trimethylhydantoins, the authors assumed that a 1:1 DPH-EtAd complex would also exist and then described three alternative hydrogen-bonding schemes that could hold such a complex together. We have crystallized DPH and EtAd with the aim of elucidating the structure of the complex and determining the exact nature of the intermolecular interactions. Comparisons of the complexes formed by both DPH and the various barbiturates with EtAd may prove helpful in understanding some modes of action of these anticonvulsant drugs. We report here the 3-dimensional structure determination of a 2:1 DPH-EtAd complex.

Approximately equimolar amounts of DPH and EtAd were dissolved in warm 2,4-pentanedione, and the solution was maintained at 45°. Solvent evaporation yielded large colorless crystals. A crystal measuring 0.58 × 0.39 × 0.17 mm was mounted along its long dimension on a glass fiber. Weissenberg and precession photographs revealed the space group to be $P\bar{1}$, with $a = 12.256 \pm 0.001$ Å, $b = 13.691 \pm 0.002$ Å, $c = 14.835 \pm 0.002$ Å, $\alpha = 112.04 \pm 0.01°$, $\beta = 98.72 \pm 0.01°$, $\gamma = 110.99 \pm 0.01°$, and $V = 2033.19$ Å^3. The measured density obtained by flotation in a KI-water solution was 1.24 ± 0.01 g/ml.

Three-dimensional X-ray intensity data were collected on a Picker FACS-1 diffractometer using nickel-filtered

This work was supported in part by National Institutes of Health Grants NS09839 and CA15879.

[1] University of Washington.

[2] University of Toronto.

[3] The abbreviations used are: DPH, diphenylhydantoin; EtAd, 9-ethyladenine.

0026-895X/83/020273-05$02.00/0

Copyright © 1983 by The American Society for Pharmacology and Experimental Therapeutics.

UM00014025
NOVARTIS EXHIBIT 1517
Novartis v. Regents, IPR2023-01347
Page 2771 of 4460

copper radiation. A θ–2θ scan was used to collect a total of 5986 unique reflections to a maximum 2θ of 120°. A total of 5263 reflections had intensity (I) greater than $2\sigma(I)$, where $\sigma(I)$ is the standard deviation in the intensity obtained from counting statistics; these reflections were classified as "observed" and were used in the structure refinement. An empirical absorption correction based on the variation of the intensity of a reflection with rotation about its scattering vector at $\chi = 90°$ was applied. The maximal correction was 14%. The structure was determined with little difficulty by direct methods (9).

Coordinates and anisotropic temperature factors of all non-hydrogen atoms were refined by least-squares. The hydrogen atom coordinates were also refined, but their temperature factors were assumed to be isotropic and equal to the average of the three diagonal elements of the anisotropic tensor of the atom to which they are bonded. Each of the final cycles of refinement was done in two blocks; blocking of the variables was changed in each cycle to compensate for possible correlation effects. The final R factor was 0.054. Table 1 lists the atom fractional coordinates; the anisotropic thermal parameters, hydrogen positional parameters, and a list of observed and calculated structure factors are available from the authors on request. Line drawings of DPH and EtAd with the numbering scheme used in the discussion are shown in Fig. 1.

Elucidation of the crystal structure of the DPH-EtAd complex crystallized from 2,4-pentanedione reveals that the asymmetrical unit contains two molecules of DPH, one molecule of EtAd, and one molecule of 2,4-pentanedione. Both DPH molecules hydrogen-bond to EtAd, thus forming a 2:1 intermolecular complex. The hydrogen-bonding scheme is illustrated in Fig. 2. DPH(I) donates its N(1) hydrogen to N(1) of EtAd while its carbonyl oxygen O(6) accepts a hydrogen from the EtAd amino group, forming a Watson-Crick type pair of hydrogen bonds. DPH(II) forms just one hydrogen bond with EtAd by donating its N(3) hydrogen to N(3) of EtAd. All three molecules in the complex also form self-associated cyclic dimers through pairs of hydrogen bonds with like molecules related through crystallographic centers of symmetry. Carbonyl O(7) is not involved in any hydrogen bonds in either of the DPH molecules. Previous structural studies of crystalline complexes of adenine derivatives with barbiturates (3–6) have shown that the carbonyl groups adjacent to the tetrahedral carbon atom tend to be weak hydrogen bond acceptors. The 2-dimensional hydrogen-bonded layer in the present complex lies approximately in the (101) plane with the 2,4-pentanedione molecules positioned above and below this plane. The pentanedione molecules are in the *enol* configuration, with an asymmetrical intramolecular hydrogen bond between O(2) and O(4). They do not participate in any hydrogen bonding with EtAd and DPH atoms. Bond distances and angles are shown in Fig. 3, which clearly illustrates the pentanedione enol structure. Conformation of both DPH molecules in this complex are very similar to the conformation of uncomplexed DPH(10) in terms of both molecular bond lengths and angles and those stereochemical parameters considered to be related to the drug's anticonvulsant properties (see Table 2).

TABLE 1

Fractional atomic coordinates (× 10^4) of all non-hydrogen atoms[a]

	X	Y	Z
DPH(I)			
N(1)	6,621(3)	6,059(2)	3,695(3)
C(2)	5,946(3)	5,730(3)	4,248(2)
N(3)	6,101(3)	4,800(3)	4,319(2)
C(4)	6,853(3)	4,497(3)	3,805(3)
C(5)	7,271(3)	5,353(3)	3,333(2)
O(6)	5,292(2)	6,148(2)	4,624(2)
O(7)	7,131(2)	3,717(2)	3,726(2)
C(8)	6,793(3)	4,623(3)	2,151(2)
C(9)	5,738(3)	4,505(4)	1,544(3)
C(10)	5,346(4)	3,844(5)	483(4)
C(11)	6,000(4)	3,300(4)	17(3)
C(12)	7,051(5)	3,422(4)	617(3)
C(13)	7,454(4)	4,071(4)	1,678(3)
C(14)	8,662(3)	6,125(3)	3,746(2)
C(15)	9,151(4)	6,865(4)	3,331(3)
C(16)	10,403(4)	7,606(4)	3,681(4)
C(17)	11,190(4)	7,603(4)	4,447(4)
C(18)	10,726(4)	6,866(5)	4,850(4)
C(19)	9,457(4)	6,126(4)	4,508(3)
DPH(II)			
N(1)	10,408(3)	1,303(2)	9,839(2)
C(2)	11,077(3)	807(3)	9,396(3)
N(3)	11,810(3)	1,565(3)	9,080(2)
C(4)	11,652(3)	2,556(3)	9,323(2)
C(5)	10,670(3)	2,449(3)	9,873(2)
O(6)	11,075(2)	−126(2)	9,272(2)
O(7)	12,162(2)	3,349(2)	9,128(2)
C(8)	9,561(3)	2,448(3)	9,244(2)
C(9)	9,723(4)	3,470(3)	9,163(3)
C(10)	8,748(4)	3,483(4)	8,565(3)
C(11)	7,615(4)	2,499(4)	8,050(3)
C(12)	7,455(4)	1,503(4)	8,143(3)
C(13)	8,424(4)	1,470(3)	8,731(3)
C(14)	11,198(3)	3,419(3)	10,995(2)
C(15)	10,440(4)	3,353(4)	11,599(3)
C(16)	10,904(6)	4,192(5)	12,638(3)
C(17)	12,105(5)	5,077(5)	13,065(3)
C(18)	12,850(4)	5,151(4)	12,472(3)
C(19)	12,391(3)	4,323(3)	11,435(3)
EtAd			
N(1)	6,122(3)	7,722(2)	3,181(2)
C(2)	6,615(3)	7,926(3)	2,489(3)
N(3)	6,810(3)	8,808(2)	2,257(3)
C(4)	6,422(3)	9,557(3)	2,832(2)
C(5)	5,880(3)	9,453(3)	3,561(2)
C(6)	5,734(3)	8,490(3)	3,746(2)
N(6)	5,223(3)	8,265(3)	4,418(2)
N(7)	5,587(2)	10,378(2)	3,985(2)
C(8)	5,960(3)	11,003(3)	3,508(3)
N(9)	6,486(3)	10,566(2)	2,809(2)
C(9)	6,996(4)	11,056(4)	2,153(3)
C(10)	6,097(8)	10,524(7)	1,140(5)
2,4-Pentanedione			
C(1)	3,332(14)	2,319(9)	2,155(9)
C(2)	2,936(6)	1,783(4)	2,821(4)
O(2)	3,647(3)	1,496(3)	3,224(3)
C(3)	1,788(7)	1,579(6)	2,986(7)
C(4)	1,399(7)	1,037(7)	3,544(6)
O(4)	2,075(5)	678(5)	4,008(4)
C(5)	139(9)	752(11)	3,719(7)

[a] Standard deviations are shown in parentheses.

NOVARTIS EXHIBIT 1517
Novartis v. Regents, IPR2023-01347
Page 2772 of 4460

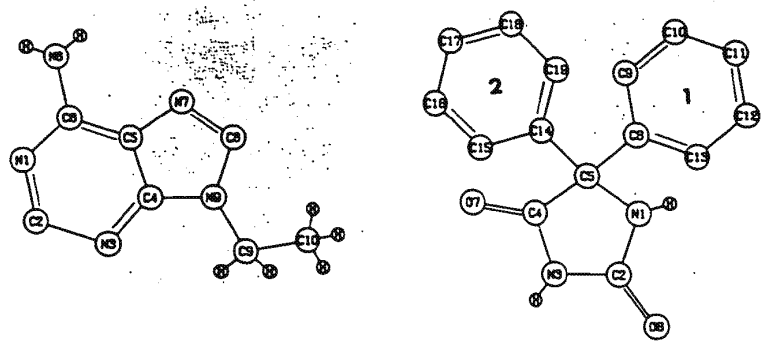


FIG. 1. *Line drawings of DPH and EtAd showing the chemical composition and numbering scheme*

Over-all, the hydrogen bonding between DPH and EtAd is very similar to that found in barbiturate-adenine complexes. Pairs of bonds formed between adenine N(1) and the amino group with an N—H and C=O of the drug are common to all. There are some differences between DPH and the barbiturate complexes, however. All of the reported barbiturate crystal structures have stoichiometries of either 1:1 or 1:2 barbiturate to adenine molecules, where the barbiturate molecule, in most cases, forms four hydrogen bonds with the adenine derivatives. This scheme is not a favorable one for the hydantoins as they possess one less carbonyl oxygen atom. As mentioned previously, the oxygen atom of one carbonyl group in both barbiturates and hydantoins is a weak hydrogen bond receptor. Thus hydantoins are left with only one site for base-pairing types of intermolecular interactions and do not readily form complexes with two adenine molecules, as is possible for the barbiturates. In none of their complexes do the barbiturates form self-associated cyclic dimers, indicating that the complex formation is energetically favored over self-association. Indeed, IR studies (2) show the association constants for various barbiturate-adenine complexes to be approximately 150 times greater than the self-association constants of the barbiturates. The association constants of the complexes also increase as the acidity of the barbiturates increases. The reported (8) association constants of various hydantoin-adenine complexes are a factor of 10 smaller than the barbiturate-adenine association constants—which is not surprising, since the hydantoins are less acidic. Evidently the hydantoin self-association is able to compete successfully with the hydantoin-adenine association, resulting in the present "mixed complex" structure. Another major difference between the barbiturate-adenine complexes and the DPH-EtAd structure is the hydrogen bond to the adenine N(3) atom. In only one of the barbiturate complexes (6) is there an interaction between a barbiturate N—H and the adenine N(3), and in that case the hydrogen bonds of that type are not strong: the reported N---N distances are 2.97 and 3.03 Å, significantly longer than the N---N distance of 2.816 Å for the comparable bond in the DPH-EtAd complex.

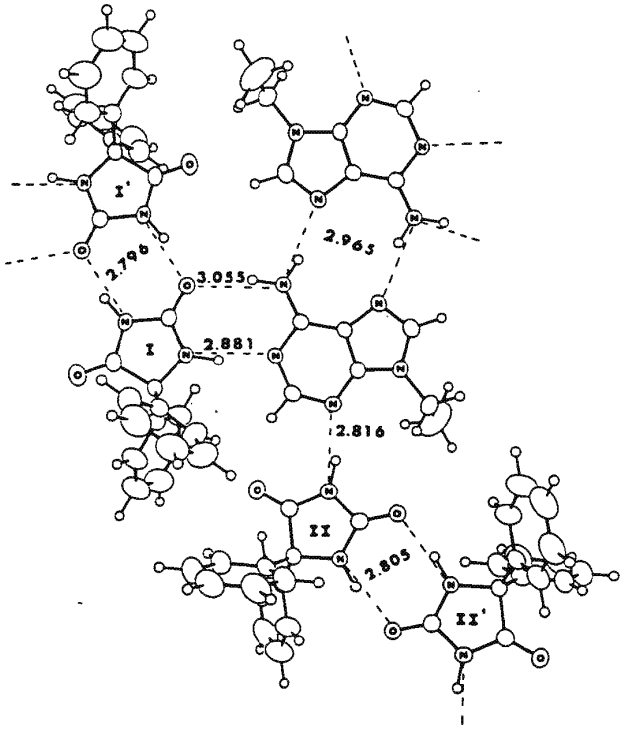


FIG. 2. *Perspective drawing showing the intermolecular hydrogen bonding*

The NMR investigation of the interaction of DPH with EtAd (8) was severely hindered by the relative insolubility of DPH in a large number of solvents. Adequate solubility was attained with dimethyl sulfoxide, but interference between the dimethyl sulfoxide proton and the DPH N—H signals and between the DPH phenyl and adenine amino hydrogen atoms made it impossible to observe concentration effects on the NMR resonance shifts. By mixing 1,5,5- and 3,5,5-trimethylhydantoins with EtAd in deuterochloroform and measuring the chemical shifts of the adenine amino and hydantoin nitrogen protons as a function of concentration, the investigators concluded that the trimethylhydantoins form 1:1 complexes with EtAd. They then suggested that, if the same relationship holds for DPH and EtAd, three different arrangements of a 1:1 DPH-EtAd complex can be postulated, depending on which DPH carbonyl oxygen atoms and nitrogen protons are utilized in the hydrogen-bonding scheme.

However, the crystal structure results show that DPH

UM00014027
NOVARTIS EXHIBIT 1517
Novartis v. Regents, IPR2023-01347
Page 2773 of 4460

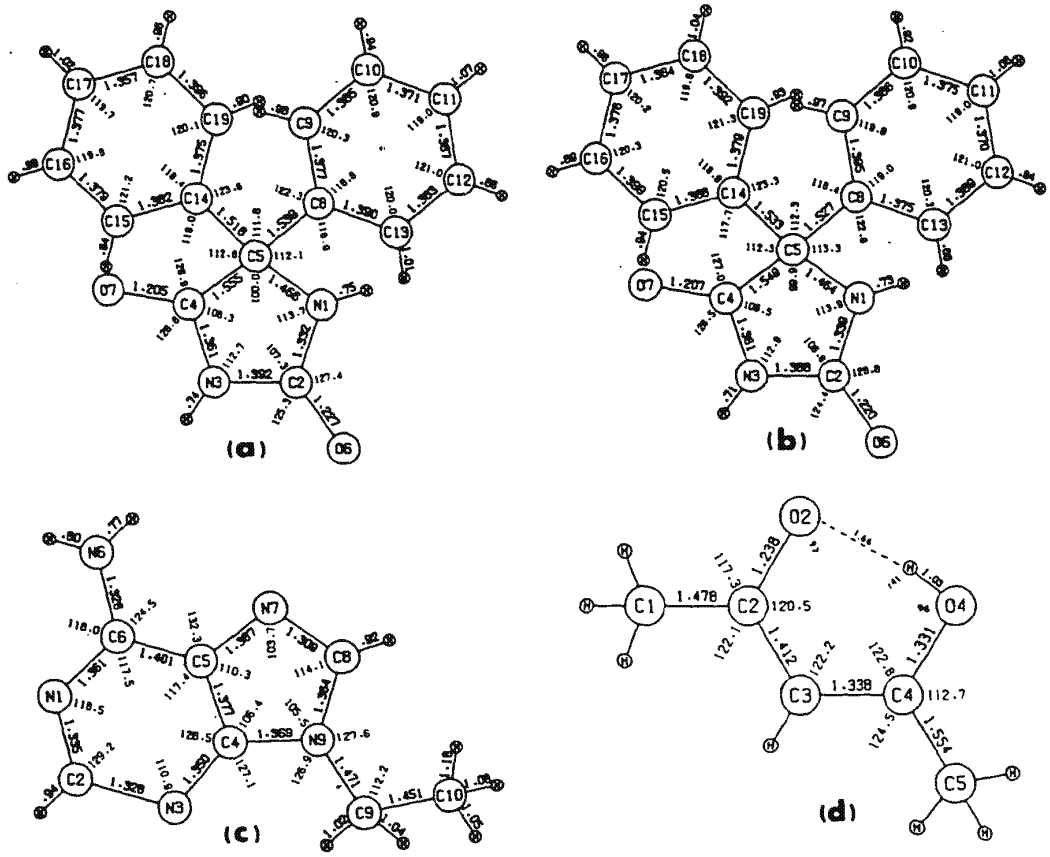


FIG. 3. *Bond distances and angles for DPH(I) (a), DPH(II) (b), EtAd (c), and 2,4-pentanedione (d)*
Additional angles not given are as follows: N(1)—C(5)—C(14) = 111.1° for DPH(I) and 110.0° for DPH(II); C(4)—C(5)—C(8) = 108.7° for DPH(I) and 108.5° for DPH(II).

TABLE 2

Comparison of selected molecular distances and angles in DPH uncomplexed and when hydrogen-bonded to EtAd

	DPH[a]	DPH(I)[b]	DPH(II)[b]
Molecular distance[c]			
O(6)-Ring 1	5.68	5.627	5.681
O(7)-Ring 1	3.97	4.054	3.975
O(6)-Ring 2	5.51	5.643	5.559
O(7)-Ring 2	4.23	4.170	4.230
O(6)-O(7)	4.56	4.571	4.557
Ring 1-Ring 2	4.84	4.796	4.878
Dihedral angle			
Hydantoin-Ring 1	114	110.6	114.9
Hydantoin-Ring 2	113	116.3	115.1
Ring 1-Ring 2	90	76.9	84.1

[a] Camerman and Camerman (10).
[b] Present study.
[c] Involving oxygen atoms and phenyl ring centroids.

can form a 2:1 hydrogen-bonded complex with EtAd in a mode that is not available to either of the trimethylhydantoins. As described above and illustrated in Fig. 2, DPH(I) interacts with EtAd using N(1) and O(6) atoms and with another DPH(I) molecule using N(3) and O(6). DPH(II) bonds to EtAd with N(3) as proton donor to adenine N(3) and with another DPH(II) by means of N(1) and O(6) hydrogen-bonding pairs. Thus all DPH N—H pairs take part in hydrogen bond formation, and EtAd accepts one H bond from one DPH molecule's N(1) and another from the second DPH molecule's N(3). Obviously, since the trimethylhydantoins have only one N—H available for hydrogen bonding, they cannot form the 2:1 complex as found for DPH. Thus extension of the NMR concentration-dependence findings from the trimethylhydantoin studies to the DPH-EtAd system is shown to be inappropriate. All of the limited NMR and IR data obtained for the DPH-EtAd complex (8) are consistent with the 2:1 complex; together with the fact that the DPH N(3)-EtAd N(3) hydrogen bond is strong, these observations suggest that the 2:1 DPH-EtAd complex is the most likely species in solution as well as in the solid state.

It is of interest to note that, even though 2,4 pentanedione (which has both hydrogen bond donor and acceptor potential) is present in the crystal lattice, there is no interaction between the solvent and DPH or EtAd. This adds to the accumulated evidence (8) that hydrogen bond formation between adenine and DPH is uniquely strong and specific. Whether this capacity to form hydrogen-bonded complexes with adenine is responsible for any of

UM00014028
NOVARTIS EXHIBIT 1517
Novartis v. Regents, IPR2023-01347
Page 2774 of 4460

DPH's pharmacological actions is not known and is not likely to be established until the drug's sites of action are more clearly identified.

REFERENCES

1. Camerman, A. and N. Camerman. Stereochemical similarities in chemically different antiepileptic drugs, in *Molecular and Quantum Pharmacology* (E. Bergman and B. Pullman, eds.). D. Reidel, Dordrecht, Holland, 213–228 (1975).
2. Kyogoku, Y., R. C. Lord, and A. Rich. Specific hydrogen bonding of barbiturates to adenine derivatives. *Nature (Lond.)* 218:69–72 (1968).
3. Kim, S. H. and A. Rich. The structure of a crystalline complex containing one phenobarbitol molecule and two adenine derivatives. *Proc. Natl. Acad. Sci. U. S. A.* 60:402–408 (1968).
4. Voet, D., and A. Rich. Barbiturates and adenine derivatives: molecular structure of a hydrogen-bonded complex. *J. Am. Chem. Soc.* 94:5888–5891 (1972).
5. Voet, D. The crystal and molecular structure of the intermolecular complex 9-ethyladenine-5,5-diethylbarbituric acid. *J. Am. Chem. Soc.* 94:8213–8222 (1972).
6. Epstein, R. H., A. V. Zeiger, C. Crocker, and D. Voet. The X-ray crystal structure of the molecular complex 8-bromo-9-ethyladenine-5-allyl-5-isobutylbarbituric acid. *Acta Crystallogr. Sect. B Struct. Crystallogr. Cryst. Chem.* 32:2180–2188 (1976).
7. Kemp, J. W., and D. M. Woodbury. Subcellular distribution of 4-^{14} C-diphenylhydantoin in rat brain. *J. Pharmacol. Exp. Ther.* 177:342–349 (1971).
8. Jones, G. L., and J. W. Kemp. Characteristics of the hydrogen bonding interactions of substituted hydantoins with 9-ethyladenine. *Mol. Pharmacol.* 10:48–56 (1974).
9. Germain, G., P. Main, and M. M. Woolfson. The application of phase relationships to complex structures. III. The optimum use of phase relationships. *Acta Crystallogr. Sect. A* 27:368–376 (1971).
10. Camerman, A., and N. Camerman. The stereochemical basis of anticonvulsant drug action. I. The crystal and molecular structure of diphenylhydantoin. *Acta Crystallogr. Sect. B Struct. Crystallogr. Cryst. Chem.* 27:2205–2211 (1971).

Send reprint requests to: Dr. Arthur Camerman, Division of Neurology, University of Washington, Seattle, Wash. 98195.

UM00014029
NOVARTIS EXHIBIT 1517
Novartis v. Regents, IPR2023-01347
Page 2775 of 4460

This Page is Inserted by IFW Indexing and Scanning Operations and is not part of the Official Record

BEST AVAILABLE IMAGES

Defective images within this document are accurate representations of the original documents submitted by the applicant.

Defects in the images include but are not limited to the items checked:

- ☐ BLACK BORDERS
- ☐ IMAGE CUT OFF AT TOP, BOTTOM OR SIDES
- ☐ FADED TEXT OR DRAWING
- ☐ BLURRED OR ILLEGIBLE TEXT OR DRAWING
- ☐ SKEWED/SLANTED IMAGES
- ☐ COLOR OR BLACK AND WHITE PHOTOGRAPHS
- ☐ GRAY SCALE DOCUMENTS
- ☐ LINES OR MARKS ON ORIGINAL DOCUMENT
- ☐ REFERENCE(S) OR EXHIBIT(S) SUBMITTED ARE POOR QUALITY
- ☐ OTHER: _____

IMAGES ARE BEST AVAILABLE COPY.
As rescanning these documents will not correct the image problems checked, please do not report these problems to the IFW Image Problem Mailbox.

μm). All solvents used were purified and/or dried by standard methods.[22]

Ethyl 3,3-Dibromopyruvate (3). A solution of ethyl bromopyruvate (5.00 g, 25.6 mmol), *N*-bromosuccinimide (4.56 g, 25.6 mmol), and azobis(isobutyronitrile) (50 mg, catalytic) in CCl_4 (100 mL) was heated at reflux for 4 h with intermittent UV irradiation from a Minerallight UVSL-25 UV lamp. The 254 μm light was held directly on the side of the flask for 2 min every 10 min during the first 30 min of the reaction. The mixture was cooled and filtered to remove succinimide, and the filtrate was evaporated to give a yellow oil. Flash chromatography (35% EtOAc/hexanes) of the crude product gave 5.60 g (80% yield) of **3** as a colorless oil: ^{1}H NMR (270 MHz, D_2O) δ 6.03 (s, 1 H), 4.24 (q, J = 7.15 Hz, 2 H), 1.22 (t, J = 7.15 Hz, 3 H); exact mass 273.87 (273.87 calcd for $C_5H_6O_3{}^{79}Br^{81}Br$).

Ethyl (*Z*)-3-Bromo-2-[(dimethoxyphosphinyl)oxy]propenoate (4a) and Ethyl (*E*)-3-Bromo-2-[(dimethoxyphosphinyl)oxy]propenoate (4b). A refluxing solution of **3** (0.274 g, 1.00 mmol) in dioxane (5 mL) was treated all at once with trimethyl phosphite (0.144 g, 1.00 mmol), and the heating was continued for 30 min. The solvent was removed on a rotary vacuum evaporator (water aspirator/35 °C). The residual colorless oil was purified by flash chromatography (70% EtOAc/hexane) followed by MPLC (20% EtOAc/hexanes) to give 0.171 g (52% yield) of **4a** and 0.061 g of **4b** (20%) as colorless oils.[23] **4a**: ^{1}H NMR (270 MHz, $CDCl_3$) δ 7.24 (d, J = 1.7 Hz, 1 H), 4.30 (q, J = 7.3 Hz, 2 H), 3.95 (d, J = 11.5 Hz, 6 H), 1.33 (t, J = 7.3 Hz, 3 H); exact mass 302.9626 (302.9633 calcd for $C_7H_{12}{}^{79}BrPO_6$). **4b**: ^{1}H NMR (270 MHz, $CDCl_3$) δ 6.96 (d, J = 2.9 Hz, 1 H), 4.34 (q, J = 7.3 Hz, 2 H), 3.87 (d, J = 11.4 Hz, 6 H), 1.26 (t, J = 7.3 Hz, 3 H).

Ethyl (*Z*)-3-Deuterio-2-[(dimethoxyphosphinyl)oxy]propenoate (5a). Bromopyruvate **4a** (0.080 g, 0.264 mmol) in 20% D_2O/THF (the THF is predried and distilled as previously described)[22] (5 mL) was treated with freshly prepared Zn/Ag couple[18] (200 mg) doped with D_2O. The progress of the reaction was monitored via TLC (silica gel/40% EtOAc/hexanes). After all the starting material has been consumed (24 h), the couple is removed by filtration. The solid was washed with diethyl ether (3 × 5 mL). The ether layer was separated from the filtrate, dried (Na_2SO_4), and evaporated under reduced pressure to give colorless oil **5a** in quantitative yield (0.059 g): ^{1}H NMR (270 MHz, $CDCl_3$) δ 5.96 (d, J = 2.4 Hz, 1 H), 4.28 (q, J = 7.3 Hz, 2 H), 3.88 (d, J = 11.4 Hz, 6 H), 1.33 (t, J = 7.3 Hz, 3 H); exact mass 225.05 (225.05 calcd for $C_7H_{12}DPO_6$).

Ethyl 3-Deuterio-3,3-dibromopyruvate (6). Ethyl dibromopyruvate (**3**) (1.00 g, 3.64 mmol) was dissolved in D_2O (25 mL), sodium bicarbonate (200 mg) was added, and the mixture was stirred overnight. Evaporation of the water layer (0.1 mm/35 °C) gave a yellowish emulsion, which was extracted with diethyl ether (3 × 10 mL). The ether layers were dried (Na_2SO_4) and evaporated to give yellow oil (1.00 g, 100% yield) **6**. The material was *not* purified by chromatography since this results in complete loss of the deuterium atom: ^{1}H NMR (270 MHz, D_2O) δ 4.24 (q, J = 7.1 Hz, 2 H), 1.22 (t, J = 7.1 Hz, 3 H); exact mass 274.88 (274.88 calcd for $C_5H_5DO_3{}^{79}Br^{81}Br$).

Ethyl (*Z*)-3-Bromo-3-deuterio-2-[(dimethoxyphosphinyl)oxy]propenoate (7a). In a procedure analogous to that used to convert **3** to **4a**, compound **6** (0.738 g, 2.68 mmol) was transformed to *Z* isomer **7a** (0.462 g) in 56% yield. The *E* isomer **7b** was obtained in 20% yield. **7a**: ^{1}H NMR (270 MHz, $CDCl_3$) δ 4.30 (q, J = 7.3 Hz, 2 H), 3.95 (d, J = 11.5 Hz, 6 H), 1.33 (t, J = 7.3 Hz, 3 H); exact mass 303.97 (303.97 calcd for $C_7H_{11}D^{79}BrPO_6$). **7b**: ^{1}H NMR (270 MHz, $CDCl_3$) δ 4.34 (q, J = 7.3 Hz, 2 H), 3.87 (d, J = 11.4 Hz, 6 H), 1.26 (t, J = 7.3 Hz, 3 H); exact mass 303.97 (303.97 calcd for $C_7H_{11}D^{79}BrPO_6$).

Ethyl (*E*)-3-Deuterio-2-[(dimethoxyphosphinyl)oxy]propenoate (5b). Compound **7a** (0.126 g, 0.45 mmol) was treated with a freshly prepared Zn/Ag couple (250 mg) doped with H_2O, in a manner similar to that reported above for the transformation of **4a** to **5a**, to give **5b** as a colorless oil (0.93 g, quantitative yield): ^{1}H NMR (270 MHz, $CDCl_3$) δ 5.62 (d, J = 2.4 Hz, 1 H), 4.28 (q, J = 7.3 Hz, 2 H), 3.88 (d, J = 11.4 Hz, 6 H), 1.33 (t, J = 7.3 Hz, 3 H).

Acknowledgment. This work was supported by U.S. Public Health Service Grant GM 36184 and an Upjohn Starter Grant from the College of Pharmacy. We are grateful to the U.S.P.H.S. and the College of Pharmacy for their contribution to the purchase of the IBM 270-MHz NMR instrument. We wish to thank Ms. Stacie Tate, a participant in the NIH sponsored College of Pharmacy Summer Minority High School Apprenticeship Program, for her expert technical assistance in the purification of the **3**, **4a**, and **4b**.

Registry No. **1** R_1 = D, R^2 = H, 56585-32-1; **1** R_1 = H, R_2 = D, 87115-15-9; **2**, 76179-25-4; **4a**, 124225-39-4; **4b**, 124225-40-7; **5a**, 87115-22-8; **5b**, 87115-21-7; **6**, 124225-41-8; **7a**, 124225-42-9; **7b**, 124225-43-0; ethyl bromopyruvate, 70-23-5; trimethyl phosphite, 121-45-9.

(22) Gordon, A. J.; Ford, R. A. *The Chemist's Companion: A Handbook of Practical Data, Techniques and References*; John Wiley and Sons: New York, 1972.

(23) The conversion of **3** to **4a** and **4b** when carried out in refluxing diglyme (bp 162 °C) yields and 82:18 *Z*/*E* ratio. The separation of the *Z* and *E* isomers can also be effected via column chromatography using 100 g of *dry* silica gel/1 g of compound. The column is eluted at 100 mL/h with 100 mL of 5% EtOAc/heptanes (vol/vol), 200 mL of 10% EtOAc/heptanes, 300 mL of 15% EtOAc/heptanes, and finally 1 L of 20% EtOAc/heptanes until the product (R_f = 0.2 30% EtOAc/heptanes) was collected in >95% optical purity.

Stereochemistry in a Medium-Sized Ring. Highly Diastereoselective N-Oxidation of a Substituted 3-Benzazonine. X-ray Crystal Structure of an Unusual Complex between an Amine *N*-Oxide and Saccharin

Bruce E. Maryanoff*,†

Chemical Research Department, McNeil Pharmaceutical, Spring House, Pennsylvania 19477

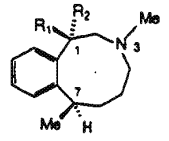
Masood Parvez and R. A. Olofson

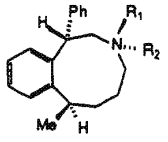
Department of Chemistry, The Pennsylvania State University, University Park, Pennsylvania 16802

Received April 11, 1989

Medium-sized cyclic compounds often adopt a wide range of low-energy conformations, which can render the control of reaction stereochemistry unpredictable or difficult.[1-4] However, with the introduction of sp^2 atoms into the ring, certain conformations may be significantly differentiated, so that impressive diastereoselection between remote sites (e.g., 1,3 and 1,4) can be achieved.[1-3] Both Still[1] and Vedejs[2] have drawn attention to local conformational effects as a source of effective stereocontrol in such molecules.

Our interest in this area stems from our work with hexahydro-1-phenyl-3-benzazonine derivatives.[3] An important problem in this earlier paper was the stereochemical assignment of *cis*- and *trans*-**1**, which was predicated





trans-**1** R_1 = H, R_2 = Ph

cis-**1** R_1 = Ph, R_2 = H

2 R_1 = Me, R_2 = O

3 R_1 = O, R_2 = Me

† Current address: Chemical Research Department, R. W. Johnson Pharmaceutical Research Institute, Spring House, PA 19477.

0022-3263/90/1955-0760$02.50/0 © 1990 American Chemical Society

UM00014031
NOVARTIS EXHIBIT 1517
Novartis v. Regents, IPR2023-01347
Page 2777 of 4460

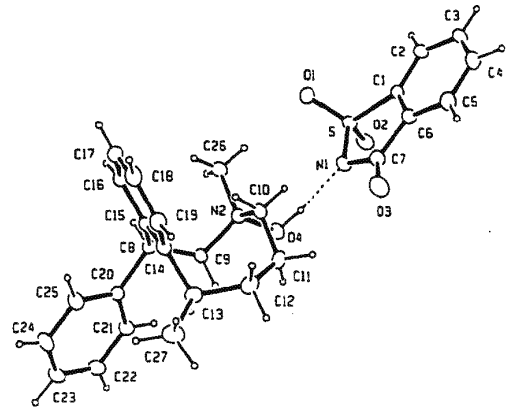


Figure 1. Molecular structure of 2·saccharin showing the crystallographic numbering scheme and the hydrogen bond involving N1 and the hydrogen atom on O4.

on ^{1}H NMR spectral data.[3] To corroborate this critical assignment, we sought a single-crystal X-ray analysis on a salt of one of these isomers. However, the preparation of adequate crystals of the perchlorate[3] of *trans*-1 or the fumarate[3] of *cis*-1 could not be fulfilled, and other salts involving *trans*-1 and 15 diverse acids were not crystalline. Ultimately, we obtained a suitable saccharin salt, X-ray analysis of which revealed, surprisingly, a complex between an *N*-oxide of *trans*-1 (i.e., 2) and saccharin. While we were naturally gratified at winning this X-ray structure and the concomitant stereochemical assignment, we were curious about where the *N*-oxide came from and fascinated by the high stereoselectivity of the N-oxidation. These issues comprise the basis of this paper.

Results and Discussion

A 100-mg sample of *trans*-1·$HClO_4$ was partitioned between aqueous NaOH and dry ethyl ether to release the free base. Treatment of the oily free base with saccharin immediately yielded a white crystalline substance (65% yield), which was recrystallized slowly to provide colorless prismatic needles. The expected 1:1 adduct (^{1}H NMR) was subjected to a single-crystal X-ray analysis, details of which are presented in the Experimental Section and the supplementary material.[5] Although the molecular structure shows the trans relationship between the substituents on positions 1 (C8) and 7 (C13), confirming our earlier assignment,[3] the compound turned out to be an *N*-oxide derivative of *trans*-1 (Figure 1, crystallographic numbering used here). The oxygen atom O4, which is cis to the pendant phenyl group on crystallographic C8 and trans to the methyl group on C13, is protonated by the saccharin, such that the molecular complex actually represents a hydroxyammonium salt. The O4–H bond distance of 0.90 Å is quite consistent with this description. Additionally, the nitrogen of the saccharinate unit is hydrogen bonded to the hydrogen on O4 with a N1-H bond distance of 1.753 Å and a nearly linear N1···H–O4 bond angle of 174.4° (the N2–O4 bond distance is a reasonable 1.43 Å).[6] The conformation of the 9-membered ring of 2 in the solid state is illustrated by the stereopair in Figure 2. The ring adopts a boat–chair conformation with the atom sequences C9–C8–C15–C14–C13–C12 and C9–N2–C10–C11–C12 defining the boat and chair segments, respectively. This X-ray structure does not precisely mimic any of the four low-energy geometries calculated for amine 1,[3] which account for 98.5% of the conformational distribution (see structures 4–7 in Figure 3), but it does come close to 4, especially in the region C10–C11–C12–C13. One key difference between the X-ray structure and 4 pertains to the nitrogen end of the ring. The 7-methyl substituent (on C13) assumes an equatorial arrangement relative to the plane defined by atoms N2, C11, and C13, while the 1-phenyl substituent is axial relative to the C8–C11–C13 plane. Since N2 marks a conformational transition in 2, it is difficult to specify the orientation of the N-substituents in terms of axial and equatorial.

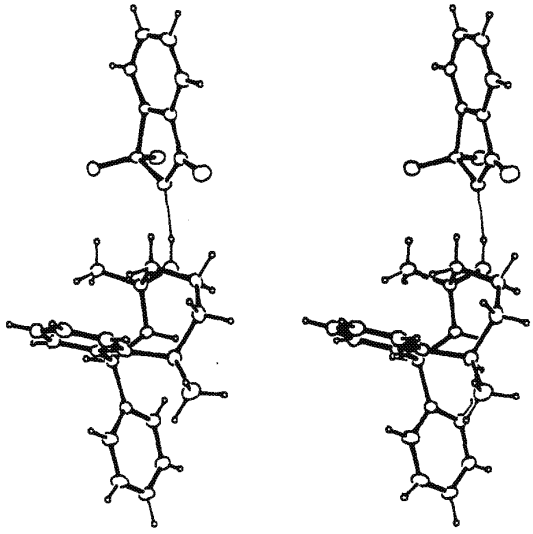


Figure 2. Stereoview of the molecular structure of 2·saccharin.

Early on, we were surprised by this peculiar *N*-oxide salt for two reasons. First, we obviously did not suspect that an *N*-oxide could form so easily during basification of *trans*-1·$HClO_4$ and subsequent salt preparation; indeed, we had generated clean samples of *trans*-1 before for NMR studies.[3] Second, we did not expect such a robust complex involving an amine *N*-oxide (weak base) and saccharin (fairly weak acid). However, there is some literature precedent for such complexes.[7,8] Etter and Baures[7] recently reported crystalline complexes between triphenylphosphine oxide and various primary and secondary amides, including saccharin.[7] They indicated that these $Ph_3P{=}O$ complexes rely on a strong hydrogen bond that imparts partial ionic character to the crystal, as seen for our complex in the solid state. Charpin et al.[8] described

(1) (a) Still, W. C.; Galynker, I. *Tetrahedron* **1981**, *37*, 3981. (b) Still, W. C.; MacPherson, L. J.; Harada, T.; Callahan, J. F.; Rheingold, A. L. *Ibid.* **1984**, *40*, 2275.
(2) Vedejs, E.; Dent, W. H., III; Gapinski, D. M.; McClure, C. K. *J. Am. Chem. Soc.* **1987**, *109*, 5437.
(3) Maryanoff, B. E.; Almond, H. R., Jr. *J. Org. Chem.* **1986**, *51*, 3295.
(4) Anet, F. A. L.; Krane, J. *Isr. J. Chem.* **1980**, *20*, 72.
(5) See paragraph at the end of this paper regarding supplementary material.
(6) For an X-ray structure determination on saccharin itself, see: Okaya, Y. *Acta Crystallogr., Sect. B* **1969**, *25*, 2257. The crystal structure showed a dimer formed by a N–H···O hydrogen bond between the imide nitrogen and the keto oxygen atoms.
(7) Etter, M. C.; Baures, P. W. *J. Am. Chem. Soc.* **1988**, *110*, 639.
(8) Charpin, P.; Dunach, E.; Kagan, H. B.; Theobald, F. R. *Tetrahedron Lett.* **1986**, *27*, 2989.

UM00014032
NOVARTIS EXHIBIT 1517
Novartis v. Regents, IPR2023-01347
Page 2778 of 4460

a stable crystalline 1:1 molecular complex between a chiral sulfoxide and a chiral secondary amide. As far as we know, complexes between amine *N*-oxides and saccharin have rarely been observed.[9]

The formation of **2** is probably connected to the use of ethyl ether in the basification of *trans*-**1**·$HClO_4$. On repeating this process with ethyl acetate or dichloromethane as the organic solvent, only the anticipated *trans*-**1** was obtained. We presume that a sufficient quantity of peroxides was present in the anhydrous ether (used in large excess) to convert almost all of the amine to the *N*-oxide.[10] This accidental oxidation was highly stereoselective since there was no evidence for the corresponding *N*-oxide diastereomer, **3**. Given this remarkable stereocontrol with a medium-sized ring, we examined the N-oxidation under more carefully controlled conditions.

A sample of *trans*-**1**, from basification of the perchlorate salt with ethyl acetate as solvent, was cleanly oxidized with *m*-chloroperbenzoic acid. ^1H NMR and FAB MS data indicated that the product was a mixture of **2** and **3** in ratio of ca. 92:8, although only **2** could be fully characterized by the ^1H NMR data. In the accidental oxidation above, **3** may have been formed to a very minor extent and then eliminated in the isolation process.

To rationalize this high stereoselectivity, we might consider ring conformations of *trans*-**1** and the approach of oxidant to the nitrogen lone pair. According to our prior report,[3] *trans*-**1** is populated mainly by two conformers, **4** (68%) and **5** (20.5%), while only two additional conformers, **6** (8%) and **7** (2%), exceed a level of 1%. The *N*-methyl in **4** is positioned exo and the lone pair is endo (1*S*,3*R*,7*R* configuration); thus, attack at nitrogen with retention would have to occur from the endo direction to generate minor diastereomer **3**. As this approach is sterically hindered, particularly by the fused benzene ring (distance of 2.6–2.8 Å), it should be unfavorable. The nitrogen lone pair in **5** is also endocyclic (1*R*,3*S*,7*S* configuration), and attack by the oxidant with retention would also produce the wrong isomer, **3**. Insofar as this avenue is hindered by transannular interaction with the ring methylene at position 6 (distances of 2.5 and 2.7 Å), it should be unfavorable as well. Production of the observed major product, **2**, from conformers **4** or **5** obviously requires inversion at nitrogen, to give significantly less stable conformations, such as **6** and **7** (1*S*,3*S*,7*R* configuration).[3] However, the nitrogen lone pair is in a hindered endocyclic orientation in these latter structures, too (distances of 2.5/2.6 Å in **6** and 2.4/3.3 Å in **7**). If we accept the force field calculations as being reasonable and the difficulty of endocyclic oxidation, then it is necessary to suggest that the high stereoselectivity stems from attack on a very minor conformation of **1** that possesses an exocyclic nitrogen lone pair (although very minor conformer **7**, being the least congested, may exhibit some competitive reactivity). This type of reactivity pattern exemplifies the well-known Curtin–Hammett principle.[11]

Experimental Section

General Procedures. Melting points are corrected. ^1H NMR spectra were recorded at 360 MHz on a Bruker AM-360WB instrument in $CDCl_3$ with Me_4Si as an internal standard, unless indicated otherwise. NMR proton assignments and coupling constants for **2** were derived with the aid of 2D COSY and homonuclear decoupling experiments. Fast-atom bombardment (FAB) mass spectral data were obtained on a VG 7070E spectrometer. TLC analysis was performed on 250-μm silica gel plates with visualization by UV fluorescence and iodine staining. The structures in Figure 3 were generated by using the SYBYL molecular modeling program (Tripos Associates, Inc., St. Louis, MO, version 5.1).

[1α,3α,7β]-2,3,4,5,6,7-Hexahydro-3,7-dimethyl-1-phenyl-1*H*-3-benzazonine *N*-Oxide (2), Compound with 1,2-Benzisothiazol-3-(2*H*)-one, 1,1-Dioxide (Saccharin). A sample of *trans*-**1**·$HClO_4$ (100 mg) was partitioned between 3 N sodium hydroxide (2 mL) and anhydrous ethyl ether (25 mL), with stirring for about 15 min to dissipate the solid. The ethereal extract was dried (Na_2SO_4) and concentrated in vacuo. The nearly colorless oil was dissolved in ethyl acetate (8 mL) and treated with a solution of saccharin (45 mg) in a small amount of warm ethyl acetate containing a drop of methanol. After addition of 2 mL of hexane, crystals began to separate. The mixture was cooled to 0 °C and filtered to give 95 mg (65%) of white powder. This material was recrystallized slowly from ethyl acetate/methanol (1:1, 3 mL) to yield 32 mg of bright colorless prismatic needles, mp 190–195 °C (turned red and intumesced), homogeneous by TLC with 1:1 chloroform/95% ethanol (R_f = 0.22); ^1H NMR δ 1.21 (d, 3, CMe, J = 6.7 Hz), 1.57–1.72 (m, 1, H6), 1.84–1.94 (m, 1, H6, ^2J = 14.2 Hz), 2.05–2.18 (m, 1, H5), 2.32–2.46 (m, 1, H5), 2.91–3.02 (m, 1, H4?), 3.61–3.73 (m, 4, s for NMe at δ 3.69), 2.74–2.83 (m, 1, H7, splitting due to Me is evident), 4.60–4.80 (m, 2, 2 H2 or H1 and H2), 4.85–4.92 (m, 1, H2 or H1), 7.13–7.35 (m, 7, Ar H in 2), 7.43–7.50 (m, 2, Ar H in 2), 7.57–7.65 (m, 2, saccharin), 7.77–7.84 (m, 2, saccharin); FAB MS, m/z 296 (M + H, 100%), 280 (loss of O, 35%).

The starting amine, *trans*-**1**, also made a fine crystalline salt with saccharin: colorless prisms from ethyl acetate/hexane, mp 148–151 °C; FAB MS, m/z 280 (M + H); ^1H NMR δ 1.12 (m, 3, Me), 1.5–1.7 (br m, 2), 1.7–1.9 (m, 1), 2.1–3.3 (m, 3), 2.86 (s, 3, NMe), 3.00 (m, 1), 3.1–3.2 (m, 1), 4.09 (dd, 1), 4.40 (m, 1), 4.6–4.7 (m, 1), 7.0–7.5 (m, 9), 7.60 (m, 2), 7.80 (m, 2); the aliphatic resonances in this spectrum were rather broad and ill-defined.

[1α,3α,7β]-2,3,4,5,6,7-Hexahydro-3,7-dimethyl-1-phenyl-1*H*-3-benzazonine *N*-Oxide (2) from MCPBA Oxidation of *trans*-1. A sample of *trans*-**1**·$HClO_4$ (20 mg) was partitioned between ethyl acetate and 1 N NaOH. The organic extract was dried (Na_2SO_4) and treated with 15 mg of MCPBA (85% assay). After 24 h, 10% aqueous Na_2CO_3 was added. The organic layer was separated, rinsed with brine, dried (Na_2SO_4), and concentrated to dryness under a stream of argon, then in vacuo, to furnish 11 mg (70%) of colorless semisolid. The product was homogeneous by TLC and gave a proper FAB MS. ^1H NMR showed one major diastereomer, **2**, and peaks attributable to the minor diastereomer, **3**. Comparison of the 7-Me and NMe in **2** and **3** gave a ratio of ca. 92:8. ^1H NMR data for **2**: δ 1.13 (d, Me, J = 6.8 Hz), 1.59 (dddd, H5a, ^2J = 14.1 Hz, ^3J(5a,6a) = 14.0 Hz, ^3J(4a,5a) = 11.6 Hz, ^3J(4e,5a) = 5.3 Hz), 1.82 (dddd, H5e, ^2J = 14.2 Hz, ^3J = 2.3, 2.3, 5.1 Hz), 1.95 (m, H6e), 2.47 (m, H6a), 2.68 (ddd, H7e, ^2J = 12.8 Hz, ^3J = 1.7, 5.8 Hz), 2.94 (ddq, H4a, ^3J(4a,5e) = ca. 2 Hz, ^3J(4a,5a) = 11.5 Hz, ^3J(4a,Me) = 6.8 Hz), 3.03 (ddd, H7a, ^2J = ca. 12 Hz, ^3J = ca. 12, ca. 1 Hz), 3.17 (s, NMe), 4.05 (dd, H3a, ^3J(2a,3a) = 13.0 Hz, ^3J(2e,3a) = 5.1 Hz), 4.45 (dd, H2a, J = 13, 13 Hz), 4.52 (dd, H2e, J = 13, 5.2 Hz), 7.0–7.4 (m, Ar). ^1H NMR data for **3**: δ 0.89 (d, Me), 2.56 (s, NMe); only these sharp signals could be assigned unambiguously to **3** because of its relatively low concentration.

Single-Crystal X-ray Analysis of 2·Saccharin. Crystals of $C_{27}H_{30}N_2O_4S$ (mw 478.61) are triclinic (space group $P\bar{1}$) with

(9) An extensive search of *Chemical Abstracts* revealed only one saccharin complex of this type. An adduct between β-narcotine *N*-oxide (an isoquinoline alkaloid structure) and saccharin was reported in a Japanese patent: *Chem. Abstr.* 1964, *52*, P5312h. Amine oxides form salts with various strong and moderate acids, and a recent paper discussed complexes between an *N*-oxide and a phenol: Toda, F.; Mori, K.; Stein, Z.; Goldberg, I. *Tetrahedron Lett.* 1989, *30*, 1841.

(10) (a) A small amount (ca. 10%) of unoxidized *trans*-**1** was found in the mother liquor from the isolation of **2**·saccharin. (b) After obtaining the X-ray result, we no longer had any original ether to evaluate the peroxide level. However, we subsequently compared the basification of *trans*-**1**·$HClO_4$ with ether that was peroxide-free and with ether that contained ca. 30 mg/L of peroxides, as assayed by Quantofix peroxide test strips. *N*-Oxide **2** was found only for the *latter* case in the residue from evaporation of the ether solvent (about 20% conversion); for either case, the ethereal extract before evaporation showed virtually no *N*-oxide.

(11) Eliel, E. L.; Allinger, N. L.; Angyal, S. J.; Morrison, G. A. *Conformational Analysis*; Wiley-Interscience: New York, 1965, p 28.

UM00014033
NOVARTIS EXHIBIT 1517
Novartis v. Regents, IPR2023-01347
Page 2779 of 4460

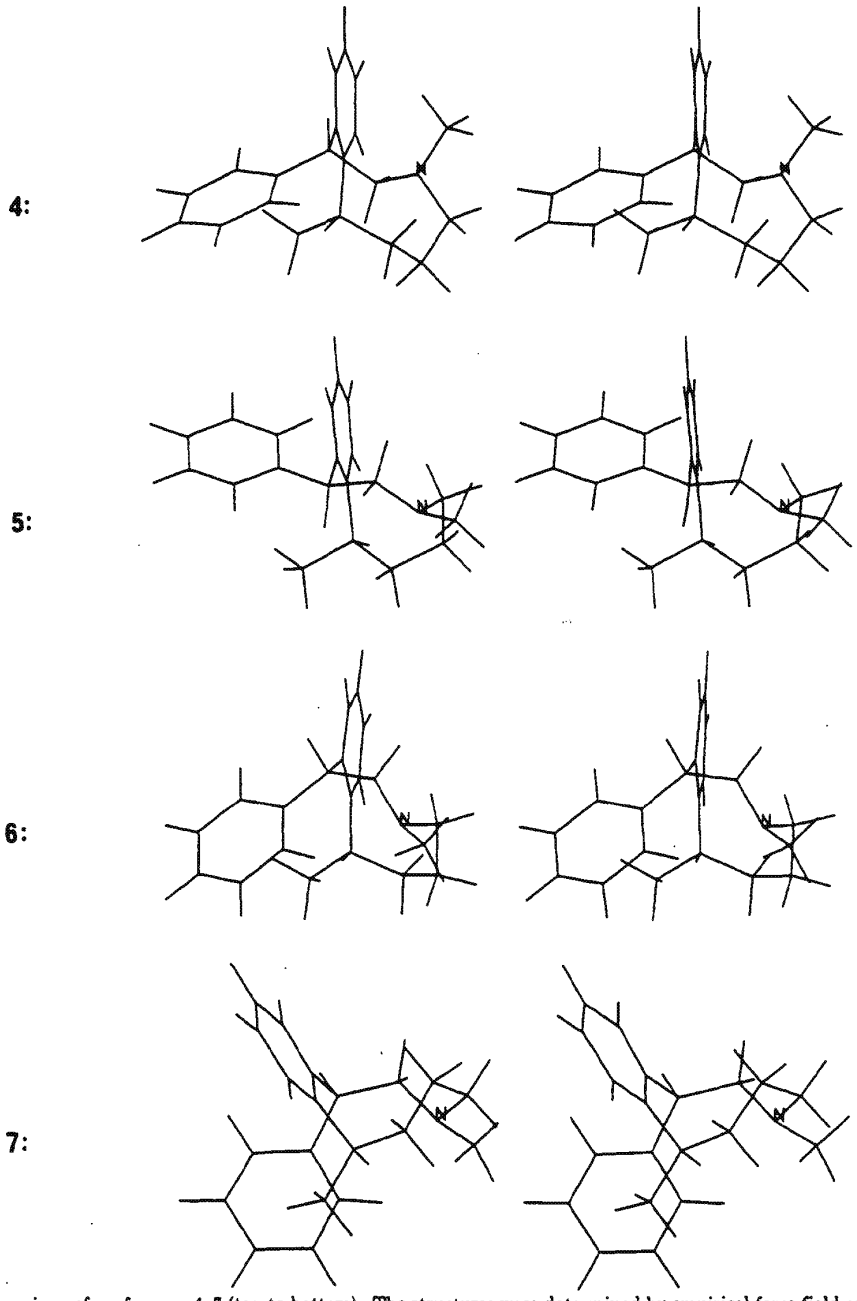


Figure 3. Stereoviews of conformers 4–7 (top to bottom). The structures were determined by empirical force field calculations[3] and generated pictorially with the SYBYL molecular modeling system.

a = 7.670 (3) Å, b = 12.516 (3) Å, c = 14.525 (4) Å, α = 64.28(2)°, β = 73.10 (2)°, γ = 82.38 (2)°, V = 1201.9 (10) Å^3, and d_{calcd} = 1.323 g cm^{-1} for Z = 2. The intensity data were collected from a single crystal on an Enraf-Nonius CAD4 diffractometer with the $\omega/2\theta$ scan method at 293 K (θ_{max} = 25°, ω-scan width = 0.80 + 0.35 tan θ, μ = 1.628 cm^{-1}) by using Mo Kα radiation (λ = 0.71073 Å). The programs employed were part of the Enraf-Nonius Structure Determination Package, as revised in 1982, implemented on a PDP 11/34 computer. The data were corrected for Lorentz and polarization factors but not for absorption. Of the 3867 total reflections, 2819 measuring greater than $3\sigma(I)$ were used. The structure was solved by direct methods and refined by full-matrix least-squares calculations. The hydrogen atoms were refined isotropically with B = 4.0 Å^2. The final discrepancy factors were R = 0.038 and $R_w = (\sum\Delta^2/\sum wF_o^2)^{1/2}$ = 0.052; the final difference map had no peaks greater than 0.26 e Å^{-3}.

Acknowledgment. We thank Dr. Harold Almond, Jr. for helpful discussions on 9-membered ring conformations.

Registry No. *trans*-1·HClO$_4$, 124439-12-9; 2, 124342-87-6; 2-saccharin, 124378-95-6; 3, 124378-96-7; saccharin, 81-07-2.

UM00014034
NOVARTIS EXHIBIT 1517
Novartis v. Regents, IPR2023-01347
Page 2780 of 4460

Supplementary Material Available: Tables of bond distances, bond angles, and positional and thermal parameters for hydrogen and non-hydrogen atoms (9 pages). Ordering information is given on any current masthead page.

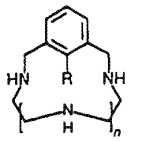
Isolation and Unusual Stability of a New Macrocyclic Polyamine Containing a Phthalimidine

Eiichi Kimura,*[†] Yukari Yoshiyama,[‡] Mitsuhiko Shionoya,[†] and Motoo Shiro*[§]

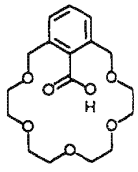
Coordination Chemistry Laboratories, Institute for Molecular Science, Okazaki National Research Institutes, Nishigonaka 38, Myodaiji, Okazaki 444, Japan, Department of Medicinal Chemistry, Hiroshima University School of Medicine, Kasumi 1-2-3, Minami-ku, Hiroshima 734, Japan, and Shionogi Research Laboratories, Shionogi & Co., Ltd., Fukushima-ku, Osaka 553, Japan

Received June 21, 1989

The host properties of macrocyclic polyamines containing a 2-hydroxy-1,3-xylyl unit as part of the large ring (1 and 2) are of great interest.[1] Effective uptake of alkaline-earth metal ions by them in MeOH has been achieved with the 1:1 complexation constants being in the order of $Mg^{2+} > Ca^{2+} > Sr^{2+} > Ba^{2+}$. Moreover, the simultaneous dissociation of the phenolic H^+ has allowed for the facile determination of complexation constants.



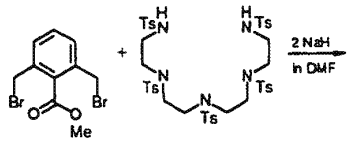
1: n = 2, R = OH
2: n = 3, R = OH
3: n = 3, R = COOH



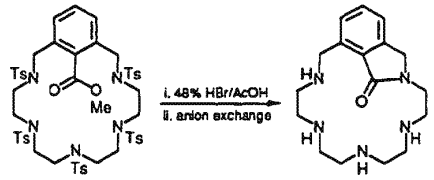
4

In order to develop further the chemistry of host polyamines, we have attempted to synthesize macrocycle 3. This putative new compound 3 would be of interest in that its benzyl nitrogens could be close enough to the carboxyl substituent so that the lone pair of each benzyl nitrogen points toward the carbonyl carbon along the axis of its π system. Such overlap could conceivably lead to some unusual properties for the carbonyl group in 3. In the polyether counterpart 4,[2] for instance, the distances of the O···C=O bond were observed to be shorter than the usual van der Waals contacts, suggesting the presence of attractive dipole–dipole interactions.[3]

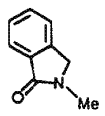
A new macrocycle (6) was prepared from dibromide 5 and tetraethylenepentamine pentatosylate in order to explore the above possibilities. Compound 6 was then heated at reflux in 48% HBr–acetic acid solution over a period of 48 h to complete the detosylation. Usual workup by anion exchange chromatography and recrystallization from acetonitrile then afforded a product as prismatic crystals, which on the basis of the reaction sequence was expected to be 3. Elemental analysis, ^1H and ^{13}C NMR, IR, and UV spectra, and other physicochemical data for this product, however, did not fit to the anticipated structure 3. This left some doubts about the structural assignment. The structure of this material was therefore



5



6 7



8

determined by X-ray diffraction analysis and on this basis assigned unequivocally as compound 7 (Figure 1).

In addition to allowing for the structural assignment, the X-ray structure provides interesting details about the macrocyclic conformation, where the planar phthalimidine ring stands almost vertically to create a shielded cavity for guest ions.

The protonation constants (pK_a) were determined by pH (see Figure 2) to be 9.9, 9.2, 5.9, and 2.2 at I = 0.1 M ($NaClO_4$), 25 °C, indicating feasible accommodation of two protons into the macrocyclic cavity. The UV spectral absorptions (220–280 nm) of the phthalimidine are substantially increased in intensity in macrocycle 7, as compared to *N*-methylphthalimidine itself (structure 8). Moreover, in 7, successive addition of protons affects the UV absorptions at 240–280 nm, whereas the UV absorption of 8, as expected, is not subject to such proton dependence.

A similar significant UV absorption change was observed upon Zn^{2+} and Cu^{2+} uptake (up to 1:1 molar ratio). The pH–titration method has established 1:1 complexation with Zn^{2+} and Cu^{2+} (Figure 2). From the titration curve the modes of complexation of Cu^{2+} and Zn^{2+} are suggested to be as shown in Scheme I.

Detailed computational analysis of the experimental curves has allowed the values of the complexation constants to be determined as log K_{CuHL} = 12.2 (K_{CuHL} = $[Cu^{II}HL]/[Cu^{II}][HL]$), log K_{CuL} = 15.3 ($K_{CuL} = K_{CuHL} \times K'_{CuL}/K_1$, where $K' = [Cu^{II}L] \times a_{H^+}/[Cu^{II}HL]$), and log K_{ZnL} = 8.1 ($K_{ZnL} = [Zn^{II}L]/[Zn^{II}][L]$).[4] The considerably smaller K values observed here relative to those for unsubstituted N_4 macrocyclic ligands[5] may indicate that the stretched N_4 ring conformation present in 7 is unfavorable for metal incorporation (due to lack of flexibility).

The amide bond in macrocyclic 7 strongly resists hydrolysis in acid (e.g., refluxing 6 N HCl) and use of Zn^{2+} or Cu^{2+} ions (which were tried in an effort to activate the

[†] Institute for Molecular Science.
[‡] Hiroshima University School of Medicine.
[§] Shionogi Research Laboratories.

(1) Kimura, E.; Kimura, Y.; Yatsunami, T; Shionoya, M.; Koike, T. *J. Am. Chem. Soc.* 1987, *109*, 6212.
(2) (a) Newcomb, M.; Cram, D. J. *J. Am. Chem. Soc.* 1975, *97*, 1257. (b) Newcomb, M.; Moore, S. S.; Cram, D. J. *J. Am. Chem. Soc.* 1977, *99*, 6405.
(3) Goldberg, I. *Acta Crystallogr.* 1976, *B32*, 41.
(4) The titration data of 7 in the presence of each metal ion (see dots on lines (b) and (c) in Figure 2) were treated by the Schwarzenbach method for the 1:1 complexation [Schwarzenbach, G. *Helv. Chim. Acta* 1950, *33*, 947]. The metal hydrolysis was taken into account, where K_{OH} (= $[M(OH)^+]/([M^{2+}]a_{OH^-})$) values are 4.6×10^6 for Cu^{II} and 1.1×10^5 for Zn^{II} [Iitaka, Y.; Koike, T.; Kimura, E. *Inorg. Chem.* 1986, *25*, 402].
(5) Kodama, M.; Kimura, E. *J. Chem. Soc., Dalton Trans.* 1977, 2269.

0022-3263/90/1955-0764$02.50/0 © 1990 American Chemical Society

UM00014035
NOVARTIS EXHIBIT 1517
Novartis v. Regents, IPR2023-01347
Page 2781 of 4460

Phytochemistry, Vol. 26, No. 1, pp 273–279, 1987
Printed in Great Britain

0031-9422/87 $3.00 + 0.00
© 1987 Pergamon Journals Ltd

THE CAFFEINE–POTASSIUM CHLOROGENATE MOLECULAR COMPLEX

RUSSELL MARTIN, TERENCE H. LILLEY, CHRISTOPHER P. FALSHAW, EDWIN HASLAM, MICHAEL J. BEGLEY* and DANIELE MAGNOLATO†

Chemistry Department, University of Sheffield, Sheffield S3 7HF, U.K.; *Chemistry Department, University of Nottingham, Nottingham NG7 2RD, U.K.; †Nestlé Research Department, Nestec Ltd., CH-1800 Vevey, Switzerland

(*Received* 17 *March* 1986)

Key Word Index *Coffea arabica*; Rubiaceae; crystal structure; caffeine potassium chlorogenate molecular complex; polyphenol association.

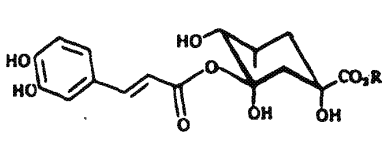
Abstract—The crystal structure of the caffeine–potassium chlorogenate 1:1 molecular complex derived from coffee beans is described. The relationship of this structure to the general question of the mechanisms of polyphenol association and precipitation is commented upon.

INTRODUCTION

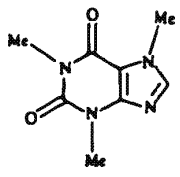
Non-covalent intermolecular forces underlie many biological phenomena enzyme catalysis, hormonal responses, membrane transport, etc. [1]. Understanding the nature of these forces—the problems of molecular recognition and discrimination—has become a major focus of attention in biological chemistry. One facet of this problem concerns plant polyphenols. The profusion and irregular distribution of phenolic compounds in plants has exercised the minds of chemists for many years. Botanists and plant physiologists have likewise pondered their function [2–5]. Plant phenols vary in complexity from the ubiquitous chlorogenic acid (1) to, for example, the complex polyphenols frequently referred to as vegetable tannins [6]. They reversibly associate with a wide range of substrates such as proteins and polysaccharides, and studies of these phenomena are not only of intrinsic scientific interest because of their possible involvement in a functional role, but they are also of undoubted practical significance. They determine, for example, the palatability of many foodstuffs [7] such as tea and coffee, wine, beers, cocoa and coca-cola; the nutritional value of crops [8]; and the rate of microbial decomposition of plant tissues in the formation of soils [9]; while extracted plant polyphenols still provide pharmaceutical preparations of medical interest and value [10]. Their ready association with proteins and other macromolecules probably forms the basis of their therapeutic action.

Recent studies [11, 12] have demonstrated some of the macroscopic features of the polyphenol molecular structure necessary for enhanced complexation with proteins and other nitrogenous metabolites. The molecular mechanisms whereby complexation is mediated have remained a subject for circumstantial speculation. Loomis [13] has suggested that hydrogen bonding and hydrophobic effects predominate. In aqueous media natural polyphenols readily associate with some alkaloids. With caffeine (3), for example, the complexation is polydentate and aggregates are ultimately formed sufficient to cause precipitation. The stoichiometry of these aggregates is similar in kind to that noted previously for polyphenols and proteins, and is directly related to the initial polyphenol concentration [14]. By extrapolation from crystal structure data it has been proposed [15] that hydrogen bonding and apolar interactions (the exclusion of the solvent water from regions between aroyl and purine rings, for example) dominate the complexation. A model for the precipitation process is suggested in Fig. 1 [15]. A further interesting facet of this work is the observation that in some polyphenolic substrates where there are multiple binding sites complexation often occurs preferentially at just one or two of these sites (C. M. Spencer, R. Martin, T. H. Lilley, E. Haslam and D. Magnolato, unpublished work).

Hydroxycinnamic acids are ubiquitous in the plant kingdom and usually occur as esters or glycosides [16]. The most familiar of these is the 5-*O*-caffeoyl ester of quinic acid, chlorogenic acid (1). It may constitute up to 0.1% of the fresh weight of many plant tissues but raw coffee is a rich source and contains 5–8% of this caffeoyl ester. Potassium chlorogenate (2) was first isolated from green coffee beans (*Coffea arabica* L.) by Gorter [17] as a crystalline 1:1 complex with caffeine (3). Gorter de-



1 R = H
2 R = K



3

UM00014036
NOVARTIS EXHIBIT 1517
Novartis v. Regents, IPR2023-01347
Page 2782 of 4460

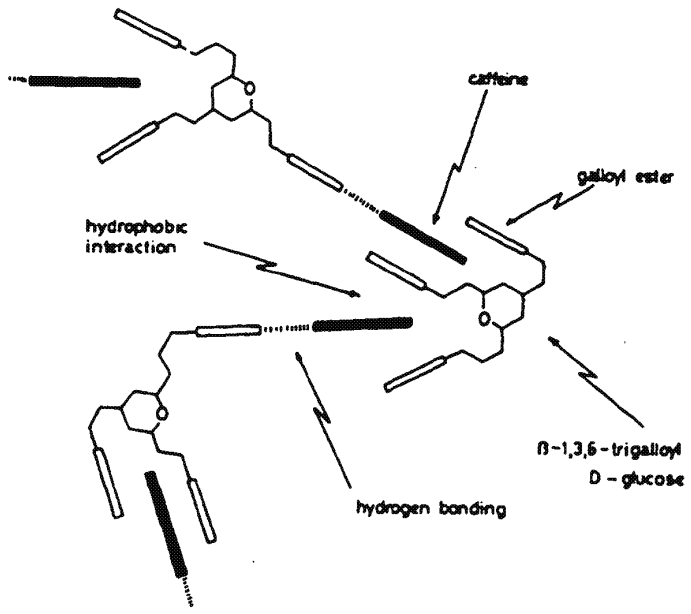


Fig. 1. Caffeine–polyphenol precipitation.

monstrated that the complex was recrystallized unchanged from aqueous ethanol, but its structure and physicochemical properties have, since that date, received scant attention. Sondheimer *et al.* [18] in a partition study considered the influence on complex stability of various stereochemical and structural features but their work failed to identify the nature of the intermolecular forces. In a later investigation, Horman and Viani [19], using NMR spectroscopy, concluded that in aqueous media the caffeine potassium chlorogenate complex was best described as a "hydrophobically bound π molecular complex" and percipiently they suggested that in solution the time-averaged conformation of the complex resembled that shown in Fig. 2. It was proposed that the plane of the caffeine molecule is parallel to the plane of the aromatic ring of the caffeoyl ester group and that the five- *and* six-membered rings of the nitrogen heterocycle are equally involved in complex formation.

RESULTS AND DISCUSSION

The structure of the caffeine potassium chlorogenate complex* was obtained from an X-ray study. Initial attempts using default values with MULTAN-80 [20] were not rewarding. Using a group scattering factor for the caffeine molecule, calculated from its published geometry [22] together with the standard weighted tangent formula [20] a partial solution was derived. Coordinates for the potassium ion and 19 of the heavy atoms comprising the chlorogenate ion were obtained in this way and refined for several cycles using the CRYSTALS [21] package. Fourier methods then allowed the location of the caffeine molecule together with the remaining atoms of the chlorogenate ion and the two oxygen atoms associated with the water of crystallization. The structure was then refined using isotropic and anisotropic temperature factors, and this process was covergent with $R = 6.99\%$. Most of the hydrogen atoms were located from a Fourier map. Where possible, hydrogen atoms were then included in their calculated positions, but hydroxyl hydrogen atoms together with those of the *N*-methyl groups at C (22) and C (23) were located in their found loci. The *N*-methyl group at C (24) was disordered and these hydrogen atoms were eventually included assuming a conformation of this *N*-methyl group similar to that reported for the caffeine barbital complex [23]. Further refinement of the parameters associated with the heavy atoms gave a final R value of 5.51%. Final atomic coordinates are contained in Table 1, and Table 2 lists inter-atomic distances and bond angles.

The structure of the asymmetric unit of the

*Crystal data for potassium chlorogenate–caffeine bishydrate, $C_{16}H_{17}O_9K \cdot C_8H_{10}N_4O_2 \cdot 2H_2O$. $M_r = 622.63$. Space group $P2_12_12_1$, $a = 7.0521$ (3), $b = 11.5848(9)$, $c = 33.8621(27)$ Å, $U = 2766.4$ Å^3, $D_c = 1.49$ g/cm^3, $Z = 4$. Cu K_α radiation ($\lambda = 1.5418$ Å), $\mu = 23.35$ cm^{-1}, $F(000) = 1304$, $R = 0.0551$, $R_w = 0.0621$ for 1682 reflections. $\theta \leq 66°$, $I \geq 2\sigma(I)$. The atomic coordinates are available on request from the Director of the Cambridge Crystallographic Data Centre, University Chemical Laboratory, Cambridge CB2 1EW, U.K.

UM00014037
NOVARTIS EXHIBIT 1517
Novartis v. Regents, IPR2023-01347
Page 2783 of 4460

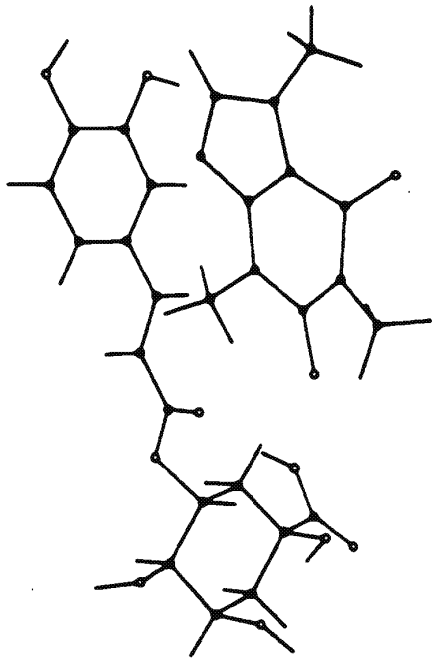


Fig. 2. Time-averaged conformation of the caffeine potassium chlorogenate complex [19].

caffeine–potassium chlorogenate complex is shown in Fig. 3 with the crystallographic numbering. The potassium ion is associated with a number of oxygen atoms (see below) but within the asymmetric unit the oxygen atoms O (6), O (7) and O (10) are coordinated to the alkali metal ion and K$^+$ ··O distances lie between 2.67 and 2.85 Å (Table 3). In addition to this feature, the asymmetric unit is further stabilized by a symmetrical hydrogen bond linking O (1), H (14) and O (12) (Table 4). The aryl ring C (1)–C (6) is planar (maximum deviation from this mean plane is 0.016 Å). Likewise the caffeine molecule is also planar (maximum deviation of 0.004 Å). Within the asymmetric unit these planes lie at an angle of 18.4° to one another.

The complex forms a layer lattice structure with the phenolic nuclei of the chlorogenate ion alternating with the caffeine molecule in stacks; Fig. 4 shows a view down the x-axis of the unit cell. Within each stack the phenolic rings are parallel and alternating caffeine molecules lie inclined at 3.6° to these rings. The centres of the adjacent planes are separated by 3.78 Å. Inspection of Fig. 4 shows that three pairs of atoms most nearly eclipse one another in this stacking array. These atoms are N (2) and C (4)—3.5 Å; N (3) and C(6)—3.62 Å; C (2) and C (10) 3.50 Å.

Two additional factors serve to stabilize this arrangement within the crystal lattice. These are respectively hydrogen bonding and coordination around the potassium ion. The hydrogen bonding network is extensive (Fig. 5; dimensions, Table 4). The potassium cation is associated with a total of seven oxygen atoms in an irregular polyhedral array. In addition to the oxygen atoms involved within the asymmetric unit (see above), also associated with the central potassium ion are both

Table 1. Caffeine-potassium chlorogenate complex. Refined atomic coordinates with e.s.d.s in parentheses

K 1	0.1893(3)	0.3071(1)	0.04616(5)
O 12	0.068(1)	0.1612(4)	0.4773(2)
O 13	0.785(1)	0.3324(5)	0.0197(2)
O 1	−0.017(1)	0.0043(4)	0.4261(1)
O 2	−0.079(1)	−0.1596(4)	0.3741(1)
O 3	0.059(1)	0.1834(5)	0.1858(2)
O 4	0.015(1)	−0.0003(5)	0.1684(2)
O 5	0.385(1)	−0.0239(5)	0.1412(2)
O 6	0.3451(9)	0.0886(5)	0.0676(2)
O 7	−0.0485(9)	0.1290(4)	0.0525(2)
O 8	−0.2699(9)	−0.1385(5)	0.0307(2)
O 9	−0.342(1)	0.0453(5)	0.0193(2)
C 1	0.003(1)	0.0860(6)	0.3070(2)
C 2	−0.033(1)	−0.0274(6)	0.3202(2)
C 3	−0.042(1)	−0.0520(6)	0.3591(2)
C 4	−0.008(1)	0.0350(6)	0.3883(2)
C 5	0.023(1)	0.1464(6)	0.3749(2)
C 6	0.028(1)	0.1710(6)	0.3346(2)
C 7	0.011(1)	0.1140(7)	0.2654(2)
C 8	0.003(1)	0.0432(7)	0.2344(2)
C 9	0.029(1)	0.0851(7)	0.1945(2)
C 10	0.056(1)	0.0227(6)	0.1273(2)
C 11	0.230(1)	−0.0479(6)	0.1160(2)
C 12	0.281(1)	−0.0284(6)	0.0730(3)
C 13	0.110(1)	−0.0542(6)	0.0647(2)
C 14	−0.070(1)	0.0084(6)	0.0588(2)
C 15	−0.113(1)	−0.0119(7)	0.1028(2)
C 16	−0.242(1)	−0.0317(7)	0.0339(2)
N 1	0.544(1)	0.3957(5)	0.1433(2)
N 2	0.499(1)	0.5792(6)	0.1162(2)
N 3	0.474(2)	0.7357(7)	0.1645(2)
N 4	0.499(1)	0.6221(7)	0.2186(2)
O 10	0.518(1)	0.4189(5)	0.0770(2)
O 11	0.557(1)	0.3672(7)	0.2113(2)
C 17	0.515(1)	0.4631(8)	0.1109(3)
C 18	0.493(1)	0.6229(8)	0.1539(3)
C 19	0.472(2)	0.7327(9)	0.2066(4)
C 20	0.509(1)	0.5545(8)	0.1859(3)
C 21	0.538(2)	0.4362(8)	0.1827(3)
C 22	0.576(2)	0.2705(8)	0.1373(3)
C 23	0.479(2)	0.6525(9)	0.0807(4)
C 24	0.499(2)	0.589(1)	0.2600(3)

phenolic oxygen atoms of a chlorogenate ion ($-x, \frac{1}{2}+y, \frac{1}{2}-z$), one of the carboxylate oxygen atoms ($\frac{1}{2}+x, \frac{1}{2}-y, -z$) and finally a water molecule ($x-\frac{1}{2}, \frac{1}{2}-y, -z$) (Fig. 6). Table 3 lists these various associated oxygen atoms.

The association of polyphenols with other molecules such as proteins and polysaccharides is a problem of very great practical significance and one with a very long history. This paper brings forward for the first time factual evidence concerning the molecular mechanisms of non-covalent interactions between the heterocycle caffeine (3) and the chlorogenate ion (2). Whilst the tendency has been to emphasize (usually on intuitive grounds) the part played by hydrogen bonding, this work unequivocally demonstrates for the first time *inter alia* the crucial importance not only of hydrogen bonding but also of hydrophobic effects and coordination around a central alkali metal ion in the complexation process. These features are additionally supported by related observations, e.g. the crystal structure of the caffeine–methyl

UM00014038
NOVARTIS EXHIBIT 1517
Novartis v. Regents, IPR2023-01347
Page 2784 of 4460

Table 2. Caffeine–potassium chlorogenate complex. Bond lengths (Å) (e.s.d.s all 0.01 Å) and bond angles (°) (e.s.d.s. 0.6 0.8° for potassium chlorogenate and 0.8 1.0° for caffeine)

	Potassium chlorogenate		
C(1)–C(2)	1.41	O(4)–C(10)	1.45
C(2)–C(3)	1.35	C(10)–C(11)	1.52
C(3)–O(2)	1.37	C(11)–O(5)	1.42
C(3)–C(4)	1.43	C(11)–C(12)	1.52
C(4)–O(1)	1.33	C(12)–O(6)	1.44
C(4)–C(5)	1.39	C(12)–C(13)	1.53
C(5)–C(6)	1.39	C(13)–C(14)	1.52
C(6)–C(1)	1.37	C(14)–O(7)	1.42
C(1)–C(7)	1.45	C(14)–C(16)	1.55
C(7)–C(8)	1.33	C(16)–O(8)	1.26
C(8)–C(9)	1.45	C(16)–O(9)	1.24
C(9)–O(3)	1.20	C(14)–C(15)	1.54
C(9)–O(4)	1.33	C(15)–C(10)	1.51
	Caffeine		
N(1)–C(17)	1.36	N(3)–C(19)	1.43
N(1)–C(22)	1.48	C(19)–N(4)	1.36
C(17)–O(10)	1.26	N(4)–C(24)	1.45
C(17)–N(2)	1.36	N(4)–C(20)	1.36
N(2)–C(23)	1.48	C(20)–C(18)	1.35
N(2)–C(18)	1.37	C(20)–C(21)	1.39
C(18)–N(3)	1.36	C(21)–O(11)	1.26
		C(21)–N(1)	1.42
	Potassium chlorogenate		
C(1)–C(2)–C(3)	121.0	O(4)–C(10)–C(15)	108.7
C(2)–C(3)–C(4)	121.1	C(15)–C(10)–C(11)	110.9
C(2)–C(3)–O(2)	124.1	C(10)–C(11)–C(12)	110.6
O(2)–C(3)–C(4)	114.7	C(10)–C(11)–O(5)	111.5
C(3)–C(4)–O(1)	117.9	O(5)–C(11)–C(12)	111.4
C(3)–C(4)–C(5)	117.1	C(11)–C(12)–C(13)	110.1
O(1)–C(4)–C(5)	124.9	C(11)–C(12)–O(6)	109.7
C(4)–C(5)–C(6)	121.0	O(6)–C(12)–C(13)	111.0
C(5)–C(6)–C(1)	121.1	C(12)–C(13)–C(14)	114.1
C(6)–C(1)–C(2)	118.4	C(13)–C(14)–C(15)	110.7
C(6)–C(1)–C(7)	119.8	C(13)–C(14)–C(16)	111.5
C(2)–C(1)–C(7)	121.8	C(13)–C(14)–O(7)	110.0
C(1)–C(7)–C(8)	128.7	O(7)–C(14)–C(16)	107.2
C(7)–C(8)–C(9)	121.5	O(7)–C(14)–C(15)	108.4
C(8)–C(9)–O(3)	124.9	C(16)–C(14)–C(15)	108.9
C(8)–C(9)–O(4)	111.2	C(14)–C(15)–C(10)	109.5
O(3)–C(9)–O(4)	123.9	C(14)–C(16)–O(8)	117.5
C(9)–O(4)–C(10)	119.1	C(14)–C(16)–O(9)	116.6
O(4)–C(10)–C(11)	107.7	O(8)–C(16)–O(9)	125.9
	Caffeine		
N(1)–C(17)–N(2)	118.2	C(19)–N(4)–C(24)	122.2
N(1)–C(17)–O(10)	119.9	C(24)–N(4)–C(20)	129.6
O(10)–C(17)–N(2)	121.6	N(4)–C(20)–C(18)	108.2
C(17)–N(2)–C(18)	119.3	N(4)–C(20)–C(21)	129.7
C(17)–N(2)–C(23)	118.0	C(18)–C(20)–C(21)	122.0
C(23)–N(2)–C(18)	122.6	C(20)–C(21)–N(1)	113.8
N(2)–C(18)–N(3)	127.0	C(20)–C(21)–O(11)	125.5
N(2)–C(18)–C(20)	121.9	O(11)–C(21)–N(1)	120.8
C(20)–C(18)–N(3)	111.1	C(21)–N(1)–C(17)	124.4
C(18)–N(3)–C(19)	103.9	C(21)–N(1)–C(22)	117.1
N(3)–C(19)–N(4)	108.7	C(22)–N(1)–C(17)	118.4
C(19)–N(4)–C(20)	122.2		

UM00014039
NOVARTIS EXHIBIT 1517
Novartis v. Regents, IPR2023-01347
Page 2785 of 4460

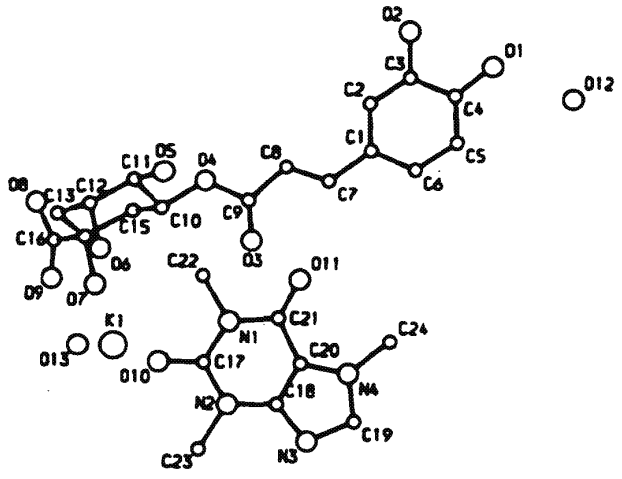


Fig. 3. Asymmetric unit of the caffeine–potassium chlorogenate 1:1 complex –crystallographic numbering.

Table 3. Contacts (Å) to and angles (°) about the potassium atom with relevant symmetry operators

Contacts (Å), symmetry operations					
O(1)	2.75	$-x, \frac{1}{2}+y, \frac{1}{2}-z$	O(9)	2.81	$\frac{1}{2}+x, \frac{1}{2}-y, z$
O(2)	2.83	$-x, \frac{1}{2}+y, \frac{1}{2}-z$	O(10)	2.85	x, y, z
O(6)	2.85	x, y, z	O(13)	2.84	$x-\frac{1}{2}, \frac{1}{2}-y, -z$
O(7)	2.67	x, y, z			

Angles (°) about the potassium atom			
O(1)-K-O(2)	56.0	O(6)-K-O(7)	62.4
O(1)-K-O(6)	144.8	O(6)-K-O(9)	140.6
O(1)-K-O(7)	109.5	O(6)-K-O(10)	90.0
O(1)-K-O(9)	74.4	O(6)-K-O(13)	66.8
O(1)-K-O(10)	81.7	O(7)-K-O(9)	119.1
O(1)-K-O(13)	147.9	O(7)-K-O(10)	146.4
O(2)-K-O(6)	88.9	O(7)-K-O(13)	77.0
O(2)-K-O(7)	81.6	O(9)-K-O(10)	94.3
O(2)-K-O(9)	130.5	O(9)-K-O(13)	75.2
O(2)-K-O(10)	79.1	O(10)-K-O(13)	110.8
O(2)-K-O(13)	153.0		

gallate 1:1 complex [24] which displays a similar stacked layer lattice structure in which in-plane cohesion is achieved by extensive hydrogen bonding, and the effect of alkali metal cations on the self-association of polyphenolic substrates in aqueous media ([15, 23]; C. M. Spencer, R. Martin, T. H. Lilley, E. Haslam and D. Magnolato, unpublished work). Bearing in mind the inherent uncertainties involved in extrapolating from crystal structure data these findings nevertheless substantiate the view that the non-covalent interactions involving phenolic substrates in aqueous media probably utilizes the range of forces outlined above. In their earlier paper, Horman and Viani [19] put forward a model for the structure of the caffeine potassium chlorogenate complex as it exists in aqueous solution (Fig. 2). The model is consistent with the known 'stacking' behaviour of aryl substrates and the magnetic anisotropy associated with such systems. There is, moreover, a striking resemblance (Figs 2 and 4) between this model and the crystal structure of the complex (they differ in the relative orientation of the caffeine and caffeoyl rings), such as to suggest that complexes of the type discussed by Horman and Viani [19] are precursors in crystal formation and growth.

Table 4. Caffeine–potassium chlorogenate complex. Hydrogen bonds (Å) with angles about hydrogen and relevant symmetry operators

	X···Y	X–H	H···Y	X–H···Y
O(1)-H(14)···O(12)	2.58	1.31	1.36	151 (x, y, z)
O(2)-H(13)···O(13)	2.73	1.16	1.78	135 ($-x, y-\frac{1}{2}, \frac{1}{2}-z$)
O(5)-H(15)···N(3)	2.96	0.97	2.09	149 ($x, 1-y, z$)
O(6)-H(16)···O(9)	2.79	0.84	2.03	150 ($1+x, y, z$)
O(12)-H(29)···O(8)	2.78	0.94	1.87	161 ($-x-\frac{1}{2}, -y, \frac{1}{2}+z$)

UM00014040
NOVARTIS EXHIBIT 1517
Novartis v. Regents, IPR2023-01347
Page 2786 of 4460

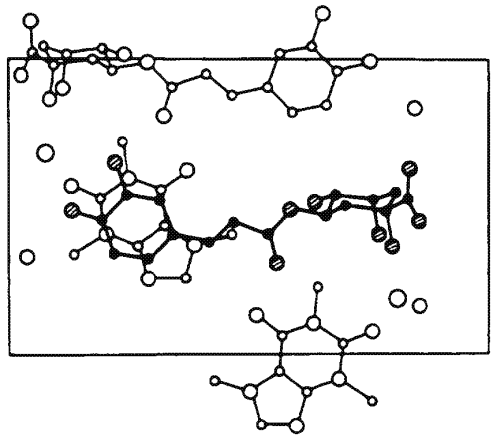


Fig. 4. Caffeine potassium chlorogenate 1:1 complex—layer lattice structure.

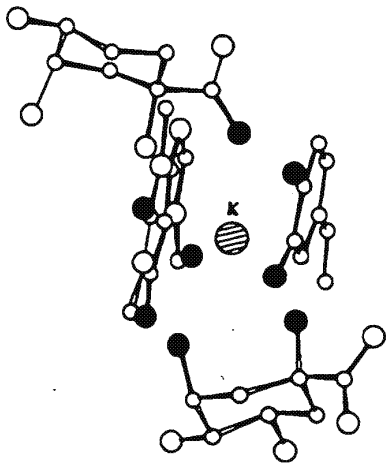


Fig. 6. Caffeine–potassium chlorogenate 1:1 complex coordination around the potassium ion.

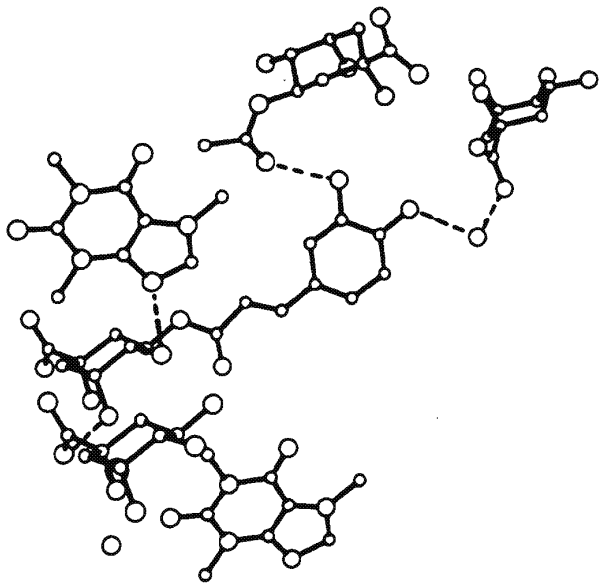
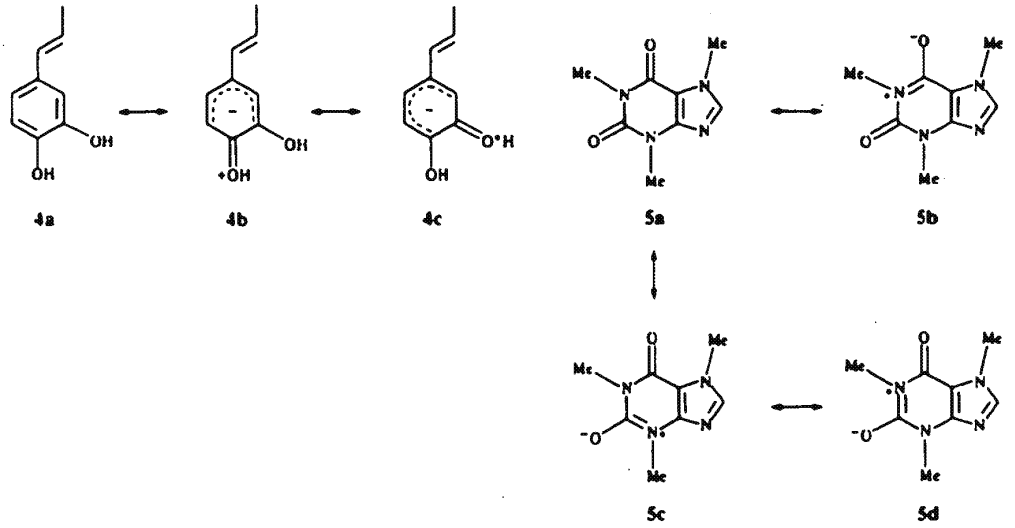


Fig. 5. Caffeine potassium chlorogenate 1:1 complex hydrogen bonding network.

Some comment should perhaps finally be made of the particular alternating plane to plane stacking arrangement of aromatic nuclei found in the caffeine-potassium chlorogenate and other phenolic–caffeine complexes [24]. π-Molecular complexes formed between aromatic electron donor and acceptor pairs display the same characteristics [25]; however, the UV absorption spectra of the caffeine–phenol complexes examined in these studies show no evidence of UV charge-transfer bonds. The term 'polarization bonding' has been used [25] to describe both charge-transfer bonding [26] and the generally weaker interactions between polar groups of one component and a polarizable second component [27]. For weak non-covalent bonding of this type the principal feature to be expected is the juxtaposition of the polarizable groups of one component and the polarizable regions of the second. It is interesting therefore to note that in the various phenol–caffeine complexes the phenolic groups and associated nuclei are stacked generally above the six-membered ring of the caffeine molecule. This suggests that

UM00014041
NOVARTIS EXHIBIT 1517
Novartis v. Regents, IPR2023-01347
Page 2787 of 4460



4a 4b 4c 5a 5b 5c 5d

in this form of association the two components develop polar characteristics of the type shown (**4a–4c**; **5a–5d**).

Acknowledgement The authors thank Nestec Ltd. Switzerland for a grant (R.M.) and for permission to publish this work.

REFERENCES

1. Creighton, T. E. (1983) *Proteins—Structure and Molecular Properties*, p. 335. Freeman, New York.
2. Feeny, P. P. (1976) *Recent Adv. Phytochem.* **10**, 1.
3. Rhoades, D. F. (1979) in *Herbivores—Their Interaction with Secondary Plant Metabolites* (Rosenthal, G. A. and Janzen, D. H., eds) p. 3. Academic Press, London.
4. Swain, T. (1977) *Annu. Rev. Plant Physiol.* **28**, 479.
5. Lilley, T. H. and Haslam, E. (1985) *Annu. Proc. Phytochem. Soc. Europe* **25**, 237.
6. Haslam, E. (1981) in *The Biochemistry of Plants* (Conn, E. E., ed.) Vol. 7, p. 527. Academic Press, London.
7. Bate-Smith, E. C. (1954) *Food* **23**, 124.
8. Price, M. L. and Butler, L. G. (1980) *Tannins and Nutrition*, Bulletin No. 272. Purdue University Agricultural Experimental Station.
9. Benoit, R. E. and Starkey, R. L. (1968) *Soil Sci.* **105**, 203, 291.
10. Perry, L. M. (1980) *Medical Plants of S. E. Asia*. MIT Press, Cambridge, MA.
11. McManus, J. P., Davis, K. G., Beart, J. E., Gaffney, S. H., Lilley, T. H. and Haslam, E. (1985) *J. Chem. Soc. Perkin Trans.* 2, 1429.
12. Beart, J. E., Lilley, T. H. and Haslam, E. (1985) *Phytochemistry* **24**, 33.
13. Loomis, W. D. (1974) *Methods Enzymol.* **31**, 528.
14. McManus, J. P., Davis, K. G., Haslam, E. and Lilley, T. H. (1981) *J. Chem. Soc. Chem. Commun.* 309.
15. Gaffney, S. H., Martin, R., Lilley, T. H., Haslam, E. and Magnolato, D. (1986) *J. Chem. Soc. Chem. Commun.* 107.
16. Herrmann, K. (1978) *Fortschr. Chem. Org. Naturst.* **35**, 73.
17. Gorter, K. (1907) *Justus Liebig's Ann. Chem.* **358**, 327; (1908) **359**, 217.
18. Sondheimer, E., Covitz, F. and Marquisee, M. J. (1961) *Arch. Biochem. Biophys.* **93**, 63.
19. Horman, I. and Viani, R. (1972) *J. Food Sci.* **37**, 925.
20. Main, P. (1900) MULTAN-80, Department of Physics, University of York, York.
21. Carruthers, J. P. (1975) *CRYSTALS User Manual* Oxford University Computing Laboratory, Oxford.
22. Sutor, D. J. (1958) *Acta Crystallogr.* **11**, 453.
23. Craven, B. M. and Gartland, G. L. (1970) *J. Pharm. Sci.* **59**, 1666.
24. Martin, R., Bailey, N. A., Falshaw, C. P., Begley, M. J., Lilley, T. H., Haslam, E. and Magnolato, D. (1986) *J. Chem. Soc. Chem. Commun.* 105.
25. Wallwork, S. C. (1961) *J. Chem. Soc.* 494.
26. Mulliken, R. S. (1952) *J. Am. Chem. Soc.* **74**, 811.
27. Prout, C. K. and Wallwork, S. C. (1966) *Acta Crystallogr.* **21**, 449.

UM00014042
NOVARTIS EXHIBIT 1517
Novartis v. Regents, IPR2023-01347
Page 2788 of 4460

Letters to the Editor

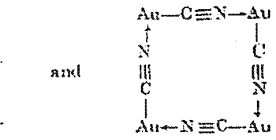
The Editor does not hold himself responsible for opinions expressed by his correspondents. He cannot undertake to return, or to correspond with the writers of, rejected manuscripts intended for this or any other part of NATURE. *No notice is taken of anonymous communications.*

NOTES ON POINTS IN SOME OF THIS WEEK'S LETTERS APPEAR ON P. 590.

CORRESPONDENTS ARE INVITED TO ATTACH SIMILAR SUMMARIES TO THEIR COMMUNICATIONS.

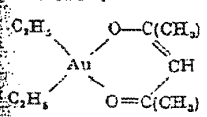
Aurous Compounds: Gold Mirrors

The volatile aurous compounds described by Dr. Gamble and Dr. A. F. Wells[1] provide further evidence of the fact that, in its aurous compounds, gold is always 2-covalent. Constitutionally analogous mercury and nitrogen compounds are also known. It is significant that whenever gold is in solution in the aurous condition, the metal is always present in the complex ion. This is shown in the cases of such compounds as potassium aurocyanide, $KAu(CN)_2$, and hydrobromoaurous acid, $HAuBr_2$. Unlike the auric ion, the aurous ion appears to be capable of existence, and some investigations[2] have indicated that the probable constitutions of the aurous ion and of aurous cyanide are respectively:



Even in its simplest compounds, aurous gold is always to be 2-covalent, while auric gold is 4-covalent and the four valencies are directed with the gold atom[3].

The production of gold mirrors by the heat decomposition of gold compounds is, of course, not new. Faraday in 1856 showed that drops of "gold solution" evaporated in watch glasses and heated over a spirit lamp produced films which exhibited by transmitted light the same colours as the gold-containing liquids (Chemistry Exhibit, 157, Science Museum). In 1930, brilliant mirrors or films of metallic gold were produced by gently heating the 2-covalent and 4-covalent gold compound, dimethylacetonegold[4]:



Some of the first pure gold films produced at low temperatures by the process recently described can be seen in the gold exhibit in the Mineral Court of the Imperial Institute.

CHARLES S. GIBSON.

Chemistry Department,
Royal Hospital Medical School,
London, S.E.1.
Sept. 20.

[1] *Nature*, **140**, 502 (Sept. 18, 1937).
[2] *Z. anorg. Chem.*, **220**, 360 (1934); **219**, 1024 (1935).
[3] Webster, *J. Chem. Soc.*, 1635 (1936). Gibson and co-workers, forthcoming publication.
[4] Simonsen, *J. Chem. Soc.*, 2532 (1930).
[5] *Nature*, **140**, 279 (Aug. 14, 1937).

Structure of Organic Molecular Compounds

THREE general conceptions are current as to the nature of the valence forces responsible for the formation of organic molecular compounds, each of which may conceivably be true as the limiting case in certain classes of compound:

(*a*) The molecular compounds are merely lattice compounds, involving no genuine chemical bonding, but depending for their formation and composition upon considerations of packing. This probably applies to such compounds[1] as $CHI_3.3S_8$.

(*b*) Combination occurs by the formation of true co-ordinate links, as in inorganic molecular compounds. This view has been developed, probably incorrectly, in connexion with the polynitrobenzene – hydrocarbon compounds[2].

(*c*) Union is effected by the forces of interaction between strongly polar groups and the highly anisotropic, polarizable aromatic systems[3]. The London forces thus involved are, in a sense, intermediate between van der Waals's attractions and true covalencies.

During the past few months, an X-ray examination has been made of the quinhydrones and related compounds, with the view of eliciting the evidence of crystal structure as to their constitution. A similar approach to the nitrobenzene – hydrocarbon compounds was made by Hertel[4], without conclusive results. The full results of the present investigation will shortly be presented elsewhere, but the following morphotropic considerations appear to lend the problem nearer to a solution.

(1) The discrete existence of quinonoid and quinoloid units in the structure, necessitated by the revised quinhydrone structure of Palacios and Fox[5], is confirmed.

(2) The identity of the *a* and *b* dimensions in ordinary quinhydrone and in α-naphthoquinone quinhydrone (see table) show that the quinone and quinol groupings lie essentially in the (001) plane, with the breadth of the molecules along *c*, as was advanced for quinhydrone[5].

(3) For dimensional reasons, the quinone and quinol units can alternate only along the *a* and *c* directions, but not along *b*. The formation of quinhydrone by a species of infinite hydrogen bond polymerization[4], which, from the orientation of the molecules, could only take place along *b*, is thereby excluded.

(4) In phenoquinone, $C_6H_4O_2.2C_6H_5OH$, *b* and *c* are essentially unchanged, whereas *a* is exactly 3/2 times the *a* dimension of quinhydrone. Clear evidence is thus afforded that the components alternate along *a*. In various *p*-substituted phenoquinones, *a* and *c* are also slightly modified (due to the bulk of the substituents and to the inclination of the molecules to (001)) while retaining the same essential characteristics.

UM00014043
NOVARTIS EXHIBIT 1517
Novartis v. Regents, IPR2023-01347
Page 2789 of 4460

(5) The relation of the remarkably stable compounds of chloranil and bromanil with hexamethyl benzene, etc.—for example, $C_6Br_2O_2.C_6(CH_3)_6$—to the quinhydrones[1] is confirmed. The same alternation of components along a is observed, with identical a spacing; this brings the planes of the bromanil and the hexamethylbenzene molecules practically into contact. In these compounds there can scarcely be any question either of hydrogen bonds or of the formation of co-ordinate links.

(6) The direction of maximum light absorption in the quinhydrones and both the maximum of light absorption and the slow vibrational direction in the even more strongly pleochroic bromanil-hexamethyl benzene compound coincide with a.

	a	b	c	β	n	Space group
Quinhydrone	7·70	6·04	21·8	90°	4	C^1_{2h}
$C_{10}H_2O_2.C_6H_4(OH)_2$	7·70	6·16	27·4	Rhombic	4	P^1
$C_6Br_2O_2.C_6(CH_3)_6$	7·40	8·83	28·7	Rhombic	4	P^5
$C_6H_4O_2.2C_6H_5OH$	11·50	6·16	22·2	100°	4	C^1_{2h}
$C_6H_4O_2.2CH_3C_6H_4OH$	11·83	6·2	24·6	97°	4	C^5_{2h}
$C_6H_4O_2.2Br.C_6H_4OH$	12·16	6·16	24·3	96°	4	C^5_{2h}
$C_6H_4O_2.2Cl.C_6H_4OH$	12·00	6·16	23·5	97°	4	C^5_{2h}

Along this direction the aromatic molecules are stacked plane to plane at a perpendicular distance of the order of 3 A. The trend of the evidence makes the conclusion inevitable that this represents also the direction of bonding, in which case the mechanism (*a*) is the most probable. The formation of hydrogen bonds in quinhydrone is not necessarily excluded, and their presence is now being sought by the elegant method of Robertson and Ubbelohde[7].

J. Stuart Anderson.

Department of Inorganic Chemistry,
Imperial College of Science,
South Kensington, S.W.7.

[1] Bernal, *Trans. Faraday Soc.*, **33**, 211 (1936).
[2] Bennett and Willis, *J. Chem. Soc.*, 256 (1929).
[3] cf. Briegleb, *Z. phys. Chem.*, B, **26**, 62 (1934).
[4] Herbst, *Z. phys. Chem.*, B, **11**, 59, 77 (1930); **22**, 289 (1933).
[5] *Anal. Fis. Quim.*, **30**, 421 (1932); **33**, 627 (1935).
[6] cf. Chem. Soc., Annual Reports, **30**, 429 (1933).
[7] Pfeiffer, *Ann.*, **404**, 1 (1914).
[8] Nature, **139**, 501 (1937).

Duality of the Coproporphyrins in Bovine Congenital Porphyrinuria

Of the four theoretically possible isomeric types of porphyrins, only those belonging to Series I and III have so far been encountered in Nature. Haemoglobin, bilirubin, cytochrome, etc., are Series III derivatives. Series III has thus come to be regarded as the normal or 'physiological' type. Excretion of excessive amounts of porphyrins belonging to Series III does, however, occur in certain pathological states including lead poisoning (Grotepass[1], Mertens[2], Fischer and Duesberg[3]), pigment cirrhosis of the liver (Dobriner[4]), hepatic tumours (Dobriner[4]) and after administration of salvarsan (Schreus[5]). The uroporphyrin excreted in acute idiopathic porphyrinuria has been shown to be uroporphyrin III (Waldenström[6], Mertens[2]), whilst Dobriner[4] has detected the simultaneous presence of coproporphyrins I and III in the stool from one such case.

The pigments formed in excessive amount by congenital porphyrinurics were until recently thought to belong exclusively to Series I, but Fischer and Hofmann[8,10], working with material from one case 'Petry', and Rimington[11,12] studying porphyrinuric bovines, have shown that large quantities of uroporphyrin III accompany coproporphyrin I in this disease.

We have now been able to isolate coproporphyrin III from the urinary and faecal pigments of a mixture of the same bovines, thus extending the duality also to the coproporphyrins. Evidence suggestive of the presence of coproporphyrin III in small amounts in the bile porphyrins of a normal bovine case had already been obtained spectroscopically by Rimington[13], but the quantities available were insufficient to allow of crystallization.

In the present instance the mixed coproporphyrin fraction (free from uroporphyrin) was esterified and the more soluble coproporphyrin III methyl ester extracted by stirring with cold methyl alcohol (compare Dobriner[4]; we are indebted to Dr. E. Mertens for first suggesting this technique). After repetitions of this procedure the coproporphyrin III ester was dissolved in a little hot dioxane, a little methyl alcohol added, and then sufficient water (about 10 per cent) to render the mixture slightly opalescent. On standing in the ice-chest, the porphyrin ester crystallized in micro-crystalline form, m.p. 138/172° (dec.). Synthetic coproporphyrin III methyl ester, kindly supplied by Prof. H. Fischer, whom we wish to thank, crystallized in the same way, had m.p. 140° (dec.) 138°. Spectrum of ester in ether: 625·7–587·5–566·7; 531·6; 498·7. Three different preparations were made.

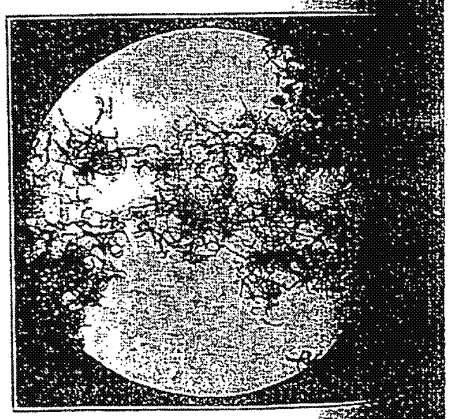


Fig. 1.

Coproporphyrin III from urine: bovine porphyrinuria. × about 100.

The occurrence of Series III porphyrins, together with those of Series I in congenital porphyrinuria, may be traceable to a secondary toxic effect (Fischer and Hofmann[10]), but is equally readily explicable on the basis of the scheme put forward by Rimington[14], picturing a catalysed synthetic mechanism in the haematopoietic tissue.

We have also encountered another porphyrin in these urines which we believe to be

UM00014044
NOVARTIS EXHIBIT 1517
Novartis v. Regents, IPR2023-01347
Page 2790 of 4460

This Page is Inserted by IFW Indexing and Scanning Operations and is not part of the Official Record

BEST AVAILABLE IMAGES

Defective images within this document are accurate representations of the original documents submitted by the applicant.

Defects in the images include but are not limited to the items checked:

- ☐ BLACK BORDERS
- ☐ IMAGE CUT OFF AT TOP, BOTTOM OR SIDES
- ☐ FADED TEXT OR DRAWING
- ☐ BLURRED OR ILLEGIBLE TEXT OR DRAWING
- ☐ SKEWED/SLANTED IMAGES
- ☐ COLOR OR BLACK AND WHITE PHOTOGRAPHS
- ☐ GRAY SCALE DOCUMENTS
- ☐ LINES OR MARKS ON ORIGINAL DOCUMENT
- ☐ REFERENCE(S) OR EXHIBIT(S) SUBMITTED ARE POOR QUALITY
- ☐ OTHER: _____

IMAGES ARE BEST AVAILABLE COPY.
As rescanning these documents will not correct the image problems checked, please do not report these problems to the IFW Image Problem Mailbox.

American Crystallographic Association - Series 2 Papers and Abstracts

L6 THE CRYSTAL STRUCTURE OF THE 1:2 ADDUCT OF POTASSIUM TRIIODIDE AND 5,5-DIETHYLBARBITURIC ACID (BARBITAL). A. H. Robbins and B. M. Craven, Department of Crystallography, University of Pittsburgh, Pittsburgh, Pa. 15213. p87 (1973)

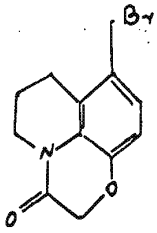
The adduct forms orthorhombic crystals, space group $Pbn2_1$, with unit cell dimensions a = 15.86, b = 13.76, and c = 11.89 Å. There are four formula units per cell. A three-circle automatic diffractometer was used to measure 1616 intensities (Zr-filtered Mo Kα radiation). All non-hydrogen atoms were located by Patterson methods and three-dimensional Fourier syntheses. Refinement of 140 atomic parameters using full-matrix least squares resulted in a final R factor of 0.067 for observed reflections.

The structure consists of triiodide ions and hydrogen-bonded barbital molecules packed in alternate sheets along (010). Potassium ions interact with both barbital oxygen atoms and triiodide ions. The triiodide ion is nearly linear.

This research was supported by Grant Nos. NS-02763 and GM-01728 of the U. S. Public Health Service, National Institutes of Health.

L7
THE CRYSTAL AND MOLECULAR STRUCTURE OF $C_{12}H_{12}NO_2Br$, A DIHYDROQUINOLINE DERIVATIVE.
T.D.Fantozzi and Gopinath Kartha, Roswell Park Memorial Institute, Buffalo, N.Y. 14203.

The compound $C_{12}H_{12}NO_2Br$ crystallizes in the monoclinic system with unit cell parameters (at 22±2° C), a = 14.985 A, b = 16.660 A, c = 9.117 A and β = 96.0°. The space group is $P2_1/a$ with two molecules in the asymmetric unit. Intensity data (to the limit of 2θ = 155°) consisting of 4105 reflections were collected manually on a G.E.XRD-5 diffractometer. The structure was solved by the heavy atom method and refined isotropically to a reliability index of 0.08. The two molecules are nearly parallel to each other. The CO groups in both molecules are preferentially oriented away from the benzene ring while the methyl groups take up the axial configuration, confirming the earlier NMR results (Nagarajan et al, Tetrahedron, 1967, 23, 1683).
This work is supported by research grants from the National Institute of Health and the National Science Foundation.



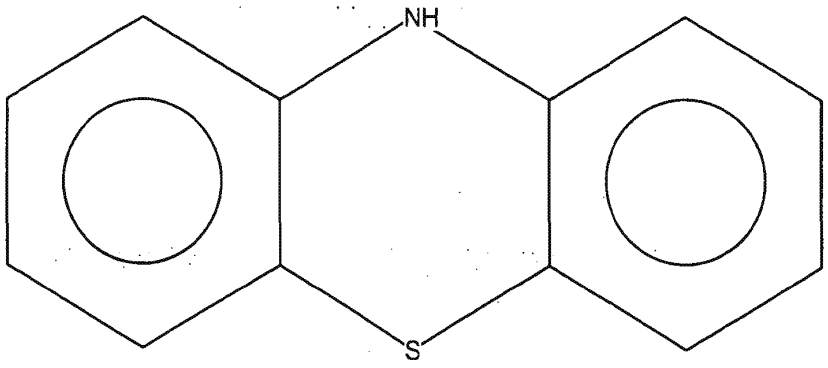
Supplied by The British Library - "The world's knowledge"

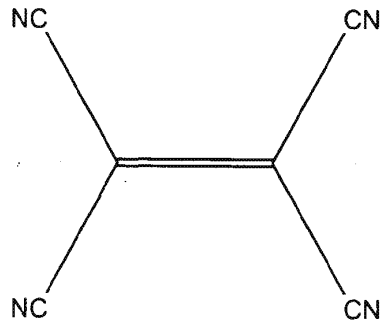
UM00014046
NOVARTIS EXHIBIT 1517
Novartis v. Regents, IPR2023-01347
Page 2792 of 4460

Reference:	P.Beerges, J.Kudnik, G.Klar, E.S.Martinez, R.D.Calleja (1994) *Private Communication* ,
Formula:	$C_{12}\,H_9\,N_1\,S_1,C_6\,N_4$
Compound Name:	Phenothiazine tetracyanoethylene

Space Group:	P21/c	***Cell:***	***a***	14.302(4)	***b***	7.408(1)	***c*** 15.207(2)
Space Group No.:	14	***(Å,°)***	α	90.00	β	95.40(1)	γ 90.00

R-Factor (%):	4.20	***Temperature(K):***	295	***Density(g/cm^3):***	1.356





Journal of Thermal Analysis and Calorimetry, Vol. 69 (2002) 281–290

THERMAL, FTIR AND XRD STUDY ON SOME 1:1 MOLECULAR COMPOUNDS OF THEOPHYLLINE

J. Madarász[1*], *P. Bombicz*[2], *K. Jármi*[1**], *M. Bán*[1], *G. Pokol*[1] *and S. Gál*[3]

[1]Institute of General and Analytical Chemistry, Budapest University of Technology and Economics, H-1521 Budapest, Hungary
[2]Institute of Chemistry, Chemical Research Centre, Hungarian Academy of Sciences, P.O. Box 17, H-1525 Budapest, Hungary
[3]Research Group for Technical Analytical Chemistry of the Hungarian Academy of Sciences, H-1521 Budapest, Hungary

Abstract

Thermal stability and structural features of three newly synthesized 1:1 lattice compounds of theophylline (**th**) with ethylenediamine carbamate (**enCO$_2$**), 1,10-phenanthroline (**phen**), and 5-sulfosalicylic acid (**sa-5-SO$_3$H**) have been studied in comparison with those of the theophylline compounds with ethanolamine (**ea**) and salicylic acid (**sa**). Simultaneous TG-DTA measurements, FTIR spectroscopy and X-ray diffraction have been carried out to get information on the various structural units of these solid inclusions, especially on the actual form (molecule, anion or cation) of theophylline moieties built in. Theophyllinate and theophyllinium ions have been found in the ethanolammonium-theophyllinate (1:1) (**1**, **eaH$^+$·th$^-$**) and the theophyllinium salicylic acid 5-sulfonate monohydrate (1:1:1), (**5**, **thH$^+$·saSO$_3^-$·H$_2$O**), respectively. Whilst the 1:1 complexes with 1,10-phenanthroline (**2**, **th·phen**), ethylenediamine carbamate (**3**, **th·enCO$_2$**), and salicylic acid (**4**, **th·sa**) contain neutral theophylline moieties associated with H-bonds. In compound (**3**) the zwitterion of N-(2-ammonium-ethyl)carbamate (NH_3^+-CH_2-CH_2-NH-CO_2^-) is present.

Keywords: ethanolamine, FTIR, 1,10-phenanthroline, salicylic acid and 5-sulfosalicylic acid, simultaneous TG-DTA, theophylline lattice compounds, ethylenediamine carbamate, unit cell parameters, XRD

Introduction

The solubility of drug theophylline in water can be increased by either basic or acidic additives. In medical injections used for treatment of acute asthma usually the base ethylenediamine (**en**) is applied, anyhow there are efforts on further improvement of this medicine based on theophylline [1]. The hydrated solid molecular compound of theophylline with ethylenediamine (in 2:1 molar ratio), called aminophylline, is a drug described in several Pharmacopeias. From the solutions prepared with additives enhanc-

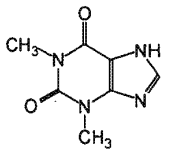
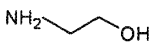
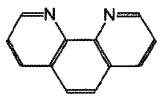
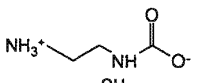
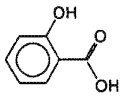
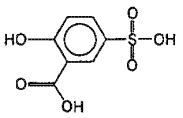
* Author for correspondence: E-mail: madarasz@tki.aak.bme.hu or madarasz@mail.bme.hu
** Present address: Alpharma Kft. H-1107 Budapest, Hungary

1418–2874/2002/ $ 5.00
Akadémiai Kiadó, Budapest
© 2002 Akadémiai Kiadó, Budapest
Kluwer Academic Publishers, Dordrecht

UM00014048
NOVARTIS EXHIBIT 1517
Novartis v. Regents, IPR2023-01347
Page 2794 of 4460

ing solubility, usually various lattice compounds of theophylline can be crystallized. Nishijo and co-workers synthesized a series of 2:1 theophylline complexes with α,ω-alkanediamines (n = 4–8) and characterized by TG-DTA, powder XRD, and IR spectroscopy [2]. They also looked for similar solid molecular compounds with several aliphatic and aromatic monoamines and aminoalcohols. The theophylline compounds formed with 1:1 molar ratio (including that of ethanolamine, **ea**) were also characterized, and a scheme for their H bonds was proposed based on their IR data [3, 4].

Table 1 Thermal behaviour and dissociation exponent(s) of the pure constituent compounds

Compounds	Name	pK_s, pK_b, pI
	Theophylline (*m.p.*: 269–270°C)	amphoteric: $pK_s = 8.6$ ($pK_b^{corr} = 5.4$) $pK_b = 13.72$ ($pK_s^{corr} = 0.28$)
	ethanolamine (*b.p.*:170°C)	$pK_b = 4.5$ ($pK_s^{corr} = 9.5$
	1,10-phenanthroline (*m.p.*: 114–117°C) 1,10-phenanthroline·H_2O (*m.p.*: 100–104°C, dec.)	$pK_{b,1} = 5.05$ ($pK_{s,1}^{corr}$ =8.95) $pK_{b,2} = 14.5$ ($pK_{s,2}^{corr} = -0.5$)
	ethylenediamine carbamate (subl.; *m.p.*: 171°C in sealed capillary [16])	isoelectric pH: $pI = 8.4$ [17]
	salicylic acid (*m.p.*: 159–161°C)	$pK_{s,1} = 3.0$ ($pK_{b,1}^{corr} = 11.0$) $pK_{s,2} = 13.4$ ($pK_{b,2}^{corr} = 0.6$)
	5-sulfosalicylic acid·$2H_2O$ (*m.p.*: 110°C, dec.)	$pK_{s,1} = 2.49$ ($pK_{b,1}^{corr} = 11.51$) $pK_{s,2} = 11.74$ ($pK_{b,2}^{corr} = 2.24$)

Sekiya and co-workers [5] found new theophylline complexes with eight differently substituted aromatic acids (including salicylic acid, **sa**) and phenols. They characterized the 1:1 compounds by elemental analyses, melting temperature ranges, and IR spectra. Structural information based on single crystal X-ray diffraction are available on non-ionic 1:1 molecular compounds with *p*-nitroaniline [6], urea [7], sulfathiazol [8], and 5-chlorosalicylic acid [9] in comparison with theophylline monohydrate [10] and anhydrous theophylline [11]. Presence of theophyllinium cat-

UM00014049
NOVARTIS EXHIBIT 1517
Novartis v. Regents, IPR2023-01347
Page 2795 of 4460

ion is structurally proved only in theophylline hydrochloride [12]. Crystal and molecular structure of 2:1 type compounds are known already for bis(theophylline) phenobarbital [13] and bis(theophylline) 5-fluorouracyl monohydrate [14].

As part of our ongoing research on preparation and structural characterization of lattice compounds and metal complexes [15] of theophylline, we report here the results of our investigation on five 1:1 type solid compounds of theophylline and various organic bases and acids (Table 1) by simultaneous TG-DTA, powder X-ray diffraction and FTIR spectroscopy prior to their single crystal X-ray diffraction studies [18].

Experimental

Preparation of 1 ($eaH^+ \cdot th^-$) and 3 ($th \cdot enCO_2$) crystals

Well-grown colourless crystals of ethanolammonium theophyllinate (1:1 compound of ethanolamine and theophylline, **1**, $eaH^+ \cdot th^-$) and theophylline N-(2-ammonium -ethyl)carbamate (1:1 compound of theophylline and ethylenediamine carbamate, **3**, $th \cdot enCO_2$) have been obtained in partially covered vessels at ambient circumstances in the laboratory after 2 weeks by slow evaporation of 6 mL aqueous solutions of theophylline (**th**, 180.2 mg, 1 mmol) and 1 mL of ethanolamine (**ea**, ca. 16.5 mmol) or ethylenediamine (**en**, ca. 15 mmol), respectively. In the latter case the ethylenediamine carbamate ($enCO_2$) formed slowly and spontaneously over the solution surface as reaction product of **en** and CO_2 from air and than this air-born fine white powder was dissolved in the solution, as well.

Preparation of crystalline 2 (th·phen), 4 (th·sa) and 5 ($thH^+ \cdot saSO_3^- \cdot H_2O$)

Anhydrous theophylline (180.2 mg, 1 mmol) was dissolved in 5 mL warm aqueous solutions containing stoichiometric amount of 1,10-phenanthroline monohydrate (198.3 mg, 1 mmol), salicylic acid (138.2 mg, 1 mmol), or 5-sulfosalicylic acid dihydrate (254.2 mg, 1 mmol), respectively. The compound with 1,10-phenanthroline (**2**, **th·phen**) was obtained immediately as fine fibers, while the compounds with salicylic acids (**4**, **th·sa** and **5**, $thH^+ \cdot saSO_3^- \cdot H_2O$) crystallized as fine needles after few days or a week.

Elemental analysis of 1–5

C, H, and N analyses of samples **1–5** were carried out at the Microanalytical Laboratory of Loránd Eötvös University of Budapest (ELTE-TTK, Budapest, Hungary) in a Heraeus-CHN-O-Rapid analyzer.

UM00014050
NOVARTIS EXHIBIT 1517
Novartis v. Regents, IPR2023-01347
Page 2796 of 4460

FTIR spectroscopy

Fourier transformed infrared spectra of compounds **1–5** and the starting substances were recorded on a Perkin Elmer FTIR System 2000 and a Biorad Excalibur FTS 3000 spectrometer in the range of 4000–400 cm^{-1} using KBr pellets.

Thermal analysis

Thermal behaviour of theophylline compounds and their pure constituents were investigated to 600°C by simultaneous TG/DTA apparatus (SDT 2960, TA Instruments). Sample size of 9–19 mg, open Pt crucibles, Al_2O_3 as reference material and a heating rate of 10°C min^{-1} were used. The measurements were carried out in flowing air atmosphere at a rate of 130 mL min^{-1}.

X-ray diffraction

Single crystal X-ray data collection of **1** (**$eaH^+ \cdot th^-$**), **3** (**$th \cdot enCO_2$**), and **5** (**$thH^+ \cdot saSO_3^- \cdot H_2O$**) were performed on an Enraf-Nonius CAD4 single crystal diffractometer using CuK_α or MoK_α radiation. X-ray powder patterns of compounds **1–5** and their starting materials were recorded on an FPM HZG4 powder diffractometer using Ni filtered CuK_α radiation. Measured and calculated powder XRD patterns were compared and are available from the authors upon request.

Table 2 Elemental (C, H, and N) composition of 1:1 compounds of theophylline **1–5** in%

Lattice compounds	Formula and formula mass FW/g mol^{-1}	Calculated/%			Found/%		
		C	N	H	C	N	H
Ethanolammonium theophyllinate (**1**, **$eaH^+ \cdot th^-$**)	$C_9H_{15}N_5O_3$ 241.25	44.81	29.0	6.27	44.90	28.61	6.32
Theophylline 1.10-phenantroline: = 1:1 (**2**, **th·phen**)	$C_{19}H_{16}N_6O_2$ 360.38	63.33	23.32	4.48	62.78	22.64	4.73
Theophylline:ethylene diamine carbamate = 1:1 (**3**, **$th \cdot enCO_2$**)	$C_{10}H_{16}N_6O_4$ 287.24	42.25	29.56	5.67	42.26	29.19	6.07
Theophylline : salicylic acid = 1:1 (**4**, **th·sa**)	$C_{14}H_{14}N_4O_5$ 318.29	52.83	17.60	4.43	52.93	17.62	4.80
Theophyllinium salicylic acid 5-sulfonate monohydrate (1:1:1) (**5**, **$thH^+ \cdot saSO_3^- \cdot H_2O$**)	$C_{14}H_{14}N_4O_8S$ 416.37	40.39	13.46	3.87	40.45	13.49	3.87

UM00014051
NOVARTIS EXHIBIT 1517
Novartis v. Regents, IPR2023-01347
Page 2797 of 4460

Results and discussion

Specific X-ray diffraction patterns of 1–5

Powders of samples **1**–**5** gave unique X-ray diffraction patterns and no traces of the parent compounds were observed. The obtained C, H, and N content of the samples (Table 2). confirmed formation of substances with molar ratio of theophylline:additives = 1:1 (in the case of **5**, **thH$^+$·saSO$_3^-$·H$_2$O** one molecule of water of crystallization is also present).

In case of ethanolammonium theophyllinate (**1**, **eaH$^+$·th$^-$**), theophylline N-(2-ammonium-ethyl)carbamate (**3**, **th·enCO$_2$**), and theophyllinium salicylic acid 5-sulfonate monohydrate (**5**, **thH$^+$·saSO$_3^-$·H$_2$O**) determination of unit cell parameters and crystal structures have been carried out by single crystal X-ray diffraction. The summary of crystal data of compound **1**, **3** and **5** is given in Table 3. Further details on the crystal and molecular structures of **1**, **3** and **5** will be published elsewhere [18].

Table 3 Crystal system, space group, unit cell data and *R*-factor of structure determination for lattice compounds **1**, **3** and **5**

Crystallographic data	Ethanolammonium theophyllinate (**1**, **eaH$^+$·th$^-$**)	Theophylline N-(2-ammonium-ethyl) carbamate (1:1) (**3**, **th·enCO$_2$**)	Theophyllinium salicylic acid 5-sulfonate monohydrate (1:1:1) (**5**, **thH$^+$·saSO$_3^-$·H$_2$O**)
Crystal system	triclinic	monoclinic	monoclinic
Space group	*P*-1 (No.2)	*Cc* (No.9)	*Cc* (No.9)
a/Å,	8.497(1)	8.949(2)	14.809(1)
b/Å,	8.581(1)	21.194(2)	8.779(1)
c/Å,	8.852(1)	7.339(2)	14.628(1)
α/°,	89.63(1)	90	90
β/°,	77.42(1)	117.85(2)	112.74(3)
γ/°,	63.53(1)	90	90
R	0.0450	0.0463	0.0388

Structural comparison based on the FTIR spectra of 1–5

The peak positions of some characteristic IR absorption bands of **1**–**5** and those of anhydrous theophylline are summarized in Table 4.

The actual positions of stretching vibrations of the two carbonyl groups in the theophylline moiety have diagnostic value. Their wavenumbers are usually lowered if the carbonyl groups take part in stronger H-bonds compared to the anhydrous theophylline. Their value decreases much more if theophylline looses its N7 proton, and becomes theophyllinate anion [15]. The observed low $\nu_{C=O}$ values for ethanol-

UM00014052
NOVARTIS EXHIBIT 1517
Novartis v. Regents, IPR2023-01347
Page 2798 of 4460

ammonium theophyllinate **1** (**eaH$^+$·th$^-$**) indicated [3] the presence of theophyllinate anion what was confirmed by our single crystal study [18]. In molecules **2**, **3** and **4** the slightly lowered $\nu_{C=O}$ values are attributed to the effect of strong H-bonds in which the neutral theophylline moiety takes part, as can be seen in the crystal structure of theophylline N-(2-ammonium-ethyl)carbamate **3** [18] and implied also by the published IR spectra of theophylline : *p*-nitrophenol (1:1) compound [5]. The protonation of theophylline on N9 position causes only a slight upward shift of $\nu_{C=O}$ wavenumbers compared to the original values of theophylline. In case of theophyllinium salicylic acid 5-sulfonate monohydrate (**5**), the protonation is also confirmed by our single crystal X-ray study [18].

Table 4 Characteristic wavenumbers of IR absorption bands of compounds **1–5**

IR absorption	$\nu_{=NH}$ cm^{-1}	$\nu_{NH_3^+}$ cm^{-1}	$\nu_{C=O}$ cm^{-1}	$\nu_{C=O}$ cm^{-1}
Theophylline (anhydrous)	3122	–	1717	1668
Ethanolammonium theophyllinate (**1**, **eaH$^+$·th$^-$**)	– –	2140 –	– 1674 (1683 [3])	– 1630 1635 [3]
Theophylline : 1,10-phenantroline=1:1 (**2**, **th·phen**)	3157	–	1703	1651
Theophylline : N-(2-ammonium-ethyl) carbamate=1:1 (**3**, **th·enCO$_2$**)	3104 3385	– 2180	1702	1651
Theophylline : salicylic acid=1:1 (**4**, **th·sa**)	3110	–	1703 1679	1650
Theophyllinium salicylic acid 5-sulfonate monohydrate (**5**, **thH$^+$·saSO$_3^-$·H$_2$O**) (**1:1:1**)	3147	–	1717	1677

Stretching absorption bands of $-NH_3^+$ groups strongly bound by H-bonds were observed in the range of 2100–2200 cm^{-1} for compound **1** and **3**. These bands are originated from ethanolammonium and (2-ammonium-ethyl)carbamate ions, respectively. Specific vibration bands of N7-H7 bonds of the theophylline molecules usually showed various changes, as mentioned in [5], whilst totally disappeared from the theophyllinate compound **1**.

UM00014053
NOVARTIS EXHIBIT 1517
Novartis v. Regents, IPR2023-01347
Page 2799 of 4460

Simultaneous TG-DTA study of 1–5

The thermal behaviour of theophylline N-(2-ammonium-ethyl)carbamate **3** (**th·enCO$_2$**) and theophylline-salicylic acid (1:1) **4** (**th·sa**) has been found to be similar to that of ethanolammonium theophyllinate **1** (**eaH$^+$·th$^-$**) [3]. Between 120 and 210°C these lattice compounds slowly release ethylenediamine carbamate, salicylic acid and ethanolamine, respectively (Fig. 1, for **1** [3]). All of these constituents, being fairly volatile in this temperature range, leave the system quantitatively, meanwhile anhydrous theophylline remains in the condensed phase. Above 200°C theophylline sublimes, then melts and evaporates, finally leaves the system without residue. The actual temperature range of elimination of the volatile constituents, the observed weight losses compared to the stoichiometric values, and the observed melting point of theophylline for **3**, **4** and **1**, are summarized in Table 5.

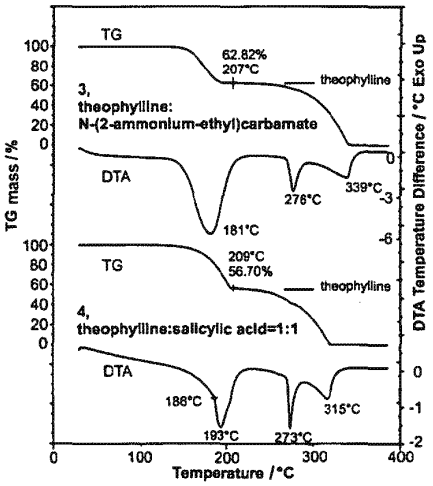


Fig. 1 Simultaneous TG-DTA curves of theophylline N-(2-ammonium-ethyl)-carbamate (1:1) **3** and theophylline salicylic acid (1:1) **4** measured in flowing air (130 mL min^{-1}) with heating rate 10 K min^{-1}, initial mass 18.77 mg and 9.45 mg for **3** and **4**, respectively

Simultaneous TG-DTA curves of **3** (**th·enCO$_2$**) and **4** (**th·sa**) are shown in Fig. 1. For the salicylic acid lattice compound **4** (**th·sa**) a melting point of 183–184°C was reported in [5]. At 186°C, in the middle of the decomposition process we have also observed a slight change in the slope of the DTA curve and which is attributable to the fusion of the non-decomposed fraction of **4**.

UM00014054
NOVARTIS EXHIBIT 1517
Novartis v. Regents, IPR2023-01347
Page 2800 of 4460

Table 5 Temperature range of the first elimination step, the observed and calculated mass losses for 1:1 compounds **1**, **3** and **4**, and the observed melting points of the residual theophylline

Compounds 1:1	Temperature range/°C	Observed mass loss/%	Calculated mass loss/%	Melting points observed for theophylline/°C
Ethanolammonium theophyllinate (**1**, $eaH^+ \cdot th^-$)	120–180	24.55	25.31 (1 mol ethanolamine)	274
Theophylline : N-(2-ammonium-ethyl)carbamate=1:1 (**3**, **th·enCO$_2$**)	130–195	37.18	36.62 (1 mol ethylenediamine carbamate)	276
Theophylline : salicylic acid=1:1 (**4**, **th·sa**)	135–210	43.30	43.40 (1 mol salicylic acid)	273

1,10-Phenanthroline compound **2** (**th·phen**) showed a sharp endothermic peak of fusion at 190°C, while the theophyllinium salicylic acid 5-sulfonate monohydrate

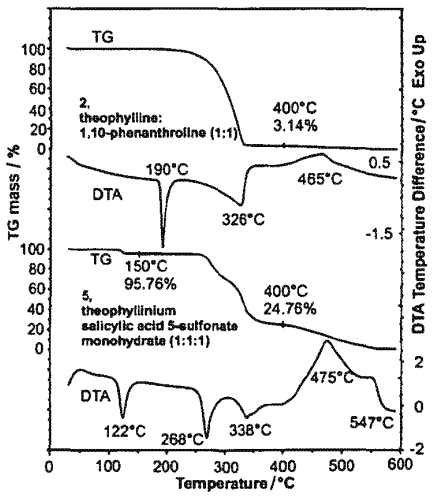


Fig. 2 Simultaneous TG-DTA curves of theophylline 1,10-phenanthroline (1:1) **2** and theophyllinium salicylic acid 5-sulfonate monohydrate (1:1:1) **5** measured in flowing air (130 mL min^{-1}) at heating rate 10 K min^{-1}, initial mass 9.67 and 9.31 mg for **2** and **5**, respectively

UM00014055
NOVARTIS EXHIBIT 1517
Novartis v. Regents, IPR2023-01347
Page 2801 of 4460

5 ($thH^+ \cdot saSO_3^- \cdot H_2O$) lost its one molecule of water of crystallisation between 110 and 135°C (mass loss observed 4.24, calculated 4.33%) and no additional melting of anhydrous **5** was observed (Fig. 2). Between 200 and 400°C both compounds **2** and **5** seemed to go through a complex degradation process, in which the theophylline moiety is also degraded. Neither stoichiometric mass losses nor melting point for theophylline occurred, although at 400°C 3.14 or 24.76% condensed phase residue of **2** and **5** were still present, respectively, which burned out only between 450–600°C.

Conclusions

Comparison of TG-DTA, XRD and FTIR data of compounds **1–5** and their parent substances gave indication on formation of new molecular compounds. Combination of TG mass losses with the results of elemental analysis helped us to determine the 1:1 composition of **1–5**. Actual form of the theophylline moieties were established according to FTIR spectra, while the structures were proven by single crystal X-ray diffraction studies. The extent of the basicity or acidity of the guest molecules is an important factor, but a certain complexity of structural features also need to stabilize the various ionic and molecular parts of the inclusion compounds [18]. Thermal stability of the five studied compounds seemed to corroborate mainly with the thermal behaviour of the guest molecules.

* * *

The authors thank to Mr. L. Sulyok and Mrs. E. Tóth for their help in preparation of samples and figures, respectively. This investigation was partially supported by the National Scientific Research Foundation (OTKA, Hungary, grant No. F 025664). J. Madarász is indebted also to the Hungarian Academy of Sciences for a Bolyai János Young Scientist Scholarship.

References

1 J. Kojima, H. Katoh, T. Taniguchi, H. Kawai, H. Fukui, A. Ohnishi and K. Onodera, Methods Find. Exp. Clin. Pharmacol., 22 (2000) 247, and references therein.
2 J. Nishijo, H. Furukawa and M. Nakano, Yakugaku Zasshi, 100 (1980) 493.
3 J. Nishijo, K. Ohno, K. Nishimura, M. Hukuda and H. Ishimura, Chem. Pharm. Bull, 30 (1982) 391.
4 J. Nishijo, K. Ohno and K. Nishimura, Chem. Pharm. Bull, 30 (1982) 2219.
5 M. Sekiya, T. Yoshino, H. Tanaka and Y. Ishido, Bull. Chem. Soc. Japan, 46 (1973) 556.
6 S. Zaitu, Y. Miwa and T. Taga, Acta Crystallogr. Sect. C (Cr. Str. Comm.), 51 (1995) 2390.
7 H. Wiedenfeld and F. Knoch, Arch. Pharm., 319 (1986) 654.
8 E. Shefter and P. Sackman, J. Pharm. Sci., 60 (1971) 282.
9 E. Shefter, J. Pharm. Sci., 58 (1969) 710.
10 D. J. Sutor, Acta Crystallogr., 11 (1958) 83.
11 Y. Ebisuzaki, P. D. Boyle and J. A. Smith, Acta Crystallogr., C 53 (1997) 777.
12 C. H. Koo, H. S. Shin and S. Oh, J. Korean Chem. Soc., 22 (1978) 86.
13 S. Nakao, S. Fujii, T. Sakaki and K. Tomita, Acta Crystallogr., Sect. B. 33 (1977) 1373.
14 S. Zaitu, Y. Miwa and T. Taga, Acta Crystallogr., Sect. C (Cr. Str. Comm.) 51 (1995) 1857.

UM00014056
NOVARTIS EXHIBIT 1517
Novartis v. Regents, IPR2023-01347
Page 2802 of 4460

15 J. Madarász, P. Bombicz, M. Czugler and G. Pokol, Polyhedron, 19 (2000) 457, and references therein.
16 E. Katchalski, C. Berliner-Klibanski and A. Berger, J. Am. Chem. Soc., 73 (1951) 1829.
17 G. L. Gainer, Jr., J. Org. Chem., 50 (1985) 410.
18 P. Bombicz, J. Madarász, M. Czugler, and A. Kálmán, Acta Cryst. B. in preparation

UM00014057
NOVARTIS EXHIBIT 1517
Novartis v. Regents, IPR2023-01347
Page 2803 of 4460

J|A|C|S
COMMUNICATIONS

Published on Web 03/23/2004

Halogen Bonding and $\pi\cdots\pi$ Stacking Control Reactivity in the Solid State

Tullio Caronna,§ Rosalba Liantonio,† Thomas A. Logothetis,† Pierangelo Metrangolo,*,† Tullio Pilati,‡ and Giuseppe Resnati*,†

Department of Chemistry, Materials, and Chemical Engineering "G. Natta", Polytechnic of Milan, Via Mancinelli 7, Milan, Italy, CNR-I.S.T.M., University of Milan, Via Golgi 19, Milan, Italy, and University of Bergamo, Faculty of Engineering, Via Marconi 5, 24044 Dalmine, Bergamo, Italy

Received December 1, 2003; E-mail: pierangelo.metrangolo@polimi.it (P.M.); giuseppe.resnati@polimi.it (G.R.)

The ultimate goal of supramolecular chemistry is to gain control over the noncovalent self-assembly of molecules in order to direct their functions.[1] Solid-state synthesis is one of the most fascinating and rapidly emerging fields of supramolecular chemistry.[2] Noncovalent interactions have recently proven fruitful in dictating the regioselectivity of solid-state reactions.[3] For instance, hydrogen bonding has been used to pin olefins to linear templates[4] and to form discrete supramolecules meeting Schmidt's requirements for UV-induced [2 + 2] cycloaddition reactions.[5] A full utilization of this innovative approach requires the successful exploitation of new and effective noncovalent interactions for the self-assembly of architectures geometrically tailored to preestablished reactions.

In this contribution we describe the first case wherein halogen bonding, namely the charge-transfer interaction between Lewis bases and halogen atoms,[6] drives the assembly of a template with an olefins' carrier, orienting double bonds for photocyclization in the crystal. To achieve this result, we engineered and synthesized the tetratopic halogen-bonding donor **3** (Scheme 1).[7]

The pentaerythritol ether **3** is obtained by a S_NAr attack of oxygen sites in **1** on iodopentafluorobenzene **2**. The reactions occur with a very high regioselectivity on the sites occupied by the para fluorine atoms. This S_NAr reaction, previously used for the preparation of ditopic halogen-bonding donors,[8] is here proven as an effective strategy to new tectons[9] for halogen-bonding-driven crystal engineering.

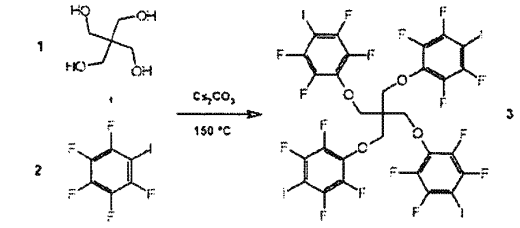
Iodoperfluoroarenes are very good halogen-bonding donors, and they easily self-assemble with nitrogen-substituted hydrocarbons.[10] To test the ability of the tetratopic tecton **3** to be involved in halogen-bonding-driven intermolecular recognition processes, we challenged it with 1,2-diaminoethane **4a** (Scheme 2). Single crystals of **5a**, melting at 435 K, were grown under isothermal conditions ($T = 298$ K) by using the diffusion technique within a chloroform–tetrachloromethane system.

The X-ray diffraction analysis of those cocrystals gave details about their supramolecular organization (Figure 1).[7,11]

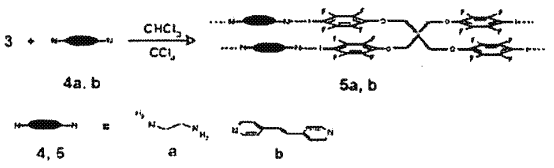
Modules **3** and **4a** are present in the cocrystal **5a** with a 2:1 ratio, and they form infinite 1D halogen-bonded ribbons.

As expected, the pentaerythritol derivative **3** behaves as a tetratopic halogen-bonding donor, while the dinitrogen module **4a** is a ditopic acceptor. The structure presents two different halogen bonds with N···I distances of 2.811 and 2.960 Å. These are, respectively, 20 and 16% shorter than the sum of the van der Waals radii for N and I (3.53 Å).[12] The N···I–C angles are 174.99 and 168.20°. This is consistent with the n → σ^* character of the halogen bonding[13] and confirms its high directionality.[14] The tecton **3** differs from the other pentaerythritol derivatives[15] in that it does not show either a planar or a tetrahedral conformation. Instead, the four arms

Scheme 1



Scheme 2



of **3** point two by two to the opposite sides. The tetrafluorophenyl rings lying on the same side are paired in a quasi-parallel fashion due to remarkable face-to-face $\pi\cdots\pi$ intramolecular interactions[16] (distances ranging from 3.551 to 3.915 Å; typical cutoff distance 3.9 Å[15]). The wider distances are observed between the carbon atoms closer to the iodine atoms. In fact, the rings slightly open up. This is probably caused by the steric hindrance of the iodine atoms, which do not show any reciprocal attraction. Thanks to the $\pi\cdots\pi$ stacking interaction forces, the iodine atoms in the periphery of module **3** stay at a distance of about 4 Å. Thus, tetratopic tecton **3** looks ideally pre-organized for enforcing topochemical alignment of the electron donor module by means of a double supramolecular control: intramolecular $\pi\cdots\pi$ stacking interaction and intermolecular halogen bonding.

With this in mind, we tried to obtain halogen-bonded adducts between **3** and *trans*-1,2-bis(4-pyridyl)ethylene (4,4′-bpe, **4b**), which is a strong halogen-bonding acceptor and easily self-assembles with iodo- and bromoperfluoroarenes.[17] Colorless cocrystals **5b** were obtained upon a slow diffusion of the volatiles in a chloroform–tetrachloromethane crystallizing system (Scheme 2).[7] The thermal analysis of **5b** gave very interesting information. The melting endotherms of the source compounds (**3**: 439 K, **4b**: 426 K) were both missing in the thermograph of **5b**, while a new endotherm, corresponding to the sample melting, appears at 494 K. This behavior is consistent with the formation of new well-defined crystalline species. The dramatic melting-point increase demonstrates the robustness of the crystal matrix of **5b**.[10] Suitable crystals of **5b** were submitted to single-crystal X-ray analysis (Figure 2).[18]

The supramolecular architecture of **5b** was also characterized by infinite 1D halogen-bonded ribbons. The similarities between

† Polytechnic of Milan.
‡ University of Milan.
§ University of Bergamo.

10.1021/ja039884n CCC: $27.50 © 2004 American Chemical Society

UM00014058
NOVARTIS EXHIBIT 1517
Novartis v. Regents, IPR2023-01347
Page 2804 of 4460

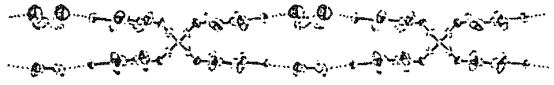


Figure 1. Infinite 1D halogen-bonded ribbons **5a** formed by self-assembling modules **3** and **4a**. Hydrogen atoms are omitted for clarity.

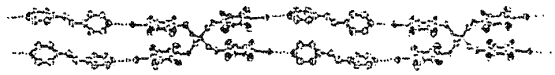
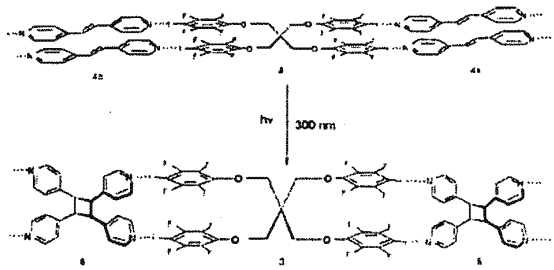


Figure 2. Infinite 1D halogen-bonded ribbons **5b** formed by self-assembling modules **3** and **4b**. Hydrogen and disordered atoms are omitted for clarity.

Scheme 3



the organization of the interacting modules in cocrystals **5a,b** are impressive and confirm the validity of our supramolecular design. The arms of the pentaerythritol derivative **3** show the same parallel arrangement with $\pi\cdots\pi$ distances ranging from 3.524 to 3.897 Å. Two different halogen bonds are present here, too, with N···I distances of 2.795−2.819 Å, about 21% shorter than the sum of the van der Waals radii for N and I (3.53 Å).[12] The N···I−C angles are 177.09 and 176.72°, respectively. In cocrystal **5b**, $\pi\cdots\pi$ stacking interactions determine the pre-organization of module **3** and the high strength and directionality of the halogen bonding transfer this topochemical information to the olefins that are pinned in the ribbons in a parallel fashion with a distance of less than 4.5 Å between the olefins' centroids. In **5b**, the olefins present the typical disorder of stilbene derivatives, which has also been observed in the structures of related supramolecules.[4b]

A powdered crystalline sample of **5b**, placed between two glass plates, was irradiated using a Rayonet at 300 nm. The cocrystal **5b** readily underwent a photochemical cycloaddition under topochemical control, producing tetrakis(4-pyridyl)cyclobutane **6** (Scheme 3). As confirmed by ^{1}H NMR spectroscopy of the crude reaction mixture and FAB-MS spectrometry, the reaction occurs stereospecifically and with high yields. After 3 h a 100% conversion of **5b** occurred, yielding 100% the *rctt* isomer only (GC analysis).[4a,7] No byproducts were revealed; in **5b**, the olefin ethylene bonds are always parallel, while the apparent cross-like feature is only due to long-range statistical disorder of these pairs (see Supporting Information). Moreover, cross-plane photoreactions are prevented by the absence of any short contacts between the olefins belonging to adjacent ribbons in the crystal stacking (inter-ribbons distance > 7 Å).[19]

In summary, we present a means to achieve supramolecular control on reactivity in the solid state using a template[4] that operates via halogen bonding. It is based on noncovalent interactions and operates at two levels. The intramolecular $\pi\cdots\pi$ interactions pre-organize the template. The intermolecular halogen bonding assembles template and olefin carrier in ribbons. As a result of the remarkable strength and directionality of the halogen bonding, the alignment of the arms of the template is translated into alignment of olefins at the distance needed for the photoreaction. Only occasional precedents have been reported wherein the halogen bonding affects solid-state photoreactions. A paper describes a chlorodiazirine that packs in infinite chains and photodecomposes with low selectivity due to intermolecular N···Cl interactions.[20] Schmidt reports how weak Cl···Cl contacts align polyenes in discrete assemblies that undergo photocyclization to cyclobutanes.[21] In contrast to Schmidt, we have used for the first time the halogen bonding in the context of a template/cocrystal system, thus inducing stereoselective photocyclization of olefins. The limited flexibility of template **3**, the strength of $\pi-\pi$ interactions between perfluorophenyl rings,[16a] and the directionality of the N···I halogen bonding[14a] suggest that the impact of the templated synthesis here described may extend to a variety of solid-state photoreactions involving nitrogen substituted partners.

Acknowledgment. We thank MIUR (PRIN 2003) and EU (HPRN-CT-2000-00002) for the fundings granted.

Supporting Information Available: Crystallographic Information Files (CIFs) for **5a,b**. Experimental data for **3**, **5a,b**, and **6**. This material is available free of charge via the Internet at http://pubs.acs.org.

References

(1) Atwood, J. L.; Steed, J. W. *Supramolecular Chemistry*; John Wiley & Sons: Ltd: Chichester, UK, 2000.
(2) Cave, G. W. V.; Raston, C. L.; Scott, J. L. *Chem. Commun.* **2001**, 2159.
(3) (a) Desiraju, G. R. *Angew. Chem., Int. Ed. Engl.* **1995**, *34*, 2311. (b) Feldman, K. S.; Campbell, R. F. *J. Org. Chem.* **1995**, *60*, 1924. (c) Coates, G. W.; Dunn, A. R.; Henling, L. M.; Ziller, J. W.; Lobkovsky, E. B.; Grubbs, R. H. *J. Am. Chem. Soc.* **1998**, *120*, 3641. (d) Rao, K. S. S. P.; Hubig, S. M.; Moorthy, J. N.; Kochi, J. K. *J. Org. Chem.* **1999**, *64*, 8098. (e) Amirsakis, D. G.; Elizarov, A. M.; Garcia-Garibay, M. A.; Glink, P. T.; Stoddart, J. F.; White, A. J. P.; Williams, D. J. *Angew. Chem., Int. Ed.* **2003**, *42*, 1158.
(4) (a) MacGillivray, L. R.; Reid, J. L.; Ripmeester, J. A. *J. Am. Chem. Soc.* **2000**, *122*, 7817. (b) Papaefstathiou, G. S.; Kipp, A. J.; MacGillivray, L. R. *Chem. Commun.* **2001**, 2462.
(5) Schmidt, G. M. J. *Pure Appl. Chem.* **1971**, *27*, 647.
(6) Metrangolo, P.; Resnati, G. Halogen Bonding. In *Encyclopedia of Supramolecular Chemistry*; Atwood, J. L., Steed, J. W., Eds.; Marcel Dekker Inc: New York, 2004. In press.
(7) For details and characterization, see Supporting Information.
(8) Liantonio, R.; Mele, M. L.; Metrangolo, P.; Pilati, T.; Resnati, G. *Supramol. Chem.* **2003**, *15*, 177.
(9) Metrangolo, P.; Resnati, G. Tectons: Definition and Scope. In *Encyclopedia of Supramolecular Chemistry*; Atwood, J. L., Steed, J. W., Eds.; Marcel Dekker Inc: New York, 2004. In press.
(10) Corradi, E.; Meille, S. V.; Messina, M. T.; Metrangolo, P.; Resnati, G. *Angew. Chem., Int. Ed.* **2000**, 39, 1782.
(11) Crystal data for **5a**: colorless prisms, crystal size 0.38 mm × 0.32 mm × 0.28 mm, monoclinic, space group C2/*c*, a = 22.805(5) Å, b = 15.455(3) Å, c = 15.417(5) Å, α = 90.00°, β = 129.68(3)°, γ = 90.00°, U = 4182(2) Å^3, 2θ = 54.74°, Mo Kα radiation (λ = 0.71073 Å) for Z = 4 and R = 0.0347. CCDC 225183.
(12) Bondi, A. *J. Phys. Chem.* **1964**, *68*, 441.
(13) Foster, R. *Organic Charge-Transfer Complexes*; Academic Press: London, 1969; p 100.
(14) (a) Metrangolo, P.; Resnati, G. *Chem. Eur. J.* **2001**, *7*, 2511. (b) Fontana, F.; Forni, A.; Metrangolo, P.; Panzeri, W.; Pilati, T.; Resnati, G. *Supramol. Chem.* **2002**, *14*, 47.
(15) Nattinen, K. I.; Rissanen, K. *Cryst. Growth Des.* **2003**, *3*, 339.
(16) (a) Liu, J.; Murray, E. M.; Young, V. G., Jr. *Chem Commun.* **2003**, 1904. (b) Messina, M. T.; Metrangolo, P.; Pappalardo, S.; Parisi, M. F.; Pilati, T.; Resnati, G. *Chem. Eur. J.* **2000**, *6*, 3495.
(17) De Santis, A.; Forni, A.; Liantonio, R.; Metrangolo, P.; Pilati, T.; Resnati, G. *Chem. Eur. J.* **2003**, *9*, 3986.
(18) Crystal data for **5b**: oblique colorless prisms, crystal size 0.40 mm × 0.32 mm × 0.16 mm, monoclinic, space group $P2_1/c$, a = 12.900(2) Å, b = 10.3505(17) Å, c = 20.172(3) Å, α = 90.00°, β = 97.446(2)°, γ = 90.00°, U = 2670.7(7) Å^3, 2θ = 48.650°, Mo Kα radiation (λ = 0.71073 Å) for Z = 2 and R = 0.0312. CCDC 225182.
(19) Friščić, T.; MacGillivray, L. R. *Chem. Commun.* **2003**, 1306.
(20) Sanrame, C. N.; Suhrada, C. P.; Dang, H.; Garcia-Garibay, M. A. *J. Phys Chem. A* **2003**, *104*, 3287.
(21) Elgavi, A.; Green, B. S.; Schmidt, G. M. J. *J. Am. Chem. Soc.* **1973**, *95*, 2058.

JA039884N

UM00014059
NOVARTIS EXHIBIT 1517
Novartis v. Regents, IPR2023-01347
Page 2805 of 4460

Steric Control of Secondary, Solid-State Architecture in 1:1 Complexes of Melamines and Barbiturates That Crystallize as Crinkled Tapes

Jonathan A. Zerkowski and George M. Whitesides*

Contribution from the Department of Chemistry, Harvard University, Cambridge, Massachusetts 02138

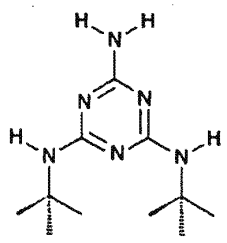
Received August 28, 1992. Revised Manuscript Received March 2, 1994®

Abstract: This paper describes the single-crystal X-ray structures of four 1:1 complexes between *N,N'*-di(*tert*-butyl)-melamine and 5,5-disubstituted barbituric acids (substituents = CH_2CH_3, CH_2CF_3, CH_3, and C_6H_5). These complexes crystallize as infinite "crinkled" tapes having components joined by a triad of hydrogen bonds. The tapes are prevented from adopting a linear motif due to steric repulsion between *tert*-butyl groups on adjacent melamines; the crinkled motif avoids such repulsion. The tape backbones deviate from planarity to permit close packing of the crinkled tapes. Crystals of these complexes of a size and shape suitable for single-crystal X-ray diffraction analysis are readily grown; this system therefore seems well-suited for systematic study of the relationships between molecular and crystalline structure.

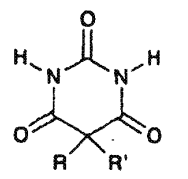
Introduction

We are studying the solid-state structures of 1:1 cocrystals of derivatives of melamine and of barbituric acid.[1-3] These cocrystals consist of crystallographically infinite hydrogen-bonded tapes that pack with their long axes parallel. By varying the steric properties of the substituents on the melamine component, we have prepared examples of linear tapes[3] and crinkled tapes.[2,4] We have also obtained one cyclic pseudo-C_3 structure (a "rosette").[2] These three structural motifs are the simplest ones that can be derived from the complex between cyanuric acid and melamine (CA-M).

Our previous work has kept the barbiturate component constant (as barbital, **Bar(Et)$_2$**), and varied the structure of the melamine. In the research reported in this paper, by contrast, we held the melamine component constant (as *N,N'*-di(*tert*-butyl)melamine, **Mel(tBu)$_2$**) and varied the barbiturate. One goal of this work was to test the hypothesis that sterically hindered substituents on the melamine would yield crinkled tapes. We chose **Mel(tBu)$_2$** because it is a truncated version of the melamine—*N,N'*-bis(4-*tert*-butylphenyl)melamine—that produced a rosette; we have rationalized the formation of the cyclic structure on the basis of the steric demands of the *tert*-butyl group.[2] We also wished simply to explore the influence of the substituents on the barbiturate on the solid-state structure: we are still surveying the range of solid-state structures accessible through manipulation of variants of CA-M, and we expect these data to complement those obtained in other studies.



Mel(tBu)$_2$



R	R'
CH_3	CH_3
CH_2CH_3	CH_2CH_3
CH_2CH_3	CH_2CF_3
C_6H_5	C_6H_5

Bar(R)(R')

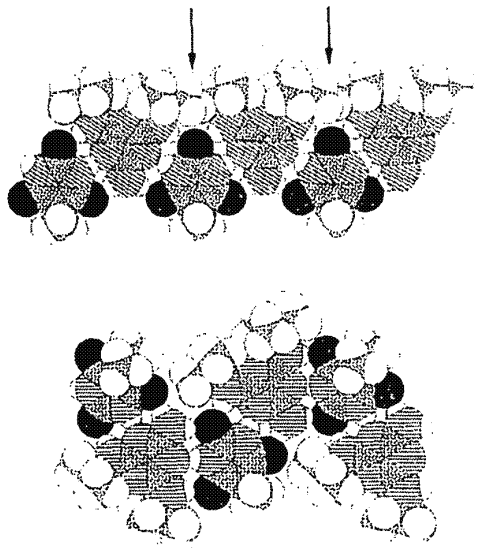


Figure 1. Top: Hypothetical linear tape of the **Mel(tBu)$_2$·Bar(CH$_3$)$_2$** complex, with regions of steric repulsion indicated by arrows. Bottom: The observed crinkled format of this complex, which relieves the steric hindrance.

Results

Formation and Features of Crinkled Tapes. The bulky *tert*-butyl substituent makes formation of linear tapes impossible for steric reasons. Figure 1 (top) shows regions of steric repulsion between the *tert*-butyl groups of adjacent melamines in a hypothetical linear tape incorporating **Mel(tBu)$_2$**. The bottom of the figure shows that the crinkled format avoids such steric repulsion: the *tert*-butyl groups are separated and are disposed on opposite sides of the tape.[3] One crystallographic axis (underlined in Table 1) is the repeat distance in a crinkled tape.

* Abstract published in *Advance ACS Abstracts*, April 1, 1994.

(1) Zerkowski, J. A.; Seto, C. T.; Wierda, D. A.; Whitesides, G. M. *J. Am. Chem. Soc.* 1990, *112*, 9025.

(2) Zerkowski, J. A.; Seto, C. T.; Whitesides, G. M. *J. Am. Chem. Soc.* 1992, *114*, 5473.

(3) Zerkowski, J. A.; MacDonald, J. C.; Seto, C. T.; Wierda, D. A.; Whitesides, G. M. *J. Am. Chem. Soc.* 1994, *116*, 2382.

(4) Zerkowski, J. A.; Mathias, J. P.; Whitesides, G. M. *J. Am. Chem. Soc.*, following paper in this issue.

0002-7863/94/1516-4298$04.50/0 © 1994 American Chemical Society

UM00014060
NOVARTIS EXHIBIT 1517
Novartis v. Regents, IPR2023-01347
Page 2806 of 4460

Table 1. Crystallographic Data for Mel(^{t}Bu)$_2$-Bar(R)(R′) Complexes

R,R′	space group	*a* (Å)	*b* (Å)	*c* (Å)	β[a] (deg)	*R*[b]	C_k*[c]	ρ[d] (g/cm^3)	solvent[e] of crystallization	deviation from planarity[f] (Å)
Et, Et	$Pna2_1$	13.634	11.708	15.739[g]		0.037	0.62	1.149	MeOH	0.54
Et, CH_2CF_3	$P2_12_12_1$	12.975	15.709	12.796		0.089	0.61	1.214	EtOH	0.78
Me, Me	$P2_1/c$	11.451	16.285	11.665	98.23	0.052	0.66	1.217	MeOH	0.29
Ph, Ph	$P2_1/c$	15.103	15.829	12.642	114.65	0.060	0.68	1.254	MeOH	0.58

[a] A blank indicates that the angle is constrained to be 90°. [b] $R = \sum|F_o - F_c|/\sum F_o$. [c] This value is the packing coefficient based on molecular volumes calculated with MacroModel (see the Results section for the definition of C_k and ref 3 for a discussion of the relationship between C_k and C_k*). [d] This value is the calculated density. [e] No solvent is included in the crystal lattice in any of these complexes. [f] This value is the average deviation of the atoms in the tape backbone from the mean plane of the backbone. [g] The underlined cell dimensions represent the repeat distance in a tape (see the Results section).

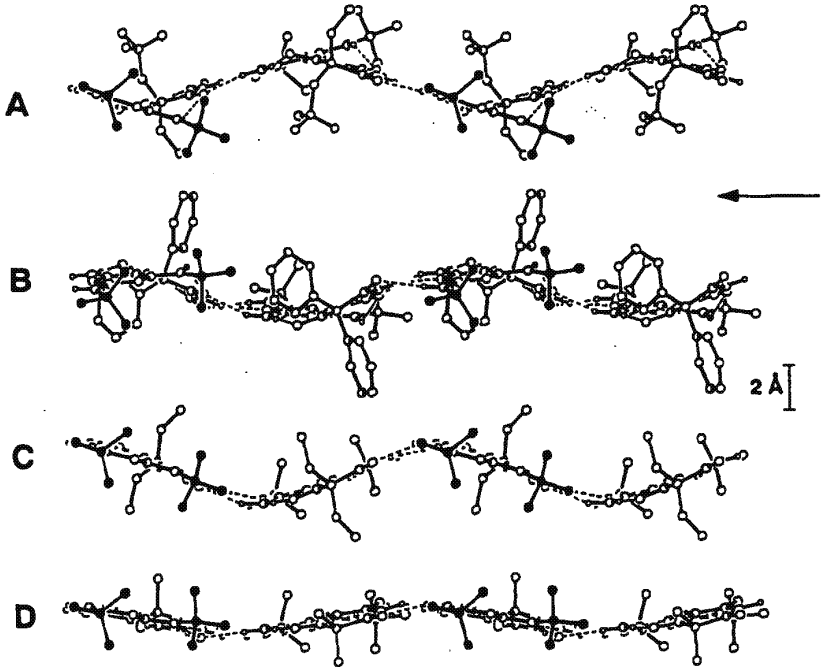


Figure 2. Side views of crinkled tapes of Mel(^{t}Bu)$_2$ complexes showing their deviation from planarity: (A) **Bar(Et)(CH$_2$CF$_3$)** complex; (B) **Bar(Ph)$_2$** complex; (C) **Bar(Et)$_2$** complex; (D) **Bar(CH$_3$)$_2$** complex. The deviation decreases from A to D (see Table 1). The arrow indicates the direction of a view down the long tape axes. The filled-in *tert*-butyl groups are on the edges of the tapes that are nearer to the viewer.

This distance is the length of a screw-related pair of Mel·Bar dimers along the tape axis, illustrated, for example, by the distance between symmetry-equivalent filled-in *tert*-butyl groups in Figure 2. Figure 2 also shows that the crinkled tapes deviate from planarity in a direction perpendicular to the infinite hydrogen-bonded axis. This deformation, or "waviness", turns the crinkled tapes into quasi-three-dimensional structures. To a first approximation, there is a rough trend between the degree of waviness and the size of the axis underlined in Table 1. The tape with the greatest deviation from planarity (the complex with **Bar(Et)-(CH$_2$CF$_3$)**) has the shortest unit projection (15.709 Å) along the tape axis.

At the macroscopic level, crystals of these crinkled tapes are blocky chunks or plates. Crystals of linear tapes, by contrast, were most frequently obtained as fine needles, a morphology that reflected the parallel packing of the linear tapes.[3] In addition, crystals of crinkled tapes were on average larger than crystals of linear tapes. A fixed-tube X-ray source, rather than a rotating anode generator, could therefore have been used for single-crystal X-ray analysis. Equally importantly, the crystals of these Mel-(^{t}Bu)$_2$ complexes were easier to grow than crystals of complexes of *para*-substituted diphenylmelamines and barbital.[3,6]

Solid-State Structures of Complexes of Mel(^{t}Bu)$_2$-Bar(R)(R′). To convey the important points of intermolecular orientation, we have constructed conglomerate pictures (Figures 3–6) showing several views of tape packing at once. The deviation from planarity of these crinkled tapes makes them appear "thicker" than linear tapes in an end-on view. Nonetheless, such a view (looking down the crystallographically infinite hydrogen-bonded axis) is still useful in showing the relative orientation, or the tertiary architecture, of tapes. Table 1 lists crystallographic data and some geometric parameters of tape packing.

***N,N′*-Di(*tert*-butyl)melamine/Barbital, Mel(^{t}Bu)$_2$-Bar(Et)$_2$ (Figure 3).** This complex was investigated to provide a comparison to our previous work on systems that contained **Bar(Et)$_2$** and substituted diphenylmelamines. The only variable structural unit in these cocrystals is thus the melamine, and crinkling can be attributed to its characteristics. The backbone of this tape is wavy (Table 1 and Figures 2 and 3): the average displacement of the atoms in the tape backbone from their own mean plane is

(5) Steric repulsion was also responsible for crinkling in the complex between *N,N′*-bis(4-methoxycarbonylphenyl)melamine and barbital that we reported previously.[2]

(6) This ready crystallization is attested to by the fact that the single crystals of Mel(^{t}Bu)$_2$-Bar(Et)$_2$ and Mel(^{t}Bu)$_2$-Bar(Et)(CH$_2$CF$_3$) used for diffraction were obtained from the very first crystallization attempts made on these complexes.

UM00014061
NOVARTIS EXHIBIT 1517
Novartis v. Regents, IPR2023-01347
Page 2807 of 4460

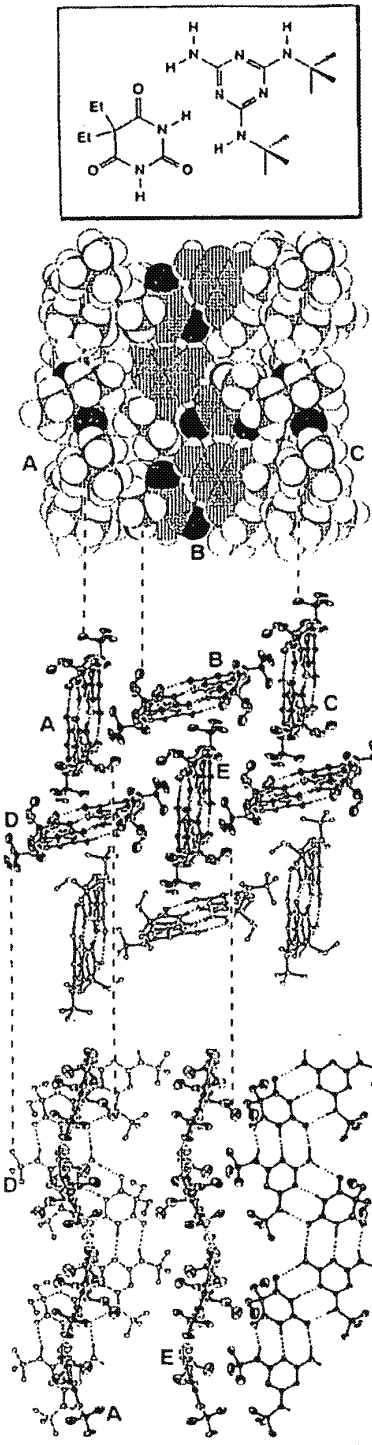


Figure 3. Views of the Mel('Bu)$_2$Bar(Et)$_2$ complex. Alkyl hydrogens have been omitted from the central and bottom views. In this and the following figures, tapes that appear in more than one view are drawn with thermal ellipsoids in the central, end-on view and are connected with vertical dotted lines. In the bottom view, the highlighted tapes are nearer to the viewer.

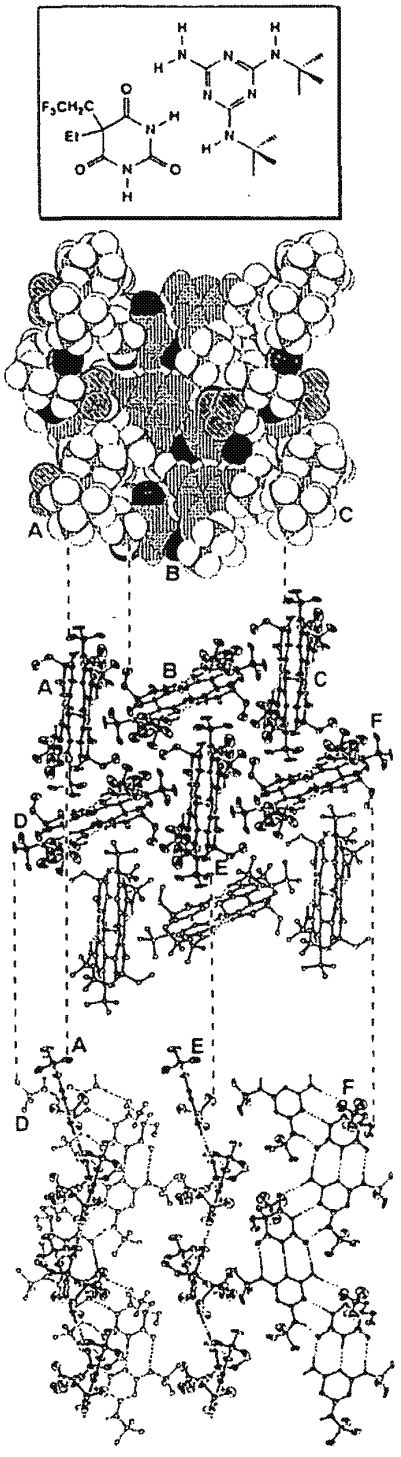


Figure 4. Views of the Mel('Bu)$_2$Bar(Et)(CH$_2$CF$_3$) complex. Alkyl hydrogens have been omitted from the central and bottom views.

0.54 Å.[7] By contrast, the seven linear tapes of complexes of *para*-substituted diphenylmelamines with barbital that we reported previously are less wavy, with an average deviation from planarity of 0.13 Å.[3]

(7) We define the mean plane of a tape as the six ring atoms of each heterocycle plus the three hydrogen-bonding exocyclic heteroatoms, three nitrogens for the melamine and three oxygens for the barbiturate.

UM00014062
NOVARTIS EXHIBIT 1517
Novartis v. Regents, IPR2023-01347
Page 2808 of 4460

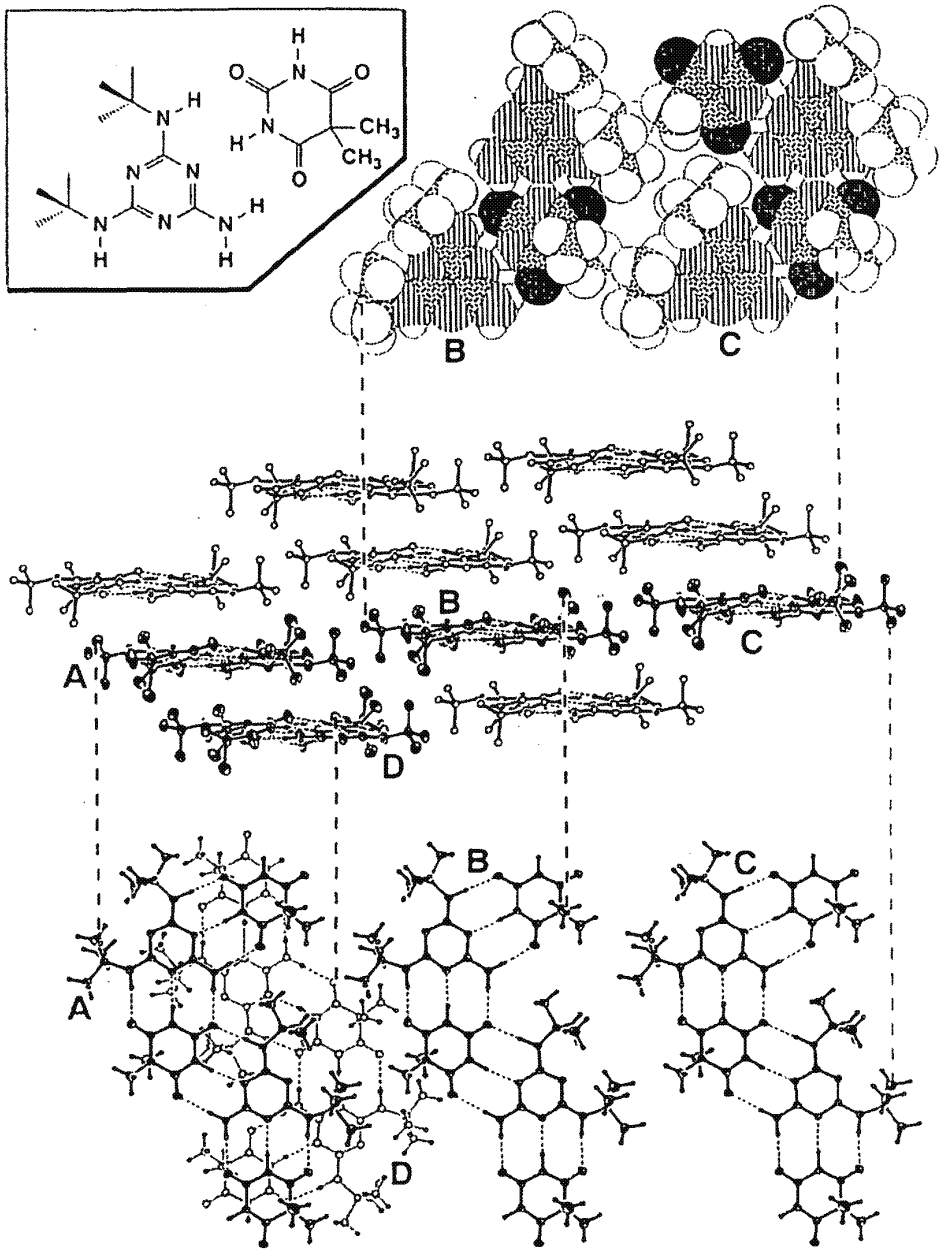


Figure 5. Views of the Mel(^{t}Bu)$_2$·Bar(CH$_3$)$_2$ complex. Alkyl hydrogens have been omitted from the central view.

N,N'-Di(*tert*-butyl)melamine/5-Ethyl-5-(2,2,2-trifluoroethyl)-barbituric Acid, Mel(^{t}Bu)$_2$/Bar(Et)(CH$_2$CF$_3$) (Figure 4). This complex represents a minimal steric perturbation on the Bar(Et)$_2$ complex. We are also interested in studying the packing of compounds containing fluorocarbon units, to see if the fluorines segregate away from hydrocarbon regions or exhibit other patterns of behavior that might be used to control solid-state structure. The stacking of the Mel(^{t}Bu)$_2$·Bar(Et)(CH$_2$CF$_3$) crinkled tapes is similar to that of the Mel(^{t}Bu)$_2$·Bar(Et)$_2$ tapes. In this solid-state structure, there are also no fluorine-rich regions and no contacts under the sums of van der Waals radii involving fluorines.

N,N'-Di(*tert*-butyl)melamine/5,5-Dimethylbarbituric Acid, Mel(^{t}Bu)$_2$·Bar(CH$_3$)$_2$ (Figure 5). We investigated this complex because it is an abbreviated analogue of the Bar(Et)$_2$ complex: that is, the size of the barbiturate substituent has been decreased. The tape backbones are less wavy than in the structures incorporating Bar(Et)$_2$ and Bar(Et)(CH$_2$CF$_3$) (Table 1).

N,N'-Di(*tert*-butyl)melamine/5,5-Diphenylbarbituric Acid, Mel(^{t}Bu)$_2$·Bar(Ph)$_2$ (Figure 6). In this complex, the steric perturbation of the barbiturate substituent is in the opposite direction from Bar(CH$_3$)$_2$: the phenyl groups are larger and more rigid than the ethyl groups. The phenyl rings are not packed in either edge-to-face or face-to-face orientations. There is, however, a CH···O contact (2.5 Å, $\sum_{vdW} \sim 2.7$ Å) between a barbiturate oxygen on one tape and an *o*-phenyl proton in an overlapping tape (e.g. tapes A and D in Figure 6).[8]

Packing Fractions (Table 1). The packing fraction C_k is a

UM00014063
NOVARTIS EXHIBIT 1517
Novartis v. Regents, IPR2023-01347
Page 2809 of 4460

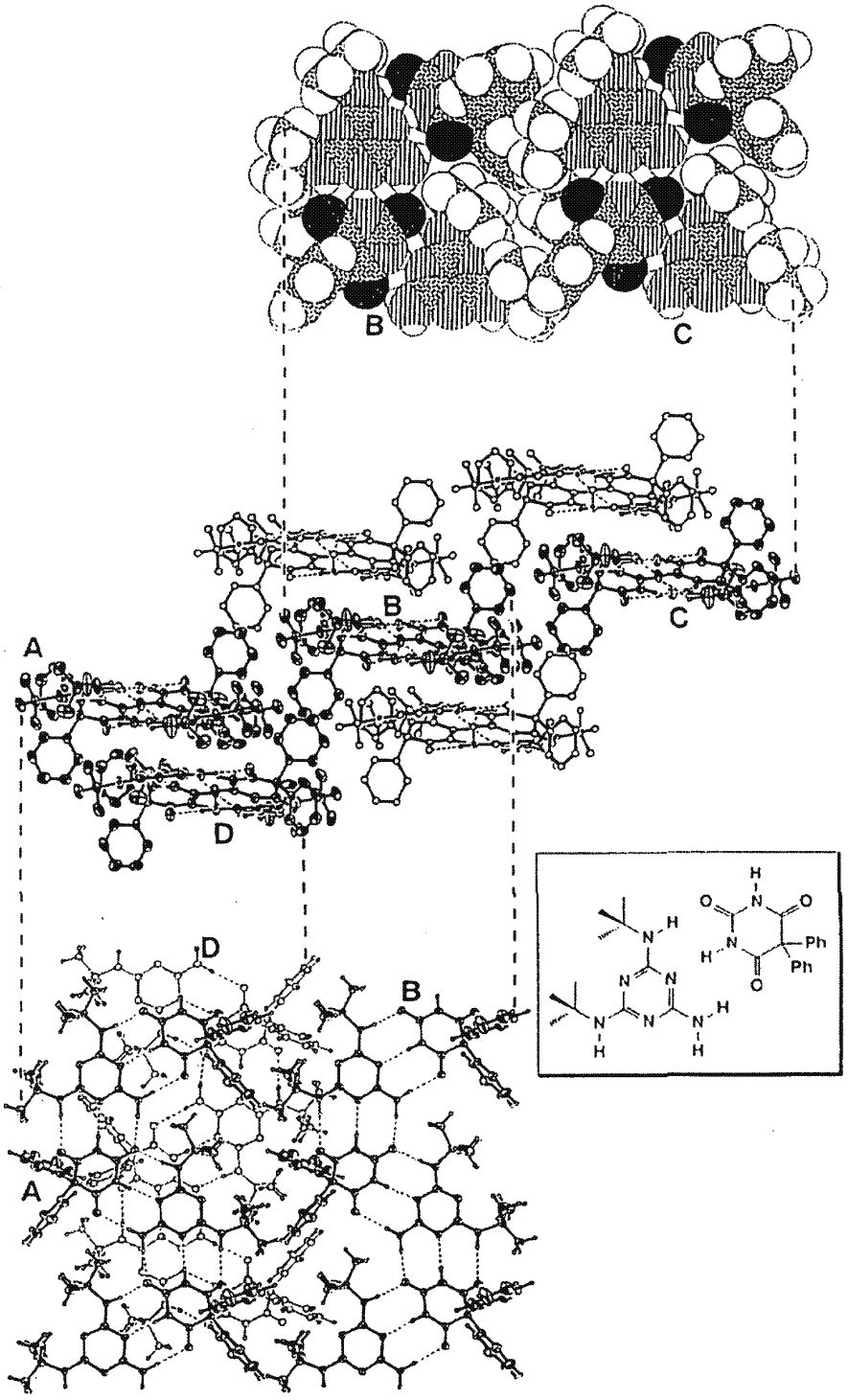


Figure 6. Views of the $MeI(^tBu)_2$·$Bar(Ph)_2$ complex. Alkyl and aryl hydrogens have been omitted from the central view.

measure of the completeness with which the molecules of a crystal fill space;[9] our modified value C_1^* is based on molecular volumes calculated using MacroModel.[10] The C_1^* values for the two herringbone complexes, $MeI(^tBu)_2$·$Bar(Et)_2$ and $MeI(^tBu)_2$·$Bar(Et)(CH_2CF_3)$, are at the lower end of the normal range.[11] Nonetheless, there are no discrete cavities large enough to allow inclusion of solvent molecules. The mean value for these four crinkled tape complexes, 0.64, is lower than that (0.69) for the

(8) We do not know if this contact is attractive or repulsive. For a discussion of CH–O contacts, see: Desiraju, G. R. *Acc. Chem. Res.* 1991, *24*, 290.

UM00014064
NOVARTIS EXHIBIT 1517
Novartis v. Regents, IPR2023-01347
Page 2810 of 4460

linear tape complexes of *para*-substituted diphenylmelamines with barbital.[3]

Discussion

The results presented here confirm our hypothesis that steric hindrance involving the *tert*-butyl substituents of the melamine would force hydrogen-bonded tapes to pack in a crinkled motif rather than in a linear motif. The most important result of this work, therefore, is that the *secondary* crystalline architecture (the tape motif: *linear*, *crinkled*, or *cyclic*) of complexes of melamines and barbiturates can be predicted and controlled using steric effects. We have not yet searched for polymorphism in these complexes, but we do believe that **Mel(tBu)$_2$** will reliably yield crinkled tapes.

At the level of tertiary architecture (the stacking of tapes in the crystal), we propose that the deviation of crinkled tapes from planarity to produce a wavy shape (Figure 2) occurs to maximize packing efficiency. This observation is consistent with the broad guideline that, in crystals in general, intermolecular contact of van der Waals surfaces tends toward a maximum.[9,11] In these crystals of crinkled tapes, regions of space that would otherwise be voids are filled by the deformation of the hydrogen-bonded backbone of tapes from planarity. The views at the bottoms of Figures 3 and 4 illustrate this increased packing efficiency for the two complexes (those with **Bar(Et)$_2$** and **Bar(Et)(CH$_2$CF$_3$)**) that adopt the herringbone pattern. Two adjacent, perpendicular tapes fit together compactly, by matching the crinkling of one and the waviness of the other. Figure 7 presents a closeup view of these relationships.

In wavy tapes, the hydrogen bonds are bent from linearity. For the N–H···O bonds, the angles at hydrogen are 167°, 145°, 175°, and 157°, and for the N–H···N bonds, the angles are 174° and 173°. The hydrogen atoms involved in these hydrogen bonds were located crystallographically from electron density maps. Bent hydrogen bonds are frequently observed in crystal structures and do not appear to be energetically unfavorable (although there must be a level of deformation beyond which the tapes would not hold together).[12,13]

Conclusions

The four crystal structures of complexes of **Mel(tBu)$_2$** with barbiturates show that the triad of hydrogen bonds that holds together crystallographically infinite tapes is robust to substitutions that cause unfavorable intratape steric interactions. The formation of crinkled tapes can be rationalized using steric arguments: bulky substituents on the melamines (here, *tert*-butyl groups) prevent adoption of a linear format and force tapes to crinkle. In terms of designing organic solids, we expect to be able to use this effect to obtain crystals built from the crinkled structural motif. In fact, the ease of crystallization of these crinkled tapes recommends their use in systematic physical–organic studies of the solid state. Another result instructive for future work is that tapes are tolerant of different classes of substituents (alkyl and aryl groups) on both melamine and barbiturate components. Systematic variation on either component is a valid approach to crystal engineering.

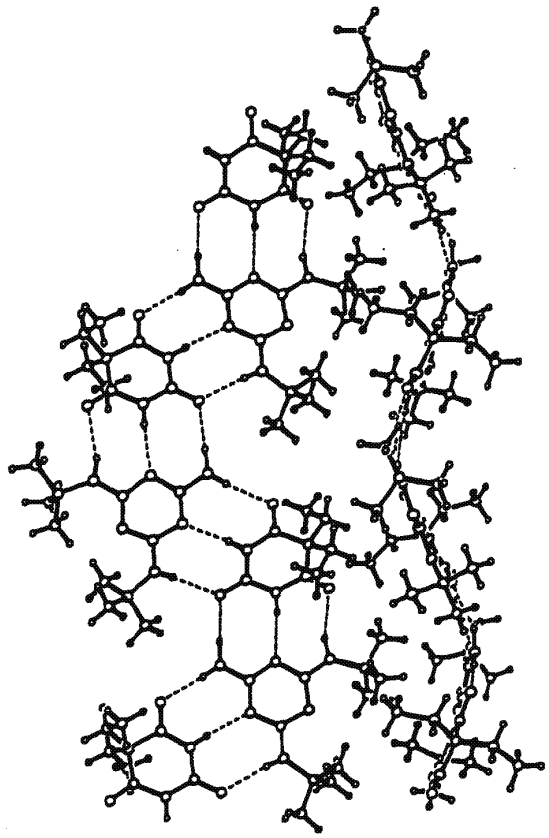


Figure 7. View of two adjacent, roughly perpendicular tapes of **Mel(tBu)$_2$·Bar(Et)$_2$** showing the steric complementarity of their fit. The tape on the right is viewed from the side; the tape on the left is tilted approximately 25° out of the plane of the page (see Figure 3). The deviations from planarity of the tape viewed perpendicularly to the mean plane of its hydrogen bond network (right) clearly are complementary to the protuberances and indentations of the quasiperpendicular tape (left).

While we still have no clear rationalization of intertape packing, we note that it is possible to relate the waviness of a tape—that is, the deviation of its hydrogen-bonded backbone from planarity—to the minimization of voids (and the maximization of the packing fraction, C_k) in the crystal. Crinkled tapes appear to deviate from planarity in order to pack as closely as possible to neighboring tapes. Since our system of tapes appears to be robust enough to tolerate a range of substitutional modifications, we believe that experiments designed to examine the consequences of steric perturbations on packing can be performed in a controlled and consistent fashion.

This system provides another model with which to study the physical–organic chemistry of the solid state. It should provide a consistent molecular framework—parallel, crinkled tapes—with which to probe relations between molecular and crystalline structure.

Experimental Section

General. *tert*-Butylamine was obtained from Aldrich Chemicals. Both 5,5-dimethylbarbituric acid[14] and 5,5-diphenylbarbituric acid[15] were prepared by literature procedures. General techniques were as previously published.[3]

(9) $C_k = N \cdot V_{mol}/V_{cell}$, where N is the number of molecules in a unit cell, V_{mol} is the molecular volume, and V_{cell} is the volume of the unit cell. Kitaigorodsky, A. I. *Organic Chemical Crystallography*; Consultants Bureau: New York, 1961.

(10) See ref 3 for a discussion of the relationship of C_k^* to C_k.

(11) Values of C_k usually range from roughly 0.65 to 0.77. Desiraju, G. R. *Crystal Engineering: The Design of Organic Solids*; Elsevier: New York, 1989.

(12) Taylor, R.; Kennard, O. *Acc. Chem. Res.* **1984**, *17*, 320.

(13) Gas-phase studies have shown that linear hydrogen bonds are the most stable (Legon, A. C.; Miller, D. J. *Acc. Chem. Res.* **1987**, *20*, 39). Crystals, however, need to balance a number of intermolecular forces, and hydrogen bonds seem to be able to deform to some extent to permit close packing between other parts of molecules.[11,12]

(14) (a) *Organic Syntheses*; Blatt, A. H., Ed.; Wiley and Sons: New York, 1943; Collect. Vol. II, p 60. (b) Thorne, J. T. *J. Chem. Soc.* **1881**, *39*, 543.

(15) McElvain, S. M. *J. Am. Chem. Soc.* **1935**, *57*, 1303.

UM00014065
NOVARTIS EXHIBIT 1517
Novartis v. Regents, IPR2023-01347
Page 2811 of 4460

2-Amino-4,6-bis(*tert*-butylamino)-1,3,5-triazine (Mel(^{t}Bu)$_2$). A solution of cyanuric chloride (2.0 g, 10.8 mmol) was prepared in 100 mL of freshly distilled THF in a round-bottomed flask and cooled in an ice-water bath. A solution of *tert*-butylamine (1.14 mL, 10.8 mmol) and diisopropylethylamine (1.88 mL, 10.8 mmol) in 20 mL of THF was added from a dropping funnel over the course of 15 min with magnetic stirring. When addition was complete, the ice-water bath was removed and stirring was continued for another hour. The mixture was heated to reflux in an oil bath and another equivalent each of *tert*-butylamine and diisopropylethylamine (in 20 mL of THF) was added. Since the boiling point of *tert*-butylamine is 46 °C, some of this compound was lost to the atmosphere, even with a water-cooled condenser affixed to the reaction flask. Over the course of another 3 h, additional portions of a *tert*-butylamine solution in THF were added to the reaction, amounting to an additional 0.4 equiv. This amount was sufficient to produce primarily one product (2-chloro-4,6-bis(*tert*-butylamino)-1,3,5-triazine) as determined by TLC. The reaction was cooled to room temperature, and solvent was removed by rotary evaporation at aspirator pressure. The residue was slurried in 100 mL of diethyl ether and solids were removed by filtration at aspirator pressure through a short plug of silica gel, which was then washed with more diethyl ether (3 × 30 mL). The ether solutions were combined, and solvent was removed by rotary evaporation at aspirator pressure.

The 2-chloro-4,6-bis(*tert*-butylamino)-1,3,5-triazine was placed in a 15-mL pressure bottle along with a magnetic stirring bar, approximately 8 mL of 2:1 1,4-dioxane/H_2O, and 3 mL of 30% NH_4OH. The pressure bottle was capped and heated in an oil bath to 100–105 °C (**CAUTION: behind a safety shield**). Heating was continued for 5 h, after which the pressure bottle was cooled to room temperature and opened. TLC indicated that some starting material remained, but the most intense spot was the product di(*tert*-butyl)melamine. The reaction mixture was poured into 150 mL of H_2O and stirred well. The precipitated product was collected by vacuum filtration, washed with H_2O (2 × 25 mL), and dried on a vacuum line at 0.1 Torr for several hours. It was then purified by chromatography on silica gel with ethyl acetate as eluant (R_f = 0.3). The product, after rotary evaporation of solvent, was a white solid (1.57 g, 61%): melting point 166–7 °C; ^{1}H NMR (300 MHz, $CDCl_3$) δ 4.85 (br s, 2 H), 4.5 (br s, 2 H), 1.4 (s, 18 H); HRMS-EI (M^+) calcd for $C_{11}H_{22}N_6$ 238.1906, found 238.1913.

5-Ethyl-5-(2,2,2-trifluoroethyl)barbituric acid. The precursor 2,2,2-trifluoroethyl trifluoromethanesulfonate was prepared by a literature procedure from 2,2,2-trifluoroethanol, $(CF_3SO_2)_2O$, and pyridine in $CFCl_3$.[16] A solution of this trifluoromethanesulfonate (2.46 g, 10.6 mmol) in 10 mL of freshly distilled diethyl ether was added over the course of 30 min from a dropping funnel to a refluxing solution of diethyl malonate (1.52 mL, 10 mmol) and NaH (80% by weight, 0.30 g, 10 mmol) in 100 mL of EtOH. Reflux was continued for 3 h, at which point an aliquot was removed, concentrated by rotary evaporation at aspirator pressure, and dried on a vacuum line at 0.1 Torr. The desired diethyl 2,2,2-trifluoroethylmalonate had been formed, as determined by ^{1}H NMR spectroscopy and comparison to literature chemical shifts.[17] Refluxing was continued for another 2 h, after which ethyl iodide (1.2 mL, 15 mmol) and powdered anhydrous K_2CO_3 (1.66 g, 12 mmol) were added to the mixture. Reflux was continued for 3 days. The reaction mixture was cooled to room temperature and solids were removed by filtration at aspirator pressure. Solvent and excess ethyl iodide were removed from the filtrate by rotary evaporation at aspirator pressure. The resulting colorless oil was judged by ^{1}H NMR spectroscopy to be sufficiently pure diethyl ethyl(2,2,2-trifluoroethyl)malonate to proceed to the next step.

A solution of the malonate (1.5 g, 5.6 mmol) in 20 mL of dry EtOH was added in one portion to a gently refluxing homogeneous solution of urea (0.53 g, 8.8 mmol) and sodium (0.37 g, 16 mmol) in 100 mL of dry EtOH in a round-bottomed flask in an oil bath. The temperature of the bath was increased to 105 °C, and reflux was continued overnight. The reaction was then cooled to room temperature and solvent was removed by rotary evaporation at aspirator pressure. The yellow residue thus obtained was dissolved in 50 mL of H_2O and washed with Et_2O (3 × 50 mL). The aqueous layer was neutralized by dropwise addition of concentrated HCl. The resulting white precipitate was collected by vacuum filtration at aspirator pressure and was recrystallized from hot water, giving 0.73 g (55%) of the barbituric acid. Chemical shifts of the ^{1}H NMR spectrum (300 MHz, acetone-d_6) agreed with literature values.[17]

Preparation of Complexes. Equimolar amounts of Mel(^{t}Bu)$_2$ and the barbiturate were dissolved together (in one flask) in THF. The solvent was removed by rotary evaporation at aspirator pressure, and the composition of the complex was checked by ^{1}H NMR spectroscopy. If integration of peaks indicated that one component was present in excess, the other component was added to bring their ratio to 1:1. The melting points of the complexes were the following: Mel(^{t}Bu)$_2$·Bar(Et)$_2$, 236–8 °C; Mel(^{t}Bu)$_2$·Bar(Et)(CH$_2$CF$_3$), 245–7 °C; Mel(^{t}Bu)$_2$·Bar(CH$_3$)$_2$, 248–50 °C; Mel(^{t}Bu)$_2$·Bar(Ph)$_2$, 264–6 °C dec.

Crystallization of Complexes. Mel(^{t}Bu)$_2$·Bar(Et)$_2$ and Mel(^{t}Bu)$_2$·Bar(Ph)$_2$: Crystals were grown by room-temperature evaporation of a solution of the complex in MeOH in a 5-mL screw-top vial with the lid resting loosely on top of the vial.

Mel(^{t}Bu)$_2$·Bar(Et)(CH$_2$CF$_3$) and Mel(^{t}Bu)$_2$·Bar(CH$_3$)$_2$: Crystals were grown by allowing a solution of the complex in boiling EtOH or MeOH, respectively, to cool to room temperature by enclosing a round-bottomed flask containing the solution in a corked Dewar flask. The Dewar flask was allowed to rest undisturbed for 24 h before opening it to check on the progress of crystal growth.

X-ray Crystallography. For details of X-ray data collection, structure solution, and refinement, see the supplementary material. Data were collected on Mel(^{t}Bu)$_2$·Bar(CH$_3$)$_2$, Mel(^{t}Bu)$_2$·Bar(Et)(CH$_2$CF$_3$), and Mel(^{t}Bu)$_2$·Bar(Ph)$_2$ by Molecular Structure Corp., The Woodlands, TX, on a Rigaku AFC5R diffractometer equipped with a rotating anode generator. These structures were solved and refined at Harvard using the Siemens SHELXTL-PLUS package of programs. Data collection, structure solution, and refinement for Mel(^{t}Bu)$_2$·Bar(Et)$_2$ were performed by Crystalytics Co., Lincoln, NE.

Acknowledgment. We acknowledge the support of the National Science Foundation through Grants CHE-91-22331 to G.M.W. and CHE-80-00670 to the Department of Chemistry for the purchase of the Siemens X-ray diffractometer.

Supplementary Material Available: Crystallographic details including tables of atomic positional parameters and bond lengths and angles (65 pages); tables of observed and calculated structure factors (44 pages). This material is contained in many libraries on microfiche, immediately follows this article in the microfilm version of the journal, and can be ordered from the ACS; see any current masthead page for ordering information.

(16) Gassman, P. G.; Harrington, C. K. *J. Org. Chem.* **1984**, *49*, 2765.
(17) Muller, N. *J. Org. Chem.* **1986**, *51*, 263.

UM00014066
NOVARTIS EXHIBIT 1517
Novartis v. Regents, IPR2023-01347
Page 2812 of 4460

The authors thank Professor M. B. Hursthouse, Department of Chemistry, University of Wales, Cardiff, for providing the three-dimensional intensity data. One of the authors (R) wishes to acknowledge the Department of Science and Technology (DST), Ministry of Science and Technology, Government of India, for the award of BOYSCAST fellowship (DST ref. SR/BY/P-04/93), and the University of Jammu, Jammu Tawi, India, for granting a years deputation.

Lists of structure factors, anisotropic displacement parameters and H-atom coordinates have been deposited with the IUCr (Reference: HU1135). Copies may be obtained through The Managing Editor, International Union of Crystallography, 5 Abbey Square, Chester CH1 2HU, England.

References

Almenningen, A. & Bastiansen, O. (1958). *K. Nor. Vidensk. Selsk. Skr.* No. 4.
Altomare, A., Burla, M. C., Cascarano, G., Giacovazzo, C. & Guagliardi, A. (1993). *Acta Cryst.* A**49**, 342–346.
Bastiansen, O. & Traetteberg, M. (1962). *Tetrahedron*, 17, 147–154.
Brock, C. P. & Haller, K. L. (1984). *J. Phys. Chem.* **88**, 3570–3574.
Brock, C. P. & Morelan, G. L. (1986). *J. Phys. Chem.* **90**, 5631–5640.
Charbonneau, G. P. & Delugeard, Y. (1976). *Acta Cryst.* B**32**, 1420–1423.
Charbonneau, G. P. & Delugeard, Y. (1977). *Acta Cryst.* B**33**, 1586–1588.
Cruickshank, D. W. J. & Sparks, R. A. (1960). *Proc. R. Soc. London Ser. A*, **258**, 270–285.
Hargreaves, A. & Rizvi, S. H. (1962). *Acta Cryst.* **15**, 365–373.
Larson, A. C. (1970). *Crystallographic Computing*, edited by F. R. Ahmed, S. R. Hall & C. P. Huber, pp. 291–294. Copenhagen: Munksgaard.
Pearce, L. J., Watkin, D. J. & Prout, C. K. (1992). *CAMERON. A Program for Plotting Molecular Structures*. Chemical Crystallography Laboratory, Univ. of Oxford, England.
Trotter, J. (1961). *Acta Cryst.* **14**, 1135–1140.
Watkin, D. J., Carruthers, J. R. & Betteridge, P. W. (1985). *CRYSTALS User Guide*. Chemical Crystallography Laboratory, Univ. of Oxford, England.

Acta Cryst. (1995). C**51**, 2390–2392

1:1 Molecular Complex of Theophylline and *p*-Nitroaniline

SHYUICHI ZAITU, YOSHIHISA MIWA AND TOORU TAGA

Faculty of Pharmaceutical Sciences, Kyoto University, Sakyo-ku, Kyoto 606-01, Japan

(*Received* 24 *April* 1995; *accepted* 26 *June* 1995)

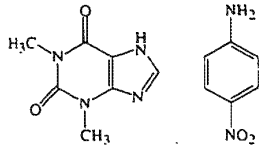
Abstract

Theophylline (3,7-dihydro-1,3-dimethyl-1*H*-purine-2,6-dione) and *p*-nitroaniline molecules in the title complex, $C_7H_8N_4O_2.C_6H_6N_2O_2$, are packed in layers. These layers are held together to form a sheet by a system of intermolecular hydrogen bonding which includes C—H···O hydrogen bonds.

©1995 International Union of Crystallography
Printed in Great Britain – all rights reserved

Comment

The structure determination of the title crystal was undertaken during the course of a study of a number of complexes involving methylxanthine. The structure of the 2:1 complex of theophylline and 5-fluorouracil has been reported (Zaitu, Miwa & Taga, 1995), and the structures of 1:1 theophylline–*p*-nitrophenol (Aoki, Ichikawa, Koinuma & Iitaka, 1987) and 1:1 theophylline–urea (Wiedenfeld & Knoch, 1986) have also been determined. Fig. 1 shows the molecular structure of the title complex, the 1:1 molecular complex of theophylline and *p*-nitroaniline, (I).



(I)

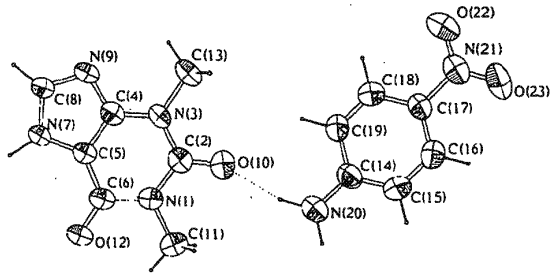


Fig. 1. Perspective view of the title complex with the atom-numbering scheme. Displacement ellipsoids are drawn at the 50% probability level.

The fused theophylline rings are essentially planar and the bond lengths and angles within the molecule are in fairly good agreement with those observed in theophylline monohydrate (Sutor, 1958) and other theophylline complexes, *e.g.* 1:1 theophylline–sulfathiazole (Shefter & Sackman, 1971). The *p*-nitroaniline molecule has practically a twofold axis collinear with the C—N bonds and, as has been observed in *p*-nitroaniline itself (Colapietro, Domenicano, Marciante & Portalone, 1982), the C—C bonds of the six-membered ring along the long molecular axis are shorter than the other C—C bonds. The planar molecules are packed by stacking forces and hydrogen bonds (Table 3) to form theophylline–*p*-nitroaniline layers (Fig. 2). C(8)—H···O(12) interactions are considered to be C—H···O hydrogen bonds; similar C(8)—H hydrogen bonds to

UM00014067
NOVARTIS EXHIBIT 1517
Novartis v. Regents, IPR2023-01347
Page 2813 of 4460

carbonyl O atoms have been observed in a number of theophylline complexes, *e.g.* 5-fluorouracil (Zaitu, Miwa & Taga, 1995), urea (Wiedenfeld & Knoch, 1986), *p*-nitrophenol (Aoki, Ichikawa, Koinuma & Iitaka, 1978), phenobarbital (Nakao, Fujii, Sakaki & Tomita, 1977) and 5-chlorosalicylic acid (Shefter, 1969). C(15)—H···O(23)^{i} interactions are also important intermolecular hydrogen bonds; these connect the theophylline–*p*-nitroaniline layers to form a sheet (Fig. 2).

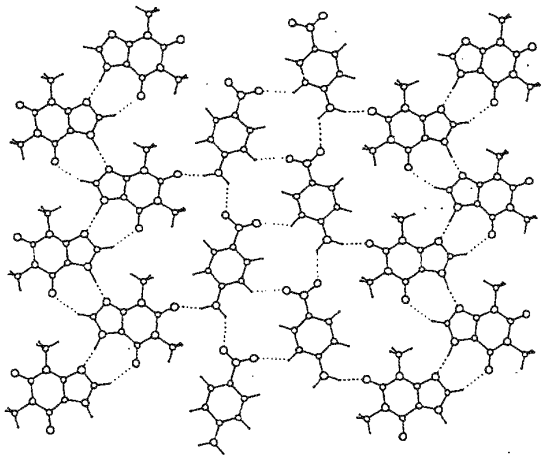


Fig. 2. A sheet of the molecular network in the crystal structure. Dotted lines indicate N—H···N, N—H···O and C—H···O hydrogen bonds.

Experimental

Crystals of the title complex were obtained at room temperature by the slow evaporation of a solution containing equimolar amounts of theophylline and *p*-nitroaniline in chloroform–methanol (10:1) solvent. The density D_m was measured by flotation.

Crystal data

$C_7H_8N_4O_2.C_6H_6N_2O_2$
M_r = 318.29
Monoclinic
$P2_1/c$
a = 7.693 (2) Å
b = 9.178 (1) Å
c = 22.982 (4) Å
β = 116.59 (2)°
V = 1451.0 Å^3
Z = 4
D_x = 1.4568 Mg m^{-3}
D_m = 1.43 Mg m^{-3}

Cu $K\alpha$ radiation
λ = 1.5418 Å
Cell parameters from 25 reflections
θ = 17.9–27.3°
μ = 0.90 mm^{-1}
T = 295.0 K
Prism
0.40 × 0.30 × 0.30 mm
Yellow

Data collection

Rigaku AFC-5 diffractometer
R_{int} = 0.021
θ_{max} = 60°
$\theta/2\theta$ scans
Absorption correction: none
2834 measured reflections
2621 independent reflections
1780 observed reflections [$F > 3\sigma(F)$]
$h = 0 \rightarrow 8$
$k = 0 \rightarrow 10$
$l = -24 \rightarrow 24$
3 standard reflections monitored every 150 reflections
intensity decay: 2%

Refinement

Refinement on F
R = 0.070
wR = 0.075
S = 0.80
1780 reflections
250 parameters
Only coordinates of H atoms refined, all from ΔF map
$w = 1/[\sigma^2(F) + 0.023F^2]$
$(\Delta/\sigma)_{max}$ = 0.05
$\Delta\rho_{max}$ = 0.38 e Å^{-3}
$\Delta\rho_{min}$ = −0.45 e Å^{-3}
Atomic scattering factors from *International Tables for X-ray Crystallography* (1974, Vol. IV, Table 2.2B)

Table 1. *Fractional atomic coordinates and equivalent isotropic displacement parameters* (Å^2)

$B_{eq} = (4/3)\sum_i\sum_j\beta_{ij}\mathbf{a}_i.\mathbf{a}_j$.

	x	y	z	B_{eq}
N(1)	0.0012 (4)	0.2614 (3)	−0.0718 (1)	4.3 (1)
C(2)	0.0330 (6)	0.1112 (4)	−0.0677 (2)	4.7 (1)
N(3)	−0.0907 (5)	0.0289 (3)	−0.1193 (2)	4.4 (1)
C(4)	−0.2398 (6)	0.0960 (3)	−0.1710 (2)	4.2 (1)
C(5)	−0.2649 (5)	0.2419 (3)	−0.1740 (2)	4.1 (1)
C(6)	−0.1446 (5)	0.3381 (4)	−0.1235 (2)	4.2 (1)
N(7)	−0.4270 (5)	0.2673 (3)	−0.2316 (1)	4.6 (1)
C(8)	−0.4889 (6)	0.1377 (4)	−0.2591 (2)	4.9 (1)
N(9)	−0.3779 (5)	0.0279 (3)	−0.2235 (1)	4.6 (1)
O(10)	0.1657 (4)	0.0566 (3)	−0.0202 (1)	6.0 (1)
C(11)	0.1377 (8)	0.3481 (5)	−0.0162 (2)	6.0 (2)
O(12)	−0.1595 (4)	0.4700 (2)	−0.1219 (1)	5.5 (1)
C(13)	−0.0649 (9)	−0.1300 (5)	−0.1186 (3)	6.4 (2)
C(14)	0.5837 (6)	−0.1073 (4)	0.1103 (2)	4.8 (1)
C(15)	0.7458 (6)	−0.1492 (4)	0.1664 (2)	5.2 (1)
C(16)	0.7967 (6)	−0.2919 (4)	0.1791 (2)	5.1 (1)
C(17)	0.6849 (6)	−0.3977 (4)	0.1358 (2)	4.7 (1)
C(18)	0.5218 (6)	−0.3592 (4)	0.0798 (2)	5.2 (1)
C(19)	0.4709 (6)	−0.2162 (4)	0.0667 (2)	5.1 (1)
N(20)	0.5302 (6)	0.0353 (4)	0.0970 (2)	6.3 (1)
N(21)	0.7388 (6)	−0.5499 (4)	0.1480 (2)	6.0 (1)
O(22)	0.6367 (6)	−0.6399 (3)	0.1081 (2)	9.1 (2)
O(23)	0.8807 (5)	−0.5835 (3)	0.1975 (2)	8.2 (1)

Table 2. *Selected bond lengths* (Å) *and angles* (°)

N(1)—C(2)	1.396 (5)	N(7)—C(8)	1.331 (4)
N(1)—C(6)	1.404 (4)	C(8)—N(9)	1.337 (4)
N(1)—C(11)	1.472 (5)	C(14)—C(15)	1.388 (5)
C(2)—N(3)	1.368 (5)	C(14)—C(19)	1.406 (5)
C(2)—O(10)	1.220 (4)	C(14)—N(20)	1.365 (5)
N(3)—C(4)	1.374 (5)	C(15)—C(16)	1.361 (5)
N(3)—C(13)	1.471 (5)	C(16)—C(17)	1.381 (5)
C(4)—C(5)	1.350 (4)	C(17)—C(18)	1.382 (5)
C(4)—N(9)	1.352 (4)	C(17)—N(21)	1.448 (5)
C(5)—C(6)	1.422 (5)	C(18)—C(19)	1.364 (5)
C(5)—N(7)	1.373 (4)	N(21)—O(22)	1.223 (5)
C(6)—O(12)	1.218 (4)	N(21)—O(23)	1.212 (5)
C(2)—N(1)—C(6)	127.0 (3)	C(5)—C(6)—O(12)	127.3 (3)
C(2)—N(1)—C(11)	116.1 (3)	C(5)—N(7)—C(8)	106.5 (3)
C(6)—N(1)—C(11)	116.9 (3)	N(7)—C(8)—N(9)	112.8 (3)
N(1)—C(2)—N(3)	117.0 (3)	C(4)—N(9)—C(8)	103.2 (3)
N(1)—C(2)—O(10)	121.2 (3)	C(15)—C(14)—C(19)	118.4 (3)
N(3)—C(2)—O(10)	121.9 (3)	C(15)—C(14)—N(20)	122.0 (3)
C(2)—N(3)—C(4)	119.3 (3)	C(19)—C(14)—N(20)	119.6 (3)

UM00014068
NOVARTIS EXHIBIT 1517
Novartis v. Regents, IPR2023-01347
Page 2814 of 4460

C(2)—N(3)—C(13)	120.0 (3)	C(14)—C(15)—C(16)	121.2 (3)
C(4)—N(3)—C(13)	120.7 (3)	C(15)—C(16)—C(17)	119.7 (3)
N(3)—C(4)—C(5)	122.3 (3)	C(16)—C(17)—C(18)	120.3 (3)
N(3)—C(4)—N(9)	125.7 (3)	C(16)—C(17)—N(21)	120.4 (3)
C(5)—C(4)—N(9)	112.1 (3)	C(18)—C(17)—N(21)	119.3 (3)
C(4)—C(5)—C(6)	123.2 (3)	C(17)—C(18)—C(19)	120.2 (3)
C(4)—C(5)—N(7)	105.4 (3)	C(14)—C(19)—C(18)	120.1 (3)
C(6)—C(5)—N(7)	131.3 (3)	C(17)—N(21)—O(22)	118.3 (3)
N(1)—C(6)—C(5)	111.2 (3)	C(17)—N(21)—O(23)	119.1 (3)
N(1)—C(6)—O(12)	121.5 (3)	O(22)—N(21)—O(23)	122.6 (4)

Table 3. *Hydrogen-bonding geometry* (Å, °)

D—H···*A*	H···*A*	*D*···*A*	*D*—H···*A*
N(7)—H(7)···N(9^{i})	1.76 (3)	2.766 (4)	171 (3)
N(20)—H(20*B*)···O(10)	1.91 (4)	2.897 (4)	163 (3)
N(20)—H(20*A*)···O(22^{ii})	2.31 (4)	3.072 (4)	132 (3)
C(8)—H(8)···O(12^{iii})	2.30 (4)	3.247 (4)	149 (2)
C(15)—H(15)···O(23^{iv})	2.45 (3)	3.218 (4)	131 (2)

Symmetry codes: (i) $-1-x, \frac{1}{2}+y, -\frac{1}{2}-z$; (ii) $x, 1+y, z$; (iii) $-1-x, y-\frac{1}{2}, -\frac{1}{2}-z$; (iv) $2-x, \frac{1}{2}+y, \frac{1}{2}-z$.

Data collection: *MSC/AFC Diffractometer Control Software*. (Molecular Structure Corporation, 1988). Cell refinement: *MSC/AFC Diffractometer Control Software*. Data reduction: *MSC/AFC Diffractometer Control Software*. Program(s) used to solve structure: *MULTAN*88 (Main *et al.*, 1988). Program(s) used to refine structure: *KPPXRAY* (Taga, Masuda, Higashi & Iizuka, 1991) including a modified version of *ORFLS* (Busing, Martin & Levy, 1962). Molecular graphics: *KPPXRAY*. Software used to prepare material for publication: *EDCIF-J* (Osaki & Taga, 1993).

Lists of structure factors, anisotropic displacement parameters, H-atom coordinates and complete geometry have been deposited with the IUCr (Reference: AS1190). Copies may be obtained through The Managing Editor, International Union of Crystallography, 5 Abbey Square, Chester CH1 2HU, England.

References

Aoki, K., Ichikawa, T., Koinuma, Y. & Iitaka, Y. (1978). *Acta Cryst.* B34, 2333–2336.

Busing, W. R., Martin, K. O. & Levy, H. A. (1962). *ORFLS. Fortran Crystallographic Function and Error Program*. Report ORNL-TM-305. Oak Ridge National Laboratory, Tennessee, USA.

Colapietro, M., Domenicano, A., Marciante, C. & Poltalone, G. (1982). *Z. Naturforsch. Teil B*, 37, 1309–1311.

Main, P., Hull, S. E., Lessinger, L., Germain, G., Declercq, J.-P. & Woolfson, M. M. (1988). *MULTAN*88. *A System of Computer Programs for the Automatic Solution of Crystal Structures from X-ray Diffraction Data*. Univs. of York, England, and Louvain, Belgium.

Molecular Structure Corporation (1988). *MSC/AFC Diffractometer Control Software*. MSC, 3200 Research Forest Drive, The Woodlands, TX 77381, USA.

Nakao, S., Fujii, S., Sakaki, T. & Tomita T. (1977). *Acta Cryst.* B33, 1373–1378.

Osaki, K. & Taga, T. (1993). *J. Crystallogr. Soc. Jpn*, 35, 223–224.

Shefter, E. (1969). *J. Pharm. Sci.* 58, 710–714.

Shefter, E. & Sackman, P. (1971). *J. Pharm. Sci.* 60, 282–286.

Sutor, D. J. (1958). *Acta Cryst.* 11, 83–87.

Taga, T., Masuda, K., Higashi, T. & Iizuka, H. (1991). *KPPXRAY. Kyoto Program Package for X-ray Crystal Structure Analysis*. Kyoto Univ., Kyoto Japan.

Wiedenfeld, H. & Knoch, F. (1986). *Arch. Pharm.* 319, 654–659.

Zaitu, S., Miwa, Y. & Taga, T. (1995). *Acta Cryst.* C51. In the press.

©1995 International Union of Crystallography
Printed in Great Britain – all rights reserved

Acta Cryst. (1995). C51, 2392–2395

α- and γ-Polymorphs of Dimethyl 9-Chloromethyl-9,10-dihydro-9,10-ethenoanthracene-11,12-dicarboxylate

RAY JONES, STEVEN J. RETTIG AND JAMES TROTTER

Department of Chemistry, University of British Columbia, Vancouver, BC, Canada V6T 1Z1

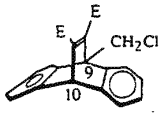
(*Received* 14 *February* 1995; *accepted* 19 *April* 1995)

Abstract

Two further polymorphic forms (α = $P2_1$ and γ = $P2_1/c$) of the title compound ($C_{21}H_{17}ClO_4$) have been obtained and their crystal structures determined. The molecular geometries and photochemical behaviour are very similar to those of the previously described β-form reported in the $P2_1/c$ space group [Chen, Pokkuluri, Scheffer & Trotter (1993). *Acta Cryst.* B49, 905–909].

Comment

The crystal structure and photochemistry of the title compound have been described previously (Chen, Pokkuluri, Scheffer & Trotter, 1991, 1993). Further study of the material (Chen, 1991) led to isolation of two other polymorphic modifications. Crystallization from chloroform/methanol gives the previously described prismatic crystals (now named the β-form). Crystallization from diethyl ether/petroleum ether gives needles (α-form) and prisms (β-form), while crystallization from acetone/hexane gives block-shaped crystals (γ-form). The α-form has a melting point 6 K higher than the other two forms, and the three forms have slightly different FTIR (Fourier transform infrared) spectra and photochromic behaviour (Chen, 1991).



E = CO_2Me

(I)

The molecules in all three polymorphic forms have very similar conformations and dimensions (Table 2). The ester group remote from the chloromethyl substituent is conjugated with the C11═C12 double bond in each molecule; the C11—C12—C15—O4 torsion angles are not far from 0 or 180°, with $\cos^2$(angle) = 0.88–1.00 (0.67 for the disordered group of the γ-form). The ester group adjacent to the chloromethyl group is not conjugated, presumably as a result of steric interactions; the

UM00014069
NOVARTIS EXHIBIT 1517
Novartis v. Regents, IPR2023-01347
Page 2815 of 4460

Monatshefte für Chemie. Vol. 80/5, pages 595-606 (1949)

Concerning organic molecular compounds and their polymorphism

by

H. Quehenberger

From the Pharmacological Institute of the University of Innsbruck

With 5 diagrams

(Submitted on February 17, 1949. Presented at the Session on February 24, 1949)

In 1924, *Hertel*[1] succeeded in demonstrating that molecular compounds can be obtained from many pairs of organic substances, whereby, with the same composition, these molecular compounds exhibit a different color, different solubility and different melting points. From the crystallographic (fine structural) viewpoint[2], the theoretical phase viewpoint[3] and the thermochemical viewpoint[4], the two forms of such systems behave like two "allotropic" modifications of a substance. At an even earlier time (1907), *H. Hantzsch*[5] drew attention to chromo-isomerism, and defined this term phenomenologically. Even if, in accordance with the work of *C. Weygand*[6], chromo-isomerism cannot be equated with polymorphism, a transition between isomerism and polymorphism is nevertheless found.

In more recent times, the investigations of *A. Kofler*[7] have generated additional insights into the polymorphism relationships of organic molecular compounds. In some cases, a connection was observed between the polymorphism of the molecular compound and that of a component, but not in other cases.

In the case of the present investigations, use has been made of the micro-melting point apparatus of *L. Kofler*[8]. The melting points were observed of microscopic preparations between the specimen slide and the cover glass.

In order to discover and investigate the molecular compounds that are indicated in the experimental part, use was made of the contact method of *A. Kofler*[9]. As a result of observing the contact zone for a single microscopic preparation, it permits one to ascertain, within an extremely short time, the eutectic temperature of two components and, in the case where one or more molecular compounds are present, the different eutectic compositions and, in addition, the melting points of the molecular compounds. This method of working also permits one to recognize and observe the polymorphism of molecular compounds; as a result of this, the graphical recording of unstable modifications is also made possible.

Following the preparative synthesis of the molecular compound in the case of the complex isomeric system 1-bromo-4-naphthylamine:2,6-dinitrophenol, *E. Hertel*[1] was successful in recording the melting points of the two modifications in a melting point diagram in the way in which this was indicated by *Rheinbold*[10].

When using the contact method[9], the thermal analysis of polymorphous compounds is found to be significantly simpler and less unambiguous in many cases.

The following working procedure was maintained for the preparation of a contact preparation. The higher melting substance is made to melt so that the melt adopts approximately one half of the space between the specimen slide and the cover glass. After solidifying the melt by cooling, the second substance is introduced at the edge of the cover glass, and heating to a few degrees above its melting point is carried out; as a result of this, the melt then flows into the space that is still free. In many cases, it is recommended that the entire preparation then be allowed to fuse together and to stay at this temperature for some time, especially if the formation of the molecular compound takes place very sluggishly. If strong affinity exists between the two components, then vigorous formation of the molecular compound takes place and one has to work especially cautiously.

Polymorphous systems can also be investigated by observing the contact zone of two components. The same method of working applies to the preparation of unstable modifications of molecular compounds as that which is used for the synthesis of unstable forms of simple chemical substances[8, 11]. The fact that organic molecular compounds, likewise, can be monotropic or enantiotropic emerges from the work of *A. Kofler*[12].

The question arises as to whether this is a general property of acid amides, whereby attention was drawn to this possibility as a result of the tendency of nicotinamide[13] to exhibit polymorphism. In order to settle this, eight acid amides were investigated with, in each case, nine carboxylic acids and, in each case, three phenols. Under the experimental conditions that were used, it was not possible to discern polymorphism in any of the molecular compounds that were obtained in this way. Without exception, however, these were acidic amides, whereas, by contrast, nicotinamide possesses a basic character. Thus the basic component of the nicotinamide [molecule] could possibly be the cause of the frequent formation of polymorphous molecular compounds. However, the pyridine component is more probable for the formation of polymorphous molecular compounds of nicotinamide with acids and phenols, as is the case with e.g. pyridine compounds[14] and phenols that has been known for a long time.

It was possible to establish polymorphous molecular compounds of nicotinamide with the following carboxylic acids:

nicotinamide:p-cresotic acid (2 MV [molecular compounds], 1:3, dimorphous)
nicotinamide:m-nitrobenzoic acid (3 MV [molecular compounds], 1:4, dimorphous)
nicotinamide:cinnamic acid (1:1, dimorphous).

A marked tendency to form molecular compounds and also to exhibit polymorphism could also be observed in the case of three of the four amines that were investigated, whereby, in each case, these were also investigated with nine different carboxylic acids and three different phenols. Thus:

benzidine and cinnamic acid give an MV [molecular compound], 1:1, dimorphous;
p-phenylenediamine and hexadecanedicarboxylic acid give a trimorphous molecular compound;
o-phenylenediamine and picric acid give a trimorphous molecular compound;
p-phenylenediamine and p-cresotic acid give a dimorphous molecular compound;
o-phenylenediamine and p-cresotic acid give three molecular compounds, 1:1, trimorphous.

The two molecular compounds of the p-phenylenediamine:cinnamic acid system are interesting since one molecular compound can be absent under certain experimental conditions and one is produced from the other. In addition, two non-homogeneously melting molecular compounds - of which the 1:1 MV [molecular compound] is dimorphous - could be established in the benzidine:methyl p-nitrobenzoate system.

Despite their polymorphous molecular compounds, the o-phenylenediamine:picric acid and p-phenylenediamine:p-cresotic acid systems were not recorded since the melting points of the individual modifications cannot be determined.

In addition, benzidine and bromural were investigated in terms of their molecular compounds with, in each case, 75 substances.

Despite the marked tendency of urea to form molecular compounds, it was established that its derivatives [bromural (monobromoisovalerylurea), adalin (bromodiethylacetylurea), and diethylurea] scarcely possess this ability any longer and, if so, then only to a much lower extent although an amino group would still be free in part.

In addition, an investigation was also made of the polymorphism of some known, medicinally utilized molecular compounds. Thus, for example, [an investigation was made of] veramon, isoamylethylbarbituric acid (hypnal), pyramidon + Orthoform-Neu (methyl m-amido-p-oxybenzoate), sarcosine anhydride + Orthoform-Neu, and antipyrine + Orthoform-Neu. These molecular compounds had already been discovered by *P. Pfeiffer* and *E. Seidel*[15]. However, polymorphism could not be observed in any of them. The dimorphous nature of trigemin is already known[8]. However, it could not be demonstrated in the contact preparation because of the exceedingly high volatility of chloral hydrate.

The molecular compounds, which were observed between nine acid amides and four amines, are arranged alphabetically in the following list. The negative cases, i.e. the cases in which the two components do not react to form a molecular compound but merely form a eutectic composition, follow as well. [Translator: the letter "E", such as in "E_1" etc., in the following diagrams and data tabulations has not been defined specifically by the author; however, "E" would seem to designate "eutectic composition", E_1 "1st eutectic composition", etc.]

In the case of the occurrence of molecular compounds, the temperatures of the eutectic compositions and their melting points and color are indicated.

A summary is then given of those systems in which the contact zone could not be made to crystallize under the experimental conditions that were used (seeding, heat, coldness).

Out of the twelve systems for which a phase diagram (designated by +) was recorded, only five have been published for reasons of saving space. For the same reason, the publication of an exact experimental description has also been dispensed with.

[Translator's Note: In the following tables, the author utilizes reference [16] (to be found at the end of this translation) to define the various symbols. As already mentioned, "E", "E_1", etc. are not specifically defined but presumably indicate "eutectic composition", 1st eutectic composition", etc.]

LIST OF THE ACID AMIDES AND AMINES[16] THAT HAVE BEEN INVESTIGATED IN TERMS OF MOLECULAR COMPOUNDS AND THEIR POLYMORPHISM

ACID AMIDES

Substances	Melting point of the molecular compounds and their eutectic compositions	Color
Benzamide	E_1 113, E_2 118, MV 120	Yellow
o-cresotic acid[17]	E_1 102, E_2 112, MV 116	
p-cresotic acid	E_1 119, E_2 114, E_3 116, E_4 115, MV 137	Yellow
m-nitrobenzoic acid	E_1 101, E_2 102, MV 111	
Picric acid	E_1 76, E_2 80,5, MV 88	
Resorcinol[18]	E_1 106, E_2 115, MV 118	
Salicylic acid		
Bromural	E_1 126, E_2 128, MV 134	
Mesaconic acid	E_1 72, E_2 100, MV 101	
1-oxy-3-ethoxybenzaldehyde	E_1 109, E_2 129, MV 131	
Picric acid		
n-butyramide	E_1 32, E_2 34, MV 35	
Pyrocatechol	E_1 77, E_2 80, MV 84	
m-nitrobenzoic acid		
Nicotinamide	E_1 115, E_2 129, MV 144	
o-cresotic acid	E_1 123, E_2 122, MV_1 124, E_3 123,5, MV_2 140, E_4 116,5, E_5 116, MV_1 II 117, E_6 104	
+ p-cresotic acid	E_1 121, E_2 123,5, E_3 128, MV_1 129, MV_2 130,5	
Hexadecanedicarboxylic acid	E_1 123, E_2 129, MV_1 131, E_3 133, MV_2 135, MV_3 150, E_4 124, E_5 121, E_6 ~70	
+ m-nitrobenzoic acid	E_1 98, E_2 103, MV_1 110, E_3 113, MV_2 115, E_4 116, MV_3 126	Yellow
p-nitrophenol	E_1 117, E_2 120, E_3 129, MV_1 129,5, MV_2 189	Yellow
Picric acid	E_1 111, E_2 119, MV 136,5	
Salicylic acid	E_1 95, E_2 96, MV_1 98,5, E_3 90, E_4 93, E_5 94,5, MV_1 II 96,5, E_6 88,5, E_7 80	
+ cinnamic acid		
Propionamide	E_1 54, E_2 70, MV 74	
m-nitrobenzoic acid	E_1 42, E_2 51, MV 58	
p-nitrophenol		
Salicylamide	E_1 123, E_2 134, MV 136	
o-cresotic acid	E_1 111, E_2 116, MV 117	
p-cresotic acid	E_1 121, E_2 122, MV 135	
m-nitrobenzoic acid		

Substances	Melting point of the molecular compounds and their eutectic compositions	Color
Picric acid	E_1 99, E_2 104, MV 106	yellow
Sulfanilamide		
Picric acid	E_1 119, E_2 147, MV 176	
	Amine.	
Benzidine		
Aspirin	E_1 105, E_2 114, MV 252	
+ azelaic acid	E_1 103, E_2 113, E_3 108, MV_1 114, MV_2 114,5, E_4 104	
Benzylic acid	E_1 116, E_2 145, MV 226	
Benzoic acid	E_1 96, E_2 101, MV 103	
+ pyrocatechol	E_1 103, E_2 108, MV 148, E_3 106, E_4 101	
o-cresotic acid	E_1 109, E_2 136, MV_1 138, E_3 143, MV_2 151	
3,4-dioxybenzaldehyde	E_1 102, E_2 110, MV ?	red
2,5-dioxybenzaldehyde	E_1 91, E_2 110, MV ?	red
Glutamic acid	E_1 119, E_2 126, MV 171	
Hexadecanedicarboxylic acid	E_1 117, E_2 119, MV 124	
Hippuric acid	E_1 116, E_2 140, MV 146	
Suberic acid	E_1 112, E_2 122, MV 124	
Lactophenin	E_1 106, E_2 108, MV 115	
d,l-mandelic acid	E_1 73, E_2 119, MV 149	
Monochloroacetic acid	E_1 44, E_2 118, E_3 135, MV_1 148, $MV_2 \approx 265$	
α-naphthol	E_1 85, E_2 86, MV 98	
β-naphthol	E_1 116, E_2 117, MV_1 132, E_3 130, MV_2 171	
+ m-nitrobenzoic acid	E_1 139, E_2 157, E_3 114, MV_1 158,5, MV_2 160,5, E_4 111, E_5 109	yellow
o-nitrobenzoic acid	E_1 120, E_2 138, MV 189	
m-nitrobenzaldehyde	E_1 52, E_2 78, MV 129	brown-yellow
o-nitrobenzaldehyde	E_1 36, E_2 82, MV 214	yellow
p-nitrobenzaldehyde	E_1 92, E_2 103, MV ?	
+ methyl p-nitrobenzoate methylester	E_1 80, E_2 77, E_3 75, MV_1 I 89, MV_1 II 86, MV_2 102	
p-nitrophenol	E_1 99, E_2 115, MV 151	
Pernocton	E_1 113, E_2 122, MV 142	
Phenylacetic acid	E_1 74, E_2 117, MV 126	
Phloroglucinol	E_1 121, E_2 163, MV ?	
Picric acid	E_1 106, E_2 119, MV ?	yellow-brown
Piperonal	E_1 31, E_2 74, MV ?	green-yellow
Pyrogallol	E_1 112, E_2 117, MV 143	
Pyrogallol-1,3-dimethyl ether	E_1 47, E_2 93, MV 106	
m-oxybenzaldehyde	E_1 89, E_2 109, MV 270	yellow
m-oxybenzoic acid	E_1 118, E_2 148, MV 151	
+ resorcinol	E_1 106, E_2 114, MV 143, E_3 103, E_4 111, E_5 109	

UM00014074
NOVARTIS EXHIBIT 1517
Novartis v. Regents, IPR2023-01347
Page 2820 of 4460

Substances	Melting point of the molecular compounds and their eutectic compositions	Color
Salicylic acid	E_1 112, E_2 147, MV 161	
o-sulfobenzoic acid	E_1 66, E_2 111, MV ?	yellow
Tetradicarboxylic acid [sic]	E_1 112, E_2 116, MV 122	
Trichloroacetic acid	E_1 49, E_2 115, MV ?	
s-trinitrobenzene	E_1 94, E_2 106, MV 131	dark violet
s-trinitrotoluene	E_1 66, E_2 90, MV 99	red-brown
o-vanillin	E_1 73, E_2 109, MV 212	yellow-red
+ cinnamic acid	E_1 112, E_2 100, MV_1 I 113, E_3 108,5, E_4 98, MV_1 II 109, E_5 97	
o-phenylenediamine		
Pyrocatechol[19]	E_1 76, E_2 76, MV 84,5	
o-cresotic acid	E_1 91, E_2 123, MV 128	
+ p-cresotic acid	E_1 96, E_2 111, MV_1 112, E_6 114, MV_2 II 116, E_4 116,5, MV_3 117 MV_2 I 123, E_5 92, E_7 110	
+ m-nitrobenzoic acid	E_1 95, E_2 132, E_3 122, MV_1 133, MV_2 138	
p-nitrophenol	E_1 68, E_2 84, MV 88	weakly yellow
Picric acid	E_1 95, E_2 119, MV ?	
Resorcinol[19]	E_1 45, E_2 47, MV 50	
Salicylic acid[20]	E_1 86, E_2 109, MV 116	
Cinnamic acid[20]	E_1 86, E_2 94, MV 95,5	
p-phenylenediamine		
Azelaic acid	E_1 78, E_2 110, MV 112	
Pyrocatechol[19]	E_1 87,5, E_2 99, MV 108	
o-cresotic acid	E_1 107, E_2 140, E_3 141, MV_1 142, MV_2 148	MV_1= brown MV_2= yellow
p-cresotic acid	E_1 126, E_2 132, MV 172	
Hexadecanedicarboxylic acid	E_1 117, E_2 128, MV_1 I 130, E_3 112, E_4 122, MV_1 II 126, E_5 117, E_6 118, MV_1 III 120	
m-nitrobenzoic acid	E_1 127, E_2 131,5, E_3 132, MV_1 136, MV_2 158,5, E_4 157,5 MV_3 163	
p-nitrophenol	E_1 114, E_2 115, MV_1 122,5, E_3 123, MV_2 139	
Resorcinol[19]	E_1 94, E_2 102, MV 116	
Salicylic acid[20]	E_1 100, E_2 107, MV 137	
+ cinnamic acid	E_1 118, E_2 123, E_3 120, MV_1 125, MV_2 128, E_4 106	
Thiosinamine		
Picric acid	E_1 73, E_2 106, MV 162	yellow

The following acid amides and amines do *not* give a molecular compound with the listed substances.

Benzamide: diallylbarbituric acid (dial), hexadecanedicarboxylic acid, p-nitrophenol, cinnamic acid.

Bromural: aconitic acid, adenine, allantoin, alloxan, anthranilic acid, benzamide, benzoic acid, naphthyl benzoate, phenyl benzoate, benzenesulfonamide, bromosuccinic acid, α-bromostearic acid, capric acid, chloral hydrate, cholanic acid, chrysophanic acid, citric acid, o-cresotic acid, p-cresotic acid, diallylbarbituric acid (dial), 3,4-dioxybenzaldehyde, gallic acid, gluconolactone, glutamic acid, glycocoll, uric acid, hexadecanedicarboxylic acid, hippuric acid, lactophenin, levulinic acid, d,l-mandelic acid, m-nitrobenzaldehyde, o-nitrobenzaldehyde, p-nitrobenzaldehyde, m-nitrobenzoic acid, o-nitrobenzoic acid, m-nitrophenol, o-nitrophenol, p-nitrophenol, isopropyl-β-bromoallylbarbituric acid (noctal), diethylaminoisopropylallylbarbituric acid (numal), m-oxybenzaldehyde, o-oxybenzoic acid, p-oxybenzoic acid, phenacetin, phenol, phenylacetic acid, phloroglucinol, phthalic acid, pimelic acid, piperonal, pyrogallol-1,3-dimethyl ether, salicylic acid guaiacol ester (guaiacolsalol), resorcinol, salicylic acid, phenyl salicylate (salol), the salicylic acid ester of acetyl-p-aminophenol (salophen), sandoptal, sorbic acid, o-sulfibenzoic acid [sic], stearic acid, tartronic acid, theobromine, theophylline, thymolnaphthalin [sic], tricarballylic acid, trichlorobutyric acid, trichloroacetic acid, d-tartaric acid, o-vanillin, veratraldehyde, cinnamic acid, cinnamic anhydride, citraconic acid.

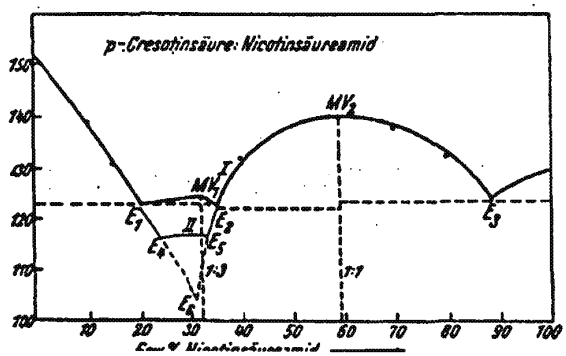


Fig. 1

Key to Figure 1:

p-Cresotinsäure:	=	p-cresotic acid:
Nicotinsäureamid		nicotinamide
MV_1	=	1st molecular compound
MV_2	=	2nd molecular compound
Gew.% Nicotinsäureamid	=	% by weight of nicotinamide

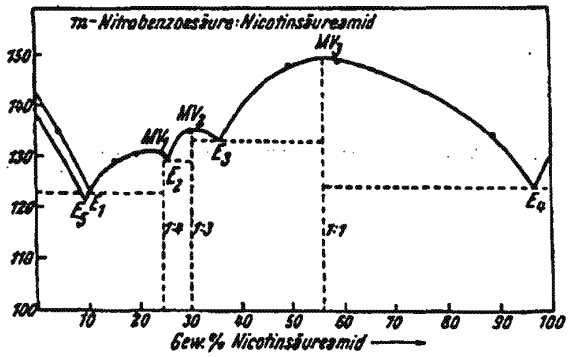


Fig. 2

Key to Figure 2:

m-Nitrobenzoesäure:	=	m-nitrobenzoic acid:
Nicotinsäureamid		nicotinamide
MV_1	=	1st molecular compound
MV_2	=	2nd molecular compound
MV_3	=	3rd molecular compound
Gew.% Nicotinsäureamid	=	% by weight of nicotinamide

n-butyramide: azelaic acid, o-cresotic acid, p-cresotic acid, diallylbarbituric acid (dial), hexadecanedicarboxylic acid, p-nitrophenol, picric acid, salicylic acid, cinnamic acid.

Nicotinamide: amidoacetanilide, amidoazobenzene, p-aminophenol, anisic acid, antipyrine, prontalbin.

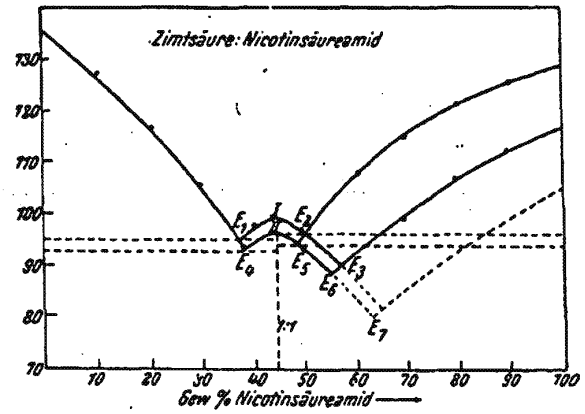


Fig. 3

Key to Figure 3:

Zimtsäure:	=	Cinnamic acid:
Nicotinsäureamid		nicotinamide
Gew.% Nicotinsäureamid	=	% by weight of nicotinamide

Propionamide: azelaic acid, o-cresotic acid, p-cresotic acid, diallylbarbituric acid (dial), hexadecanedicarboxylic acid, picric acid, salicylic acid, cinnamic acid.

Salicylamide: azelaic acid, pyrocatechol, diallylbarbituric acid (dial), hexadecanedicarboxylic acid, p-nitrophenol, resorcinol, salicylic acid, cinnamic acid.

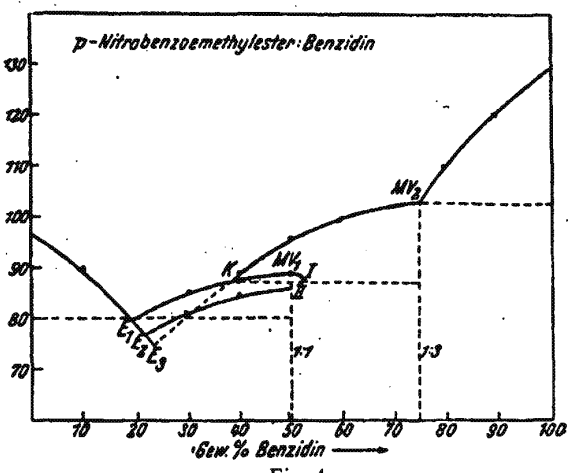


Fig. 4

Key to Figure 4:

p-Nitrobenzoemethylester:	=	Methyl p-nitrobenzoate:
Benzidin		benzidine
MV_1	=	1st molecular compound
MV_2	=	2nd molecular compound
Gew.% Benzidin	=	% by weight of benzidine

Sulfanilamide: azelaic acid, pyrocatechol, o-cresotic acid, p-cresotic acid, diallylbarbituric acid (dial), hexadecanedicarboxylic acid, m-nitrobenzoic acid, p-nitrophenol, resorcinol, salicylic acid, cinnamic acid.

p-toluenesulfonamide: azelaic acid, pyrocatechol, o-cresotic acid, p-cresotic acid, diallylbarbituric acid (dial), hexadecanedicarboxylic acid, m-nitrobenzoic acid, p-nitrophenol, picric acid, resorcinol, salicylic acid, cinnamic acid.

Trichloroacetamide: azelaic acid, pyrocatechol, o-cresotic acid, p-cresotic acid, diallylbarbituric acid (dial), hexadecanedicarboxylic acid, m-nitrobenzoic acid, p-nitrophenol, picric acid, resorcinol, salicylic acid, cinnamic acid.

Benzidine: acetanilide, amidoacetanilide, amidoazobenzene, m-amidobenzoic acid, o-amidobenzoic acid, p-amidobenzoic acid, antipyrine, azobenzene, benzil, benzylaniline, naphthyl benzoate, phenyl benzoate, bromosuccinic acid, capric acid, citric acid, diallylbarbituric acid (dial), urea, mesaconic acid, α-naphthylamine, β-naphthylamine, nicotinamide, nipabenzyl, the ethyl ester of p-oxybenzoic acid (Nipagin A), the propyl ester of p-oxybenzoic acid (Nipasol), phenacetin, phenanthrene, p-oxybenzoic acid, salicylic acid guaiacol ester (guaiacolsalol), the salicylic acid ester of acetyl-p-aminophenol (salophen), sorbic acid, trichlorobutyric acid, d-tartaric acid, xylene musk.

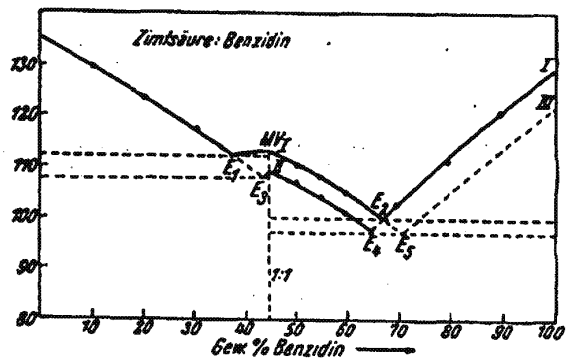


Fig. 5

Key to Figure 5:

Zimtsäure:	=	Cinnamic acid:
Benzidin		benzidine
MV	=	Molecular compound
Gew.% Benzidin	=	% by weight of benzidine

o-phenylenediamine: azelaic acid, diallylbarbituric acid (dial), hexadecanedicarboxylic acid.

p-phenylenediamine: diallylbarbituric acid (dial).

Thiosinamine: azelaic acid, pyrocatechol, o-cresotic acid, p-cresotic acid, diallylbarbituric acid (dial), hexadecanedicarboxylic acid, m-nitrobenzoic acid, p-nitrophenol, resorcinol, salicylic acid, cinnamic acid.

It was not possible to make the contact zone crystallize in the case of the following systems:

bromural: monochloroacetic acid; n-butyramide: resorcinol; nicotinamide: mandelic acid; nicotinamide: resorcinol; propionamide: pyrocatechol; propionamide: resorcinol.

I. Nicotinamide (N): p-cresotic acid (C) (Fig. 1)

E_1 123, E_2 122, E_3 123,5, MV_1 I 124, MV_2 140, E_4 116,5, E_5 116, MV_1 II 117, E_6 106.

Gew.-% N:	0	10	15	20	30	40	50	60	70	80	90	100
Schmp.:	151	138	130	123	123,5	132	138	140	137	132	124	129

MV_1 = 1 : 3 (32,7% N : 67,7% C).
MV_2 = 1 : 1 (59,3% N : 40,7% C).

Key to Data I:
MV = Molecular compound
Gew.-% N = % by weight of N
Schmp. = Melting point

II. Nicotinamide (N): m-nitrobenzoic acid (Nb) (Fig. 2)

E_1 123, E_2 129, MV_1 131, E_3 133, MV_2 135, MV_3 150, E_4 124, E_5 121, E_6 70.

Gew.-% N:	0	5	10	15	20	30	35	40	50	60	70	80	90	100
Schmp.	142	135	125	129	130	134,5	133,5	139	148	149	146	141	134	129

MV_1 = 1 : 4 (24,8% N : 75,2% Nb), MV_2 = 1 : 3 (30,7% N : 69,3% Nb),

MV_3 = 1 : 1 (57% N : 43% Nb).

Key to Data II:
MV = Molecular compound
Gew.-% N = % by weight of N
Schmp. = Melting point

III. Nicotinamide (N): cinnamic acid (Z) (Fig. 3)

E_1 95, E_2 96, MV_1 I 98,5, E_3 90, E_4 93, E_5 94,5, MV_1 II 96,5, E_6 88,5, E_7 80.

Gew.-% N:	0	10	20	30	40	50	60	70	80	90	100
Schmp. der MV_1 I:	135	126	116	106	97	96	107	115	122	126	129
Schmp. der MV_1 II:					94	94	93	99	107		

MV_1 = 1 : 1 (45,19% N : 54,81% Z).

Key to Data III:
MV_1 = 1st molecular compound]
Gew.-% N = % by weight of N
Schmp. der MV_1 I = Melting point of MV_1 I [MV_1 = 1st molecular compound]
Schmp. der MV_1 II = Melting point of MV_1 II [MV_1 = 1st molecular compound]

IV. Benzidine (B): methyl p-nitrobenzoate (N) (Fig. 4)

E_1 80, E_2 77, MV_1 I 89, MV_2 102, MV_1 II 86, E_3 75.

Gew.-% B:	0	10	20	30	40	50	60	70	80	90	100
Schmp.:	96	90	81	85,5	89	95,5	99	101	110	120	129
Schmp. der MV_1 I:					88	89					
Schmp. der MV_2 II:				82	85						

MV_1 = 1 : 1 (50,33% B : 49,67% N).
MV_2 = 1 : 3 (75,33% B : 24,67% N).

Key to Data IV:
MV_1 = 1st molecular compound]
MV_2 = 2nd molecular compound]
Gew.-% B = % by weight of B
Schmp. = Melting point
Schmp. der MV_1 I = Melting point of MV_1 I [MV_1 = 1st molecular compound]
Schmp. der MV_2 II = Melting point of MV_2 II [MV_2 = 2nd molecular compound]

NOVARTIS EXHIBIT 1517
Novartis v. Regents, IPR2023-01347
Page 2825 of 4460

V. Benzidine (B): cinnamic acid (Z) (Fig. 5)

E_1 112, E_2 100, MV_1 I 113, E_3 108, E_4 98, MV_1 II 109, E_5 97.

Gew.-% B:	0	10	20	30	40	45	50	55	60	70	80	90	100
Schmp. d. MV I:	135	129	123	117	112,5	113	110,5	108	105	102	111	120	129
Schmp. d. MV II:						108,5	107	104	101				

MV = 1:1 (44,5% B: 55,5% Z).

Key to Data IV:

MV_1	=	1st molecular compound]
Gew.-% B	=	% by weight of B
Schmp. der MV_1 I	=	Melting point of MV_1 I [MV_1 = 1st molecular compound]
Schmp. der MV_2 II	=	Melting point of MV_2 II [MV = Molecular compound]

The investigations of the individual modifications took place in the contact apparatus with use being made of the surface preparation. A mixture of the two components, which form the molecular compound in the appropriate molar ratio, is fused between the cover glass and the specimen slide. Any excess melt is suctionally removed with the help of filter paper. The melt is then rapidly made to solidify in accordance with the modification which one wishes to achieve. Stable and unstable forms are not infrequently produced side by side using the same cooling conditions.

It was not always possible to make the unstable forms melt prior to their transformation in the contact preparation or surface preparation. In such cases, it is best if a pull-off preparation is prepared. A thoroughly fused surface preparation is used and the cover glass is pulled off before the melt crystallizes; droplet formation of the melt is produced as a result of this. Since these droplets are located in an isolated manner and they are usually formed only from one modification, one is frequently successful in seeing this modification melt away since - as a result of its isolated position - infection with another modification is, by far, not as extensive as would otherwise be the case. It is not possible to compile one particular working procedure that could be used for all systems; this is because every system exhibits special features. Experimental conditions that lead to the production of different modifications in one system fail completely in the case of other systems.

After clarity in regard to the basic form of the diagram has been generated via the contact method, the points of primary crystallization are determined[21] using expedient mixtures of the two components.

Summary

The tendency of nicotinamide to form polymorphous molecular compounds with carboxylic acids and phenols is not brought about by the acid amide as such but, rather, by its pyridine component; this is so because, under the experimental conditions that were used, polymorphism could not be observed in the molecular compounds that are formed with the eight acid amides that were investigated, in terms of their molecular compounds, with, in each case, nine carboxylic acids and, in each case, three phenols.

It was possible to ascertain three further molecular compounds of nicotinamide and carboxylic acids.

A marked tendency to exhibit molecular compounds and, in addition, to exhibit polymorphism was found in the case of three out of four amines, namely benzidine, o-phenylenediamine and p-phenylenediamine that were, likewise, made to combine with, in each case, nine carboxylic acids and, in each case, three phenols. Benzidine and bromural were examined in terms of their molecular compounds with, in each case, 75 further substances.

It was observed that, despite the marked tendency of urea to form molecular compounds, its derivatives (bromural, adalin, diethylurea) scarcely possess this capability any longer.

Polymorphism did not materialize with the medicinally utilized molecular compounds veramon, isoamylethylbarbituric acid (hypnal), pyramidon + Orthoform-Neu, sarcosine anhydride + Orthoform-Neu and antipyrine + Orthoform-Neu.

References

1 *E. Hertel*, Ber. Dtsch. chem. Ges. **57**, 1559 (1924); Liebigs Ann. Chem. **179**, 1451 (1926).

2 *E. Hertel* and *Schneider*, Z. physik. Chem. Abt. B **13**, 387 (1931).

3 *E. Hertel* and *v. Cleef*, Ber. dtsch. chem. Ges. **61**, 1545 (1928).

4 *E. Hertel* and *H. Frank*, Z. physik. Chem. Abt. B **27**, 460 (1934).

5 *A. Hantzsch, S. Angew.* Chem. **20**, 1889 (1907).

6 *C. Weygand*, "Chemical morphology of liquids and crystals". Leipzig. 1941.

7 *A. Kofler*, Z. Elektrochem. **50**, 200 (1944). - *L.* and *A. Kofler*, Ber. dtsch. chem. Ges. **76**, 718 (1943). *A. Kofler*, Z. physik. Chem. Abt. A **187**, 363 (1941); **190**, 291 (1942).

8 *A.* and *L. Kofler*, "Micro-methods for the characterization of organic substances and mixtures of substances". Innsbruck: Universitäts-Verlag Wagner. 1948

9 *A.Kofler*, Z. physik. Chem. Abt. A **187**, 363 (1941).

10 *H. Rheinbold*, J. prakt. Chem. (2) **3**, 242 (1925).

11 *A. Kofler*, Microchem. **34**, 15 (1948).

12 *A. Kofler*, Z. Elektrochem. **50**, 200 (1944)

13 *L.* and *A. Kofler*, Ber. dtsch. chem. Ges. **76**, 718 (1943).

14 *W.H. Hatcher*, Chem. Zbl. **1918**, I, 338

15 *P. Pfeiffer*, Z. physik. Chem.. Abt. A **137**, 107 (1928.

16 Symbol clarification: MV: molecular compound melts with decomposition; MV_1II: the unstable modification of MV_1 [the first molecular compound]; +: a phase diagram was recorded for this system; //: dimorphous molecular compound; ///" trimorphous molecular compound.

17 *R. Kremann*, Mh. Chem. **39**, 441 (1918).

18 *R. Kremann*, Mh. Chem. **39**, 441 (1918).

19 *R. Kremann*, Mh. Chem. **39**, 505 (1918).

20 *R. Kremann*, Mh. Chem. **46**, 193 (1925).

21 *A.Kofler*, Z. physik. Chem. Abt. A **187**, 363 (1941); Naturwiss. **31**, 553 (1943).

Monatsh. Chem. 80, 595-606 (1949)

Über organische Molekülverbindungen und deren Polymorphie.

Von

H. Quehenberger.

Aus dem Pharmakognostischen Institut der Universität Innsbruck.

Mit 5 Abbildungen.

(Eingelangt am 17. Febr. 1949. Vorgelegt in der Sitzung am 24. Febr. 1949.)

1924 gelang es *Hertel*[1] nachzuweisen, daß von vielen organischen Substanzpaaren Molekülverbindungen zu erhalten sind, die bei gleicher Zusammensetzung verschiedene Farbe, verschiedene Löslichkeit und verschiedene Schmelzpunkte aufweisen. In kristallographischer (feinstruktureller),[2] phasentheoretischer[3] und thermochemischer[4] Hinsicht verhalten sich die beiden Formen derartiger Systeme wie zwei „allotrope" Modifikationen eines Stoffes. Schon früher (1907) hat *H. Hantzsch*[5] auf die Chromoisomerie hingewiesen und diesen Begriff phänomenologisch definiert. Wenn auch Chromoisomerie nach *C. Weygand*[6] nicht der Polymorphie gleichzusetzen ist, so stellt sie doch einen Übergang zwischen Isomerie und Polymorphismus dar.

In neuerer Zeit haben Untersuchungen von *A. Kofler*[7] weitere Einblicke in die Polymorphieverhältnisse organischer Molekülverbindungen gebracht. In einigen Fällen wurde ein Zusammenhang zwischen der

---

[1] *E. Hertel*, Ber. dtsch. chem. Ges. **57**, 1559 (1924); Liebigs Ann. Chem. **170**, 1451 (1926).

[2] *E. Hertel* und *Schneider*, Z. physik. Chem., Abt. B **18**, 387 (1931).

[3] *E. Hertel* und *v. Cleef*, Ber. dtsch. chem. Ges. **61**, 1545 (1928).

[4] *E. Hertel* und *H. Frank*, Z. physik. Chem., Abt. B **27**, 460 (1934).

[5] *H. Hantzsch*, Z. angew. Chem. **20**, 1889 (1907).

[6] *C. Weygand*, Chemische Morphologie der Flüssigkeiten und Kristalle. Leipzig. 1941.

[7] *A. Kofler*, Z. Elektrochem. **50**, 200 (1944). — *L.* und *A. Kofler*, Ber. dtsch. chem. Ges. **76**, 718 (1943). — *A. Kofler*, Z. physik. Chem., Abt. A **187**, 363 (1941); **190**, 291 (1942).

UM00014082
NOVARTIS EXHIBIT 1517
Novartis v. Regents, IPR2023-01347
Page 2828 of 4460

Polymorphie der Molekülverbindung und derjenigen einer Komponente beobachtet, in anderen Fällen dagegen nicht.

Bei den vorliegenden Untersuchungen wurde der Mikro-Schmelzpunktapparat von *L. Kofler*[8] verwendet. Die Schmelzpunkte wurden an mikroskopischen Präparaten zwischen Objektträger und Deckglas beobachtet.

Zur Auffindung und Untersuchung der im experimentellen Teil angegebenen Molekülverbindungen wurde die Kontaktmethode von *A. Kofler*[9] benützt. Sie erlaubt es, durch Beobachtung der Kontaktzone an einem einzigen mikroskopischen Präparat die eutektische Temperatur zweier Komponenten und bei Vorhandensein einer oder mehrerer Molekülverbindungen sowohl die verschiedenen Eutektika als auch die Schmelzpunkte der Molekülverbindungen in kürzester Zeit zu ermitteln. Ferner gestattet diese Arbeitsweise ein Erkennen und Beobachten der Polymorphie von Molekülverbindungen, wodurch auch die graphische Erfassung der instabilen Modifikationen ermöglicht wird.

E. Hertel[1] gelang es im Falle des komplexisomeren Systems 1-Brom-4-naphthylamin : 2,6-Dinitrophenol, nach präparativer Herstellung der Molekülverbindung die Schmelzpunkte der beiden Modifikationen in der von *Rheinbold*[10] angegebenen Weise in einem Schmelzdiagramm festzuhalten.

Bei Verwendung der Kontaktmethode[9] gestaltet sich in vielen Fällen die Thermoanalyse polymorpher Verbindungen wesentlich einfacher und eindeutiger.

Bei der Herstellung eines Kontaktpräparates wurde folgender Arbeitsgang eingehalten: Die höherschmelzende Substanz wird zum Schmelzen gebracht, so daß die Schmelze ungefähr die Hälfte des Raumes zwischen Objektträger und Deckglas einnimmt. Nach Erstarren der Schmelze durch Abkühlung wird die zweite Substanz an den Deckglasrand gegeben und einige Grade über ihren Schmelzpunkt erwärmt, wodurch dann die Schmelze in den noch freien Raum einfließt. In manchen Fällen empfiehlt es sich, das ganze Präparat anschließend durchzuschmelzen und einige Zeit bei dieser Temperatur liegen zu lassen, zumal wenn sich die Bildung der Molekülverbindung sehr träge vollzieht. Besteht eine starke Affinität zwischen den beiden Komponenten, so kommt es zu einer stürmischen Bildung der Molekülverbindung und es muß besonders vorsichtig gearbeitet werden.

Durch Beobachtung der Kontaktzone zweier Komponenten lassen sich auch polymorphe Systeme untersuchen. Für die Herstellung der instabilen Modifikationen von Molekülverbindungen gilt dieselbe Arbeitsweise, wie sie bei der Darstellung instabiler Formen einfacher chemischer

---

[8] *A.* und *L. Kofler*, Mikromethoden zur Kennzeichnung organischer Stoffe und Stoffgemische. Innsbruck: Universitäts-Verlag Wagner. 1948.

[9] *A. Kofler*, Z. physik. Chem., Abt. A 187, 363 (1941).

[10] *H. Rheinbold*, J. prakt. Chem. (2) 3, 242 (1925).

UM00014083
NOVARTIS EXHIBIT 1517
Novartis v. Regents, IPR2023-01347
Page 2829 of 4460

Substanzen verwendet wird.[8, 11] Daß auch organische Molekülverbindungen monotrop oder enantiotrop sein können, geht aus der Arbeit von *A. Kofler*[12] hervor.

Aufmerksam gemacht durch die Neigung des Nikotinsäureamids[13] zur Polymorphie, tauchte die Frage auf, ob dies eine allgemeine Eigenschaft der Säureamide ist. Um dies zu klären, wurden acht Säureamide mit je neun Carbonsäuren und je drei Phenolen untersucht. Es konnte bei allen so gewonnenen Molekülverbindungen keine Polymorphie unter den angewandten Versuchsbedingungen erkannt werden. Allerdings handelte es sich dabei durchwegs um saure Amide, wohingegen Nikotinsäureamid basischen Charakter besitzt. Es könnte eventuell also die basische Komponente des Nikotinsäureamids die Ursache für die häufige Bildung polymorpher Molekülverbindungen sein. Wahrscheinlicher ist jedoch für die Bildung polymorpher Molekülverbindungen des Nikotinsäureamids mit Säuren und Phenolen die Pyridinkomponente, wie z. B. Pyridinverbindungen[14] mit Phenolen lange schon bekannt sind.

Weiters konnten polymorphe Molekülverbindungen des Nikotinsäureamids mit folgenden Carbonsäuren festgestellt werden:

Nikotinsäureamid : p-Cresotinsäure (2 MV, 1 : 3, dimorph);

Nikotinsäureamid : m-Nitrobenzoesäure (3 MV, 1 : 4, dimorph);

Nikotinsäureamid : Zimtsäure (1 : 1, dimorph).

Eine große Neigung zu Molekülverbindungen und auch zur Polymorphie konnte weiters bei dreien der vier untersuchten Amine wahrgenommen werden, die auch jeweils mit neun verschiedenen Carbonsäuren und je drei verschiedenen Phenolen untersucht wurden. So gibt:

Benzidin mit Zimtsäure, MV 1 : 1, dimorph;

p-Phenylendiamin mit Hexadecandicarbonsäure eine trimorphe Molekülverbindung;

o-Phenylendiamin mit Pikrinsäure eine trimorphe Molekülverbindung;

p-Phenylendiamin mit p-Cresotinsäure, eine dimorphe Molekülverbindung;

o-Phenylendiamin mit p-Cresotinsäure drei Molekülverbindungen, 1 : 1, trimorph.

Die beiden Molekülverbindungen des Systems p-Phenylendiamin : Zimtsäure sind deshalb interessant, da bei bestimmten Versuchsbedingungen eine Molekülverbindung ausbleiben kann und eine aus der anderen entsteht. Außerdem konnten im System Benzidin : p-Nitrobenzoesäuremethylester zwei inhomogen schmelzende Molekülverbindungen, von denen MV 1 : 1 dimorph ist, festgestellt werden.

---

[11] *A. Kofler*, Mikrochem. **34**, 15 (1948).
[12] *A. Kofler*, Z. Elektrochem. **50**, 200 (1944).
[13] *L.* und *A. Kofler*, Ber. dtsch. chem. Ges. **76**, 718 (1943).
[14] *W. H. Hatcher*, Chem. Zbl. **1918 I**, 338.

UM00014084
NOVARTIS EXHIBIT 1517
Novartis v. Regents, IPR2023-01347
Page 2830 of 4460

Die Systeme o-Phenylendiamin : Pikrinsäure und p-Phenylendiamin : p-Cresotinsäure wurden trotz ihrer polymorphen Molekülverbindungen nicht aufgenommen, da sich die Schmelzpunkte der einzelnen Modifikationen nicht bestimmen lassen.

Außerdem wurde Benzidin und Bromural mit je weiteren 75 Substanzen auf Molekülverbindungen untersucht.

Festgestellt wurde, daß trotz der großen Neigung des Harnstoffes zur Bildung von Molekülverbindungen seine Derivate [Bromural (Monobromisovalerianylharnstoff), Adalin (Bromdiäthylacetylharnstoff), Diäthylharnstoff] diese Fähigkeit kaum mehr und wenn, nur in einem viel geringeren Ausmaß besitzen, obwohl teilweise noch eine Aminogruppe frei wäre.

Ferner wurden auch einige bekannte, medizinisch verwendete Molekülverbindungen auf Polymorphismus untersucht. So z. B. Veramon, Isoamyläthylbarbitursäure (Hypnal), Pyramidon + Orthoform-Neu (m-Amido-p-oxybenzoesäuremethylester), Sarkosinanhydrid + Orthoform-Neu, Antipyrin + Orthoform-Neu. Diese Molekülverbindungen sind bereits von *P. Pfeiffer* und *E. Seidel*[15] ermittelt worden. Es konnte jedoch bei keiner eine Polymorphie beobachtet werden. Die Dimorphie von Trigemin ist bereits bekannt.[8] Sie konnte aber im Kontaktpräparat nicht nachgewiesen werden wegen der überaus großen Flüchtigkeit des Chloralhydrats.

In der folgenden Liste sind die zwischen neun Säureamiden und vier Aminen beobachteten Molekülverbindungen alphabetisch angeordnet. Weiters folgen die negativen Fälle, das heißt Fälle, bei denen die beiden Komponenten nicht unter Bildung einer Molekülverbindung reagieren, sondern nur ein Eutektikum bilden.

Bei Auftreten von Molekülverbindungen sind die Temperaturen der Eutektika und Schmelzpunkte sowie die Farbe angegeben.

Anschließend sind diejenigen Systeme zusammengefaßt, bei denen die Kontaktzone unter den angewandten Versuchsbedingungen (Impfen, Wärme, Kälte) nicht zur Kristallisation gebracht werden konnte.

Von den zwölf Systemen, von denen ein Zustandsdiagramm (mit + bezeichnet) aufgenommen wurde, wurden nur fünf aus Gründen der Platzersparnis veröffentlicht. Außerdem wurde aus demselben Grunde von der Veröffentlichung der genauen Versuchsbeschreibung Abstand genommen.

[15] *P. Pfeiffer*, Z. physik. Chem., Abt. A 187, 107 (1928).

UM00014085
NOVARTIS EXHIBIT 1517
Novartis v. Regents, IPR2023-01347
Page 2831 of 4460

Liste der auf Molekülverbindungen und deren Polymorphie untersuchten Säureamide und Amine.[16]

Säureamide.

Substanzen	Schmelzpunkt der Molekülverbindungen und ihre Eutektika	Farbe
Benzamid:		
o-Cresotinsäure[17]	E_1 113, E_2 118, MV 120	
p-Cresotinsäure	E_1 102, E_2 112, MV 116	
m-Nitrobenzoesäure	E_1 119, E_2 114, E_3 116, E_4 115, MV 137	
Pikrinsäure	E_1 101, E_2 102, MV 111	gelb
Resorcin[18]	E_1 76, E_2 80,5, MV 88	
Salicylsäure	E_1 106, E_2 115, MV 118	
Bromural:		
Mesaconsäure	E_1 126, E_2 128, MV 134	
1-Oxy-3-äthoxybenzaldehyd	E_1 72, E_2 100, MV 101	
Pikrinsäure	E_1 109, E_2 129, MV 131	
n-Butyramid:		
Brenzkatechin	E_1 32, E_2 34, MV 35	
m-Nitrobenzoesäure	E_1 77, E_2 80, MV 84	
Nikotinsäureamid:		
o-Cresotinsäure	E_1 115, E_2 129, MV 144	
+ p-Cresotinsäure //	E_1 123, E_2 122, MV_1 124, E_3 123,5, MV_2 140, E_4 116,5, E_5 116, MV_1 II 117, E_6 104	
Hexadecandicarbonsäure	E_1 121, E_2 123,5, E_3 128, MV_1 129, MV_2 130,5	
+ m-Nitrobenzoesäure //	E_1 123, E_2 129, MV_1 131, E_3 133, MV_2 135, MV_3 150, E_4 124, E_5 121, E_6 ~ 70	
p-Nitrophenol	E_1 98, E_2 103, MV_1 110, E_3 113, MV_2 115, E_4 116, MV_3 126	gelb
Pikrinsäure	E_1 117, E_2 120, E_3 129, MV_1 129,5, MV_2 189	gelb
Salicylsäure	E_1 111, E_2 119, MV 136,5	
+ Zimtsäure //	E_1 95, E_2 96, MV_1 98,5, E_3 90, E_4 93, E_5 94,5, MV_1 II 96,5, E_6 88,5, E_7 80	
Propionamid:		
m-Nitrobenzoesäure	E_1 54, E_2 70, MV 74	
p-Nitrophenol	E_1 42, E_2 51, MV 58	
Salicylamid:		
o-Cresotinsäure	E_1 123, E_2 134, MV 136	
p-Cresotinsäure	E_1 111, E_2 116, MV 117	
m-Nitrobenzoesäure	E_1 121, E_2 122, MV 135	

[16] Zeichenerklärung: MV ?: Molekülverbindung schmilzt unter Zersetzung; MV_1 II: die instabile Modifikation der MV_1; +: von diesem System wurde ein Zustandsdiagramm aufgenommen; //: dimorphe MV, ///: trimorphe MV.

[17] *R. Kremann*, Mh. Chem. **39**, 441 (1918).

[18] *R. Kremann*, Mh. Chem. **39**, 441 (1918).

UM00014086
NOVARTIS EXHIBIT 1517
Novartis v. Regents, IPR2023-01347
Page 2832 of 4460

Substanzen	Schmelzpunkt der Molekülverbindungen und ihre Eutektika	Farbe
Pikrinsäure	E_1 99, E_2 104, MV 106	gelb
Sulfanylsäureamid:		
Pikrinsäure	E_1 119, E_2 147, MV 176	
	Amine.	
Benzidin:		
Aspirin	E_1 105, E_2 114, MV 252	
+ Azelainsäure	E_1 103, E_2 113, E_3 108, MV_1 114, MV_2 114,5, E_4 104	
Benzilsäure	E_1 116, E_2 145, MV 226	
Benzoesäure	E_1 96, E_2 101, MV 103	
+ Brenzkatechin	E_1 103, E_2 108, MV 148, E_3 106, E_4 101	
o-Cresotinsäure	E_1 109, E_2 136, MV_1 138, E_3 143, MV_2 151	
3,4-Dioxybenzaldehyd	E_1 102, E_2 110, MV ?	rot
2,5-Dioxybenzaldehyd	E_1 91, E_2 110, MV ?	rot
Glutaminsäure	E_1 119, E_2 126, MV 171	
Hexadecandicarbonsäure	E_1 117, E_2 119, MV 124	
Hippursäure	E_1 116, E_2 140, MV 146	
Korksäure	E_1 112, E_2 122, MV 124	
Lactophenin	E_1 106, E_2 108, MV 115	
d-l-Mandelsäure	E_1 73, E_2 119, MV 149	
Monochloressigsäure	E_1 44, E_2 118, E_3 135, MV_1 148, $MV_2 \approx 265$	
α-Naphthol	E_1 85, E_2 86, MV 98	
β-Naphthol	E_1 116, E_2 117, MV_1 132, E_3 130, MV_2 171	
+ m-Nitrobenzoesäure	E_1 139, E_2 157, E_3 114, MV_1 158,5, MV_2 160,5, E_4 111, E_5 109	gelb
o-Nitrobenzoesäure	E_1 120, E_2 138, MV 189	
m-Nitrobenzaldehyd	E_1 52, E_2 78, MV 129	braungelb
o-Nitrobenzaldehyd	E_1 36, E_2 82, MV 214	gelb
p-Nitrobenzaldehyd	E_1 92, E_2 103, MV ?	
+ p-Nitrobenzoesäure-methylester //	E_1 80, E_2 77, E_3 75, MV_1 I 89, MV_1 II 86, MV_2 102	
p-Nitrophenol	E_1 99, E_2 115, MV 151	
Pernocton	E_1 113, E_2 122, MV 142	
Phenylessigsäure	E_1 74, E_2 117, MV 126	
Phloroglucin	E_1 121, E_2 163, MV ?	
Pikrinsäure	E_1 106, E_2 119, MV ?	gelbbraun
Piperonal	E_1 31, E_2 74, MV ?	grüngelb
Pyrogallol	E_1 112, E_2 117, MV 143	
Pyrogallol-1,3-dimethyläther	E_1 47, E_2 93, MV 106	
m-Oxybenzaldehyd	E_1 89, E_2 109, MV 270	gelb
m-Oxybenzoesäure	E_1 118, E_2 148, MV 151	
+ Resorcin	E_1 106, E_2 114, MV 143, E_3 103, E_4 111, E_5 109	

UM00014087
NOVARTIS EXHIBIT 1517
Novartis v. Regents, IPR2023-01347
Page 2833 of 4460

Substanzen	Schmelzpunkt der Molekülverbindungen und ihre Eutektika	Farbe
Salicylsäure	E_1 112, E_2 147, MV 161	
o-Sulfobenzoesäure	E_1 66, E_2 111, MV ?	gelb
Tetradicarbonsäure	E_1 112, E_2 116, MV 122	
Trichloressigsäure	E_1 49, E_2 115, MV ?	
s-Trinitrobenzol	E_1 94, E_2 106, MV 131	dunkelviolett
s-Trinitrotoluol	E_1 66, E_2 90, MV 99	rotbraun
o-Vanillin	E_1 73, E_2 109, MV 212	gelbrot
+ Zimtsäure //	E_1 112, E_2 100, MV_1 I 113, E_3 108,5, E_4 98, MV_1 II 109, E_5 97	
o-Phenylendiamin:		
Brenzkatechin[19]	E_1 76, E_2 76, MV 84,5	
o-Cresotinsäure	E_1 91, E_2 123, MV 128	
+ p-Cresotinsäure //	E_1 96, E_2 111, MV_1 112, E_6 114, MV_2 II 116, E_4 116,5, MV_3 117, MV_2 I 123, E_5 92, E_7 110	
+ m-Nitrobenzoesäure	E_1 95, E_2 132, E_3 122, MV_1 133, MV_2 138	
p-Nitrophenol	E_1 68, E_2 84, MV 88	schwach gelb
Pikrinsäure ///	E_1 95, E_2 119, MV ?	
Resorcin[19]	E_1 45, E_2 47, MV 50	
Salicylsäure[20]	E_1 86, E_2 109, MV 116	
Zimtsäure[20]	E_1 86, E_2 94, MV 95,5	
p-Phenylendiamin:		
Azelainsäure	E_1 78, E_2 110, MV 112	
Brenzkatechin[19]	E_1 87,5, E_2 99, MV 108	
o-Cresotinsäure	E_1 107, E_2 140, E_3 141, MV_1 142, MV_2 148	
p-Cresotinsäure //	E_1 126, E_2 132, MV 172	
Hexadecandicarbonsäure ///	E_1 117, E_2 128, MV_1 I 130, E_3 112, E_4 122, MV_1 II 126, E_5 117, E_6 118, MV_1 III 120	
m-Nitrobenzoesäure	E_1 127, E_2 131,5, E_3 132, MV_1 136, MV_2 158,5, E_4 157,5, MV_3 163	
p-Nitrophenol	E_1 114, E_2 115, MV_1 122,5, E_3 123, MV_2 139	MV_1 = braun MV_2 = gelb
Resorcin[19]	E_1 94, E_2 102, MV 116	
Salicylsäure[20]	E_1 100, E_2 107, MV 137	
+ Zimtsäure	E_1 118, E_2 123, E_3 120, MV_1 125, MV_2 128, E_4 106	
Thiosinamin:		
Pikrinsäure	E_1 73, E_2 106, MV 162	gelb

Folgende Säureamide und Amine geben mit den angeführten Substanzen *keine* Molekülverbindung:

Benzamid: Diallylbarbitursäure (Dial), Hexadecandicarbonsäure, p-Nitrophenol, Zimtsäure.

[19] *R. Kremann*, Mh. Chem. 39, 505 (1918).
[20] *R. Kremann*, Mh. Chem. 46, 193 (1925).

UM00014088
NOVARTIS EXHIBIT 1517
Novartis v. Regents, IPR2023-01347
Page 2834 of 4460

Bromural: Aconitsäure, Adenin, Allantoin, Alloxan, Anthranilsäure, Benzamid, Benzoesäure, Benzoesäurenaphthylester, Benzoesäurephenylester, Benzoesäuresulfonamid, Brombernsteinsäure, α-Bromstearinsäure, Caprinsäure, Chloralhydrat, Cholaninsäure, Chrysophansäure, Citronensäure, o- und p-Cresotinsäure, Diallylbarbitursäure (Dial), 3,4-Dioxybenzaldehyd, Gallussäure, Gluconsäurelacton, Glutaminsäure, Glykokoll, Harnsäure, Hexa-

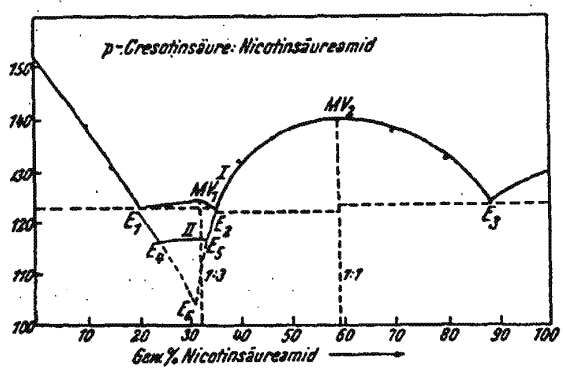


Abb. 1.

decandicarbonsäure, Hippursäure, Lactophenin, Lävulinsäure, d,l-Mandelsäure, m-, o- und p-Nitrobenzaldehyd, m- und o-Nitrobenzoesäure, m-, o- und p-Nitrophenol, Isopropyl-β-bromallylbarbitursäure (Noctal), Diäthylaminisopropylallylbarbitursäure (Numal), m-Oxybenzaldehyd, o- und p-

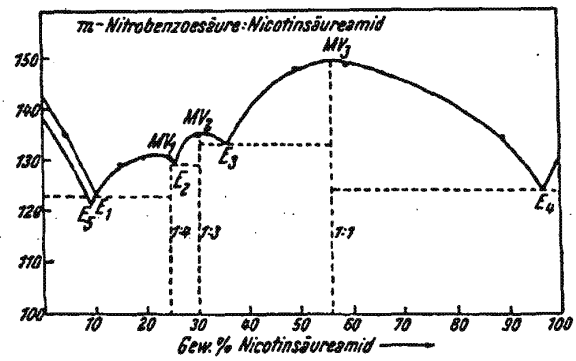


Abb. 2.

Oxybenzoesäure, Phenacetin, Phenol, Phenylessigsäure, Phloroglucin, Phthalsäure, Pimelinsäure, Piperonal, Pyrogallol-1,3-dimethyläther, Salicylsäureguajacolester (Guajakolsalol), Resorcin, Salicylsäure, Phenylsalicylat (Salol), Salicylsäureester des Acetyl-p-aminophenol (Salophen), Sandoptal, Sorbinsäure, o-Sulfibenzoesäure, Stearinsäure, Tartronsäure, Theobromin, Theophyllin, Thymolnaphthalin, Tricarballylsäure, Trichlorbuttersäure, Trichloressigsäure, d-Weinsäure, o-Vanillin, Veratrumaldehyd, Zimtsäure, Zimtsäureanhydrid, Zitakonsäure.

n-Butyramid: Azelainsäure, o- und p-Cresotinsäure, Diallylbarbitursäure

UM00014089
NOVARTIS EXHIBIT 1517
Novartis v. Regents, IPR2023-01347
Page 2835 of 4460

(Dial). Hexadecandicarbonsäure, p-Nitrophenol, Pikrinsäure, Salicylsäure, Zimtsäure.

Nicotinsäureamid: Amidoacetanilid, Amidoazobenzol, p-Aminophenol, Anissäure, Antipyrin, Prontalbin.

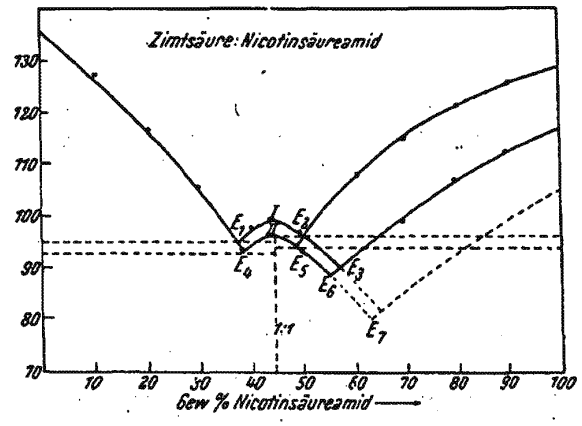


Abb. 3.

Propionamid: Azelainsäure, o- und p-Cresotinsäure, Diallylbarbitursäure (Dial), Hexadecandicarbonsäure, Pikrinsäure, Salicylsäure, Zimtsäure.

Salicylamid: Azelainsäure, Brenzkatechin, Diallylbarbitursäure (Dial), Hexadecandicarbonsäure, p-Nitrophenol, Resorcin, Salicylsäure, Zimtsäure.

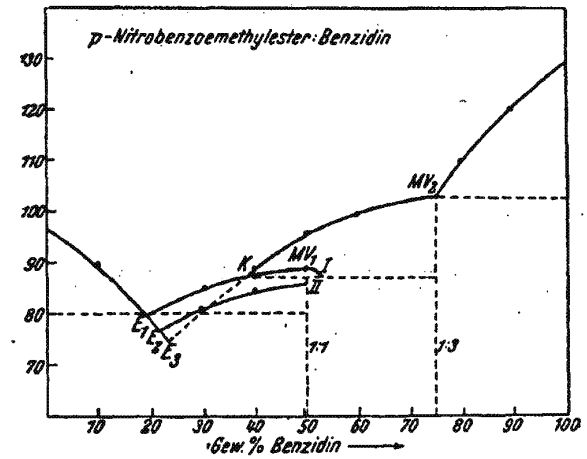


Abb. 4.

Sulfanylsäureamid: Azelainsäure, Brenzkatechin, o- und p-Cresotinsäure, Diallylbarbitursäure (Dial), Hexadecandicarbonsäure, m-Nitrobenzoesäure, p-Nitrophenol, Resorcin, Salicylsäure, Zimtsäure.

p-Toluolsulfonsäureamid: Azelainsäure, Brenzkatechin, o- und p-Cresotinsäure, Diallylbarbitursäure (Dial), Hexadecandicarbonsäure, m-Nitrobenzoesäure, p-Nitrophenol, Pikrinsäure, Resorcin, Salicylsäure, Zimtsäure.

UM00014090
NOVARTIS EXHIBIT 1517
Novartis v. Regents, IPR2023-01347
Page 2836 of 4460

Trichloracetamid: Azelainsäure, Brenzkatechin, o- und p-Cresotinsäure, Diallylbarbitursäure (Dial), Hexadecandicarbonsäure, m-Nitrobenzoesäure, p-Nitrophenol, Pikrinsäure, Resorcin, Salicylsäure, Zimtsäure.

Benzidin: Acetanilid, Amidoacetanilid, Amidoazobenzol, m- und o-Amidobenzoesäure, p-Amidobenzoesäure, Antipyrin, Azobenzol, Benzil, Benzylanilin, Benzoesäurenaphthylester, Benzoesäurephenylester, Brombernsteinsäure, Caprinsäure, Citronensäure, Diallylbarbitursäure (Dial), Harnstoff, Mesaconsäure, α-Naphthylamin, β-Naphthylamin, Nicotinsäureamid, Nipabenzyl, Äthylester der p-Oxybenzoesäure (Nipagin A), Propylester der p-Oxybenzoesäure (Nipasol), Phenacetin, Phenanthren, p-Oxybenzoesäure, Salicylsäureguajacolester (Guajakolsalol), Salicylsäureester des Acetyl-p-aminophenols (Salophen), Sorbinsäure, Trichlorbuttersäure, d-Weinsäure, Xylolmoschus.

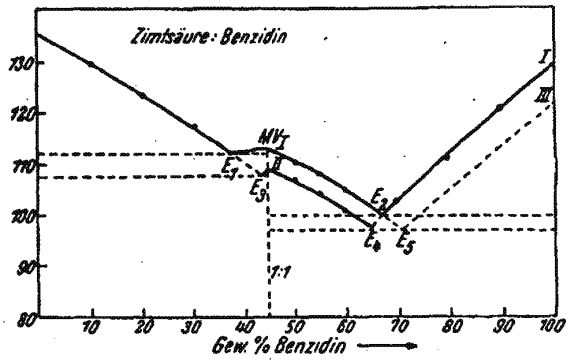


Abb. 5.

o-Phenylendiamin: Azelainsäure, Diallylbarbitursäure (Dial), Hexadecandicarbonsäure.

p-Phenylendiamin: Diallylbarbitursäure (Dial).

Thiosinamin: Azelainsäure, Brenzkatechin, o- und p-Cresotinsäure, Diallylbarbitursäure (Dial), Hexadecandicarbonsäure, m-Nitrobenzoesäure, p-Nitrophenol, Resorcin, Salicylsäure, Zimtsäure.

Bei folgenden Systemen konnte die Kontaktzone nicht zur Kristallisation gebracht werden:

Bromural: Monochloressigsäure; n-Butyramid: Resorcin; Nicotinsäureamid: Mandelsäure; Nicotinsäureamid: Resorcin; Propionamid: Brenzkatechin; Propionamid: Resorcin.

I. Nicotinsäureamid (N): p-Cresotinsäure (C) (Abb. 1).

E_1 123, E_2 122, E_3 123,5, MV_1 I 124, MV_2 140, E_4 116,5, E_5 116, MV_1 II 117, E_6 106.

Gew.-% N:	0	10	15	20	30	40	50	60	70	80	90	100
Schmp.:	151	138	130	123	123,5	132	138	140	137	132	124	129

MV_1 = 1 : 3 (32,7% N : 67,7% C).

MV_2 = 1 : 1 (59,3% N : 40,7% C).

II. Nicotinsäureamid (N): m-Nitrobenzoesäure (Nb) (Abb. 2).

E_1 123, E_2 129, MV_1 131, E_3 133, MV_2 135, MV_3 150, E_4 124, E_5 121, E_6 70.

Gew.-% N:	0	5	10	15	20	30	35	40	50	60	70	80	90	100
Schmp.	142	135	125	129	130	134,5	133,5	139	148	149	146	141	134	129

MV_1 = 1 : 4 (24,8% N : 75,2% Nb), MV_2 = 1 : 3 (30,7% N : 69,3% Nb),

UM00014091
NOVARTIS EXHIBIT 1517
Novartis v. Regents, IPR2023-01347
Page 2837 of 4460

MV_3 = 1 : 1 (57% N : 43% Nb).

III. Nicotinsäureamid (N) : Zimtsäure (Z) (Abb. 3).

E_1 95, E_2 96, MV_1 I 98,5, E_3 90, E_4 93, E_5 94,5, MV_1 II 96,5, E_6 88,5, E_7 80.

Gew.-% N:	0	10	20	30	40	50	60	70	80	90	100
Schmp. der MV_1 I:	135	126	116	106	97	96	107	115	122	126	129
Schmp. der MV_1 II:					94	94	93	99	107		

MV_1 = 1 : 1 (45,19% N : 54,81% Z).

IV. Benzidin (B) : p-Nitrobenzoemethylester (N) (Abb. 4).

E_1 80, E_2 77, MV_1 I 89, MV_2 102, MV_1 II 86, E_3 75.

Gew.-% B:	0	10	20	30	40	50	60	70	80	90	100
Schmp.:	96	90	81	85,5	89	95,5	99	101	110	120	129
Schmp. der MV_1 I:					88	89					
Schmp. der MV_2 II:				82	85						

MV_1 = 1 : 1 (50,33% B : 49,67% N).

MV_2 = 1 : 3 (75,33% B : 24,67% N).

V. Benzidin (B) : Zimtsäure (Z) (Abb. 5).

E_1 112, E_2 100, MV_1 I 113, E_3 108, E_4 98, MV_1 II 109, E_5 97.

Gew.-% B:	0	10	20	30	40	45	50	55	60	70	80	90	100
Schmp. d. MV I:	135	129	123	117	112,5	113	110,5	108	105	102	111	120	129
Schmp. d. MV II:						108,5	107	104	101				

MV = 1 : 1 (44,5% B : 55,5% Z).

Die Untersuchungen der einzelnen Modifikationen erfolgten im Kontaktpräparat und im Flächenpräparat. Ein Gemisch beider die Molekülverbindung bildenden Komponenten im entsprechenden molaren Verhältnis wird zwischen Deckglas und Objektträger geschmolzen. Eventuell überflüssige Schmelze wird mit Hilfe von Filterpapier abgesaugt. Die Schmelze wird dann rasch zum Erstarren gebracht, je nachdem, zu welcher Modifikation man gelangen will. Nicht selten entstehen bei gleichen Abkühlungsbedingungen stabile und instabile Formen nebeneinander.

Nicht immer ist es möglich, die instabilen Modifikationen vor ihrer Umwandlung im Kontaktpräparat oder Flächenpräparat zum Schmelzen zu bringen. In solchen Fällen bereitet man sich am besten ein Abreißpräparat. Bei einem durchgeschmolzenen Flächenpräparat wird das Deckglas vor dem Auskristallisieren der Schmelze abgerissen, wodurch es zu einer Tröpfchenbildung der Schmelze kommt. Da nun diese Tröpfchen isoliert liegen und meist nur von einer Modifikation gebildet werden, gelingt es häufig, diese Modifikation abschmelzen zu sehen, da die Infektion mit einer anderen Modifikation wegen der isolierten Lage bei weitem nicht so groß ist wie sonst. Ein bestimmter Arbeitsgang, der sich für alle Systeme anwenden ließe, kann nicht aufgestellt werden, da jedes System Sonderheiten aufweist. Versuchsbedingungen, die bei einem System zur Erzeugung verschiedener Modifikationen führen, versagen bei einem anderen System vollkommen.

Nachdem man sich durch die Kontaktmethode über die Grundform des Diagramms Klarheit verschafft hat, werden an zweckmäßigen Gemischen der beiden Komponenten die Punkte der primären Kristallisation bestimmt[21].

Zusammenfassung.

Die Neigung des Nikotinsäureamids zur Bildung polymorpher Molekülverbindungen mit Carbonsäuren und Phenolen ist nicht durch das Säure-

[21] *A. Kofler*, Z. physik. Chem., Abt. A 187, 363 (1941); Naturwiss. 31, 553 (1943).

UM00014092
NOVARTIS EXHIBIT 1517
Novartis v. Regents, IPR2023-01347
Page 2838 of 4460

amid als solches, sondern durch die Pyridinkomponente bedingt; denn bei den acht Säureamiden, die mit je neun Carbonsäuren und je drei Phenolen auf Molekülverbindungen untersucht wurden, konnten unter den angewandten Versuchsbedingungen keine Polymorphie an den von ihnen gebildeten Molekülverbindungen beobachtet werden.

Es konnten weitere drei Molekülverbindungen des Nikotinsäureamids mit Carbonsäuren festgestellt werden.

Bei drei von vier Aminen, nämlich Benzidin, o-Phenylendiamin und p-Phenylendiamin, die ebenfalls mit je neun Carbonsäuren und je drei Phenolen in Verbindung gebracht wurden, zeigte sich eine große Neigung zu Molekülverbindungen und auch zur Polymorphie. Benzidin und Bromural wurden mit je 75 weiteren Substanzen auf Molekülverbindungen geprüft.

Es wurde beobachtet, daß trotz der großen Tendenz des Harnstoffes zur Bildung von Molekülverbindungen seine Derivate (Bromural, Adalin, Diäthylharnstoff) diese Fähigkeit kaum mehr besitzen.

An den medizinisch verwendeten Molekülverbindungen Veramon, Isoamyläthylbarbitursäure (Hypnal), Pyramidon + Orthoform-Neu, Sarkosinanhydrid + Orthoform-Neu und Antipyrin + Orthoform-Neu trat kein Polymorphismus zutage.

UM00014093
NOVARTIS EXHIBIT 1517
Novartis v. Regents, IPR2023-01347
Page 2839 of 4460

This Page is Inserted by IFW Indexing and Scanning Operations and is not part of the Official Record

BEST AVAILABLE IMAGES

Defective images within this document are accurate representations of the original documents submitted by the applicant.

Defects in the images include but are not limited to the items checked:

- ☐ BLACK BORDERS
- ☐ IMAGE CUT OFF AT TOP, BOTTOM OR SIDES
- ☐ FADED TEXT OR DRAWING
- ☐ BLURRED OR ILLEGIBLE TEXT OR DRAWING
- ☐ SKEWED/SLANTED IMAGES
- ☐ COLOR OR BLACK AND WHITE PHOTOGRAPHS
- ☐ GRAY SCALE DOCUMENTS
- ☐ LINES OR MARKS ON ORIGINAL DOCUMENT
- ☐ REFERENCE(S) OR EXHIBIT(S) SUBMITTED ARE POOR QUALITY
- ☐ OTHER: _____

IMAGES ARE BEST AVAILABLE COPY.
As rescanning these documents will not correct the image problems checked, please do not report these problems to the IFW Image Problem Mailbox.

Arch. Pharm. (Weinheim) *319*, 654-659 (1986)

The Crystal Structure of the Theophylline-Urea Complex

Helmut Wiedenfeld* and Falk Knoch**)

Pharmaceutical Institute of the University, An der Immenburg 4, D-5300 Bonn-Endenich
**) Inorganic Chemistry Institute of the University, Gerhard-Domagk-Strasse 1, D-5300 Bonn-Endenich

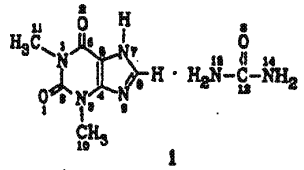
Received on June 25, 1985

The Crystal Structure of the Theophylline-Urea complex

The solubilization of theophylline by urea depends on complexation. The structure of the crystalline 1:1 compound was determined by X-ray analysis to be screw shaped (helical).

Urea is known as a complexing agent. For example, compounds with dicarboxylic acids[1)], glucose[2)], barbituric acid[3)], purine[4)], gramicidin[5)] and salicylic acid[6)] have been described in this regard.

The theophylline-urea complex **1** has been investigated by means of x-ray structural analysis within the framework of studies on the spatial structure of urea compounds. It has been shown that the compound crystallizes in a 1:1 ratio. The spatial structure of the complex gave rise to a screw-like helical structure. This structure arises as a result of hydrogen bond formation.



1

Crystal data

In order to crystallize the complex, cold saturated solutions of urea and theophylline in ethanol were combined and then stirred for 30 minutes at 50 °C. After 2 to 4 days, the compound crystallized out in rectangular parallelepipeds monoclinic crystal system in the C 2/c space group. Melting point: 215 °C (decomposition). Lattice constants: a = 16.294 Å; b = 7.552 Å; c = 17.751 Å; $\beta = 91.71°$. The cell volume amounts to 2184.3 Å^3; eight formula units are to be found in the unit cell, and the x-ray density is calculated to be 1.46 g/cm^3.

Structure elucidation and refinement

2633 independent reflections were measured in the range $3° < 2\Theta < 56°$. The measurement was carried out using an automatic four-circle diffractometer (Nicolet R 3 m) with a graphite monochromator using the ω-scan procedure (Mo-K_α radiation: 0.7107 Å). Following Lorentz polarization corrections, use was made of 1474 structure factors with $F > 4\,\sigma(F)$ in order to solve the structure. Use was made of direct methods (SHELXTL) in this connection. Refinement took place using the method of least squares. The hydrogen atoms of the methyl groups were calculated for ideal tetrahedra and were rotated about their central atom during the refinement. The other hydrogen atoms were determined by means of differential Fourier synthesis and were inserted into the model. Following the refining of all the parameters (heavy atoms anisotropic; H atoms isotropic), the R value converged to 0.063 ($R_\omega = 0.050$; $\omega = 1/\sigma^2$). Use was made of scattering factors for uncharged atoms (International Tables). Table 1 gives the atomic parameters, Table 2 gives the bond lengths and angles, and Table 3 gives the anisotropic temperature factors.

Table 1: *Atomic coordinates* (x 10^4) *and temperature factors* (Å x 10^3)

atom	x	y	z	U_{eq}
C 6	6093(2)	3596(5)	5664(2)	39(1)*
O 2	5404(1)	2947(4)	5605(1)	58(1)*
N 1	6474(2)	3845(4)	6384(1)	39(1)*
C11	6016(2)	3294(6)	7040(2)	59(1)*
C 2	7259(2)	4559(4)	6524(2)	40(1)*
O 1	7530(1)	4710(4)	7181(1)	56(1)*
N 3	7702(2)	5064(4)	5925(1)	37(1)*
C10	8544(2)	5748(5)	6029(2)	53(1)*
C 4	7367(2)	4838(4)	5197(2)	33(1)*
C 5	6604(2)	4160(4)	5086(2)	33(1)*
N 7	6491(2)	4113(4)	4310(1)	39(1)*
C 8	7174(2)	4756(5)	4023(2)	40(1)*
N 9	7741(2)	5232(4)	4548(1)	38(1)*

atom	x	y	z	U_{eq}
O 3	5266(1)	2960(3)	3427(1)	51(1)*
C12	4595(2)	2276(5)	3573(2)	43(1)*
N13	4069(2)	1838(5)	2995(2)	58(1)*
N14	4362(2)	1949(5)	4268(2)	56(1)*
C11-H_a	5521	2681	6893	72
C11-H_b	5885	4286	7352	72
C11-H_c	6376	2504	7316	72
C10-H_a	8578	6913	5815	64
C10-H_b	8924	4978	5787	64
C10-H_c	8679	5804	6559	64
N 7-H	6000(16)	3691(35)	4040(15)	45
C 8-H	7255(16)	4826(39)	3432(16)	49
N13-H_a	4243(18)	2141(42)	2490(17)	67
N13-H_b	3616(20)	1406(50)	3142(20)	67
N14-H_a	3871(20)	1354(46)	4349(19)	62
N14-H_b	4667(18)	2244(41)	4608(16)	62

*Equivalent isotropic U defined as one third of the trace of the orthogonalised U_{ij} tensor

Table 2: *Bond lengths* (Å) *and angles* (degrees)

C6 – O2	1.227(4)	C(1)–N(1)	1.416(4)
C6 – C5	1.407(4)	N(1)–C(6)	1.461(4)
N1 – C2	1.404(4)	C(2)–O(2)	1.240(3)
C2 – N3	1.358(4)	N(2)–C(7)	1.472(4)
N3 – C4	1.398(3)	C(3)–C(4)	1.353(4)
C4 – N9	1.352(4)	C(4)–N(3)	1.385(3)
N7 – C8	1.331(4)	C(5)–N(4)	1.342(4)
O3 – C12	1.245(4)	C(8)–N(5)	1.358(4)
C12 – N14	1.324(4)		

O2 – C6 – N1	120.4(3)	O2 – C6 – C5	128.2(3)
N1 – C6 – C5	111.4(3)	C6 – N1 – C11	117.5(3)
C6 – N1 – C2	125.6(2)	C11 – N1 – C2	116.9(2)
N1 – C2 – O1	119.9(3)	N1 – C2 – N3	118.2(2)
O1 – C2 – N3	121.9(3)	C2 – N3 – C10	121.0(2)
C2 – N3 – C4	119.2(2)	C10 – N3 – C4	119.7(2)
N3 – C4 – C5	120.8(2)	N3 – C4 – N9	125.9(3)
C5 – C4 – N9	113.3(2)	C6 – C5 – C4	124.7(3)
C6 – C5 – N7	130.8(3)	C4 – C5 – N7	104.4(2)
C5 – N7 – C8	106.5(2)	N7 – C8 – N9	113.4(3)
C4 – N9 – C8	102.4(2)	O3 – C12 – N13	118.9(3)
O3 – C12 – N14	123.3(3)	N13 – C12 – N14	117.8(3)

UM00014096
NOVARTIS EXHIBIT 1517
Novartis v. Regents, IPR2023-01347
Page 2842 of 4460

Table 3: *Anisotropic temperature factors* (Å x 10^3)

atom	U_{11}	U_{22}	U_{33}	U_{23}	U_{13}	U_{12}
C 6	40(2)	45(2)	32(2)	1(2)	-0(1)	-1(2)
O 2	44(1)	87(2)	42(1)	4(1)	-1(1)	-25(2)
N 1	41(2)	48(2)	28(1)	3(1)	-2(1)	-1(1)
C11	64(2)	74(3)	37(2)	8(2)	4(2)	-7(2)
C 2	45(2)	41(2)	34(2)	0(2)	-2(2)	11(2)
O 1	56(1)	85(2)	26(1)	-1(1)	-11(1)	7(1)
N 3	34(1)	49(2)	28(1)	-3(1)	-8(1)	-3(1)
C10	43(2)	69(3)	46(2)	2(2)	-17(2)	-7(2)
C 4	33(2)	39(2)	27(2)	-0(2)	-5(1)	3(2)
C 5	30(2)	42(2)	27(1)	1(1)	-3(1)	-1(2)
N 7	36(2)	52(2)	28(1)	-3(1)	-5(1)	-8(1)
C 8	39(2)	55(2)	26(2)	1(2)	-0(1)	-5(2)
N 9	33(2)	49(2)	32(1)	-0(1)	-4(1)	-6(1)
O 3	36(1)	80(2)	36(1)	-1(1)	-4(1)	-22(1)
C12	39(2)	48(2)	41(2)	-1(2)	-4(2)	-1(2)
N13	41(2)	88(3)	44(2)	-1(2)	-7(1)	-25(2)
N14	43(2)	82(3)	42(2)	-1(2)	-3(1)	-26(2)

The anisotropic temperature factor exponent takes the form: $-2\pi^2(h^2a^{*2}U_{11} + k^2b^{*2}U_{22} + \ldots\ldots + 2hka^*b^*U_{12})$

Results and discussion

The molecular weight of 240.1 can be calculated from the x-ray density of 1.46 g/cm^3 using the relationship $\rho_D \cdot V \cdot N_L/Z$ (ρ_D = x-ray density; V = volume of the unit cell; N_L = Loschmidt's Number (6.023 x 10^{23}); Z = number of formula units in the unit cell). In the present case, one must therefore be dealing with a 1:1 complex, whereby the smallest asymmetrical unit (unit cell) consists of four complex molecules. Each complex molecule exhibits two hydrogen bonds: from the N14-H to the O2 (2.18 Å) and from the N7-H to the O3 of the urea (1.69 Å). The Ortep plot of a complex molecule is illustrated in Fig. 1[7].

The individual complex molecules are connected to one another by additional H bonds: from the N9 to the second hydrogen of the N14-H_2 group of symmetry 5 (2.07 Å), and from the O1 to both the hydrogen of an N13-H2 group of symmetry 8 (2.56 Å) and also to the C8-H of a theophylline molecule that has been shifted by translation in the y direction and obeys symmetry 4 (2.31 Å).

The urea molecules are, likewise, mutually connected by hydrogen bonds in such a way that the last "free" proton of an N13-H_2 group is connected to the O3 of the adjacent molecule (1.94 Å) that, likewise, exhibits only one H bond to the theophylline. A surprising aspect is the fact that only one single H bond is formed to the O2 and not in this way to the O3.

Thus each theophylline molecule exhibits five hydrogen bonds and each urea molecule exhibits six H bonds. The aforementioned screw-like arrangement of the helical structure results from this. A segment of this structure is illustrated in Fig. 2.

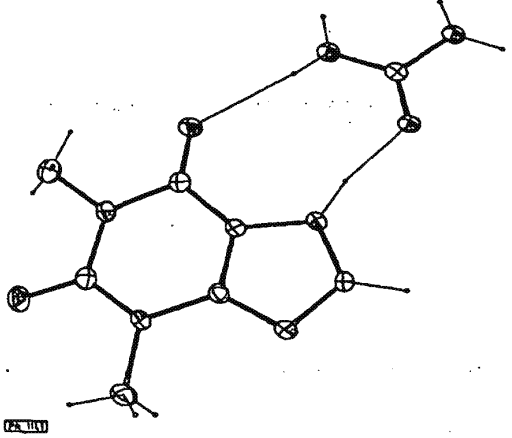


Fig. 1: ORTEP plot of the complex molecule

UM00014097
NOVARTIS EXHIBIT 1517
Novartis v. Regents, IPR2023-01347
Page 2843 of 4460

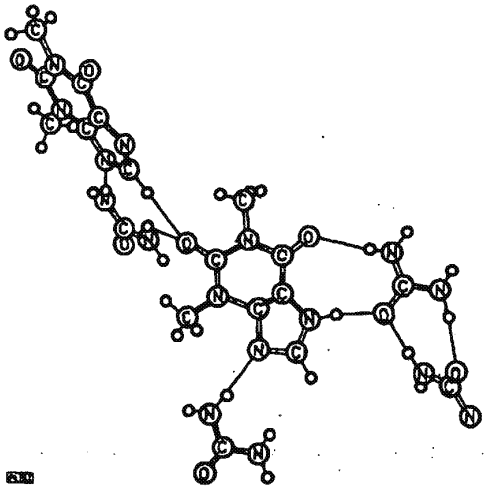


Fig. 2: Segment from the structure of the complex

Bibliography

1 S. Harkema, J.W. Bats, A.M. Weyenberg and D. Feil, Acta Crystallogr. Sect, *B 28*, 1646 (1972).
2 R.L. Snyder and R.D. Rosenstein, Acta Crystallogr. Sect, *B 27*, 1969 (1971).
3 G.L. Gartland and B.M. Craven, Acta Crystallogr. Sect, *B 30*, 980 (1974).
4 A. Itai, H. Yamada, T. Okamoto and Y. Iitaka, Acta Crystallogr. Sect, *B 33*, 1816 (1977).
5 S.E. Hull, R. Karlsson, P. Main, M.M. Woolfson and E.J. Dodson, Nature (London) *275*, 206 (1978).
6 I-NAN HSU and R.W. Gellert, J. of Crystallogr. Spectroscop. Res. *13*, 43 (1983).
7 C.H. Johnson, Oak-Ridge National Laboratory Report, ORNL-3794 (1965).

[Ph 111]

NOVARTIS EXHIBIT 1517
Novartis v. Regents, IPR2023-01347
Page 2844 of 4460

8 So auch jetzt (siehe Exp. Teil) die vorher nicht beschriebene 3,3-Dimethyl-Verbindung.
9 Eastman Kodak Co (P.W. Jenkins), Franz. Pat. 2.099.780; C.A. *78*, 17648a (1973).
10 C.A. *95* (1981), Formula Index: $C_6H_4N_2O_4$.
11 C.A. *95* (1981) 152152 a.
12 Ciba Geigy AG (S.R. Postle), Eur. Pat. 29.412.
13 In der Reihe der 3,5-Pyrazolidindione wurden derartige Betaine erstmals hergestellt aus dem 1,2-Diphenyl-Derivat: A. Hochrainer, Monatsh. Chem. *97*, 823 (1966).
14 D.T. Cromer und J.T. Waber, International Tables for X-ray Crystallography, Vol. IV, S. 71, Kynoch Press, Birmingham, U.K., 1974.
15 C.K. Johnson, ORTEP II, Report ORNL-5138, Oak Ridge National Laboratory, Oak Ridge, Tenn., USA, 1976.
16 J. Godin und A.Le Berre, Bull. Soc. Chim. Fr. *10*, 4210 (1968).
17 G. Fritsch, G. Zinner und L. Ernst, Arch. Pharm. (Weinheim) *319*, 537 (1986).

[Ph 109]

Arch. Pharm. (Weinheim) *319*, 654–659 (1986)

Zur Kristallstruktur des Theophyllin-Harnstoff-Komplexes

Helmut Wiedenfeld* und Falk Knoch**)

Pharmazeutisches Institut der Universität, An der Immenburg 4, D-5300 Bonn-Endenich
**) Anorganisch-Chemisches Institut der Universität, Gerhard-Domagk-Straße 1, D-5300 Bonn-Endenich

Eingegangen am 25. Juni 1985

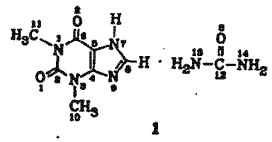
Die Lösungsvermittlung von Theophyllin durch Harnstoff beruht auf Komplexbildung. Durch Röntgenstrukturanalyse wird die Kristallstruktur dieser 1:1-Verbindung geklärt. Es wird ein schraubenartiger Aufbau (Helix-Struktur) gefunden.

The Crystal Structure of the Theophylline-Urea Complex

The solubilisation of theophylline by urea depends on complexation. The structure of the crystalline 1:1 compound was determined by X-ray analysis to be screwshaped (helical).

Harnstoff ist als Komplexbildner bekannt. So sind z.B. Verbindungen mit Dicarbonsäuren[1], Glucose[2], Barbitursäure[3], Purin[4], Gramicidin[5] und Salicylsäure[6] beschrieben.

Im Zuge der Untersuchungen zum räumlichen Aufbau von Harnstoff-Verbindungen wurde der Theophyllin-Harnstoff-Komplex **1** durch Röntgenstrukturanalyse untersucht. Es wurde gezeigt, daß die Verbindung im Verhältnis 1:1 kristallisiert. Der räumliche Aufbau des Komplexes ergab eine schraubenartige Anordnung von helixartiger Struktur. Diese Struktur kommt durch Wasserstoffbrückenbildung zustande.



1

Kristalldaten

Zur Kristallisation des Komplexes wurden kalt gesättigte Lösungen von Harnstoff und Theophyllin in Ethanol vereinigt und 30 min bei 50° gerührt. Die Verbindung kristallisierte nach 2 bis 4 Tagen in rechteckigen Quadern und monoklin in der Raumgruppe C 2/c aus. Schmp.: 215° (Zers.). Gitterkonstanten: a = 16.294 Å; b = 7.552 Å; c = 17.751 Å; β = 91.71°. Das Zellvol. beträgt 2184.3 $Å^3$; in der Elementarzelle befinden sich acht Formeleinheiten und die Röntgendichte errechnet sich zu 1.46 g/cm^3.

Strukturaufklärung und Verfeinerung

Es wurden 2633 unabhängige Reflexe im Bereich $3° < 2\Theta < 56°$ vermessen. Die Messung wurde auf einem automatischen Vierkreisdiffraktometer (Nicolet R 3 m) mit Graphitmonochromator im ω-Scan-Verfahren durchgeführt (Mo-K_α-Strahlung: 0.7107 Å). Nach Lorentz- und Polarisationskorrektur wurden 1474 Strukturfaktoren mit $F > 4\sigma(F)$ zur Lösung der Struktur verwendet. Dabei wurden direkte Methoden (SHELXTL) eingesetzt. Die Verfeinerung erfolgte nach der Methode der kleinsten Fehlerquadrate. Die Wasserstoffatome der Methylgruppen wurden für ideale Tetraeder berechnet und während der Verfeinerung um ihr Zentralatom rotiert. Die übrigen Wasserstoffatome wurden durch Differenz-Fourier-Synthese ermittelt und in das Modell eingefügt. Nach Verfeinerung aller Parameter (schwere Atome anisotrop; H-Atome isotrop) konvergierte der R-Wert gegen 0.063 (R_w = 0.050; $\omega = 1/\sigma^2$). Es wurden Streufaktoren für ungeladene Atome (International Tables) verwendet. Tab. 1 gibt die Atomparameter, Tab. 2 die Abstände und Winkel und Tab. 3 die anisotropen Temperaturfaktoren wieder.

Tab. 1: *Atomkoordinaten* (x 10^4) *und Temperaturfaktoren* (Å x 10^3)

atom	x	y	z	U_{eq}
C 6	6093(2)	3596(5)	5664(2)	39(1)*
O 2	5404(1)	2947(4)	5605(1)	58(1)*
N 1	6474(2)	3845(4)	6384(1)	39(1)*
C11	6016(2)	3294(6)	7040(2)	59(1)*
C 2	7259(2)	4559(4)	6524(2)	40(1)*
O 1	7530(1)	4710(4)	7181(1)	56(1)*
N 3	7702(2)	5064(4)	5925(1)	37(1)*
C10	8544(2)	5748(5)	6029(2)	53(1)*
C 4	7367(2)	4838(4)	5197(2)	33(1)*
C 5	6604(2)	4160(4)	5086(2)	33(1)*
N 7	6491(2)	4113(4)	4310(1)	39(1)*
C 8	7174(2)	4756(5)	4023(2)	40(1)*
N 9	7741(2)	5232(4)	4548(1)	38(1)*

UM00014099

NOVARTIS EXHIBIT 1517
Novartis v. Regents, IPR2023-01347
Page 2845 of 4460

Forts. **Tab. 1:**

atom	x	y	z	U_{eq}
O 3	5266(1)	2960(3)	3427(1)	51(1)*
C12	4595(2)	2276(5)	3573(2)	43(1)*
N13	4069(2)	1838(5)	2995(2)	58(1)*
N14	4362(2)	1949(5)	4268(2)	56(1)*
C11-H_a	5521	2681	6893	72
C11-H_b	5885	4286	7352	72
C11-H_c	6376	2504	7316	72
C10-H_a	8578	6913	5815	64
C10-H_b	8924	4978	5787	64
C10-H_c	8679	5804	6559	64
N 7-H	6000(16)	3691(35)	4040(15)	45
C 8-H	7255(16)	4826(39)	3432(16)	49
N13-H_a	4243(18)	2141(42)	2490(17)	67
N13-H_b	3616(20)	1406(50)	3142(20)	67
N14-H_a	3871(20)	1354(46)	4349(19)	62
N14-H_b	4667(18)	2244(41)	4608(16)	62

*Equivalent isotropic U defined as one third of the trace of the orthogonalised U_{ij} tensor

Tab. 2: *Bindungslängen* (Å) *und Winkel* (Grad)

C6 – O2	1.227(4)	C(1)–N(1)	1.416(4)
C6 – C5	1.407(4)	N(1)–C(6)	1.461(4)
N1 – C2	1.404(4)	C(2)–O(2)	1.240(3)
C2 – N3	1.358(4)	N(2)–C(7)	1.472(4)
N3 – C4	1.398(3)	C(3)–C(4)	1.353(4)
C4 – N9	1.352(4)	C(4)–N(3)	1.385(3)
N7 – C8	1.331(4)	C(5)–N(4)	1.342(4)
O3 – C12	1.245(4)	C(8)–N(5)	1.358(4)
C12 – N14	1.324(4)		

O2 – C6 – N1	120.4(3)	O2 – C6 – C5	128.2(3)
N1 – C6 – C5	111.4(3)	C6 – N1 – C11	117.5(3)
C6 – N1 – C2	125.6(2)	C11 – N1 – C2	116.9(2)
N1 – C2 – O1	119.9(3)	N1 – C2 – N3	118.2(2)
O1 – C2 – N3	121.9(3)	C2 – N3 – C10	121.0(2)
C2 – N3 – C4	119.2(2)	C10 – N3 – C4	119.7(2)
N3 – C4 – C5	120.8(2)	N3 – C4 – N9	125.9(3)
C5 – C4 – N9	113.3(2)	C6 – C5 – C4	124.7(3)
C6 – C5 – N7	130.8(3)	C4 – C5 – N7	104.4(2)
C5 – N7 – C8	106.5(2)	N7 – C8 – N9	113.4(3)
C4 – N9 – C8	102.4(2)	O3 – C12 – N13	118.9(3)
O3 – C12 – N14	123.3(3)	N13 – C12 – N14	117.8(3)

Tab. 3: *Anisotrope Temperaturfaktoren* (Å x 10^3)

atom	U_{11}	U_{22}	U_{33}	U_{23}	U_{13}	U_{12}
C 6	40(2)	45(2)	32(2)	1(2)	–0(1)	–1(2)
O 2	44(1)	87(2)	42(1)	4(1)	–1(1)	–25(2)
N 1	41(2)	48(2)	28(1)	3(1)	–2(1)	–1(1)
C11	64(2)	74(3)	37(2)	8(2)	4(2)	–7(2)
C 2	45(2)	41(2)	34(2)	0(2)	–2(2)	11(2)
O 1	56(1)	85(2)	26(1)	–1(1)	–11(1)	7(1)
N 3	34(1)	49(2)	28(1)	–3(1)	–8(1)	–3(1)
C10	43(2)	69(3)	46(2)	2(2)	–17(2)	–7(2)
C 4	33(2)	39(2)	27(2)	–0(2)	–5(1)	3(2)
C 5	30(2)	42(2)	27(1)	1(1)	–3(1)	–1(2)
N 7	36(2)	52(2)	28(1)	–3(1)	–5(1)	–8(1)
C 8	39(2)	55(2)	26(2)	1(2)	–0(1)	–5(2)
N 9	33(2)	49(2)	32(1)	–0(1)	–4(1)	–6(1)
O 3	36(1)	80(2)	36(1)	–1(1)	–4(1)	–22(1)
C12	39(2)	48(2)	41(2)	–1(2)	–4(2)	–1(2)
N13	41(2)	88(3)	44(2)	–1(2)	–7(1)	–25(2)
N14	43(2)	82(3)	42(2)	–1(2)	–3(1)	–26(2)

The anisotropic temperature factor exponent takes the form: $-2\pi^2(h^2a^{*2}U_{11} + k^2b^{*2}U_{22} + \ldots\ldots + 2hka^*b^*U_{12})$

Ergebnisse und Diskussion

Aus der Röntgendichte von 1.46 g/cm³ läßt sich nach der Beziehung $\varrho_D \cdot V \cdot N_L/Z$ (ϱ_D = Röntgendichte; V = Vol. der Elementarzelle; N_L = Loschmidt'sche Zahl ($6.023 \cdot 10^{23}$); Z = Anzahl der Formeleinheiten in der Elementarzelle) das Molekulargewicht von 240.1 errechnen. Somit muß es sich im vorliegenden Fall um einen 1:1-Komplex handeln, wobei die kleinste asymmetrische Einheit (Elementarzelle) aus vier Komplexmolekülen besteht. Jedes Komplexmolekül weist zwei Wasserstoffbrücken auf: Vom N 14-H zum 02 (2.18 Å) und vom N7-H zum 03 des Harnstoffes (1.69 Å). In Abb. 1 ist der Ortep-Plot eines Komplexmoleküls wiedergegeben[7].

Die einzelnen Komplexmoleküle sind durch weitere H-Brücken miteinander verbunden: Vom N9 zum zweiten Wasserstoff der N14-H_2-Gruppe der Symmetrie 5 (2.07 Å, vom 01 sowohl zum Wasserstoff einer N13-H_2-Gruppe der Symmetrie 8 (2.56 Å) als auch zum C8-H eines Theophyllin-Moleküls, das um eine Translation in y-Richtung verschoben ist und der Symmetrie 4 gehorcht (2.31 Å).

Die Harnstoff-Moleküle sind ebenfalls untereinander durch Wasserstoffbrücken verbunden, in der Weise, daß das letzte „freie" Proton einer N13-H_2-Gruppe mit dem 03 des Nachbarmoleküls, das ja ebenfalls erst eine H-Brücke zum Theophyllin aufweist, verbunden ist (1.94 Å). Überraschend ist die Tatsache, daß zum 02 – nicht wie zum 03 – nur eine einzige H-Brücke ausgebildet wird.

Somit weist jedes Theophyllin-Molekül fünf und jedes Harnstoff-Molekül sechs H-Brücken auf. Hieraus resultiert die bereits erwähnte schraubenartige Anordnung der Helixstruktur. Ein Ausschnitt aus dieser Struktur ist in Abb. 2 wiedergegeben.

UM00014100

NOVARTIS EXHIBIT 1517
Novartis v. Regents, IPR2023-01347
Page 2846 of 4460

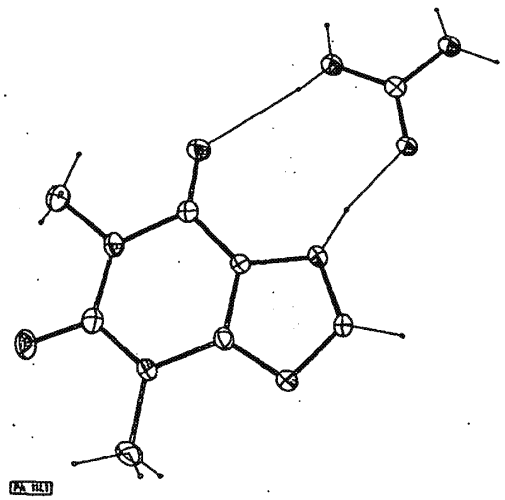


Abb. 1: ORTEP-Plot des Komplexmoleküls

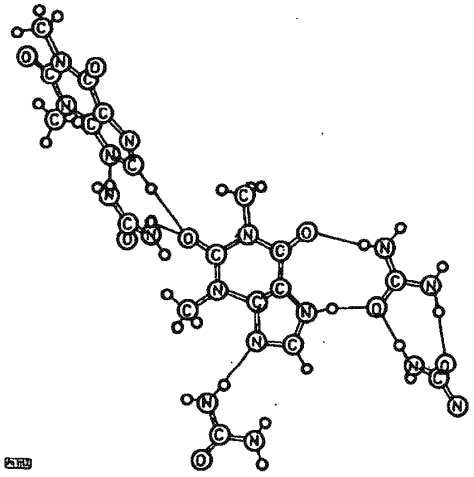


Abb. 2: Ausschnitt aus der Struktur des Komplexes

Literatur

1 S. Harkema, J.W. Bats, A.M. Weyenberg und D. Feil, Acta Crystallogr. Sect. *B 28*, 1646 (1972).
2 R.L. Snyder und R.D. Rosenstein, Acta Crystallogr. Sect. *B 27*, 1969 (1971).
3 G.L. Gartland und B.M. Craven, Acta Crystallogr. Sect. *B 30*, 980 (1974).
4 A. Itai, H. Yamada, T. Okamoto und Y. Iitaka, Acta Crystallogr. Sect. *B 33*, 1816 (1977).
5 S.E. Hull, R. Karlsson, P. Main, M.M. Woolfson und E.J. Dodson, Nature (London) *275*, 206 (1978).
6 I-NAN HSU and R.W. Gellert, J. of Crystallogr. Spectroscop. Res. *13*, 43 (1983).
7 C.H. Johnson, Oak-Ridge National Laboratory Report, ORNL-3794 (1965).

[Ph 111]

Kurzmitteilungen

Arch. Pharm. (Weinheim) *319*, 659–661 (1986)

Anellierungsreaktionen von α-(Dihydro-β-carbolinium)-keton-Derivaten

Annellation Reactions of α-(Dihydro-β-carbolinium)-ketone-Derivatives

Hans Möhrle* und Peter Schillings

Institut für Pharmazeutische Chemie der Universität Düsseldorf, Universitätsstr. 1, 4000 Düsseldorf 1
Eingegangen am 3. Februar 1986

Um die Anwendungsbreite unserer Methode zur Darstellung anellierter Imidazole[1,2] zu überprüfen, wurde 9-Methyl-3,4-dihydro-β-carbolin (**1**) in die Untersuchungen[3] einbezogen. **1** ergab mit α-Bromacetophenon das Iminiumperchlorat **2**.

Aus **2** entstand mit Hydroxylamin in acetatgepufferter Essigsäure das Imidazol-Derivat **3**, das in geringerer Ausbeute auch durch Umsatz von **2** mit Ammoniumacetat/Essigsäure erhalten werden konnte.

Die Reaktion von **2** mit Hydrazin lieferte das Tetrahydrotriazin **4**, das mit Quecksilber(II)-EDTA zum anellierten Dihydrotriazin **5** dehydriert wurde.

Dem Fonds der Chemischen Industrie danken wir für die finanzielle Unterstützung unserer Arbeit.

UM00014101

NOVARTIS EXHIBIT 1517
Novartis v. Regents, IPR2023-01347
Page 2847 of 4460

This Page is Inserted by IFW Indexing and Scanning Operations and is not part of the Official Record

BEST AVAILABLE IMAGES

Defective images within this document are accurate representations of the original documents submitted by the applicant.

Defects in the images include but are not limited to the items checked:

- ☐ BLACK BORDERS
- ☐ IMAGE CUT OFF AT TOP, BOTTOM OR SIDES
- ☐ FADED TEXT OR DRAWING
- ☐ BLURRED OR ILLEGIBLE TEXT OR DRAWING
- ☐ SKEWED/SLANTED IMAGES
- ☐ COLOR OR BLACK AND WHITE PHOTOGRAPHS
- ☐ GRAY SCALE DOCUMENTS
- ☐ LINES OR MARKS ON ORIGINAL DOCUMENT
- ☐ REFERENCE(S) OR EXHIBIT(S) SUBMITTED ARE POOR QUALITY
- ☐ OTHER: _____

IMAGES ARE BEST AVAILABLE COPY.
As rescanning these documents will not correct the image problems checked, please do not report these problems to the IFW Image Problem Mailbox.

F8 A THIOPHENYL ETHER OF USNIC ACID, A MODEL COMPOUND FOR SELECTIVE ALKYLATION BY αβ-UNSATURATED TUMOR INHIBITORS. R.F. Bryan, Chemistry Department University of Virginia, Charlottesville, Virginia

(-)-Usnic acid shows inhibitory activity against Lewis lung carcinoma in live mice [S.M. Kupchan & H.L. Kopperman, *Experientia*, 31, 625 (1975)].

Nucleophilic addition of enzyme thiol groups to α,β-unsaturated systems may be involved in the tumor inhibitory properties of compounds of this type.

The crystal structure of the ether formed by reaction of usnic acid with thiophenol has been determined as a model for such a system. Reaction takes place at C(4a) of the unsaturated system and places the thiol residue *cis* to the C(1a) methyl group.

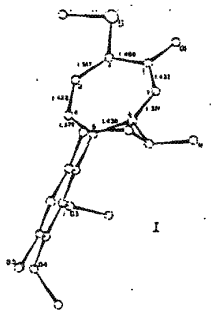
The molecule contains three intramolecular O-H...O hydrogen bonds of length 2.663(4), 2.522(4), and 2.417(4) Å, the last of these apparently symmetrical. The ether thus has the same tautomeric form as the parent acid and shows the same delocalization of electrons among atoms involved in the keto-enol system associated with the short hydrogen bond.

Crystal data: $C_{24}H_{22}O_7S$, mol. wt. 454.5; Orthorhombic, *Pbca*, a = 13.439(2), b = 23.645(3), c = 13.318(2) Å, Z = 8.

2588 reflections measured by counter diffractometry, *MULTAN*, least-squares, C, O, S anisotropic, H isotropic, R = 0.056, R_w = 0.048.

F9 COLCHICINE RELATED MICROTUBULE INHIBITORS. T.N. Margulis Department of Chemistry, University of Massachusetts-Boston Boston, Massachusetts 02125.

Microtubules are implicated in many cell processes involving biological motility and morphology. Colchicine and its analogs interfere with these processes probably by binding to tubulin, the protein from which microtubules are formed. Colchicine is used in the treatment of gout and some derivatives are being tested as anti-tumor agents. N-deacetylthiocolchicine(I), $C_{20}H_{24}NO_4S^+Cl^-\cdot 2H_2O$, is as active as colchicine. Crystals are orthorhombic, space group $P2_12_12_1$; a = 7.538, b = 11.663, c = 25.375 Å; Z = 4 molecules/cell.[1] The structure is similar to that of other colchicine derivatives. Demethyl-iso-thiocolchicine(II), $C_{21}H_{23}NO_5S\cdot H_2O$ is an inactive substance forming monoclinic crystals, space group $P2_1$; a = 11.906, b = 8.713, c = 10.004 Å, β = 89.44°, Z = 2 molecules/cell. It is missing the methyl group on O5 and has C=O and S-CH_3 positions interchanged on the troponoid ring. A prominent difference between these structures is the conformation of the methoxy groups on the benzenoid ring.



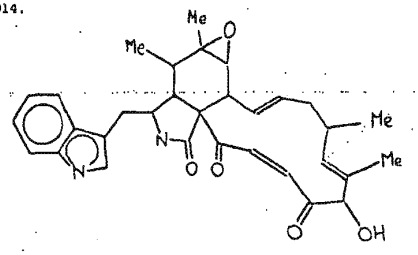
I

This investigation was supported by Public Health Service Research Grant No. CA-17340 from the National Cancer Institute.

F10 THE CRYSTAL AND MOLECULAR STRUCTURE OF THE COMPLEX 2,6-DIAMINO-9-ETHYLPURINE · 5,5-DIETHYLBARBITURIC ACID. G. J. Bunick and D. Voet, Department of Chemistry and Laboratory for Research on the Structure of Matter, University of Pennsylvania, Philadelphia, Pennsylvania 19174

Crystals of the molecular complex 2,6-diamino-9-ethylpurine · 5,5-diethylbarbituric acid crystallize from aqueous solution in the space group $P\bar{1}$ with one complex per asymmetric unit. The unit cell parameters are a = 9.610(2), b = 9.972(3), c = 11.021(4) Å, α = 66.69(2), β = 69.24(2), and γ = 74.74(2)°. The structure was solved by direct methods and refined by least-squares to a final R factor of 0.049 based on 2766 unique reflections. The structure is extensively base paired such that all possible hydrogen bonds are utilized. Several of the hydrogen bonds in which the barbiturate carbonyl is the acceptor group are quite long as is commonly observed in barbiturate containing complexes. The dihedral angle between the least-squares planes of the adenine residue and the barbiturate rings to which it forms a Watson-Crick type base pair is 52°. Such a base pairing configuration has not been observed among the over 30 such structures reported to date.

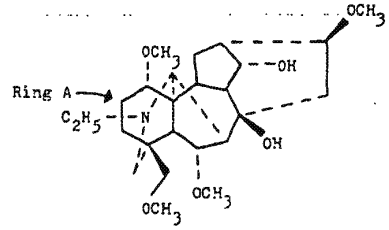
F11 THE CRYSTAL AND MOLECULAR STRUCTURE OF THE MOLD TOXIN, CHAETOGLOBOSIN, $C_{32}H_{32}N_2O_6$. J. V. Silverton, T. Akiyama and C. Kabuto, Laboratory of Chemistry, NHLI, NIH, Bethesda, MD 20014.



The compound shown above crystallizes in $P2_12_12_1$ (a=10.036(1) b=16.888(1), c=17.092(2)Å, Z=4, MW=528). 3207 reflections were measured with an automatic diffractometer (468 unobserved; 1σ). The final R-factor is 0.033 with all hydrogen atoms included in the refinement. The structure was solved by direct methods with the use of "negative quartets". The asymmetric unit includes one molecule of water and there is extensive hydrogen bonding.

F12 PROOF OF THE STRUCTURE OF CHASMANINE: THE CRYSTAL AND MOLECULAR STRUCTURE OF CHASMANINE 14α-BENZOATE HYDROCHLORIDE. Wilson H. De Camp and S. W. Pelletier, Natural Products Laboratory, Department of Chemistry, University of Georgia, Athens, Georgia 30602.

Chasmanine is a C_{19} diterpene alkaloid which is found in the roots of Aconitum chasmanthum Stapf. The structures of several other alkaloids depend on the correlation of chasmanine with browniine (Edwards, Fonzes & Marion, Can. J. Chem., 44,583 (1966)), which has recently been questioned (Pelletier, Djarmati & De Camp, Xth IUCr, paper 6.1-34, Acta Cryst. A31, S111 (1975)). The crystal structure of the title compound has been solved, confirming the structure shown below for chasmanine.



Supplied by The British Library - "The world's knowledge"

BEST AVAILABLE COPY

UM00014103

NOVARTIS EXHIBIT 1517
Novartis v. Regents, IPR2023-01347
Page 2849 of 4460

ELSEVIER

Journal of Molecular Structure 436–437 (1997) 143–151

Journal of
MOLECULAR
STRUCTURE

Crystal structure and vibrational spectra of the 1:1 and 1:2 complexes of pyridine betaine with pentachlorophenol[1]

Grzegorz Buczak, Zofia Dega-Szafran, Andrzej Katrusiak, Mirosław Szafran*

Faculty of Chemistry, A. Mickiewicz University, Grunwaldzka 6, PL-60780 Poznań, Poland

Received 24 December 1996; accepted 28 January 1997

Abstract

Crystalline complexes of pyridine betaine (PBET) with pentachlorophenol (PCP) have been synthesized and characterized by X-ray diffraction and FTIR spectroscopy: PBET·$(PCP)_2$ (space group $P\bar{1}$ with $a = 8.748(4)$, $b = 11.855(6)$, $c = 13.221(6)$ Å, $\alpha = 66.70(5)$, $\beta = 74.06(4)$, $\gamma = 77.97(4)°$), PBET·PCP·H_2O (space group $P2_1/c$ with $a = 8.616(2)$, $b = 27.610(6)$, $c = 7.0760(10)$, $\alpha = 90$, $\beta = 104.82(3)$, $\gamma = 90°$), PBET·PCP·HOMe and PBET·PCP. In PBET·$(PCP)_2$ the betaine carboxylate group is linked to two phenol molecules by hydrogen bonds of 2.582(6) and 2.611(6) Å. In PBET·PCP·H_2O a centrosymmetric molecular complex is formed by two formula units, where two carboxylate groups are bridged by two water molecules to form an eight membered ring with four O–H···O hydrogen bonds of 2.703(4) and 2.715(5) Å, respectively; each water molecule, in turn, forms a hydrogen bond of 2.580(4) Å to PCP. The IR spectrum of PBET·PCP·HOMe is consonant with a structure in which the betaine carboxylate group accepts both PCP and HOMe. © 1997 Elsevier Science B.V.

Keywords: Pyridine betaine; Pentachlorophenol; Hydrogen bond; X-rays; FTIR spectroscopy

1. Introduction

Betaines are zwitterions generally containing a carboxylate group and a quaternary ammonium or pyridinium groups. The chemistry of betaines has become a subject of particular interest due to their role in biological research, especially in amino acid syntheses as a methyl transfer agent [1]. Interesting physical properties, like ferroelectric, antiferroelectric and ferroelastic phase transitions, were reported for a series of betaine complexes [2]. Betaines containing a hydrophobic chain of 8 to 20 carbon atoms are surface active agents often added to other surfactants to largely improve their performance, mildness, foaming, viscosity or other properties [3].

The crystal structures of pyridine betaine [4], its complexes with hydrochloric [5] and sulphuric [6] acids and 2,6-dichloro-4-nitrophenol [7] have been determined. Recently we have shown that pyridine betaine forms complexes with one or two molecules of 2,6-dichloro-4-nitrophenol ($pK_a = 3.54$ [8]) [7]. In this paper we describe its complexes with pentachlorophenol, which is a weaker proton donor ($pK_a = 4.5$ [9]a, 4.82 [9]b).

2. Experimental

Pyridine betaine, 1-(carboxymethyl)pyridinium

* Corresponding author. Tel.: +48 61 699181; fax: +48 61 658008, e-mail: szafran@chem.amu.edu.pl

[1] Dedicated to Professor Henryk Ratajczak on the occasion of his 65th birthday.

0022-2860/97/$17.00 © 1997 Elsevier Science B.V. All rights reserved
PII S0022-2860(97)00121-X

UM00014104
NOVARTIS EXHIBIT 1517
Novartis v. Regents, IPR2023-01347
Page 2850 of 4460

inner salt (PBET), was prepared by a modified procedure of von Gerichten as described previously [10].

The complex of pyridine betaine with 2 molecules of pentachlorophenol [PBET·(PCP)$_2$], was obtained by adding two moles of PCP in acetonitrile solution to 1 mole of pyridine betaine in methanol. The resulting product was recrystallized from CH_3CN–CH_3OH mixture (1:1) and dried over P_2O_5, m.p. 147–150°C decomp. Analysis for $C_{19}H_9Cl_{10}NO_4$ calcd. C, 34.07; H, 1.35; N, 2.09, found C, 34.07; H, 1.11; N, 2.01%.

PBET·PCP·HOMe, complex of pyridine betaine with pentachlorophenol and methanol was prepared by mixing equivalents in a little hot methanol, m.p. 143–145°C. Analysis for $C_{14}H_{12}Cl_5NO_4$: Calcd. C, 38.61; H, 2.78; N, 3.22; Found C, 38.61; H, 2.70; N, 3.18%. The complex lost methanol molecule at 50° during the night. Recrystallization of PBET·PCP·HOMe from 4:1 mixture of methanol with water gave PBET·(PCP)$_2$. To avoid a surface effect due to small amounts of absorbed water, a sample of PBET·PCP.HOMe was left in room atmosphere until it was completely hydrated; for details see Ref. [11]. PBET·PCP·H_2O, m.p. 144–145°C. Analysis for $C_{13}H_8Cl_5NO_3 \cdot H_2O$: Calcd. C, 37.05; H, 2.39; N, 3.32; Found C, 37.26; H, 1.96; N, 3.31%.

The FTIR spectra were recorded using Bruker IFS 113v spectrometer with resolution of 2 cm^{-1} in Nujol and Fluorolube suspensions on KBr plates.

X-Ray measurements were carried out at room temperature on a KUMA diffractometer with a graphite monochromator; ω–2θ scan mode was applied. The structures were solved by direct methods [12] and refined by full matrix least-squares on F^2 using the SHELXL 93 program [13]. Anisotropic thermal factors

Table 1
Crystal data and structure refinement for PBET·(PCP)$_2$ and PBET·PCP·H_2O

	PBET·(PCP)$_2$	PBET·PCP·H_2O
Formula	$C_{19}H_9Cl_{10}NO_4$	$C_{13}H_{10}Cl_5NO_4$
Formula weight	669.77	421.47
Temperature (K)	293(2)	293(2)
Wavelength (Å)	0.71073	1.54178
Crystal size (mm)	0.2 × 0.2 × 0.15	0.4 × 0.2 × 0.1
Crystal system	triclinic	monoclinic
Space group	$P\bar{1}$	$P2_1/c$
Unit cell dimensions:		
a (Å)	8.748(4)	8.616(2)
b (Å)	11.855(6)	27.610(6)
c (Å)	13.221(6)	7.0760(10)
α (deg)	66.70(5)	90
β (deg)	74.06(4)	104.82(3)
γ (deg)	77.97(4)	90
V (Å^3)	1203.1(10)	1627.3(6)
Z	2	4
D_x (g cm^{-3})	1.849	1.720
μ (mm^{-1})	1.189	8.299
Theta max. (deg)	1. 72 to 24.05	3.20 to 70.32
Index ranges	$-9 \le h \le 10$, $-12 \le k \le 13$, $0 \le l \le 15$	$0 \le h \le 10$, $0 \le k \le 30$, $-8 \le l \le 8$
F(000)	664	848
Reflections collected	3941	3104
Independent reflections	3754 [R(int) = 0.0431]	2905 [R(int) = 0.1382]
Data/restraints/parameters	3753/1/344	2903/2/249
Goodness-of-fit on F^2	1.137	1.052
Final R indices [$I > 2\sigma(I)$]	$R1$ = 0.0487, w$R2$ = 0.1209	$R1$ = 0.0583, w$R2$ = 0.1396
R indices (all data)	$R1$ = 0.1229, w$R2$ = 0.1472	$R1$ = 0.0802, w$R2$ = 0.1638
Extinction coefficient	0.0015(6)	0.0038(6)
Largest diff. peak and hole (eÅ^{-3})	0.437 and −0.441	0.821 and −0.571

UM00014105
NOVARTIS EXHIBIT 1517
Novartis v. Regents, IPR2023-01347
Page 2851 of 4460

Table 2
Atomic coordinates ($\times 10^4$ and $\times 10^3$ for H-atoms) and equivalent isotropic thermal parameters ($Å^2 \times 10^3$) for PBET·(PCP)$_2$ and PBET·PCP·H$_2$O. U(eq) is defined as one third of the trace of the orthogonalized U_{ij} tensor

	x	y	z	U(eq)
PBET·(PCP)$_2$				
Cl(2)	2376(2)	9193(2)	6576(1)	45(1)
Cl(Y)	−82(2)	4628(2)	7292(2)	53(1)
Cl(2')	4134(2)	6646(2)	9126(2)	58(1)
Cl(6')	−1651(2)	6227(2)	8785(2)	45(1)
C1(3')	5737(2)	5094(2)	7614(2)	56(1)
Cl(3)	4023(2)	7704(2)	5018(2)	50(1)
C1(6)	−3386(2)	8583(2)	6337(2)	53(1)
Cl(5)	−1772(2)	7082(2)	4762(2)	55(1)
Cl(4')	3639(2)	4148(2)	6627(2)	52(1)
Cl(4)	1942(2)	6667(2)	4072(2)	60(1)
C(1)	−412(7)	8813(5)	6365(5)	33(1)
O(1')	616(5)	7121(4)	9444(4)	47(1)
C(3)	1965(7)	7944(5)	5356(5)	34(1)
C(1')	1331(7)	6406(5)	8822(5)	35(2)
O(1)	−1201(5)	9451(4)	7038(4)	47(1)
C(4')	2754(7)	4964(5)	7505(5)	34(1)
C(2)	1227(7)	8606(5)	6062(5)	33(1)
C(5')	1095(7)	5191(5)	7793(5)	33(1)
C(3')	3690(7)	5401(5)	7913(5)	36(2)
C(4)	1035(7)	7490(5)	4944(5)	36(2)
C(5)	−615(7)	7687(6)	5243(5)	38(2)
C(2')	2977(7)	6139(5)	8574(5)	35(1)
C(6)	−1351(7)	8353(6)	5951(5)	39(2)
C(6')	405(7)	5915(5)	8448(5)	31(1)
O(2)	−414(5)	10039(4)	8496(4)	54(1)
O(3)	1763(5)	9099(4)	9202(4)	45(1)
C(7)	849(8)	10018(6)	8748(5)	40(2)
C(8)	1300(8)	11300(6)	8479(7)	41(2)
N(1)	2857(6)	11318(4)	8669(4)	37(1)
C(9)	2952(8)	11733(6)	9456(6)	48(2)
C(10)	4408(10)	11761(8)	9628(8)	65(2)
C(11)	5807(10)	11398(7)	8976(8)	60(2)
C(12)	5654(9)	10977(7)	8175(7)	59(2)
C(13)	4197(8)	10921(6)	8041(6)	50(2)
H(81)	30(8)	1164(5)	887(5)	43(17)
H(82)	135(6)	1177(5)	779(5)	24(16)
H(9)	174(7)	1199(5)	986(5)	40(16)
H(10)	436(13)	1199(10)	1016(9)	128(43)
H(11)	690(8)	1140(6)	905(5)	52(20)
H(12)	664(9)	1069(6)	773(6)	64(21)
H(13)	381(10)	1053(8)	742(7)	101(29)
H(1)	−60(7)	932(6)	750(5)	40(19)
H(1')	140(8)	750(6)	954(6)	64(23)
PBET·PCP·H$_2$O				
C(1)	2283(4)	3274(1)	174(5)	42(1)
O(1)	1979(4)	3753(1)	132(5)	53(1)
C(2)	3808(4)	3071(1)	444(5)	41(1)
C1(2)	5437(1)	3447(1)	702(2)	58(1)
C(3)	4014(4)	2571(1)	470(5)	40(1)
C1(3)	5903(1)	2333(1)	786(2)	57(1)
C(4)	2700(4)	2265(1)	251(5)	40(1)
C1(4)	2961(1)	1649(1)	298(2)	56(1)
C(5)	1176(4)	2465(1)	−13(5)	40(1)
C1(5)	−462(1)	2092(1)	−287(2)	60(1)
C(6)	972(4)	2964(1)	−25(5)	42(1)
C1(6)	−902(1)	3213(1)	−348(2)	57(1)
O(2)	5532(4)	5453(1)	3250(5)	66(1)
O(3)	2941(4)	5254(1)	2147(4)	56(1)
C(7)	4103(5)	5465(1)	3265(6)	47(1)
C(8)	3767(6)	5801(2)	4849(8)	58(1)
N(1)	2220(4)	5712(1)	5323(5)	42(1)
C(9)	2223(5)	5555(2)	7125(6)	50(1)
C(10)	807(6)	5471(2)	7607(7)	56(1)
C(11)	−629(6)	5541(2)	6221(7)	58(1)
C(12)	−605(5)	5696(2)	4382(7)	53(1)
C(13)	821(5)	5783(1)	3976(6)	47(1)
O(1W)	3867(4)	4487(1)	327(5)	54(1)
H(1)	269(7)	399(3)	22(8)	101(22)
H(81)	375(5)	614(2)	443(6)	46(11)
H(82)	444(7)	570(2)	595(8)	85(19)
H(9)	331(6)	551(2)	800(7)	61(13)
H(10)	79(6)	535(2)	898(8)	77(15)
H(11)	−163(6)	546(2)	646(7)	57(13)
H(12)	−156(6)	576(2)	348(7)	63(14)
H(13)	104(6)	594(2)	284(7)	82(17)
H(1W)	351(6)	475(1)	53(8)	74(17)
H(2W)	393(7)	454(2)	−90(6)	84(19)

were refined for all non-hydrogen atoms. All hydrogen atoms were located in a difference Fourier maps and their positions and isotropic thermal parameters were refined. The crystal data and details of data collections and structure refinements are given in Table 1. The fractional atomic coordinates and equivalent thermal parameters for the crystal structures of PBET·(PCP)$_2$ and PBET·PCP·H$_2$O are presented in Table 2.

3. Results and discussion

3.1. X-Ray structural analyses

Perspective drawings of the hydrogen bonded molecular complexes and the numbering schemes of their atoms are shown in Fig. 1. The bond lengths and valency angles are listed in Table 3. In PBET·(PCP)$_2$, each phenol molecule forms a donor hydrogen bond

UM00014106
NOVARTIS EXHIBIT 1517
Novartis v. Regents, IPR2023-01347
Page 2852 of 4460

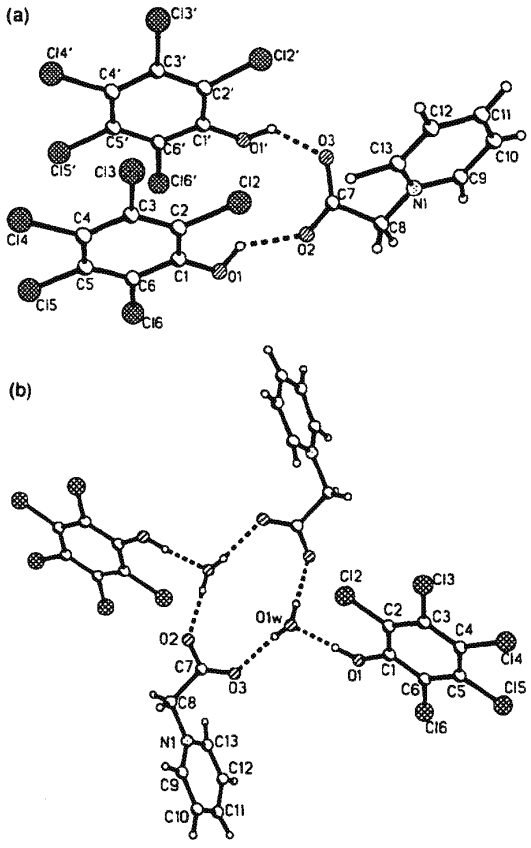


Fig. 1. Perspective view showing the hydrogen bonding scheme and atom labelling in (a) $C_5H_5N^+CH_2COO^-(HOC_6Cl_5)_2$ and (b) $C_5H_5N^+CH_2COO^-\cdot HOC_6Cl_5\cdot H_2O$.

with one molecule of betaine (Table 4). The measured values for the carboxylate group in PBET·$(PCP)_2$ (Table 3) depart from the literature dimensions (C–O, 1.25(2) Å; C–C–O, 117(2)°, O–C–O, 126(2)° [14]) in that the C(8)–C(7)–O(3) angle exceeds the C(8)–C(7)–O(2) angle by 3.8°.

In elementary resonance theory, the carboxylate anion is represented as a hybrid of the following forms:



In the unperturbed anion both forms contribute equally, so the C–O distances and C–C–O angles are equal. The close proximity of O(3) to N(1) in the crystallographically determined betaine complexes (see Fig. 1 and torsion angles in Table 3) facilitates internal charge neutralization and stabilizes one of the COO^- forms. The relevant intermolecular distances N(1)···O(2) and N(1)···O(3) are 3.604(7) and 2.747(6) Å in PBET·$(PCP)_2$ and 3.598(4) and 2.784(4) Å in PBET·PCP·H_2O, respectively.

The mean C(1)–O bond length and the mean C(2)–C(1)–C(6) bond angle for pentachlorophenol and its six molecular complexes are 1.332(8) Å and 117.8(9), respectively [15]. In PBET·$(PCP)_2$ the C(1)–O bonds and the C(2)–C(1)–C(6) bond angles in A and B moieties (Table 3) are very close to those in the free phenol and its molecular complexes, confirming the proton locations at PCP.

Conformation of PBET·$(PCP)_2$ can be described by five planes. The least-squares planes fitted to the rings of phenol ring A (r. m. s deviation from the coplanarity 0.002 Å) and B (r.m.s. deviation from the coplanarity 0.014 Å) form an angle of 3.3(4)°. The dihedral angle between CH_2COO^- residue (the r.m.s deviation of atoms O(2), O(3), C(7) and C(8) from their least-squares plane being 0.004 Å) and pyridine ring (atoms N(1), C(9) – C(13), r.m.s. deviation 0.010 Å) is 60.0(3)°. The fifth plane through atoms O(2), O(3), C(7) C(8), C(1) and C(11) (r.m.s. deviation is 0.056 Å) indicates that the betaine residue forms a quasiplanar molecule comprising all non-hydrogen atoms, except the α, α' and β, β' carbon atoms of the pyridine ring. The latter are arranged symmetrically with respect to this plane.

Recently, we have described a complex of PBET with two molecules of 2,6-dichloro-4-nitro-phenol (DCNP) [7], which is a stronger proton donor than PCP. As consequence, betaine being protonated, two H-bonds in PBET·$(DCNP)_2$ are considerably different, O(2)H···O(1) of 2.452(4) Å and O(3)···H–O(1′) of 2.623(4) Å, and the phenol residues are unequivalent.

In PBET·PCP.H_2O two water molecules form donor H-bonds to a pair of betaine molecules interconnecting them into an eight-membered ring with four H-bonds of 2.703(4) and 2.715(5) Å (Fig. 1), typical for hydrates [16]. Each water molecule additionally accepts a PCP molecule. The H-bonds between PCP and bonded water molecules are much

UM00014107
NOVARTIS EXHIBIT 1517
Novartis v. Regents, IPR2023-01347
Page 2853 of 4460

Table 3
Bond lengths (Å) and bond angles (deg) in PBET·$(PCP)_2$ and PBET·PCP·H_2O

	PBET·$(PCP)_2$	PBET·PCP·H_2O
Bond length		
Cl(2)–C(2)	1.731(6)	1.718(4)
Cl(3)–C(3)	1.723(6)	1.715(4)
Cl(6)–C(6)	1.707(6)	1.716(4)
Cl(5)–C(5)	1.719(6)	1.718(4)
Cl(4)–C(4)	1.724(6)	1.716(4)
C(1)–O(1)	1.348(7)	1.345(5)
C(1)–C(2)	1.375(8)	1.397(5)
C(1)–C(6)	1.394(8)	1.396(5)
C(3)–C(4)	1.380(8)	1.389(5)
C(3)–C(2)	1.394(8)	1.391(5)
C(4)–C(5)	1.384(8)	1.392(5)
C(5)–C(6)	1.399(8)	1.388(5)
O(2)–C(7)	1.231(7)	1.250(5)
O(3)–C(7)	1.254(8)	1.235(5)
C(7)–C(8)	1.528(9)	1.537(6)
C(8)–N(1)	1.457(8)	1.475(5)
N(1)–C(9)	1.343(8)	1.346(5)
N(1)–C(13)	1.353(8)	1.346(5)
C(9)–C(10)	1.362(11)	1.369(6)
C(10)–C(11)	1.386(12)	1.382(6)
C(11)–C(12)	1.382(12)	1.374(7)
C(12)–C(13)	1.353(11)	1.353(6)
H(1)–O(1)	0.86(4)	
H(1′)–O(1′)	0.95(7)	
Cl(5′)–C(5′)	1.720(6)	
Cl(2′)–C(2′)	1.710(6)	
Cl(6′)–C(6′)	1.727(6)	
Cl(3′)–C(3′)	1.717(6)	
Cl(4′)–C(4′)	1.722(6)	
O(1′)–C(1′)	1.354(7)	
C(1′)–C(6′)	1.372(8)	
C(1′)–C(2)	1.384(8)	
C(4′)–C(3′)	1.368(8)	
C(4′)–C(5′)	1.393(8)	
C(5′)–C(6′)	1.392(8)	
C(3′)–C(2′)	1.412(8)	
O(2)···H(1)	1.87(5)	
O(3)···H(1′)	1.84(7)	
Bond angles		
O(1)–C(1)–C(2)	124.5(6)	124.7(3)
O(1)–C(1)–C(6)	116.5(5)	116.9(3)
C(2)–C(1)–C(6)	119.0(5)	118.4(3)
C(4)–C(3)–C(2)	119.5(5)	120.2(3)
C(4)–C(3)–Cl(3)	121.3(4)	120.1(3)
C(2)–C(3)–Cl(3)	119.2(5)	119.7(3)
C(1)–C(2)–C(3)	121.5(5)	120.9(3)

Table 3. (*Continued*)

	PBET·$(PCP)_2$	PBET·PCP·H_2O
C(1)–C(2)–Cl(2)	118.5(4)	119.0(3)
C(3)–C(2)–Cl(2)	120.0(4)	120.1(3)
C(3)–C(4)–C(5)	119.8(5)	119.2(3)
C(3)–C(4)–Cl(4)	119.6(5)	120.1(3)
C(5)–C(4)–Cl(4)	120.5(5)	120.7(3)
C(4)–C(5)–C(6)	120.5(6)	120.6(3)
C(4)–C(5)–Cl(5)	119.8(4)	119.7(3)
C(6)–C(5)–Cl(5)	119.7(5)	119.7(3)
C(1)–C(6)–Cl(5)	119.7(5)	120.7(3)
C(1)–C(6)–Cl(6)	119.5(5)	118.5(3)
C(5)–C(6)–Cl(6)	120.8(5)	120.8(3)
O(2)–C(7)–O(3)	128.5(6)	128.4(4)
O(2)–C(7)–C(8)	113.8(6)	113.3(4)
O(3)–C(7)–C(8)	117.6(6)	118.3(4)
N(1)–C(8)–C(7)	115.5(5)	114.5(3)
C(9)–N(1)–C(13)	120.7(6)	120.1(4)
C(9)–N(1)–C(8)	120.0(5)	119.1(4)
C(13)–N(1)–C(8)	119.3(6)	120.8(4)
N(1)–C(9)–C(10)	120.1(7)	120.3(4)
C(9)–C(10)–C(11)	120.8(8)	119.5(4)
C(12)–C(11)–C(10)	117.2(8)	119.2(4)
C(13)–C(12)–C(11)	121.1(7)	119.4(4)
C(12)–C(13)–N(1)	120.1(7)	121.4(4)
O(2)–H(1)–O(1)	138(5)	
O(3)–H(1′)–O(1′)	136(6)	
O(1′)–C(1′)–C(6′)	119.5(5)	
O(1′)–C(1′)–C(2′)	121.3(5)	
C(6′)–C(1′)–C(2′)	119.2(5)	
C(3′)–C(4′)–C(5′)	119.8(5)	
C(3′)–C(4′)–Cl(4′)	119.7(4)	
C(5′)–C(4′)–Cl(4′)	120.4(4)	
C(6′)–C(5′)–C(4′)	119.6(5)	
C(6′)–C(5′)–Cl(5′)	120.5(4)	
C(4′)–C(5′)–Cl(5′)	119.9(4)	
C(4′)–C(3′)–C(2′)	120.0(5)	
C(4′)–C(3′)–Cl(3′)	121.1(4)	
C(2′)–C(3′)–Cl(3′)	118.9(5)	
C(1′)–C(2′)–C(3)	120.1(6)	
C(1′)–C(2′)–Cl(2′)	119.7(4)	
C(3′)–C(2′)–Cl(2′)	120.2(5)	
C(1′)–C(6′)–C(5′)	121.2(5)	
C(1′)–C(6′)–Cl(6′)	118.9(4)	
C(5′)–C(6′)–Cl(6′)	119.9(5)	
Selected torsion angles		
N(1)–C(8)–C(7)–O(2)	−174.7(6)	−161.9(4)
N(1)–C(8)–C(7)–O(3)	6.5(9)	19.9(6)
C(9)–N(1)–C(8)–C(7)	−115.8(7)	115.3(5)
C(13)–N(1)–C(8)–C(7)	64.7(8)	−64.2(6)

UM00014108
NOVARTIS EXHIBIT 1517
Novartis v. Regents, IPR2023-01347
Page 2854 of 4460

Table 4
Geometries of the hydrogen bonds and short N⁺···O contacts in PBET·(PCP)$_2$ and PBET·PCP·H$_2$O crystals

X–H···O	Distance (Å)			Angle (deg)
	X···O	X–H	H···O	O–H···O
PBET·(PCP)$_2$				
O(1)–H···O(2)	2.582(6)	0.86(4)	1.87(5)	136(5)
O(1')–H···O(3)	2.611(6)	0.95(7)	1.84(7)	136(6)
N(1)···O(2)	3.604(7)			
N(1)···O(3)	2.747(6)			
N(1)···O(2) [a]	3.669(7)			
N(1)···O(3) [a]	4.241(7)			
PBET·PCP·H$_2$O				
O(1w)–H···O(2)	2.715(5)	0.90(4)	1.84(4)	165(5)
O(1w')–H···O(3)	2.703(4)	0.83(4)	1.93(4)	155(5)
O(1)–H···O(1w)	2.580(4)	0.88(7)		
N(1)···O(2)	3.598(4)			
N(1)···O(3)	2.784(4)			

[a] Intermolecular contact, symmetry code $-x, 2-y, 2-z$.

shorter, O···O distance is 2.580(4) Å. As shown in Fig. 2(a) and 2(b), in both crystals of PBET and PCP the molecular arrangement in the lattice can be described by layers of PBET and PCP molecules, nearly parallel to crystal plane (011) in PBET·(PCP)$_2$ and (010) in PBET·PCP·H$_2$O.

3.2. FTIR spectra

The FTIR spectra of powdered samples of PBET·(PCP)$_2$, PBET·PCP, PBET·PCP·HOMe and PBET·PCP·H$_2$O recorded at room temperature are shown in Fig. 3. The bands observed can conveniently be divided into these which arise from the hydrogen bond vibrational modes and the internal vibrations.

3.2.1. Hydrogen bond vibrations

In the investigated complexes there are three distinct hydrogen bonds; a rather strong one with the O···O distance of ca. 2.6 Å, between phenol molecules acting as the proton donor and betaine or water molecules acting as proton acceptors, a relatively weaker one of ca. 2.7 Å in which the water molecule acts as the proton donor and the betaine molecule as the proton acceptor (Table 4), and the longest (weakest) hydrogen bond formed by methanol.

The shorter hydrogen bond displays a poorly defined AB structure (Fig. 3) with maxima at approximately 2900 (A) and 2500 (B) cm^{-1}. Such a band structure may be explained on the basis of Fermi resonance between the OH stretching and the overtone 2δOH [17]. The δOH bond was found at ca. 1270 cm^{-1}. The hydrogen bonds between water molecule and betaine manifest themselves as broad absorption at ca. 3200 cm^{-1}.

The structures of PBET·PCP and PBET·PCP·HOMe crystals have not been determined. Hydrogen bonds formed by PCP are expected in these complexes of about ca. 2.6 Å, because they display an absorption in the 3000–2200 cm^{-1} region similar to that in PBET·(PCP)$_2$. Absorption due to the νOH vibration of bonded methanol molecule in PBET·PCP·HOMe was found at 3359 cm^{-1} as a sharp band. Its structure is probably similar to that in PBET·(PCP)$_2$ where one PCP is replaced by methanol. Frequency of the bonded methanol suggests O···O distance of about 2.8 Å [18].

3.2.2. Internal vibrations of pyridine betaine and pentachlorophenol

The ν_{as}COO mode of the carboxylate group is easily identified at 1627 cm^{-1} in all investigated complexes. In PBET·PCP the ν_{as}COO band is split into doublet (1637 and 1627 cm^{-1}). The strong band in the 1368–62 cm^{-1} region is due to the ν_sCOO mode. In anhydrous PBET ν_{as}COO and ν_sCOO frequencies are at 1632 and 1344 cm^{-1}, respectively [4]. Note that

UM00014109
NOVARTIS EXHIBIT 1517
Novartis v. Regents, IPR2023-01347
Page 2855 of 4460

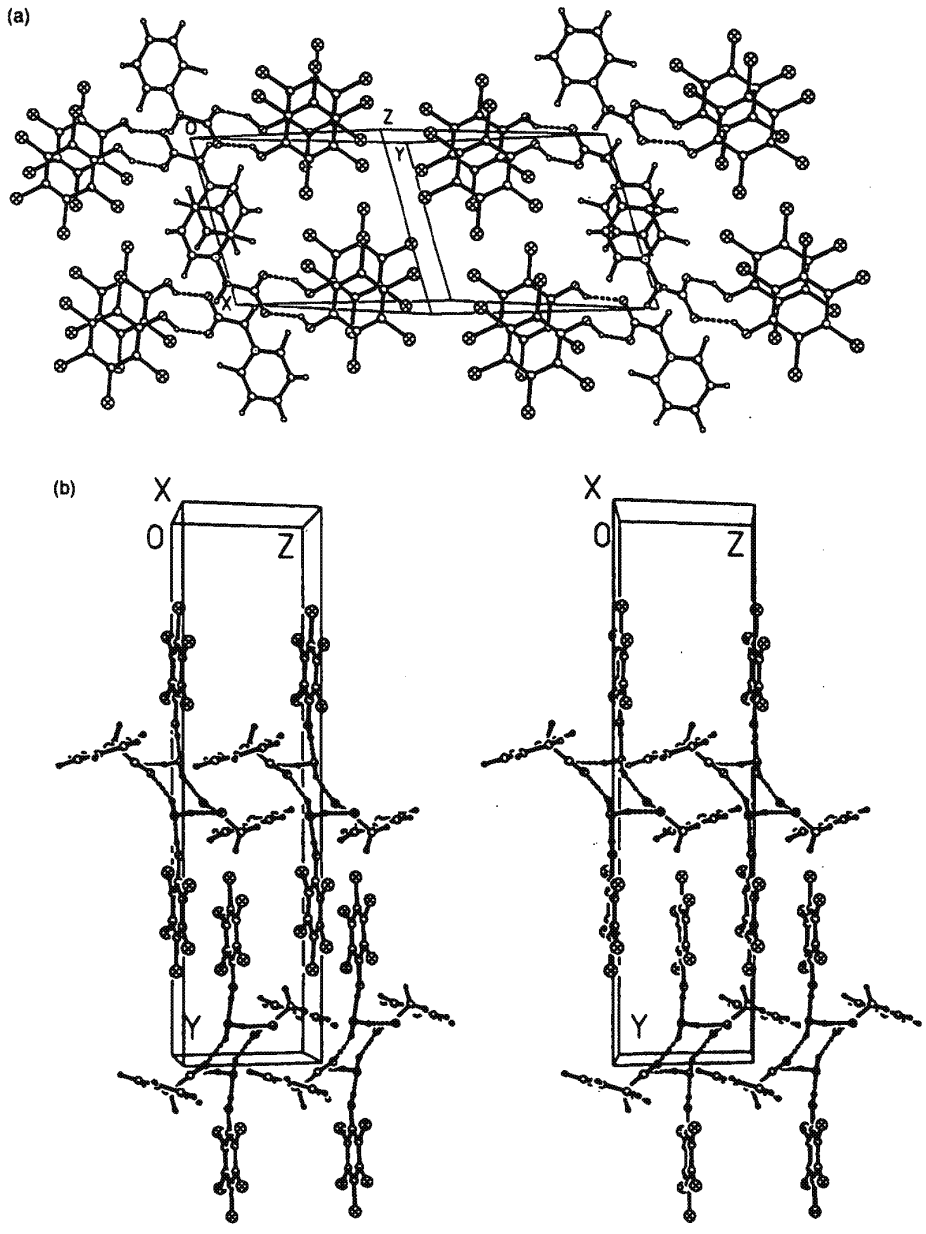


Fig. 2. Molecular arrangements in structure of (a) $C_5H_5N^+CH_2COO^-(HOC_6Cl_5)_2$, a perspective view down [011]; (b) a $C_5H_5N^+CH_2COO^-\cdot HOC_6Cl_5\cdot H_2O$, sterreoview down [100].

UM00014110
NOVARTIS EXHIBIT 1517
Novartis v. Regents, IPR2023-01347
Page 2856 of 4460

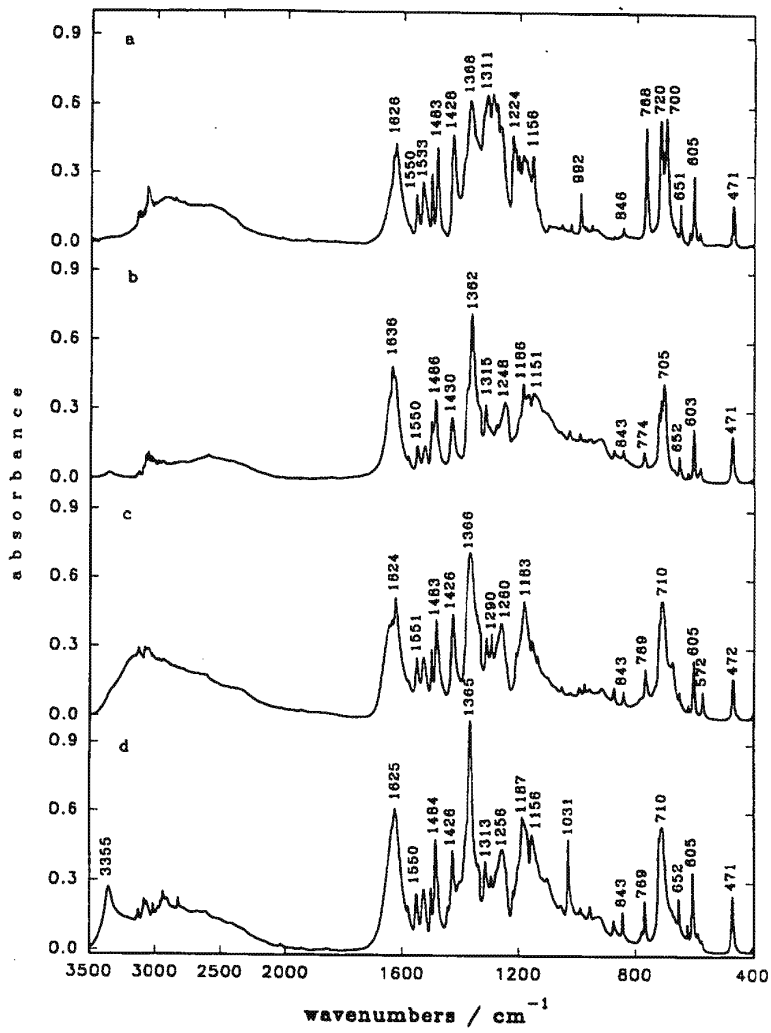


Fig. 3. FTIR spectra of (a) PBET·$(PCP)_2$; (b) PBET·PCP; (c) PBET·PCP·H_2O; (d) PBET·PCP·HOMe.

PBET·$(PCP)_2$ and PBET·PCP·H_2O both oxygen atoms of betaine are engaged in hydrogen bonds (Table 4). In such a case C(7)–O(2) and C(7)–O(3) would be comparable. The observed difference in their bond lengths (Table 4) is caused by electrostatic interaction with the positive charged nitrogen atom. A separation of vibration of the pyridine ring from benzene ring in the investigated complexes is a formidable task and needs the use of powerful computer to calculate their wavenumbers.

4. Conclusions

Formation of the crystalline complex of pyridine betaine with two molecules of pentachlorophenol, PBET·$(PCP)_2$, have been described. One of the PCP molecules can be replaced by H_2O or $HOCH_3$ to given PBET·PCP·H_2O or PBET·PCP·HOMe, respectively. The latter complex lost methanol on heating at 50°C and was transferred into PBET·PCP. Methanol molecules were also replaced by water molecules when a

UM00014111
NOVARTIS EXHIBIT 1517
Novartis v. Regents, IPR2023-01347
Page 2857 of 4460

PBET·PCP·HOMe sample was left at room atmosphere for several days. The structures of PBET·$(PCP)_2$ and PBET·PCP·H_2O have been determined by X-ray diffraction. Assignments of the hydrogen bonded vibrational modes of all investigated complexes and the molecular structures for PBET·PCP·HOMe and PBET·PCP are proposed.

Acknowledgements

We thanks the State Committee for Scientific Research, Grant (KBN grant no. 2P303 06907) for financial support.

References

[1] G. Blunden, S.M. Gordon, Prog. Phycol. Res. 4 (1986) 39.
[2] G. Schaack, Ferroelectrics 104 (1990) 147 and references cited therein.
[3] E.G. Lomax (Ed.), Amphoteric Surfactants, Marcel Dekker, New York, 1996, pp. 76–190.
[4] See, for example, M. Szafran, J. Koput, J. Mol. Struct. 381 (1996) 157 and references cited therein.
[5] (a) T.C.W. Mak, J. Mol. Struct. 220 (1990) 13; (b) Z. Dega-Szafran, M. Gdaniec, M. Grundwald-Wyspiańska, I. Kowalczyk, M. Szafran, J. Mol. Struct. 322 (1994) 297. (c) M. Szafran, J. Koput, J. Baran, T. Głowiak, J. Mol. Struct., 123–142.
[6] J. Baran, Z. Dega-Szafran, M. Jaskólski, M.K. Marchewka, H. Ratajczak, M. Szafran, J. Mol. Struct., 406 (1997) 127.
[7] M. Szafran, Z.Dega-Szafran, G. Buczak, A. Katrusiak, M.J. Potrzebowski, A. Komasa, J. Mol. Struct., 416 (1997) 145–160.
[8] R. Nouwen, P. Huyskens, J. Mol. Struct. 16 (1973) 459.
[9] (a) E.P. Serjeant, B. Dempsey, Ionization Constants of Organic Acids in Aqueous Solution (IUPAC Chemical Data Series no. 23), Pergamon Press, Oxford, 1979. (b) Z. Pawlak, R.G. Bates, J. Chem. Thermodynam. 14 (1982) 1035.
[10] Z. Dega-Szafran, I. Kowalczyk, M. Szafran, Bull. Pol. Acad. Sci. Chem. 43 (1995) 303.
[11] P.L. Toccalino, K.M. Harmon, J. Harmon, J. Mol. Struct. 189 (1988) 373.
[12] G.M. Sheldrick, SHELXS 86, Program for the Solution of Crystal Structures, University of Göttingen, Germany, 1986.
[13] G.M. Sheldrick, SHELXL 93, Program for the Refinement of Crystal Structures, University of Göttingen, Germany, 1993.
[14] P.W. Borthwick, Acta Crystallogr. B36 (1980) 628.
[15] CSD; F.H. Allen, O. Kennard, Chemical Design Automation News, 1993, 8.1.31-37.
[16] (a) T.C.W. Mak, J. Mol. Struct. 178 (1988) 169 and references cited therein. (b) H.D. Lutz, Struct. Bonding 69 (1988) 97.
[17] M.F. Claydon, N. Sheppard, Chem. Commun. (1969) 1431.
[18] A. Noval, Struct. Bonding 18 (1974) 177.

UM00014112
NOVARTIS EXHIBIT 1517
Novartis v. Regents, IPR2023-01347
Page 2858 of 4460

Acta Cryst. (1972). B28, 1646

The crystal structure of urea oxalic acid (2:1).

By S. HARKEMA, J. W. BATS, A. M. WEYENBERG* and D. FEIL, *Chemical Physics Laboratory, Twente University of Technology, Enschede, The Netherlands.*

(*Received* 1 *March* 1971)

The crystal structure of urea oxalic acid, $2[CO(NH_2)_2].(COOH)_2$ has been determined using three-dimensional X-ray data, collected on an automatic diffractometer. The space group is $P2_1/c$. The lattice constants are: $a = 5{\cdot}058$ (3), $b = 12{\cdot}400$ (3), $c = 6{\cdot}964$ (2) Å, $\beta = 98{\cdot}13$ (7)°. The number of molecules in the unit cell is two. The structure consists of layers of urea and oxalic acid molecules held together by hydrogen bonds. The positions of all hydrogen atoms have been found. The compound is not a uronium salt.

Introduction

The structures of protonated urea and thiourea cations have been investigated in recent years by a number of methods. These techniques include infrared spectroscopy (Janssen, 1961; Kutzelnigg & Mecke, 1961), nuclear magnetic resonance (Stewart & Siddall, 1970), X-ray and neutron diffraction. The work done on uronium nitrate by the last two methods (Harkema & Feil, 1969; Worsham & Busing, 1969) shows that the extra proton is attached to the oxygen atom of urea and that measurable changes in geometry occur when urea is protonated. The same applies to the structure of *N*-methyluronium nitrate (Bryden, 1957; Selman & Harkema, 1971). As part of our investigations on bonding in urea compounds we decided to determine accurately the structure of urea oxalic acid. A preliminary report on the determination of this structure has been given by Schuch, Merritt & Sturdivant (1950).

Experimental

Crystals of urea oxalic acid (2:1) were prepared by evaporation of an aqueous solution of urea and oxalic acid in the stoichiometric ratio. The crystals formed in this way have a pronounced cleavage plane which indicates a two-dimensional hydrogen-bonding network.

Data were collected on a Nonius automatic diffractometer at room temperature. A crystal of size $0{\cdot}3 \times 0{\cdot}2 \times 0{\cdot}2$ mm was mounted with the b axis parallel to the goniometer axis. Reflexions with $\theta < 35°$ were measured with Zr-filtered Mo $K\alpha$ radiation ($\lambda = 0{\cdot}70926$ Å) using the θ–2θ scanning technique. In this way 1058 independent reflexions were measured, each having an intensity greater than twice the corresponding standard deviation from counting statistics. The space group of the crystal is $P2_1/c$, in accordance with previous work (Lonsdale, 1941).

The cell dimensions found are: $a = 5{\cdot}058$ (3), $b = 12{\cdot}400$ (3), $c = 6{\cdot}964$ (2), $\beta = 98{\cdot}13$ (7)° (here as in the rest of the paper the values given in brackets represent the standard deviation in the last decimal place of the number given). The number of molecules in the unit cell is 2, consisting of 2 molecules of oxalic acid and 4 molecules of urea (Lonsdale, 1941). From the very strong $10\bar{2}$ reflexion it is clear that all molecules must be approximately parallel to the $(10\bar{2})$ plane. No correction for absorption was applied ($\mu = 1{\cdot}3$ cm^{-1}).

Structure determination

As the general position in the space group $P2_1/c$ is fourfold, the oxalic acid molecules must lie on centres of symmetry. With the help of the known molecular geometries, a model of the structure was constructed and rotated in the plane containing the molecules until an acceptable hydrogen bonding scheme was found. Coordinates for the heavy atoms obtained in this way were used as input for the least-squares program. The identity of the atoms in the urea molecule was established from the isotropic temperature factors resulting from refinement with one atomic form factor (that of nitrogen) for all atoms.

The weighting scheme used in the refinement was the same as that reported for uronium nitrate (Harkema & Feil, 1969). Four cycles of refinement with anisotropic temperature factors gave an R factor of 7·1%.

A difference Fourier synthesis made at this stage clearly revealed the hydrogen atoms. Inclusion of the hydrogen atoms and refinement of their positions and isotropic temperature factors, together with the positions and anisotropic temperature factors of the other atoms, gave a final R value of 4·0%. In the last stages of refinement a secondary-extinction correction was applied (Zachariasen, 1963; Larson, 1970). Observed and calculated structure factors are collected in Table 1.

Final positional parameters are given in Table 2. Table 3 shows the vibration parameters obtained from the least-squares analysis. The labelling of the atoms is given in Fig. 1, which shows a projection of the structure on the $(10\bar{2})$

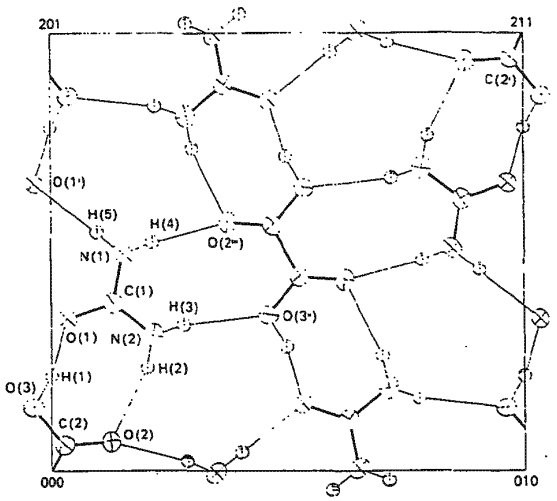


Fig. 1. Projection of the crystal structure of urea oxalic acid on $(10\bar{2})$. The vibration ellipsoids of the heavy atoms are scaled to include 50% probability. The hydrogen atoms have arbitrary, small isotropic vibration parameters.

* Present address: AKZO research, Arnhem, The Netherlands.

UM00014113
NOVARTIS EXHIBIT 1517
Novartis v. Regents, IPR2023-01347
Page 2859 of 4460

Table 1. *Observed and calculated structure factors* ($\times 10$) *for urea oxalic acid*



plane. This figure was prepared with the *ORTEP*-program (Johnson, 1965).

Table 2. *Final atomic parameters*

	x/a	*y/b*	*z/c*
N(1)	0·9970 (3)	0·1507 (2)	0·4857 (2)
N(2)	0·6215 (3)	0·2136 (1)	0·3047 (2)
O(1)	0·7033 (2)	0·0348 (1)	0·3319 (2)
O(2)	0·1552 (2)	0·1245 (2)	0·0388 (2)
O(3)	0·2864 (2)	−0·0380 (1)	0·1502 (2)
C(1)	0·7709 (3)	0·1307 (1)	0·3729 (2)
C(2)	0·1237 (2)	0·0284 (1)	0·0517 (2)
H(1)	0·446 (4)	0·002 (2)	0·211 (3)
H(2)	0·475 (4)	0·201 (2)	0·227 (3)
H(3)	0·680 (4)	0·278 (2)	0·319 (3)
H(4)	0·049 (4)	0·213 (2)	0·513 (3)
H(5)	0·090 (4)	0·095 (2)	0·537 (3)

Discussion of the results

The structure of urea oxalic acid consists of nearly planar urea and oxalic acid molecules held together by a two-dimensional hydrogen-bonding network. The acidic proton is attached to the oxalic acid molecule. The compound, unlike uronium nitrate, is not a uronium salt. This difference may be related to the difference in acid strength between oxalic acid and nitric acid.

The bond distances and angles found in the title compound are given in Tables 4 and 5 respectively. These geometric data are compared with the results of recent structure determinations on related compounds. In accordance with the fact that the compound studied is an addition compound, differences in bond lengths and angles are very small when one compares the urea and oxalic acid molecules in this compound with urea and oxalic acid dihydrate. As usual, bond lengths involving hydrogen atoms determined by X-ray diffraction are shorter than the ones determined by neutron diffraction. This effect is due to the assumption commonly made in X-ray analysis that the electron density of bonded atoms is spherically symmetric. A theoretical study of the geometry of the uronium ion and the urea molecule is in progress.

References

BRYDEN, J. H. (1957). *Acta Cryst.* **10**, 714.
HARKEMA, S. & FEIL, D. (1969). *Acta Cryst.* B**25**, 589.
JANSSEN, M. J. (1961). *Spectrochim. Acta*, **17**, 475.
JOHNSON, C. K. (1965). *ORTEP*. ORNL-3794, Oak Ridge National Laboratory, Oak Ridge, Tennessee.

UM00014114
NOVARTIS EXHIBIT 1517
Novartis v. Regents, IPR2023-01347
Page 2860 of 4460

Table 3. *Vibration parameters*

The temperature factor for the heavy atoms was: $\exp[-2\pi^2(h^2 a^{*2} U_{11} + 2h k a^* b^* U_{12} + \cdots)]$.
The temperature factor for the hydrogen atoms was: $\exp[-(B \sin^2\theta/\lambda^2)]$.

	U_{11}	U_{22}	U_{33}	U_{12}	U_{13}	U_{23}
N(1)	0·0396 (6)	0·0312 (8)	0·0578 (10)	−0·0069 (6)	−0·0136 (5)	−0·0043 (9)
N(2)	0·0480 (8)	0·0281 (8)	0·0635 (10)	0·0025 (6)	−0·0127 (7)	−0·0017 (9)
O(1)	0·0331 (5)	0·0257 (8)	0·0537 (7)	−0·0022 (3)	−0·0129 (3)	−0·0030 (4)
O(2)	0·0377 (5)	0·0234 (8)	0·0602 (7)	−0·0016 (3)	−0·0093 (5)	0·0013 (4)
O(3)	0·0289 (5)	0·0288 (8)	0·0498 (7)	−0·0006 (3)	−0·0096 (3)	0·0035 (4)
C(1)	0·0317 (6)	0·0281 (8)	0·0347 (7)	−0·0022 (6)	0·0007 (5)	−0·0022 (4)
C(2)	0·0266 (5)	0·0257 (16)	0·0344 (7)	0·0025 (6)	0·0009 (5)	−0·0004 (4)
H(1)	7·3 (6)					
H(2)	4·8 (4)					
H(3)	4·9 (5)					
H(4)	6·1 (6)					
H(5)	4·9 (5)					

Table 4. *Bond distances* (Å)

	Urea–oxalic acid (*a*), (*d*), (*g*)	Oxalic acid dihydrate (*b*), (*e*), (*g*)	Urea (*c*), (*e*), (*f*)
C(2)–C(2′)	1·521 (5)	1·536 (3)	
C(2)–O(2)	1·209 (3)	1·212 (4)	
C(2)–O(3)	1·289 (5)	1·291 (5)	
O(3)–H(1)	0·96 (4)	1·026 (7)	
C(1)–N(1)	1·318 (6)		1·352 (2)
C(1)–N(2)	1·321 (4)		
C(1)–O(1)	1·260 (3)		1.260 (3)
N(2)–H(3)	0·86 (2)		1·003 (4)
N(1)–H(4)	0·84 (2)		
N(2)–H(2)	0·86 (4)		0·998 (5)
N(1)–H(5)	0·88 (3)		
O(1)···O(3)	2·472 (5)		
O(2)···N(2)	2·999 (5)		
O(3″)···N(2)	3·123 (3)		
O(2‴)···N(1)	2·911 (3)		
O(1′)···N(1)	2·941 (4)		

(*a*) Present work.
(*b*) Sabine, Cox & Craven (1969).
(*c*) Pryor & Sanger (1970).
(*d*) X-ray.
(*e*) Neutron.
(*f*) Bond lengths corrected for thermal motion.
(*g*) Bond lengths not corrected for thermal motion.

Table 5. *Bond angles* (°)

	Urea-oxalic acid (*a*), (*d*), (*g*)	Oxalic acid dihydrate (*b*), (*e*), (*g*)	Urea (*c*), (*e*), (*f*)
C(2′)–C(2)–O(2)	121·8 (2)	121·0 (3)	121·7 (1)
C(2′)–C(2)–O(3)	112·3 (3)	112·4 (3)	
O(2)–C(2)–O(3)	125·9 (2)	126·6 (3)	
C(2)–O(3)–H(1)	110 (3)	114·4 (6)	
O(1)–C(1)–N(1)	119·8 (3)		121·7 (1)
O(1)–C(1)–N(2)	122·2 (2)		
N(1)–C(1)–N(2)	118·1 (3)		116·6 (1)
C(1)–N(1)–H(5)	118 (3)		119·0 (3)
C(1)–N(2)–H(2)	118 (2)		
C(1)–N(1)–H(4)	122 (3)		120·2 (3)
C(1)–N(2)–H(3)	123 (2)		
H(4)–N(1)–H(5)	120 (3)		
H(2)–N(2)–H(3)	118 (4)		

(*a*) Present work.
(*b*) Sabine, Cox & Craven (1969).
(*c*) Pryor & Sanger (1970).
(*d*) X-ray.
(*e*) Neutron.
(*f*) Bond lengths corrected for thermal motion.
(*g*) Bond lengths not corrected for thermal motion.

KUTZELNIGG, W. & MECKE, R. (1961). *Chem. Ber.* **94**, 1706.
LARSON, A. C. (1970). *Crystallographic Computing*, pp. 291-294. Copenhagen: Munksgaard.
LONSDALE, K. (1941). *Proc. Roy. Soc.* A177, 272.
PRYOR, A. W. & SANGER, P. L. (1970). *Acta Cryst.* A26, 543.
SABINE, T. M., COX, G. W. & CRAVEN, B. M. (1969). *Acta Cryst.* B25, 2437.
SCHUCH, A. F., MERRITT, L. L. & STURDIVANT, J. H. (1950). Amer. Crystallogr. Assoc., Abstracts of Meeting, April 10-12, p. 21. (see also *Structure Reports* **13**, 477.)
SELMAN, W. F. & HARKEMA, S. (1971). Prog. Report, Chem. Phys. Lab., Twente Univ. of Technology.
STEWART, W. E. & SIDDALL, T. H. (1970). *Chem. Rev.* **70**, 517.
WORSHAM, J. E. & BUSING, W. R. (1969). *Acta Cryst.* B25, 572.
ZACHARIASEN, W. H. (1963). *Acta Cryst.* **16**, 1139.

Acta Cryst. (1972). B28, 1648

Structural studies of metal dithiocarbamates. V. The crystal and molecular structure of bis-(*N*,*N*-diethyldithiocarbamato)tellurium(II)

By C. FABIANI, R. SPAGNA, A. VACIAGO and L. ZAMBONELLI, *Laboratorio di Strutturistica Chimica 'Giordano Giacomello', CNR, Città Universitaria*, 00100 *Roma, Italy*

(*Received* 9 *November* 1971)

A correction to a reference in *Acta Cryst.* (1971) B27, 1499 is given.

In a paper of the above title (Fabiani, Spagna, Vaciago & Zambonelli, 1971) the reference to the structure of lead(II) bis-(*O*,*O*-diisopropylphosphorodithioate) is incorrect. On page 1504, column 1, line 20 (Guzy, Raynor & Stodulski, 1969) should read (Lawton & Kokotailo, 1969) and in the list of references GUZY, C. M., RAYNOR, J. B. & STODULSKI, L. P. (1969). *Nature, Lond.* **221**, 550 should read LAWTON, S. L. & KOKOTAILO, G. T. (1969). *Nature, Lond.* **221**, 550.

Reference

FABIANI, C., SPAGNA, R., VACIAGO, A. & ZAMBONELLI, L. (1971). *Acta Cryst.* B27, 1499.

UM00014115

NOVARTIS EXHIBIT 1517
Novartis v. Regents, IPR2023-01347
Page 2861 of 4460

This Page is Inserted by IFW Indexing and Scanning Operations and is not part of the Official Record

BEST AVAILABLE IMAGES

Defective images within this document are accurate representations of the original documents submitted by the applicant.

Defects in the images include but are not limited to the items checked:

- ☐ BLACK BORDERS
- ☐ IMAGE CUT OFF AT TOP, BOTTOM OR SIDES
- ☐ FADED TEXT OR DRAWING
- ☐ BLURRED OR ILLEGIBLE TEXT OR DRAWING
- ☐ SKEWED/SLANTED IMAGES
- ☐ COLOR OR BLACK AND WHITE PHOTOGRAPHS
- ☐ GRAY SCALE DOCUMENTS
- ☐ LINES OR MARKS ON ORIGINAL DOCUMENT
- ☐ REFERENCE(S) OR EXHIBIT(S) SUBMITTED ARE POOR QUALITY
- ☐ OTHER: _____

IMAGES ARE BEST AVAILABLE COPY.
As rescanning these documents will not correct the image problems checked, please do not report these problems to the IFW Image Problem Mailbox.

Sodium Theophylline Glycinate*

By JOHN C. KRANTZ, JR., JAMES M. HOLBERT, HARRY K. IWAMOTO, and C. JELLEFF CARR

A method of preparation and the characterization of Sodium Theophylline Glycinate are described. This new combination produces a typical theophylline response in animals and it is well tolerated in large amounts in man.

IT IS WELL established that alkali salts of organic acids render theophylline water-soluble. Owing to the slightly acidic property of the principle (dissociation constant 1.62×10^{-11} at 25°) (1) it has been combined with ethylene diamine to form one of its most popular dosage forms.

Intensive therapy with the available combinations of theophylline is limited by the gastric irritation produced by the principle. Gastric hydrochloric acid readily decomposes the theophylline complexes and liberates the free amine which produces irritation to the mucosa.

It occurred to one of the authors (J. C. K.) that the use of an amino acid instead of such acids as acetic or salicylic might obviate this difficulty. Having used glycine successfully in the buffering of gastric acidity combined with aluminum hydroxide (2) we chose this amino acid.

EXPERIMENTAL

Preparation.—Sodium theophylline glycinate was prepared as follows:

One mole (198 Gm.) of theophylline U. S. P. was added to 1 L. of 1 *N* NaOH (40 Gm., 1 mole). The theophylline did not completely dissolve but remained as a ropy suspension. To this mixture was added 2 moles (150 Gm.) of glycine. Solution was effected with gentle heat and then filtered to remove any suspended material. The solution was evaporated to dryness at reduced pressure and at a temperature not exceeding 70°. More drastic conditions of drying resulted in discoloration of the product. The product is a white, almost anhydrous material containing approximately 50% theophylline.

Physical Properties.—Sodium theophylline glycinate has no melting point; however, it darkens at 190° and the entire mass becomes black at 210°. It is soluble in water to the extent of approximately 18% (*w/v*). In the preparation of a saturated solution, care must be taken not to use too great an excess of the solid, for under these conditions preferential solution of sodium glycinate occurs with the resulting precipitation of theophylline. A saturated solution of the material has a *p*H of 8.7 to 9.1, a density at 20° of 1.05, and exhibits unusual stability to carbon dioxide.

Structure.—In our opinion the structure of sodium theophylline glycinate is best represented by the equilibrium:

$$C_7H_7O_2N_4Na + NH_2CH_2COOH \rightleftarrows C_7H_8O_2N_4 + NH_2CH_2COONa$$

This is concluded from the fact that solution of sodium theophylline glycinate of the same physical characteristics may be prepared from a mixture of sodium theophylline and glycine or from a mixture of theophylline and sodium glycinate. The following results illustrate this experimentally.

Four grams of theophylline were dissolved in 20 cc. of 1 *N* NaOH and diluted to 70 cc. The weights of the reactants represent equivalent amounts. The sodium theophylline formed is not completely soluble but remained as a ropy suspension. Glycine was then added in the ratio of 1/4 molar unite until the glycine-theophylline ratio was 5:1. The first addition of glycine caused the solution to clear. The *p*H of the solution was determined after each addition of glycine. The results are recorded below.

TABLE I.—THEOPHYLLINE SODIUM-GLYCINE RATIOS AND *p*H

Test No.	Molar Ratio of Glycine	*p*H
1	0	10.48
2	0.25	9.72
3	0.50	9.50
4	0.75	9.37
5	1.00	9.26
6	1.25	9.17
7	1.50	9.12
8	1.75	9.06
9	2.00	9.01
10	2.25	8.98
11	2.50	8.93
12	2.75	8.90
13	3.00	8.86
14	3.50	8.82
15	4.00	8.77
16	5.00	8.69

If the glycine concentration is plotted against *p*H, a smooth curve of diminishing *p*H results. There is no break in the curve to suggest compound or complex formation.

* Received Dec. 23, 1946, from the Dept. of Pharmacology School. University of Maryland, Baltimore, Md.

UM00014117
NOVARTIS EXHIBIT 1517
Novartis v. Regents, IPR2023-01347
Page 2863 of 4460

TABLE II.—LD_{50} RAT INTRAPERITONEAL INJECTION

Aminophylline				Sodium Theophylline Glycinate			
No. Rats	Mg./Kg.	Alive	Dead	No. Rats	Mg./Kg.	Alive	Dead
2	100	2	0	2	100	2	0
4	200	2	2	4	200	4	0
4	300	0	4	4	300	4	0
4	400	0	4	4	400	0	4
4	500	0	4	2	450	0	2
4	600	0	4	4	500	0	4
.	. . .	.	.	4	600	0	4

The solutions prepared in the foregoing studies were then compared with similar solutions prepared from theophylline and sodium glycinate. Accordingly, in an attempt to duplicate solution Test Number 5 in Table I, 2 Gm. of sodium glycinate and 4 Gm. of theophylline were dissolved in the correct volume of water. The *p*H of this solution was 9.22 as compared to 9.26 for Number 5. An additional 1.5 Gm. of glycine was added to the solution, thus making its composition similar to that of Test Number 9. The *p*H of this solution was 9.00 as compared to 9.01 for Number 9.

Thus it may be concluded from these results that the same mixture is formed with a combination of sodium theophylline and glycine as with a combination of theophylline and sodium glycinate. Since there is no evidence of compound formation, the composition is best expressed by the foregoing equilibrium equation:

Pharmacodynamic Studies

To ascertain whether or not full theophylline activity was exhibited by sodium theophylline glycinate (amino acetate) the following experiments were conducted.

LD_{50} Rat.—The LD_{50} of sodium theophylline glycinate was determined in the rat upon intraperitoneal injection, time period three hours, and compared with that of aminophylline. Each compound was injected in 2% aqueous solution. The results are shown in Table II.

This first approximation of the LD_{50} of the 2 compounds shows for aminophylline a value of 200 mg./Kg., and for sodium theophylline glycinate approximately 350 mg./Kg. The onset of the terminal convulsive syndrome at the same dosage levels was invariably more rapid with aminophylline than with sodium theophylline glycinate.

Blood Pressure Studies (Dog).—Dogs under ether anesthesia were injected intravenously with 2% aqueous solutions of aminophylline and sodium theophylline glycinate, respectively. Injections were made in 2 animals, alternating the 2 compounds. Aminophylline injections caused a precipitous fall in blood pressure to approximately two-thirds of the pre-injection level, with a prompt return to normal. Similar injections of sodium theophylline glycinate elicited falls in blood pressure to about 85% of the normal value. Injections of 20 to 50 mg./Kg. of ethylene diamine in aqueous solution

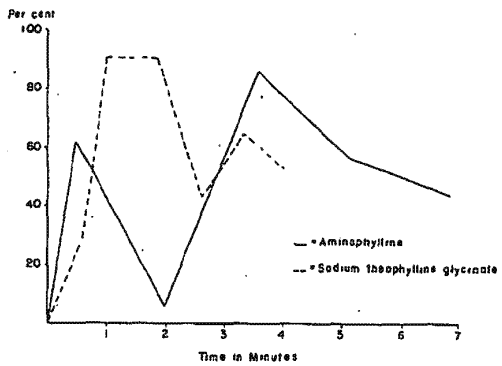


Figure 1

produced falls in blood pressure to approximately 75% of the pre-injection level. Theophylline sodium salicylate in comparable doses caused no significant change in arterial tension.

Coronary Flow Experiments (Dog).—Coronary flow experiments were carried out on the dog *in situ* by the Moravitz-Zahn technique (3). The animals were anesthetized with morphine and chlorobutanol. Heparin sodium 20 mg./Kg. was used as an anticoagulant. The right atrium was not clamped prior to the insertion of the Moravitz cannula, as rapid manipulations with sutures already in place made it possible to eliminate this feature of the experiment. The blood was collected in 5 to 20 cc. volumes and returned immediately through a Liebig condenser at 37° to the circulation through the jugular vein. The carotid blood pressure was recorded.

Aminophylline and sodium theophylline glycinate, respectively, were injected intravenously in 10 cc. volumes of 2% solution. Typical responses from the experiments on 4 dogs are shown on a percentile basis in Chart I. It is evident from the data in Chart I that each compound elicits acute coronary dilatation of approximately the same magnitude and duration.

Therapeutic Studies.—In an eighteen-month clinical trial with sodium theophylline glycinate, W. D. Paul (4) used this dosage form of theophylline in more than 300 patients. It elicited a typical theophylline therapeutic response. It was tolerated without nausea or vomiting in quantities up to 4 Gm. in twenty-four hours; i.e., 2 Gm. of theophylline. A detailed account of these studies will appear in a subsequent communication to another journal.

UM00014118
NOVARTIS EXHIBIT 1517
Novartis v. Regents, IPR2023-01347
Page 2864 of 4460

SUMMARY

1. A new simple theophylline combination has been prepared, namely, sodium theophylline glycinate.

2. Sodium theophylline glycinate is soluble in water, 1 part in 5 parts. Its solutions are slightly alkaline and stable in the air.

3. Sodium theophylline glycinate elicits a typical theophylline response in animals and is tolerated in unusually large amounts in man.

REFERENCES

(1) "Physikalischchemische Tabellen-Landolt-Bornstein," Julius Springer, Berlin, 1923, p. 1161.
(2) Krantz, J. C., Jr., Kibler, D. V., and Bell, F. K., *J. Pharmacol.*, 82, 247(1944).
(3) Moravitz P. and Zahn, A., *Zentr. Physiol.*, 26, 405(1912).
(4) Paul, W. D., Personal communication, 1946.

Chemical Examination of *Daemia extensa* R. Br. I.*

By ASHUTOSH DUTTA and SUDHAMOY GHOSH

A chemical study of *Daemia extensa* is described. Three sterols were isolated in pure form and characterized. In addition, a glycosidic bitter principle with pituitrin-like action is described. Other minor constituents are described briefly.

DAEMIA *extensa* R. Br. (syn. *Pergularia extensa* N. E. Br.) belongs to the Natural Order Asclepiadaceae, and grows throughout the hotter parts of India, often at an altitude of 3000 feet, and in Afghanistan and Ceylon. It is a perennial twining herb with much milky juice and is foetid when bruised.

Leaves.—The leaves are thin, broadly ovate or suborbicular, acuminate, glabrous, more or less shortly pubescent above, usually velvety pubescent beneath, the margins ciliate, base deeply cordate, flowers greenish yellow or dull white, calyx pubescent divided to the base. The plant is known in Sanskrit as Chandal Dudhika or Yugmaphala, in Bengal as Chaggalbati, in Hindi as Jutak or Zitran, in Bombay as Utrani, and in Punjab as Karial.

Uses in India.—Many medicinal properties are attributed to it in the Indian indigenous systems of medicine. It is said to be pungent, cooling, anthelmintic, laxative, antiperiodic, useful in eye troubles, urinary discharges, leucoderma, uterine complaints, stranguary, inflammations, and in facilitating parturition. The juice of the leaves is used as an expectorant in the treatment of catarrhal affections. It is also given in asthma and applied to rheumatic swellings. In combination with lime or ginger it is used in amenorrhea and dysmenorrhea. All the parts of the plant are used in medicine.

Dymock (1) in his Pharmacographia Indica mentions the presence of an alkaloid which he designated as "daemine." Hartwich (2) mentions the presence of a bitter glucoside, but no details about its properties or its pharmacological action are stated in literature. As the drug finds such an important place in the Indian indigenous systems of medicine, a detailed chemical investigation was found desirable in order to find its important constituents. The material employed was the entire plant consisting of the roots, stems, leaves, and fruits. The plant was collected locally and identified by a botanist. The fresh plant when dried in the air lost about 86 per cent of its weight. The dried plant was coarsely powdered and used for all the experiments.

* Received Oct. 11, 1946, from the Department of Chemistry, School of Tropical Medicine, Calcutta, India.

Test for All
drug was thor
the solvent re
1% HCl. The
the filtrate tes
loid, as sugge
however, be d
Preliminary
the powdered
different solve
tracts were fr
weighed with
ether (b. p. 4
chloroform 0.(
4.43%; total
extracts was t
extract: neut
fats, fatty oil
tract: acid t
with ferric ch
tions for car
acid to litmus
stances. (*d*)
tastes extrem
dirty green c
shows strong
soluble extra
bitter; aque
cipitate with
strongly posi
Detailed I
grams of the
several chan
alcohol extra
Usually, 6 to
alcoholic extr
distilled off
evaporated t
residue whic
weighed 403
drug. This
water and su
extract was a
Examinati
the Alcoholi
insoluble resi
with petrole
the residue
ether extract
dark colored
hundred gra
of drug was
for six hou
saponified p
alcohol remo
emulsion ext
The ethereal
hydrated wi
ether distille
yellow color
and the crys

UM00014119
NOVARTIS EXHIBIT 1517
Novartis v. Regents, IPR2023-01347
Page 2865 of 4460

This Page is Inserted by IFW Indexing and Scanning Operations and is not part of the Official Record

BEST AVAILABLE IMAGES

Defective images within this document are accurate representations of the original documents submitted by the applicant.

Defects in the images include but are not limited to the items checked:

- ☐ BLACK BORDERS
- ☐ IMAGE CUT OFF AT TOP, BOTTOM OR SIDES
- ☐ FADED TEXT OR DRAWING
- ☐ BLURRED OR ILLEGIBLE TEXT OR DRAWING
- ☐ SKEWED/SLANTED IMAGES
- ☐ COLOR OR BLACK AND WHITE PHOTOGRAPHS
- ☐ GRAY SCALE DOCUMENTS
- ☐ LINES OR MARKS ON ORIGINAL DOCUMENT
- ☐ REFERENCE(S) OR EXHIBIT(S) SUBMITTED ARE POOR QUALITY
- ☐ OTHER: _____

IMAGES ARE BEST AVAILABLE COPY.
As rescanning these documents will not correct the image problems checked, please do not report these problems to the IFW Image Problem Mailbox.

CRYSTAL STRUCTURES OF DRUGS: ADVANCES IN DETERMINATION, PREDICTION AND ENGINEERING

Sharmistha Datta and David J. W. Grant

Most marketed pharmaceuticals consist of molecular crystals. The arrangement of the molecules in a crystal determines its physical properties and, in certain cases, its chemical properties, and so greatly influences the processing and formulation of solid pharmaceuticals, as well as key drug properties such as dissolution rate and stability. A thorough understanding of the relationships between physical structures and the properties of pharmaceutical solids is therefore important in selecting the most suitable form of an active pharmaceutical ingredient for development into a drug product. In this article, we review the different crystal forms of pharmaceuticals, the challenges that they present and recent advances in crystal structure determination. We then discuss computational approaches for predicting crystal properties. Finally, we review the analysis of crystal structures in furthering crystal engineering to design novel pharmaceutical compounds with desired physical and mechanical properties.

Department of Pharmaceutics, College of Pharmacy, University of Minnesota, Weaver-Densford Hall, 308 Harvard Street SE, Minneapolis, Minnesota 55455-0343, USA.
Correspondence to D.J.W.G.
e-mail: grant001@umn.edu
doi:10.1038/nrd1280

Pharmaceutical solids can be classified as either crystalline solids, which have regular arrangements of molecules that repeat in three dimensions, or amorphous solids, which lack the long-range order present in crystals[1]. These differences in the long-range periodicity of the molecules result in the substantially different physical and chemical properties of crystals and amorphous solids[2,3]. Although amorphous solids often have desirable pharmaceutical properties — such as faster dissolution rates — than their crystalline counterparts, they are not marketed as widely as the crystalline forms because of their lower chemical stability and their innate tendency to crystallize. Most marketed pharmaceuticals therefore consist of molecular crystals[4].

The arrangement of the molecules in a crystal determines its physical properties and, in certain cases, its chemical properties[5]. The physicochemical properties of the solid drug can affect its performance. The shape and particle size of the solid drug can influence pharmaceutical operations, such as filtration, washing, drying, milling, mixing, tableting, dissolution, recrystallization of a suspension and lyophilization[2,6]. Several pharmaceutical crystals — for example, theophylline[7], chlorpropamide[8], carbamazepine[9,10], phenobarbital[11], lactose[12], chlorpromazine hydrochloride[13], uricosuric agent FR76505 (REF. 14) and pentamidine isethionate[15] — are known to undergo a variety of PHASE TRANSFORMATIONS during their processing and formulation[16,17]. These phase transformations can affect the stability of the product and, in some cases, even the bioavailability of the drug[18]. An understanding of the relationship between the solid-state properties and the crystal structure of the likely phases might be utilized for optimizing operational and formulation strategies and in designing suitable stability protocols to avoid later problems[19–23]. The characterization and understanding of the crystal properties is also important for quality control and regulatory purposes[24].

Pharmaceutical crystals can exist as single molecular entities or as MOLECULAR ADDUCTS[5]. As single molecular entities, organic solids can show polymorphism, which is frequently defined as the ability of a substance to exist as two or more crystalline phases that have different arrangements and/or conformations of the molecules in the crystal lattice[25]. BOX 1 lists the differences that can

UM00014121
NOVARTIS EXHIBIT 1517
Novartis v. Regents, IPR2023-01347
Page 2867 of 4460

Box 1 | Polymorph property differences

Packing properties
- Molar volume and density
- Refractive index, optical properties
- Conductivity, electrical and thermal
- Hygroscopicity

Thermodynamic properties
- Melting and sublimation temperatures
- Internal energy
- Enthalpy
- Heat capacity
- Entropy
- Free energy and chemical potential
- Thermodynamic activity
- Vapour pressure
- Solubility

Spectroscopic properties
- Electronic transitions, ultraviolet-visible spectra
- Vibrational transitions, infrared and Raman spectra
- Rotational transitions
- Nuclear magnetic resonance chemical shifts

Kinetic properties
- Dissolution rate
- Rates of solid state reactions
- Stability

Surface properties
- Surface free energy
- Interfacial tensions
- Habit

Mechanical properties
- Hardness
- Tensile strength
- Compactibility, tabletability
- Handling, flow and blending

PHASE TRANFORMATION
The transformation of a solid from one physical form to another. Phase transformation can involve the transformation of a single component into one or more components, and can result from changes in physical conditions, as in pharmaceutical processing. Examples of phase transformation include polymorphic transitions, crystallization of amorphous solids, and solid-state solvation and desolvation.

MOLECULAR ADDUCT
A crystal is termed a molecular adduct when its lattice consists of more than one chemical component.

SOLVATE
A solid phase that contains solvent molecules, in addition to molecules of the major component, in the crystal lattice.

HYDRATE
A solid phase that contains water molecules, in addition to molecules of the major component, in the crystal lattice.

HYDROGEN BOND
An attractive interaction between two electronegative atoms through a hydrogen bridge. The hydrogen bond is partly electrostatic and partly covalent in nature, with limited orbital overlap between the participating atoms. Of the two electronegative atoms, one is the proton donor and the other is a proton acceptor. When present within the same molecule, a hydrogen bond is termed intramolecular. When present between two molecules, a hydrogen bond is termed intermolecular.

SLIP SYSTEM
The term slip refers to the translational motion of lattice planes relative to each other. Such planes are termed slip planes. A family of slip planes, together with the slip direction, is termed a slip system.

be shown by different polymorphs[19], many of which might be important in drug performance. A recent case that exemplifies the importance of polymorphism in pharmaceuticals is highlighted in BOX 2.

Molecular adducts include SOLVATES and HYDRATES, which can be stoichiometric or nonstoichiometric in nature[26]. Clathrates are a special type of molecular adduct in which the guest molecules occupy, fully or partially, cages in the crystal lattice of the host[27,28] without specifically interacting with the host molecules. Solvates and hydrates generally demonstrate different solubilities and consequently different intrinsic dissolution rates (dissolution rates per unit surface area) than their unsolvated counterparts[29]. Moreover, the stability profiles of hydrates and solvates at various temperatures and at different vapour pressures of water or organic solvents differ from those of the unsolvated crystal form[30]. These differences can influence formulation, processing and stability under various storage conditions of the drug compound, as well as the pharmaceutical product.

Pharmaceutical salts can exist in any of the above solid forms. However, the presence of ions strongly influences the physicochemical properties of the crystals, including solubility, dissolution rate, stability and hygroscopicity[31–34]. Recently, interest in the physical properties and crystal structures of chiral drugs has also grown[35,36]. It is well recognized that the pharmacological, toxicological, pharmacodynamic and pharmacokinetic properties can differ markedly between the opposite enantiomers and the racemates of a chiral drug[37,38]. The molecular environments in each of these solids are unique and impart different physicochemical properties to the crystals[39].

The structure of a crystal also affects its mechanical properties and thereby its processability. For example, Agbada and York[40] showed that the monohydrate of theophylline possesses higher mechanical strength than anhydrous theophylline, by virtue of the greater number of intermolecular HYDROGEN BONDS in its crystal structure. The weaker mechanical strength of the anhydrate makes it more brittle than the monohydrate. Similarly, Sun and Grant[41] showed that the presence of water molecules in the crystal structure of 4-hydroxybenzoic acid facilitates plastic deformation as compared with that of 4-hydroxybenzoic acid anhydrate. Bandopadhyay and Grant[42] showed that knowledge of the crystal structure and the SLIP SYSTEMS can be used to model the tableting and compaction behaviour of molecular crystals, such as the anhydrate and dihydrate forms of L-lysine hydrochloride. Furthermore, comparing the crystal structures of two polymorphs of sulfamerazine (FIG. 1), Sun and Grant[43] showed that polymorph I, which has well-defined slip planes, gives greater plasticity, compressibility and tabletability than polymorph II, which has no discernible slip planes.

In summary, an understanding of the crystalline state leads to an understanding of the drug properties, which is crucial for many of the activities of the pharmaceutical industry. In this article, we review the different crystal forms of pharmaceuticals, the challenges that they present and recent advances in crystal structure determination. We emphasize the computational approaches for predicting crystal properties, and also review the analysis of crystal structures in furthering crystal engineering to design novel pharmaceutical compounds with desired physical and mechanical properties.

Crystalline state: fundamental concepts

Crystal systems. Crystals, following the discussion above, consist of minimal building blocks, each of which contains all the structural features and symmetry elements, and which is repeated regularly in three-dimensional space. The minimal building block is termed the unit cell[44] (FIG. 2), and contains at least one molecule. Symmetry considerations show 230 unique arrangements of points in space, termed space groups. These 230 space groups describe all the possible ways in

UM00014122
NOVARTIS EXHIBIT 1517
Novartis v. Regents, IPR2023-01347
Page 2868 of 4460

Box 2 | Importance of pharmaceutical polymorphism: ritonavir

Ritonavir (Norvir; Abbott) is a drug for treating patients infected with human immunodeficiency virus-1 (HIV-1) that acts by inhibiting the HIV-1 protease[185]. When it was first discovered in late 1992, ritonavir crystallized as Form I. Other crystal forms of ritonavir were not discovered at that time. A New Drug Application for ritonavir was filed in 1995 and ritonavir was launched on to the market in 1996. The drug was formulated as soft gelatin capsules and as oral solutions. Early in 1998, some lots of ritonavir capsules failed the dissolution test. Investigation of this phenomenon revealed that a new crystal form of ritonavir precipitated from the formulation. The new crystal form, named Form II, is less soluble than Form I, and is therefore thermodynamically more stable. The lower solubility of Form II as compared with that of Form I resulted in the precipitation of the drug and also decreased the dissolution rate of the marketed formulations. Within days–weeks, the new form, Form II, was produced in all the production lines, resulting in the failure of the established formulation. To investigate whether any significant changes had been made to the bulk manufacturing process of ritonavir, a team of scientists who had been exposed to Form II in the United States visited the facility manufacturing ritonavir in Italy. Until then, Form II had not been detected in the bulk drug lots in the Italian sites. However, soon after this visit, significant amounts of Form II appeared in the bulk drug manufactured in Italy, perhaps as a result of accidental seeding with Form II. The adverse effect of the decreased dissolution rate on the bioavailability of ritonavir led to withdrawal of the extant formulated products. Eventually, after considerable effort and expense, a new formulation of ritonavir was developed, submitted to the FDA, approved and launched onto the market[186].

which identical objects can be arranged in an infinite lattice[45]. Certain space groups are seen frequently, whereas other space groups have never been found in crystals[46]. According to the Cambridge Structural Database (CSD), ~76% of all organic and organometallic compounds crystallize in only five space groups — $P2_1/c$, $P2_12_12_1$, $P\bar{1}$, $P2_1$ and $C2/c$ — and ~90% of all organic and organometallic crystal structures belong to the 17 most common space groups[47].

ENANTIOTROPE
The members of a pair of polymorphs are termed enantiotropes when their mutual transition temperature is less than the melting point of either polymorph. Each enantiotrope has its own temperature range of stability.

Forces responsible for crystal packing. The packing energy of a crystal, termed the lattice energy, is the summation of a large number of relatively weak intermolecular interactions (0.5–2 kJ per mol), relatively strong intermolecular interactions (~30 kJ per mol), and especially strong intramolecular and interionic interactions (~150 kJ per mol)[48]. Although the intramolecular interactions bond the atoms in the molecule, the intermolecular forces minimize the energy of the molecules in the crystal and are primarily responsible for the formation of organic crystals[49]. The intermolecular forces, which can be attractive or repulsive in nature, consist of non-bonded (sometimes termed non-covalent) interactions, such as van der Waals forces and hydrogen bonds[50–52], and ionic and electrostatic interactions. Hydrogen bonds and van der Waals interactions, both of which are attractive interactions, are the major intermolecular forces in most pharmaceutical crystals[53–56]. However, if the molecule is polar and charged, ion–ion contributions can significantly affect the overall crystal packing energy[57].

Crystalline states. Crystalline solids can exist as polymorphs, hydrates or solvates, or combinations thereof. According to the corresponding thermodynamic relationships, polymorphs can be classified as either ENANTIOTROPES or MONOTROPES, depending on whether or not one form can transform reversibly to another[58–66]. Organic molecules are capable of forming different crystal lattices through two different mechanisms. One mechanism, termed packing polymorphism or orientational polymorphism, represents instances in which molecules that are conformationally relatively rigid can be assembled into different three-dimensional structures through different intermolecular juxtapositions. The other mechanism, termed conformational polymorphism, arises when a flexible molecule bends into different conformations, which subsequently can be packed into alternative crystal structures. The structural aspects associated with polymorphs have been reviewed recently, as have the analogous features of solvates and hydrate systems[16].

Approximately one-third of active pharmaceutical substances are capable of forming crystalline hydrates[67]. The water molecule, because of its small size, can often fill structural voids and, because of its ability to participate in multidirectional hydrogen bonding, is also capable of linking to most drug molecules to form new crystal structures. On the basis of the location of water in their structures, crystalline hydrates can be classified into three categories[68,69]: ISOLATED SITE HYDRATES (for example, cephadrine dihydrate[70]); ION-ASSOCIATED HYDRATES (for example, dihydrate and trihydrate of disodium adenosine 5′-triphosphate[16,71]); and CHANNEL HYDRATES (for example, theophylline monohydrate[72]), which can be further classified into two subcategories, the EXPANDED CHANNEL or nonstoichiometric hydrates (for example, cromolyn sodium[73–75]) and the PLANAR HYDRATES (for example, nedocromil zinc[76]). On account of the multiple roles of water, some hydrates can comprise more than one category; for example, the nedocromil bivalent metal salt hydrates[77]. The mere presence of water in a system is not sufficient for hydrate formation. The molecular (and crystal) structure, the activity of water in the crystallization medium and the temperature determine whether a given hydrate structure will form[78].

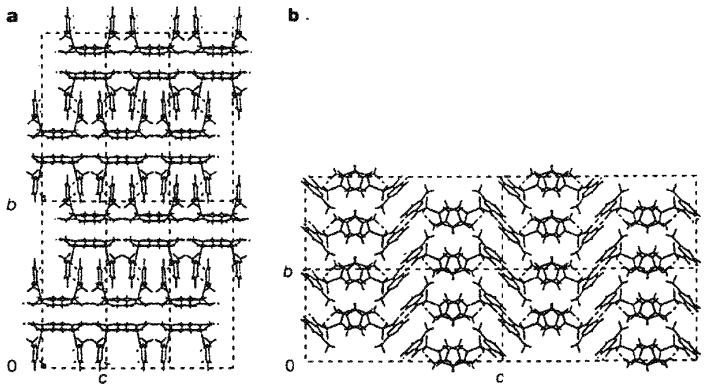


Figure 1 | **Influence of crystal structure on properties of polymorphs.** The crystal structures of sulfamerazine polymorphs looking into the *a* axis. **a** | Polymorph I, in which the slip planes are parallel to the *ac* plane of the unit cell. **b** | Polymorph II, in which no slip plane is observed. The hydrogen bonds are indicated by dotted lines between molecules[168]. Reproduced, with permission, from REF. 43 © (2001) Kluwer Academic Press.

UM00014123
NOVARTIS EXHIBIT 1517
Novartis v. Regents, IPR2023-01347
Page 2869 of 4460

MONOTROPE
The members of a pair of polymorphs are termed monotropes when they have no mutual transition temperature. One monotrope is always more stable than the other polymorph under all conditions in which the solid state can exist.

ISOLATED SITE HYDRATE
In an isolated site hydrate, the water molecules in the crystal lattice of the hydrate are isolated from direct contact with other water molecules by intervening molecules of the major component.

ION-ASSOCIATED HYDRATE
In an ion-associated hydrate, the water molecules in the crystal lattice of the hydrate are coordinated to certain ions (often metal ions).

CHANNEL HYDRATE
In a channel hydrate, the water molecules present in the crystal lattice of the hydrate lie next to other water molecules of adjoining unit cells, forming channels through the crystals along a direction in the lattice.

EXPANDED CHANNEL HYDRATE
An expanded channel hydrate can take up water into the channels when exposed to relatively high humidity and can release water from the channels when exposed to relatively low humidity. The crystal lattice can expand or contract as hydration or dehydration proceeds, changing the dimensions of the unit cell.

PLANAR HYDRATE
A planar hydrate is a channel hydrate in which water molecules are localized in a plane, corresponding to two-dimensional order.

SOLID SOLUTION
A solid solution can be substitutional or interstitial. A substitutional solid solution is a homogeneous crystalline phase in which some of the constituent molecules are substituted by foreign molecules that possess sufficient similarity that the lattice dimensions are changed only slightly. In an interstitial solid solution, the foreign molecules are inserted into interstitial positions, such that the lattice dimensions are changed only slightly.

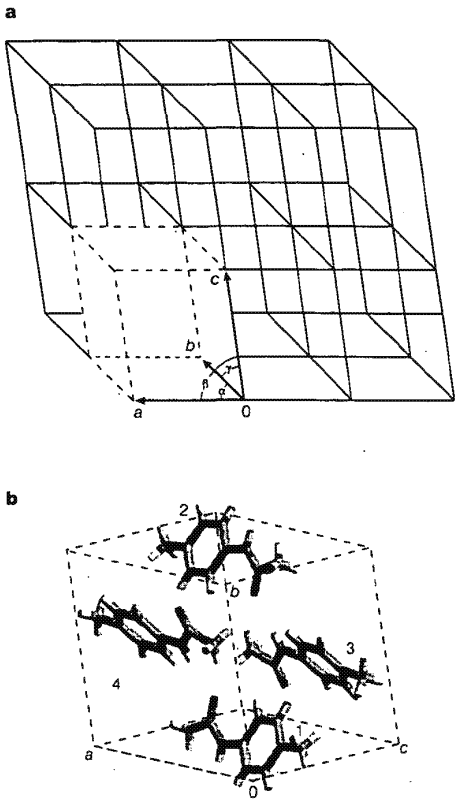


Figure 2 | **Fundamentals of crystal structure. a** | Crystals consist of minimal building blocks, termed unit cells, each of which contains all the structural features and symmetry elements and is repeated regularly in three-dimensional space. The dimensions of the unit cell are characterized by six quantities; three axial lengths (*a*, *b*, *c*) and three interaxial angles (α, β, γ). Each unit cell contains at least one molecule and can be classified by one of the seven three-dimensional coordinate systems, which are the seven primitive crystal systems. Each of these crystal systems has one or more symmetry elements that describe the internal symmetry of the unit cell. The different symmetry elements comprise rotation, mirror, screw, glide, and rotation-inversion operations. There are 32 possible unique combinations of the different crystallographic symmetry elements, each defined by a point group. Bravais discovered that some crystal lattices are more complex but still conform to the seven crystal systems. In these so-called nonprimitive lattices, each lattice point and every symmetry element in the primitive lattice are reproduced with a corresponding offset. In total, there are 14 Bravais lattices consisting of seven primitive and seven nonprimitive lattices. The combination of 32 point groups with 14 Bravais lattices leads to 230 unique arrangements of points in space, termed space groups. **b** | The features and symmetry elements of space group $P2_1/c$ (in which pharmaceuticals often crystallize) is exemplified with the unit cell of 4-methylacetanilide (CSD Refcode ACTOLD01), which contains two independent symmetry elements: (i) rotary inversion (about the centre of the unit cell), and (ii) screw symmetry (with rotation parallel to *b*-axis and translation along *c*-axis). The molecular pair (1, 2) and (3, 4) are related by symmetry of rotary inversion. The molecular pair (1, 3), (1, 4), (2, 4) and (3, 4) are related by the screw symmetry.

More than half of all marketed drug molecules contain one or more chiral centres. No matter whether a racemate or an enantiomer is chosen for administration, the physical properties of the chiral drug must be thoroughly characterized during the development of the drug to provide a safe, efficacious and stable pharmaceutical formulation[28,79,80]. Most chiral drugs are marketed as racemates. Three known types of racemates — racemic conglomerate, racemic compound and pseudoracemate — are shown schematically in FIG. 3 (REF. 81). Because of the strict spatial requirements for formation of SOLID SOLUTIONS, pseudoracemates are rare racemic species. Racemic compounds and pseudoracemates comprise heterochiral crystals. The differences in properties between the two enantiomers in a conglomerate and a racemic compound arise from the different interactions between the homochiral or heterochiral molecules and from their different packing arrangements in the crystal structures. These differences in crystal structures lead to different physical properties and/or biological activities of racemic conglomerates and racemic compounds. The elements of inverse symmetry present in the achiral space groups of the racemates contribute to close packing, leading to greater stability of the racemic compound compared with that of homochiral mixtures or conglomerates[82].

Polymorphism and solid-state solvation are common among chiral drugs. Polymorphism can be shown by individual enantiomers (for example, carvoxime[82] and nitrendipine[83]) as well as by racemates (for example, mandelic acid[84]). The existence of polymorphism of a chiral drug will not only affect its pharmaceutically relevant properties, but can also result in interconversion between the different types of racemates, as shown by nicotine derivatives[85] and sodium ibuprofen[86].

Certain chiral drugs can form solvates. In chiral systems, the racemic compound and the enantiomer undergo different degrees of solvation under given conditions. For example, enantiomeric histidine hydrochloride forms a monohydrate when crystallized from water, whereas racemic histidine hydrochloride forms a dihydrate[87]. Diastereomeric pairs also form solvates with different degrees of solvation that can affect their individual solubilities.

The non-superimposibility of a chiral molecule on its mirror image is reflected in the crystal structure[88]. Although chirality does not imply a total lack of symmetry (asymmetry), the existence of chirality in a crystal does require the absence of an IMPROPER ROTATION ELEMENT. Consequently, the overall crystal structure of an enantiomer must be dissymmetric. Enantiomers can therefore crystallize in only 66 of the 230 space groups. A survey of 430 cases of enantiomers[89] revealed that enantiomers crystallize preferentially in certain selected space groups: 67% in the $P2_12_12_1$ space group, 27% in the $P2_1$ space group, 1% in the $C2$ space group, and 5% in some of the other 63 space groups. Racemic compounds, on the other hand, can crystallize in any one of the 164 achiral space groups. However, a study of 792 cases of racemic compounds revealed

UM00014124
NOVARTIS EXHIBIT 1517
Novartis v. Regents, IPR2023-01347
Page 2870 of 4460

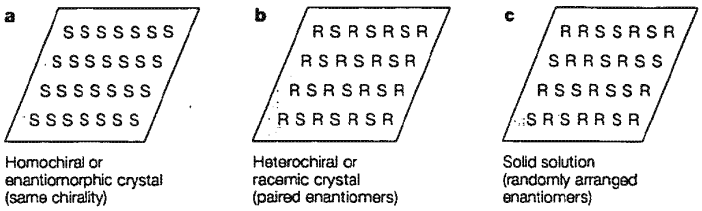


Figure 3 | **Types of racemate.** Schematic representation of the molecular arrangements in the following three types of racemic species. **a** | Racemic conglomerate (Type I) is a 1:1 physical mixture of homochiral crystals of the enantiomers, for example, asparagine or sodium ibuprofen. **b** | Racemic compound (Type II) is a homogeneous solid phase with the two enantiomers present in equal amounts in each unit cell of the crystal lattice, for example, ibuprofen free acid or ephedrine free base. **c** | Pseudoracemate (Type III) is a homogeneous solid solution containing equimolar amounts of the opposite enantiomers more or less unordered in the crystal, for example, camphor[77]. Reproduced, with permission, from REF. 82 © (1981) John Wiley.

that 56% crystallized in the $P2_1/c$ space group, 15% in the $C2/c$ space group and 13% in the $P\bar{1}$ space group, whereas 16% crystallized in some of the other 161 achiral space groups[89].

IMPROPER ROTATION ELEMENT
A 360°/*n* rotation about an *n*-fold axis of improper rotation, followed by a reflection through a mirror plane perpendicular to the rotation axis.

SYNCHROTRON
An electron accelerator that uses synchronized magnetic fields. When the high-speed electrons are directed to collide with an appropriate target, high-energy X-ray radiation or ultraviolet radiation is produced.

MELT
When a solid is heated beyond its melting temperature, it fuses (melts) to produce a liquid that can be termed a melt.

EPITAXIAL GROWTH
The growth of one crystal on the surface of another crystal (the substrate), on which the growth of the deposited crystal is oriented by the lattice structure of the substrate.

CAPILLARY CRYSTALLIZATION
A specific crystallization technique in which the crystals nucleate and grow inside a capillary as a result of slow solvent evaporation.

SYSTEMATIC ABSENCES
The systematic absence of specific groups of reflections in a diffraction pattern of a crystal indicates the presence of certain symmetry elements and enables the crystallographic space group of the crystal lattice to be defined.

Crystal structure determination

Crystallization techniques. Determination of the crystal structure by conventional single-crystal X-ray diffractometry (SCXRD) requires crystals of suitable size and quality[90,91]. In general, the minimum dimension along each axis of the crystal should exceed 0.05 mm, unless a heavy atom (atomic number >17) is present in the constituent molecules. However, with the advancement of SYNCHROTRON and neutron scattering techniques, the minimum crystal size required has considerably decreased. The crystal should also possess uniform internal structure. Special procedures are often used to prepare satisfactory crystals[92]. These techniques include slow cooling of saturated solutions, slow diffusion of a non-solvent liquid or vapour into a saturated solution, diffusion of reacting solutions and the use of seed crystals to obtain larger crystals[92–95]. A variety of methods can be used for preparing polymorphs of drugs, such as crystallization from different solvents at different temperatures, crystallization from supercritical fluids, addition of non-solvents, pH adjustment, sublimation and crystallization from the MELT[94]. Furthermore, various combinations of the above techniques are used in a systematic manner to rapidly screen polymorphs, solvates and salt forms, to establish which are most suitable for further development and scale-up. In recent years, polymorphs have also been intentionally crystallized by EPITAXIAL GROWTH[96] and CAPILLARY CRYSTALLIZATION[97]. Zaccaro *et al.* have shown that the exposure of a supersaturated solution to light from a laser can result in the nucleation of hitherto unknown polymorphs[98]. The crystals obtained, even if not suitable for single-crystal studies, can be used as seeds for the growth of larger crystals[99]. However, in many cases, it is difficult to obtain the desired compound as a single crystal of sufficient size and quality. The material might be available only as a polycrystalline powder. Further, solving the crystal structure of certain types of substance might be beyond the capability of SCXRD, even when performing microcrystal diffraction with a synchrotron radiation source. Substances that undergo rapid transformation under conditions of SCXRD, such as metastable polymorphic forms, solvates and hydrates, might be highly flawed crystals. Twinned crystals have two different orientations of the lattice in an apparently single crystal, making their structural solution difficult[100,101]. In spite of these various drawbacks, structure solution by SCXRD is the most reliable technique for crystal structure determination.

Single-crystal X-ray diffractometry. If a satisfactory crystal is available, the crystal structure is determined by SCXRD, which is the most unambiguous way of solving crystal structures[90]. Crystals diffract X-rays in a pattern that is unique to the respective crystals and depends on their internal structure, and so X-ray diffraction can be used to determine crystal structure (BOX 3)[102–104]. The structure solution, which essentially provides the atomic positions of all the atoms in their regular, repeating positions in the crystal, is determined from the intensities and phases of the diffracted X-rays. The intensities can be determined directly from the diffraction pattern. However, the phases cannot be determined unambiguously, a limitation that is termed the phase problem (see below)[90,104].

To solve the crystal structure, the unit-cell type and the space group are first identified by acquiring a few diffraction frames and then comparing the observed pattern for missing diffraction intensities (called SYSTEMATIC ABSENCES)[105]. Knowledge of the space group can simplify the analysis of the diffraction pattern and can reveal the important symmetry element(s) within the unit cell[106]. Next, the phase problem is solved using one of the several available complex and elaborate methods; that is, the PATTERSON METHOD, ISOMORPHOUS REPLACEMENT METHOD or the direct method[106]. The direct method is normally used to determine the crystal structures of organic compounds, including drugs, and is described very briefly in BOX 4 (REFS 107,108).

Computational techniques. When the determination of a crystal structure using SCXRD is difficult because of the nonavailability of suitable single crystals, computational techniques can be utilized to predict crystal structures.

Several predictive techniques have now been developed, as described below, and the programs are being refined to generate more reliable results[109–111]. The accuracy of a predicted structure can be initially assessed by visual comparison with the experimentally determined structure. The similarity between the predicted and the experimental structure can also be judged qualitatively by comparing their space groups and can be quantified by measuring the differences between their corresponding lattice parameters, crystal structure densities and root mean square deviations for the molecular conformation and crystal packing[112,113]. Usually, a predicted structure is considered to be successful if the lattice parameters differ by less than ±5%, the molecular positions by less than ±1% and the molecular orientations by less than ±5° (REF. 113). Most methods

UM00014125
NOVARTIS EXHIBIT 1517
Novartis v. Regents, IPR2023-01347
Page 2871 of 4460

Box 3 | Fundamentals of X-ray crystallography

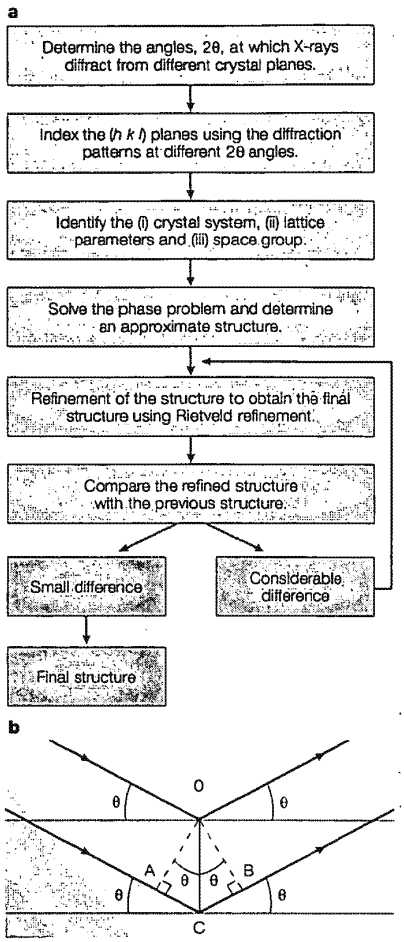
The diffraction of X-rays by crystals was discovered by M. von Laue in 1912 (see part a for steps in determining crystal structure from X-ray diffraction patterns and part b for diffraction of X-rays by the planes in a crystal). He showed that the phenomenon could be described in terms of diffraction from a three-dimensional grating[102]. However, W. L. Bragg was the first to exploit the similarity of diffraction to ordinary reflection. He deduced a simple equation, now known as the Bragg equation — $n\lambda = 2d\sin\theta$ — in which d is the distance between the crystal planes, θ is the angle of diffraction of the X-rays, λ is the wavelength of the X-rays and n is an integer[103,104]. The intensity of diffracted electromagnetic radiation is maximized when the path difference between the incident and the diffracted beam is an integral multiple, n, of the wavelength of the radiation, λ. When X-rays diffract from a given crystal plane ($h\,k\,l$), the intensity is maximized at a particular angle of incidence when the path difference of the radiation is equal to twice the distance, d, between the ($h\,k\,l$) planes multiplied by the sine of the angle of incidence of the X-ray beam. So, for monochromatic X-rays impinging on a single crystal, diffraction by each of the various planes ($h\,k\,l$) will be observed only for certain values of the angle of incidence, θ.

Using the principles of the Bragg equation, the crystal structure is determined by following a series of discrete steps[104]:

- Indexing the diffraction pattern and determination of the crystal system and lattice parameters.
- Identification of the space group.
- Conversion of the experimentally determined intensities into an image of the atoms in the unit cell, by performing a three-dimensional Fourier summation equation 1:

$$\rho(x, y, z) = \frac{1}{V}\sum_{h}\sum_{k}\sum_{l} F_{hkl}e^{-2\pi(hx + ky + lz)} \qquad (1)$$

where ρ is the electron density at point (x, y, z), V is the volume of the unit cell, and F_{hkl} is the structure factor for each plane of the corresponding Miller index ($h\,k\,l$). The structure factor depends on both the intensity and the phase of the diffracted radiation (which requires solution of the phase problem; see main text and BOX 4).



PATTERSON METHOD
The Patterson method employs the relatively large electron diffraction resulting from the presence of heavy atoms (atomic number >17) to determine the crystal structures of inorganic and organic compounds.

ISOMORPHOUS REPLACEMENT METHOD
In the isomorphous replacement method, a heavy atom is introduced into the crystal lattice without disrupting the original crystal structure. The new crystal obtained is known as the derivative crystal. The aim of isomorphous replacement is to obtain the structure of the original crystal by constructing a map (that is, a Patterson map) of the difference in electron density between the diffraction pattern of the derivative crystal and that of the heavy atom. This method is used to determine the crystal structures of proteins.

for solving crystal structures use a partial or full Rietveld analysis for the final refinement of the structure, which is discussed in detail in BOX 5.

Ab initio *crystal structure prediction*. The ability to predict the crystal structure from the molecular structure of a compound is the ultimate goal in crystal structure prediction. Although the structures of many small molecules (organic, organometallic and inorganic) have been solved successfully by this technique, it is still not widespread because of the complexity of the task[113–116].

The *ab initio* method consists of calculating lattice energies of molecular crystals followed by ranking of these structures according to their structural stabilities, thereby using purely energetic criteria for predictions[117–119]. When no previous information is available, such as unit-cell dimensions, it is recommended to search the seven most probable space groups; that is, $P2_1/c$, $P2_12_12_1$, $P2_1$, $P\bar{1}$, $C2/c$, $Pbca$ and $Pnma$[120]. The probable number of molecules in the unit cell can be estimated from the unit-cell volume, if available, or from the true density of the material. The lattice energies of the crystals are calculated using force fields, which assign parametric potentials to various atoms in their different hybridization states. The potentials of each of the atoms can be calculated from first principles when the molecule consists of fewer than 50 atoms[121]. Because typical organic molecules consist of more than 50 atoms, it is difficult to calculate real potentials for each of the atoms in these molecules using current technology. As a result, parametric expressions are used[122]. A short description of the definition and the various force fields in current use is given in ONLINE TABLE S1. The derivation of the necessary parameters can use several experimental quantities to improve the fit, such as heats of sublimation and melting, and lattice vibrations and intermolecular distances that have previously been reported for related crystal structures. If the molecules in the crystal structure show conformational

UM00014126
NOVARTIS EXHIBIT 1517
Novartis v. Regents, IPR2023-01347
Page 2872 of 4460

Box 4 | Direct method for structure determination from single crystals

The direct method attempts to derive relationships among the phases of different reflections[107]. These relationships predict the phases of other reflections and also provide a probability that the phase is correct. The phases are used to map the electron densities in space defined by the crystal. In some cases, several electron-density maps must be calculated and inspected until a chemically reasonable structure is recognized. Once rough atomic positions are determined from electron-density maps, the structure is refined by least-squares minimization of the difference between the calculated intensities and the observed intensities. When this refinement process converges, accurate atomic positions and atomic displacement parameters, known as temperature factors, are obtained. The resulting atomic positions can then be used to construct images of the molecule and/or contents of the unit cell. Hence, the crystal structure is determined[108].

flexibility, the complexity of finding adequate parameters increases greatly[123]. The effect of internal vibrations and kinetic energies can be incorporated into the calculation by introducing suitable corrections. Once suitable parameters have been obtained and the interacting atom types are identified, the interacting atom–atom potentials are added in lattice summations, to produce the total lattice energy[124].

It should be stressed that when predicting crystal structures using energetics, the differences between the lattice energies of the probable structures seldom exceed 20 kJ per mol, which is usually less than 5% of the total lattice energy[125]. For this reason, it is most important that the selected force field be as accurate and as robust as possible. Any source of inaccuracy in the energy function, corresponding to an error of a few kJ per mol in the lattice energy, can lead to inaccurate prediction.

However, the lattice energy is not the only factor that influences the crystal structure. The kinetics of crystallization are an important factor in influencing not only the size and morphology of the crystals but also the structure of the crystals that crystallize. Recent advances in the field of *ab initio* crystal structure prediction have incorporated the kinetic factor during crystallization into the overall prediction process[126]. Information from factors such as space group symmetry, relative crystal stability and the physicochemical properties of phase transitions has also been utilized to arrive at more plausible crystal structures[127].

Ab initio crystal structure prediction requires the determination of the correct molecular conformation of the constituent molecules. Although for a rigid molecule this step poses no problem, for a conformationally flexible molecule, or for a molecule exhibiting TAUTOMERISM, the process can be more complicated[128,129]. A full systematic search might be required in such cases, which can involve an iterative search using lattice energy and other structural information, such as the X-ray diffraction profile of the crystal. It might also be instructive to make use of the observed conformational preferences by examining the conformations found in similar molecules in the CSD, which is a storehouse of more than 250,000 organic and organometallic crystal structures consisting of small molecules[129–131].

TAUTOMERISM
An equilibrium, usually under ambient conditions, of two isomers of a compound.

The method of *ab initio* crystal structure prediction has been used to predict the crystal structure of many small organic molecules, such as methanol, propanol, benzene, terephthalic acid, and pharmaceutically relevant molecules, such as estrone and theophylline[114,116,132,133]. The trial crystal structure for anhydrous theophylline derived by a systematic search elucidated two different crystal structures, which were indistinguishable in terms of lattice energy calculated using the isotropic atom–atom approximation, and fitting of the X-ray diffraction pattern to experimental data. More sophisticated analysis of the lattice energy hypersurfaces, using a distributed multipole-based intermolecular potential, was able to distinguish between the stability of the two structures. The most stable predicted structure resembles the experimentally obtained polymorph of anhydrous theophylline[120]. In another study, Dong *et al.* reported that the crystal structure of neotame anhydrate polymorph G, determined by simulation, closely resembles the experimental crystal structure only when the correct conformation of the neotame molecule is selected beforehand[134]. The crystal structure of 3-hydroxy-4-methyl-2(3H)-thiazolethione was determined experimentally using a synchrotron radiation source. In this case, powder X-ray diffraction data and *ab initio* crystal structure prediction were utilized to compare the predicted crystal structures with the experimentally determined structures. The *ab initio* method was successful when an initial pseudo-centrosymmetric subunit constructed via O-H···S hydrogen bonds was specified[115].

Simulated annealing and energy minimization. Methods of predicting crystal structures that rely on minimization of the lattice energy are based on the assumption that the structure with the least lattice energy is the most plausible. This simple model has two inherent weaknesses: the omission of the entropy term, which contributes to the free-energy and explicit dynamic effects; and the local minimum problem, which is explained below[126]. The simulated annealing algorithm developed by Kirkpatrick *et al.* in 1983 has been utilized to overcome this problem[109]. In this method, the temperature of the physical system is elevated, which permits the system to attain a range of higher energy states. The subsequent gradual reduction in temperature shifts the equilibrium until low energy states dominate. This method introduces the possibility of accepting energy-increasing moves or 'uphill' moves in the minimization of a given function and therefore prevents the system from becoming trapped in a local minimum. The relative probabilities of existence of two states at a given temperature are represented by Boltzmann statistics. A criterion of acceptance of structures generated by simulated annealing is developed on the basis of the statistics of the Boltzmann distribution. A variety of schemes for governing the annealing of the system have been developed. For example, the effective heat capacity can be monitored to detect the onset of melting and

UM00014127
NOVARTIS EXHIBIT 1517
Novartis v. Regents, IPR2023-01347
Page 2873 of 4460

freezing. Alternatively, the rate of cooling applied to the system can be determined by monitoring the jumps, termed the Metropolis moves, in the simulated annealing step. Predictive capabilities of crystal structures have been strengthened by the use of this technique[135]. Gdanitz *et al.* used the simulated annealing technique to predict the crystal structures of hexamethylbenzene and ethene, and the accuracies of the predicted structures were better than 0.02Å and 0.1Å, respectively, when compared with the optimized experimental structure[136]. The simulated annealing technique is now used in conjunction with other methods for improved predictions.

Powder X-ray diffractometry (PXRD). It is sometimes difficult to obtain single crystals of sufficient size and purity for SCXRD, such that only powders, which are actually polycrystalline forms, are available. If the sample is available in powder form and is of high purity, then the solution of the crystal structure can be attempted using the powder X-ray diffraction pattern[111,137]. Because the diffraction pattern is collected on a sample of crystallites of random orientation, structure solution by the powder method circumvents the problem of small size and twinning of the crystals[138].

Crystal structure determination from PXRD patterns can, however, be complicated by a variety of factors.

Box 5 | Rietveld method for refinement

The information required for a full Rietveld analysis are the unit-cell parameters, the experimental or the observed diffraction intensities (such as powder X-ray diffractometry (PXRD) profile parameters), the calculated diffraction intensities (from any predictive methodologies) and the background contribution. In the classical Rietveld method, the weighted sum of square difference between the observed and calculated reflected X-ray intensity, y, is minimized. Refinement is usually performed in sets of two to five cycles at a time. The progress of the refinement is monitored by the profile fit and the nature of the parameter shifts. The fit of the calculated pattern to the observed data can be presented quantitatively in terms of agreement indices or R values[187]. The weighted-profile R value, R_{wp}, is defined as shown in equation 2:

$$R_{wp} = \left\{ \sum_i w_i [y_{iobs} - y_{icalc}]^2 / \sum_i w_i [y_{iobs}]^2 \right\}^{1/2} \quad (2)$$

where y_{iobs} is the observed intensity at step i, y_{icalc} the calculated intensity and w_i the weighting factor. The expression in the numerator is the value that is minimized during a Rietveld refinement. In order to evaluate the goodness of fit of the peaks, an R_{wp} value for which the background contribution has been eliminated should also be calculated.

Ideally, the final R_{wp} should approach the statistically expected R value, R_{exp}, as defined in equation 3:

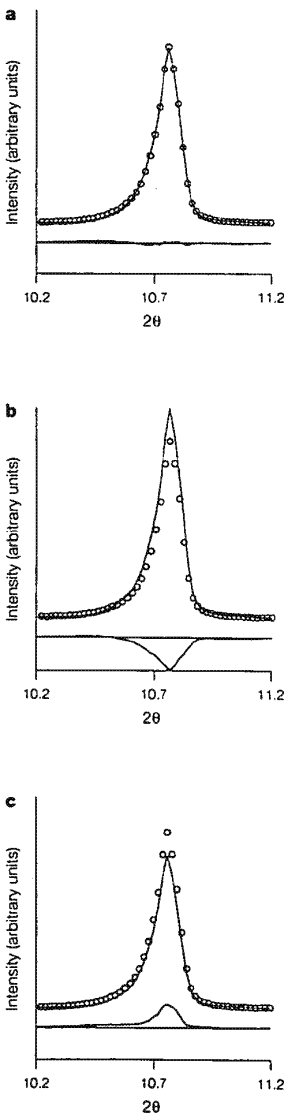
$$R_{exp} = \left\{ [(N-P)/\sum_i^N w_i y^2_{iobs}] \right\}^{1/2} \quad (3)$$

where N is the number of observations, P is the number of parameters and R_{exp} reflects the quality of the data. The ratio R_{wp}: R_{exp} is termed the goodness of fit and is represented as χ^2 (REF. 188).

The difference profile plot, which is the difference between the observed and calculated intensities, is the visual way to check the profile fit. It should be emphasized that profile plots are much more informative than R values, because they can indicate whether a high R value is due to a profile parameter problem or to a total deficiency in the structural model as shown in the figure.

Quantitative phase analysis by means of the Rietveld method is now an especially important ancillary procedure to refine crystal structures[189]. The Rietveld method has also been applied to improve the crystal structure prediction from PXRD patterns[190,191]. The main drawback of the conventional powder method for determining crystal structures is that the patterns grossly overlap, thereby preventing maximum utilization of the experimental information. The Rietveld method was developed to separate effectively these overlapping data, thereby allowing accurate determination of the structure.

The figure shows the observed (circles), calculated (line) and difference (bottom) profiles for a good fit of a peak (a), a calculated intensity that is too high (b) and a calculated intensity that is too low (c). The characteristic difference profile for intensity is either positive or negative and is concentrated at the centre of the peak[188]. Reproduced, with permission, from REF. 188 © (1999) International Union of Crystallography.



UM00014128
NOVARTIS EXHIBIT 1517
Novartis v. Regents, IPR2023-01347
Page 2874 of 4460

For powder diffraction patterns, the reflections from different crystal planes are averaged over directions and projected onto a single variable, the diffraction angle 2θ. This averaging makes the reconstruction of the underlying crystal structure much more difficult than for single-crystal diffraction patterns[139]. Space group determination using powders is more ambiguous than with single-crystal diffraction. This problem arises because the regions in the pattern, which should be free of peaks because of the systematic absences, are often overlaid with peaks of other reflections. Also, poor quality PXRD patterns, obtained from solid samples of poor crystallinity or solid samples with considerable amorphous content, preclude their successful indexing. When the crystals have a strongly anisotropic morphology, such as flat plates or long needles, then the crystallites tend to align along a certain direction. The nonrandom distribution of crystallite orientation affects the relative intensities of given peaks and hinders the correct solution of the pattern[140]. These problems notwithstanding, crystal structure determination from PXRD data is an important and emerging discipline. To determine the crystal structure from the PXRD pattern, it is essential that the powder diffraction data be collected appropriately. Factors to consider before data collection are the geometry of the diffractometer, the quality of the alignment and calibration of the instrument, the most suitable radiation, the wavelength, appropriate sample preparation and thickness, slit widths and necessary counting time. Here, we outline some of the basic concepts and recent developments. Structure solution from PXRD data falls into two classes: traditional methods and direct-space approaches.

Traditional methods include the Patterson method, direct methods that differ from direct-space approaches, and the method of entropy maximization and likelihood ranking. The traditional approach to crystal structure solution from PXRD data attempts to extract the integrated Bragg intensities of individual reflections directly from the PXRD pattern[141]. Once the integrated intensities are known, an electron-density map is constructed using the same techniques that have been developed for single-crystal diffraction data[142] (for particularly informative papers on pattern decomposition, see REFS 143–146). Variants of this basic idea have been applied successfully to organic systems with up to 31 non-hydrogen atoms. Although traditional techniques for structure solution from PXRD data have been applied successfully in several cases, these techniques have certain intrinsic limitations[126]. For example, peak overlap can create major difficulties in extracting intensities from PXRD patterns, which limits the complexity of structures that can be solved by traditional methods. Because of the above limitation, much recent interest has focused on the development of new methods for solving crystal structures directly from PXRD data. The direct-space approach is such a method that is particularly well suited for molecular crystals.

In direct-space approaches, trial structures are generated in direct space — that is, they are generated independently of the experimental powder diffraction pattern. The suitability of each trial structure is assessed by comparing the powder diffraction pattern calculated for the trial structure and the experimental powder diffraction data[139] via a least-squares fit of the calculated diffraction pattern to the experimental diffraction pattern. The agreement factor for the trial configuration is denoted $R_{wp(trial)}$ and is calculated using equation 4 (REF. 111).

$$R_{wp(trial)} = 100 \times \sqrt{\frac{\sum w_i (y_i - y_{ci})^2}{\sum w_i y_i^2}} \quad (4)$$

in which y_i is the intensity of the ith observed point in the experimental powder diffraction profile, y_{ci} is the intensity of the corresponding point in the calculated powder diffraction profile from the trial structure, and w_i is a weighted factor for the ith point in the powder diffraction profile. The aim is to find the trial structure with the lowest value of $R_{wp(trial)}$. The process is therefore equivalent to exploring a hypersurface $R_{wp}(\Gamma)$ to find the global minimum, where Γ represents the set of variables that define the structure in direct space. Methods that can be used to locate the global minimum, within strategies for direct-space structure solution, include simulated annealing by the Monte Carlo method[111,147], genetic algorithm techniques[148,149] and techniques employing a systematic search approach using a grid-based search with lattice energy calculations[150].

Most direct-space approaches are stochastic in nature, and so it is recommended that the calculation of the structure solution be repeated several times from different random starting populations.

Monte Carlo method. The Monte Carlo method is a technique for surveying the hypersurface as defined above. In this approach, starting from a random configuration of atoms in the unit cell, each atom is displaced by a random amount in a random direction to generate a trial configuration[151]. The powder diffraction pattern corresponding to the trial configuration is calculated. After a sufficient number of configurations have been generated via the Monte Carlo algorithm, the best configuration — that is, the one that with the lowest $R_{wp(trial)}$ — is considered further[151]. This configuration then provides the structural model for the initial conventional Rietveld refinement calculation. Occasionally, the structures obtained by the Monte Carlo procedure are incomplete and further development through difference Fourier methods might be required. When a complete structural model has been obtained, a full Rietveld refinement calculation is carried out to give the final refined crystal structure.

Bond and Jones successfully predicted the crystal structure of a series of divalent complexes of the cyclic thiohydroxamic acids pyrithione, methylpyrithione and methylthiazolethione with zinc, copper and nickel from PXRD data using a combination of a Monte Carlo procedure, the refinement of cell parameters using the Rietveld method, and energy minimization within the constrained unit cell[111]. ONLINE TABLE S2 compares the

UM00014129
NOVARTIS EXHIBIT 1517
Novartis v. Regents, IPR2023-01347
Page 2875 of 4460

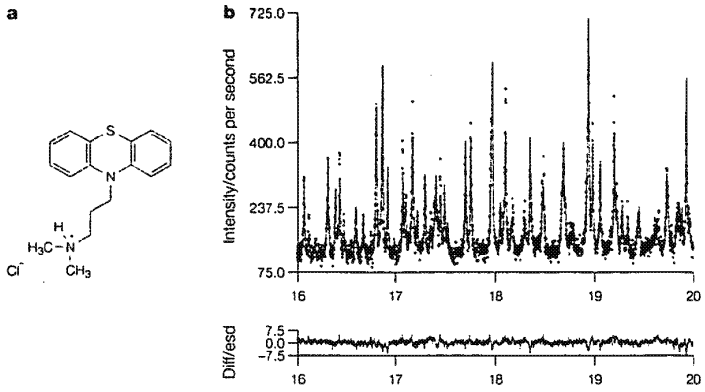


Figure 4 | **Application of the Monte Carlo method in crystal structure solution. a** | The molecular structure of promazine hydrochloride. **b** | The observed powder diffraction data, the calculated powder pattern resulting from the Rietveld refinement of the structure obtained from Monte Carlo simulated annealing of the structure generated from the experimental powder pattern, and the difference shown below[147]. Reproduced, with permission, from REF. 147 © (1998) Royal Society of Chemistry.

single-crystal structures and predicted structures of these compounds. The authors judged the success of each predicted structure by comparing the simulated PXRD patterns of the predicted structure with that of the corresponding experimental structure, in addition to comparing the space group, lattice parameters and lattice energies, as mentioned earlier.

David *et al.* determined the crystal structure of capsaicin, thiothixene and promazine hydrochloride from their powder diffraction data[147]. FIGURE 4 shows the observed powder diffraction data and the calculated powder pattern resulting from the Rietveld refinement of the structure obtained by simulated annealing using the Monte Carlo method of the structure generated from the experimental powder pattern.

Genetic algorithms. In the genetic algorithm (GA) method, a population of trial crystal structures is allowed to evolve and optimize, subject to the rules and operations that govern evolution in biological systems[152,153]. The set, Γ, can be regarded as the genetic code. The initial population of structures is allowed to evolve through subsequent generations by applying the evolutionary operations of mating, mutating and natural selection. Through these operations, a given population is converted to the next generation, and the number of structures remains unchanged. The quality of each structure depends on its value of R_{wp} and fitness is defined as an appropriate function of R_{wp} or by the figure of merit, χ^2, as described in Rietveld analysis (BOX 5).

In the mating procedure, pairs of structures are first selected from the population. The probability of selecting a given structure as a parent is proportional to its fitness. For each pair of parents, two offspring are generated by distributing parts of the genetic codes of the two parents between the two offspring. In the mutating procedure, new values of individual genetic variables are introduced into the population. In the natural selection procedure, only the structures with the lowest R_{wp} are allowed to pass from one generation to the next[152].

Among the recent improvements in the GA technique for crystal structure solution is the implementation of a Lamarckian approach to evolution, rather than the more commonly used Darwinian evolution[154]. In the Lamarckian procedure, each new structure generated by a GA calculation is subjected to local minimization of R_{wp} with respect to the structural variables in the set Γ. Only these minimized structures are used subsequently in the GA calculation. This procedure therefore combines the stochastic and deterministic components within the global minimization strategy.

The analysis of the evolutionary history of a GA structure can provide important insights into the development of the algorithm itself, which can be utilized to improve the quality of prediction, as well as to decrease the time required for the prediction[155]. These analytical methods are the evolutionary progress plot, evolutionary distribution plot and evolutionary trajectory plot.

Another development in crystal structure prediction by GA has been the addition of the energy minimization component into the algorithm to generate the most probable structure. Both the potential energy $E(\Gamma)$ function and the $R_{wp}(\Gamma)$ function are minimized together in an appropriate functional form to define a new hybrid hypersurface $G(\Gamma)$[156]. The hybrid function $G(\Gamma)$ is designed to behave as an energy term, when the value of potential energy, E, is high, and to give increasing importance (ultimately absolute importance) to R_{wp} as lower values of E are approached. This behaviour is achieved by means of a sliding weighting parameter $w(\Gamma)$, which is defined as an appropriate function of E. As the energy of the system increases, the weighting function has greater values, which implies greater significance of $E(\Gamma)$ in determining $G(\Gamma)$. $G(\Gamma)$ therefore guides one property — that is, the $E(\Gamma)$ — to enable another property — that is, the $R(\Gamma)$ — to reach the optimum value. The guiding function can itself be derived by several techniques. FIGURE 5 illustrates the application of the GA method by Harris *et al.* to structure solution of 4-methoxybenzoic acid and formylurea[149].

Maximum entropy algorithm. The maximum entropy (ME) method for solving crystal structures views the unknown crystal structure as consisting of atoms of known chemical identity but with unknown positions, and considers the latter as random, with an initially uniform distribution in the asymmetric unit of the crystal[157]. Structure determination involves the gradual removal of that randomness. The ME algorithm is a deconvolution technique that utilizes Bayesian statistics to generate the most probable structures by comparing the calculated structures with the experimental structures obtained from PXRD. This method purports to generate an electron-density map from the PXRD pattern, which can then be used to solve the structure of the crystal.

UM00014130
NOVARTIS EXHIBIT 1517
Novartis v. Regents, IPR2023-01347
Page 2876 of 4460

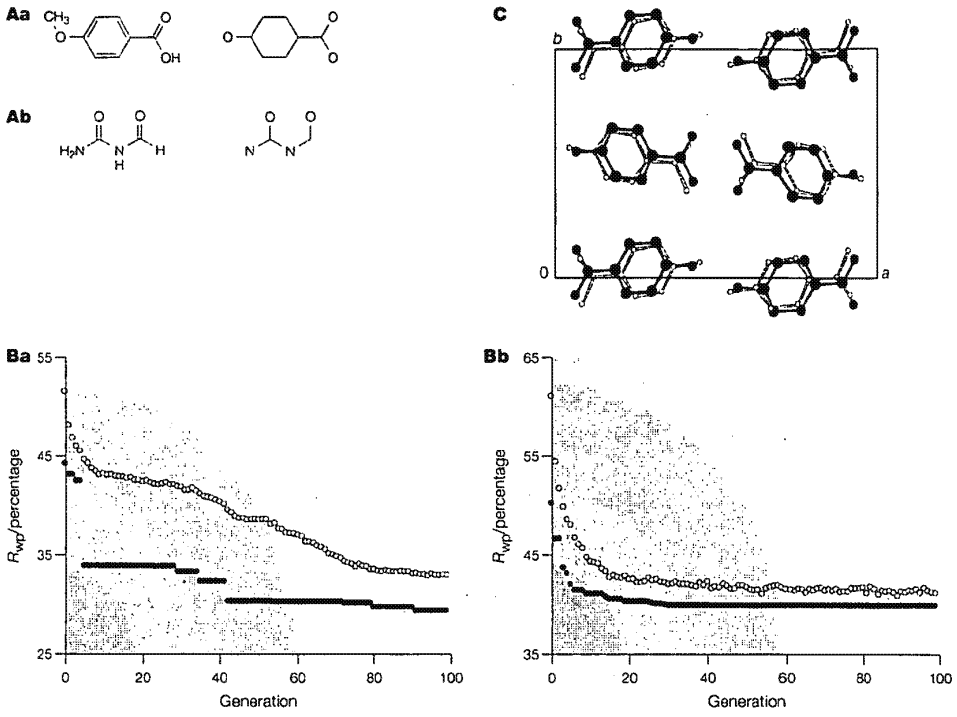


Figure 5 | **Application of the genetic algorithm (GA) method in crystal structure solution. A** | Molecular structures and definitions of the structural fragments used in the GA structure solution calculations for: 4-methoxybenzoic acid (**a**) and formylurea (**b**)[149]. **B** | The evolutionary progress plot for 4-methoxybenzoic acid (**a**) and formylurea (**b**), showing the evolution of R_{min} (filled circles) and R_{ave} (open circles) as a function of generation number[149]. **C** | Comparison between the position of the structural fragment in the best structure solution obtained in the GA calculation for 4-methoxybenzoic acid (open circles) and the position of the corresponding atoms in the known crystal structure (filled circles)[149]. Reproduced from REF. 149 © (1998) International Union of Crystallography.

The crystal structure of perchlorocoronene, $C_{24}Cl_{12}$, was solved by Gilmore *et al.* using the ME method[158]. The Fourier transformation of the reflection data of the compound yielded four phases, which were used as a basis set for further analysis. The electron-density map obtained from the Fourier transformation of the electron microscope image is shown in FIG. 6a. Routine phase extension using ME procedures led to a map in which the diffraction intensities are phased, as shown in FIG. 6b.

Crystal engineering

Nobel laureate Richard Feynman once remarked that if the arrangement of things can be controlled on a small scale, then the possible properties of the material can be modulated to a greater extent and the range of applications to which it can be applied can be greatly enhanced[159]. In accordance with this idea, crystal engineering is defined as the modelling, design, synthesis and application of crystalline solids with predefined and desired aggregation of molecules and ions[160]. The aim of crystal engineering is to design and synthesize crystals in which the arrangement of the constituent molecules is controlled so as to elicit one or more desired functional properties from the crystal. Pepinsky first introduced the concept of crystal engineering in a seminal paper[161], and Schmidt was the first to show the importance of this field to the solid-state photodimerization of olefins[162].

Crystals can be assumed to be *de facto* manifestations of self-recognition and self-organization of molecules by means of intermolecular interactions and packing preferences. The self-assembly of molecules to form crystals confers distinct physical and chemical properties to the crystal as compared with the individual molecules that constitute the crystal. Molecular crystals can therefore be viewed as supermolecules with characteristic physical and chemical properties. An essential requirement in designing crystals is understanding the intermolecular interactions involved in crystal packing, and utilizing such understanding in the design of new solids with desired physical and chemical properties[163]. Though the physical nature of the forces acting between organic molecules in crystals is usually quite well understood, it is still difficult to grasp the complex spatial pattern of such forces[164]. The term supramolecular synthon was developed to define the structural units that result from known or conceivable synthetic operations involving intermolecular interactions among

UM00014131
NOVARTIS EXHIBIT 1517
Novartis v. Regents, IPR2023-01347
Page 2877 of 4460

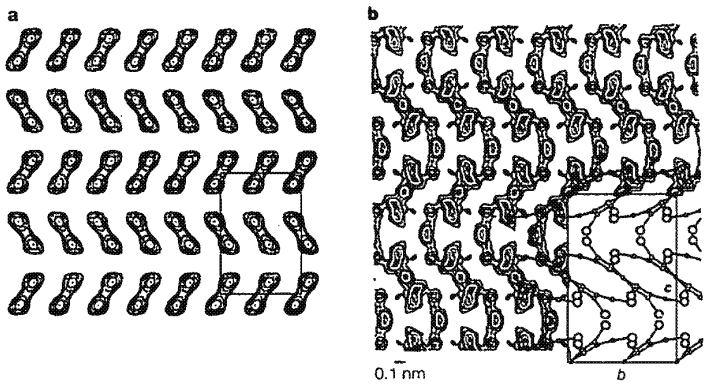


Figure 6 | **Application of the maximum entropy (ME) method to crystal structure solution.** Perchlorocoronene crystal structures are shown. **a** | Projection down the *a* axis of an electrostatic potential map based on four reflections obtained from the Fourier transformation of the electron microscope image. **b** | Electrostatic potential map derived from ME phasing. The refined structure from a single crystal X-ray analysis is superimposed in the bottom right-hand corner[158]. Reproduced, with permission, from REF. 158 © (1993) The Royal Society.

constituent molecules of a crystal which, when extended in three-dimensional space, result in a crystal[165]. The available crystal structures give insight into the varieties of supramolecular synthons that exist. The goal in crystal engineering is to attain collective crystal properties by an adequate choice of the building blocks (molecules) that can be modulated to self-assemble in accordance with suitable synthons to form desired crystals.

The properties of crystalline matter are manifold and diverse. As discussed in the introduction to this review, the crystalline form affects such physical properties as the solubility, stability, dissolution rate, bioavailability and mechanical properties of the solid drug. Using crystal engineering, new phases of pharmaceuticals can be synthesized to improve, and ultimately to optimize, these properties.

The design of binary compounds using complementary molecules is an application of crystal engineering. Pharmaceutical molecules inherently contain molecular recognition sites that bind selectively to biomolecules. These sites have the potential to be used to form supramolecular self-assemblies with desired physicochemical properties. For example, Walsh *et al.* co-crystallized the anti-inflammatory molecules *rac*-ibuprofen and *rac*-flubiprofen (shown in FIG. 7A) with 4,4′-dipyridyl to yield co-crystals with a 2:1 stoichiometry[166]. The co-crystals exhibit heterosynthons formed by the interaction between the drug molecules and 4,4′-dipyridyl, whereas the pure drug components exhibit dimeric homosynthons formed by the interaction between two drug molecules. The co-crystals exhibit physical properties different from those of the parent compounds as a direct result of hydrogen-bonding interactions between the binary components of the crystal.

Similarly, drugs, such as indomethacin, phenobarbital, aspirin and carbamazepine, were co-crystallized with a number of secondary molecules, such as acetone, benzoquinone and 1,2-bis(4-pyridyl)ethylene[167,168]. The physical characteristics of the co-crystals are reported to be considerably different from those of the pure drug molecules[169]. However, the utility of the co-crystal formers in pharmaceutical products is limited by their pharmacological and toxicological properties. Nevertheless, food additives and selected 'generally regarded as safe' compounds have also been used as co-crystal formers. For example, itraconazole, a poorly water-soluble antifungal drug, forms co-crystals with a number of pharmaceutically acceptable acids, such as fumaric acid, succinic acid and L-, D- or DL-tartaric acid, when crystallized from polar aprotic solvents or from mixtures of hydrocarbons and polar aprotic solvents. FIGURE 7B shows that co-crystallization increases the dissolution rate of the drug[170]. This example shows that, with a suitable application of supramolecular chemistry, it should be possible to rationally design co-crystals of compounds with significantly complex molecular structures.

The relationship describing the influence of crystallographic structure on the mechanical properties of crystals and powders is another area in which crystal engineering can be utilized, but which has received little attention so far. In one such study, the YOUNG'S MODULUS of aspirin was estimated from its crystal structure[171]. In another study, Roberts *et al.*[172] showed that the mechanical properties of aspirin, sulphathiazole, carbamazepine and polymorphs of primidone (forms A and B) can be

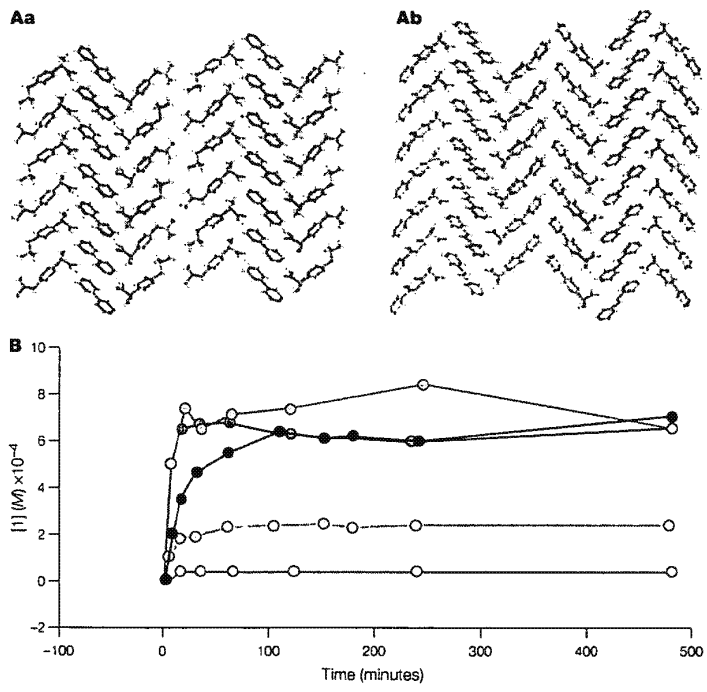


Figure 7 | **Crystal engineering. A** | The 1:2 adducts of 4,4′-dipyridyl with ibuprofen (a) and flubiprofen (b)[166]. **B** | A comparison of the dissolution profiles of crystalline itraconazole (grey) and co-crystals of itraconazole with succinic acid (orange), L-malic acid (red), L-tartaric acid (dark blue) and SPORANOX BEADS (light blue) in 0.1 M hydrochloric acid at 25°C[170]. Part **A, b** reproduced from REF. 166 © (2003) Royal Society of Chemistry. Part **B** reproduced from REF. 170 © (2003) American Chemical Society.

UM00014132
NOVARTIS EXHIBIT 1517
Novartis v. Regents, IPR2023-01347
Page 2878 of 4460

predicted by applying lattice dynamics to the atom–atom potential model. In this case, the crystal morphology was taken into account when considering the experimental results. Although the mechanical properties of a compound can be predicted from its crystal structure, crystal engineering of pharmaceuticals has not yet resulted in the design of crystals with desired mechanical properties. If a molecular basis for the origins and magnitude of mechanical properties can be developed, then the required controlled modification might be achieved by analysis of the structural and constituent molecular information[173–175]. Then, the knowledge gained might be utilized to design crystals with desired mechanical properties[176].

Afterword

Statistical analysis of structural data in the CSD provides a better understanding of the nature of hydrogen bonds and intermolecular interactions, and facilitates the identification of frequently occurring interaction patterns and supramolecular synthons[177]. With enhanced knowledge of hydrogen-bond synthons in crystals, novel strategies can be designed for the self-assembly of supramolecular architectures from multifunctional molecules. Using the database, the twin phenomena of polymorphism and solid-state solvation (pseudopolymorphism) are being studied by examining the information on molecular conformations and solvent inclusion. The hydrogen-bonding patterns elucidated in small molecules are used as models in structure-based drug design and pharmacophore mapping. So the implications of crystal engineering extend far beyond organic and organometallic crystal design into supramolecular materials, nanotechnology, ligand–protein binding and crystal structure prediction[177].

The field of crystal structure prediction has recently made significant progress. However, certain factors have not yet been considered when predicting crystal structures. These factors include the enthalpy force field issue, intra–intermolecular energy issues, the entropy issue, the temperature issue, kinetic energy issues and the kinetic dynamic issues. Incorporation of these factors into the prediction process is expected to improve the overall results generated[178].

Modelling techniques have also been successful in determining the energetics and location of sorbed molecules within solids, especially in inorganic solids. Their use in studies of organic solids is still at an early stage. Computational techniques are progressively becoming more common for morphology prediction[179]. Simulation techniques are expected to have an expanded role in solving the problems involved in the determination and study of the crystallographic and molecular sites occupied by sorbed molecules on the surfaces of solids or within solids. Other analytical techniques, especially vibrational spectroscopy (for example, infrared spectroscopy and Raman spectroscopy) and nuclear magnetic resonance (NMR) spectroscopy, might complement the results obtained from computational studies. For example, the structure of *N*-(*p*-tolyl)-dodecylsulfonamide was determined from PXRD data and was validated by solid-state NMR spectroscopy[180] (for recent reviews on the application of spectroscopic techniques to the characterization of pharmaceuticals, see REFS 181–184).

We hope this review has highlighted the major advances in crystal structure solution and prediction, as well as the utilization of this information in designing solids with desired physical properties. Increased computational speed and memory will further improve the analytical procedures and the modelling of the crystal structure and energy calculations. Much scope remains for improving the modelling of intermolecular interactions. Such improvements will also enhance the engineering of new crystal forms with novel properties and for novel applications.

SPORANOX BEAD
An amorphous capsule that is used to achieve the required oral bioavailability of extremely water-insoluble drugs, such as itraconazole.

YOUNG'S MODULUS
A measure of a material's elasticity, which is defined as the force per unit cross-section of the material divided by the fractional increase in length that results from the stretching of a standard specimen of the material.

1. Vippagunta, S. R., Brittain, H. G. & Grant, D. J. W. Crystalline solids. *Adv. Drug Deliv. Rev.* **48**, 3–26 (2001). **Review of the structure and properties of crystalline pharmaceuticals.**
2. Byrn, S. R., Pfeiffer, R. R. & Stowell, J. G. *Solid State Chemistry of Drugs* (SSCI, West Lafayette, 1999).
3. Hancock, B. C. & Zografi, G. Characteristics and significance of the amorphous state in pharmaceutical systems. *J. Pharm. Sci.* **86**, 1–12 (1997).
4. Borka, L. & Haleblian, J. K. Crystal polymorphism of pharmaceuticals. *Acta Pharm. Jugosl.* **40**, 71–94 (1990).
5. Haleblian, J. K. Characterization of habits and crystalline modification of solids and their pharmaceutical applications. *J. Pharm. Sci.* **64**, 1269–1288 (1975).
6. Brittain, H. G. & Fiese, E. F. in *Polymorphism in Pharmaceutical Solids* (ed. Brittain, H. G.) 331–362 (Marcel Dekker, New York, 1999).
7. Phadnis, N. V. & Suryanarayanan, R. Polymorphism in anhydrous theophylline: implications on the dissolution rate of theophylline tablets. *J. Pharm. Sci.* **86**, 1256–1263 (1997).
8. Otsuka, M. & Matsuda, Y. Effects of environmental temperature and compression energy on polymorphic transformation during tableting. *Drug Dev. Ind. Pharm.* **19**, 2241–2269 (1993).
9. Otsuka, M., Hasegawa, H. & Matsuda, Y. Effect of polymorphic transformation during the extrusion-granulation process on the pharmaceutical properties of carbamazepine granules. *Chem. Pharm. Bull.* **45**, 894–898 (1997).
10. Otsuka, M., Hasegawa, H. & Matsuda, Y. Effect of polymorphic forms of bulk powders on pharmaceutical properties of carbamazepine granules. *Chem. Pharm. Bull.* **47**, 852–856 (1999).
11. Otsuka, M., Nakanishi, M. & Matsuda, Y. Effects of crystalline form on the tableting compression mechanism of phenobarbital polymorphs. *Drug Dev. Ind. Pharm.* **25**, 205–215 (1999).
12. Otsuka, M., Ohtani, H., Otsuka, K. & Kaneniwa, N. Effect of humidity on solid-state isomerization of various kinds of lactose during grinding. *J. Pharm. Pharmacol.* **45**, 2–5 (1993).
13. Wong, M. W. Y. & Mitchell, A. G. Physicochemical characterization of a phase change produced during the wet granulation of chlorpromazine hydrochloride and its effects on tableting. *Int. J. Pharm.* **88**, 261–273 (1992).
14. Miyamae, A. *et al.* X-ray powder diffraction study on the grinding effect of the polymorphs of a novel and orally effective uricosuric agent: FR76505. *Drug Dev. Ind. Pharm.* **20**, 2881–2897 (1994).
15. Chongprasert, S. *et al.* Effects of freeze-dry processing conditions on the crystallization of pentamidine isethionate. *J. Pharm. Sci.* **87**, 1155–1160 (1998).
16. Morris, K. R., Griesser, U. J., Eckhardt, C. J. & Stowell, J. G. Theoretical approaches to physical transformations of active pharmaceutical ingredients during manufacturing processes. *Adv. Drug Deliv. Rev.* **48**, 91–114 (2001). **Explains the importance of crystal structure in pharmaceutical processing.**
17. Morris, K. R. *et al.* Advances in pharmaceutical materials and processing. *Pharm. Sci. Technol. Today* **1**, 235–245 (1998).
18. Khankari, R. K. & Grant, D. J. W. Pharmaceutical hydrates. *Thermochim. Acta* **248**, 61–79 (1995).
19. Grant, D. J. W. in *Polymorphism in Pharmaceutical Solids* (ed. Brittain, H. G.) 1–33 (Marcel Dekker, New York, 1999).
20. Ghosh, S., Ojala, W. H., Gleason, W. B. & Grant, D. J. W. Relationships between crystal structures, thermal properties and solvate stability of dialkylhydroxypyridones and their formic acid solvates. *J. Pharm. Sci.* **84**, 1392–1399 (1995).
21. Ojala, W. H., Khankari, R. K., Grant, D. J. W. & Gleason, W. B. Crystal structures and physical chemical properties of nedocromil zinc heptahydrate and nedocromil magnesium pentahydrate. *J. Chem. Crystallog.* **26**, 167–178 (1996).
22. Giordiano, F. *et al.* Physical properties of parabens and their mixtures: solubility in water, thermal behavior, and crystal structures. *J. Pharm. Sci.* **88**, 1210–1216 (1999).
23. Zhu, H. J., Young, V. G. Jr & Grant, D. J. W. Crystal structure and thermal behavior of nedocromil nickel octahydrate. *Int. J. Pharm.* **232**, 23–33 (2002).
24. Brittain, H. G. The impact of polymorphism on drug development: a regulatory viewpoint. *Am. Pharm. Rev.* **3**, 67–68, 70 (2000). **Explains the regulatory issues related to the polymorphism of pharmaceuticals.**
25. Bernstein, J. *Polymorphism in Molecular Crystals* (Oxford Univ. Press, New York, 2002).

UM00014133
NOVARTIS EXHIBIT 1517
Novartis v. Regents, IPR2023-01347
Page 2879 of 4460

Comprehensively summarizes the current knowledge and understanding of the polymorphism of molecular crystals.
26. Morris, K. R. in *Polymorphism in Pharmaceutical Solids* (ed. Brittain, H. G.) 125–181 (Marcel Dekker, New York, 1999).
27. Andreetti, G. D. Crystallographic studies of inclusion compounds. *Inclusion Compounds* **3**, 129–146 (1984).
28. Lipkowski, J. in *Crystallography of Supramolecular Compounds* NATO Science Series C Vol. 480 (eds Tsoucaris, G. *et al.*) 265–283 (Kluwer Academic, Boston, 1996).
29. Brittain, H. G. & Grant D. J. W. in *Polymorphism in Pharmaceutical Solids* (ed. Brittain, H. G.) 279–330 (Marcel Dekker, New York, 1999).
30. Bechtloff, B., Nordhoff, S. & Ulrich, J. Pseudopolymorphs in industrial use. *Cryst. Res. Technol.* **36**, 1315–1328 (2001).
Explains the importance of pseudopolymorphs (solvates and hydrates) in the pharmaceutical industry.
31. Berge, S. M., Bighley, L. D. & Monkhouse, D. C. Pharmaceutical salts. *J. Pharm. Sci.* **66**, 1–19 (1977).
32. Neau, S. H. in *Water-Insoluble Drug Formations* (ed. Liu, R.) 405–425 (Interpharm, Buffalo Grove, 2000).
33. Puddipeddi, M., Serajuddin, A. T. M., Grant, D. J. W. & Stahl, P. H. in *Handbook of Pharmaceutical Salts: Properties, Selection, and Use* (eds Stahl, P. H. & Wermuth, C. G.) 19–38 (Wiley, Weinheim, 2002).
34. Giron, D. & Grant, D. J. W. in *Handbook of Pharmaceutical Salts: Properties, Selection, and Use* (eds Stahl, P. H. & Wermuth, C. G.) 41–81 (Wiley, Weinheim, 2002).
Explains the importance of salt forms of pharmaceuticals in the stabilization and processing of pharmaceutical formulations.
35. Stahl, P. H. & Byrn, S. R. in *Molecular Modeling Applications in Crystallization* (ed. Myerson, A. S.) 313–345 (Cambridge Univ. Press, New York, 1999).
36. Shah, R. D. & Natie, L. A. Spectroscopic methods for determining enantiomeric purity and absolute configuration in chiral pharmaceutical molecules. *Curr. Opin. Drug Discov. Devel.* **4**, 764–775 (2001).
37. van Eikeren, P. Commercial manufacture of chiral pharmaceuticals. *Chiral Separations* 9–35 (1997).
38. Gu, C. H. & Grant, D. J. W. in *Handbook of Experimental Pharmacology: Stereochemical Aspects of Drug Action and Disposition* Vol. 153 (eds Eichelbaum M., Testa, B. & Somogyi, A.) 113–137 (Springer, Berlin, 2003).
Explains the structural basis of the solid-state properties of chiral pharmaceuticals.
39. Li, Z. J. & Grant, D. J. W. Relationship between physical properties and crystal structures of chiral drugs. *J. Pharm. Sci.* **86**, 1073–1078 (1997).
40. Abgada, C. O. & York, P. Dehydration of theophylline monohydrate powder: effects of particle size and sample weight. *Int. J. Pharm.* **106**, 33–40 (1994).
41. Sun, C. & Grant, D. J. W. Improved tableting properties of p-hydroxybenzoic acid by water of crystallization – a molecular insight. *Pharm. Res.* (in the press).
42. Bandopadhyay, R. & Grant, D. J. W. Plasticity and slip system of plate-shaped crystals of L-lysine monohydrochloride dihydrate. *Pharm. Res.* **19**, 491–496 (2002).
43. Sun, C. & Grant, D. J. W. Influence of crystal structure on the tableting properties of sulfamerazine polymorphs. *Pharm. Res.*, **18**, 274–280 (2001).
44. Cullity, B. D. *Elements of X-ray Diffraction* 3rd edn (Prentice Hall, New Jersey, 2001).
Provides an excellent introduction to crystal structures and X-ray crystallography.
45. Buerger, M. J. *Elementary Crystallography* 253–273 (Wiley Interscience, New York, 1963).
46. Zorky, P. M. Symmetry, pseudosymmetry and hypersymmetry of organic crystals. *J. Mol. Struct.* **374**, 9–28 (1996).
47. Cambridge Crystallographic Data Centre, Cambridge Structural Database, University Chemical Laboratory, Cambridge, UK (1999).
This databank includes more than 250,000 crystal structures and is a site reference for crystal structure reports.
48. Perlstein, J. in *Crystal Engineering: from Molecules and Crystals to Materials* NATO Science Series C Vol. 538 (eds Braga, D., Grepini, F. & Orpen, G. A.) 23–42 (Kluwer Academic, Boston, 1999).
49. Buckingham, A. D. in *Crystal Engineering: the Design and Application of Functional Solids* NATO Science Series C Vol. 539 (eds Seddon, K. R. & Zaworotko, M.) 49–68 (Kluwer Academic, Boston, 1999).
50. Pimentel, G. C. & McClennan, A. L. *The Hydrogen Bond* (W. H. Freeman, San Francisco, 1960).
51. Scheiner, S. *Hydrogen Bonding: A Theoretical Perspective* (Oxford Univ. Press, Oxford, 1997).
52. Desiraju, G. R. Hydrogen bridges in crystal engineering: interactions without borders. *Acc. Chem. Res.* **35**, 565–573 (2002).
53. Jeffrey, G. A. *An Introduction to Hydrogen Bonding* (Oxford Univ. Press, New York, 1997).
54. Desiraju, G. R. & Steiner, T. *The Weak Hydrogen Bond in Structural Chemistry and Biology* (IUCr Monographs on Crystallography 9) 15–47 (Oxford Univ. Press, New York, 1999).
55. Beyer, A., Karpfen, A. & Schuster, P. Energy surfaces of hydrogen complexes in the vapour phase. *Topics Curr. Chem.* **120**, 1–40 (1984).
56. Perlstein, J. Molecular self-assemblies 4. Using Kitaigorodskii's Aufbau principle for quantitatively predicting the packing geometry of semiflexible organic molecules in translation monolayer aggregates. *J. Am. Chem. Soc.* **116**, 11420–11432 (1994).
57. Smith, E. R. Electrostatic energy in ionic crystals. *Proc. R. Soc. Lond. A* **375**, 475–505 (1981).
58. Haleblian, J. K. & McCrone, W. C. Pharmaceutical applications of polymorphism. *J. Pharm. Sci.* **58**, 911–929 (1969).
59. Burger, A. & Ramberger, R. On the polymorphism of pharmaceuticals and other molecular crystals. I. Theory of thermodynamic rules. *Mikrochim. Acta* **II**, 259–271 (1979).
60. Burger, A. & Ramberger, R. On the polymorphism of pharmaceuticals and other molecular crystals. II. Applicability of thermodynamic rules. *Mikrochim. Acta* **II**, 273–316 (1979).
61. Henck, J. O. & Kuhnert-Brandstatter, M. Demonstration of the terms enantiotropy and monotropy in polymorphism research exemplified by flurbiprofen. *J. Pharm. Sci.* **88**, 103–108 (1999).
62. Yu, L., Reutzel, S. M. & Stephenson, G. A. Physical characterization of polymorphic drugs: an integrated characterization strategy. *Pharm. Sci. Technol. Today* **1**, 118–127 (1998).
63. Grunenberg, A., Henck, J. O. & Siesler, H. W. Theoretical derivation and practical application of energy/temperature diagrams as an instrument in preformulation studies of polymorphic drug substances. *Int. J. Pharm.* **129**, 147–158 (1996).
64. Yu, L. Inferring thermodynamic stability relationship of polymorphs from melting data. *J. Pharm. Sci.* **84**, 966–974 (1995).
65. Gu, C. H., Young, V. Jr & Grant, D. J. W. Polymorph screening: influence of solvents on the rate of solvent-mediated polymorphic transformation. *J. Pharm. Sci.* **90**, 1878–1890 (2001).
66. Toscani, S. An up-to-date approach to drug polymorphism. *Thermochim. Acta* **321**, 73–79 (1998).
67. Stahl, P. H. in *Towards Better Safety of Drugs and Pharmaceutical Products* (ed. Braimer, D. D.) 265–280 (Elsevier/North-Holland Biomedical, Amsterdam, 1980).
68. Giron, D. *et al.* Solid state characterizations of pharmaceutical hydrates. *J. Thermal Anal. Cal.* **68**, 453–465 (2002).
69. Morris, K. & Rodriguez-Hornedo, N. in *Encyclopaedia of Pharmaceutical Technology* Vol. 7 (eds Swarbrick, J. & Boylan, J. C.) 393–440 (Marcel Dekker, New York, 1993).
70. Florey, K. in *Analytical Profiles of Drug Substances* Vol. 2 (ed. Florey, K.) 1–62 (Academic, New York, 1973).
71. Sugawara, Y., Kamiya, N., Iwasaki, H., Ito, T. & Satow, Y. Humidity controlled reversible structure transition of disodium adenosine 5'-triphosphate between dihydrate and trihydrate in a single crystal state. *J. Am. Chem. Soc.* **113**, 5440–5445 (1991).
72. Sun, C., Zhou, D., Grant, D. J. W. & Young, V. G. Jr. Theophylline monohydrate. *Acta Cryst. E* **58**, O368–O370 (2002).
73. Cox, J. S. G., Woodgard, G. D. & McCrone, W. C. Solid state chemistry of cromolyn sodium (disodium cromoglycate). *J. Pharm. Sci.* **60**, 1458–1465 (1971).
74. Stephenson, G. A. & Diseroad, B. A. Structural relationship and desolvation behaviour of cromolyn cefazolin and fenoprofen sodium hydrates. *Int. J. Pharm.* **198**, 167–177 (2000).
75. Chen, L. R., Young, V. G., Lechuga-Ballesteros, D. & Grant D. J. W. Solid state behavior of cromolyn sodium hydrates. *J. Pharm. Sci.* **88**, 1191–1200 (1999).
76. Zhu, J., Padden, B. E., Munson, E. J. & Grant, D. J. W. Physicochemical characterization of nedocromil bivalent metal salt hydrates. 2. Nedocromil zinc. *J. Pharm. Sci.* **86**, 418–428 (1997).
77. Khankari, R. K., Ojala, W. H., Gleason, W. B. & Grant, D. J. W. Crystal structure of nedocromil sodium heptahemihydrate and its comparison with that of nedocromil sodium trihydrate. *J. Chem. Crystallogr.* **25**, 859–866 (1995).
78. Ahlqvist, M. U. A. & Taylor, L. S. Water dynamics in channel hydrates investigated using H/D exchange. *Int. J. Pharm.* **241**, 253–261 (2002).
79. Li, Z. J. & Grant, D. J. W. Relationship between physical properties and crystal structures of chiral drugs. *J. Pharm. Sci.* **86**, 1073–1078 (1997).
80. Reddy, I. K., Kommuru, T. R., Zaghloul, A. A. & Khan, M. A. Chirality and its implications in transdermal drug development. *Crit. Rev. Ther. Drug Carrier Syst.* **17**, 285–325 (2000).
81. Collet, A. & Vigne-Maeder, F. Increase of the occurrence of spontaneous resolution due to the crystallization of racemates under high pressure. *New J. Chem.* **19**, 877–880 (1995).
82. Jacques, J., Collet, A. & Wilen, S. H. *Enantiomers, Racemates, and Resolutions* 3–213 (John Wiley & Sons, New York, 1981).
83. Burger, A., Rollinger, J. M. & Brueggeller, P. Binary system of (*R*)- and (*S*)-nitrendipine-polymorphism and structure. *J. Pharm. Sci.* **86**, 674–679 (1997).
84. Kuhnert-Brandstaetter, M. & Ulmer, R. Contribution to the thermal analysis of optical antipodes-mandelic acid. *Mikrochim. Acta* **5**, 927–935 (1974).
85. Langhammer, L. Binary systems of enantiomeric nicotine derivatives. *Arch. Pharm.* **308**, 933–939 (1975).
86. Zhang, G. G. Z., Paspal, S. Y. L., Suryanarayanan, R. & Grant, D. J. W. Racemic species of sodium ibuprofen: characterization and polymorphic relationships. *J. Pharm. Sci.* **92**, 1356–1366 (2003).
87. Jacques, J. & Gabard, J. Optical antipode mixtures. III. Solubility diagrams for several types of racemates. *Bull. Soc. Chim. Fr.* **1**, 342–350 (1972).
88. Flack, H. D. Chiral and achiral crystal structure. *Helv. Chim. Acta* **86**, 907–921 (2003).
89. Bel'skii, V. K. & Zorkii, P. M. Distribution of organic homomolecular crystals by chiral types and structural classes. *Acta Cryst.* **A33**, 1004–1006 (1977).
90. Stout, G. H. & Jensen, L. H. *X-Ray Structure Determination: A Practical Guide* 2nd edn (John Wiley & Sons, New York, 1989).
91. Fagan, P. G., Hammond, R. B., Roberts K. J., Docherty, R. & Edmondson, M. in *Crystal Growth of Organic Materials* Third International Workshop on Crystal Growth of Organic Materials Conference (eds Myerson, A., Green, D.A. & Meenan, P.) 22–27 (Oxford Univ. Press, New York, 1996).
92. Jones, P. G. Crystal growing. *Chem. Br.* **17**, 222–225 (1981).
Describes the common methods for growing single crystals.
93. Threlfall, T. L. Analysis of organic polymorphs. a review. *Analyst* **120**, 2435–2460 (1995).
94. Guillory, J. K. in *Polymorphism in Pharmaceutical Solids* (ed. Brittain, H. G.) 183–226 (Marcel Dekker, New York, 1999).
95. Mullin, J. W. *Crystallization* 4th edn (Butterworth–Heinemann, Boston, 2001).
96. Mitchell, C. A., Yu, L. & Ward, M. D. Selective nucleation and discovery of organic polymorphs through epitaxy with single crystal substrate. *J. Am. Chem. Soc.* **123**, 10830–10839 (2001).
97. Hilden, J. L. *et al.* Capillary precipitation of a highly polymorphic organic compound. *Cryst. Growth Des.* **3**, 921–926 (2003).
98. Zaccaro, J., Matic, J., Myerson, A. S. & Garetz, B. A. Nonphotochemical, laser-induced nucleation of supersaturated aqueous glycine produces unexpected γ-polymorph. *Cryst. Growth Des.* **1**, 5–8 (2001).
References 96–98 describe newer methods of generating polymorphs: epitaxy, capillary crystallization and laser-induced nucleation.
99. Beckmann, W., Otto, W. & Budde, U. Crystallization of the stable polymorph of hydroxytriendione: seeding process and effects of purity. *Org. Process Res. Dev.* **5**, 387–392 (2001).
100. Wang, B., Lu, Z. P., Shi, E. W. & Zhong, W. Z. Twinning morphologies and mechanisms of β-BaB2O4 (BBO) crystal grown by TSSG method. *Cryst. Res. Technol.* **33**, 929–935 (1998).
101. Wadhawan, V. K. A tensor classification of twinning in crystals. *Acta Cryst. A* **53**, 546–555 (1997).
102. von Laue, M. Eine quantitative prüfung der theorie für die interferenz-erscheinungen bei röntgenstrahlen. *Sitz. Math. Phys. Klasse Bayer. Akad. Wiss.* 363–373 (1912).
103. Bragg, W. L. Diffraction of short electromagnetic waves by a crystal. *Proc. Cambridge Philos. Soc.* **17**, 43–57 (1913).

UM00014134
NOVARTIS EXHIBIT 1517
Novartis v. Regents, IPR2023-01347
Page 2880 of 4460

104. Giacovazzo, C. *Fundamentals of Crystallography* (Oxford Univ. Press, New York, 2002).
105. Hanh, T. *International Table of Crystallography* Vol. A 5th edn (Kluwer Academic, Dordrecht, 2002).
106. Sayre, D. in *Computational Crystallography* (ed. Sayre, D.) 65–140 (Claredon, Oxford, 1982).
107. Giacovazzo, C. in *International Tables for Crystallography* 2nd edn Vol. B (ed. Shmueli, U.) 210–234 (Kluwer Academic, Dordrecht, 2002).
108. Giacovazzo, C. *Direct Phasing in Crystallography: Fundamentals and Applications* (Oxford Univ. Press, Oxford, 1998).
Explains the most common technique for solving crystal structures from single crystal X-ray diffraction patterns.
109. Kirkpatrick, S., Gelatt, C. D. & Vecchi, M. P. Optimization by simulated annealing. *Science* **220**, 671–680 (1983).
This seminal paper explains the value and the process of simulated annealing.
110. Catlow, C. R. A., Thomas, J. M., Freeman, C. M., Wright, P. A. & Bell, R. G. Simulating and predicting crystal structures. *Proc. R. Soc. Lond. A* **442**, 85–96 (1993).
111. Bond, A. D. & Jones, W. Structure prediction as a tool for solution of the crystal structures of metallo-organic complexes using powder X-ray diffraction data. *Acta Cryst. B* **58**, 233–243 (2002).
112. Gavezzotti, A. & Filippini, G. Polymorphic forms of organic crystals at room conditions: thermodynamic and structural implications. *J. Am. Chem. Soc.* **117**, 12299–12305 (1995).
113. Lommerse, J. P. M. *et al.* A test of crystal structure prediction of small organic molecules. *Acta Cryst. B* **56**, 697–714 (2000).
114. Giovannini, J., Perrin, M. A., Louer, D. & Leveiller, F. *Ab initio* crystal structure determination of three pharmaceutical compounds from X-ray powder diffraction data. *Mater. Sci. Forum* **2**, 582–587 (2001).
115. Bond, A. D., Feeder, N., Teat, S. J. & Jones, W. The solid-state structure of 3-hydroxy-4-methyl-2(3H)-thiazolethione: prediction and measurement. *Tetrahedron* **56**, 6617–6624 (2000).
116. Motherwell, W. D. S. *et al.* Crystal structure prediction of small molecules: a second blind test. *Acta Cryst. B* **58**, 647–661 (2002).
Describes the results from the most recent Cambridge Crystallographic Data Centre (CCDC) workshop for testing the feasibility of the various programs in predicting the crystal structure of three compounds from their individual molecular structures only.
117. Freeman, C. M. & Catlow, C. R. A. Structure predictions in inorganic solids. *J. Chem. Soc. Chem. Comm.* **2**, 89–91 (1992).
118. Gdanitz, R. J. in *Theoretical Aspects and Computer Modeling of the Molecular Solid State* (ed. Gavezzotti, A.) 185–201 (Wiley, Chichester, 1997).
Explains the *ab initio* method of crystal structure prediction.
119. Karfunkel, H. R. & Gdanitz, R. J. *Ab initio* prediction of possible crystal structures for general organic molecules. *J. Comp. Chem.* **13**, 1171–1183 (1992).
120. Smith, E. D. L. *et al.* The determination of the crystal structure of anhydrous theophylline by X-ray powder diffraction with a systematic search algorithm, lattice energy calculations, and ^{13}C and ^{15}N solid-state NMR: a question of polymorphism in a given unit cell. *J. Phys. Chem. B* **105**, 5818–5826 (2001).
121. Ko, G. H. & Fink, W. H. A combined quantum chemistry and classical molecular interaction energy method for the determination of crystal geometries and energies. *J. Chem. Phys.* **116**, 747–754 (2002).
122. Gavezzotti, A. Organic crystals: engineering and design. *Curr. Opin. Solid State Mater. Sci.* **1**, 501–505 (1996).
123. Buttar, D., Charlton, M. H., Docherty, R. & Starbuck, J. Theoretical investigations of conformational aspects of polymorphism. Part 1: o-acetamidobenzamide. *J. Chem. Soc. Perkin Trans. I* **2**, 763–772 (1998).
124. Childs, S. L. *Nonbonded Interactions in Molecular Crystal Structures* (Emory Univ., Atlanta, 2001).
125. Filippini, G., Gavezzotti, A. & Novoa, J. J. Modeling the crystal structure of the 2-hydronitronylnitroxide radical (HNN): observed and computer-generated polymorphs. *Acta Cryst. B* **55**, 543–553 (1999).
126. Gavezzotti, A. Methods and current trends in the simulation and prediction of organic crystal structures. *Nova Acta Leopold.* **79**, 33–46 (1999).
127. Gao, D. W. & Donald, E. Molecular packing groups and *ab initio* crystal-structure prediction. *Acta Cryst. A* **55**, 621–627 (1999).
128. Williams, D. E. I. in *Crystal Engineering: From Molecules and Crystals to Materials* NATO Science Series C Vol. 538 (eds Braga, D., Grepini, F. & Orpen, G. A.) 295–310 (Kluwer Academic, Boston, 1999).
129. Mooij, W. T. M., van Eijck, B. P. & Kroon, J. *Ab initio* crystal structure predictions for flexible hydrogen-bonded molecules. *J. Am. Chem. Soc.* **122**, 3500–3505 (2000).
130. Allen, F. H., Kennard, O. & Taylor, R. Systematic analysis of structural data as a research technique in organic chemistry. *Acc. Chem. Res.* **16**, 146–153 (1983).
131. Sarma, J. A. R. P. & Desiraju, G. R. The supramolecular synthon approach to crystal structure prediction. *Cryst. Growth Des.* **2**, 93–100 (2002).
132. Mooij, W. T. M., van Eijck, B. P. & Kroon, J. Transferable *ab initio* intermolecular potentials. 2. Validation and application to crystal structure prediction. *J. Phys. Chem. A* **103**, 9883–9890 (1999).
133. Leusen, F. J. J. *Ab initio* prediction of polymorphs. *J. Cryst. Growth* **166**, 900–903 (1996).
134. Dong, Z. *et al.* Crystal structure of neotame anhydrate polymorph G. *Pharm. Res.* **19**, 1549–1553 (2002).
135. Chin, D. N. Improving the efficiency of predicting hydrogen-bonded organic molecules. *Trans. Am. Cryst. Assoc.* **33**, 33–43 (1999).
136. Gdanitz, R. J. Prediction of molecular crystal structures by Monte Carlo simulated annealing without reference to diffraction data. *Chem. Phys. Lett.* **190**, 391–396 (1992).
Explains the application of the Monte Carlo method in predicting crystal structures.
137. Hammond, R. B., Roberts, K. J., Docherty, R. & Edmondson, R. B. in *Crystal Growth of Organic Materials* International Workshop 4th edn (ed. Ulrich, J.) 53–60 (Shaker, Aachen, 1997).
138. Hammond, R. B. *et al.* Determining the crystal structures of organic solids using x-ray powder diffraction together with molecular and solid state modeling techniques. *Molecular Crystals and Liquid Crystals Science and Technology A* **356**, 389–405 (2001).
139. Harris, K. D. M. & Tremayne, M. Crystals structure determination from powder diffraction data. *Chem. Mater.* **8**, 2554–2570 (1996).
Explains the prediction of the crystal structure of compounds from their powder diffraction data only.
140. Aakeroy, C. B., Beatty, A. M., Tremayne, M., Rowe, D. M. & Seaton C. C. A combination of X-ray single crystal diffraction and Monte Carlo structure solution from X-ray powder diffraction data in a structural investigation of 5-bromo-nicotinic acid and solvates thereof. *Cryst. Growth Des.* **1**, 377–382 (2001).
141. Will, G. POWLS: a powder least-squares program. *J. Appl. Cryst.* **12**, 483–485 (1979).
142. Pawley, G. S. Unit-cell refinement from powder diffraction scans. *J. Appl. Cryst.* **14**, 357–361 (1981).
143. Langford, J. I. & Louer, D. High-resolution powder diffraction studies of copper (II) oxide. *J. Appl. Cryst.* **24**, 149–155 (1991).
144. Langford, J. I., Cernik, R. J. & Louer, D. The breadth and shape of instrumental line profiles in high-resolution powder diffraction. *J. Appl. Cryst.* **24**, 912–918 (1991).
145. Will, G., Parrish, W. & Huang, T. C. Crystal-structure refinement by profile fitting and least-squares analysis of powder diffractometer data. *J. Appl. Cryst.* **16**, 611–622 (1983).
146. Langford, J. I., Louer, D., Sonneveld, E. J. & Visser, J. W. Applications of total pattern fitting to a study of crystallite size and strain in zinc oxide powder. *Powder Diffract.* **1**, 211–221 (1986).
147. David, W. I. F., Shankland, K. & Shankland, N. Routine determination of molecular crystal structures from powder diffraction data. *Chem. Commun. (Camb.)* **8**, 931–932 (1998).
148. Shankland, K., David, W. I. F. & Csoka, T. Crystal structure determination from powder diffraction data by the application of a genetic algorithm. *Zeit. fuer Kristall.* **212**, 550–552 (1997).
149. Harris, K. D. M., Johnston, R. L. & Kariuki, B. M. The genetic algorithm: foundations and applications in structure solution from powder diffraction data. *Acta Cryst. A* **54**, 632–645 (1998).
Explains the use of the genetic algorithm for predicting the crystal structure of compounds from their powder diffraction pattern.
150. Hammond, R. B., Roberts, K. J., Docherty, R. & Edmondson, M. Computationally assisted structure determination for molecular materials from X-ray powder diffraction data. *J. Phys. Chem. B* **101**, 6532–6536 (1997).
151. Harris, K. D. M., Tremayne, M., Lightfoot, P. & Bruce P. G. Crystal structure determination from powder diffraction data by Monte Carlo methods. *J. Am. Chem. Soc.* **116**, 3543–3547 (1994).
152. Harris, K. D. M., Johnston, R. L., Kariuki, B. M. & Tremayne, M. A genetic algorithm for crystal structure solution from powder diffraction data. *J. Chem. Res. Synop.* **7**, 390–391 (1998).
153. Harris, K. D. M. *et al.* Recent advances in opportunities for solving molecular crystal structures directly from powder diffraction data: new insights in crystal engineering contexts. *Cryst. Eng. Comm.* **4**, 356–367 (2002).
154. Turner, G. W., Tedesco, E., Harris, K. D. M., Johnston, R. L. & Kariuki, B. M. Implementation of Lamarckian concepts in a genetic algorithm for structure solution from powder diffraction data. *Chem. Phys. Lett.* **321**, 183 (2000).
155. Habershon, S., Turner, G. W., Harris, K. D. M., Johnston, R. L. & Johnston, J. M. Gaining insights into the evolutionary behavior in genetic algorithm calculations, with applications in structure solution from powder diffraction data. *Chem. Phys. Lett.* **353**, 185–194 (2002).
156. Lanning, O. J. *et al.* Definition of a 'guiding function' in global optimization: a hybrid approach combining energy and R-factor in structure solution from powder diffraction data. *Chem. Phys. Lett.* **317**, 296–303 (2000).
157. Gilmore, C. Maximum entropy and Bayesian statistics in crystallography: a review of practical applications. *Acta Cryst. A* **52**, 561–589 (1996).
Explains the use of the maximum entropy algorithm for the prediction of the crystal structures of compounds and reviews its application.
158. Gilmore, C. J., Shankland, K. & Bricogne, G. Applications of the maximum entropy method to powder diffraction and electron crystallography. *Proc. R. Soc. Lond. A* **442**, 97–111 (1993).
159. Presented at the fifteenth annual meeting of the National Science Teachers Association, 1966 in New York City, and reprinted from The Physics Teacher Vol. 7, issue 6, 1968, pp. 313–320 by permission of the editor and the author.
160. Braga, D., Desiraju, G. R., Miller, J. S., Guy Orpen, A. & Price, S. Innovation in crystal engineering. *Cryst. Eng. Comm.* **4**, 500–509 (2002).
161. Pepinsky, R. Crystal engineering-new concept in crystallography. *Phys. Rev. II* **100**, 971 (1955).
162. Schmidt, G. M. J. Photodimerization in solid state. *Pure Appl. Chem.* **647**, 647–678 (1971).
163. Panunto, T. W., Lipkowska, Z. U., Johnson, R. & Etter, M. C. Hydrogen-bond formation in nitroanilines: the first step in designing acentric materials. *J. Am. Chem. Soc.* **109**, 7786–7797 (1987).
164. Braga, D. & Fabrizia, G. in *Crystal Engineering: From Molecules and Crystals to Materials* (eds Braga, D., Grepioni, F. & Guy Orpen, A.) 421–441 (Kluwer Academic, Boston, 1999).
Comprehensive work summarizing the recent achievements and future trends in crystal engineering.
165. Desiraju, G. R. Supramolecular synthons in crystal engineering — a new organic synthesis. *Angew. Chem. Int. Edn Eng.* **34**, 2311–2327 (1995)
166. Walsh, R. B. R. D. *et al.* Crystal engineering of the composition of pharmaceutical phases. *Chem. Commun.* **2**, 186–187 (2003).
167. Bis, J. A., Shattock, T. R. & Zaworotko, M. J. Design of binary crystals that contain pharmaceutical molecules. Abstracts of Papers, 225th ACS National Meeting, New Orleans, LA, United States, March 23–27 (2003).
168. McMahon, J. A. & Zaworotko, M. J. Crystal engineering of novel pharmaceutical phases. Abstracts of Papers, 225th ACS National Meeting, New Orleans, LA, United States, March 23–27 (2003).
169. Fleischman, S., Morales, L. A. & Zaworotko, M. J. Crystal engineering of binary crystals that contain pharmaceutical molecules. Abstracts of Papers, 223rd ACS National Meeting, Orlando, FL, United States, April 7–11 (2002).
170. Remenar, J. F. *et al.* Crystal engineering of novel cocrystals of a triazole drug with 1,4-dicarboxylic acids. *J. Am. Chem. Soc.* **125**, 8456–8457 (2003).
171. Payne, R. S., Roberts, R. J. & Rowe, R. C. The mechanical properties of two forms of primidone predicted from their crystal structures. *Int. J. Pharm.* **145**, 165–173 (1996).
172. Roberts, R. J., Payne, R. S. & Rowe, R. C. Mechanical property predictions for polymorphs of sulphathiazole and carbamazepine. *Eur. J. Pharm. Sci.* **9**, 277–283 (2000).
173. Roberts, R. J., Rowe, R. C. & Kendall, K. Brittle–ductile transitions in die compaction of sodium chloride. *Chem. Eng. Sci.* **44**, 1647–1651 (1989).
174. Roberts, R. J. & Rowe, R. C. Determination of the critical stress intensity factor (KIC) of microcrystalline cellulose using radially edge-cracked tablets. *Int. J. Pharm.* **52**, 213–219 (1989).

UM00014135
NOVARTIS EXHIBIT 1517
Novartis v. Regents, IPR2023-01347
Page 2881 of 4460

175. Bassam, F., York, P., Rowe, R. C. & Roberts, R. J. Young's modulus of powders used as pharmaceutical excipients. *Int. J. Pharm.* **64**, 55–60 (1990).
176. Roberts, R. J., Rowe, R. C. & York, P. The relationship between Young's modulus of elasticity of organic solids and their molecular structure. *Powder Technol.* **65**, 139–146 (1991).
177. Nangia, A. Database research in crystal engineering. *Cryst. Eng. Comm.* **4**, 93–101 (2002).
178. Gavezzotti, A. Ten years of experience in polymorph prediction: what next? *Cryst. Eng. Comm.* **4**, 343–347 (2002).
179. Rohl, A. L. Computer prediction of crystal morphology. *Curr. Opin. Solid State Mater. Sci.* **7**, 21–26 (2003).
180. Rajeswaran, M. *et al.* Three-dimensional structure determination of N-(p-tolyl)-dodecylsulfonamide from powder diffraction data and validation of structure using solid-state NMR spectroscopy. *J. Am. Chem. Soc.* **124**, 14450–14459 (2002).
181. Tishmack, P. A., Bugay, D. E. & Byrn, S. R Solid-state nuclear magnetic resonance spectroscopy — pharmaceutical applications. *J. Pharm. Sci.* **92**, 441–474 (2003).
182. Reutzel-Edens, S. M. & Bush, J. K. Solid-state NMR spectroscopy of small molecules: from NMR crystallography to the characterization of solid oral dosage forms. *Am. Pharm. Rev.* **5**, 112–115 (2002).
183. Bugay, D. E. Characterization of the solid-state:spectroscopic techniques. *Adv. Drug Del. Rev.* **48**, 43–65 (2001).
184. Taylor, L. S. & Langkilde, F. W. Evaluation of solid-state forms present in tablets by Raman spectroscopy. *J. Pharm. Sci.*, **89**, 1342–1353 (2000).
185. Kempf, D. J. *et al.* ABT-538 is a potent inhibitor of human immunodeficiency virus protease and has high oral bioavailability in humans. *Proc. Natl Acad. Sci. USA* **92**, 2484–2488 (1995).
186. Chemburkar, S. R. *et al.* Dealing with the impact of ritonavir polymorphs on the late stages of bulk drug process development. *Org. Process Res. Dev.* **4**, 413–417 (2000).
187. Young, A. *The Rietveld Method* International Union of Crystallography (Oxford Univ. Press, New York, 1993). **Explains the Rietveld refinement method in detail.**
188. McCusker, L. B., von Dreele, R. B., Cox, D. E., Louer, D. & Scardi, P. Rietveld refinement guidelines. *J. Appl. Cryst.* **32**, 36–50 (1999).
189. Stephenson, G. A. & Young, R. Potential applications of Rietveld analysis in the pharmaceutical industry. *Am. Pharm. Rev.* **4**, 46–51 (2001).
190. Kisi, E. H. Rietveld analysis of powder diffraction patterns. *Mater. Forum* **18**, 135–153 (1994).
191. Rietveld, H. M. Profile refinement method for nuclear and magnetic structures. *J. Appl. Cryst.* **2**, 65–71 (1969).

Acknowledgement
We thank A. Sheth for kindly reviewing the manuscript and for his valuable suggestions.

Competing interest statement
The authors declare that they have no competing financial interests.

Online links

FURTHER INFORMATION
Cambridge Crystallographic Data Centre: http://www.ccdc.cam.ac.uk/
International Union of Crystallography: http://www.iucr.org/
Access to this interactive links box is free online.

UM00014136
NOVARTIS EXHIBIT 1517
Novartis v. Regents, IPR2023-01347
Page 2882 of 4460

J|A|C|S
ARTICLES
Published on Web 09/24/2004

Crystal Engineering Approach To Forming Cocrystals of Amine Hydrochlorides with Organic Acids. Molecular Complexes of Fluoxetine Hydrochloride with Benzoic, Succinic, and Fumaric Acids

Scott L. Childs,*,† Leonard J. Chyall,‡ Jeanette T. Dunlap,‡ Valeriya N. Smolenskaya,‡ Barbara C. Stahly,‡ and G. Patrick Stahly‡

SSCI, Inc., 3065 Kent Avenue, West Lafayette, Indiana 47906, and Design Science Research, LLC, 1256 Briarcliff Road, Atlanta, Georgia 30306

Received April 1, 2004; E-mail: scott@design-science.info

Abstract: A crystal engineering strategy for designing cocrystals of pharmaceuticals is presented. The strategy increases the probability of discovering useful cocrystals and decreases the number of experiments that are needed by selecting API:guest combinations that have the greatest potential of forming energetically and structurally robust interactions. Our approach involves multicomponent cocrystallization of hydrochloride salts, wherein strong hydrogen bond donors are introduced to interact with chloride ions that are underutilized as hydrogen bond acceptors. The strategy is particularly effective in producing cocrystals of amine hydrochlorides with neutral organic acid guests. As an example of the approach, we report the discovery of three cocrystals containing fluoxetine hydrochloride (**1**), which is the active ingredient in the popular antidepressant Prozac. A 1:1 cocrystal was prepared with **1** and benzoic acid (**2**), while succinic acid and fumaric acid were each cocrystallized with **1** to provide 2:1 cocrystals of fluoxetine hydrochloride:succinic acid (**3**) and fluoxetine hydrochloride:fumaric acid (**4**). The presence of a guest molecule along with fluoxetine hydrochloride in the same crystal structure results in a solid phase with altered physical properties when compared to the known crystalline form of fluoxetine hydrochloride. On the basis of intrinsic dissolution rate experiments, cocrystals **2** and **4** dissolve more slowly than **1**, and **3** dissolves more quickly than **1**. Powder dissolution experiments demonstrated that the solid present at equilibrium corresponds to the cocrystal for **2** and **4**, while **3** completely converted to **1** upon prolonged slurry in water.

Introduction

An important part of the drug development process involves devising a method for delivering the active pharmaceutical ingredient (API). Most APIs are crystalline solids at room temperature and are commonly delivered as a solid oral dosage form such as a tablet. The efficacy of the drug is often dependent on the physical properties of the dosage form, and it is well-established that different solid forms of the same compound have different chemical and physical properties.[1] When improvements in the properties of the API are needed, pharmaceutical scientists often evaluate different solid forms of the API. For an ionizable API, a common approach involves the generation and testing of different salt forms. Salts can effectively provide improved stability, solubility, and crystallinity of the API. Different crystalline polymorphs, hydrates, solvates, and amorphous forms of the API can also provide property improvements, although they are not used as often as salts.

Cocrystallization offers another option that has enormous potential to provide new, stable structures that may improve the properties of an API.[2] A cocrystal is a molecular complex that contains two or more different molecules in the same crystal lattice. Cocrystallization has been underutilized in the pharmaceutical industry, despite the many years API cocrystals have been known.[3-5] However, interest in the subject has grown recently, and a number of new binary cocrystals of APIs have been reported,[6] although in many cases the guest molecules are not pharmaceutically acceptable.

Through a crystal engineering approach, we have developed a method of obtaining multicomponent cocrystals of amine hydrochloride APIs using pharmaceutically acceptable compounds as guests. There is a special and significant opportunity for effective cocrystal formation with amine hydrochlorides that has not been previously recognized. The chloride ion is one of the most preferred anions for salts of cationic APIs. It has been estimated that approximately half of the salts of cationic drugs are marketed as hydrochloride salts.[7] Cocrystallizing the hydrochloride salt of an API presents an opportunity to alter the physical properties of the solid dosage form while simulta-

† Design Science Research, LLC.
‡ SSCI, Inc.

(1) (a) Curatolo, W. *Pharm. Sci. Technol. Today* **1998**, *1*, 387–393. (b) Huang, L. F.; Tong, W. Q. *Adv. Drug Delivery Rev.* **2004**, *56*, 321–334. (c) Bastin, R. J.; Bowker, M. J.; Slater, B. J. *Org. Process Res. Dev.* **2000**, *4*, 427–435. (d) Morris, K. R.; Fakes, M. G.; Thakur, A. B.; Newman, A. W.; Singh, A. K.; Venit, J. J.; Spagnuolo, C. J.; Serajuddin, A. T. M. *Int. J. Pharm.* **1994**, *105*, 209–217.

(2) (a) Datta, S.; Grant, D. J. W. *Nat. Rev. Drug Discov.* **2004**, *3*, 42–57. (b) Rodriguez-Spong, B.; Price, C. P.; Jayasankar, A.; Matzger, A. J.; Rodriguez-Hornedo, N. *Adv. Drug Delivery Rev.* **2004**, *56*, 241–274.

10.1021/ja048114o CCC: $27.50 © 2004 American Chemical Society

UM00014137
NOVARTIS EXHIBIT 1517
Novartis v. Regents, IPR2023-01347
Page 2883 of 4460

neously retaining the hydrochloride salt of the API in the crystal structure. This methodology is illustrated by the rational synthesis, structural characterization, and dissolution properties of three cocrystals of fluoxetine hydrochloride, which is the API in the popular antidepressant Prozac.

Experimental Section

Fluoxetine hydrochloride (**1**) was obtained from the U.S. Pharmacopeia and used as received. Solvents and reagents were obtained from various commercial suppliers and used as received.

X-ray powder diffraction (XRPD) analyses were carried out on a Shimadzu XRD-6000 diffractometer using Cu Kα radiation. The instrument is equipped with a long fine focus X-ray tube. The tube voltage and amperage were set to 40 kV and 40 mA, respectively. The divergence and scattering slits were set at 1°, and the receiving slit was set at 0.15 mm. Diffracted radiation was detected by a NaI scintillation detector. A $\theta-2\theta$ continuous scan at 3°/min (0.4 s/0.02° step) from 2.5 to 40° 2θ was used. Samples were packed into silicon sample holders. The peak position calibration was verified using a silicon reference standard.

Differential scanning calorimetry (DSC) analyses were carried out on a TA Instruments 2920 differential scanning calorimeter. Each sample was placed into a hermetically sealed aluminum DSC pan containing a pinhole. The sample cell was equilibrated at 25 °C and then heated under a nitrogen purge at a rate of 10 °C/min. Indium metal was used as the calibration standard. Thermogravimetric analyses (TGA) were performed using a TA Instruments Model 2950 thermogravimetric analyzer. Nickel and Alumel were used as the calibration standards. Samples were heated in either aluminum or platinum pans under a stream of nitrogen at rate of 10 °C/min.

Raman spectroscopic analyses were carried out on a Thermo Nicolet 960 spectrometer equipped with an indium gallium arsenide (InGaAs) detector. An excitation wavelength of 1064 nm and approximately 0.4 W of Nd:YVO_4 laser power were used. Each sample was analyzed in a 5 mm diameter glass tube. A total of 256 scans were collected from 3600 to 100 cm^{-1} at a spectral resolution of 4 cm^{-1}. Wavelength calibration was performed using sulfur and cyclohexane.

Moisture sorption/desorption data were collected on a VTI SGA-100 Vapor Sorption Analyzer over a range of 5−95% relative humidity (RH) at 10% RH intervals under a nitrogen purge. Samples were not dried prior to analysis. Equilibrium criteria used for analysis were less than 0.0100% weight change in 5 min. Sodium chloride and poly(vinylpyrrolidone) were used as calibration standards.

Ultraviolet (UV) analyses were carried out on a Beckman-Coulter DU-640 spectrophotometer. The wavelength accuracy of this instrument was verified by calibration with a holmium oxide standard. The photometric accuracy of the instrument was verified by measuring the intensity of the light at the detector when filters of known optical density were placed in the path of the beam. Samples were analyzed in 1 cm cells at 227 nm.

Fluoxetine Hydrochloride Benzoic Acid 1:1 Molecular Complex (2). Fluoxetine hydrochloride (5.00 g, 14.5 mmol) and benzoic acid (1.76 g, 14.4 mmol) were dissolved in 50 mL of acetonitrile with warming. The solution was placed into an open evaporating dish under ambient conditions and allowed to evaporate to a volume of approximately 5 mL. Crystals were isolated by filtration and allowed to dry in the air to give 5.40 g (80% yield) of **2**. Crystals suitable for single-crystal X-ray analysis were obtained by allowing a saturated acetonitrile solution to slowly evaporate.

Fluoxetine Hydrochloride Succinic Acid 2:1 Molecular Complex (3). Fluoxetine hydrochloride (5.00 g, 14.5 mmol) and succinic acid (0.85 g, 7.2 mmol) were dissolved in 55 mL of acetonitrile with warming. The solution was placed into an open evaporating dish under ambient conditions and allowed to evaporate to a volume of approximately 4 mL. Crystals were isolated by filtration and allowed to dry in the air to give 5.40 g (92% yield) of **3**. Crystals suitable for single-crystal X-ray analysis were obtained by seeding a saturated acetonitrile solution and allowing it to evaporate slowly at room temperature.

Fluoxetine Hydrochloride Fumaric Acid 2:1 Molecular Complex (4). Fluoxetine hydrochloride (6.00 g, 17.4 mmol) and fumaric acid (1.01 g, 8.7 mmol) were dissolved in 20 mL of ethanol with warming. The solution was filtered through a 0.2 μm nylon filter, concentrated to a volume of about 8 mL, and cooled in an ice bath for 6 h. The crystals were isolated by filtration and allowed to dry in the air to give 5.74 g (82% yield) of **4**. Crystals suitable for single-crystal X-ray analysis were obtained by allowing a saturated ethanol solution to evaporate slowly at room temperature.

Single-Crystal X-ray Diffraction. Suitable crystals of **2**−**4** were coated with Paratone N oil, suspended in small fiber loops. Crystals of **2** and **3** were placed in a cooled nitrogen gas stream at 100 K on a Bruker D8 APEX CCD sealed-tube diffractometer with graphite-monochromated Mo Kα (0.710 73 Å) radiation, while a crystal of **4** was placed in a cooled nitrogen gas stream at 100 K on a Bruker D8 SMART 1000 CCD sealed-tube diffractometer with graphite-monochromated Cu Kα (1.54178 Å) radiation. Data were measured using a

(3) Examples of API:guest cocrystals are as follows. (a) CSD refcode LABZUJ: Prasad, G. S.; Vijayan, M. *Acta Crystallogr., Sect. B: Struct. Commun.* **1993**, *49*, 348−356. (b) CSD refcode TOPPNP: Aoki, K.; Ichikawa, T.; Koinuma, Y.; Iitaka, Y. *Acta Crystallogr., Sect. B: Struct. Commun.* **1978**, *34*, 2333−2336. (c) CSD refcode ZAYLOA: Zaitu, S.; Miwa, Y.; Taga, T. *Acta Crystallogr., Sect. C: Cryst. Struct. Commun.* **1995**, *51*, 1857−1859. (d) CSD refcode ZEXTIF: Zaitu, S.; Miwa, Y.; Taga, T. *Acta Crystallogr., Sect. C: Cryst. Struct. Commun.* **1995**, *51*, 2390−2392. (e) CSD refcode GEYSAE: Patel, U.; Haridas, M.; Singh, T. P. *Acta Crystallogr., Sect. C: Cryst Struct. Commun.* **1988**, *44*, 1264−1267. (f) CSD refcode VUGMOZ: Caira, M. R. *J. Crystallogr. Spectrosc. Res.* **1992**, *22*, 193−200. (g) CSD refcode PEQBES: Krajewski, K.; Ciunik, Z. *Pol. J. Chem.* **1999**, *73*, 1687−1696. (h) CSD refcode SAGQEW: Caira, M. R.; Dekker, T. G.; Liebenberg, W. *J. Chem. Crystallogr.* **1998**, *28*, 11−15. (i) CSD refcode JATMEW: Ishida, T.; In, Y.; Doi, M.; Inoue, M. *Acta Crystallogr., Sect. B: Struct. Commun.* **1989**, *45*, 505−512. (j) CSD refcode SOSBAD: van Roey, P.; Bullion, K. A.; Osawa, Y.; Browne L. J.; Bowman R. M.; Braun D. G. *J. Enzyme Inhib. Med. Chem.* **1991**, *5*, 119−226. (k) CSD refcode LOKRAE: Krajewski, K.; Ciunik, Z. *Pol. J. Chem.* **1999**, *73*, 1687−1696. (l) CSD refcode TAJVOP: van Roey, P.; Bullion, K. A.; Osawa, Y.; Bowman, R. M.; Braun, D. G. *Acta Crystallogr., Sect. C: Cryst. Struct. Commun.* **1991**, *47*, 1015−1018.

(4) Examples of API:API cocrystals are as follows. (a) CSD refcode THOPBA: Nakao, S.; Fujii, S.; Sakaki, T.; Tomita, K. I. *Acta Crystallogr., Sect. B: Struct. Commun.* **1977**, *33*, 1373−1378. (b) CSD refcode VIGVOW: Ghosh, M.; Basak, A. K.; Mazumdar, S. K.; Sheldrick, B. *Acta Crystallogr., Sect. C: Cryst. Struct. Commun.* **1991**, *47*, 577−580. (c) CSD refcode BIGCUP: Shimizu, N.; Nishigaki, S.; Nakai, Y.; Osaki, K. *Acta Crystallogr., Sect. B: Struct. Commun.* **1982**, *38*, 2309−2311. (d) CSD refcode HEKRUK: Giuseppetti, G.; Tadini, C.; Bettinetti, G. P. *Acta Crystallogr., Sect. C: Cryst. Struct. Commun.* **1994**, *50*, 1289−1291. (e) CSD refcode RASSUZ: Bettinetti, G.; Sardone, N. *Acta Crystallogr., Sect. C: Cryst. Struct. Commun.* **1997**, *53*, 594−597. (f) CSD refcode RIWLOY: Sardone, N.; Bettinetti, G.; Sorrenti, M. *Acta Crystallogr., Sect. C: Cryst. Struct. Commun.* **1997**, *53*, 1295−1299. (g) CSD refcode QQQEYV10: Patel, U.; Singh, T. P. *Indian J. Phys., A* **1985**, *59*, 185. (h) CSD refcode APYSAL: Singh, T. P.; Vijayan, M. *Acta Crystallogr., Sect. B: Struct. Commun.* **1974**, *B30*, 557−562.

(5) (a) Bettis, J. W.; Lach, J. L.; Hood, J. *Am. J. Hosp. Pharm.* **1973**, *30*, 240−243. (b) Amos, J. G.; Indelicato, J. M.; Pasini, C. E.; Reutzel, S. M. U.S. Patent 5,412,094, May 2, 1995. (c) *The Merck Index*, 13th ed.; O'Neil, M. J., Ed.; Merck: Whitehouse Station, NJ, 2001; p 325. (d) Bartoszak-Adamska, E.; Wojciechowski, G.; Jaskolski, M.; Brzezinski, B. *J. Mol. Struct.* **2001**, *595*, 21−28. (e) Sangster, J. *J. Phys. Chem. Ref. Data* **1999**, *28*, 889−930.

(6) (a) Walsh, R. D. B.; Bradner, M. W.; Fleischman, S.; Morales, L. A.; Moulton, B.; Rodriguez-Hornedo, N.; Zaworotko, M. J. *Chem. Commun.* **2003**, 186−187. (b) Oswald, I. D. H.; Allan, D. R.; McGregor, P. A.; Motherwell, W. D. S.; Parsons, S.; Pulham, C. R. *Acta Crystallogr., Sect. B* **2002**, *58*, 1057−1066. (c) Bettinetti, G.; Caira, M. R.; Callegari, A.; Merli, M.; Sorrenti, M.; Tadini, C. *J. Pharm. Sci.* **2000**, *89*, 478−489. (d) Oguchi, T.; Tozuka, Y.; Hanawa, T.; Mizutani, M.; Sasaki, N.; Limmatvapirat, S.; Yamamoto, K. *Chem. Pharm. Bull.* **2002**, *50*, 887−891. (e) Remenar, J. F.; Morissette, S. L.; Peterson, M. L.; Moulton, B.; MacPhee, J. M.; Guzman, H. R.; Almarsson, O. *J. Am. Chem. Soc.* **2003**, *125*, 8456−8457. (f) Fleischman, S. G.; Kuduva, S. S.; McMahon, J. A.; Moulton, B.; Walsh, R. D. B.; Rodriguez-Hornedo, N.; Zaworotko, M. J. *Cryst. Growth Des.* **2003**, *3*, 909−919. (g) Oswald, I. D. H.; Motherwell, W. D. S.; Parsons, S.; Pulham, C. R. *Acta Crystallogr., Sect. E: Struct. Rep. Online* **2002**, *58*, 1290−1292.

(7) Stahl, P. H., Wermuth, C. G., Eds. *Handbook of Pharmaceutical Salts: Properties, Selection, and Use*; Wiley: Weinheim, Germany, 2002.

UM00014138
NOVARTIS EXHIBIT 1517
Novartis v. Regents, IPR2023-01347
Page 2884 of 4460

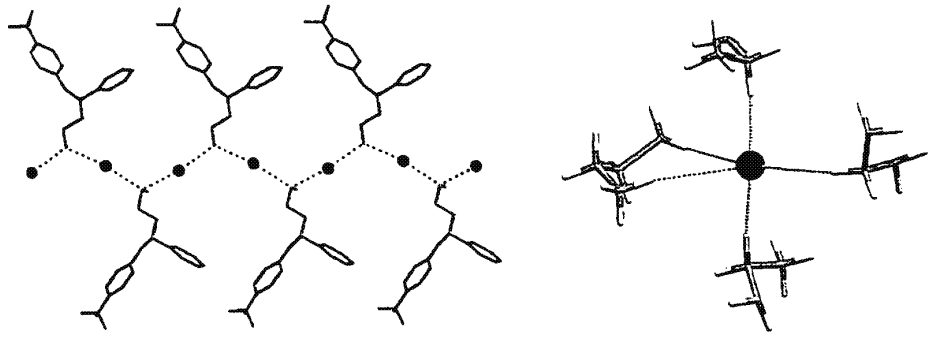


Figure 1. (Left) One-dimensional rod dominant hydrogen bonding motif in the structure of **1**. (Right) Coordination sphere around the chloride ion in **1**, shown with normalized N−H···Cl⁻ and C−H···Cl⁻ distances up to 2.8 Å.

series of combinations of ψ and ω scans with 10 s frame exposures and 0.3° frame widths. Data collection, indexing, and initial cell refinements were all carried out using SMART[8] software. Frame integration and final cell refinements were done using SAINT[9] software. The SADABS[10] program was used to carry out absorption corrections.

The structures were solved using direct methods and difference Fourier techniques (SHELXTL version 5.10).[11] Hydrogen atoms were placed at their expected chemical positions using the HFIX command and were included in the final cycles of least squares with isotropic U_{ij}'s related to the atom's ridden upon. The C−H distances were fixed at 0.93 Å (aromatic and amide), 0.98 Å (methine), 0.97 Å (methylene), and 0.96 Å (methyl). All non-hydrogen atoms were refined anisotropically. Scattering factors and anomalous dispersion corrections are taken from ref 12. Structure solution and refinement were performed by using SHELXTL version 5.10 software. Additional details of data collection and structure refinement are given in Table 2.

Dissolution Experiments. Concentrations of fluoxetine hydrochloride in water were determined by UV spectrophotometry at 227 nm. For experiments involving compounds **1**, **3**, and **4**, absorbance values were related to solution concentrations using a calibration curve for **1** ($\epsilon_{227} = 1.23 \times 10^4$ M^{-1}). This was possible since succinic acid and fumaric acid do not absorb at 227 nm and, therefore, did not interfere with determination of the concentration of **1**. Since benzoic acid absorbs at 227 nm, absorbance values for **2** were related to solution concentrations using a calibration curve for **2** ($\epsilon_{227} = 2.06 \times 10^4$ M^{-1}).

For powder dissolution studies of **1**−**4** the starting solids were sieved using ASTM standard mesh sieves to provide samples with approximate particle size ranges of 53−150 μm. In each experiment, a flask containing 30 mL of water was equilibrated at 20.0 °C in a constant-temperature bath. Approximately 800 mg of sample was added to the flask, and the resulting slurry was stirred at 144 rpm using an overhead stirrer equipped with a poly(tetrafluoroethylene) paddle. At each time interval an aliquot of the slurry was withdrawn from the flask and filtered through a 0.2 μm nylon filter. A 0.50 mL portion of the filtered aliquot was diluted to 50.0 mL with water, and a 1.00 mL portion of the diluted solution was then diluted to 10.0 mL with water to provide a total dilution factor of 1000. After the last aliquot was collected, the remaining solids were collected by vacuum filtration, vacuum-dried, and analyzed by XRPD.

(8) SMART, Version 5.624; Bruker AXS, Inc., Analytical X-ray Systems, 5465 East Cheryl Parkway, Madison, WI 53711-5373, 2000.
(9) SAINT, Version 6.02; Bruker AXS, Inc., Analytical X-ray Systems, 5465 East Cheryl Parkway, Madison, WI 53711-5373, 2000.
(10) Sheldrick, G. M. SADABS, Version 2.03; University of Göttingen, Göttingen, Germany, 2001.
(11) SHELXTL, Version 5.10; Bruker AXS, Inc., Analytical X-ray Systems, 5465 East Cheryl Parkway, Madison, WI 53711-5373, 2000.
(12) Wilson, A. J. C., Ed. *International Tables for X-ray Crystallography*; Kluwer Academic: Dordrecht, The Netherlands, 1992; Vol. C, Tables 6.1.1.4 (pp 500−502) and 4.2.6.8 (pp 219−222).

Table 1. Hydrogen Bond Distances and Angles to the Chloride Ion in **1**[a]

atom–H···atom	atom–H (Å)	H···atom (Å)	atom···atom (Å)	atom–H···atom (deg)
N(1)−H(10)···Cl(1)	1.009	2.092	3.099	175.3
N(1)−H(11)···Cl(1)	1.009	2.117	3.115	169.6
C(2)−H(4)···Cl(1)	1.083	2.693	3.773	175.2
C(10)−H(14)···Cl(1)	1.083	2.756	3.818	166.7
C(1)−H(2)···Cl(1)	1.083	2.769	3.819	163.4

[a] Values are determined using normalized hydrogen distances (N−H = 1.009 Å and C−H = 1.083 Å).

A modified Wood apparatus[17b] was used for intrinsic dissolution experiments. About 200 mg of each sample was compressed into a 0.50 cm^2 disk using a hydraulic press at a nominal gauge pressure of 10 000 psig for 5 min. The disk was compressed to provide a flat surface at one end of the die, and the other end of the die was sealed. A jacketed vessel of about 10 cm internal diameter and 22 cm depth was charged with approximately 1000 mL of an accurately weighed amount of water. The flask was chilled with a circulating bath to provide a water temperature of 10.0 °C, and the assembly containing the compressed sample was placed at the bottom of the vessel with the sample pointing upward. A USP standard paddle was positioned 25 mm above the die, and the solution was stirred at 300 rpm. At each time interval a 6.0 mL aliquot of the solution was withdrawn from the flask and filtered through a 0.2 μm nylon filter. Certain aliquots that were collected toward the end of the run were further diluted with water prior to UV analysis. The linear region of the plot of amount of material dissolved vs time was used to determine the intrinsic dissolution rates, expressed in (mmol of fluoxetine HCl) cm^{-2} min^{-1}.

Results and Discussion

Our strategy is to use the chloride ion as an anchor in the construction of multicomponent amine hydrochloride:guest cocrystals. The exceptional ability of the chloride ion to act as a hydrogen bond acceptor is the key to the approach. In the crystal structure of an amine hydrochloride salt, a charge-assisted hydrogen bond will almost invariably form between the amine cation and the chloride ion. Steiner has noted that "if the cation is capable of donating hydrogen bonds, X−H···Hal$^-$ hydrogen bonds are normally formed and constitute one of the largest contributors to crystal stability."[13] In addition, chloride ions may form hydrogen bonds to weaker, neutral hydrogen bond donors available in the system. These neutral donors play a role in the chloride coordination sphere. For example, when a stronger

(13) Steiner, T. *Acta Crystallogr., Sect. B* **1998**, *54*, 456−463.

UM00014139
NOVARTIS EXHIBIT 1517
Novartis v. Regents, IPR2023-01347
Page 2885 of 4460

Table 2. Crystallographic Data for Cocrystals 2–4

	2	3	4
empirical formula	$C_{24}H_{25}ClF_3NO_3$	$C_{38}H_{44}Cl_2F_6N_2O_6$	$C_{38}H_{42}Cl_2F_6N_2O_6$
formula wt	467.90	809.06	807.64
temp, K	100(2)	100(2)	100(2)
wavelength, Å	0.710 73	0.710 73	1.541 78
cryst syst	monoclinic	orthorhombic	orthorhombic
space group	$P2_1/n$	*Pbcn*	*Pbcn*
unit cell dimens			
a, Å	14.806(5)	26.620(2)	26.691(8)
b, Å	13.179(4)	7.2147(7)	7.1907(3)
c, Å	24.417(7)	20.8315(19)	20.6546(7)
α, deg	90	90	90
β, deg	97.738(13)	90	90
γ, deg	90	90	90
V, Å^3	4721(2)	4000.8(6)	3958.7(2)
Z	8	4	4
calcd density, Mg/m^3	1.317	1.344	1.355
abs coeff, mm^{-1}	0.210	0.236	2.130
F(000)	1952	1688	1680
cryst size, mm^3	0.47 × 0.15 × 0.10	0.21 × 0.18 × 0.09	0.20 × 0.14 × 0.08
θ range for data collecn, deg	1.52–33.07	1.53–27.50	3.31–58.93
index ranges	$-22 \le h \le 22$, $-20 \le k \le 20$, $-37 \le l \le 37$	$-34 \le h \le 34$, $-9 \le k \le 9$, $-26 \le l \le 27$	$-24 \le h \le 29$, $-7 \le k \le 7$, $-21 \le l \le 22$
no. of rflns collected	82 494	37 123	15 698
no. of indep rflns	17 030 (R(int) = 0.0751)	4600 (R(int) = 0.0748)	2823 (R(int) = 0.1693)
completeness to θ = 33.07°, %	95.0	100.0	99.7
abs cor	semiempirical from equivalents	semiempirical from equivalents	none
refinement method	full-matrix least squares on F^2	full-matrix least squares on F^2	full-matrix least squares on F^2
no. of data/restraints/params	17 030/0/603	4600/0/257	2823/0/257
goodness of fit on F^2	1.052	1.195	1.004
final R indices ($I > 2\sigma(I)$)	R1 = 0.0852, wR2 = 0.1930	R1 = 0.0767, wR2 = 0.1855	R1 = 0.0470, wR2 = 0.0927
R indices (all data)	R1 = 0.1330, wR2 = 0.2165	R1 = 0.0892, wR2 = 0.1928	R1 = 0.0941, wR2 = 0.1202
largest diff peak and hole, e Å^{-3}	2.574 and −0.689	0.432 and −0.662	0.561 and −0.747

donor is not available, the ubiquitous C–H donors will often occupy available acceptor sites on the chloride ion.[14] In systems with only a few strong hydrogen bond donors, the hydrogen bond accepting ability of the chloride ion will often be underutilized, and the addition of another strong hydrogen bond donor guest molecule can be accommodated, often by displacing one of the weaker C–H···Cl$^-$ interactions. In comparison to other hydrogen bond acceptors, the chloride ion has several distinct attributes. It is able to accommodate different combinations and numbers of weak and strong hydrogen bond donors, the point location of the negative charge allows it to be placed on symmetry elements such as inversion centers, and its malleable geometric preferences allow it to adopt a variety of hydrogen bonding geometries.

The application of the crystal engineering strategy of combining an amine hydrochloride salt with an additional neutral, strong hydrogen bond donor molecule is demonstrated using fluoxetine hydrochloride as the model API. This approach is expected to be applicable to a variety of pharmaceuticals, because a large percentage of APIs are capable of existing as crystalline hydrochloride salts. For fluoxetine hydrochloride (**1**) only one crystalline phase is known, which is a water- and solvent-free structure.[15] To evaluate the potential for cocrystallization, the structure of **1** was analyzed in terms of the relative strengths of the available hydrogen bond donors and acceptors. The strongest hydrogen bonds in **1**, which are those between the protonated amine donor and the chloride acceptor, form a one-dimensional network (Figure 1). The next strongest donors available are the C–H groups. These form weak hydrogen bonds and complete the nonbonded coordination sphere around the chloride ion (nonbonded distances in Table 1). The chloride ion is an underutilized hydrogen bond acceptor in **1** and may be considered as the focus of attempts to disrupt the homomeric crystal of **1** in favor of a cocrystal by displacing the weak C–H···Cl$^-$ interactions with stronger interactions involving the intended guest molecule.

Of the available pharmaceutically acceptable guest candidates, neutral carboxylic acids stand out as having the best ability to hydrogen bond with chloride ions.[16] We therefore investigated cocrystal formation between fluoxetine hydrochloride and selected pharmaceutically acceptable carboxylic acids. Three cocrystals were isolated. They are cocrystals of **1** with benzoic acid (1:1) (**2**), succinic acid (2:1) (**3**), and fumaric acid (2:1) (**4**). The structure of each cocrystal was determined by single-crystal X-ray diffraction. The relevant crystallographic data are displayed in Table 2. Note that the relative amount of fluoxetine hydrochloride for each cocrystal is high on a weight percent basis: **2**, 74%; **3**, 85%; **4**, 85%. The expected carboxylic acid to chloride hydrogen bond is present in all three structures.

The asymmetric unit of cocrystal **2** is shown in Figure 2. Hydrogen bond parameters are shown in Table 3. The central hydrogen-bonding interactions in **2** result in a zero-dimensional aggregate via the association of two fluoxetine hydrochloride and two benzoic acid molecules (Figure 3). All four of the molecules in the aggregate are crystallographically unique, the independent molecules differing mostly in the region of the $-CF_3$ group on the fluoxetine cation. The aggregate is held

(14) (a) Aakeroy, C. B.; Evans, T. A.; Seddon, K. R.; Palinko, I. *New J. Chem.* **1999**, *23*, 145–152. (b) Aullon, G.; Bellamy, D.; Brammer, L.; Bruton, E. A.; Orpen, A. G. *Chem. Commun.* **1998**, 653–654.

(15) Robertson, D. W.; Jones, N. D.; Swartzendruber, J. K.; Yang, K. S.; Wong, D. T. *J. Med. Chem.* **1988**, *31*, 185–189.

(16) Thallypally, P. K.; Nangia, A. *CrystEngComm* **2001**, 27.

UM00014140
NOVARTIS EXHIBIT 1517
Novartis v. Regents, IPR2023-01347
Page 2886 of 4460

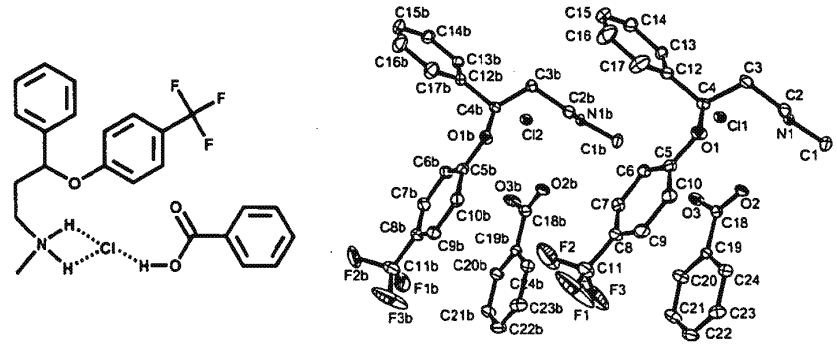


Figure 2. Molecular diagram (left) and ORTEP drawing (right) of the asymmetric unit of **2** (ellipsoids shown at the 50% probability level). Hydrogen atoms have been removed for clarity.

Table 3. Hydrogen Bond Parameters for **2**[a]

atom–H···atom	atom–H (Å)	H···atom (Å)	atom··· atom (Å)	atom–H··· atom (deg)
N(1)–H(1D)···O(2)	0.92	2.10	2.789(3)	130.5
N(1)–H(1D)···Cl(1)	0.92	2.56	3.2352(2)	130.3
N(1)–H(1E)···Cl(2)#1	0.92	2.24	3.149(2)	169.2
O(3)–H(3)···Cl(1)	0.84	2.18	3.0197(18)	177.6
N(1B)–H(1B4)···O(2B)	0.92	2.05	2.760(3)	132.8
N(1B)–H(1B4)···Cl(2)	0.92	2.67	3.326(2)	128.7
N(1B)–H(1B5)···Cl(1)#1	0.92	2.22	3.130(2)	168.8
O(3B)–H(3B3)···Cl(2)	0.84	2.19	3.0281(19)	174.7

[a] Symmetry transformations used to generate equivalent atoms: (#1) $-x+1, -y+1, -z$.

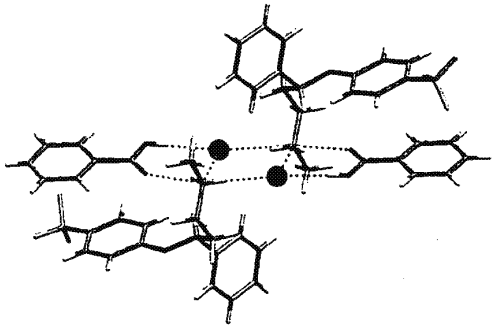


Figure 3. Zero-dimensional aggregate from cocrystal **2**.

together by a cooperative arrangement of N–H···Cl^-, O–H···Cl^-, and N–H···O hydrogen bonds. The aggregates pack (Figure 4) with a combination of van der Waals forces complemented by an aromatic C–H···Cl^- interaction and one activated $-CH_3$···Cl^- interaction.

The asymmetric units of the isostructural cocrystals **3** and **4**, which consist of one complete fluoxetine hydrochloride molecule and half of one succinic (**3**) or fumaric acid (**4**) molecule, are shown in Figures 5 and 6, respectively. Hydrogen bond parameters are shown in Tables 4 and 5, respectively. The carboxylic acid guest in **3** and **4** is located on an inversion center. The protonated amine forms a bifurcated hydrogen bond to both the carbonyl of the acid group and the chloride ion. The other N–H donor forms a hydrogen bond with the chloride, as does the neutral carboxylic acid. Thus, the chloride accepts three strong hydrogen bonds. There is a two-dimensional layer defined by the carboxylic acid to chloride and protonated amine to

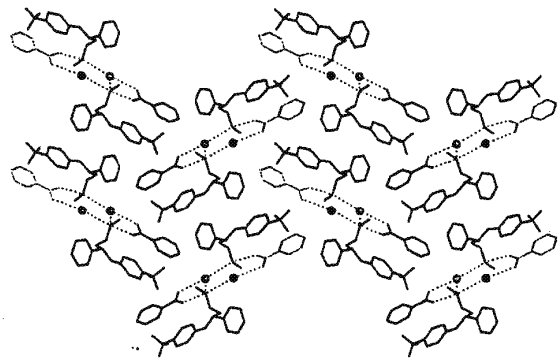


Figure 4. Packing diagram of **2**, with the *bc* plane parallel to the page and symmetry-equivalent molecules shown in solid colors. The fluoxetine cation and the benzoic acid are shown in stick format, and the chloride ions are shown as balls. Hydrogen bonds are shown in blue.

chloride hydrogen bonds (Figure 7). These layers are stacked as shown in Figure 8.

Each cocrystal was characterized using X-ray powder diffraction (XRPD), differential scanning calorimetry (DSC), thermogravimetric analysis (TGA), Raman spectroscopy, and automated moisture sorption/desorption analysis. These data are available in the Supporting Information. The XRPD patterns obtained for each cocrystal were compared to the pattern of the fluoxetine HCl starting material in order to confirm that new solid phases were formed (Figure 9). The Raman spectra also indicated new solid phases. Moisture sorption/desorption experiments showed that each cocrystal is nonhygroscopic, undergoing less than 0.2% weight gain up to 95% relative humidity.

The melt endotherms obtained from the DSC data are shown in Table 6 along with the literature melting points for the corresponding cocrystal components. The melting points of cocrystals **2** and **4** are between the melting points of the pure starting materials (**1** and the acid guest), while the melting point of **3** is lower than that of either component. Although cocrystals **3** and **4** are isostructural, the melting points are quite different. The melting point of **3** is lower than that of either succinic acid or fluoxetine hydrochloride, while the melting point of **4** is higher than that of fluoxetine hydrochloride but lower than that of fumaric acid. The melting points of these two isostructural cocrystals highlight the difficulty in correlating the effect of structural variation with the resulting change in physical properties.

UM00014141
NOVARTIS EXHIBIT 1517
Novartis v. Regents, IPR2023-01347
Page 2887 of 4460

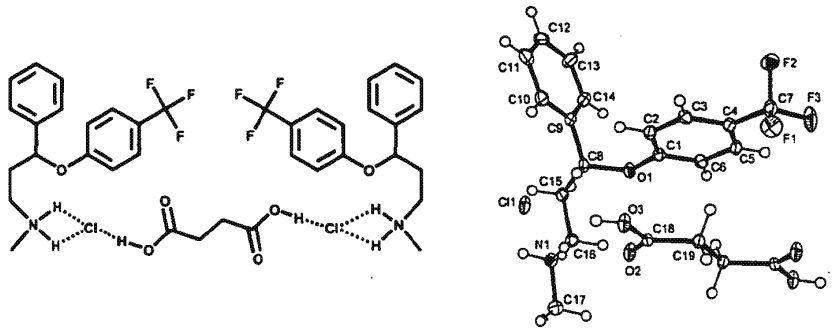


Figure 5. Molecular diagram (left) and ORTEP drawing (right) of the asymmetric unit of **3** (ellipsoids shown at the 50% probability level).

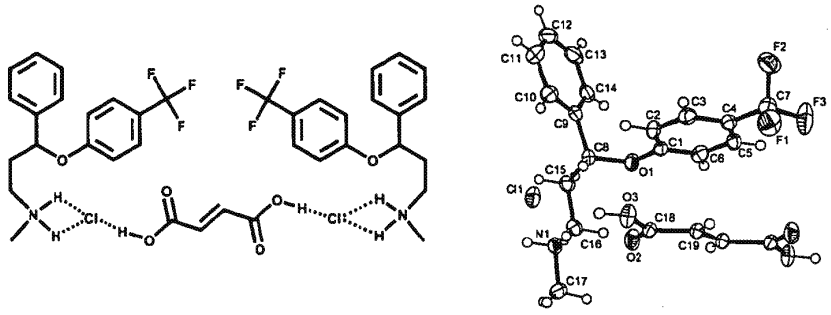


Figure 6. Molecular diagram (left) and ORTEP drawing (right) of the asymmetric unit of **4** (ellipsoids at the 50% probability level).

Table 4. Hydrogen Bond Parameters for **3**[a]

atom-H···atom	atom–H (Å)	H···atom (Å)	atom··· atom (Å)	atom-H··· atom (deg)
O(3)–H(3A)···Cl(1)	0.82(4)	2.21(4)	3.028(2)	173(4)
N(1)–H(1A)···O(2)	0.85(4)	2.22(4)	2.842(3)	130(4)
N(1)–H(1B)···Cl(1)#2	0.89(5)	2.26(5)	3.128(3)	164(4)
N(1)–H(1A)···Cl(1)	0.85(4)	2.61(4)	3.258(3)	135(3)

[a] Symmetry transformations used to generate equivalent atoms: (#1) $-x$, $-y+1$, $-z$; (#2) $-x+{}^1/_2$, $y-{}^1/_2$, z.

Table 5. Hydrogen Bond Parameters for **4**[a]

atom–H···atom	atom–H (Å)	H···atom (Å)	atom··· atom (Å)	atom–H···atom (deg)
N(1)–H(1A)...Cl(1)	0.92(4)	2.55(4)	3.230(3)	131(3)
N(1)–H(1A)...O(2)	0.92(4)	2.19(4)	2.871(4)	131(3)
N(1)–H(1B)...Cl(1)#2	0.91(3)	2.24(3)	3.136(3)	169(3)
O(3)–H(3A)...Cl(1)	0.88(3)	2.14(3)	3.015(2)	173(3)

[a] Symmetry transformations used to generate equivalent atoms: (#1) $-x+2$, $-y+2$, $-z+2$; (#2) $-x+{}^3/_2$, $y-{}^1/_2$, z.

Powder dissolution profile experiments were carried out on compounds **1**–**4** at 20 °C. All compounds dissolve at a rapid rate such that differences in the powder dissolution rates could not be discerned at the early time points. These results are presented in graphical form in Figure 10. The data for the cocrystals is normalized such that the solution concentration of fluoxetine hydrochloride (mM) is plotted for each compound. This type of analysis permits a direct comparison of the effect of the acid guest molecule in the cocrystal on the solubility of the API. The solubility values for the cocrystals expressed in mg/mL of the fluoxetine component as well as the cocrystal are provided in Table 7. Since solubility and bioavailability are often related, these results demonstrate that, in principle, cocrystals can be used to tune the bioavailability of an API.

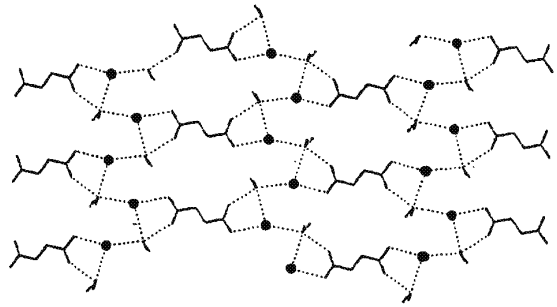


Figure 7. Layered structure in cocrystal **3**. The fluoxetine atoms have been removed, except for the cationic $C-NH_2^+-C$ moiety, for clarity. Intra-ion bonding forms a one-dimensional, charge-assisted motif along the *b* axis (vertical), which is bridged by neutral succinic acid interactions along the *a* axis (horizontal). An identical motif exists in **4**.

Fluoxetine hydrochloride and cocrystals **2** and **4** were stable in water at 20 °C such that the equilibrium solubility values could be obtained at this temperature (Table 7). The stability of **1**, **2**, and **4** was demonstrated by isolating the undissolved solids after several hours and then analyzing the solids by XRPD. In these three experiments, the corresponding XRPD patterns matched those obtained for the starting solid phases. For cocrystal **3**, XRPD analysis of the solids isolated after several hours provided a pattern corresponding to fluoxetine hydrochloride, which demonstrates that **3** dissociated and recrystallized to fluoxetine hydrochloride under the conditions of the powder dissolution experiment. The succinic acid component of this cocrystal remains in solution due to its high solubility, and consequently succinic acid is not observed in

UM00014142
NOVARTIS EXHIBIT 1517
Novartis v. Regents, IPR2023-01347
Page 2888 of 4460

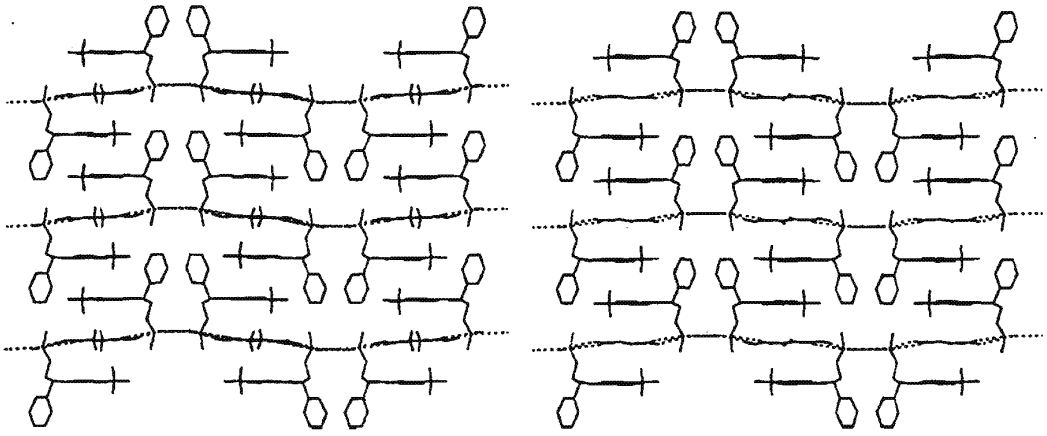


Figure 8. Isostructural cocrystals of fluoxetine hydrochloride with succinic acid (3, left) and fumaric acid (4, right). View is of the *ac*-plane. Hydrogen atoms on the fluoxetine cation have been removed, and entire molecules appear in a single color for clarity.

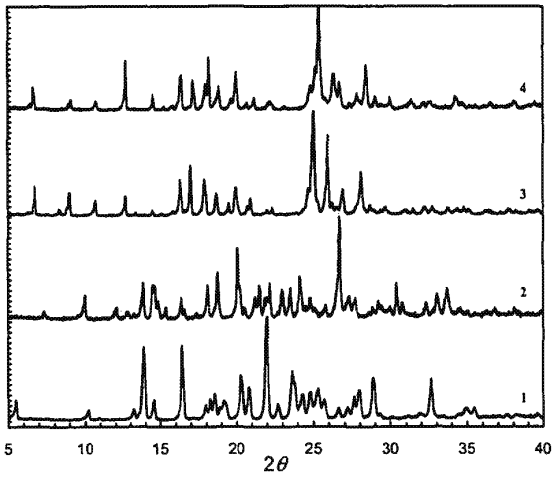


Figure 9. Comparison of the experimental XRPD patterns for **1**−**4**.

Table 6. Melting Point and DSC Data for Cocrystals 2−4 and the Related Individual Components

compd	endotherm onset (°C)	heat of fusion (J/g)	lit. mp[a] (°C)
fluoxetine HCl (**1**)	157.2	105	158.4−158.9
fluoxetine HCl:benzoic acid (1:1) (**2**)	131.5	119	
benzoic acid			122.4
fluoxetine HCl:succinic acid (2:1) (**3**)	134.1	109	
succinic acid			185−187
fluoxetine HCl:fumaric acid (2:1) (**4**)	161.1	108	
fumaric acid			~287

[a] Values obtained from ref 12.

the XRPD pattern of the recovered solids after the powder dissolution experiment. The instability of **3** in water is also characterized by the powder dissolution profile of this cocrystal (Figure 10). Unlike the other systems studied, the rapid increase in fluoxetine hydrochloride concentration at the early time points is followed by a decrease in concentration, which is a result of the recrystallization of the cocrystal to fluoxetine hydrochloride. The peak fluoxetine hydrochloride concentration for **3** is roughly double that for API alone, while the equilibrium concentration

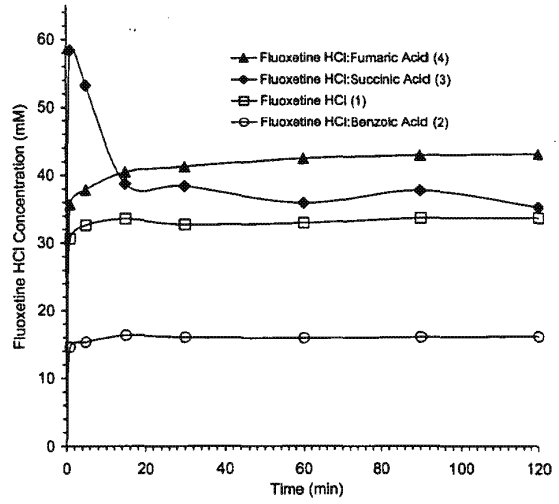


Figure 10. Powder dissolution profiles for **1** (□), **2** (○), **3** (◆), and **4** (▲) in water at 20 °C.

of the API in **4** is approximately 30% higher than **1** alone (Table 7). The increase in solubility of **3** and **4** relative to **1** demonstrates the potential for cocrystal engineering to increase the bioavailability of an API.

Intrinsic dissolution rate experiments[17] were performed in order to obtain quantitative information on the dissolution rates of compounds **1**−**4**, which were not apparent from the powder dissolution experiments described above. The intrinsic dissolution studies were carried out in water at 10 °C in order to decrease further the dissolution rates such that they could be measured reliably. These results are graphed in Figure 11. The data have been normalized to represent the rate of dissolution of the fluoxetine hydrochloride component for each of the cocrystals so that an evaluation of the dissolution of the API could be directly compared. Only the linear region of the dissolution profile is shown in Figure 11, which roughly

(17) (a) Milosovich, G. J. *J. Pharm. Sci.* **1964**, *53*, 484−487. (b) Wood, J. H.; Syarto, J. E.; Letterman, H. *J. Pharm. Sci.* **1964**, *53*, 1068−1077. (c) Grant, D. J. W.; Higuchi, T. *Solubility Behavior of Organic Compounds*; Techniques of Chemistry Series 21; Wiley: New York, 1990; Chapter XI.

UM00014143
NOVARTIS EXHIBIT 1517
Novartis v. Regents, IPR2023-01347
Page 2889 of 4460

Table 7. Aqueous Solubility and Intrinsic Dissolution Rates for 1−4 at 20 °C

	equilibrium solubility at 20 °C			intrinsic dissolution rate at 10 °C	
compd	[fluoxetine HCl] (mM)	[fluoxetine HCl] (mg/mL)	[cocrystal] (mg/mL)	fluoxetine HCl (mmol cm^{-2} min^{-1})	k_{rel} ($k(n)/k(1)$)
fluoxetine HCl (1)	33.1	11.4	n/a	6.8×10^{-3}	1
fluoxetine HCl:benzoic acid (1:1) (2)	16.1	5.6	7.5	3.4×10^{-3}	0.5
fluoxetine HCl:succinic acid (2:1) (3)	58.4[a]	20.2[a]	23.6[a]	$>1.9 \times 10^{-2}$ [b]	>2.9[b]
fluoxetine HCl:fumaric acid (2:1) (4)	42.9	14.8	17.3	6.1×10^{-3}	0.9

[a] Maximum concentration measured at 1 min. [b] Intrinsic dissolution rate of 3 was too rapid to provide an accurate value.

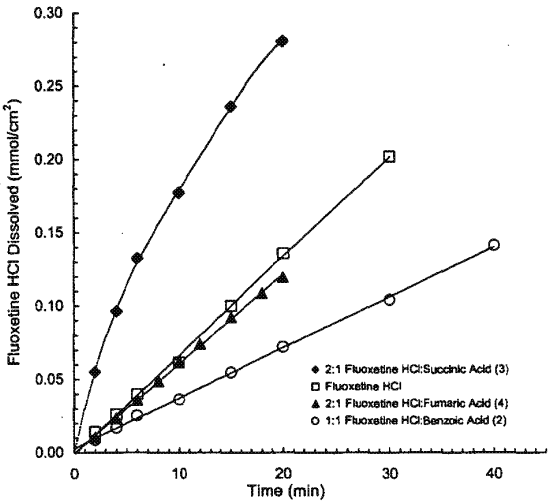


Figure 11. Intrinsic dissolution profiles for 1 (□), 2 (○), 3 (◆), and 4 (▲) in water at 10 °C.

corresponds to 10% dissolution of the total charge of starting material. The dissolution of **3** was too fast to measure an accurate value for the intrinsic dissolution rate at this temperature. The values for **1**, **2**, and **4** obtained by least-squares analysis of the linear regions are provided in Table 7. For **3** an approximate 3-fold increase in the dissolution of the API relative to **1** can be estimated from the early points in the experiment. In contrast, cocrystal **2** dissolves at a rate that is approximately half of the rate for the API alone, while the dissolution rate for **4** is roughly similar to that for **1**. These results demonstrate that, by cocrystallizing an API with different guest molecules, it is possible to increase or decrease the dissolution rate of the API or to leave the effective dissolution rate essentially unchanged.

The manner in which the structural and thermodynamic factors influence the corresponding dissolution rate is presently unknown for these compounds. Regardless of these factors, it is interesting to note that the aqueous solubility of the guest molecule appears to correlate to the aqueous dissolution rates of the corresponding cocrystal with fluoxetine hydrochloride. Approximate solubilities in water are as follows: benzoic acid, 0.34 g/100 g at 25 °C;[18] succinic acid, 7.5 g/100 g at 25 °C;[19] fumaric acid, 0.61 g/100 g at 25 °C.[20] These follow the same ordering as the values for the intrinsic dissolution rate (Table 7).

Conclusions

The ability to alter the physical properties of a crystalline solid containing an API by incorporating a pharmaceutically acceptable molecular species into a unique crystal lattice presents an opportunity to tailor the properties of a solid-state dosage form at the molecular level. By using crystal engineering strategies[21] to guide the selection of API:guest combinations that are preorganized to form complementary intermolecular hydrogen bonds, the potential for discovering useful cocrystals is increased and the number of API:guest combinations that must be empirically examined is reduced.

The viability of a crystal engineering approach to the identification of stable cocrystals has been demonstrated through the rational synthesis of cocrystals of fluoxetine hydrochloride with fumaric, succinic, and benzoic acids. In all three cases the organic acid was found to engage in a hydrogen bond with the targeted chloride ion. These three cocrystals were prepared in gram quantities using standard techniques. The solubility and intrinsic dissolution rate experiments conducted on fluoxetine hydrochloride and the corresponding cocrystals demonstrated that these species have significantly different solubilities and dissolution rates. These results indicate that it is possible to alter the physical properties of the solid-state form of an API through the application of API:guest cocrystals.

We have tested this crystal engineering approach with five other amine hydrochloride APIs in order to determine if the neutral carboxylic acid guest to chloride acceptor synthon is a robust and reliable design tool. Cocrystals with neutral carboxylic acids have been observed in all cases, and the expected neutral organic acid to chloride hydrogen bond is present in all of the structures. These results will be the subject of future contributions.

Acknowledgment. We thank Dr. Kenneth Hardcastle and Dr. Karl Hagen from the Emory University X-ray Diffraction Center for determining the crystal structures reported in this paper.

Supporting Information Available: X-ray crystallographic information files (CIF) for cocrystals **2**−**4** and figures giving Raman, XRPD, TGA, DSC, and moisture sorption/desorption data for compounds **1**−**4**. This information is available free of charge via the Internet at http://pubs.acs.org.

JA048114O

(18) *The Merck Index*, 13th ed.; Merck & Co.: Whitehouse Station, NJ, 2001 (CD-ROM).
(19) Wermuth, C. G.; Stahl, P. H. In *Handbook of Pharmaceutical Salts: Properties, Selection, and Use*; Stahl, P. H., Wermuth, C. G., Eds.; Verlag Helvitica Chimica Acta: Zurich and Wiley-VCH: Weinheim, Germany, 2002; p 306.
(20) Reference 13, p 282.
(21) (a) Aakeroy, C. B. *Acta Crystallogr., Sect. B: Struct. Commun.* **1997**, *53*, 569−586. (b) Bilton, C.; Allen, F. H.; Shields, G. P.; Howard, J. A. K. *Acta Crystallogr. Sect. B: Struct. Commun.* **2000**, *56*, 849−856. (c) Coe, S.; Kane, J. J.; Nguyen, T. L.; Toledo, L. M.; Wininger, E.; Fowler, F. W.; Lauher, J. W. *J. Am. Chem. Soc.* **1997**, *119*, 86−93. (d) Desiraju, G. R. *Angew. Chem., Int. Ed. Engl.* **1995**, *34*, 2311−2327. (e) Desiraju, G. R. *Chem. Commun.* **1997**, 1475−1482. (f) Nangia, A.; Desiraju, G. R. *Acta Crystallogr., Sect. A* **1998**, *54*, 934−944. (g) Videnova-Adrabinska, V. *Acta Crystallogr., Sect. B* **1996**, *B52*, 1048−1056.

UM00014144
NOVARTIS EXHIBIT 1517
Novartis v. Regents, IPR2023-01347
Page 2890 of 4460

that this synthesis concept is potentially expandable toward other metal systems. Mixed-metal clusters containing both lanthanides and d block transition elements such as copper, iron, and manganese, for example, may be prepared.[14] The synthetic opportunities abound when the rich varieties of amino acids and transition metals including lanthanide elements are considered. Furthermore, these pentadecanuclear clusters possess unprecedented layered structures that are complex yet architecturally pleasing. The highly ordered arrangement of the metal centers in these nano-sized clusters is expected to yield useful magnetic properties.[5, 7, 8] We believe that the novel structural patterns (and any accompanying physical/chemical properties), coupled with the ability to construct a huge variety of lanthanide clusters will undoubtedly enhance our understanding of lanthanide-based molecular magnetic materials.

Experimental Section

Tyrosine (0.181 g, 1.0 mmol) was added as a solid to an aqueous solution of $Eu(ClO_4)_3$ prepared by dissolution of Eu_2O_3 (1.408 g, 4.0 mmol) in 70% perchloric acid. To this clear solution was added one drop of 1.0 M aqueous HCl and the mixture was stirred at 80 °C for 5 min. The pH value of the above solution was then carefully adjusted by slow addition of 0.5 M aqueous NaOH until the precipitate thus formed remained. The mixture was then filtered and the filtrate was allowed to stand at room temperature. Parallelepipeds of the lanthanide complexes appeared in about one week. The complex was synthesized in a typical yield of 60% (based on tyrosine). Elemental analysis calcd: Eu 37.41; found: 37.36; ESI-MS: *m/z* (%): 1936.1 (30) $[(M^+ + H) - 5H_2O - 2ClO_4^-]^{3+}$, 1474.7 (100) $[(M^+ + 2H) - 2ClO_4^-]^{4+}$, 1150.9 (40) $[(M^+ + 3H) - 8H_2O - 2ClO_4^-]^{5+}$.

Received: January 4, 1999 [Z12870IE]
German version: *Angew. Chem.* **1999**, *111*, 1929–1932

Keywords: amino acids · cluster compounds · coordination modes · lanthanides · template synthesis

[1] D. Gatteschi, A. Caneschi, R. Sessoli, A. Cornia, *Chem. Soc. Rev.* **1996**, 101.
[2] G. L. Abbati, A. Cornia, A. C. Fabretti, A. Caneschi, D. Gatteschi, *Inorg. Chem.* **1998**, *37*, 3759.
[3] a) R. C. Squire, S. M. J. Aubin, K. Folting, W. E. Streib, D. N. Hendrickson, G. Christou, *Inorg. Chem.* **1995**, *34*, 6463; b) S. P. Watton, P. Fuhrmann, L. Pence, A. Caneschi, A. Cornia, G. L. Abbati, S. J. Lippard, *Angew. Chem.* **1997**, *109*, 2917; *Angew. Chem. Int. Ed. Engl.* **1997**, *36*, 2774.
[4] A. Caneschi, A. Cornia, S. J. Lippard, *Angew. Chem.* **1995**, *107*, 511; *Angew. Chem. Int. Ed. Engl.* **1995**, *34*, 467.
[5] G. L. Abbati, A. Cornia, A. C. Fabretti, A. Caneschi, D. Gatteschi, *Inorg. Chem.* **1998**, *37*, 1430.
[6] D. Gatteschi, L. Pardi, A. L. Barra, A. Müller, J. Döring, *Nature* **1991**, *354*, 463.
[7] a) "Magnetism: A Supramolecular Functions": G. Christou, *NATO ASI Ser.* **1996**, *484*, 383; b) A. Caneschi, D. Gatteschi, L. Pardi, R. Sessoli, *J. Chem. Soc. Dalton Trans.* **1997**, 3963.
[8] a) L. Thomas, F. Lionti, R. Ballou, D. Gatteschi, R. Sessoli, B. Barbara, *Nature* **1996**, *383*, 145; b) S. M. J. Aubin, Z. Sun, I. A. Guzei, A. L. Rheingold, G. Christou, D. N. Hendrickson, *Chem. Commun.* **1997**, 2239.
[9] "Magnetic Molecular Materials": C. Benelli, A. Caneschi, D. Gatteschi, L. Pardi, *NATO ASI Ser.* **1991**, *198*, 233.
[10] J. Legendziewicz, E. Huskowska, G.Y. Argay, A. Waśkowska, *J. Less-Common Met.* **1989**, *146*, 33, and references therein.
[11] Crystal structure determination of **1**: A colorless crystal (ca. 0.15 × 0.15 × 0.10 mm) was analyzed with a Bruker SMART CCD-based diffractometer at 213 K with $Mo_{K\alpha}$ radiation ($\lambda = 0.71073$ Å). Monoclinic, space group C_2, $a = 32.259(3)$, $b = 20.926(2)$, $c = 22.037(2)$ Å, $\beta = 130.956(4)°$, $V = 11234(2)$ Å^3, $Z = 2$, $\rho_{calcd} = 1.801$ Mg m^{-3}, $\mu(Mo_{K\alpha}) = 4.254$ mm^{-1}, $F(000) = 5956$. ω–2θ scans, 29805 reflections measured ($2\theta_{max} = 50°$), of which 13780 were independent and all are observed [$I = 2\sigma(I)$], 528 refined parameters, $R = 0.0812$, $wR_2 = 0.2096$, residual electron density max./min. 2.229/−1.294 e Å^{-3}, max./min. transmission 0.9583/0.7456. Data reduction was performed with the SAINT software, which corrects for Lorentz and polarization factors as well as decay. Absorption corrections were applied with SADABS supplied by G. Sheldrick. The structure was solved by the direct method with the SHELXS-97 program and refined by least squares method on F^2, SHELXL-97, incorporated in SHELXTL-PC version 5.10. Only the metal atoms were refined anisotropically. Hydrogens were calculated by geometrical methods for the ligand and refined as a riding model. The solvated water molecules were found by using the program XWAT, supplied within SHELXTL. No hydrogen atoms were modeled for the hydroxides or water molecules in the cluster or solvated. Further details on the crystal structure investigation may be obtained from the Fachinformationszentrum Karlsruhe, D-76344 Eggenstein-Leopoldshafen, Germany (fax: (+49) 7247-808-666; e-mail: crysdata@fiz-karlsruhe.de) on quoting the depository number CSD-410601.
[12] R. Anwander, *Angew. Chem.* **1998**, *110*, 619; *Angew. Chem. Int. Ed.* **1998**, *37*, 599.
[13] J. L. Sessler, P. I. Sansom, A. Andrievsky, V. Kral in *Supramolecular Chemistry of Anions* (Eds.: A. Bianchi, K. Bowman-James, E. Garcia-Espana), WILEY-VCH, New York, **1997**, p. 355.
[14] X. Chen, S. M. J. Aubin, Y. Wu, Y. Yang, T. C. W. Mak, D. N. Hendrickson, *J. Am. Chem. Soc.* **1995**, *117*, 9600.

A Versatile Route to Porous Solids: Organic–Inorganic Hybrid Materials Assembled through Hydrogen Bonds**

Christer B. Aakeröy,* Alicia M. Beatty, and Destin S. Leinen

One of the many promising applications of supramolecular chemistry is in the design of crystalline host–guest materials, which have been pursued through two principal routes. First, coordination polymers[1] have been shown to form porous materials whose host frameworks can withstand the removal/addition of guest molecules[2] or exhibit high shape specificity in clathration.[3] Second, organic networks have been assembled through directional intermolecular forces[4] to form porous frameworks, which can be applied to homogeneous and heterogeneous[5, 6] separations. Remarkably, some three-dimensional (3D) organic frameworks assembled through hydrogen bonds are rugged enough for reversible guest

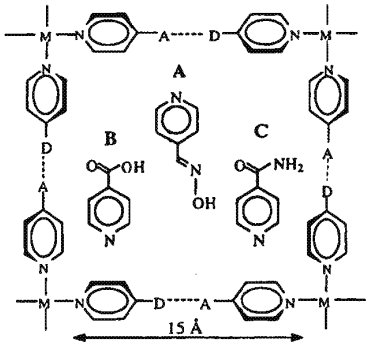
[*] Dr. C. B. Aakeröy, Dr. A. M. Beatty, D. S. Leinen
Department of Chemistry, Kansas State University
Manhattan, Kansas, 66506 (USA)
Fax: (+1) 785-532-6666
E-mail: aakeroy@ksu.edu

[**] We acknowledge financial support from Kansas State University, NSF-EPSCoR (OSR-9550487), and DuPont, and we thank Dr. R. Rogers and L. Rogers at the University of Alabama, Tuscaloosa (USA) for the X-ray diffraction data for **4**.

UM00014145
NOVARTIS EXHIBIT 1517
Novartis v. Regents, IPR2023-01347
Page 2891 of 4460

inclusion.[6] While it is unlikely that molecular host–guest complexes will be as robust as naturally occurring zeolites, these systems have the advantage of "tunability" where the nature and size of the pore may be altered.[7] We are interested in a crystal engineering strategy based on a combination of the above approaches:[8] while we are inclined to use hydrogen bonds as crystal engineering tools[9] (they can *flex* to accommodate entering and departing guest molecules), we also recognize the advantage of using metal centers (square-planar or octahedral geometries are not easily accessible in organic chemistry). The aim is to assemble metal complexes through hydrogen bonds to form porous materials for inclusion/separation.

The assembly of the materials described herein relies on the ability of Pt^{II} and Ni^{II} ions to coordinate to four pyridine-based ligands in a square-planar arrangement. The ligands are substituted with oxime (**A**), carboxylic acid (**B**), and carboxamide (**C**) moieties (Scheme 1); such functional groups can



Scheme 1. A = Hydrogen-bond acceptor, D = hydrogen-bond donor, M = metal ion.

overcome competition from solvent molecules and counterions to assemble linear silver(I) complexes through complementary hydrogen bonds.[10] Successful assembly of square-planar complexes through head-to-head hydrogen-bond interactions between the ligands affords the potential for large cavities, 15 Å × 15 Å, that are suitable for inclusion of guest molecules (Scheme 1; cavity sizes are consistently estimated allowing for van der Waals radii). As ever, the possibility for interpenetration exists,[11] but even in that case, such large voids should only be partially filled (although examples to the contrary have been reported[12]). Herein, we describe four structures which demonstrate the proclivity of platinum(II) and nickel(II) complexes to form crystalline host–guest materials.

In compound **1**,[13] the metal complexes link through four unique N–H···O amide–amide hydrogen bonds to form cationic sheets (Figure 1); the hydrogen-bond motif results in

$[Ni(C)_4(H_2O)_2][ClO_4]_2 \cdot 2H_2O$ **1**

the formation of two unique holes in each parallel sheet. The smaller, $R_4^4(16)$ hole[14] is blocked by nickel(II) ions in the sheets above and below, but the larger, $R_2^2(28)$ holes only partially overlap, forming channels for the perchlorate

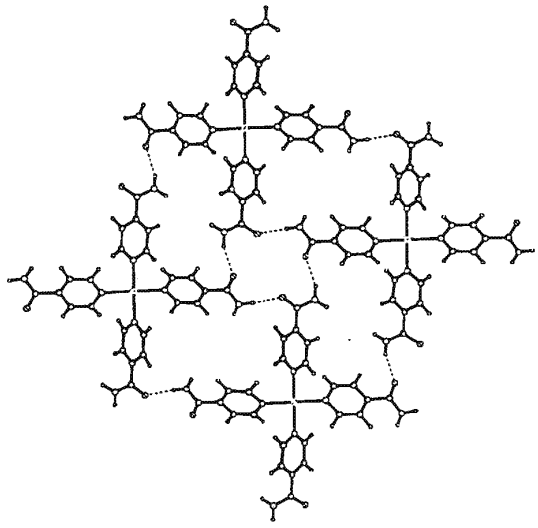


Figure 1. An infinite cationic layer in **1**, in which two unique holes $R_4^4(16)$ and $R_2^2(28)$ are formed.

counterions.[15] Additional hydrogen bonds between coordinated water molecules and amide oxygen atoms connect the sheets above and below to generate the three-dimensional network. As the amide–amide hydrogen bonds display catemer-type interactions (instead of head-to-head), the large holes predicted for these assemblies are not realized, and instead small channels containing counterions are present.

The versatility of the strategy is demonstrated in compound **2**, which utilizes a different type of hydrogen-bonding moiety (oxime instead of amide). The oxime hydroxy groups link

$[Ni(A)_4(H_2O)_2]Br_2 \cdot 2A$ **2**

through complementary O–H···O hydrogen bonds to form sheets with large, $R_4^4(64)$ hourglass-shaped holes (22 Å long, 15 Å wide at the ends, 7 Å wide at the waist). The sheets are cross-linked by hydrogen bonds between the axially coordinated water molecules and the bromide counterions, forming a 3D network, where the large holes are aligned into channels. Twofold interpenetration of the 3D networks blocks the center of the large hole, leaving two smaller channels at each end. In this case, a host–guest complex is formed, and the guest molecules, 4-aldoximepyridine, are contained inside the channels (Figure 2), held in the lattice by hydrogen bonds to the bromide ion and the ligated oxime moieties.[16] Thus, the structure of **2** demonstrates that an octahedral system can generate a 3D network with holes large enough to hold small organic molecules.

A similar square-planar system can also create a host–guest complex, as evidenced by compound **3**. In this case, *trans* ligands are linked linearly by head-to-head $[R_2^2(8)]$

$[Pt(C)_4]Cl_2 \cdot 4C$ **3**

amide–amide hydrogen bonds; the resulting chains are arranged parallel to each other. The linear assemblies are

 © WILEY-VCH Verlag GmbH, D-69451 Weinheim, 1999 1433-7851/99/3812-1816 $ 17.50+.50/0 *Angew. Chem. Int. Ed.* 1999, *38*, No. 12

UM00014146
NOVARTIS EXHIBIT 1517
Novartis v. Regents, IPR2023-01347
Page 2892 of 4460

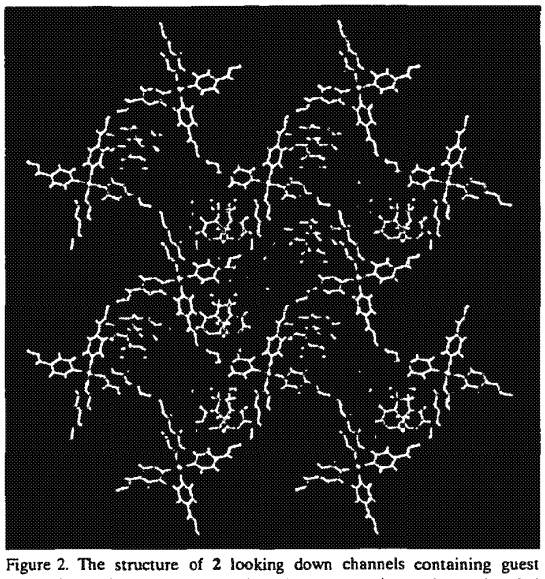


Figure 2. The structure of **2** looking down channels containing guest 4-aldoximepyridine molecules, where interpenetrating hydrogen-bonded nets are depicted in yellow and red, respectively.

interconnected perpendicular to the propagation of the chains through two inequivalent N–H···Cl interactions, creating a three-dimensional network which contains large square channels (Figure 3 left). The guest isonicotinamide molecules occupy these channels (Figure 3 right), and are anchored to the lattice by hydrogen bonds. Compound **3** demonstrates that even if the structure manifests head-to-head hydrogen bonds in chains (1D), rather than the sheets (2D) proposed in Scheme 1, other hydrogen-bonding interactions can create a 3D framework, and the smaller channels are still large enough to hold small organic molecules.

While the amide and oxime ligands remain protonated, thus necessitating the presence of counteranions, carboxylic acid moieties can become deprotonated, and the lattices can be constructed without counterions. Thus compound **4**, unlike

$Pt(HB)_2(B)_2 \cdot 2H_2O$ **4**

1–**3**, is a neutral metal complex which forms two crystallographically unique square nets, assembled through charge-assisted carboxylate–carboxylic acid hydrogen bonds [$R_4^4(56)$] (Figure 4). The distance between the platinum(II) ions in each

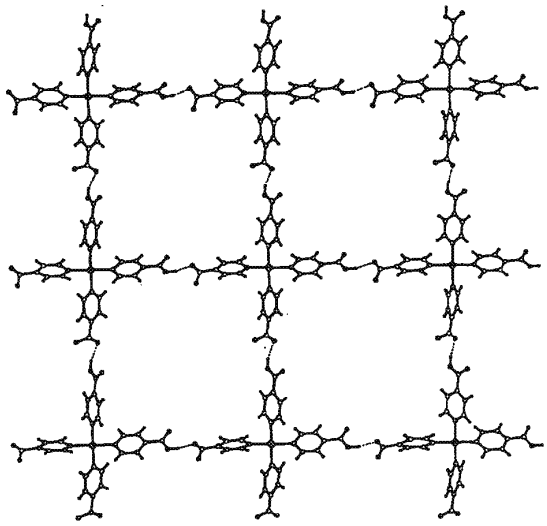


Figure 4. One of the 2D hydrogen-bonded nets in **4**, showing the large square cavities generated by hydrogen-bonded metal–complex cations.

sheet is >15 Å, leading to large square cavities. The crystal structure of **4** provides a rare example of inclined interpenetration of (4,4) nets in three mutually perpendicular planes.[11] Each square cavity of one of the unique nets is

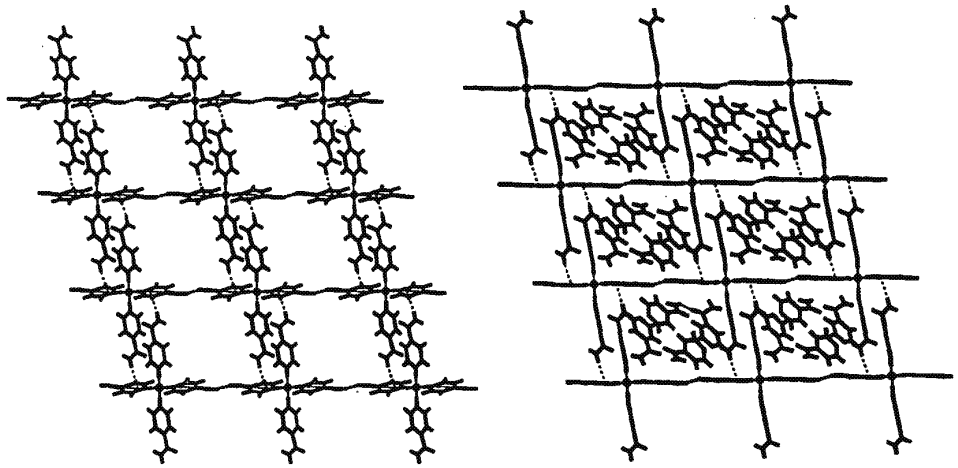


Figure 3. The structure of **3** without (left) and with (right) guest isonicotinamide molecules. In the structure with guest molecules, the ligand pyridine rings are replaced with a line for clarity.

UM00014147
NOVARTIS EXHIBIT 1517
Novartis v. Regents, IPR2023-01347
Page 2893 of 4460

interwoven by three other nets, while those of the other unique net are interwoven by five nets. Despite this interpenetration, channels are present which host disordered water molecules (Figure 5). The complex is thermally stable, with a melting point of > 300 °C, indicating that the structure could remain intact for reversible addition of water or other guests in the channels.

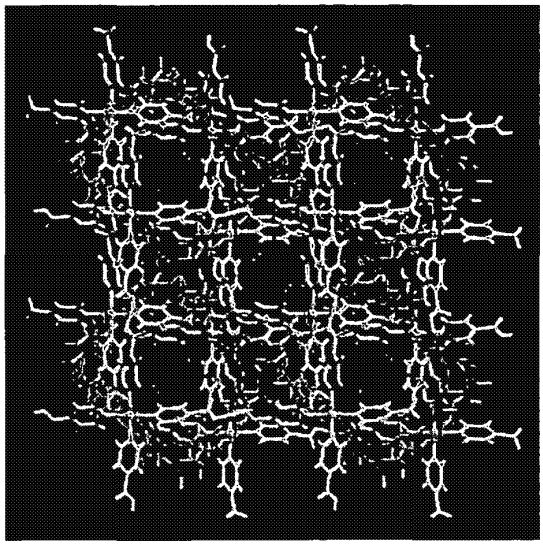


Figure 5. The structure of **4**, viewed down channels resulting from interpenetrating hydrogen bonded nets. The three mutually perpendicular nets are shown in purple, yellow, and green. The red spheres are guest water molecules.

Experimental Section

1: An aqueous solution (20 mL) of isonicotinamide (0.30 g, 2.5 mmol) was slowly added to an aqueous solution (10 mL) of $Ni(ClO_4)_2 \cdot 6H_2O$ (0.18 g, 0.49 mmol). The solution was allowed to evaporate at room temperature. Irregular blue crystals formed in a few weeks (m.p. > 300 °C).

2: A solution of 4-aldoximepyridine (0.20 g, 1.64 mmol) in ethanol was slowly added to an aqueous solution of $NiBr_2 \cdot x H_2O$ (0.14 g). The flask was covered and left to stand in ambient conditions. Slow evaporation of solvent produced blue, platelike crystals (m.p. > 300 °C).

3: An aqueous solution of isonicotinamide (0.08 g, 0.66 mmol) was added to an aqueous solution of $[NH_4]_2[PtCl_4]$ (0.05 g, 0.13 mmol), and allowed to evaporate at room temperature. After about one week, a yellow powder was filtered off and washed with ethanol. The ethanolic filtrate and the mother liquor were mixed and allowed to evaporate, yielding irregular colorless crystals (m.p. > 300 °C).

4: A 1:2 ethanol:water solution (30 mL) of isonicotinic acid (0.13 g, 0.94 mmol) was added to an aqueous solution (15 mL) of $K_2[PtCl_4]$ (0.07 g, 0.17 mmol) and allowed to evaporate, yielding conical colorless crystals (m.p. > 300 °C). Typically, the yields were over 80 % except in the case of **4**, which was below 40 %.

Crystallographic data (excluding structure factors) for the structures reported in this paper have been deposited with the Cambridge Crystallographic Data Centre as supplementary publication nos. CCDC-108604 – CCDC-108607 (**1** – **4**). Copies of the data can be obtained free of charge on application to CCDC, 12 Union Road, Cambridge CB2 1EZ, UK (fax: (+44) 1223-336-033; e-mail: deposit@ccdc.cam.ac.uk).

Received: November 16, 1998 [Z12665IE]
German version: *Angew. Chem.* **1999**, *111*, 1932 – 1936

Keywords: crystal engineering · host – guest chemistry · hydrogen bonds · nickel · platinum

[1] a) O. M. Yaghi, H. Li, *J. Am. Chem. Soc.* **1996**, *118*, 295; b) S. Subramanian, M. J. Zaworotko, *Angew. Chem.* **1995**, *107*, 2295; *Angew. Chem. Int. Ed. Engl.* **1995**, *34*, 2127; c) L. Carlucci, G. Ciani, D. M. Proserpio, A. Sironi, *Chem. Commun.* **1996**, 1393.

[2] a) H. Li, C. E. Davis, T. L. Groy, D. G. Kelley, O. M. Yaghi, *J. Am. Chem. Soc.* **1998**, *120*, 2186; b) G. B. Gardner, D. Venkataraman, J. S. Moore, S. Lee, *Nature* **1995**, *374*, 792.

[3] M. Fujita, Y. J. Kwon, S. Washizu, K. Ogura, *J. Am Chem. Soc.* **1994**, *116*, 1151.

[4] a) M. C. Etter, *Acc. Chem. Res.* **1990**, *23*, 120; b) G. R. Desiraju, *Crystal Engineering. The Design of Organic Solids*, Elsevier, Amsterdam, **1989**.

[5] V. A. Russell, C. Evans, W. Li, M. D. Ward, *Science* **1997**, *276*, 575.

[6] a) P. Brunet, M. Simard, J. D. Wuest, *J. Am. Chem. Soc.* **1997**, *119*, 2737; b) X. Wang, M. Simard, J. D. Wuest, *J. Am. Chem. Soc.* **1994**, *116*, 12119; c) Y. Aoyama, *Top. Curr. Chem.* **1998**, *198*, 131; d) K. Endo, T. Koike, T. Sawaki, O. Hayashida, H. Masuda, Y. Aoyama, *J. Am. Chem. Soc.* **1997**, *119*, 4117.

[7] C. Janiak, *Angew. Chem.* **1997**, *109*, 1499; *Angew. Chem. Int. Ed. Engl.* **1997**, *36*, 1431.

[8] Examples of assembly of metal complexes with intermolecular interactions: a) M. M. Chowdhry, D. M. P. Mingos, A. J. P. White, D. J. Williams, *Chem. Commun.* **1996**, 899; b) A. D. Burrows, D. M. P. Mingos, A. J. P. White, D. J. Williams, *Chem. Commun.* **1996**, 97; c) Z.-N. Chen, H.-X. Zhang, K. B. Yu, K. C. Zheng, H. Cai, B.-S. Kang, *J. Chem. Soc. Dalton Trans.* **1998**, 1133; d) L. Carlucci, G. Ciani, D. M. Proserpio, A. Sironi, *J. Chem. Soc. Dalton Trans.* **1997**, 1801; e) C. B. Aakeröy, A. M. Beatty, B. A. Helfrich, *J. Chem. Soc. Dalton Trans.* **1998**, 1943; f) D. Braga, F. Grepioni, G. R. Desiraju, *Chem. Rev.* **1998**, *98*, 1375; g) M. Munakata, L. P. Wu, M. Yamamoto, T. Kurodo-Sowa, M. Maekawa, *J. Am. Chem. Soc.* **1996**, *118*, 3117; h) R. K. Kumar, S. Balasubramanian, I. Goldberg, *Chem. Commun.* **1998**, 1435; i) B. R. Cameron, S. S. Corrent, S. J. Loeb, *Angew. Chem.* **1995**, *107*, 2900; *Angew. Chem. Int. Ed. Engl.* **1995**, *34*, 2689; j) J. C. M. Rivas, L. Brammer, *New J. Chem.* **1998**, *22*, 1315.

[9] C. B. Aakeröy, *Acta Crystallogr. Sect. B.* **1997**, *53*, 569.

[10] a) C. B. Aakeröy, A. M. Beatty, *Chem. Commun.* **1998**, 1067; b) C. B. Aakeröy, A. M. Beatty, D. S. Leinen, *J. Am. Chem. Soc.* **1998**, *120*, 7383.

[11] S. R. Batten, R. Robson, *Angew. Chem.* **1998**, *110*, 1558; *Angew. Chem. Int. Ed.* **1998**, *37*, 1460.

[12] H.-P. Wu, C. Janiak, L. Uehlin, P. Klüfers, P. Mayer, *Chem. Commun.* **1998**, 2637.

[13] X-ray diffraction studies were performed on single crystals using $Mo_{K\alpha}$ radiation ($\lambda = 0.71073$ Å) at 173 K, and Lorentz and polarization corrections, and semiempirical absorption corrections were applied for all compounds. Structure solutions were determined from Patterson methods using SHELXS-86 with a full-matrix least-squares refinement on F^2 using SHELXL-93 (G. Sheldrick, Universität Göttingen). Hydrogen atoms were located from the difference map, and a riding model with fixed thermal parameters [$u_{ij} = 1.2U_{ij}$(eq)] for the atom to which they are bonded] was used for subsequent refinements. Crystal data: Compound **1**, 0.4 × 0.3 × 0.1 mm, monoclinic, space group $C2/c$, $a = 18.492(3)$, $b = 10.076(1)$, $c = 18.665(4)$ Å, $\beta = 91.03(1)°$, $V = 3477(1)$ Å^3, $\rho = 1.563$ Mg m^{-3}, 3066 unique reflections, 2251 observed ($I > 2\sigma I$), 261 parameters, $R = 0.0491$, $R_w = 0.1085$. Compound **2**, 0.4 × 0.3 × 0.3 mm, orthorhombic, space group $Aba2$, $a = 22.414(2)$, $b = 23.753(2)$, $c = 8.0830(7)$ Å, $V = 4303.6(7)$ Å^3 $\rho = 1.524$ Mg m^{-3}, 2888 unique reflections, 2191 observed ($I > 2\sigma I$), 268 parameters, $R = 0.0494$, $R_w = 0.1171$. Compound **3**, 0.4 × 0.2 × 0.2 mm, monoclinic, space group $P2_1/c$, $a = 13.533(1)$, $b = 9.6166(8)$, $c = 20.787(2)$ Å, $V = 2569.4(4)$ Å^3, $\rho = 1.607$ Mg m^{-3}, 4530 unique reflections, 3444 observed ($I > 2\sigma I$), 340 parameters, $R = 0.0281$, $R_w = 0.0723$. Compound **4**, 0.7 × 0.2 × 0.2 mm, tetragonal, space group $P4_32_12$, $a = 16.2242(4)$, $c = 22.8441(8)$ Å, $V = 6013.1(3)$ Å^3, $\rho = 1.585$ Mg m^{-3}, 7137 unique reflections, 6079 observed ($I > 2\sigma I$), 356 parameters, $R = 0.0584$, $R_w = 0.1436$, a disordered carboxylate unit was restrained with fixed distances (rC–C 1.54; rC–O 1.26).

 © WILEY-VCH Verlag GmbH, D-69451 Weinheim, 1999 1433-7851/99/3812-1818 $ 17.50+.50/0

UM00014148
NOVARTIS EXHIBIT 1517
Novartis v. Regents, IPR2023-01347
Page 2894 of 4460

[14] For information about graph-set notation; J. Bernstein, R. E. Davis, L. Shimoni, N.-L. Chang, *Angew. Chem.* **1995**, *107*, 1689; *Angew. Chem. Int. Ed. Engl.* **1995**, *34*, 1555.
[15] A crystalline metal complex with anions in hydrophobic channels has been shown to undergo ion exchange: C. V. K. Sharma, S. T. Griffin, R. D. Rogers, *Chem. Commun.* **1998**, 215.
[16] For an up-to-date database study of of hydrogen-bond distances to halide ions: T. Steiner, *Acta Crystallogr. Sect. B.* **1998**, *54*, 456.

Photoionization and Electron Transfer of Biphenyl within the Channels of Al-ZSM-5 Zeolites

Isabelle Gener, Guy Buntinx, and Claude Brémard*

There is considerable interest in the use of crystalline aluminosilicate porous materials such as zeolites to study and try to control the photophysical and photochemical properties of the occluded molecules.[1] The ability of zeolites to stabilize radical cations and trap electrons is now firmly established.[2, 3] In contrast, the reverse situation in which zeolites act as electron donors is far less documented.[4, 5] The ZSM-5 zeolites with straight (0.54×0.56 nm) and zigzag (0.51×0.55 nm) channels have been reported previously to generate radical cations spontaneously and stabilize them in the void space.[6] While the mechanism of oxidation remains unclear today, it appears that the presence of aluminum in the zeolite is a requirement for persistent radical cations. Herein we present our most striking results concerning the photolysis of biphenyl ($C_{12}H_{10}$, BP) occluded at low coverage in nonacidic ZSM-5 zeolites. The emphasis of the paper is mainly set on the photoionization of biphenyl and electron transfer. The zeolite – radical cation – electron interactions have been tuned by varying the silicon:aluminum ratio, by using charge-balancing cations, and without any additional molecules.

Weighted amounts of bisublimated BP (0.5 – 1 BP per unit cell) were mixed with freshly dehydrated $M_n[Al_nSi_{96-n}O_{192}]$ ($M = Na^+$, K^+, Cs^+; $n = 0$, 3, 6) zeolites under an inert atmosphere in a silica cell. The FT-Raman and diffuse reflectance UV/Vis absorption spectra of the mechanical powder mixtures were recorded as a function of time. All the spectroscopic data recorded after the required equilibration period of one month at a gentle temperature (50 °C) are typical of occluded BP at low coverage within the void space. The aluminum content, the extraframework cations M^+, and the cosorbed gas (argon or helium) do not induce dramatic effects upon the molecular conformation of ground state BP ($BP(S_0)$) as evident from similar vibrational spectroscopic characteristics to that reported previously for $BP(S_0)$ in fluid solution and attributed to a twisted structure.[7] The ground-state absorption electronic spectra of BP occluded at low coverage in ZSM-5 are typical of isolated chromophores.[7]

Molecular mechanics calculations (MM), Monte Carlo simulations (MC), and molecular dynamics calculations (MD) provide evidence of the expected location, the structure as well as the diffusion of $BP(S_0)$ within the void space of the $Na_4[Al_4Si_{92}O_{192}]$ zeolites.[8] The $BP(S_0)$ molecules were found to be located preferentially in the straight channels in the vicinity of the intersection with zigzag channels (Figure 1).

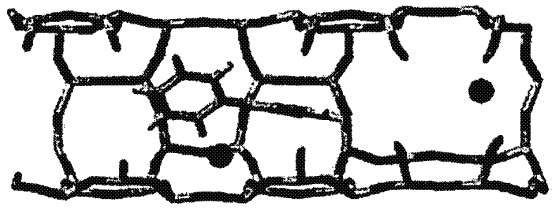


Figure 1. Cross-sectional view of biphenyl (BP, S_0) occluded in the straight channel of $Na_4Si_{92}Al_4O_{192}$ zeolite perpendicular to the b axis. The yellow Si, blue Al, and red O cylinders represent the ZSM-5 framework, the pink balls represent the extra-framework Na^+ cations, the shaded and white cylinders represent the C and H atoms of BP, respectively.

The expected site of $BP(S_0)$ in ZSM-5 is in reasonable agreement with preliminary X-ray diffraction data performed at high coverage.[9]

It should be noted that the nearest C···Na and C···Al distances are found to be 4.66 and 7.1 Å, respectively. From MD simulations data the main role of the zeolite framework appears to be to reduce the mobility of BP within the void space, and the $BP(S_0)$ molecule performs only vibrational, internal rotation, and translational motions in the vicinity of the sorption site.[8]

An excimer laser (248 nm, 15 ns, 0.12 – 30 mJ cm^{-2}) was used as pump excitation within the $S_3 \leftarrow S_0$ ($\pi^* \leftarrow \pi$) transition of occluded BP in $M_n[Al_nSi_{96-n}O_{192}]$. This transition exhibits an intense electronic absorption around 250 nm. Decays in the UV/Vis spectra up to 300 μs were recorded after the laser photolysis of the $1BP/Si_{96}O_{192}$ and $1BP/Na_3[Al_3Si_{93}O_{192}]$ samples by the transient diffuse reflection technique.[10] It should be noted that with the pump excitation power used, no transient spectra were obtained after photolysis of the bare zeolites.

The data processing[11] of the transient spectra provides clear evidence of the pure component spectra and concentrations of the lowest triplet state $BP(T_1)$ (355 nm) and the radical cation $BP^{+\cdot}$ (380, 660 nm) within the experimental pump energy range.[7] No spectral evidence of both the radical anion and trapped electron was found in either $1BP/Si_{96}O_{192}$ or $1BP/Na_3[Al_3Si_{93}O_{192}]$ samples under the experimental conditions used.[7, 8, 12, 13] The short lifetime of $BP(T_1)$ is found to be shorter in $1BP/[Si_{96}O_{192}]$ (3×10^{-7} s) than in $1BP/Na_3[Al_3Si_{93}O_{192}]$ (2.4×10^{-6} s). In contrast, the lifetime of $BP^{+\cdot}$

[*] Dr. C. Brémard, I. Gener, Dr. G. Buntinx
Laboratoire de Spectrochimie Infrarouge et Raman UMR-CNRS 8516
Centre d' Etudes et de Recherches Lasers et Applications
Bât. C5 Université des Sciences et Technologies de Lille
59655 Villeneuve d'Ascq cedex (France)
Fax: (+33) 3-20-436755
E-mail: bremard@univ-lille1.fr

 © WILEY-VCH Verlag GmbH, D-69451 Weinheim, 1999 1433-7851/99/3812-1819 $ 17.50+.50/0

UM00014149
NOVARTIS EXHIBIT 1517
Novartis v. Regents, IPR2023-01347
Page 2895 of 4460

This Page is Inserted by IFW Indexing and Scanning Operations and is not part of the Official Record

BEST AVAILABLE IMAGES

Defective images within this document are accurate representations of the original documents submitted by the applicant.

Defects in the images include but are not limited to the items checked:

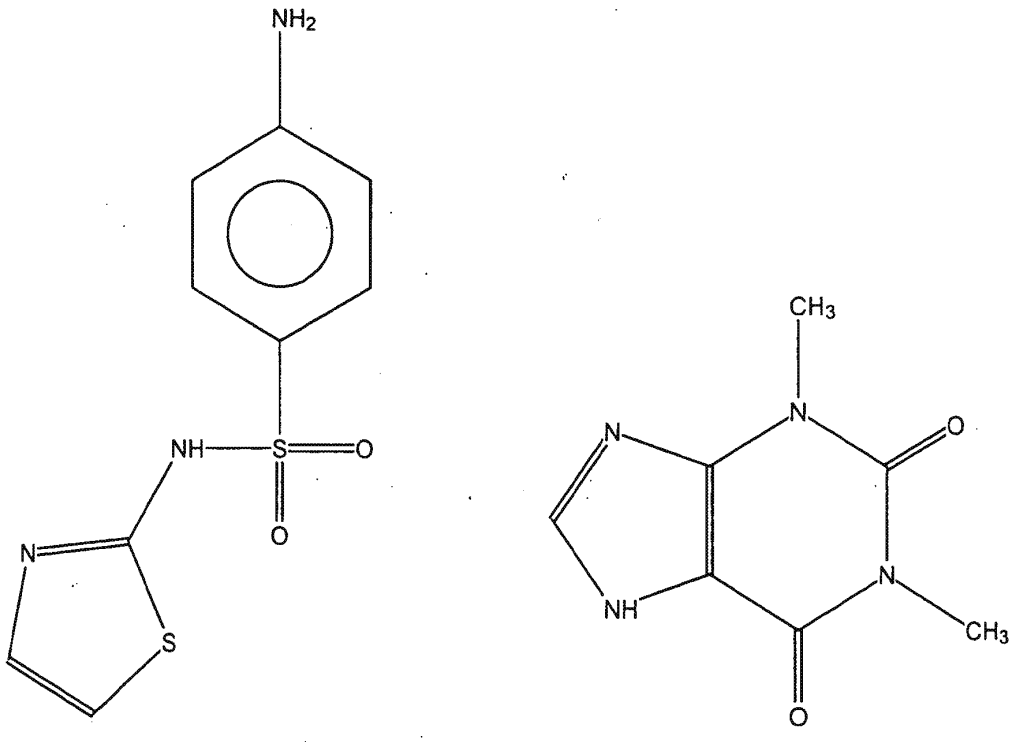
- ☐ BLACK BORDERS
- ☐ IMAGE CUT OFF AT TOP, BOTTOM OR SIDES
- ☐ FADED TEXT OR DRAWING
- ☐ BLURRED OR ILLEGIBLE TEXT OR DRAWING
- ☐ SKEWED/SLANTED IMAGES
- ☐ COLOR OR BLACK AND WHITE PHOTOGRAPHS
- ☐ GRAY SCALE DOCUMENTS
- ☐ LINES OR MARKS ON ORIGINAL DOCUMENT
- ☐ REFERENCE(S) OR EXHIBIT(S) SUBMITTED ARE POOR QUALITY
- ☐ OTHER: _____

IMAGES ARE BEST AVAILABLE COPY.
As rescanning these documents will not correct the image problems checked, please do not report these problems to the IFW Image Problem Mailbox.

Reference:	E.Shefter, T.F.Brennan, P.Sackman (1970) *ACS,Abstr.Papers(Summer)* ,35
Formula:	$C_9 H_9 N_3 O_2 S_2$,$C_7 H_8 N_4 O_2$
Compound Name:	Sulfathiazole-theophylline complex

Space Group:	P21/c	***Cell:***	***a***	11.020	***b***	9.010	***c*** 20.186
Space Group No.:	14	***(Å,°)***	α	90.00	β	113.68	γ 90.00

R-Factor (%):	0.00	***Temperature(K):***	295	***Density(g/cm^3):***	0.000



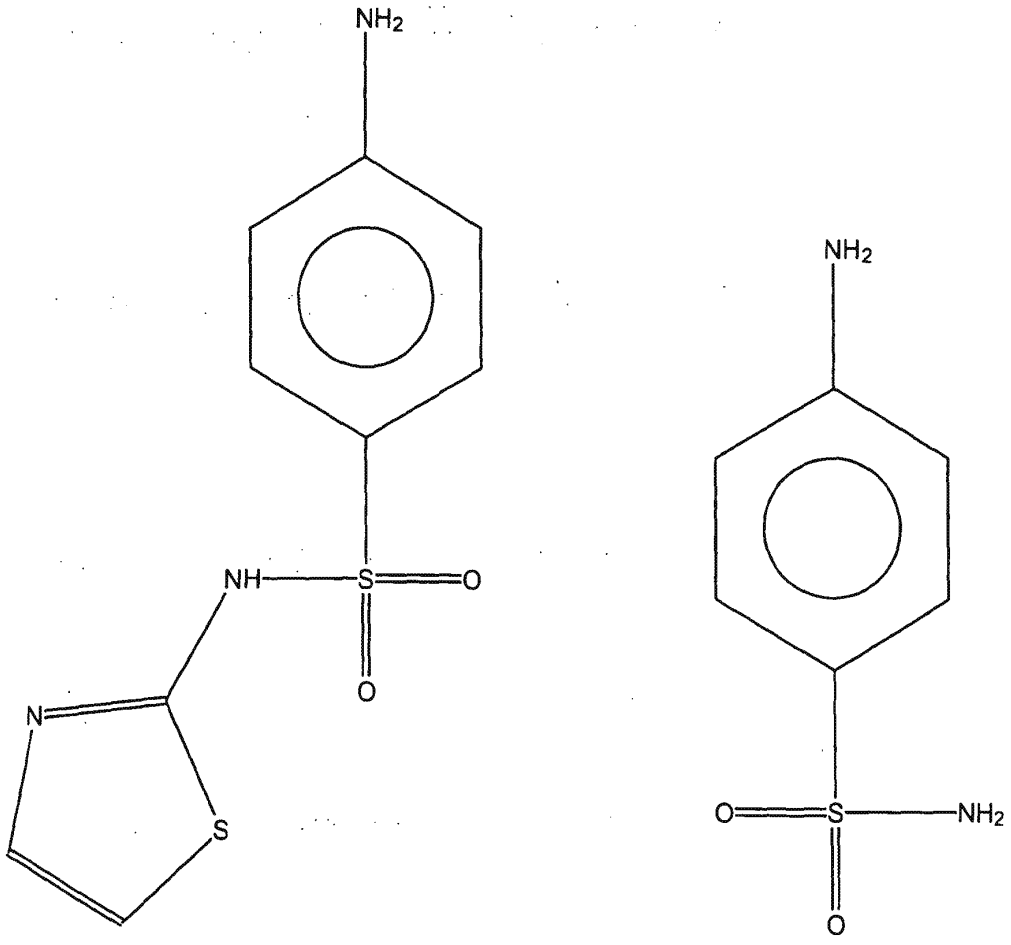
Reference: E.Shefter, T.F.Brennan, P.Sackman (1970)
ACS,Abstr.Papers(Summer) ,35

Formula: $C_9 H_9 N_3 O_2 S_2, C_6 H_8 N_2 O_2 S_1$

Compound Name: Sulfathiazole-sulfanilamide complex

Space Group:	P21/c	***Cell:***	***a***	9.135	***b***	5.379	***c*** 36.630
Space Group No.:	14	***(Å,°)***	α	90.00	β	91.17	γ 90.00

R-Factor (%): 0.00 ***Temperature(K):*** 295 ***Density(g/cm³):*** 0.000



NOVARTIS EXHIBIT 1517
Novartis v. Regents, IPR2023-01347
Page 2898 of 4460

CRYSTAL GROWTH & DESIGN
2003
VOL. 3, NO. 5
783–790

Molecular Complexes of Homologous Alkanedicarboxylic Acids with Isonicotinamide: X-ray Crystal Structures, Hydrogen Bond Synthons, and Melting Point Alternation

Peddy Vishweshwar,[†] Ashwini Nangia,*[,†] and Vincent M. Lynch[‡]

School of Chemistry, University of Hyderabad, Hyderabad 500 046, India, and Department of Chemistry and Biochemistry, University of Texas, Austin, Texas 78712

Received March 7, 2003

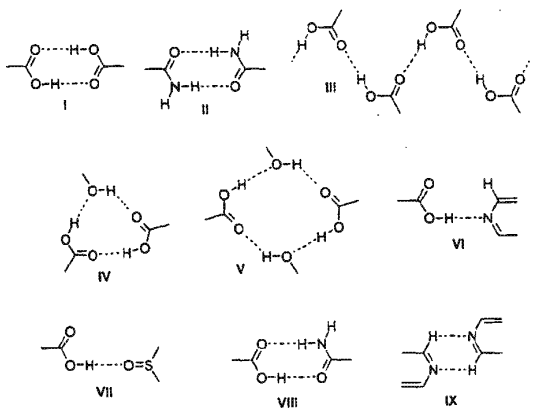
ABSTRACT: Crystallization of α,ω-alkanedicarboxylic acids (HOOC−$(CH_2)_{n-2}$−COOH, n = 2−6) with isonicotinamide (IN) is carried out in 1:2 and 1:1 stoichiometry. Five cocrystals of (diacid)·$(IN)_2$ composition (diacid = oxalic acid, malonic acid, succinic acid, glutaric acid, and adipic acid) are characterized by X-ray diffraction at 153(2) K. Tapes of acid−pyridine O−H···N and amide−amide N−H···O hydrogen bond synthons stabilize these five crystal structures as predicted by the hierarchic model: the best donor (COOH) and best acceptor group (pyridine N) hydrogen bond as acid−pyridine and the second best donor−acceptor group ($CONH_2$) aggregates as an amide dimer. Glutaric acid and adipic acid cocrystallize in 1:1 stoichiometry also, (diacid)·(IN), with acid−pyridine and acid−amide hydrogen bonds. Synthon energy calculations ($\Delta E_{synthon}$, RHF/6-31G**) explain the observed hydrogen bond preferences in 1:2 (five examples) and 1:1 (two examples) cocrystals. The acid−pyridine hydrogen bond is favored over the acid−amide dimer for strong carboxylic acids because the difference between $\Delta E_{acid-pyridine}$ and $\Delta E_{acid-amide}$ (−2.21 kcal mol^{-1}) is greater than the difference for weak acids (−0.77 kcal mol^{-1}), which cocrystallize with both of these hydrogen bond synthons. We suggest $\Delta E_{synthon}$ as a semiquantitative parameter to rank hydrogen bond preferences and better understand supramolecular organization in the multifunctional acid−IN system. Melting point alternation in five homologous (diacid)·$(IN)_2$ cocrystals is correlated with changes in crystal density and packing fraction.

Introduction

Hydrogen bonding is the master key in crystal engineering, supramolecular chemistry, and biological recognition.[1−3] The strong and directional nature of hydrogen bonds is exploited in the organized self-assembly of molecules in solution and the solid state. Carboxylic acids and amides are two commonly used functional groups in crystal engineering because they generally form robust architectures via O−H···O and N−H···O hydrogen-bonded dimers.[4,5] However, our understanding of the factors that direct hydrogen-bonding motifs when other functional groups are also present in the molecule is still evolving.[6] The main challenge in carrying out crystal design with multifunctional molecules is that one is unable to predict when a particular functional group (e.g., hydroxyl, halogen, pyridine, ester, amide) will perturb the normal hydrogen bond motif of a given functional group (say COOH). The exercise is further complicated because the way in which the hydrogen bond motif changes in a particular system could subtly depend on the molecular structure.[6f] Therefore, research on understanding the forces that govern recognition between multifunctional molecules is of fundamental importance in supramolecular chemistry. For the successful implementation of target crystal synthesis, it is necessary to understand the synergy, interplay, and competition between different functional groups during self-assembly.[7]

A current theme in crystal engineering is to use strong and weak hydrogen bonds (O−H···O, O−H···N, N−H···O, C−H···O) for building nanoscale architectures from molecular scaffolds via multipoint recognition supramolecular synthons.[8] Statistical trends retrieved from the Cambridge Structural Database (CSD)[9] are a better guide in crystal design than the observed interaction patterns in a subset of structures. For two common bimolecular synthons, carboxylic acid dimer I occurs in 33% crystal structures and amide dimer II is very rare (8%) in the global archive.[10] Apart from homodimer I, carboxylic acids also aggregate via catemer III and hydrated motifs IV and V (Scheme 1). On the other hand, the success rate of carboxylic acid hydrogen bonding with complementary functional groups is much higher: acid−pyridine VI (91%), acid−sulfoxide VII (78%), and acid−amide VIII (78%).[11] The synthesis of binary crystals[12] (molecular complexes of two neutral

Scheme 1. Hydrogen Bond Synthons Discussed in This Paper

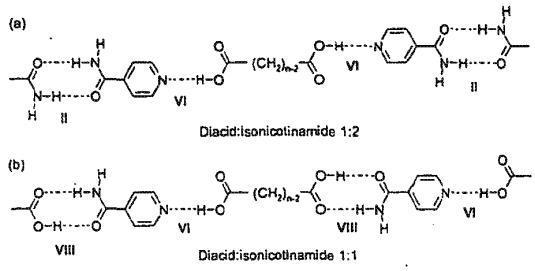


* Corresponding author. Tel.: 91 40 3011338. Fax: 91 40 3010567. E-mail: ansc@uohyd.ernet.in.
† University of Hyderabad.
‡ University of Texas.

10.1021/cg034037h CCC: $25.00 © 2003 American Chemical Society
Published on Web 06/20/2003

UM00014152
NOVARTIS EXHIBIT 1517
Novartis v. Regents, IPR2023-01347
Page 2899 of 4460

Scheme 2[a]



[a] (a) Acid–pyridine VI and amide–amide II synthons in diacid·$(IN)_2$ cocrystals (n = 2–6). (b) Acid–pyridine VI and acid–amide VIII synthons in diacid·(IN) cocrystals (n = 5, 6).

components, cocrystals) mediated via heterosynthons rapidly affords a large number of crystal structures for analysis.

Carboxylic acid–pyridine synthon VI has emerged as a robust and recurring design strategy in crystal engineering.[13] A modular self-assembly approach to carboxylic acid·isonicotinamide (IN) cocrystals stabilized by acid–pyridine synthon VI and amide–amide dimer II was recently proposed by Aakeröy[14] based on the hydrogen bond hierarchy (ranking) rules formulated by Etter:[15] the best donor (COOH) hydrogen bonds to the best acceptor (pyridine N), and the second best donor and acceptor groups hydrogen bond next (amide dimer). Notwithstanding the synthetic ease of building nanostructures through such a supramolecular synthesis protocol, the factors that control self-assembly in competitive hydrogen bond situations are still not properly understood. For example, different combinations of O–H···O, O–H···N, and N–H···O hydrogen bonds in the carboxylic acid–IN system can result in at least four different synthons (I, II, VI, VIII; Scheme 1) with the preference order acid–pyridine VI > acid–amide VIII > amide–amide II > acid–acid I. However, subtle molecular features, crystallization conditions, and small differences in hydrogen bond energy could alter this hierarchy in favor of one motif or another, particularly between heterosynthons VI and VIII. It is therefore ideal to probe hydrogen bonding in such (almost) isoenergetic synthons in X-ray crystal structures with systematic variation of molecular structure. We have synthesized cocrystals of IN with homologous α,ω-alkanedicarboxylic acids (HOOC–$(CH_2)_{n-2}$–COOH): oxalic acid (OA, n = 2), malonic acid (MA, n = 3), succinic acid (SA, n = 4), glutaric acid (GA, n = 5), and adipic acid (AA, n = 6). These five acids afford the expected 1:2 complex of diacid and IN stabilized by acid–pyridine VI and amide–amide II hydrogen bonds (Scheme 2a). GA and AA also cocrystallize in 1:1 stoichiometry with acid–pyridine VI and acid–amide hydrogen bond VIII (Scheme 2b).[16] The idea of using symmetrical dicarboxylic acid with chemically equivalent COOH groups is to study supramolecular organization in competitive hydrogen bond situations. We explain through computation of hydrogen bond synthon energy ($\Delta E_{synthon}$, Spartan, RHF/6-31G**) the formation of 1:2 cocrystals and rationalize why 1:1 cocrystals are isolated in two out of five cases. Melting point alternation in diacid·$(IN)_2$ cocrystals is correlated with alternation in crystal density and packing fraction.

Results

The molecular complex of the appropriate dicarboxylic acid (HOOC–$(CH_2)_{n-2}$–COOH, n = 2–6) and IN was obtained by dissolving the components in 1:2 stoichiometry in suitable solvent(s). Slow evaporation at room temperature gave diffraction quality crystals after a few days. Binary crystals were characterized by Fourier transform infrared, melting point (differential scanning calorimetry; DSC), and X-ray diffraction (XRD) (see Experimental Section). Similarly, 1:1 cocrystals of diacid (n = 5, 6) and IN were grown and analyzed. Crystallographic details are summarized in Table 1, and hydrogen bond metrics are listed in Table 2. ORTEP plots of crystal structures are displayed in the Supporting Information.

The crystal structure of OA·$(IN)_2$ contains half a molecule of OA and one molecule of IN in the monoclinic space group $C2/c$ (Table 1). The OA molecule resides on the 2-fold rotation axis in *syn*-planar conformation. The COOH group hydrogen bonds to pyridine N, and carboxamide groups aggregate as a centrosymmetric dimer (O–H···N: 1.58 Å, 2.5636(13) Å, 179.5°; N–H···O: 1.91 Å, 2.9168(13) Å, 173.8°). Linear tapes of synthons VI and II are connected via N–H···O hydrogen bond to acid carbonyl group of inversion-related tapes as shown in Figure 1a (2.00 Å, 3.0079(13) Å, 170.9°). The overall structure is stabilized by numerous C–H···O interactions.[17] The crystal structure of MA·$(IN)_2$ in the triclinic space group $P\bar{1}$ has three symmetry-independent diacid molecules and six crystallographically unique IN molecules.[18] Symmetry-independent MA and IN molecules constitute the zigzag tape of acid–pyridine and amide–amide hydrogen bonds, which are in turn connected via amide N–H···O hydrogen bonds (Figure 1b). Metrics of hydrogen bonds and C–H···O interactions are in the usual range (Table 2). The crystal structure of SA·$(IN)_2$ (at 203 K) was published[14] while this work was in its final stages. We present our crystallographic result (at 153 K, Figure 1c) because it is part of the homologous series. The fact that an identical crystal structure of the same complex is obtained in different laboratories means that polymorphism, the existence of the same chemical substance in different crystalline modifications, is not a complication in the present family of compounds. The tape structure in GA·$(IN)_2$ has two symmetry-independent diacid molecules and four IN molecules (space group $P2_1/n$, Figure 1d). In both diacid molecules, one of the O–H···N hydrogen bonds is shorter than the other contact (O···N: 2.58, 2.66; 2.59, 2.68 Å). AA·$(IN)_2$ crystallizes in the triclinic space group $P\bar{1}$ with Z' of half for diacid and one molecule of IN (Figure 1e).

Upon isolation of 1:2 cocrystals for five homologous dicarboxylic acids with IN, we posed the question: Is it possible for COOH groups of the α,ω-alkanedicarboxylic acid to hydrogen bond via acid–pyridine and acid–amide synthons in the same crystal? Our experiment with 1:1 cocrystallization was successful with two out of five diacids tried, GA and AA. In the 1:1 complex of GA·IN and AA·IN (both in $P2_1/c$), one molecule of each component is present in the asymmetric unit. What is of note in the 1:1 cocrystal is that the identical COOH group of diacid hydrogen bonds via different synthons, acid–pyridine VI and acid–amide VIII (Figure 2).

UM00014154
NOVARTIS EXHIBIT 1517
Novartis v. Regents, IPR2023-01347
Page 2900 of 4460

Table 1. Crystallographic Data and Structure Refinement Parameters (CCDC Deposit Nos. 199970−199976)

compound	OA·(IN)$_2$	MA·(IN)$_2$	SA·(IN)$_2$	GA·(IN)$_2$	AA·(IN)$_2$	GA·IN	AA·IN
empirical formula	$(C_2H_2O_4)_{0.5}\cdot(C_6H_6N_2O)$	$(C_3H_4O_4)_3\cdot(C_6H_6N_2O)_6$	$(C_4H_6O_4)_{0.5}\cdot(C_6H_6N_2O)$	$(C_5H_8O_4)_2\cdot(C_6H_6N_2O)_4$	$(C_6H_{10}O_4)0.5\cdot(C_6H_6N_2O)$	$(C_5H_8O_4)\cdot(C_6H_6N_2O)$	$(C_6H_{10}O_4)\cdot(C_6H_6N_2O)$
formula wt	167.15	1044.95	181.17	752.74	195.20	254.24	268.27
crystal system	monoclinic	triclinic	triclinic	monoclinic	triclinic	monoclinic	monoclinic
space group	*C*2/*c*	$P\bar{1}$	$P\bar{1}$	$P2_1/n$	$P\bar{1}$	$P2_1/c$	$P2_1/c$
a (Å)	11.7466(2)	11.9420(2)	6.8198(2)	14.0439(2)	5.2522(1)	9.8980(3)	13.6429(4)
b (Å)	10.0164(2)	14.8580(2)	7.0650(2)	10.9859(1)	9.1180(2)	16.7520(6)	9.6159(2)
c (Å)	12.1967(2)	15.6820(2)	9.0971(3)	23.0238(4)	10.4487(3)	7.3150(5)	9.8215(2)
α (°)	90.0	65.6990(6)	80.509(1)	90.0	104.473(1)	90.0	90.0
β (°)	102.395(1)	85.5740(6)	77.614(1)	97.5560(5)	103.477(1)	95.479(2)	97.562(1)
γ (°)	90.0	67.3070(6)	72.838(1)	90.0	100.811(1)	90.0	90.0
Z	8	2	2	4	2	4	4
volume (Å^3)	1401.60(4)	2328.62(6)	406.62(2)	3521.4(12)	454.824(19)	1207.37(10)	1277.26(5)
D_{calc} (g cm^{-3})	1.584	1.490	1.480	1.420	1.425	1.399	1.395
μ (mm^{-1})	0.126	0.117	0.115	0.109	0.109	0.112	0.110
2θ (°)	5.96−54.96	5.82−54.94	6.08−54.98	5.82−54.96	5.82−54.96	5.82−54.96	5.82−54.96
range *h*	−15 to 15	−15 to 15	−8 to 7	−18 to 18	−6 to 6	−12 to 12	−17 to 17
range *k*	−12 to 12	−15 to 19	−9 to 8	−14 to 12	−10 to 11	−21 to 18	−10 to 12
range *l*	−15 to 15	−20 to 20	−11 to 11	−29 to 29	−10 to 13	−9 to 9	−12 to 12
reflns collected	2980	16180	2738	13721	3003	4619	4705
unique reflns	1596	10660	1818	7966	2012	2710	2803
observed reflns	1428	6898	1565	5020	1582	1966	2235
R_1 [$I > 2\sigma(I)$][a]	0.0329	0.0463	0.0348	0.0439	0.0393	0.0392	0.0394
wR_2 (all)	0.0916	0.1017	0.0880	0.0990	0.0946	0.0900	0.1091
goodness-of-fit	1.064	1.031	1.048	0.982	1.052	1.049	1.060
C_k* (%)[b]	77.1	73.1	74.1	71.8	73.0	70.3	71.6

[a] R_1, crystallographic reliability index. [b] C_k*, Packing fraction calculated with PLATON.

Table 2. Geometrical Parameters of Hydrogen Bonds

cocrystal	H-bond	*d* (Å)[c]	*D* (Å)	θ (°)	H-bond	*d* (Å)[c]	*D* (Å)	θ (°)
OA·(IN)$_2$	O−H···N	1.58	2.5636(13)	179.5	C−H···O	2.43	3.2853(14)	134.9
	N−H···O	1.91	2.9168(13)	173.8	C−H···O	2.48	3.3055(13)	131.6
	N−H···O	2.00	3.0079(13)	170.9	C−H···O	2.60	3.5317(14)	143.8
	C−H···O	2.38	3.2109(13)	132.2				
MA·(IN)$_2$	O−H···N	1.57	2.5475(18)	168.4	N−H···O	1.91	2.9095(18)	168.4
	O−H···N	1.57	2.5517(18)	175.9	N−H···O	1.92	2.9115(18)	167.1
	O−H···N	1.57	2.5523(20)	172.2	N−H···O	1.91	2.9190(20)	175.6
	O−H···N	1.57	2.5545(18)	173.2	N−H···O	1.92	2.9119(18)	166.5
	O−H···N	1.59	2.5642(18)	171.9	N−H···O	1.95	2.9630(20)	177.3
	N^+−H···O^-	1.55	2.5559(18)	171.2	N−H···O	1.97	2.9820(20)	175.7
	N−H···O	1.86	2.8538(18)	167.9	N−H···O	1.99	2.9644(18)	161.9
	N−H···O	1.86	2.8740(20)	176.6	C−H···O	2.17	3.2382(18)	166.0
	N−H···O	1.89	2.8697(18)	161.7	C−H···O	2.19	3.2549(18)	166.8
	N−H···O	1.89	2.8990(20)	178.2	C−H···O	2.21	3.2843(18)	168.7
	N−H···O	1.89	2.9030(20)	175.1	C−H···O	2.24	3.2877(19)	161.4
SA·(IN)$_2$	O−H···N	1.65	2.6149(14)	165.6	C−H···O	2.66	3.4368(16)	127.8
	N−H···O	1.91	2.9211(13)	177.8	C−H···O	2.69	3.4356(15)	125.1
	N−H···O	1.97	2.9487(14)	162.5	C−H···O	2.70	3.6053(16)	141.0
	C−H···O	2.55	3.4897(15)	144.5				
GA·(IN)$_2$	O−H···N	1.61	2.5822(18)	168.7	N−H···O	1.98	2.9789(19)	168.3
	O−H···N	1.63	2.5957(17)	166.0	N−H···O	1.99	2.9952(18)	170.1
	O−H···N	1.68	2.6684(17)	177.2	N−H···O	2.09	3.0725(19)	162.4
	O−H···N	1.70	2.6818(17)	174.0	N−H···O	2.11	3.0871(19)	161.6
	N−H···O	1.83	2.8341(19)	174.0	C−H···O	2.22	3.2820(20)	165.1
	N−H···O	1.84	2.8510(19)	174.6	C−H···O	2.27	3.3280(20)	163.1
	N−H···O	1.91	2.9149(19)	174.2	C−H···O	2.36	3.3570(20)	151.9
	N−H···O	1.95	2.9607(19)	173.3	C−H···O	2.37	3.3710(20)	152.9
AA·(IN)$_2$	O−H···N	1.64	2.6179(15)	170.0	C−H···O	2.39	3.4304(19)	161.1
	N−H···O	1.87	2.8794(15)	178.1	C−H···O	2.46	3.4508(18)	150.6
	N−H···O	2.04	3.0275(16)	164.6	C−H···O	2.54	3.5401(19)	153.4
	C−H···O	2.35	3.4299(19)	172.1	C−H···O	2.65	3.2665(17)	115.1
GA·IN	O−H···O	1.64	2.6047(14)	165.4	C−H···O	2.41	3.4844(17)	172.3
	O−H···N	1.77	2.6710(15)	150.9	C−H···O	2.41	3.4509(17)	160.5
	N−H···O	1.85	2.8360(16)	163.5	C−H···O	2.45	3.2228(17)	127.3
	N−H···O	1.90	2.9109(17)	173.4				
AA·IN	O−H···O	1.66	2.6323(15)	167.3	C−H···O	2.43	3.4376(17)	154.2
	O−H···N	1.65	2.6301(15)	170.6	C−H···O	2.45	3.4318(19)	149.8
	N−H···O	1.91	2.9055(17)	167.6	C−H···O	2.47	3.2452(16)	127.3
	N−H···O	1.96	2.9616(16)	170.5				

[c] O−H, N−H, and C−H distances are neutron-normalized.

UM00014155
NOVARTIS EXHIBIT 1517
Novartis v. Regents, IPR2023-01347
Page 2901 of 4460

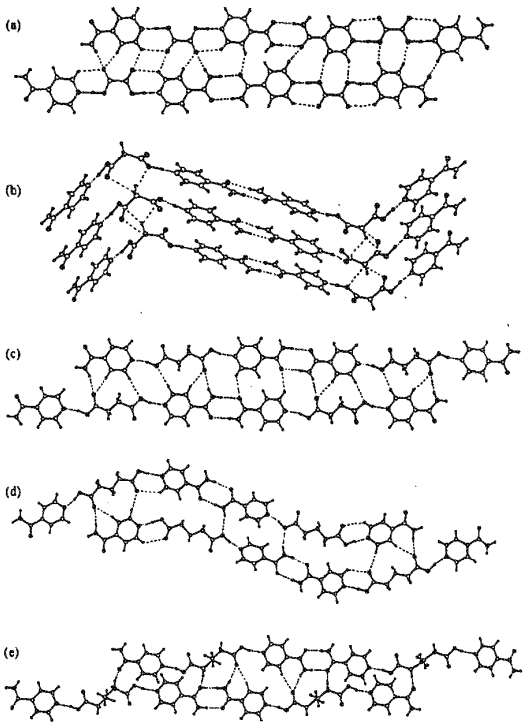


Figure 1. Hydrogen-bonded tapes of diacid and IN molecules assembled via synthons VI and II and N−H···O and C−H···O interactions between the tapes. (a) OA·$(IN)_2$, (b) MA·$(IN)_2$, (c) SA·$(IN)_2$, (d) GA·$(IN)_2$, and (e) AA·$(IN)_2$. The central carbon atoms of AA are not clearly visible in (e) because it is present in a folded conformation (Figure 3). Hydrogen bonds are shown as dash lines in this and subsequent figures.

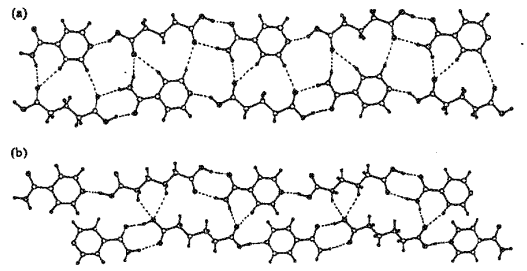


Figure 2. Hydrogen-bonded tapes of diacid and IN molecules assembled via synthons VI and VIII and N−H···O and C−H···O interactions between the tapes. (a) GA·IN and (b) AA·IN.

Discussion

Structural Analysis. Crystal structures of diacid·IN 1:2 complexes presented in this paper have predictable tapes of synthons VI and II. While there are differences in the way these hydrogen-bonded tapes aggregate as layers and then stack to form the three-dimensional crystal, these details are specific to each structure and therefore not discussed. We highlight only those structural features that deal with an unusual molecular conformation or facilitate our understanding of the variable stoichiometry in these cocrystals.

OA usually exists in the anti conformation in its crystal structure and also in many molecular complexes. The anti conformation is more stable than the syn conformation by <0.5 kcal mol^{-1}.[19] OA is present in the *syn*-planar conformation in OA·$(IN)_2$. There are three occurrences of syn conformation in the literature,[20] and all of these are cocrystals of OA. The first occurrence of *syn*-OA in the solid state was reported by Leiserowitz[20a] in the 1:1 complex with acetamide (space group *A*2/*a*, $Z' = 2$ molecules of each component). The less stable syn conformation of OA in OA·$(IN)_2$ is stabilized by O−H···N and C−H···O hydrogen bonds of synthon VI together with a N−H···O hydrogen bond from $CONH_2$ (Table 2, Figure 1a). Salient bond angles and torsion angles of *syn*-planar COOH groups of OA are listed in Table 3. The *syn*-planar conformation of OA in its complex with IN is the most planar among published examples, with a O=C−C=O torsion angle of 0.13(15)° as compared to 2.1° in OA·(acetamide). A molecule like OA can reside either on the inversion center (anti conformation) or on the 2-fold rotation axis (syn conformation) in a space group like *C*2/*c*, *A*2/*a*. Generally, diacids occupy the inversion center special position in a near planar anti orientation of C=O groups in the crystal. However, if the diacid occupies the 2-fold rotation axis, the syn C=O groups are usually inclined.[21] The present case is unique in that OA occupies the 2-fold axis special position in a perfect *syn*-planar conformation. We believe that the C=O groups can be in close proximity (O···O 2.76 Å) despite the severe lone-pair repulsion because the oxygen atoms are engaged in extensive hydrogen bonding and this minimizes their mutual repulsion.

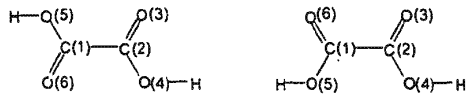
The MA·$(IN)_2$ cocrystal structure has three symmetry-independent MA molecules and six unique IN molecules. The crystallographic-independent MA molecules have different bond angles and torsion angles (Supporting Information), i.e., they adopt different conformations in the crystal. The phenomenon of multiple molecules in the asymmetric unit ($Z' > 1$) continues to interest crystallographers and structural chemists.[22] Database analyses have been carried out to understand high Z' structures, but the exact reasons are still not fully understood. We note that O−H···N hydrogen bonds in symmetry-independent occurrences of synthon VI are short (strong) with a typical O···N distance of ca. 2.55 Å (Table 2). Crystallization of multiple conformations of a molecule from solution to the solid state is common in structures stabilized by strong hydrogen bonds (e.g., alcohols).

GA and AA cocrystals were obtained with 1:2 and 1:1 composition. The three molecules of GA, two in the 1:2 crystal and one in the 1:1 crystal, have a syn orientation (O=C- - -C=O = 4.5, 6.1, 2.5°). There are many occurrences of the syn conformer of GA in the CSD. AA is present in the extended zigzag conformation in AA·IN but in the folded S-shaped conformation in AA·$(IN)_2$. The S-shaped conformation is stabilized by an intramolecular C−H···O hydrogen bond (2.65 Å, 115.1°) in a six member ring (Figure 3).[23] The folded conformation is more stable than the extended, zigzag conformation by 0.63 kcal mol^{-1}, as calculated in Cerius[2] using the Dreiding force field.

GA·IN and AA·IN cocrystals (1:1) have tapes of acid−pyridine VI and acid−amide VIII synthons connected

UM00014156
NOVARTIS EXHIBIT 1517
Novartis v. Regents, IPR2023-01347
Page 2902 of 4460

Table 3. Conformation of OA in OA·(IN)$_2$ and Some Structures in the CSD



	OA·(IN)$_2$[a] (this paper)	OXLACM[a] (ref 20a)	COGREV[a] (ref 20b)	FUNCUM[a,b] (ref 20c)	OXALAC05[c] (ref 27)
		bond length (Å)			
C(1)−C(2)	1.5601(14)	1.529(7)	1.534	1.539	1.542
C(2)=O(3)	1.2172(13)	1.212(6)	1.199	1.189 1.195	1.218
C(2)=O(4)	1.2923(13)	1.298(6)	1.298	1.304 1.304	1.303
O(4)···O(5)	2.621	2.590	2.574	2.573	
O(3)···O(6)	2.763	2.728	2.754	2.768	
		bond/torsion angle (°)			
C(1)−C(2)=O(3)	119.61(9)	119.6(5)	120.248	120.796 121.136	122.07
C(1)−C(2)-O(4)	114.24(9)	114.1(4)	113.169	113.251 113.362	110.89
O(3)=C(2)−O(4)	126.14(10)	126.2(5)	126.581	125.947 125.482	127.04
O(3)=C(2)−C(1)=O(6)	0.13(15)	2.1	13.81	5.621	180.0

[a] *syn*-Planar conformation in cocrystal. [b] Full molecule in asymmetric unit. [c] *anti*-Planar conformation in pure OA.

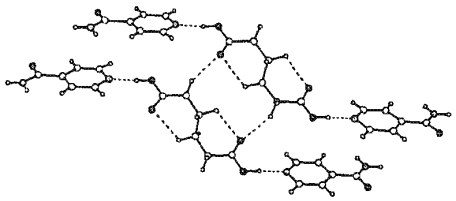


Figure 3. Folded S-conformer of AA in AA·(IN)$_2$. The intramolecular C−H···O hydrogen bond is shown with bold dash lines.

via N−H···O and C−H···O hydrogen bonds (Figure 2). Dicarboxylic acids (e.g., SA, fumaric acid)[14] hydrogen bond with the pyridine acceptor of IN in a symmetrical motif (1:2 cocrystal). It is possible that hydrogen bonding of one COOH will slightly alter the acidity of second COOH (e.g., in cocrystal of OA),[20a] in effect differentiating between the two donor groups. However, such inductive effects will fall off over a long range in GA and AA. Second, the change in stoichiometry may not be due to orientation of donor groups[13h] because 1:1 cocrystals are obtained with both even and odd member diacids. In the 1:1 cocrystal, the same COOH donor groups hydrogen bond with the best acceptor (pyridine N) and second best acceptor ($CONH_2$) via synthons VI and VIII. The reasons for alternative crystallization pathways are discussed next.

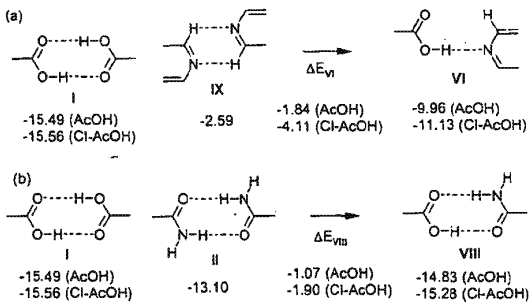
Synthon Energy and Database Analysis. Hydrogen bond synthon energies were calculated in Spartan using the RHF 6-31G** basis set. To cover dicarboxylic acids with different strengths in the present series (Table 4),[24] chloroacetic acid and acetic acid were taken to represent strong and weak acids, respectively. A reason for selecting Cl−AcOH is that it is a strong acid that hydrogen bonds with IN in a neutral cocrystal without transfer of proton. Computed synthon energies on model complexes AcOH·pyridine, AcOH·CH_3CONH_2, Cl−AcOH·pyridine, and Cl−AcOH·CH_3CONH_2 (Scheme 3) are used for further discussion of hydrogen bonding

Table 4. pK_a (First Step) of Carboxylic Acids[a]

acid	pK_a	acid	pK_a
OA	1.23	AA	4.43
MA	2.83	acetic acid	4.75
SA	4.16	chloroacetic acid	2.85
GA	4.31		

[a] Ref 24.

Scheme 3. Energy of Hydrogen Bond Synthons Calculated in Spartan (RHF/6-31G, kcal mol^{-1})[a]**



[a] $E_{synthon}$ refers to the energy of the hydrogen bond motif and $\Delta E_{synthon}$ is the stabilization of heterosynthon as compared to homodimers. (a) CH_3COOH·pyridine, $ClCH_2COOH$·pyridine. (b) CH_3COOH·CH_3CONH_2, $ClCH_2COOH$·CH_3CONH_2.

in the diacid·IN system. $E_{synthon}$ is the energy of the hydrogen bond motif and $\Delta E_{synthon}$ is the energy difference between the heterosynthon and the constituent homosynthons. $\Delta E_{synthon}$ calculations for VI and VIII show that acid−pyridine and acid−amide heterosynthon is favored over the constituent homosynthons for both Cl−AcOH and AcOH but to different extents. ΔE_{VI} and ΔE_{VIII} for complex with Cl−AcOH are quite different (−4.11, −1.90 kcal mol^{-1}), but the energy difference for AcOH is small (−1.84, −1.07 kcal mol^{-1}). Heterosynthon VI is generally favored when COOH, pyridine, and $CONH_2$ groups compete for hydrogen bonding ($\Delta E_{VI} < \Delta E_{VIII}$). For strong carboxylic acids, VI is always formed

UM00014157
NOVARTIS EXHIBIT 1517
Novartis v. Regents, IPR2023-01347
Page 2903 of 4460

in preference to VIII ($\Delta E_{VI} - \Delta E_{VIII} = -2.21$ kcal mol^{-1}, Cl–AcOH), but for weak acids, the selectivity is moderate ($\Delta E_{VI} - \Delta E_{VIII} = -0.77$ kcal mol^{-1}, AcOH). We assume that entropy (kinetic factors) is equally important in these recognition events because they are bimolecular synthons and so differences in enthalpy are an indication of free energy differences. If a product heterosynthon is more stable relative to starting homosynthons, then it is more likely to be formed. That such an assumption is reasonable in the present family of crystal structures is validated by CSD statistics. In the subdatabase of 63 organic crystal structures containing COOH, pyridine (C=N–C), and CONH functional groups, the acid–pyridine hydrogen bond is present in 39 hits as compared to only five hits for acid–amide when O···O and O···N distances within the van der Waals sum were considered.

The variation of $\Delta E_{synthon}$ with donor acidity may be explained as follows. Acid–pyridine recognition VI has a single hydrogen bond (O–H···N) with auxiliary contribution (occasionally) from a weak C–H···O interaction. The energy of synthon VI decreases for weak carboxylic acids (compare E_{VI} for Cl–AcOH and AcOH, Scheme 3), and this is also reflected in the lengthening of the O–H···N hydrogen bond in 1:2 cocrystals (Table 2, O···N (Å): OA, 2.56; AA, 2.62). However, because numerous directional (long range) and isotropic (short range) forces determine the geometry of a particular interaction in the crystal, a regular increase in the O···N distance with increasing pK_a is not observed in the series. In acid–amide VIII, as the O–H···O bond lengthens, the N–H···O interaction becomes shorter (because C=O is a better acceptor) and hence the synthon energy is not so sensitive to donor strength[25] (compare E_{VIII} for Cl–AcOH and AcOH, Scheme 3). The difference in $\Delta E_{synthon}$ for VI and VIII diminishes for weak acid because VI becomes weaker but the energy of VIII is largely invariant.

Finally, we note that success in cocrystallization depends not only on the choice of complementary molecules but also on many other critical factors such as similar solubility, size match, solvent, and temperature. Hence, the cocrystals isolated in our experiments represent only a subset of possible combinations. Several attempts to identify a 1:1 cocrystal of OA, MA, and SA gave 1:2 stoichiometry even when diacid was used in excess.[26] Results reported in this paper were confirmed in multiple experiments. We are carrying out crystallization under different solvent/temperature conditions and with mechanical grinding to discover other forms and stoichiometry. Our attempts to correlate calculated lattice energies of crystals (Mimimizer, Cerius^2) were thwarted because the space group, number of symmetry-independent molecules, and molecular conformation change from structure to structure.

Melting Point Alternation. The observed melting point (by DSC) and density, the packing fraction (from X-ray structure) in diacid·(IN)$_2$ cocrystals, and the corresponding pure α,ω-alkanedicarboxylic acids[27] are displayed in Figure 4. Melting point alternation in pure diacids is explained through differences in molecular conformation and packing motifs: even diacids close pack in a parallelogram shape with no voids whereas odd diacids adopt less stable conformations and pack as trapezoids with small voids. Cocrystals have higher melting points than the corresponding pure diacids (Table 5) because strong hydrogen bonds and efficient close packing stabilize the structures of molecular complexes. The T_m values of cocrystals with $n = 2-6$ carbon atoms show an alternation of even series having a higher melting point than odd members. Both D_{calc} and C_k* alternate in these cocrystals, although the correlation is somewhat superior with packing fraction. Inasmuch as enthalpy factors determine the melting point, D_{calc} (or C_k*) is correlated with T_m of the crystal. Our results together with data on (acid)$_2$·(pyrazine)[28] cocrystals suggest that melting point alternation is a property of the pure carboxylic acids as well as their crystalline complexes.

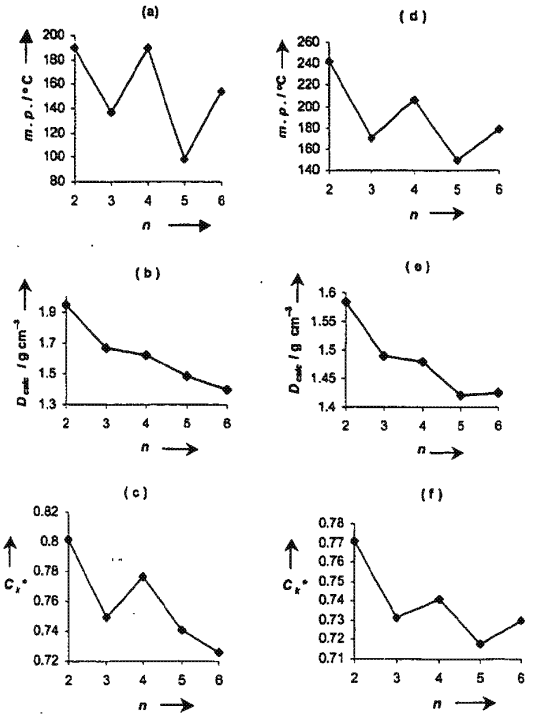


Figure 4. Melting point (a), crystal density (b), and packing fraction (c) for α,ω-alkanedicarboxylic acids using data taken from ref 27. Melting point (d), crystal density (e), and packing fraction (f) for diacid·(IN)$_2$ cocrystals. Note that melting point alternation in cocrystals correlates with D_{calc} and C_k* values.

Table 5. Melting Point of Aliphatic Dicarboxylic Acids and Their 1:2 Cocrystals with IN, Diacid·(IN)$_2$

dicarboxylic acid	mp (°) of diacid[a]	mp (°) of cocrystal
OA	190	243
MA	137	170
SA	193	206
GA	98	149
AA	155	178

[a] Ref 27.

Conclusions

We have analyzed carboxylic acid–IN crystal structures in a family of homologous α,ω-alkanedicarboxylic

UM00014158
NOVARTIS EXHIBIT 1517
Novartis v. Regents, IPR2023-01347
Page 2904 of 4460

acids to better understand competition and interplay between acid–pyridine and acid–amide hydrogen bond synthons. Five cocrystals of diacid·IN with 1:2 stoichiometry are isolated and characterized by XRD. Hydrogen bonding in these five structures obeys hierarchy rules. Furthermore, two cocrystals with 1:1 composition are characterized in which hydrogen bonding does not follow from the best donor–best acceptor order. The reason for an alternative crystallization pathway in acid–IN complexes is explained by a combination of synthon energy and structural database derived arguments. Acid–pyridine synthon is favored over acid–amide for strong carboxylic acid, but the preference is marginal for weak acid. That there are no formal rules for predicting crystal structures with competing supramolecular organization was noted very recently in the same journal.[6f] We make a beginning toward understanding hydrogen bond preferences in multifunctional systems with a semiquantitative synthon energy-based approach. The observed melting point alternation in diacid·$(IN)_2$ cocrystals is correlated with a change in crystal density and packing fraction.

Note Added in Proof

After submitting this paper, we reported the crystal structure of 4-hydroxybenzoic acid·IN that has phenol–pyridine and acid–amide hydrogen bonds and not the expected acid–pyridine and amide–amide synthons. Vishweshwar, P.; Nangia, A.; Lynch, V. M. *CrystEngComm* **2003**, *5*, 164–168.

Experimental Section

Crystallization. All chemicals were purchased from Lancaster and used as such for crystallization. The components were well ground and dissolved in appropriate solvents. All crystallization experiments were carried out under near identical conditions and gave recurring results in at least three batches. The melting point was recorded on a Fisher-Johns apparatus and also from the onset temperature of endotherm in DSC.

OA·$(IN)_2$. OA dihydrate (26 mg, 0.2 mmol) and IN (50 mg, 0.4 mmol) were dissolved in a hot water–ethanol (1:1) mixture. Colorless cubelike crystals were formed after a few days upon evaporation of the solvent; mp 241–243 °C. IR (KBr): 3385, 3161, 1686, 1404, 1236, 1032, 852, 653 cm^{-1}.

MA·$(IN)_2$. A 1:2 mixture of MA (21 mg, 0.2 mmol) and IN (50 mg, 0.4 mmol) was dissolved in hot ethanol. Needlelike colorless crystals were obtained after a few days; mp 167–170 °C. IR (KBr): 3389, 3178, 1722, 1392, 1153, 1055, 856, 650 cm^{-1}.

SA·$(IN)_2$. SA (24 mg, 0.2 mmol) was dissolved in hot ethyl acetate–methanol (1:1) together with IN (50 mg, 0.4 mmol). Colorless crystals were formed after 1 week upon evaporation of the solvent; mp 205–206 °C (134–136 °C).[14] IR (KBr): 3395, 3171, 1686, 1413, 1317, 1184, 1063, 1014, 798, 619 cm^{-1}.

GA·$(IN)_2$. Light brown platelike crystals of the complex were obtained upon crystallization of a 1:2 mixture of GA (27 mg, 0.2 mmol) and IN (50 mg, 0.4 mmol) from hot methanol solution; mp 148–149 °C. IR (KBr): 3410, 3175, 1682, 1556, 1418, 1387, 1283, 1182, 1016, 852, 642 cm^{-1}.

AA·$(IN)_2$. A powdered mixture of AA (30 mg, 0.2 mmol) and IN (50 mg, 0.4 mmol) was dissolved in hot methanol. Needle-shaped crystals were obtained after a few days; mp 177–178 °C. IR (KBr): 3399, 3158, 2957, 1686, 1410, 1258, 1016, 852, 804, 754, 644 cm^{-1}.

GA·IN. A 1:1 mixture of GA (54 mg, 0.4 mmol) and IN (50 mg, 0.4 mmol) was dissolved in hot methanol. Light brown crystals were collected after a few days; mp 134–135 °C. IR (KBr): 3391, 3194, 1701, 1589, 1545, 1414, 1281, 1186, 1065, 1005, 883, 858, 756, 638 cm^{-1}.

AA·IN. AA (60 mg, 0.4 mmol) and IN (50 mg, 0.4 mmol) were dissolved in hot methanol. Needle-shaped crystals were formed after a few days; mp 163–165 °C. IR (KBr): 3354, 3169, 2932, 1705, 1601, 1555, 1501, 1466, 1412, 1269, 1186, 1063, 1016, 941, 854 cm^{-1}.

XRD. Reflections were collected on Nonius Kappa CCD diffractometer at 153(2) K with incident X-ray radiation Mo Kα (λ = 0.71073 Å). The crystals were cooled with an Oxford Cryosystem device attached to a CCD machine. Data reductions were performed using DENZO-SMN.[29] Structures were solved by direct methods using the SHELXS-97 program and refined by full-matrix least-squares refinement on F^2 with anisotropic displacement parameters for the non-H-atoms using SHELXL-97.[30] The function, $\sum w(|F_o|^2 - |F_c|^2)^2$, was minimized, where $w = 1/[(\sigma(F_o))^2 + (0.0415*P)^2 + (0.9360*P)]$ and $P = (|F_o|^2 + 2|F_c|^2)/3$. Equations for calculating $R(F)$, $R_w(F^2)$, and the goodness of fit, S, are given below. Neutral atom scattering factors and values used to calculate the linear absorption coefficient are taken from the International Tables for X-ray Crystallography. Geometrical analysis was carried out in PLATON[31] on a Silicon Graphics Octane2 workstation. Details of cell parameters, data collection, and structure refinement are summarized in Table 1. Hydrogen bond metrics are listed in Table 2.

$$R_w(F^2) = \{\sum w(|F_o|^2 - |F_c|^2)^2 / \sum w(|F_o|)^4\}^{1/2}$$

where w is the weight given to each reflection.

$$R(F) = \sum(|F_o| - |F_c|)\sum|F_o|$$

for reflections with $F_o > 4(\sum(F_o))$ and

$$S = [\sum w(|F_o|^2 - |F_c|^2)^2/(n - p)]^{1/2}$$

where n is the number of reflections and p is the number of refined parameters.

Computations. Hydrogen bond energy was calculated in the RHF 6-31G** basis set with Spartan[32] on a Pentium PC. The crystal lattice energy was calculated in Cerius[233] with Dreiding force field on an Octane2 workstation.

Crystallography Database. The CSD,[9a] ConQuest version 1.4 (April 2002 update), operating on a Pentium PC was used for statistical analysis. Searches were carried out on organic crystal structures with standard distance and angle cutoff criteria.[9b]

DSC. DSC was recorded on a Perkin-Elmer DSC4 at a scan rate of 10° min^{-1}.

Acknowledgment. A.N. thanks the CSIR (01/1738/02/EMR-II) for research funding. The UPE program of UGC supports UoH. P.V. thanks the CSIR for a fellowship. V.M.L. thanks the NSF (CHE-9807702) for funding.

Supporting Information Available: ORTEP plots and X-ray crystallographic files (CIF). This material is available free of charge via the Internet at http://pubs.acs.org.

References

(1) Desiraju,G. R. *Crystal Engineering: The Design of Organic Solids*; Elsevier: New York, 1989.
(2) Steed, J. W.; Atwood, J. L. *Supramolecular Chemistry*; Wiley: Chichester, 2000.
(3) Jeffrey, G. A.; Saenger, W. *Hydrogen Bonding in Biological Structures*; Springer-Verlag: Berlin, 1991.
(4) (a) Leiserowitz, L. *Acta Crystallogr.* **1976**, *B32*, 775–802. (b) Bernstein, J.; Etter, M. C.; Leiserowitz, L. In *Structure*

UM00014159
NOVARTIS EXHIBIT 1517
Novartis v. Regents, IPR2023-01347
Page 2905 of 4460

Correlation; Bürgi, H.-B., Dunitz, J. D., Eds.; VCH: Weinheim, 1994; pp 431–507. (c) Kolotuchin, S. V.; Fenlon, E. E.; Wilson, S. R.; Loweth, C. J.; Zimmerman, S. C. *Angew. Chem., Int. Ed. Engl.* **1995**, *34*, 2654–2657. (d) Jetti, R. K. R.; Xue, F.; Mak, T. C. W.; Nangia, A. *J. Chem. Soc., Perkin Trans. 2* **2000**, 1223–1232.

(5) (a) Leiserowitz, L.; Schmidt, G. M. J. *J. Chem. Soc. Sect. A* **1969**, 2372–2382. (b) Leiserowitz, L.; Tuval, M. *Acta Crystallogr.* **1978**, *B34*, 1230–1247. (c) Meléndez, R. E.; Hamilton, A. D. *Top. Curr. Chem.* **1998**, *198*, 97–130. (d) Palmore, G. T. R.; MacDonald, J. C. In *The Amide Linkage: Selected Structural Aspects in Chemistry, Biochemistry, and Materials Science*; Greenberg, A., Breneman, C. M., Liebman, J. F., Eds.; Wiley: New York, 2000; pp 291–336.

(6) (a) Leiserowitz, L.; Nader, F. *Acta Crystallogr.* **1977**, *B33*, 2719–2733. (b) Wash, P. L.; Maverick, E.; Chiefari, J.; Lightner, D. A. *J. Am. Chem. Soc.* **1997**, *119*, 3802–3806. (c) Chang, Y.; West, M.; Fowler, F. W.; Lauher, J. W. *J. Am. Chem. Soc.* **1993**, *115*, 5991–6000. (d) Kuduva, S. S.; Craig, D. C.; Nangia, A.; Desiraju, G. R. *J. Am. Chem. Soc.* **1999**, *121*, 1936–1944. (e) Moorthy, J. N.; Natarajan, R.; Mal, P.; Venugopalan, P. *J. Am. Chem. Soc.* **2002**, *124*, 6530–6531. (f) Baures, P. W.; Rush, J. R.; Wiznycia, A. V.; Desper, J.; Helfrich, B. A.; Beatty, A. M. *Cryst. Growth Des.* **2002**, *2*, 653–664.

(7) (a) Desiraju, G. R. *Angew. Chem., Int. Ed. Engl.* **1995**, *34*, 2311–2327. (b) Nangia, A.; Desiraju, G. R. *Top. Curr. Chem.* **1998**, *198*, 57–95.

(8) Some recent examples: (a) Kumar, V. S. S.; Nangia, A.; Katz, A. K.; Carrell, H. L. *Cryst. Growth Des.* **2002**, *2*, 313–318. (b) Edwards, M. R.; Jones, W.; Motherwell, W. D. S. *Cryst. Eng.* **2002**, *5*, 25–35. (c) Vishweshwar, P.; Thaimattam, R.; Jaskólski, M.; Desiraju, G. R. *Chem. Commun.* **2002**, 1830–1831. (d) MacGillivray, L. R. *CrystEngComm* **2002**, *4*, 37–41. (e) Kumar, V. S. S.; Nangia, A.; Kirchner, M. T.; Boese, R. *New J. Chem.* **2003**, *27*, 224–226.

(9) (a) Allen, F. H. *Acta Crystallogr.* **2002**, *B58*, 380–388. (b) Nangia, A. *CrystEngComm* **2002**, *4*, 93–101.

(10) Allen, F. H.; Motherwell, W. D. S.; Raithby, P. R.; Shields, G. P.; Taylor, R. *New J. Chem.* **1999**, *23*, 25–34.

(11) Steiner, T. *Acta Crystallogr.* **2001**, *B57*, 103–106.

(12) (a) Moulton, B.; Zaworotko, M. J. *Chem. Rev.* **2001**, *101*, 1629–1658. (b) Walsh, R. D. B.; Bradner, M. W.; Fleischman, S.; Morales, L. A.; Moulton, B.; Rodríguez-Hornedo, N.; Zaworotko, M. J. *Chem. Commun.* **2003**, 186–187.

(13) (a) Vishweshwar, P.; Nangia, A.; Lynch, V. M. *J. Org. Chem.* **2002**, *67*, 556–565. (b) Bhogala, B. R.; Vishweshwar, P.; Nangia, A. *Cryst. Growth Des.* **2002**, *2*, 325–328. (c) Kane, J. J.; Liao, R.-F.; Lauher, J. W.; Fowler, F. W. *J. Am. Chem. Soc.* **1995**, *117*, 12003–12004. (d) Palmore, G. T. R.; Luo, T.-J. M.; McBride-Wieser, M. T.; Picciotto, E. A.; Reynoso-Paz, C. M. *Chem. Mater.* **1999**, *11*, 3315–3328. (e) Pedireddi, V. R.; Chatterjee, S.; Ranganathan, A. *Tetrahedron* **1998**, *54*, 9457–9474. (f) Shan, N.; Bond, A. D.; Jones, W. *Cryst. Eng.* **2002**, *5*, 9–24. (g) Aakeröy, C. B.; Beatty, A. M.; Tremayne, M.; Rowe, D. M. *Cryst. Growth Des.* **2001**, *1*, 377–382. (h) Batchelor, E.; Klinowski, J.; Jones, W. *J. Mater. Chem.* **2000**, *10*, 839–848. (i) Olenik, B.; Smolka, T.; Boese, R.; Sustmann, R. *Cryst. Growth Des.* **2003**, *3*, 183–188.

(14) Aakeröy, C. B.; Beatty, A. M.; Helfrich, B. A. *J. Am. Chem. Soc.* **2002**, *124*, 14425–14432.

(15) (a) Etter, M. C. *Acc. Chem. Res.* **1990**, *23*, 120–126. (b) Etter, M. C. *J. Phys. Chem.* **1991**, *95*, 4601–4610.

(16) (a) While ternary crystals of isonicotinamide with two different carboxylic acids have been synthesized with synthons VI and VIII (ref 16b), we show herein that even symmetrical diacids aggregate via different hydrogen bond synthons. (b) Aakeröy, C. B.; Beatty, A. M.; Helfrich, B. A. *Angew. Chem., Int. Ed.* **2001**, *40*, 3240–3242.

(17) Monographs on hydrogen bonding: (a) Jeffrey, G. A. *An Introduction to Hydrogen Bonding*; OUP: Oxford, 1997. (b) Desiraju, G. R.; Steiner, T. *The Weak Hydrogen Bond in Structural Chemistry and Biology*; OUP: Oxford, 1999.

(18) Acid–pyridine recognition can result in proton transfer for strong organic acids or with mineral acids. We observe neutral cocrystals for all diacids studied except a single occurrence of proton transfer in one of the symmetry-independent molecules of MA·(IN)$_2$ (N^+–H, 1.170 Å; O···N, 2.556 Å). The theme of our discussion is not altered because acid–pyridine hydrogen bonding is preserved.

(19) (a) Maçôas, E. M. S.; Fausto, R. *J. Phys. Chem.* **2000**, *A104*, 6956–6961. (b) Godfrey, P. D.; Mirabella, M. J.; Brown, R. D. *J. Phys. Chem.* **2000**, *A104*, 258–264. (c) Nieminen, J.; Räsänen, M.; Murto, J. *J. Phys. Chem.* **1992**, *96*, 5303–5308.

(20) (a) Leserowitz, L.; Nader, F. *Angew. Chem., Int. Ed. Engl.* **1972**, *11*, 514–515. (b) Zukerman-Schpector, J.; Castellano, E. E.; Oliva, G.; Massabni, A. C.; Pinto, A. D. *Can. J. Chem.* **1984**, *62*, 725–728. (c) Doedens, R. J.; Meier, G. P.; Overman, L. E. *J. Org. Chem.* **1988**, *53*, 685–690.

(21) Dunitz, J. D. *Chem. Eur. J.* **1998**, *4*, 745–746.

(22) (a) Padmaja, N.; Ramakumar, S.; Viswamitra, M. A. *Acta Crystallogr.* **1990**, *A46*, 725–730. (b) Brock, C. P.; Dunitz, J. D. *Chem. Mater.* **1994**, *6*, 1118–1127. (c) Steiner, T. *Acta Crystallogr.* **2000**, *B56*, 673–676. (d) Steed, J. W. *CrystEngComm* **2003**, *5*, 169–179.

(23) The role of C–H···O interaction towards stabilization of folded conformation has not been mentioned in the published molecular complexes of AA with S-conformation. (a) Garcia-Tellado, F.; Goswami, S.; Chang, S. K.; Geib, S. J.; Hamilton, A. D. *J. Am. Chem. Soc.* **1990**, *112*, 7393–7394. (b) Liao, R.-F.; Lauher, J. W.; Fowler, F. W. *Tetrahedron* **1996**, *52*, 3153–3162. (c) Ref 13e.

(24) *CRC Handbook of Chemistry and Physics*, 65th ed.; CRC Press: Boca Raton, FL, 1984; p D-165.

(25) That a stronger N–H···O bond makes up for a weaker O–H···O interaction in acid–amide synthon is confirmed by CSD scatter plot (79 hits). O–H···O and N–H···O hydrogen bonds in synthon VIII show an inverse correlation, i.e., the N–H···O is generally short when the O–H···O contact is long. In some acid–urea complexes with synthon VIII, O···O and N···O values are (Å): 2.48, 3.00 (OA, UROXAL01); 2.50, 3.00 (fumaric acid, TIPWIY01); 2.53, 2.99 (SA, VEJXAJ01); 2.71, 2.84 (GA, ZODWIY). Such an inverse correlation is absent between O–H···N and C–H···O hydrogen bonds in acid–pyridine synthon VI.

(26) The reported 1:2 structures are the major products isolated from more than one batch. Under similar conditions, GA and AA gave 1:1 crystals. The uniqueness of the bulk solid phase in each experiment is yet to be fully established by DSC and PXRD.

(27) Thalladi, V. R.; Nusse, M.; Boese, R. *J. Am. Chem. Soc.* **2000**, *122*, 9227–9236.

(28) Bond, A. D. *Chem. Commun.* **2003**, 250–251.

(29) Otwinowski, Z.; Minor, W. DENZO-SMN. In *Methods in Enzymology, Macromolecular Crystallography, Part A*; Carter, C. W., Jr., Sweets, R. M., Eds.; Academic Press: New York, 1997; p 276.

(30) Sheldrick, G. M. *SHELX-97, Program for the Refinement and Solution of Crystal Strucutres*; University of Göttingen: Germany, 1997.

(31) Spek, A. L. *PLATON*; Bijvoet Center for Biochemical Research, Vakgroep Kristal-en Structure-Chemie, University of Utrecht: The Netherlands.

(32) *Spartan Pro 1.0*; Wave Function Inc.: 18401 von Karman Avenue, Suite 370, Irvine, CA 92612.

(33) *Cerius*^{2}; Accelrys Ltd.: 334 Cambridge Science Park, Cambridge CB4 0WN, U.K.

CG034037H

UM00014160
NOVARTIS EXHIBIT 1517
Novartis v. Regents, IPR2023-01347
Page 2906 of 4460

This Page is Inserted by IFW Indexing and Scanning Operations and is not part of the Official Record

BEST AVAILABLE IMAGES

Defective images within this document are accurate representations of the original documents submitted by the applicant.

Defects in the images include but are not limited to the items checked:

- ☐ BLACK BORDERS
- ☐ IMAGE CUT OFF AT TOP, BOTTOM OR SIDES
- ☐ FADED TEXT OR DRAWING
- ☐ BLURRED OR ILLEGIBLE TEXT OR DRAWING
- ☐ SKEWED/SLANTED IMAGES
- ☐ COLOR OR BLACK AND WHITE PHOTOGRAPHS
- ☐ GRAY SCALE DOCUMENTS
- ☐ LINES OR MARKS ON ORIGINAL DOCUMENT
- ☐ REFERENCE(S) OR EXHIBIT(S) SUBMITTED ARE POOR QUALITY
- ☐ OTHER: _____

IMAGES ARE BEST AVAILABLE COPY.
As rescanning these documents will not correct the image problems checked, please do not report these problems to the IFW Image Problem Mailbox.

Original Paper

European Neurology

Eur Neurol 1999;41:37–43

Received: June 22, 1998
Accepted: August 13, 1998

Comparative Efficacy and Safety of Calcium Carbasalate plus Metoclopramide versus Ergotamine Tartrate plus Caffeine in the Treatment of Acute Migraine Attacks

C. Le Jeunne[a] J. Pascual Gómez[e] A. Pradalier[b] F. Titus i Albareda[f] A. Joffroy[i] H. Liaño[g] P. Henry[c] J.M. Lainez[h] G. Geraud[d]

[a]Department of Internal Medicine, Laennec Hospital, Paris, [b]Department of Internal Medicine, Louis Mourier Hospital, Colombes, [c]Department of Neurology, Tripode Hospital, Bordeaux, [d]Department of Neurology, Rangueil Hospital, Toulouse, France; [e]Department of Neurology, Hospital Universitario 'Marqués de Valdecilla', Santander, [f]Department of Neurology, Clínica Dexeus, Barcelona, [g]Department of Neurology, Clínica Puerta de Hierro, Madrid, [h]Department of Neurology, Hospital General Universitario, Valencia, Spain; [i]Department of Neurology, Erasme Hospital, Brussels, Belgium

Key Words

Migraine · Acute treatment · Calcium carbasalate · Metoclopramide · Ergotamine tartrate · Caffeine

Abstract

This randomized, double-blind, double-dummy, multicenter, parallel-group study aimed at comparing the efficacy and safety of calcium carbasalate (equivalent to 900 mg aspirin) plus metoclopramide 10 mg (CM) with ergotamine tartrate 1 mg plus caffeine 100 mg (EC) administered in the treatment of 2 acute migraine attacks. A total of 296 patients fulfilling the International Headache Society diagnostic criteria for migraine were enrolled. In total, one or two migraine attacks were treated in 268 and 235 patients, respectively. The primary endpoint for the first treated attack was headache relief, with intensity decreasing from moderate or severe to mild or absent 2 h after drug intake. Usual secondary efficacy endpoints were assessed. A superiority of CM over EC was observed for both treated attacks for the main endpoint: success in 54 versus 36%, p = 0.003 for the first attack and 60 versus 44%, p = 0.02 for the second attack. CM was also significantly superior to EC during the first attack for complete headache relief (20 vs. 8%, p = 0.006), nausea (42 vs. 63%, p = 0.007) and willingness to take the drug again (90 vs. 80%, p = 0.043). The global efficacy evaluation, rated by the investigators, was significantly more favorable to CM for both attacks (p = 0.001 for the first attack and p = 0.02 for the second). The patients'

Principal Investigators of the Study

Belgium: Dr. Joffroy (Brussels); *France*: Dr. Allain (Saint-Denis), Dr. Baudesson (Colombes), Prof. Bes (Toulouse), Dr. Cajfinger (Verneuil-sur-Seine), Dr. Cenraud (Pau), Dr. Cohen (Saint-Ouen), Dr. Dahan (Aulnay-sous-Bois), Dr. Donnet (Marseille), Dr. Dujardin (Evreux), Prof. Geraud (Toulouse), Prof. Henry (Bordeaux), Dr. Jouan (Gennevilliers), Dr. Kichelewski (Saint-Ouen), Dr. Lacoste (Paris), Dr. Lancret (Paris), Dr. Lanteri-Minet (Nice), Dr. Le Guyader (Brest), Prof. Le Jeunne (Paris), Dr. Louiset (Bordeaux), Dr. Mekies (Toulouse), Dr. Nataf (Saint-Denis), Prof. Pradalier (Colombes), Dr. Puymirat (Bordeaux), Dr. Ratinahirana (Ste-Geneviève-des-Bois), Dr. Sahloul (Colombes), Dr. Veyrie-Courtade (Toulouse); *Spain*: Dr. Lainez (Valencia), Dr. Liaño (Madrid), Dr. Pascual Gómez (Santander), Dr. Titus i Albareda (Barcelona).

KARGER

Fax + 41 61 306 12 34
E-Mail karger@karger.ch
www.karger.com

© 1999 S. Karger AG, Basel
0014–3022/99/0411–0037$17.50/0

Accessible online at:
http://BioMedNet.com/karger

Prof. C. Le Jeunne
Department of Internal Medicine
Laennec Hospital, 42, rue de Sèvres
F-75007 Paris (France)
Tel. +33 1 44 39 67 31, Fax +33 1 44 39 67 36

UM00014162
NOVARTIS EXHIBIT 1517
Novartis v. Regents, IPR2023-01347
Page 2908 of 4460

evaluation was significant for the first attack (p = 0.002). The global incidence of adverse events was 45% higher with EC, though not significant (32 vs. 22%, p = 0.075). They were most often unspecific and mild to moderate in intensity. Gastrointestinal side effects were significantly less frequent with CM than EC (7 vs. 21%, p = 0.001). Thus, CM is more effective and has a better gastrointestinal safety than EC in the acute treatment of migraine attacks.

Introduction

Migraine is a very common disease. Recent European [1, 2] and American [3] population-based studies (all of them using the diagnostic criteria of the International Headache Society; IHS) [4] indicate a prevalence of migraine between 12 and 16%. A wide range of medications have been used for the acute treatment of migraine attacks. Among these, ergotamine tartrate (ET) has long been widely used, most often in combination with caffeine that enhances its absorption [5], and is considered a reference treatment. However, gastrointestinal side effects limit its use, and the abuse of ET may result in rebound headache. In addition, ET is not devoid of potentially severe adverse events linked to its nonspecific vasoconstrictor activity that may lead to peripheral gangrene in some cases.

Among nonsteroidal anti-inflammatory drugs, aspirin is commonly used and effective in the treatment of acute migraine attacks [6, 7]. However, absorption of aspirin is known to be impaired during migraine attacks due to gastric stasis. Metoclopramide associated to aspirin has been shown to accelerate gastric emptying and to enhance the absorption of aspirin [8]. Furthermore, metoclopramide is effective in relieving nausea and vomiting frequently associated with migraine. A combination of 900 mg aspirin and 10 mg metoclopramide in the treatment of migraine attacks has been shown to be more effective than placebo [9, 10] and as effective as oral sumatriptan [11]. Calcium carbasalate is a soluble complex of aspirin that has been shown to be less harmful to the stomach than plain aspirin [12]. Its combination with metoclopramide is known to be well tolerated [13]. The present study was designed to compare the efficacy and safety of calcium carbasalate (equivalent to 900 mg aspirin) plus metoclopramide (CM) with ergotamine tartrate 1 mg plus caffeine (EC) in the acute treatment of migraine attacks.

Patients and Methods

Patients

The study was conducted in 31 centers in France, Spain and Belgium after approval by the local Ethics Committees. Patients were included from November 1994 to April 1996. The study was conducted in accordance with the Declaration of Helsinki, and written informed consent was obtained from each patient prior to entering the study. Patients of either sex, aged 18–65 years with a diagnosis of migraine attacks with or without aura according to the IHS criteria were included in the study. Patients were required to have a history of migraine of at least a year (first attack before the age of 50), with 1 to 6 moderate or severe attacks per month, and at least 3 attacks in the last 3 months. Neither patients with known intolerance or contraindication to any of the study drugs nor pregnant or lactating women, or women at risk of pregnancy with no adequate contraception could be included. Concomitant treatments with salicylates, ET, nonsteroidal anti-inflammatory drugs, macrolides, heparin, vitamin K antagonists, neuroleptic or antiepileptic drugs were not allowed throughout the study. Migraine prophylaxis was not allowed, unless started at least 3 months before inclusion and without any modification throughout the study.

Study Design and Schedule

A randomized, double-blind, double-dummy, multicenter, parallel-group study was performed to compare the association of CM with EC for the treatment of 2 migraine attacks in the same patient.

Three visits were scheduled: patients' characteristics and migraine history were recorded at the inclusion visit. Following a predetermined randomization list, eligible patients were supplied with a pack of medication for the treatment of the first migraine attack. The pack contained either one sachet of calcium carbasalate 1,144.8 mg (equivalent to 900 mg acetylsalicylic acid) plus 10 mg metoclopramide and one tablet of a placebo of EC or one tablet of 1 mg ET plus 100 mg caffeine and one sachet of a placebo of CM. Patients were asked to treat their migraine attack as soon as the intensity of headache was moderate or severe. They were given a diary card to record the details of the attack: intensity of headache and of associated symptoms whenever present (nausea, vomiting, photophobia, phonophobia) before and 2 h after treatment, recurrence of migraine attack (if any) within the 24 h following study drug intake, influence on usual activities, use of rescue medication after the 2 h following study drug intake, adverse events, global judgement on the treatment efficacy and willingness to take the study medication again.

Within 15 days following the treatment of the first attack, patients had to return for the second visit to the investigator, who assessed the safety and the global efficacy of the treatment of the first attack, delivered a new diary card and the same treatment pack for the second attack.

A final evaluation was scheduled within 15 days of the second migraine attack and no more than 3 months after the inclusion visit.

Efficacy and Safety Assessment

The primary endpoint was headache relief for the first attack. Success was defined as a reduction in headache intensity from severe or moderate (grade 3 or 2) at baseline, to mild (grade 1; improved) or none (grade 0; cured) 2 h after study drug intake. Treatment was considered to have failed in all other patients including those who took rescue medication within 2 h of study drug intake. Secondary efficacy endpoints included for each migraine attack: cure at 2 h; intensity

UM00014163
NOVARTIS EXHIBIT 1517
Novartis v. Regents, IPR2023-01347
Page 2909 of 4460

of associated symptoms expressed as present (mild, moderate or severe) or absent 2 h after drug intake; recurrence of migraine within 24 h after initial relief (grade 0 or 1 at 2 h); use of rescue medication after the assessment at 2 h; willingness to take the study treatment for other migraine attacks; global efficacy evaluation by both the investigator and the patient separately, and headache relief for the second attack. Safety was evaluated based on the adverse events reported by the patients.

Statistical Considerations

Assuming a success rate of 60–70% with CM [13], the size of the sample calculated was 100 patients per group, in order to detect a 20% difference between treatments (two-sided) with a 5% type I error and an 80% power. More patients were included in order to take into account nonevaluable patients. A predetermined randomization code was used to allocate treatment to patients in blocks of 4.

Analysis was conducted on the intent-to-treat population defined as all randomized patients who took the study drug. All tests were two-sided at the 5% significance level.

The primary efficacy criterion and other binary variables were analyzed by means of a χ^2 test. The 95% confidence interval on the difference of the rates of success between treatment groups was also calculated for the primary criterion. Additional analyses were performed using the Cochran-Mantel-Haenszel test stratified by baseline evaluation for the primary criterion and other criteria when considered relevant. Cumulative logits were used for the analysis of associated symptoms and other ordered categorical variables.

The analysis was performed with the software SAS, release 6.10 (SAS Institute, Cary, N.C., USA).

Results

Patients' Characteristics

A total of 296 patients were randomized for treatment. Twenty-eight did not receive any study treatment (their baseline characteristics did not differ markedly from the patients in the intent-to-treat population). Two hundred and sixty-eight patients treated 1 migraine attack (136 in the CM group and 132 in the EC group) and were included in the safety analysis. Two of them did not return the patient diary card. Hence, 266 patients were included in the efficacy analysis for all variables derived from the patient diary card for the first migraine attack. Thirty-three patients (19 with CM and 14 with EC) did not treat a second migraine attack with the study medication for the following reasons: 23 had no second migraine attacks, 4 were lost to follow-up, 3 withdrew their consent, 2 had an adverse event and 1 patient was pregnant. Thus, the efficacy analysis for the second attack was based on 235 patients.

Treatment groups did not differ significantly for both demographic characteristics and migraine history (table 1). The characteristics of the attacks for headache

Table 1. Patients' demographics data and migraine history

	CM	EC
Total patients	151	145
Males	24 (16)	23 (16)
Females	127 (84)	122 (84)
Mean age, years ± SD	37 ± 11	37 ± 11
Range, years	18–63	18–65
Migraine history		
Duration, years		
Mean ± SD	16 ± 10	17 ± 11
Range	3–52	2–58
Frequency of attacks per month		
Mean ± SD	3.0 ± 1.3	3.0 ± 1.4
Range	1–6	1–7
Type of migraine		
With aura	20 (13)	21 (14)
Without aura	87 (58)	75 (52)
Alternating	44 (29)	49 (34)
Previous use of ergotamine	21 (14)	22 (15)

Figures in parentheses are percentages.

Table 2. Baseline characteristics of the attacks

	CM		EC	
	1st attack[1] n = 134	2nd attack[1] n = 115	1st attack n = 132	2nd attack[2] n = 117
Headache				
Mild	0 (0)	0 (0)	1 (1)	1 (1)
Moderate	82 (61)	65 (56)	72 (54)	63 (54)
Severe	52 (39)	50 (44)	59 (45)	53 (45)
Nausea				
None	45 (34)	40 (35)	37 (28)	34 (29)
Mild	54 (40)	44 (38)	59 (45)	48 (41)
Moderate	25 (19)	24 (21)	31 (23)	27 (23)
Severe	10 (7)	7 (6)	5 (4)	8 (7)
Vomiting				
None	115 (86)	100 (87)	119 (90)	102 (87)
Mild	16 (12)	7 (6)	5 (4)	6 (5)
Moderate	2 (1)	8 (7)	8 (6)	7 (6)
Severe	1 (1)	0 (0)	0 (0)	2 (2)

Figures in parentheses are percentages.
[1] For each attack, 2 patients did not return their diary card.
[2] One patient did not return the diary card for the 2nd attack.

UM00014164
NOVARTIS EXHIBIT 1517
Novartis v. Regents, IPR2023-01347
Page 2910 of 4460

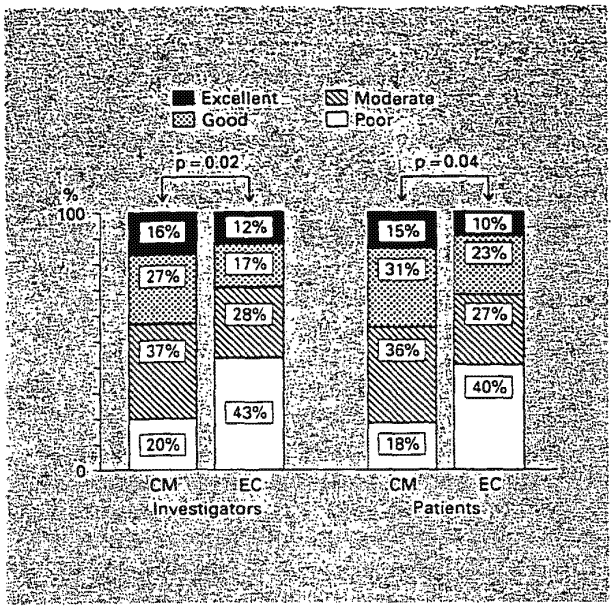


Fig. 1. Investigators' and patients' global efficacy assessment for the first attack.

Table 3. Efficacy criteria

	CM	EC	p
Effect on headache 1st attack			
Patients, n	134	132	
Success, %	54	36	0.003
Cured, %	20	8	0.006
Effect on headache 2nd attack			
Patients, n	115	117	
Success, %	60	44	0.02
Cured, %	24	17	NS
Presence of nausea 1st attack			
Patients, n	134	132	
Prior to treatment, %	66	72	
2 h after treatment, %	42	63	0.007[1]
Presence of nausea 2nd attack			
Patients, n	114	117	
Prior to treatment, %	65	71	
2 h after treatment, %	47	59	NS[1]

[1] The cumulative logit test was performed on the 4-point categorical variable: none, mild, moderate, severe.

intensity and associated symptoms before treatment were similar in both groups (table 2).

Efficacy (table 3)

CM was significantly more effective than EC at providing headache relief with 54% (73/134) and 36% (48/132) of patients, respectively, for the first attack (p = 0.003, 95%, confidence interval 6–30%). This result was confirmed when stratifying the analysis with baseline headache intensity (p = 0.004). CM was also significantly better than EC at relieving headache during the second attack, with respective success rates of 60% (69/115) and 44% (52/117) (p = 0.02). The proportion of patients with complete relief 2 h after drug intake was higher with CM compared with EC, 20% (27/134) and 8% (11/132), respectively, for the first attack (p = 0.006), and 24% (28/115) and 17% (20/117) for the second attack (not significant, NS). The rates of recurrence of migraine for patients with treatment success at 2 h were 16% (12/73) and 8% (4/48), respectively, in the CM and EC groups for the first attack, and 19% (13/69) and 11% (6/52) for the second attack (NS).

For this first attack, CM was significantly better than EC at relieving nausea: at 2 h, nausea was absent in 58%

Table 4. Number of patients with an adverse event

	CM	EC	p
Total patients	136	132	
Patients with at least 1 adverse event	30 (22)	42 (32)	0.075 (NS)
Patients with at least 1 gastrointestinal adverse event	9 (7)	28 (21)	0.001
Main adverse events[1]			
Somnolence	6 (4.4)	5 (3.8)	
Abdominal pain	5 (3.7)	12 (9.1)	
Nausea	5 (3.7)	11 (8.3)	
Vomiting	1 (0.7)	6 (4.5)	
Asthenia	5 (3.7)	2 (1.5)	

Figures in parentheses are percentages.
[1] Adverse events reported with an incidence ≥ 3.5% in at least one group.

UM00014165
NOVARTIS EXHIBIT 1517
Novartis v. Regents, IPR2023-01347
Page 2911 of 4460

(78/134) of patients in the CM group versus 37% (49/132) of patients in the EC group, p = 0.007. This result was confirmed with an analysis of the presence or absence of nausea at baseline (p = 0.001). Although the rate of patients without nausea at 2 h was higher in the CM compared with the EC group – 53% (60/114) and 41% (48/117), respectively – no significant difference between treatments was observed for the second attack. Due to the small number of patients with vomiting at baseline, cumulative logit tests were not performed.

Thirty-seven percent (49/134) and 47% (61/131) of patients in the CM and EC group, respectively, took rescue medication within 24 h for treatment of the first attack (NS), and 33% (38/115) and 45% (53/117) did so for the second attack (NS).

The global efficacy evaluation rated by the investigators was significantly more favorable to CM for both attacks (p = 0.001 for the first attack and p = 0.02 for the second). The patients' evaluation was significant for the first attack (p = 0.002). For the first attack, significantly more investigators and patients considered that CM had a good or excellent efficacy compared with EC, p = 0.02 and p = 0.04, respectively (fig. 1). After the first attack, twice as many patients treated with EC would refuse to take the medication again for the treatment of a subsequent attack compared with CM: 20% (26/131) versus 10% (13/134), p = 0.043. No significant difference was shown for the second attack.

Safety

During the study, adverse events were less frequently reported with CM than EC: 22% (30/136) versus 32% (42/136) of the patients, but the trend in favor of CM was not statistically significant (p = 0.075). In total, 54 and 69 adverse events were reported in the CM and EC groups, respectively. The most frequently reported adverse events (≥ 3.5% in at least one group) are shown in table 4. Most of them were mild to moderate in intensity. They were usually nonspecific (somnolence and asthenia), considered by the investigator to be unrelated or possibly related to the study drugs, and resolved spontaneously. One patient in each group withdrew because of an adverse event not related to the study drug: a pulmonary embolism in the CM group and back pain in the EC group.

Significantly more patients experienced gastrointestinal events in the EC group compared with the CM group: 21% (28/132) versus 7% (9/136), p = 0.001. All gastrointestinal adverse events (abdominal pain, nausea, vomiting, diarrhea and flatulence) were more frequent with EC than with CM treatment.

Discussion

The results obtained in terms of efficacy demonstrate the significant superiority of the combination of calcium carbasalate 1,144.8 mg + metoclopramide 10 mg over ET 1 mg + caffeine 100 mg in providing headache relief and alleviation of nausea in patients with acute migraine attacks.

Although treatment groups did not differ significantly for headache intensity and associated symptoms at baseline, slightly more patients had severe headache and nausea in the EC group.

Additional analyses, stratified with baseline headache intensity or presence/absence of nausea at baseline showed that CM was more effective than EC.

The rate of success obtained with CM was similar to what has been previously published with the association aspirin plus metoclopramide [9–11, 13]. In two double-blind, placebo-controlled studies, the efficacy rates of the association aspirin (900 mg) plus metoclopramide (10 mg) at relieving and curing headache were 58 and 18% [9], and 54 and 14% [10]. In one double-blind study of combined oral lysine acetylsalicylate and metoclopramide versus oral sumatriptan, the success rate was 57% of which 22% of patients were cured [11]. Only in one study of CM versus oral dihydroergotamine were the efficacy rates higher than in our study; 64% for success, of which 41% of the patients were cured [13]. In the literature, some studies have looked at the efficacy of EC at a 2-mg dose [14–20] or of ET alone [21]. However, in all except three [16, 19, 20], the number of patients was low. More important, in all studies except one [20], the IHS diagnostic criteria for migraine were not used, and the results were usually expressed as mean reduction of headache intensity rather than using the IHS definition of success. No comparative efficacy data are available with 1 mg EC. In one study [20] comparing oral ET (2 mg) plus caffeine with oral sumatriptan (100 mg), 48% (118/246) of the patients had headache relief with EC. This rate was slightly higher than the 36% rate observed with EC in our study for the first attack, but was similar to the rate of 44% obtained for the second attack. In our study, the 1-mg dose was chosen for the following reasons: on one hand, 1 mg of ET has shown to be more effective than placebo in the treatment of acute migraine attacks [21]; on the other hand, the use of a higher dose of ET is limited by its gastrointestinal adverse events and by the risk of enhancement of general malaise in some patients. Mathew [22] recommends a dose of ET of 1 or 2 mg at the start of an attack [22]. As ET-naive patients could be in-

UM00014166
NOVARTIS EXHIBIT 1517
Novartis v. Regents, IPR2023-01347
Page 2912 of 4460

cluded in the study (85% of the patients in each treatment group were ET naive), it was considered that 2 mg should not be administered for the first time to this population.

For the first attack, CM was more effective than EC in relieving nausea. The results are consistent with data from the study comparing aspirin plus metoclopramide with oral sumatriptan [11] and from the study comparing EC with oral sumatriptan [20]. The number of patients with vomiting at baseline was too low to expect a significant difference between treatment groups.

Though this was not significant, less patients took another analgesic within 24 h in the CM group compared to the EC group. Both treatments did not differ significantly in terms of headache recurrence within 24 h. The proportion of patients with headache recurrence was very low compared to the results reported with oral sumatriptan [20]. The significantly higher overall benefit of CM compared with EC was confirmed by the global assessment of efficacy by the investigators and the patients for the first attack.

In our study, results were consistent across the 2 attacks for relief of headache and nausea. Efficacy rates for the second migraine attack were slightly higher for both treatment groups.

Both treatments were generally well tolerated, and adverse events were usually transient and mild in intensity. Although not statistically significant, there was a trend for a better safety profile for CM. The percentage of patients with an adverse event in the CM group was consistent with other studies in which CM has been shown not to be significantly different from placebo as far as safety is concerned [10, 11]. The percentage of adverse events with EC was lower than the rate observed in studies with 2 mg ET: 39% [20], 41% [15] and 64% [16]. Moreover, 0.7% of the patients withdrew from our study in the EC group compared with 3% [17] and 5% [21] in the literature. Statistically more gastrointestinal adverse events occurred with EC. Between two and three times more patients in the EC group had nausea de novo 2 h after study drug intake. In a review of placebo-controlled trials, Dahlöf [23] found that treatment with ET or EC was associated with increased severity of nausea and vomiting compared with placebo in 5 out of 7 studies. These data are consistent with the clinical observation that nausea is usually the principal adverse effect limiting the use of ET [24]. The fairly good safety profile of EC in our study could be related to the 1-mg dose used compared to other trials with 2-mg doses. The global superiority of CM over EC in terms of efficacy and safety was confirmed by the willingness of patients to take the study drug again.

Conclusion

The combination of calcium carbasalate (equivalent to 900 mg aspirin) and 10 mg metoclopramide has been shown to be significantly more effective than 1 mg ET and 100 mg caffeine in relieving headache and nausea in patients with acute migraine attacks.

Both treatments were globally well tolerated. However, there were significantly less gastrointestinal adverse events with CM treatment and a global trend for a better tolerability of CM compared with EC.

Because of its safety, efficacy and low cost, CM should be the first-choice treatment for acute migraine attacks.

References

1 Henry P, Michel P, Brochet B, Dartigues JF, Tison S, Salamon R, the GRIM: A nationwide survey of migraine in France: Prevalence and clinical features in adults. Cephalalgia 1992;12:229–237.

2 Rasmussen BK: Epidemiology of migraine. Biomed Pharmacother 1995;49:452–455.

3 Stewart WF, Lipton RB, Celentano DD, Reed ML: Prevalence of migraine headache in the United States. Relation to age, income, race and other sociodemographic factors. JAMA 1992;267:64–69.

4 Headache Classification Committee of the International Headache Society: Diagnostic Criteria. Cephalalgia 1988;8:19–28.

5 Berde B, Cerletti A, Dengler HJ, Zoglio MA: Studies of the interaction between ergot alkaloids and xanthine derivatives; in Cochrane AL (ed): Background to Migraine. London, Heinemann, 1970, pp 80–102.

6 Wilkinson M: The treatment of acute migraine attacks. Headache 1976;15:291.

7 Thrush D: Treatment of migraine. Br Med J 1978;i:1004.

8 Volans GN: Absorption of effervescent aspirin during migraine. Br Med J 1974;4:265–269.

9 Chabriat H, Joire JE, Danchot J, Grippon P, Bousser MG: Combined lysine acetylsalicylate and metoclopramide in the acute treatment of migraine: A multicentre double-blind placebo-controlled study. Cephalalgia 1994;14:297–300.

10 Henry P, Hiesse-Provost O, Dillenschneider A, Ganry H, Insuasty J: Efficacité et tolérance de l'association of effervescente aspirine-métoclopramide dans le traitement de la crise de migraine sans aura. Essai randomisé en double aveugle contre placebo. Presse Méd 1995;24:254–258.

11 Tfelt-Hansen P, Henry P, Mulder LJ, Scheidewaert RG, Schoenen J, Chazot G: The effectiveness of combined oral lysine acetylsalicylate and metoclopramide compared with oral sumatriptan for migraine. Lancet 1995;346:923–926.

UM00014167
NOVARTIS EXHIBIT 1517
Novartis v. Regents, IPR2023-01347
Page 2913 of 4460

12 Murray FE, Hudson N, Atherton JC, Cole AT, Scheck F, Hawkey CJ: Comparison of effects of calcium carbasalate and aspirin on gastroduodenal mucosal damage in human volunteers. Gut 1996;38:11–14.
13 Pradalier A, Guérard des Lauriers A, Scheck F, Peraudeau P, Lacoste JP, Cajfinger F: Association carbasalate calcique-métoclopramide versus dihydroergotamine dans le traitement de la crise de migraine. Pathol Biol 1995;43:806–813.
14 Waters WE: Controlled clinical trial of ergotamine tartrate. Br Med J 1970;2:325–327.
15 Ryan RE: Double-blind clinical evaluation of the efficacy and safety of ergostine-caffeine, ergotamine-caffeine and placebo in migraine headache. Headache 1970;9:212–220.
16 Pradalier A, Rancurel G, Dordain G, Verdure L, Rascol A, Dry J: Acute migraine attack therapy: Comparison of naproxen sodium and an ergotamine tartrate compound. Cephalalgia 1985;5:107–113.
17 Sargent JD, Baumel B, Peters K, Diamond S, Saper JR, Eisner LS, Solbach P: Aborting a migraine attack: Naproxen sodium vs. ergotamine plus caffeine. Headache 1988;28:263–266.
18 Kinnunen E, Erkinjuntti T, Färkkilä M, Palomäki H, Porras J, Teirmaa H, Freudenthal Y, Andersson P: Placebo-controlled double-blind trial of pirprofen and an ergotamine tartrate compound in migraine attacks. Cephalalgia 1988;8:175–179.
19 Friedman AP, Di Serio FJ, Hwang DS: Symptomatic relief of migraine: Multicenter comparison of Cafergot® P-B, Cafergot®, and placebo. Clin Ther 1989;11:170–182.
20 The Multinational Oral Sumatriptan and Cafergot Comparative Study Group: A randomised, double-blind comparison of sumatriptan and Cafergot in the acute treatment of migraine. Eur Neurol 1991;31:314–322.
21 Hakkarainen H, Vapaatalo H, Gothoni G, Parantainen J: Tolfenamic acid is as effective as ergotamine during migraine attacks. Lancet 1979;ii:326–328.
22 Mathew NT: Dosing and administration of ergotamine tartrate and dihydroergotamine. Headache 1997;37(suppl 1):S26–S32.
23 Dahlöf C: Placebo-controlled trials with ergotamine in the acute treatment of migraine. Cephalalgia 1993;13:166–171.
24 Tfelt-Hansen P, Johnson ES: Ergotamine; in Olesen J, Tfelt-Hansen P, Welch KMA (eds): The Headaches. New York, Raven Press, 1993, pp 313–322.

UM00014168
NOVARTIS EXHIBIT 1517
Novartis v. Regents, IPR2023-01347
Page 2914 of 4460

This Page is Inserted by IFW Indexing and Scanning Operations and is not part of the Official Record

BEST AVAILABLE IMAGES

Defective images within this document are accurate representations of the original documents submitted by the applicant.

Defects in the images include but are not limited to the items checked:

- ☐ BLACK BORDERS
- ☐ IMAGE CUT OFF AT TOP, BOTTOM OR SIDES
- ☐ FADED TEXT OR DRAWING
- ☐ BLURRED OR ILLEGIBLE TEXT OR DRAWING
- ☐ SKEWED/SLANTED IMAGES
- ☐ COLOR OR BLACK AND WHITE PHOTOGRAPHS
- ☐ GRAY SCALE DOCUMENTS
- ☐ LINES OR MARKS ON ORIGINAL DOCUMENT
- ☐ REFERENCE(S) OR EXHIBIT(S) SUBMITTED ARE POOR QUALITY
- ☐ OTHER: _____

IMAGES ARE BEST AVAILABLE COPY.
As rescanning these documents will not correct the image problems checked, please do not report these problems to the IFW Image Problem Mailbox.

Journal of Chemical Crystallography, Vol. 32, No. 12, December 2002 (© 2002)

Separation of 4-aminobenzoic acid by cocrystallization: Crystal structure of the complex of 4-aminobenzoic acid with (2*R*,3*R*)-tartaric acid

Ziqiang Hu,[1,2] Jiageng Liu,[1] Liang Shen,[2] Duanjun Xu,[1]* and Yuanzhi Xu[1]

Received September 21, 2001

4-Aminobenzoic acid (PABA) has been successfully separated from a mixture containing 2-aminobenzoic acid and (2*R*,3*R*)-tartaric acid. X-ray structure analysis confirms the separating result. The molecular complex formed by PABA and tartaric acid in 1:1 molar ratio crystallizes in the orthorhombic space group $P2_12_12_1$ with cell dimensions of $a = 7.329(1)$ Å, $b = 12.095(2)$ Å, $c = 15.231(3)$ Å, $V = 1350.1(4)$ Å^3, $Z = 4$. The crystal structure comprises protonated PABA, monoanion of tartaric acid, and crystalline water. The extensive H-bonding network exists in the crystal structure. H bonding between tartaric acid and both terminal groups on para position of PABA is considered as a possible reason for the successful separation.

KEY WORDS: 4-Aminobenzoic acid; (2*R*,3*R*)-tartaric acid; crystal structure; separation.

Introduction

4-Aminobenzoic acid (PABA) is reported to be an effective sunscreen agent and can be used to soften or regress fibrotis tissue in peyronie's disease and pemphigus.[1] It is usually obtained as a mixture with its isomer 2-aminobenzoic acid. Although it is obviously meaningful to separate 4-aminobenzoic acids from the mixture, the separation is difficult owing to their similar structures and properties. Several procedures for the separation of PABA have been reported with the expensive chemical modification of cyclodextrin.[2–4] We have made efforts in the separation of PABA using cheaper organic acid as separation reagent and finally successfully obtained PABA from an isomer mixture through cocrystallization with a chiral reagent of (2*R*,3*R*)-tartaric acid. We present here the separation procedure and X-ray crystal structure of the complex formed from PABA and tartaric acid.

[1] Department of Chemistry, Zhejiang University, Hangzhou 310027, People's Republic of China.
[2] Department of Chemistry, Hangzhou Teachers College, Hangzhou 310012, People's Republic of China.
* To whom correspondence should be addressed. E-mail: h8804110@163.com

Experimental

A hot 95% ethanol solution (20 mL) containing PABA (about 15 mmol) and 2-aminobenzoic acid (about 15 mmol) was mixed with a hot 95% ethanol solution (10 mL) containing DHBA (about 15 mmol). The pale-yellow precipitate was obtained by allowing the solution to stand for several days at room temperature. Recrystallization of the precipitate from ethanol (95%) gave well-shaped single crystals.

1074-1542/02/1200-0525/0 © 2002 Plenum Publishing Corporation

UM00014170
NOVARTIS EXHIBIT 1517
Novartis v. Regents, IPR2023-01347
Page 2916 of 4460

Table 1. Crystal Data and Summary of Data Collection and Structure Refinement

Compound	$C_7H_9NO_2^+ \cdot C_4H_5O_6^- \cdot H_2O$
CCDC deposit no.	CCDC-1003/6154
Color/shape	Colorless/parallelepiped
Empirical	$C_{11}H_{15}NO_9$
Formula weight	305.24
Temperature, K	295(2)
Crystal system	Orthorhombic
Space group	$P2_12_12_1$
Unit cell dimensions	$a = 7.329(1)$ Å
	$b = 12.095(2)$ Å
	$c = 15.231(3)$ Å
Volume, Å^3	1350.1(4)
Z	4
D_{calcl} Mg/m^3	1.502
Absorption coefficient, mm^{-1}	0.133
Diffractometer/scan	Siemens P4/ω
Radiatiation/wavelength	Mo Kα (graphite monochromator)/0.71073 Å
$F(000)$	640
Crystal size, mm	0.52 × 0.36 × 0.20
2θ range, deg	5.34–57.50
Range of h, k, l	$0 \le h \le 9, 0 \le k \le 16, -1 \le l \le 20$
Reflections collected	2152
Independent/observed reflections	2030 [R(int) = 0.0234], 1508
Refinement method	Full-matrix least-squares on F^2
Decay of standard, %	1.73
Data/restraints/parameters	2030/0/236
Goodness of fit on F^2	0.951
Final R indices [$I/\sigma(I) > 2.0$]	$R1 = 0.039$, $wR2 = 0.086$
R indices (all data)	$R1 = 0.057$, $wR2 = 0.091$
Extinction coefficient	0.026(2)
Largest diff. peak and hole, e/Å^3	0.237 and −0.207

Table 2. Atomic Coordinates and Equivalent Isotropic Displacement Parameters

Atom	x	y	z	Ueq (Å^2)
O(1)	0.1781(4)	0.1996(2)	0.3620(1)	0.059(1)
O(2)	0.1492(4)	0.0718(2)	0.4662(2)	0.056(1)
O(3)	0.0745(3)	0.1908(2)	0.8611(2)	0.037(1)
O(4)	0.0930(3)	0.3597(2)	0.9197(1)	0.037(1)
O(5)	−0.2755(3)	0.1946(2)	0.8505(2)	0.040(1)
O(6)	−0.1870(3)	0.4176(2)	0.7782(1)	0.030(1)
O(7)	−0.5638(2)	0.3462(2)	0.9114(1)	0.033(1)
O(8)	−0.5400(3)	0.4690(2)	0.8029(1)	0.039(1)
O(9)	−0.3983(3)	0.5799(2)	0.6555(1)	0.034(1)
N	0.1434(3)	0.4941(2)	0.7136(2)	0.028(1)
C(1)	0.1572(4)	0.4131(2)	0.6421(2)	0.028(1)
C(2)	0.1453(6)	0.4459(2)	0.5562(2)	0.045(1)
C(3)	0.1517(6)	0.3680(2)	0.4907(2)	0.047(1)
C(4)	0.1685(4)	0.2569(2)	0.5108(2)	0.033(1)
C(5)	0.1825(6)	0.2261(3)	0.5977(2)	0.054(1)
C(6)	0.1797(6)	0.3042(3)	0.6633(2)	0.053(1)
C(7)	0.1672(4)	0.1744(2)	0.4384(2)	0.038(1)
C(8)	0.0046(3)	0.2738(2)	0.8915(2)	0.025(1)
C(9)	−0.2029(3)	0.2839(2)	0.8981(2)	0.026(1)
C(10)	−0.2655(3)	0.3953(2)	0.8617(2)	0.023(1)
C(11)	−0.4747(3)	0.4034(2)	0.8576(2)	0.024(1)

Salt

Table 3. Selected Bond Distances (Å) and Bond Angles (Deg)

Bond length			
O(1)–C(7)	1.204(4)	O(2)–C(7)	1.319(4)
O(3)–C(8)	1.219(3)	O(4)–C(8)	1.297(3)
O(5)–C(9)	1.405(3)	O(6)–C(10)	1.422(3)
O(7)–C(11)	1.256(3)	O(8)–C(11)	1.246(3)
N–C(1)	1.468(3)	C(8)–C(9)	1.529(4)
C(9)–C(10)	1.527(4)	C(10)–C(11)	1.538(4)
Bond angle			
O(1)–C(7)–O(2)	123.7(3)	O(1)–C(7)–C(4)	123.1(3)
O(2)–C(7)–C(4)	113.2(3)	O(3)–C(8)–O(4)	125.1(2)
O(3)–C(8)–C(9)	120.5(2)	O(4)–C(8)–C(9)	114.3(2)
O(8)–C(11)–O(7)	126.0(2)	O(8)–C(11)–C(10)	116.8(2)
O(7)–C(11)–C(10)	117.2(2)		

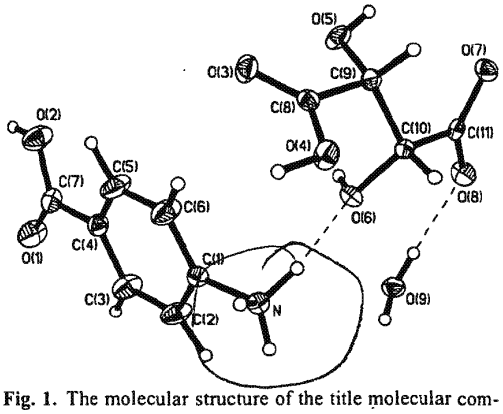


Fig. 1. The molecular structure of the title molecular complex, showing 30% probability displacement ellipsoids, and dashed lines showing H bonding.

The pale-yellow precipitate was also obtained from the mixture of PABA and tartaric acid, but not obtained from the mixture of 2-aminobenzoic acid and tartaric acid.

A similar procedure was repeated using acetone in stead of ethanol as solvent, and the same separation phenomenon was observed.

The pale-yellow precipitate (2.08 g) was dissolved in hot water. Crystals with needle shape were obtained when the solution was cooled to room temperature. The melting point of 186°C for the needle crystal agrees well with 186.5–188.5°C for PABA but disagrees with 144–147°C for 2-aminobenzoic acid.

A single crystal of the title complex was mounted on the Siemens P4 diffractometer for data collection. The structure was solved by direct methods and expanded using Fourier techniques. Non-H atoms were refined anisotropically. All H atoms were reasonably located on a difference Fourier map and refined with fixed thermal parameter U_{iso} of 0.08 Å^2. The weighting scheme used at the final stage was $w = [\sigma^2(F_o^2) + (0.0440P)^2]^{-1}$, where $P = (F_o^2 + 2F_c^2)/3$. Atomic scattering factors used were taken from International Tables for X-ray Crystallography.[5] A summary of data collection and structure refinement is given in Table 1.

Table 4. H-Bonding Geometry Parameters[a]

D–H···A	D–H (Å)	H···A (Å)	D···A (Å)	D–H···A (deg)
N–H(1A)···O(6)	0.97(4)	1.83(4)	2.773(3)	163(4)
N–H(1B)···O(8)[a]	0.97(4)	1.74(4)	2.706(3)	172(4)
N–H(1C)···O(3)[b]	0.91(4)	2.38(4)	3.083(3)	134(4)
N–H(1C)···O(5)[b]	0.91(4)	1.94(4)	2.787(3)	154(4)
O(9)–H(9A)···O(3)[b]	0.81(4)	1.94(4)	2.738(3)	168(4)
O(9)–H(9B)···O(8)	0.94(4)	1.90(4)	2.813(3)	163(4)
O(2)–H(20)···O(9)[c]	0.87(4)	1.77(4)	2.631(3)	168(4)
O(4)–H(40)···O(7)[a]	1.05(4)	1.48(4)	2.524(3)	173(4)
O(5)–H(50)···O(9)[d]	0.86(4)	2.02(4)	2.766(3)	144(4)
O(6)–H(60)···O(1)[e]	0.81(5)	1.98(5)	2.748(3)	160(4)

Note: Symmetry codes: (a) $1 + x, y, z$; (b) $-x, 0.5 + y, 1.5 - z$; (c) $0.5 + x, 0.5 - y, 1 - z$; (d) $-1 - x, -0.5 + y, 1.5 - z$; (e) $0.5 + x, 0.5 - y, 1 - z$.

[a] D: donor; A: acceptor.

UM00014172
NOVARTIS EXHIBIT 1517
Novartis v. Regents, IPR2023-01347
Page 2918 of 4460

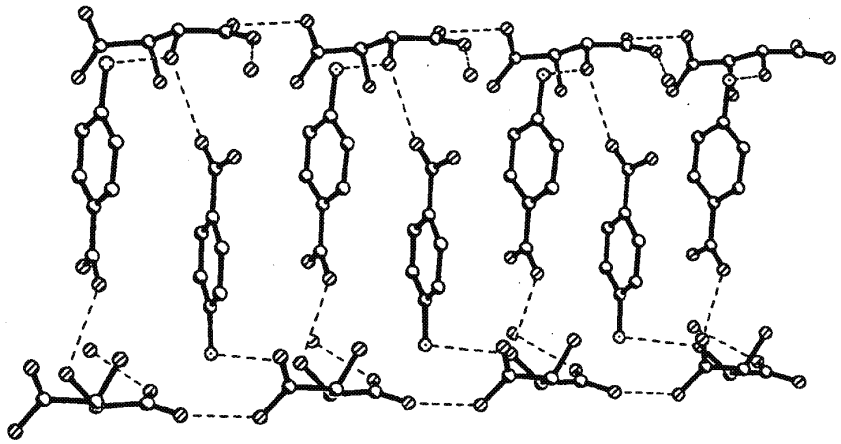


Fig. 2. A diagram showing molecule assembly through H-bonding network.

Results and discussion

The final atomic positional parameters and selected bond lengths and bond angles are given in Tables 2 and 3, respectively. The molecular structure is illustrated in Fig. 1. The molecular structure consists of discrete PABA, tartaric acid, and crystalline water, which link to each other through H bonding to form the molecular complex.

A lot of structure determinations showed the following rule for C—O bond distances of carboxyl group: both C—O bond distances are almost identical in a carboxylate anion but significantly different in a neutral carboxylic acid.[6] Within the tartaric acid moiety, as shown in Table 3, the C—O bond distances are almost identical for the C(11) carboxyl group but much different for the C(8) carboxyl group. This fact strongly suggests that the present tartaric acid is a monoanion. While different C—O bond distances were also observed in the carboxyl group of the PABA, three H atoms were clearly found around the N atom with reasonable distances and angle in a difference Fourier map. This means that the PABA is an amine salt. The carbon skeleton of tartrate assumes a coplanar arrangement in the structure with a C(8)—C(9)—C(10)—C(11) torsion angle of 173.6(2)°, which is similar to 178.3 and 181.5° found in ammonium *D*-tartrate.[7,8]

The extensive H-bonding network exists in the crystal structure. H-bonding geometry parameters are presented in Table 4. With the aid of intermolecular H bonds between carboxylic groups of adjacent PABA, tartaric acid molecules link to each other to form the layer structures as shown in Fig. 2. PABA molecules H bond to adjacent layers with the aid of both terminal groups on para position to form the sandwich-like structure, which looks rather stable and is considered as a possible reason for this successful separation.

Acknowledgment

The project was supported by the National Natural Science Foundation of China (No. 29973036).

References

1. *Remington's Pharmaceutical Sciences 1980*; Mack Publishing Co.: Easton, Pennsylvania, p 730.
2. Chang, C.L.; Wu, Q.; Tan, L. *J. Chromatogy*, **1986**, *361*, 199.

UM00014173
NOVARTIS EXHIBIT 1517
Novartis v. Regents, IPR2023-01347
Page 2919 of 4460

3. Tanaka, M.; Iked, H.; Shono, T. *J. Chromatogr.* **1987**, *398*, 165.
4. Fanali, S.; Sinibaldi, M. *J. Chromatogr.* **1988**, *442*, 371.
5. *International Tables for X-Ray Crystallography*; Kluwer Academic Publisher: Dordrecht, 1992; Vol. C.
6. Nic, J.J.; Xu, D.J.; Wu, J.Y.; Chiang, M.Y. *Acta Crystallogr., Sect. C* **2001**, *57*, o428–o429.
7. Nic, J.J.; Xu, D.J.; Wu, J.Y.; Chiang, M.Y. *Chin. J. Struct. Chem.* **2001**, *20*(6), 470–472.
8. Spek, A.L. *Acta Crystallogr., Sect. C* **1987**, *43*, 1633.

UM00014174
NOVARTIS EXHIBIT 1517
Novartis v. Regents, IPR2023-01347
Page 2920 of 4460

Molecular Self-Assembly in the Solid State. The Combined Use of Solid-State NMR and Differential Scanning Calorimetry for the Determination of Phase Constitution

Donna Guarrera, Lloyd D. Taylor, and John C. Warner*

Media Systems Research Laboratories, 730 Main St., Polaroid Corporation, Cambridge, Massachusetts 02139

Received February 2, 1994. Revised Manuscript Received March 21, 1994

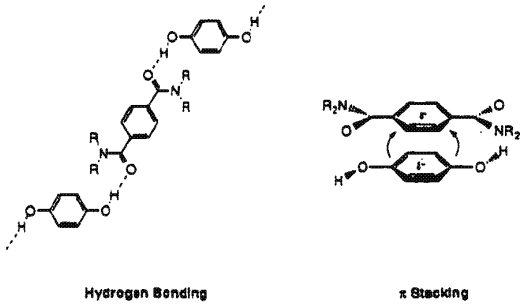
The construction and use of phase diagrams for the study of self-assembled systems are extremely useful. While well-known in various fields of metallurgy, phase diagrams have not been widely applied to multicomponent organic systems of contemporary interest. The blending of hydroquinone (1) with bis(*N*,*N*-diethyl)terephthalamide (2) or bis(*N*,*N*-dimethyl)terephthalamide (3) in the solid state has been demonstrated to generate stable binary phases as determined by both solid-state NMR and differential scanning calorimetry. Compounds 1 and 2 form a single phase of a 1:1 composition, while compounds 1 and 3 form two stable phases, one of a 1:1 composition and the other of a hydroquinone/terephthalamide composition of 2:1. Phase diagrams of these systems are constructed and structural features discussed.

Introduction

Hydroquinones have found widespread use as developers in photographic systems.[1] At sufficiently elevated pH hydroquinones are fully deprotonated, forming anionic species which are both soluble and mobile in aqueous media, including thin-film photographic systems. At neutral pH, on the other hand, hydroquinones are nonionic, and therefore in such systems insoluble and immobile. Quinones, the oxidation products of hydroquinones, cannot undergo deprotonation in alkaline solution. Therefore, in aqueous environments at both high and neutral pH, quinones are insoluble and immobile. These phenomena are exploited in diffusion-controlled, silver halide photographic imaging systems such as Polaroid instant photography. In such systems a multilayer, thin-film negative (which is coated from water at neutral pH) is treated after exposure with a highly alkaline reagent to solubilize the hydroquinones and allow them to effect silver halide developement.

While a simple description of the diffusivities of hydroquinones and their reaction products is adequate to explain the general principle of diffusion-controlled imaging, in practice the situation is unfortunately not so straightforward. Some photographically useful hydroquinones have sufficient aqueous solubility in their protonated state to present a particular problem. In these cases, the marginal solubility may lead to migration of reagents in the multilayer film structure prior to pH elevation. This compromises the performance of the imaging system and must be anticipated and compensated for in some way. Our research efforts have been directed toward more effectively controlling hydroquinone immobilization at neutral pH while not interfering with the solubility, and therefore reactivity, of the deprotonated species.

The formation and properties of quinhydrones have been thoroughly investigated.[2] A quinhydrone may be thought of as a bulk 1:1 stoichiometric complex of a hydroquinone with a quinone, held together by a network of hydrogen bonds and π-stacking. These complexes are often insoluble in aqueous environments at neutral pH. At high pH, the hydroquinone component of the quinhydrone is deprotonated, disrupting the hydrogen bonding. The absence of the hydrogen bonding network allows for the dissociation of the solid complex, thereby allowing the deprotonated hydroquinone to dissolve. Such a solubility modification of hydroquinones could accomplish our task of immobilization. Unfortunately however, quinones, being oxidizing reagents which are reactive in photographic systems, cannot be used to form the complex. Some other molecule would be needed to mimic the behavior of the quinone in forming complexes with hydroquinones. We expected that the complexes of hydroquinones with bis(*N*,*N*-dialkyl)terephthalamides would resemble quinhydrones as π-stacked extended hydrogen bonded networks.



Results and Discussion

The two complex systems investigated were those of hydroquinone 1 with bis(*N*,*N*-diethyl)terephthalamide (2, system 1), and hydroquinone (1) with bis(*N*,*N*-dimethyl)-

* Abstract published in *Advance ACS Abstracts*, August 15, 1994.

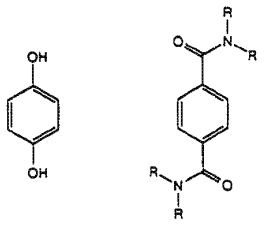
(1) Lee, W. E.; Brown, E. R. In *The Theory of the Photographic Process*, 4th ed.; James, T. H., Ed.; Macmillan: New York, 1977; Chapter 11.

(2) Patil, A. O.; Pennington, W. T.; Desiraju, G. R.; Curtin, D. Y.; Paul, I. C. *Mol. Cryst. Liq. Cryst.* **1986**, *134*, 279.

0897-4756/94/2806-1293$04.50/0 © 1994 American Chemical Society

UM00014175
NOVARTIS EXHIBIT 1517
Novartis v. Regents, IPR2023-01347
Page 2921 of 4460

terephthalamide (3, system 2). To characterize the phase behavior of these systems, mixtures of the components at various molar ratios were prepared. Following examples of Etter[3] and Lehn,[4] we prepared mixtures of the components by solid-state grinding.[5]



1 2: R = Et 3: R = Me

Examination of the ^{13}C CP/MAS spectra (Figure 1) of pure hydroquinone (1), pure bis(*N,N*-diethyl)terephthalamide (2), and the five mixtures of 1 and 2 of molar ratios 3:1, 2:1, 1:1, 1:2, and 1:3 (**2a–e**, respectively, system 1) shows the presence of a unique spectrum which is derived from the 1:1 mixture, **2c**. The nonequivalent mixtures give spectra that are the simple sums of the excess constituent component 1 or 2, and the 1:1 mixture, **2c**. In pure **1**, the 1 and 4 phenolic carbons display a triplet resonance at 148.1 ppm. In the 1:1 mixture, **2c**, this resonance is simplified to a singlet at 149.2 ppm. The 3:1 and 2:1 mixtures, **2a** and **2b**, display combinations of these peaks that are proportional to the excess hydroquinone, 1, and the 1:1 mixture, **2c**. In the 1:2 and 1:3 mixtures, **2d** and **2e**, where there is no excess hydroquinone 1, but there is excess bis(*N,N*-diethyl)terephthalamide **2**, no triplet resonances at 148.1 ppm appear at all.

The chemical shifts of the two, three, five, and six carbons of bis(*N,N*-diethyl)terephthalamide (2) serve as diagnostic resonances for the mixtures which have this compound in excess. In pure **2**, these atoms display a doublet at 124.0 ppm. The 1:1 mixture, **2c**, displays a doublet at 126.0 ppm. The 1:2 and 1:3 mixtures, **2d** and **2e**, show the 124.0 and 126.0 doublets in proportion to the excess of **2** with respect to **2c**. In the 3:1 and 2:1 mixtures, **2a** and **2b**, where no free **2** exists, only the doublet at 126.0 ppm is observed. Each of the other carbon resonances show analogous behavior.

These dramatic variations in spectra are quite remarkable in light of the fact that these mixtures were prepared by simple solid grinding at room temperature.[5] To obtain a thermodynamic measure of the complexation, differential scanning calorimetry was performed on the mixtures of 1 and 2. The phase diagram so derived exhibits the thermal behavior that can be expected from a binary mixture that forms a stable 1:1 complex (Figure 2). Pure hydroquinone (1) has a melting endothermic transition at 173 °C and

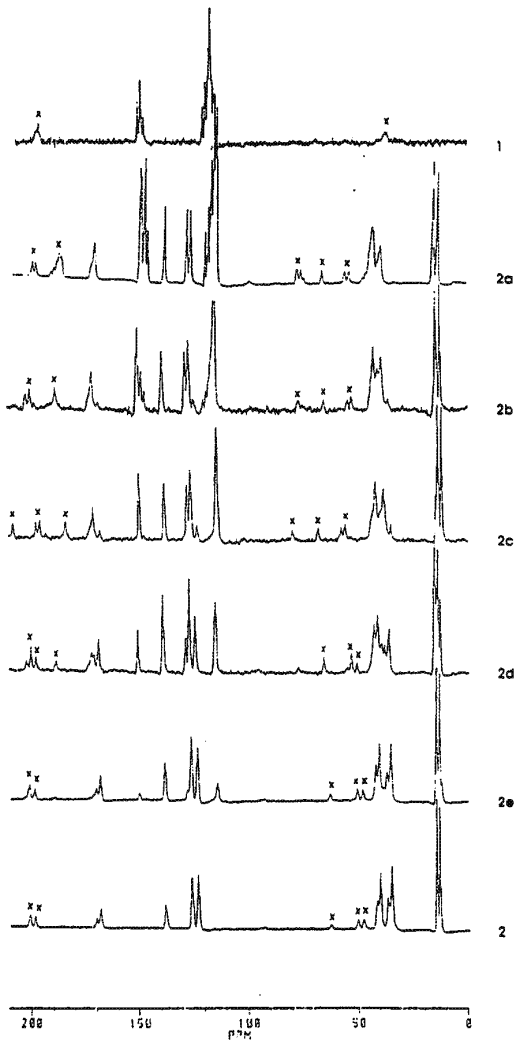


Figure 1. ^{13}C CP/MAS spectra for the hydroquinone–bis(*N,N*-diethyl)terephthalamide system (system 1). Lines marked by an × indicate spinning sidebands.

pure bis(*N,N*-diethyl)terephthalamide (2) displays a melting endothermic transition at 129 °C. The 1:1 mixture, **2c**, exhibits a sharp endotherm at 147 °C. The 3:1 and 2:1 mixtures, **2a** and **2b**, indicate the presence of a eutectic with an endothermic transition at 122 °C, while the 1:2 and 1:3 mixtures, **2d** and **2e**, indicate the presence of a different eutectic with an endotherm at 118 °C. This thermal behavior is typical of a mixture where the components form a stable complex;[6] for instance, phenol and aniline display this property.[7]

When bis(*N,N*-dimethyl)terephthalamide (3) was used in place of bis(*N,N*-diethyl)terephthalamide (2) to form similar mixtures **3a–e** (system 2), we were surprised to find significantly different phase behavior. In addition to the formation of the new stable phase of 1:1 composition, **3c**, the 2:1 mixture, **3b**, also formed a stable binary phase.

(3) (a) Etter, M. C.; Hoye, R. C.; Vojta, G. M. *Cryst. Rev.* **1988**, *1*, 281. (b) Etter, M. C.; Frankenbach, G. M.; Bernstein, J. *Tetrahedron Lett.* **1989**, *30*, 3617. (c) Etter, M. C. *J. Phys. Chem.* **1991**, *95*, 4601. (d) Etter, M. C. *J. Am. Chem. Soc.* **1991**, *113*, 2586. (e) Etter, M. C. *Acc. Chem. Res.* **1990**, *23*, 120. (f) Etter, M. C.; Reutzel, S. M.; Choo, C. G. *J. Am. Chem. Soc.* **1993**, *115*, 4411.

(4) Lehn, J.-M. *Angew. Chem., Int. Ed. Engl.* **1990**, *29*, 1304.

(5) The ability to use solid grinding techniques to form new molecular phases has been elegantly demonstrated by Etter with hydrogen-bonded cocrystals. This work represents an application of this methodology to explore phase constitution in hydroquinone/terephthalamide mixtures. The kinetics and efficiency of this technique is being explored for these and similar binary systems.

(6) Gutt, W.; Majumdar, A. J. In *Differential Thermal Analysis*; Mackenzie, R. C.; Ed.; Academic: London, 1972; Chapter 29.

(7) Moore, W. J. *Physical Chemistry*; Prentice-Hall: Englewood Cliffs, NJ, 1972; Chapter 7.

UM00014176
NOVARTIS EXHIBIT 1517
Novartis v. Regents, IPR2023-01347
Page 2922 of 4460

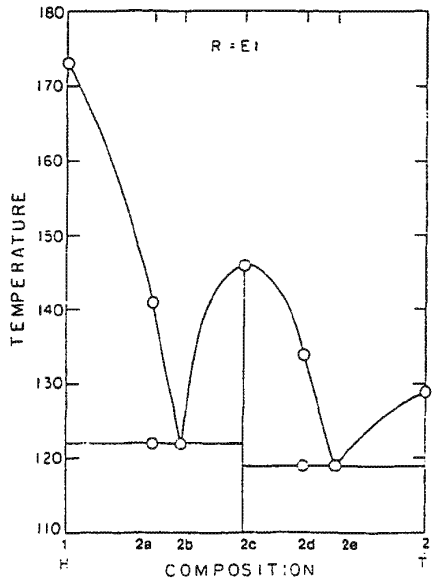


Figure 2. Phase diagram for the hydroquinone–bis(*N*,*N*-diethyl)terephthalamide system (system 1). The eutectic compositions were estimated (not experimentally determined).

The formation of a nonequivalent molar complex of a hydroquinone has to our knowledge been described only once,[8] in a case where the complexing molecules reported contain just one amide functionality.

The ^{13}C CP/MAS spectra of these mixtures (Figure 3) with **3** are somewhat more complicated than those of the mixtures with **2**. Consideration of the one and four phenolic carbons of hydroquinone reveals the triplet resonance at 148.1 of pure **1** to emerge as a very tight doublet at 148.5 ppm for the 2:1 mixture, **3b**. In the 1:1 mixture this resonance appears as a singlet at 151.0 ppm. The 3:1 mixture, **3a**, appears to be a mixture of **1** and **3b**, while **3d** and **3e** are proportional mixtures of **3** and **3c**.

This same additivity is observed for the two, three, five, and six carbons of **3**. Pure bis(*N*,*N*-dimethyl)terephthalamide (**3**) exhibits a singlet resonance at 126.7 ppm. The 1:1 mixture, **3c**, displays an asymmetric pair of peaks at 129.0 and 124.9 ppm, and the 2:1 mixture, **3b**, shows a tight doublet at 125.4 ppm.

The phase diagram derived from differential scanning calorimetry of the binary mixtures was difficult to interpret. It was necessary to prepare and examine several additional ratios of hydroquinone (**1**), and bis(*N*,*N*-dimethyl)terephthalamide (**3**). Having these additional data, we were able to construct a phase diagram consistent with the NMR data (Figure 4). Pure bis(*N*,*N*-dimethyl)-terephthalamide (**3**) displays a melting endotherm at 203 °C. The 2:1 mixture **3b** exhibits a sharp endothermic transition at 198 °C, and the 1:1 mixture **3c** has its endotherm at 169 °C. A eutectic appears between the 1:1 mixture **3c** and pure **3** at 163 °C. Another eutectic is apparent between the 2:1 mixture **3b** and pure **1** at 161 °C. The eutectic between the 2:1 mixture **3b** and the 1:1 mixture **3c** appears to be exhibited at 167 °C.

Pure samples of the complexes could be prepared by cocrystallization of hydroquinone with the terephthalamides from solvent. These samples showed the same spectral and thermodynamic properties as those obtained by grinding, and most importantly allowed the determination of structure by X-ray crystallography.[9]

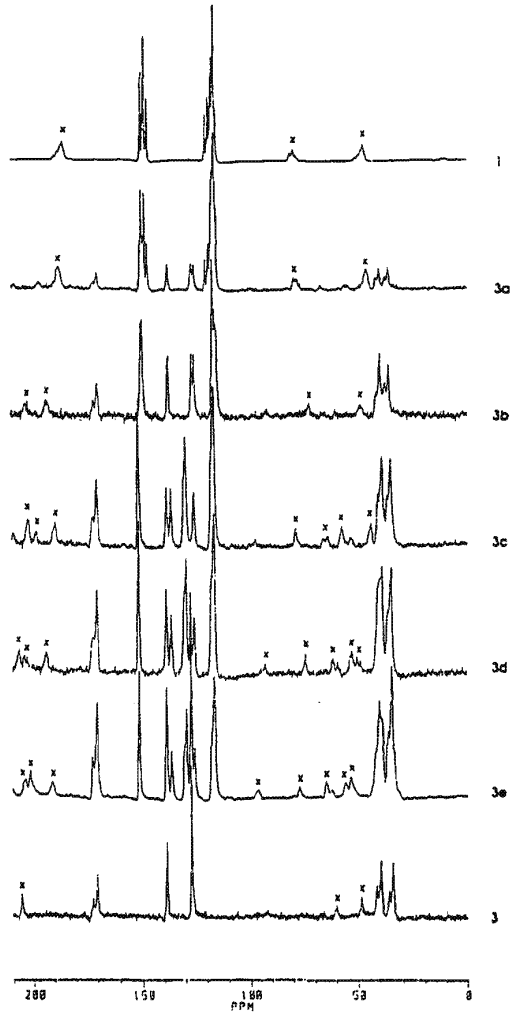


Figure 3. ^{13}C CP/MAS spectra for the hydroquinone–bis(*N*,*N*-dimethyl)terephthalamide system (system 2). Lines marked by an × indicate spinning sidebands.

An examination of the preliminary X-ray crystal structures of **2c**, **3b**, and **3c** have provided some structural insights. Upon examination of the structure of **2c**, the 1:1 complex of system 1, the extended hydrogen bonding network is evident. We were surprised to find that the hydroquinone and terephthalamides were not π-stacked in a *face-to-face* manner but were actually packed *edge-to-face*. Examples of this type of aryl interaction have been well documented.[10] The X-ray crystal structure of **3b**, the 2:1 complex of system 2, shows similar hydrogen bonding features to that of **2c**. The absence of the methylene carbons in the dimethyl amides of **3b** allows room to accommodate the extra hydroquinone molecule.

(8) Barry, J. E.; Cipollini, N. E.; Finkelstein, M.; Ross, S. D. *Tetrahedron* **1981**, *37*, 1669.

(9) Foxman, B.; Guarrera, D.; Taylor, L. D.; Van Engen, D.; Warner, J. C., unpublished observations.

(10) Muehldorf, A. V.; Van Engen, D.; Warner, J. C.; Hamilton, A. D. *J. Am. Chem. Soc.* **1988**, *110*, 6561.

UM00014177
NOVARTIS EXHIBIT 1517
Novartis v. Regents, IPR2023-01347
Page 2923 of 4460

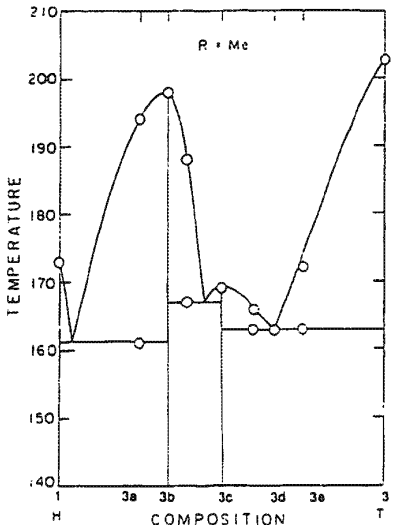


Figure 4. Phase diagram for the hydroquinone–bis(*N*,*N*-dimethyl)terephthalamide system (system 2). The eutectic compositions were estimated (not experimentally determined).

In the case of **3c**, the 1:1 complex of system 2, extended networks of hydrogen bonds are not observed. The X-ray crystal structure of **3c** shows the presence of isolated rings consisting of two hydroquinones and two terephthalamides connected by hydrogen bonds.

Conclusions

These results demonstrate the valuable information that can be obtained by the combination of solid-state NMR and differential scanning calorimetry, allowing the construction and use of phase diagrams for the study of self-assembled systems. While well-known in various fields of metallurgy, phase diagrams have not been applied to multicomponent organic systems of contemporary interest. The differences in behavior between the mixtures of hydroquinone (**1**) with bis(*N*,*N*-diethyl)terephthalamide (**2**, system 1), and bis(*N*,*N*-dimethyl)terephthalamide (**3**, system 2) probably arise from the steric interactions produced by the alkyl substituents. When the alkyl substituents are ethyl groups, only a 1:1 ratio can be accommodated in the molecular assembly. When the less sterically imposing methyl substituents are present, the additional "fitting" of a second hydroquinone is possible and thus two stable binary phases can be observed. Interestingly, our initial expectation that complexes of hydroquinone with terephthalamides would be structurally similar to quinhydrones was only partially fulfilled. As anticipated, a hydrogen-bonding network was evident; but *face-to-face* π stacking was not. Fortunately, however, the complexes have indeed proven useful as solubility inhibitors in photographic systems, as intended.[11]

Experimental Section

Hydroquinone (**1**) was purchased from Aldrich Chemical and used without further purification. Bis(*N*,*N*-diethyl)terephthalamide (**2**) and bis(*N*,*N*-dimethyl)terephthalamide (**3**) were prepared from the condensation of terephthaloyl chloride and the appropriate amine. The products were purified by recrystallization from ethanol and confirmed by comparison to literature properties.[12]

Solid-state grinding was performed with either a Bel-Art Products Micro-Millmill for combined weights exceeding 2.0 g for 4 h or by shaking less than 2.0 g of combined weight in a Nalgene container with a Teflon-coated stirring bar on a Vortex stirrer for 4 h. Pure samples of each complex were prepared by dissolving the appropriate molar amounts of hydroquinone with the terephthalamides in a mutually miscible solvent (typically ethanol or acetonitrile) and allowing the complexes to crystallize slowly at room temperature.

^{13}C CP/MAS spectra were obtained on a Bruker 200-MHz FT NMR spectrometer equipped with a Doty solid-state probe. Differential scanning calorimetry (DSC) scans were obtained on a DuPont 9900 DSC and a Perkin-Elmer DSC4. The samples were weighed into aluminum sample pans, where the sample size ranged from 1 to 3 mg. The samples were then heated at a rate of 10 °C/min under a nitrogen atmosphere. Nitrogen gas purged the DSC at a rate of 30 mL/min.

Acknowledgment. We are grateful to many members of the Polaroid Chemical Research division for helpful discussions. NMR spectra and some of the DSC data were obtained at the Polymer Central Facility, Center for Materials Science and Engineering, at MIT by C. V. Berney. We wish to thank Joy Rogers, Polaroid Student Intern, Southern University, for obtaining some of the DSC scans. X-ray crystallography was performed by Donna van Engen at Princeton University and Bruce Foxman at Brandeis University.

(11) Taylor, L. D.; Warner, J. C. US Patent 5,177,262, Jan 5, 1993.
(12) Beilstein E IV 9 p 3321. Syst.-Nr. 978/H 845; E III 4253.

UM00014178
NOVARTIS EXHIBIT 1517
Novartis v. Regents, IPR2023-01347
Page 2924 of 4460

Conformational Study of a Potent Human Renin Inhibitor: X-Ray Crystal Structure of Isopropyl (2*R*,3*S*)-4-Cyclohexyl-2-hydroxy-3-{*N*-[(2*R*)-2-morpholinocarbonylmethyl-3-(1-naphthyl)propionyl]-L-histidylamino}butyrate (KRI-1314), a Pentapeptide Analogue with Amino Acid Sequence Corresponding to the Cleavage Site of Angiotensinogen

Mitsunobu Doi,[a] Yasuko In,[a] Masatoshi Inoue,[a] Toshimasa Ishida,*[,a] Kinji Iizuka,[b] Kenji Akahane,[b] Hiromu Harada,[b] Hideaki Umeyama[c] and Yoshiaki Kiso*[,d]

[a] *Department of Physical Chemistry, Osaka University of Pharmaceutical Sciences, 2-10-65 Kawai, Matsubara, Osaka 580, Japan*

[b] *Central Research Laboratories, Kissei Pharmaceutical Co., Ltd., Yoshino, Matsumoto, Nagano 339, Japan*

[c] *School of Pharmaceutical Sciences, Kitasato University, Shirokane, Minato-ku, Tokyo 108, Japan*

[d] *Department of Medicinal Chemistry, Kyoto Pharmaceutical University, Yamashita-ku, Kyoto 607, Japan*

A potent inhibitor of renin, isopropyl (2*R*,3*S*)-4-cyclohexyl-2-hydroxy-3-{*N*-[(2*R*)-2- morpholinocarbonylmethyl-3-(1-naphthyl)propionyl]-L-histidylamino}butyrate (KRI-1314), was crystallized as a cinnamic acid salt. The crystal structure of KRI-1314 was determined by X-ray analysis, and the conformation is discussed in relation to the inhibitory activity. The backbone chain of the molecule was largely twisted at the unusual amino acid residue of cyclohexylnorstatine. The observed conformation was compared with that of the model pentapeptide corresponding to the scissile site of angiotensinogen. The stacking interaction was formed between the histidine side-chains related by the crystallographic 2-fold screw axis. The histidine imidazole rings were further fixed by hydrogen bonds with the cinnamic acid. The water molecule of crystallization mediated the hydrogen-bonding bridge of the cinnamic acid with the hydroxy oxygen of the cyclohexylnorstatine. Such interactions appear to be very important in considerations of inhibitor- or substrate-binding mechanisms against renin.

Renin is an aspartic protease (EC 3.4.23.15), which generates a decapeptide of angiotensin I (Asp-Arg-Val-Try-Ile-His-Pro-Phe-His-Leu) from the circulation glycoprotein, angiotensinogen. Angiotensin I is further cleaved by angiotensin-converting enzymes (ACE) to yield the dipeptide His-Leu and angiotensin II (octapeptide).[1] Angiotensin II exhibits strong vasoconstrictor activity and correlates with the maintenance of normal blood pressure.[2] Therefore, the route of the renin–angiotensin system has been a target for antihypertensive therapy.[3]

It is well known that captopril[4] and enalapril[5] are potent ACE inhibitors. The hypertensive state which is related to the imbalance of the renin–angiotensin pathway is improved by the administration of these and relating drugs. Many investigations have been focussed on peptide inhibitors effective against renin. Most of them possess a partial amino acid sequence corresponding to the scissile P5-P3′ site * of angiotensinogen.[7,8] Our strategy for the development of a useful renin inhibitor is aimed at achieving high affinity and selectivity for the protease without incurring accompanying hydrolysis. Boger *et al.* designed potent renin inhibitors (pepstatin derivatives),[9] which contained an unusual amino acid, statine[10] [(3*S*,4*S*)-4-amino-3-hydroxy-6-methylheptanoic acid; see Fig. 1a]. Statine could possibly mimic a dipeptide,[11] wherein the amide bond (ψ[CONH]) is replaced by the ψ[CH(OH)CH_2] bond, as in pepstatin. Consequently, statine in the peptide chain blocks hydrolysis of several proteases, such as renin.

By the aid of comparative model-building techniques,[12] Akahane *et al.* attempted to design structures suitable for binding to renin.[13] Isopropyl (2*R*,3*S*)-4-cyclohexyl-2-hydroxy-3-{*N*-[(2*R*)-2-morpholinocarbonylmethyl-3-(1-naphthyl)-propionyl]-L-histidylamino}butyrate (KRI-1314) was developed as a potent human renin inhibitor (Fig. 1b)[14] and contained a novel cyclohexylnorstatine structure. This compound has the structure corresponding to the P4-P1′ site of angiotensinogen, and its two amide bonds are replaced by unusual bonds to suppress cleavage by proteases. KRI-1314 exhibits high inhibitory activity against renin (IC_{50} 2.4 × 10^{-9} mol dm^{-3}), though this compound shows no significant inhibitory activity against other proteases, such as cathepsin D and chymotrypsin.[15,16] Therefore, we thought it of interest to analyse the conformation of KRI-1314 in order to gain insight into the substrate specificity of renin. The conformational analysis would, furthermore, give useful information on inhibitor design based on the structure–activity relationship of the renin P4-P1′ site, owing to its mimic structure.

* Nomenclature of positions (P) is in accordance with a previous report (ref. 6).

Results and Discussion

Molecular Structure.—Fig. 2 shows the molecular conformation of KRI-1314, where backbone chain assumes an L-shape in the crystal. The morpholine (Mrp), an *N*-terminal residue, is linked by an amide bond with 2-(1-naphthylmethyl)succinate (Nps), and this linkage is a *retro-inverso*[17] type compared with that of normal peptides. The geometry of the amide bond is different from that of a normal peptide (Fig. 3a). However, the conformation of the Mrp^1 residue is similar to that of proline (*trans*-isomer), except for the steric hindrance from the side chain; the torsional angles related to the Mrp^1 residues are C(1′)–N(1A)–C(1)–C(2′) −175(1)° and N(1A)–C(1)–C(2′)–C(2A) 175.7(7)°. The main chain Nps^2–His^3 takes a *trans-zigzag* form. The torsional angles are C(1)–C(2′)–C(2A)–C(2) −65.1(6), C(2′)–C(2A)–C(2)–N(3) 144.4(7), C(2A)–C(2)–N(3)–C(3A) 168.8(7), C(2)–N(3)–C(3A)–C(3) −140.2(7), N(3)–C(3A)–C(3)–N(4) 167.9(7) and C(3A)–C(3)–N(4)–C(4A) 176.9(7)°. The backbone is twisted mainly at the cyclohexylnorstatine (Chs) and isopropyl ester (Isp) groups; C(3)–N(4)–C(4A)–C(4) −94.1(7) and N(4)–C(4A)–C(4)–C(5) 60.0(6)°. The

NOVARTIS EXHIBIT 1517
Novartis v. Regents, IPR2023-01347
Page 2925 of 4460

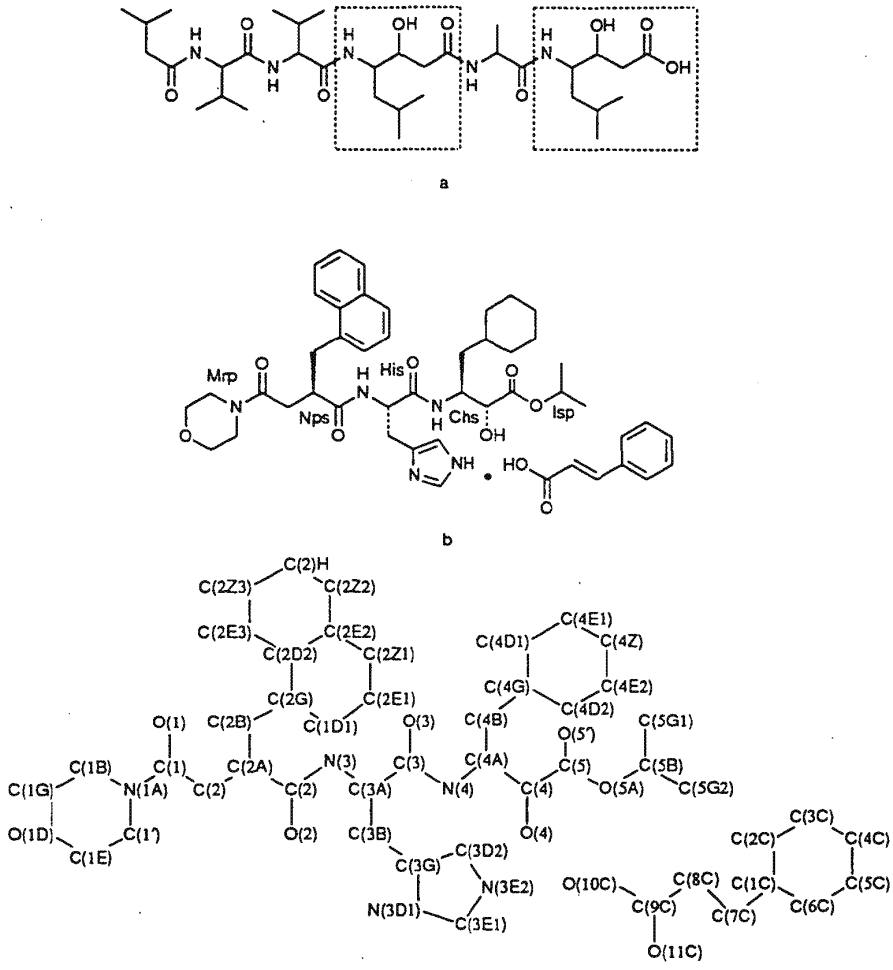


Fig. 1 Chemical structures of renin inhibitors and atomic numbering of KRI-1314. (a) Pepstatin (ref. 10), (b) KRI-1314, and (c) atomic numbering. Statine residues in (a) are boxed by dotted lines.

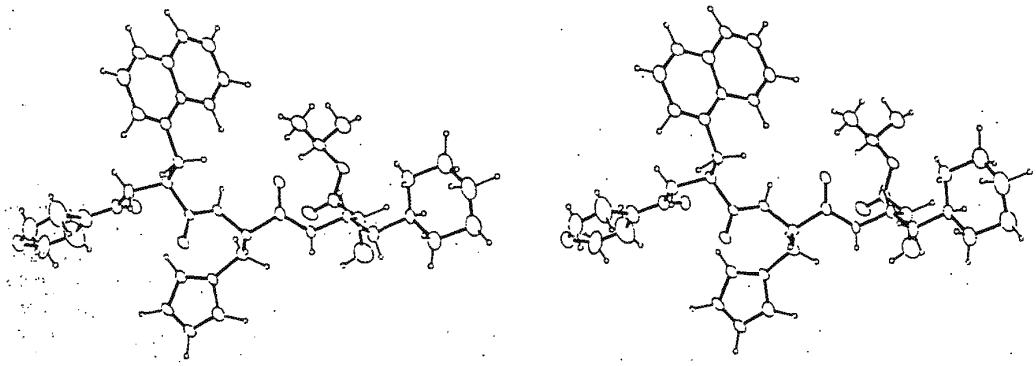


Fig. 2 Molecular conformation of KRI-1314

torsional angle C(4A)–C(4)–C(5)–O(5A) is 86.3(7)°, which corresponds to the peptide ω angle (normally 180°[18]). Although the conformation of KRI-1314 is different from that of the corresponding pepstatin derivative observed in the crystal structure,[19] it is interesting to note that a similarly twisted conformation of the backbone chain is observed at the statine residue of pepstatin bound to a carboxy proteinase.[20]

The torsional angles of side-chains are as follows; C(1')–N(1A)–C(1B)–C(1G) (χ_1) 10.0(1), C(2')–C(2A)–C(2B)–C(2G) (χ_2) −74.1(7), N(3)–C(3A)–C(3B)–C(3G) (χ_3) −69.6(6) and N(4)–C(4A)–C(4B)–C(4G) (χ_4) −168.8(7)°. The side-chains of Nps[2] and His[3] are orientated *gauche*. Although the Chs[4] side-chain is in a *trans* position, such a conformation avoids short contacts with the L-shaped main chain.

Geometry of Non-peptide Linkages.—Since the non-peptide linkages [C(1)–C(2') and C(4)–C(5)] of KRI-1314 are important for the inhibitory activity, the geometry observed was

UM00014180
NOVARTIS EXHIBIT 1517
Novartis v. Regents, IPR2023-01347
Page 2926 of 4460

compared with that of the normal peptide as shown in Fig. 3. The bond lengths and angles are slightly different. The bond lengths N(1A)–C(1) and C(1)–C(2′), however, correspond essentially to the respective C–N and C_α–N bond (Fig. 3a), and the spatial dispositions of the N(1A), C(1), O(1) and C(2′) atoms are almost the same as those of the corresponding atoms in the normal peptide. Although the partial double-bond character for the C(1)–C(2′) bond could not be expected to be similar to that of an amide bond (ψ[CONH]), the N(1A)–C(1)–C(2′)–C(2A) bond sequence achieves conformational planarity (torsional angle 176°). Therefore, the linkage between Mrp[1] and Nps[2] is similar in size to that of an amide bond.

Contrary to this, however, the geometry of the linkage between the Chs[4] and Isp[5] moieties is significantly different from that of an amide bond (Fig. 3b). The hydroxy bond C(4)–O(4) is much longer than the C=O bond, and the C(4)–C(5) bond is also longer than the corresponding C–N bond. The existence of the oxygen atom O(5) causes a large spatial attraction from that of an amide bond. It could be that these structural characteristics help to achieve tight binding with renin, considering the strong inhibitory activity of KRI-1314.

In both linkages shown in Fig. 3 the geometries of the amide and ester bonds, which correspond to the scissile site of the protease substrate, disagree with those of the amide bond in the normal peptide. Furthermore, the O(4) atom of Chs[4] acts as both a donor and an acceptor for hydrogen bond formation, though this atom in the normal peptide acts only as an acceptor. The O(5) atom could be a hydrogen-bonding acceptor, while the nitrogen atom of the amide bond is a hydrogen-bonding donor. Thus, the arrangement of KRI-1314's polar atoms which are able to participate in hydrogen-bond formation is rather different from that of normal substrate polar atoms.

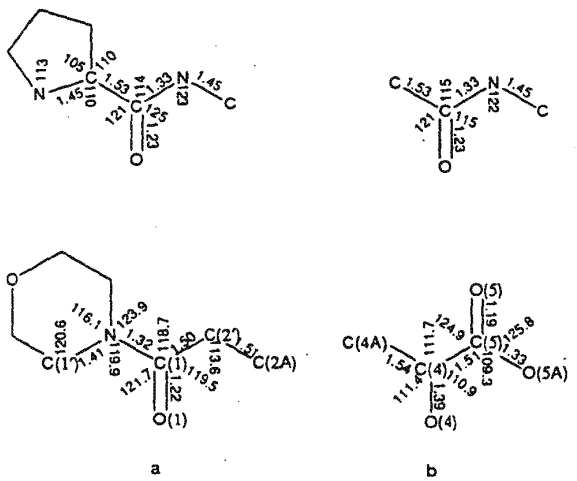


Fig. 3 Geometrical comparison of the non-peptide bond of KRI-1314 with a normal peptide bond, formed between the Mrp[1] and Nps[2] (a), and the Chs[4] and Isp[5] (b), residues. The geometry of the normal peptide corresponds to the upper pair, and that of the KRI-1314 to the lower pair, respectively.

Possible Conformation of P4–P1′ Site.—To compare the present conformation with that of the normal peptide corresponding to the P4–P1′ site, the model pentapeptide Pro-Phe-His-Leu-Val was built up by three-dimensional graphics and by energy minimization (see Experimental section). The superimposition of the pentapeptide with KRI-1314 is shown in Fig. 4. The white and black sticks represent the molecules of the model peptide and KRI-1314, respectively. Large deviations are observed in the residues of the non-peptide linkage. The Pro residue is rotated almost at right angles to the Mrp[1] residue. The side-chain of the Nps[2] residue takes a different conformation from that of the Phe side-chain, because of differences in ring bulkiness. The backbone chain is slightly shifted at the *C*-terminal residue. This would be due to the existence of the carboxy terminal in the model peptide. However, a good fit is achieved on the His[3] residue.

Molecular Association.—Intermolecular interactions are observed in the crystal. Fig. 5 shows the important molecular associations. Although no significant interaction is observed among the side-chains of the Mrp[1], Nps[2], Chs[4] and Isp[5] residues, electrostatic forces could exist between the His[3] residues of neighbouring molecules. The molecules in Fig. 5 are related to each other by the 2-fold screw axis, and projected on the imidazole rings of the His[3] residues. The imidazole rings overlap each other between the translated molecules, and the two ring planes are almost parallel; the dihedral angle between the rings is 18.3°. The interplanar spacing is 3.1–3.3 Å, which is somewhat shorter than the van der Waals separation distance (3.4 Å). Therefore, the imidazole rings could be stacked by partial π–π charge-transfer force. Furthermore, the carboxy oxygens of the cinnamic acids are hydrogen-bonded to the nitrogen atoms of the His[3] imidazole ring; N(3D1) · · · O(11C) 2.69(1) and N(3E2) · · · O(10C) 2.59(1) Å. Both the N(3D1) and N(3E2) atoms of the protonated imidazole ring act as donor atoms for the hydrogen bond, and the positive charge is delocalized on the ring. The histidine side-chain is thus linked with the cinnamic acid by two hydrogen bonds. A weak interaction is observed between the C(3E1) and keto oxygen O(2) atoms; C(3E1) · · · O(2) 3.08(1) Å. The water molecule of crystallization is located in the internal space between the KRI-1314 molecule and the cinnamic acid, and is hydrogen-bonded to both molecules; O(4) · · · W(1) 2.61(1), N(4) · · · W(1) 3.18(1), O(10C) · · · W(1) 2.64(1) and O(11C) · · · W(1) 2.55(1) Å. It is noticeable that the Chs[4] moiety of KRI-1314, which is linked with the water through a hydrogen bond, is the residue corresponding to the cleavage (P1) site[6] of angiotensinogen (discussed later).

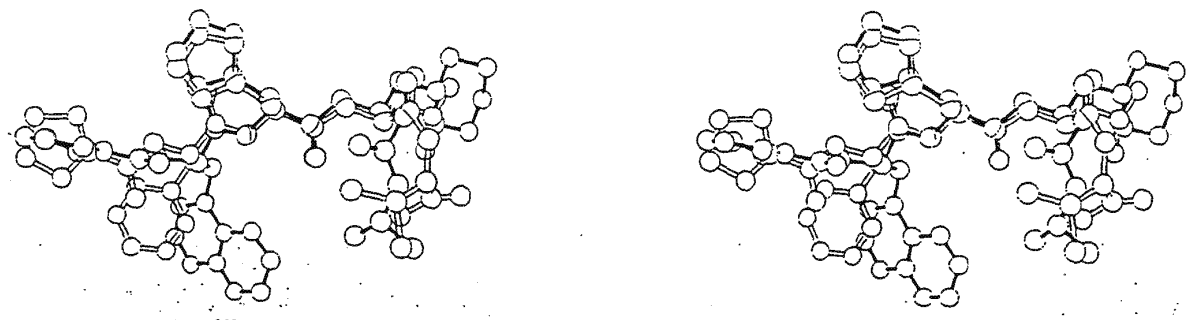


Fig. 4 Superimposition of KRI-1314 and model pentapeptide. The white and black sticks represent the model peptide and KRI-1314, respectively.

NOVARTIS EXHIBIT 1517
Novartis v. Regents, IPR2023-01347
Page 2927 of 4460

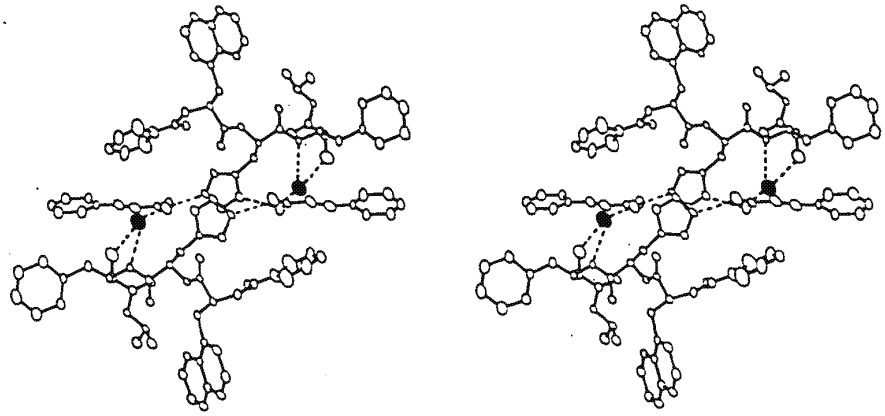


Fig. 5 Molecular association. Dotted lines represent hydrogen bonds. Filled circles represent water molecules of crystallization.

Possible Binding Mode to Renin.—The aforementioned intermolecular interactions (i, hydrophobicity of Nps and Chs side-chains; ii, stacking between His residues; iii, hydrogen bonds with cinnamic acid; and iv, hydrogen bonds with water) are important in considering the possible binding of the inhibitor to renin, as follows: (1) The three-dimensional structure of recombinant renin has been reported,[21] where the active site region consists of the hydrophobic residues of leucine, isoleucine and valine. These amino acid residues could generate hydrophobic forces for the interaction with the KRI-1314 molecule. The residues Nps[2] and Chs[4] have more bulky and hydrophobic side-chains compared with the normal amino acids. These side-chains would be convenient for binding to renin *via* hydrophobic interaction. (2) Potent peptide inhibitors of renin usually contain a histidine residue at the position corresponding to the P2 site.[7,8] The present simulation suggested that the conformation of the His[3] residue was similar to that in the renin inhibitor KRI-1314 and that in the model substrate. Since it has already been shown that there were electron-rich amino acids such as tryptophan and tyrosine in the active-site region of renin,[21] they could be expected to bind the histidine side-chain by a stacking interaction, just like the interaction observed in the present crystal structure. (3) In the present crystal structure, the hydrogen bonds were formed between the His[3] residue and the carboxy group of the cinnamic acid. Judging from molecular models of human renin,[12,13] it is most probable that the His[3] residue of KRI-1314 is fixed by a hydrogen bond with the serine-233 OH side-chain of renin. In addition to the stacking interaction of the His[3] imidazole rings (ii, above), such a hydrogen bond would enhance the specificity of the inhibitor to renin.[22] (4) For the hydrolysis by aspartic protease a tetrahedral complex model has been proposed, where the substrate interacts with the Asp and Gly residues, and with a water molecule which locates at a position near to the amide bond of the cleavage site (P1).[20] The water molecule of crystallization is likely to be that one used for the hydrolysis of the substrate. In the present crystal structure, the water of crystallization is located 2.6 Å away from the O(4) atom of the Chs[4] residue corresponding to the P1 site, and participated in the formation of hydrogen bonds. Furthermore, (5) the dispositions of hydrogen bond-donor and -acceptor atoms on the Mrp[1] and Chs[4] residues could give a potential for diversity of binding of the inhibitor to the active site of renin, compared with the substrate.

Experimental

Crystal Data.—$C_{38}H_{51}N_5O_7 \cdot C_9H_8O_2 \cdot H_2O$, molecular weight in an asymmetric unit 856.04, monoclinic, $P2_1$, a = 23.076(8), b = 6.200(1), c 16.582(7) Å, β = 108.64(5)°, V = 2248(1) Å^3, Z = 2, D_x = 1.255 g cm^{-3}.

Data Collection.—Attempted crystallization of KRI-1314 from several solvents and with several different counter-anion salts finally yielded needle crystals of KRI-1314 from aq. methanol solution as a cinnamic acid salt monohydrate by slow evaporation at room temperature. The dimensions were *ca.* 0.07 × 0.07 × 0.6 mm along edges. Cell constants were determined by a least-squares fitting of 24 reflections on a Rigaku diffractometer equipped with a graphite monochromator using Cu-Kα radiation (λ 1.5418 Å). Intensities were collected by the ω–2θ scan mode using variable speed (2–4° min^{-1}). Standard reflections monitored during the measurement indicated stable X-ray output and no significant decay of the crystal. The data were corrected for Lorentz and polarization effects. Absorption correction was also applied according to the method[23] based on a φ-scan along the b-axis of the crystal. Unique data of 3234 reflections were measured within 2θ 110°. The reflective intensities of this crystal largely decreased depending on the 2θ angle, and reflections for $2\theta > 110°$ were weak because of the small size of the crystal.

Structure Determination and Refinement.—The backbone structure was solved by MULTAN87,[24] and the remaining atoms were picked out from successive weighted Fourier maps. The structure was refined by the 'blocked' full-matrix least-squares method using SHELX-76[25] minimizing the quantity $\Sigma w(|F_o| - |F_c|)^2$. Anisotropic temperature factors were applied for non-hydrogen atoms. Hydrogens were calculated at geometrically ideal position, and were included in the refinement with isotropic temperature factors. The y-co-ordinate of the N(1) atom was fixed during the refinement to avoid divergence of the molecular co-ordinates along the b-axis. In the final cycle, the weight was calculated as $w = 1.0/[\sigma^2(F_o) + 0.000\,63F_o^2]$, and R and R_w were reduced to 0.0692 and 0.0658 for 2475 reflections with $F_o > 3.0\sigma(F_o)$, where $\sigma(F_o)$ was the standard deviation in F_o. All crystallographic calculations were performed on a MicroVAX-II computer at Osaka University of Pharmaceutical Sciences. The obtained atomic co-ordinates are listed in Table 1,* and the atomic numbering used in this work is indicated in Fig. 1c. The averaged standard deviations for bond lengths and angles are 0.1 Å and 0.6°, respectively. Owing to the

* *Supplementary data* (see section 5.6.3 of Instruction for Authors, in the January issue). Anisotropic temperature factors of non-hydrogen atoms, the hydrogen atomic co-ordinates, bond lengths and angles, torsion angles, and hydrogen bonds and short contacts have been deposited at the Cambridge Crystallographic Data Centre.

UM00014182
NOVARTIS EXHIBIT 1517
Novartis v. Regents, IPR2023-01347
Page 2928 of 4460

Table 1 Fractional co-ordinates with esds in parentheses

Atom	x	y	z	Atom	x	y	z
C(1')	0.0395(6)	0.591(2)	0.1786(3)	C(3)	0.2561(3)	0.519(1)	0.6746(4)
N(1A)	0.0797(3)	0.7599[a]	0.2159(5)	O(3)	0.3028(2)	0.499(1)	0.6557(3)
C(1B)	0.0687(6)	0.967(2)	0.1707(8)	N(4)	0.2541(2)	0.493(1)	0.7537(3)
C(1G)	0.0212(6)	0.988(2)	0.1101(7)	C(4A)	0.3070(3)	0.434(1)	0.8264(4)
O(1D)	−0.0179(3)	0.820(1)	0.0676(3)	C(4B)	0.3044(3)	0.556(2)	0.9026(4)
C(1E)	−0.0069(6)	0.625(2)	0.1099(7)	C(4G)	0.3617(3)	0.550(2)	0.9816(4)
C(1)	0.1251(4)	0.725(2)	0.2867(5)	C(4D1)	0.3474(4)	0.663(2)	1.0546(6)
O(1)	0.1377(2)	0.544(1)	0.3158(3)	C(4E1)	0.4031(6)	0.658(3)	1.1380(7)
C(2')	0.1640(3)	0.912(1)	0.3294(4)	C(4Z)	0.4549(6)	0.775(2)	1.1154(7)
C(2A)	0.2115(3)	0.854(1)	0.4132(4)	C(4E2)	0.4708(5)	0.652(2)	1.0439(7)
C(2B)	0.2551(3)	1.042(1)	0.4495(4)	C(4D2)	0.4176(4)	0.639(2)	0.9644(5)
C(2G)	0.3007(3)	1.080(1)	0.4033(4)	C(4)	0.3098(3)	0.189(1)	0.8402(5)
C(2D1)	0.2933(3)	1.252(1)	0.3490(5)	O(4)	0.2599(3)	0.115(1)	0.8623(4)
C(2E1)	0.3354(4)	1.292(2)	0.3019(5)	C(5)	0.3150(4)	0.070(1)	0.7635(5)
C(2Z1)	0.3833(3)	1.152(2)	0.3124(5)	O(5')	0.2727(2)	0.003(1)	0.7066(4)
C(2E2)	0.3934(3)	0.980(2)	0.3685(5)	O(5A)	0.3736(2)	0.056(1)	0.7686(3)
C(2Z2)	0.4433(3)	0.837(2)	0.3785(5)	C(5B)	0.3881(3)	−0.039(1)	0.6924(5)
C(2H)	0.4523(3)	0.676(2)	0.4320(6)	C(5G1)	0.4056(3)	0.141(2)	0.6464(6)
C(2Z3)	0.4124(4)	0.630(2)	0.4822(5)	C(5G2)	0.4387(4)	−0.198(2)	0.7290(5)
C(2E3)	0.3631(3)	0.764(2)	0.4711(5)	W(1)[b]	0.1464(3)	0.211(2)	0.7798(6)
C(2D2)	0.3503(3)	0.942(1)	0.4146(4)	C(1C)	0.1734(3)	0.733(2)	0.9981(4)
C(2)	0.1811(3)	0.787(1)	0.4776(4)	C(2C)	0.2058(4)	0.920(2)	1.0310(5)
O(2)	0.1364(2)	0.8879(9)	0.4848(3)	C(3C)	0.2374(4)	0.949(2)	1.1169(5)
N(3)	0.2087(2)	0.633(1)	0.5307(3)	C(4C)	0.2341(4)	0.775(2)	1.1685(6)
C(3A)	0.1954(3)	0.564(1)	0.6065(4)	C(5C)	0.2027(4)	0.585(2)	1.1385(5)
C(3B)	0.1573(3)	0.358(1)	0.5899(4)	C(6C)	0.1709(3)	0.564(2)	1.0521(5)
C(3G)	0.0928(3)	0.383(1)	0.5320(4)	C(7C)	0.1419(4)	0.663(3)	0.9155(5)
N(3D1)	0.0454(3)	0.421(1)	0.5657(4)	C(8C)	0.1263(4)	0.726(2)	0.8453(5)
C(3E1)	−0.0066(3)	0.425(1)	0.5026(6)	C(9C)	0.0919(5)	0.706(2)	0.7591(5)
N(3E2)	0.0049(2)	0.399(1)	0.4310(4)	O(10C)	0.0829(3)	0.865(2)	0.7122(5)
C(3D2)	0.0671(3)	0.371(1)	0.4478(4)	O(11C)	0.0730(4)	0.527(2)	0.7307(4)

[a] Fixed. [b] W Represents the water molecule of crystallization.

relatively low number of reflections compared with the atom number of the molecule, these values are rather high, and their bonding parameters are somewhat imprecise. However, this would not seriously affect the molecular conformation discussed in the text.

Molecular Modelling and Fitting of P4-P1' *Peptide.*—The pentapeptide Pro-Phe-His-Leu-Val (the P4-P1' site of angiotensinogen[6]) was built up by three-dimensional graphics on an IRIS computer. The peptide structure was energy-refined by the molecular mechanics force-field method[26] on the CHEMLAB system.[27] The molecular steric energy converted to −24.8 kcal mol^{-1}.*

The molecular superposition between the pentapeptide and KRI-1314 was fitted by a least-squares method. For the fitting calculations, the root-mean-square error was within 0.88 Å between the main-chain atoms of both molecules.

* 1 cal = 4.184 J.

References

1 M. J. Peach, *Physiol. Rev.*, 1977, **57**, 313.
2 R. R. Smeby, *Chemistry and Biochemistry of Amino Acids, Peptides, and Proteins*, ed. B. Weinstein, Marcel Dekker, New York, 1978, vol. 5, p. 117.
3 L. C. Skeggs, F. E. Dorer, M. Levine, K. E. Lentz and J. R. Kahm, *The Renin Angiotensin System*, ed. J. A. Johnson and R. R. Anderson, Plenum, New York, 1980, p. 1.
4 M. A. Ondetti, B. Rubin and B. W. Cushman, *Science*, 1976, **196**, 441.
5 A. A. Patchett, E. Harris, E. W. Tristam, M. J. Wycratt, M. T. Wu, D. Taub, E. R. Peterson, T. J. Ikeler, J. TenBroke, L. G. Payne, D. L. Ondeyka, E. D. Thorset, W. J. Greenlee, S. R. Lohr, R. D. Hoffsommer, H. Joshua, W. W. Ruyle, J. W. Rothrock, S. D. Aster, A. L. Maycock, F. M. Robinson, R. Hirschmann, C. S. Sweet, E. H. Ulm, D. H. Gross, T. C. Vassil and C. A. Stone, *Nature (London)*, 1980, **228**, 280.
6 I. Schechter and A. Berger, *Biochem. Biophys. Res. Commun.*, 1968, **32**, 898.
7 R. Guegan, J. Diaz, C. Cazaubon, M. Beaumont, C. Carlet, J. Cément, H. Demarne, M. Mellet, J.-P. Richaud, D. Segondy, M. Vedel, J.-P. Gagnol, R. Roncucci, B. Castro, P. Corvol, G. Evin and B. P. Roques, *J. Med. Chem.*, 1986, **29**, 1152.
8 M. G. Bock, R. M. DiPardo, B. E. Evans, K. E. Rittle, J. S. Boger, R. M. Freidinger and D. F. Veber, *J. Chem. Soc., Chem. Commun.*, 1985, 109.
9 J. Boger, N. S. Lohr, E. H. Ulm, M. Poe, E. H. Blaine, G. M. Fanelli, T.-Y. Lin, L. S. Payne, T. W. Schorn, B. I. LaMont, T. C. Vassil, I. I. Stabilito, D. F. Veber, D. H. Rich and A. S. Bopari, *Nature (London)*, 1983, **303**, 81.
10 W. Umezawa, T. Aoyagi, H. Morishima, M. Matsuzaki, M. Hamada and T. Takeuchi, *J. Antibiot.*, 1970, **23**, 259.
11 J. Boger, *Peptides Structure and Function*, Proceedings of the 8th American Peptide Symposium, ed. V. J. Hruby and D. H. Rich, Pierce Chemical Co., Rockford, IL, 1983, p. 569.
12 K. Akahane, H. Umeyama, S. Nakagawa, I. Moriguchi, S. Hirose, K. Iizuka and K. Murakami, *Hypertension*, 1985, **7**, 3.
13 K. Akahane, T. Kamijo, K. Iizuka, T. Taguchi, Y. Kobayashi, Y. Kiso and H. Umeyama, *Chem. Pharm. Bull.*, 1988, **36**, 3447.
14 K. Iizuka, T. Kamijo, H. Harada, K. Akahane, T. Kubota, H. Umeyama and Y. Kiso, *J. Chem. Soc., Chem. Commun.*, 1989, 1678; H. Harada, A. Iyobe, A. Tsubaki, T. Yamabuchi, K. Hirata, T. Kamijo, K. Iizuka and Y. Kiso, *J. Chem. Soc., Perkin Trans. 1*, 1990, 2497.
15 K. Iizuka, T. Kamijo, H. Harada, K. Akahane, T. Kubota, Y. Etoh, I. Shimaoka, A. Tsubaki, M. Murakami, T. Yamaguchi, A. Iyobe, H. Umeyama and Y. Kiso, *Chem. Pharm. Bull.*, 1990, **38**, 2487.
16 K. Iizuka, T. Kamijo, H. Harada, K. Akahane, T. Kubota, H. Umeyama, T. Ishida and Y. Kiso, *J. Med. Chem.*, 1990, in the press.
17 H. Harada, K. Iizuka, T. Kamijo, K. Akahane, R. Yamamoto, Y. Nakano, A. Tsubaki, T. Kubota, I. Shimaoka, H. Umeyama and Y. Kiso, *Chem. Pharm. Bull.*, 1990, in the press.
18 G. E. Schulz and R. H. Schirmer, *Springe Advanced Texts in Chemistry: Principles of Protein Structure*, ed. C. R. Cantor, Springer-Verlag, New York, 1979, p. 1.

NOVARTIS EXHIBIT 1517
Novartis v. Regents, IPR2023-01347
Page 2929 of 4460

19 G. Precigoux, S. Geoffre and E. Quvrad, *Acta Crystallogr., Sect. C*, 1986, **42**, 721.
20 R. Bott, E. Subramanian and R. D. Davies, *Biochemistry*, 1982, **21**, 6956.
21 A. R. Sielecki, K. Hayakawa, M. Fujinaga, E. P. M. Murphy, M. Fraster, A. K. Muir, C. T. Carilli, J. A. Lewicki, J. D. Baxter and M. N. G. James, *Science*, 1989, **243**, 1346.
22 K. Iizuka, T. Kamijo, T. Kubota, K. Akahane, H. Umeyama and Y. Kiso, *J. Med. Chem.*, 1988, **31**, 701.
23 A. C. T. North, P. C. Phillips and F. S. Mathews, *Acta Crystallogr., Sect. A*, 1968, **24**, 351.
24 T. Debaerdemaeker, G. Germain, P. Main, C. Tate and M. M. Woolfson, MULTAN87, Computer Programs for the Automatic Solution of Crystal Structures from X-Ray Diffraction Data, Universities of York, England, and Louvain, Belgium, 1987.
25 G. M. Sheldrick, SHELX-76, Program for Crystal Structure Determination, University of Göttingen, Göttingen, 1976.
26 A. J. Hopfinger and R. A. Pearlstein, *J. Comput. Chem.*, 1984, **5**, 486.
27 CHEMLAB-II, A Molecular Modeling Software System, Molecular Design, Ltd., San Diego, CA, 1986.

Paper 0/04527F
Received 8*th October* 1990
Accepted 22*nd November* 1990

UM00014184
NOVARTIS EXHIBIT 1517
Novartis v. Regents, IPR2023-01347
Page 2930 of 4460

This Page is Inserted by IFW Indexing and Scanning Operations and is not part of the Official Record

BEST AVAILABLE IMAGES

Defective images within this document are accurate representations of the original documents submitted by the applicant.

Defects in the images include but are not limited to the items checked:

- ☐ BLACK BORDERS
- ☐ IMAGE CUT OFF AT TOP, BOTTOM OR SIDES
- ☐ FADED TEXT OR DRAWING
- ☐ BLURRED OR ILLEGIBLE TEXT OR DRAWING
- ☐ SKEWED/SLANTED IMAGES
- ☐ COLOR OR BLACK AND WHITE PHOTOGRAPHS
- ☐ GRAY SCALE DOCUMENTS
- ☐ LINES OR MARKS ON ORIGINAL DOCUMENT
- ☐ REFERENCE(S) OR EXHIBIT(S) SUBMITTED ARE POOR QUALITY
- ☐ OTHER: _____

IMAGES ARE BEST AVAILABLE COPY.
As rescanning these documents will not correct the image problems checked, please do not report these problems to the IFW Image Problem Mailbox.

CRYSTAL GROWTH & DESIGN
2003
VOL. 3, NO. 3
313–320

Crystal Engineering through Halogen Bonding. 2. Complexes of Diacetylene-Linked Heterocycles with Organic Iodides

April Crihfield,[†] Joshua Hartwell,[†] Dustin Phelps,[†] Rosa Bailey Walsh,[‡] Jeffery L. Harris,[‡] John F. Payne,[‡] William T. Pennington,*[,‡] and Timothy W. Hanks*[,†]

Department of Chemistry, Furman University, Greenville, South Carolina, 29613, and Department of Chemistry, Hunter Chemistry Laboratories, Clemson University, Clemson, South Carolina 29634

Received January 9, 2003; Revised Manuscript Received January 27, 2003

ABSTRACT: The bis(aryl)diacetylenes 1,4-bis(3-quinolyl)-1,3-butadiyne (**1**), 1,4-bis(4-isoquinolyl)-1,3-butadiyne (**2**), and 1,4-bis(3-pyridyl)-1,3-butadiyne (**3**) form strongly halogen bonded complexes with organic iodides, including tetraiodoethylene (TIE), 1,4-diiodotetrafluorobenzene (F_4DIB), and 1,4-diiodooctafluorobutane (F_8DIBut). The crystal structures for the new donor, **2**, as well as for six complexes, **1**·TIE, **1**·F_4DIB, **2**·TIE, **2**·F_4DIB, **3**·(F_4DIB)$_2$, and **3**$_2$·(F_8DIBut)$_2$, are reported. Extended chain structures consisting of donor and acceptor molecules are observed in all cases, except that of **3**$_2$·(F_8DIBut)$_2$, which forms a molecular adduct. In most cases, the complexes segregate into columns of donors and acceptors, as is typical for this class of complexes. However, **1**·F_4DIB displays an unusual "crosshatched" pattern with each acceptor directly above the diacetylene moiety of another donor along the *b*-axis. In addition to **1**·F_4DIB, **3**$_2$·(F_8DIBut)$_2$ also exhibits packing that does not consist of segregated stacks (i.e., the acceptor in the chain sits on top of one end of the donor and the uncomplexed F_4DIB sits on top of the other end). Neither diacetylene **2**, nor any of the complexes, pack in a manner that would allow for topotactic polymerization of the diacetylene moiety.

Introduction

Bis(aryl)diacetylenes are intriguing building blocks for supramolecular synthesis. They are rigid and planar, and a variety of systems can be easily synthesized from readily available components. The most widely investigated approach to supramolecular construction in these systems takes advantage of the fact that the diacetylene (DA) moiety has a strong tendency to stack into columnar arrays. If the packing of the arrays falls within certain empirically determined parameters (Figure 1), the DAs may undergo photoinduced topopolymerization.[2] The resulting polymers are highly conjugated, deeply colored, and display interesting optical and nonlinear optical properties.[2b] In general, the polymerization reaction proceeds best when the DAs stack at a 45° angle from the long axis of the molecule. This puts the 1 and 4 positions of the DA moiety close enough to each other that atomic motion required on polymerization (Figure 1a) is minimized. These packing requirements are particularly strict with completely conjugated bis(aryl)diacetylenes, since their rigidity permits little motion during the polymerization reaction. A second packing motif has also been observed, where the DAs pack directly over one another.[3] This presumably results in a head-to-head polymerization (Figure 1b).

When the aryl groups are heterocycles, other types of supramolecular structures may be formed. For example, the heterocycle can act as a ligand to form coordination polymers. The linear compound 1,4-bis(4-pyridyl)butadiyne has most often been used to form extended complexes with metals.[4] However, there appear to be no examples of DA coordination polymers of this type that are capable of topopolymerization at the diacetylene.[5] This is not surprising, as we are aware of only one symmetrical bis(heterocycle)DA, 1,4-bis(3-quinolyl)-1,3-butadiyne, that photopolymerizes in the solid state.[6] While it may be possible to use the coordination of a metal (or some other species) to manipulate the packing of the DAs into a more favorable geometry for DA polymerization, the formation of an extended chain structure would be expected to greatly restrict the motion of the reacting centers. This would increase the

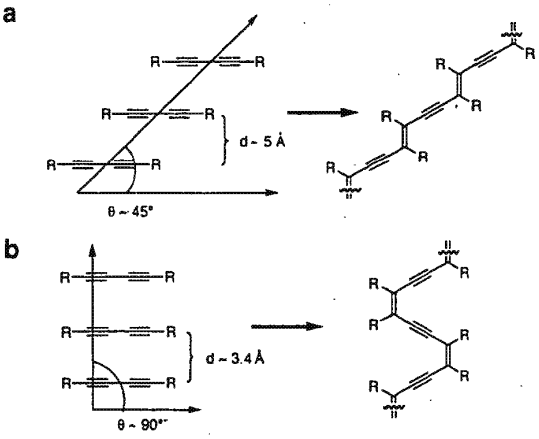


Figure 1. Geometrical requirements for (a) head-to-tail and (b) head-to-head topopolymerization of DAs.

[†] Furman University.
[‡] Clemson University.
* To whom correspondence should be addressed. BillP@Clemson.edu; Tim.Hanks@Furman.edu.

10.1021/cg0340042 CCC: $25.00 © 2003 American Chemical Society
Published on Web 02/22/2003

UM00014186
NOVARTIS EXHIBIT 1517
Novartis v. Regents, IPR2023-01347
Page 2932 of 4460

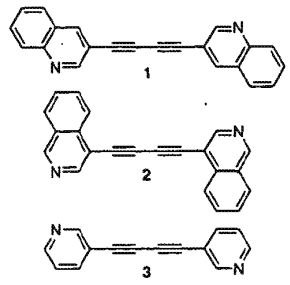


Figure 2. Diacetylene donor compounds **1**–**3**.

strain that the crystal lattice would experience during the topopolymerization reaction, making the formation of crystalline polymers more challenging. This is unfortunate, since the resulting highly organized, three-dimensional polymers would be of both theoretical and practical importance.[7]

While there are a number of examples of host–guest complexes formed from DAs attached to aliphatic carbons,[8] reports of complexes built from crystals of bis(heterocyclic)DAs, where the heterocycle is in direct conjugation with the DA, are much less common. In one important example, Rodriquez methylated members of the bis(pyridyl)butadiyne family to give salts that are capable of forming $\pi-\pi$ charge-transfer complexes with tetramethyl-*p*-phenylenediamine.[9] Interestingly, quaternization of the pyridine nitrogen seems to encourage polymerization of the DA moiety (although not in any of the charge-transfer complexes). The reaction is not the topotactic 1–4 reaction described above, but a random radical polymerization to give a highly cross-linked material.[10]

We have long been interested in the halogen bonding interaction between N-heterocycles and organoiodides.[1,11] Like hydrogen bonding, the halogen bond is a highly directional and relatively strong noncovalent bond. Nominally, the interaction involves the donation of the nitrogen lone pair into the C–I σ^* antibonding orbital (a more detailed quantum mechanical description is available[11c]) and is therefore strengthened by electron withdrawing groups on the acceptor. While halogen bonding was first reported some 140 years ago,[12] it has only recently been seriously investigated as a tool for crystal engineering.[13]

Herein we report the synthesis and structural characterization of a series of halogen-bonded complexes involving 1,4-bis(3-quinolyl)-1,3-butadiyne (**1**), its isomer 1,4-bis(4-isoquinolyl)-1,3-butadiyne (**2**), and 1,4-bis(3-pyridyl)-1,3-butadiyne (**3**) (Figure 2). While DA **3** does not undergo ready solid-state photopolymerization, DA **1**, which differs only in the addition of a fused benzene ring, does. DA **2** has not been previously reported. This compound is an isomer of **1** and retains the 1,3-relationship between the nitrogen atom and the diacetylene. This paper looks for a simple relationship between DA molecular structure, DA crystal packing, and solid-state photoreactivity. In addition, we examine the influence of halogen bonding on the propensity of the DAs toward photopolymerization.

Experimental Section

Materials and Methods. All reagents were purchased from Aldrich and were used as received. Solvents were purchased from commercial sources and distilled under argon from appropriate drying agents immediately before use. Carbon, hydrogen, and nitrogen analyses were performed by Atlantic Microlabs, Norcross, GA and were satisfactory for all compounds. Proton NMR data were collected at 500 MHz on a Varian INOVA 500 spectrometer and carbon-13 data were collected on a Varian VXR-300 spectrometer at 75 MHz. IR data were collected on a Nicolet Magna IR-750 Fourier Transform spectrometer. Melting point data were collected on at Mel Temp II apparatus and are uncorrected. Compounds **1** and **3** were prepared as previously reported, and their spectroscopic characterization was consistent with those reports.[6,9]

X-ray Crystallographic Studies. Specific details of the crystallographic experiment and results for each compound are given in Table 1. The data were measured at room temperature (295 ± 1 K) with graphite-monochromated Mo Kα radiation (λ = 0.71073 Å) on either a four-circle diffractometer (Nicolet R3mV or Rigaku AFC7R-18) with serial detection or on a three-circle diffractometer equipped with a CCD area detector (Rigaku AFC8/Mercury CCD). The data were corrected for Lorentz and polarization effects. The intensities of three reflections, remeasured periodically throughout data collection for **1**·TIE and **2**·TIE, declined by 9.6 and 4.8%, respectively. A linear correction was applied to the data for the latter two compounds to account for crystal decomposition. An absorption correction, based on either azimuthal scans of several intense reflections or on a multiscan technique,[14] was applied to the data for each compound. All structures were solved by direct methods and refined (on F^2) using full-matrix, least-squares techniques. All non-hydrogen atoms were refined anisotropically. Hydrogen atoms were either refined isotropically (compound **2**) or were included in the structure factor calculation at optimized positions with isotropic displacement parameters fixed at values 20% greater than that of their host atom. Structure solution, refinement, and calculation of derived results was performed with the SHELXTL[15] package of computer programs. Neutral atom scattering factors and the real and imaginary anomalous dispersion corrections were taken from *International Tables for X-ray Crystallography*, Vol. C.[16]

Synthesis of 2-Methyl-4-(4-isoquinolyl)but-3-yn-2-ol (4). To a 250 mL round-bottomed flask was added triethylamine (70 mL), 2-methylbut-3-yn-2-ol (3.36 g, 0.040 mol), 4-bromoisoquinoline (4.16 g, 0.020 mol), and tetrakis(triphenylphosphine)palladium (0.50 g, 1.1 mmol). The flask was flushed with dry N_2 and a solution containing CuBr (0.20 g, 1.4 mmol) and LiBr (0.7 g, 8.1 mmol) in 10 mL of anhydrous THF was added with stirring. The mixture was heated at reflux under dry N_2 for 3 h, cooled to room temperature, and the inorganic salts removed by vacuum filtration. The triethylamine was removed under vacuum. Water was added to the crude product, and the resulting solution was extracted with diethyl ether. The organic layer was dried with $MgSO_4$, and the product was recrystallized from ethyl acetate/hexane to give white needles (85%), mp 107–108 °C ^{1}H NMR (500 MHz, $CDCl_3$) δ_H 1.78 (s, 6H), 7.66 (dd, 1H), 7.79 (dd, 1H), 7.98 (d, 1H), 8.19 (d 1H), 8.68 (s, 1H), 9.19 (s, 1H).

Synthesis of 4-Isoquinoylacetylene (5). Toluene (300 mL), finely ground NaOH (5 g), and **4** (4.22 g, 0.020 mol) were placed in a 500 mL round-bottom flask and heated to reflux under nitrogen for 5 h The mixture was filtered and the toluene was removed under vacuum. The crude product was dissolved in diethyl ether and washed with water. The organic layer was dried with $MgSO_4$ and the product was recrystallized from ethyl acetate/hexane to give a pale yellow solid (80%), mp 79–80 °C. ^{1}H NMR (500 MHz, $CDCl_3$) δ_H 3.55 (s, 1H), 7.66 (dd, 1H), 7.80 (dd, 1H), 7.95 (d, 1H), 8.26, (d, 1H), 8.73 (s, 1H), 9.21 (s, 1H).

Synthesis of 1,4-Bis(4-isoquinolyl)-1,3-butadiyne (2). A solution of CuCl (198 mg, 2.0 mmol), **5** (1.53 g, 0.010 mol), and TMEDA (2 mL) in 35 mL of DME was stirred rapidly as

UM00014187
NOVARTIS EXHIBIT 1517
Novartis v. Regents, IPR2023-01347
Page 2933 of 4460

Table 1. Crystal Data for 1·TIE, 1·F_4DIB, 2,2·TIE, 2·F_4DIB, 3_2·F_8DIBut, and 3·$(F_4DIB)_2$

	1·TIE	1·F_4DIB	2	2·TIE	2·F_4DIB	3·$(F_4DIB)_2$	3_2·F_8DIBut
formula	$C_{24}H_{12}N_2I_4$	$C_{28}H_{12}N_2F_4I_2$	$C_{22}H_{12}N_2$	$C_{24}H_{12}N_2I_4$	$C_{28}H_{12}N_2F_4I_2$	$C_{28}H_8N_2F_8I_4$	$C_{32}H_{16}N_4F_8I_2$
M_w	835.96	706.20	304.34	835.96	706.20	1007.94	862.29
crystal color, habit	light-yellow, needle	light-blue, needle	yellow, needle	light-yellow, needle	light-yellow, plate	light-yellow, needle	yellow, parallelepiped
crystal dimensions (mm)	0.12 × 0.14 × 0.28	0.07 × 0.07 × 0.43	0.10 × 0.10 × 0.60	0.12 × 0.22 × 0.41	0.11 × 0.24 × 0.36	0.11 × 0 12 × 0 36	0 07 × 0.19 × 0 48
crystal system	triclinic	monoclinic	monoclinic	triclinic	triclinic	triclinic	monoclinic
space group	$P\bar{1}$ (no. 2)	$C2/c$ (no. 15)	$P2_1n$ (no. 14)	$P\bar{1}$(no. 2)	$P\bar{1}$(no. 2)	$P\bar{1}$ (no. 2)	$P2_1/c$ (no. 14)
a, Å	7.1360(5)	19.293(4)	3.816(2)	7.362(1)	4.023(2)	7.479(2)	18.7594(5)
b, Å	8.9258(7)	9.546(2)	25.504(13)	19.278(4)	7.540(4)	11.186(2)	7.2538(11)
c, Å	10.2314(7)	15.771(3)(7)	7 767(4)	4.2134(5)	20.239(11)	17 454(4)	12.0581(9)
α, (°)	95.699(5)	90	90	94.07(1)	80.97(3)	81.880(14)	90
β, (°)	108.631(5)	121.770(6)	93.988(9)	98.13(1)	85.29(4)	87.58(2)	101.7708(10)
γ, (°)	91.813(6)	90	90	97 22(1)	84.00(3)	79.740(12)	90
V, Å^3	613.09(8)	2469(1)	764.0(6)	584.9(2)	601.6(5)	1422.2(6)	1606.3(3)
Z	1	4	2	1	1	2	2
D_{calc}, g cm^{-3}	2.26	1.90	1.34	2.37	1.95	2.35	1.78
diffractometer	Siemens R3mV	Rigaku AFC8/ Mercury CCD	Rigaku AFC8/ Mercury CCD	Rigaku AFC7R-18	Rigaku AFC8/ Mercury CCD	Rigaku AFC8/ Mercury CCD	Rigaku AFC8/ Mercury CCD
θ_{range} (°)	2.11–27.57	2.47–26.73	2.75–25.67	2.14–27.48	2 78–26.37	2.80–26.50	3.33–26.37
μ, mm^{-1}	5.10	2.60	0.079	5.34	2 66	4.45	2.03
transmission coefficients	0.73–1.00	0.67–1.00	0.77–1.00	0.57–1.00	0 54–1.00	0.61–1.00	0.66–1.00
reflections collected	3067	11368	4390	2909	5574	13885	23586
reflections unique (R_{int})	2843 (0.015)	2534 (0.032)	1426 (0.046)	2869 (0.029)	2334 (0.157)	5784 (0.047)	3252 (0.034)
reflections observed ($I > 2\sigma(I)$)	2399	2484	1153	2660	1902	4887	3251
R_1[a]	0 0246 (0.0311)	0 0492 (0.0530)	0 0856 (0.1033)	0.0599 (0.0693)	0.1471 (0.1633)	0.0671 (0.0812)	0.0469 (0.0801)
wR_2[b]	0.0609 (0.0622)	0.0861 (0.0869)	0 1345 (0.1420)	0.1514 (0.1555)	0.2818 (0.2916)	0.1362 (0.1454)	0.1076 (0 1260)

[a] $R_1 = \Sigma||F_o| - |F_c||/\Sigma|F_o|$ for observed data ($I > 2\sigma(I)$); number in parentheses is for all data. [b] $wR_2 = \{\Sigma[w(F_o^2 - F_c^2)^2]/\Sigma[w(F_o^2)^2]\}^{1/2}$ for observed data ($I > 2\sigma(I)$); number in parentheses is for all data.

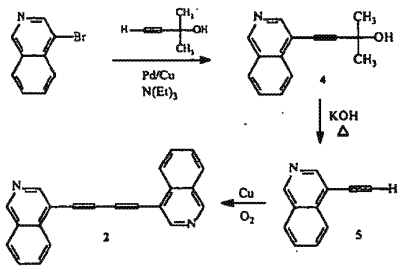


Figure 3. Synthesis of diacetylene donor 2.

O_2 was bubbled through it. After 3 h, the solvent was removed and the solid was extracted with chloroform, washed with water, and dried of $MgSO_4$. The product was then recrystallized from chloroform to give a yellow solid (40%), mp 242–243. ^{1}H NMR (500 MHz, $CDCl_3$) δ_H 7.72 (dd, 2H), 7.86 (dd, 2H), 8.04 (d, 2H), 8.34, (d, 2H), 8.84 (s, 2H), 9.26 (s, 2H).

Preparation of Charge-Transfer Complexes, General Procedure. Equal molar amounts of the diacetylene donor and either tetraiodoethylene (TIE) or 1,4-diiodotetrafluorobenzene (F_4DIB) were dissolved in methylene chloride. Slow evaporation of the solvent gave crystalline solids suitable for single-crystal analysis.

Results and Discussion

Synthesis and Photostability of Diacetylene Donors. The diacetylene donors were prepared by the classic route shown in Figure 3. Donors 1 and 3 have been previously reported, while the isoquinoline derivative 2 is a new compound. The route involves the Sonogashira coupling[17] of a protected acetylene to an aryl halide. Base-catalyzed deprotection followed by a copper-catalyzed oxidative coupling gives the corresponding diacetylene in good yields. As previously noted, 1 is light sensitive, photopolymerizing slowly in ambient light to form a blue solid. This compound was stored cold and in the dark. Fortunately, the polymer is completely insoluble and the inevitable slight contamination of the monomer did not interfere with the preparation of charge-transfer complexes. Donors 2 and 3 did not undergo solid-state polymerization even when irradiated with intense UV light for a period of days. Thus, it seems that neither the relative location of the DA to the nitrogen nor the presence of a fused ring systems are sufficient for solid-state photopolymerization.

Structure Discussion of Complexes. All of the compounds crystallize with significant halogen bonding between the organoiodide acceptor and the nitrogen heterocycle donor to form either extended chain structures, or in the case of 3_2·F_8DIBut, a molecular adduct. In all complexes involving 2, the chains are oriented to give segregated stacks of donors and acceptors with no significant interaction between adjacent members of a stack. More varied interaction is seen with complexes involving 1 and 3. Although many of the donor diacetylene molecules are within the required contact distance for solid-state polymerization, none are at the proper stacking angle to provide the slipped-stack necessary for this phenomenon. Selected bond distances and angles for halogen bonding between the donor and acceptor and for the diacetylene moiety are given in Table 2.

Crystal Structure of 1·TIE. Molecules of 1 and TIE, shown in Figure 4, are each situated about inversion

UM00014188
NOVARTIS EXHIBIT 1517
Novartis v. Regents, IPR2023-01347
Page 2934 of 4460

Table 2. Selected Distances (Å) and Angles (°)[a]

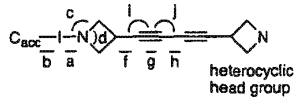
Donor·Acceptor Parameters

compound	(a) N···I (Å)	(b) N···I–C (°)	(c) I···N–C (°)	(d) C–N–C (°)	(e) C–X[b] (Å)
1[19]				117.4(6)	
3[20]				117.3(2)	
F_4DIB[21]					2.075(8)
TIE[11b]					2.095(14)
					2.100(16)
					2.112(16)
					2.164(22)
1·TIE	2.884(3)	174.75(11)	125.80(19), 115.9(2)	118.3(3)	2.115(3), (2.104(4))
1·F_4DIB	2.916(4)	168.37(15)	132.3(3), 109.1(3)	118.4(4)	2.096(4)
2				116.8(3)	
2·TIE	2.949(11)	175.4(5)	129.8(9), 114.5(9)	115.4(12)	2.086(11), (2.080(13))
2·F_4DIB	2.913(15)	176.6(6)	128.3(14), 113.2(13)	118.3(18)	2.103(18)
3·(F_4DIB)$_2$	2.895(9)	174.4(3)	126.9(8), 114.9(7)	118.1(10)	2.094(10), 2.086(9)
	2.913(9)	172.4(3)	127.2(8), 115.2(7)	117.6(10)	(2.083(11)), (2.070(11))
3_2·F_8DIBut	2.858(4)	174.9(3)	129.3(3), 111.9(3)	117.4(4)	2.156(2)

Diacetylene Parameters

compound	(f) C–C (Å)	(g) C≡C (Å)	(h) C–C (Å)	(i) C_f–C≡C (°)	(j) C≡C–C_h (°)
1[19]	1.431(3)	1.199(3)	1.371(3)	178.1(2)	179.7(2)
3[20]	1.442(8)	1.192(7)	1.369(11)	178.4(6)	178.7(7)
1·TIE	1.431(4)	1.192(5)	1.375(6)	177.2(4)	179.3(5)
1·F_4DIB	1.433(6)	1.192(5)	1.375(6)	177.2(4)	179.3(5)
2	1.431(4)	1.193(7)	1.366(9)	177.2(4)	179.3(5)
2·TIE	1.422(18)	1.211(18)	1.38(3)	175.5(16)	176(2)
2·F_4DIB	1.44(3)	1.18(3)	1.41(4)	175(2)	177(3)
3·(F_4DIB)$_2$	1.372(16)	1.177(15)	1.425(15)	176.4(14)	177.8(13)
	1.422(14)	1.173(15)		177.0(13)	175.8(14)
3_2·F_8DIBut	1.431(6)	1.195(6)	1.376(7)	179.7(5)	178.7(5)
		1.197(6)		178.4(6)	

[a] Distances and angles refer to the figure below. [b] Atom labels with a subscripted letter also refer to this figure.



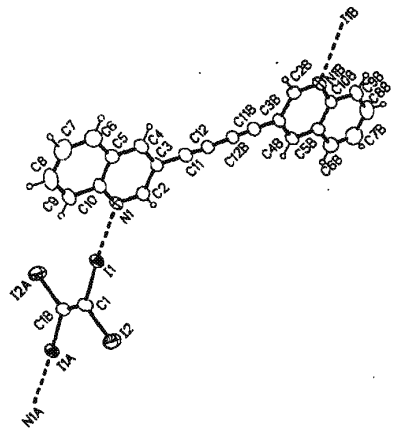


Figure 4. Thermal ellipsoid plot (50% probability) of 1·TIE (symmetry related atoms are generated by operations listed in Table 2).

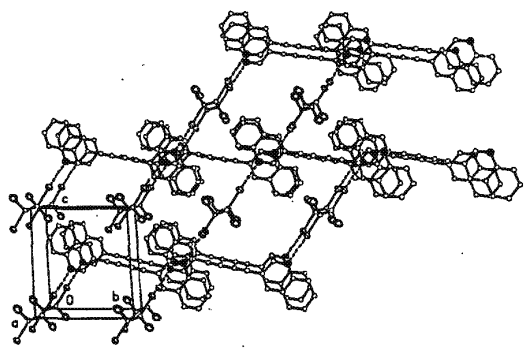


Figure 5. Crystal packing of 1·TIE, viewed down the *a*-axis.

centers: the TIE molecule at the origin and the diacetylene at (1 2 1). The two are linked by halogen bonding into zigzag chains that run along the (1 2 1) direction. The donor and acceptor molecules are both planar (rms deviations of 0.0028 and 0.0657 Å, respectively) and are nearly orthogonal (dihedral angle of 72.66(2)°). Chains stack along the *a*-axis (Figure 5) with neighboring chains related by inversion centers: (0 1/2 1/2) and (1/2 1/2 1/2), with heterocycle interplanar spacings of 3.42(2) and 3.28(2) Å, respectively. The general packing of the TIE molecules is similar to that observed in many halogen-bonded complexes of this acceptor,[11b] but whereas those complexes are dominated by I···I interactions there are no such close contacts in this complex.

Crystal Structure of 1·F_4DIB. Donor and acceptor molecules, shown in Figure 6, are both situated about inversion centers: the F_4DIB molecule at (1/4 3/4 1/2) and the diacetylene at (−1/4 1/4 0). The two are linked by halogen bonding into zigzag chains that run along the body diagonal ((1 1 1) direction). The donor and acceptor molecules are both planar (rms deviations of 0.0184 and 0.0489 Å, respectively) and are nearly orthogonal (dihedral angle of 86.70(5)°). Chains are

UM00014189
NOVARTIS EXHIBIT 1517
Novartis v. Regents, IPR2023-01347
Page 2935 of 4460

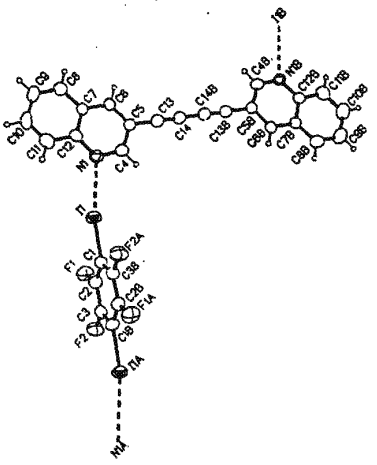


Figure 6. Thermal ellipsoid plot (50% probability) of 1·F_4DIB (symmetry related atoms are generated by operations listed in Table 2).

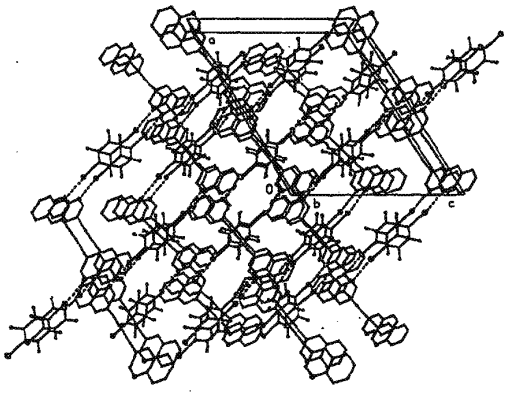


Figure 7. Crystal packing of 1·F_4DIB, viewed down the *b*-axis

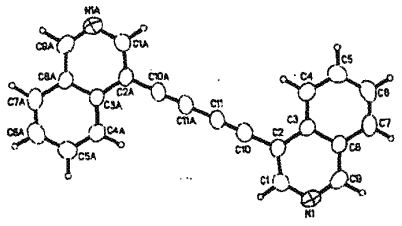


Figure 8. Thermal ellipsoid plot (50% probability) of **2** (symmetry related atoms are generated by operations listed in Table 2).

oriented such that the acceptor is situated directly above the center of the diacetylene moiety along the *b*-axis (Figure 7).

Crystal Structure of 2. Molecules of **2**, shown in Figure 8, are planar to within 0.0528 Å. The molecule is situated about an inversion center (1/2 1/2 1/2) and stack along the *a*-axis with adjacent molecules in the stack related by translation and separated by an inter-

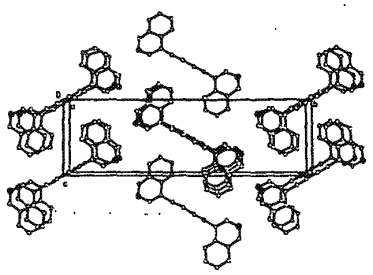


Figure 9. Crystal packing of **2**, viewed down the *a*-axis.

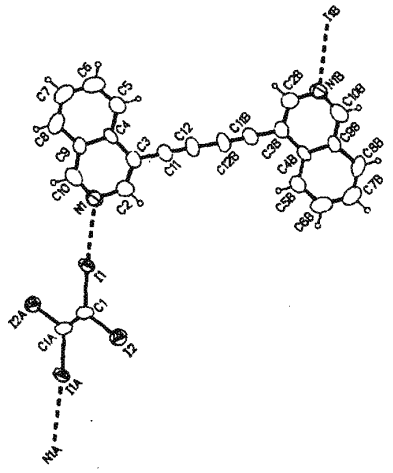


Figure 10. Thermal ellipsoid plot (50% probability) of **2**·TIE (symmetry related atoms are generated by operations listed in Table 2).

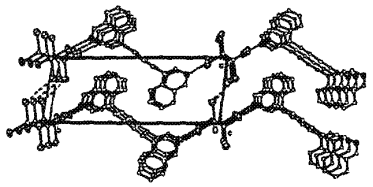


Figure 11. Crystal packing of **2**·TIE, viewed down the *c*-axis.

planar spacing of 3.56(5) Å. Weak C–H···N interactions (H···N = 2.48(3) Å; C···N = 3.499(5) Å; C–H···N = 165(3)°) join molecules along the (1 1 1) direction (see Figure 9).

Crystal Structure of 2·TIE. Molecules of **2** and TIE, shown in Figure 10, are each situated about inversion centers: the TIE molecule at the origin and the diacetylene at (0 1/2 1/2). The two are linked by halogen bonding into zigzag chains that run along the (0 1 1) direction. The donor and acceptor molecules are both planar (rms deviations of 0.0004 and 0.0609 Å, respectively), but are closer to parallel than to orthogonal (dihedral angle of 35.85(13)°). Chains stack along the *c*-axis (Figure 11) with neighboring chains related by translation. The general packing is similar to that observed in many halogen-bonded complexes of this acceptor,[11b] with I···I interactions of 3.8692(19) and

UM00014190
NOVARTIS EXHIBIT 1517
Novartis v. Regents, IPR2023-01347
Page 2936 of 4460

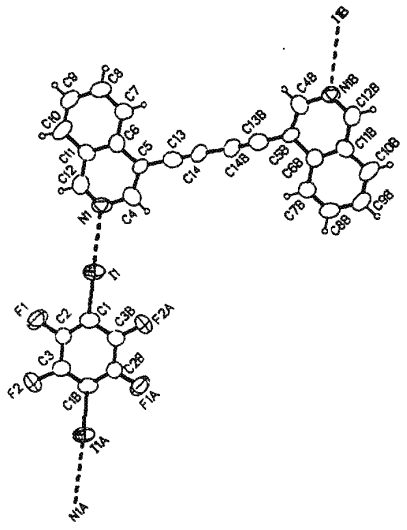


Figure 12. Thermal ellipsoid plot (50% probability) of **2**·F_4DIB (symmetry related atoms are generated by operations listed in Table 2).

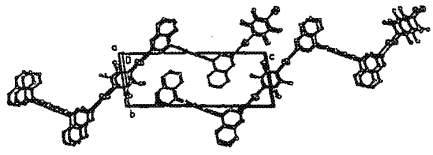


Figure 13. Crystal packing of **2**·F_4DIB, viewed down the *a*-axis.

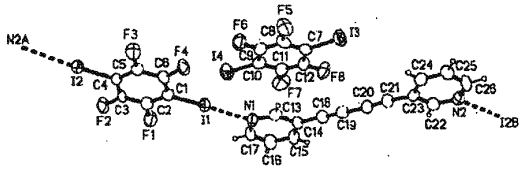


Figure 14. Thermal ellipsoid plot (50% probability) of **3**·$(F_4DIB)_2$ (symmetry related atoms are generated by operations listed in Table 2).

4.1486(14) Å. As has been previously noted, this packing is quite similar to the packing of TIE itself, but it should be pointed out that this is also quite similar to the packing of **2**, with the TIE molecule taking the place of alternating diacetylene molecules of the C−H···N linked chains.

Crystal Structure of 2·F_4DIB. Molecules of **2** and F_4DIB, shown in Figure 12, are situated about inversion centers of (0 0 1/2) and (1/2 1/2 0), respectively. Halogen bonding links them into extended chains which run in the (1 1 1) direction. Both the donor and acceptor molecules are planar (rms deviations of 0.0071 and 0.0600 Å, respectively) with a dihedral angle between them of 14.2(8)°. As in **2**·TIE, the complex crystallizes in a manner very similar to the donor, **2**,[18] with extended chains of alternating donors and acceptors, which are positioned to give segregated stacks of donors and acceptors (see Figure 13) running along the shortest unit cell axis (*a*). The interplanar spacing for the F_4-DIB acceptors is 3.579(8) Å and for the donors the spacing is 3.65(6) Å.

Crystal Structure of 3·$(F_4DIB)_2$. The complex of **3** with F_4DIB includes an additional uncomplexed molecule of the latter, and all three molecules sit on general positions within the unit cell (see Figure 14). The diacetylene donor, the F_4DIB acceptor, and the additional F_4DIB molecule are planar (rms deviations of 0.0289, 0.0024, and 0.0146 Å, respectively) and are nearly parallel, with a dihedral angle of 3.5(3)° between the donor and acceptor and dihedral angles to the uncomplexed molecule of 4.2(3)° for the donor and 7.8(4)° for the acceptor. Pairs of zigzag *X*-bonded chains related by inversion symmetry at the origin stack along the *a*-axis. This results in stacks of alternating complexed F_4DIB molecules and pyridyl rings from one end of the donor (atoms N2 and C22−C26). The interplanar spacings for this stack are 3.45(5) and 3.50(5) Å. The uncomplexed F_4DIB molecule forms alternating stacks with the other end of the diacetylene molecule (N1 and C13−C17) with interplanar spacings of 3.50(9) and 3.63(8) Å. The crystal packing is shown in Figure 15.

3_2·F_8DIBut. The bulkier F_8DIBut acceptor crystallizes with two molecules of **3** (see Figure 16). As only one end of the diacetylene is *X*-bonded to the acceptor a molecular adduct is formed rather than an extended chain. The diacetylene donor is planar (rms of 0.0423 Å), and the donors of adducts related by a 2_1 screw operation (about 1/2 y 1/4) are interdigitated to form stacks up the *b*-axis (shown in Figure 17). The interplanar spacings between donors in the stack are 3.6(1) and 3.7(1) Å. It is interesting to note that, unlike all the other donors which possess crystallographic or local inversion symmetry, the molecule of **3** in this complex does not (i.e., both nitrogen atoms are on the same side of the plane parallel to the diacetylene group and bisecting the pyridine rings).

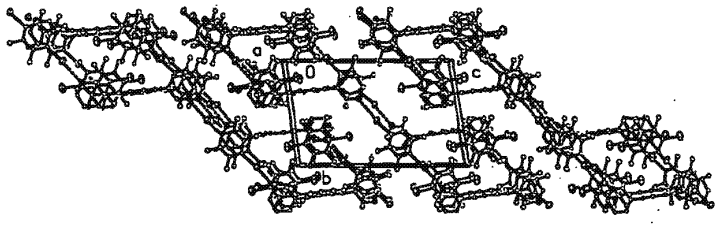


Figure 15. Crystal packing of **3**·$(F_4DIB)_2$, viewed down the *a*-axis.

UM00014191
NOVARTIS EXHIBIT 1517
Novartis v. Regents, IPR2023-01347
Page 2937 of 4460

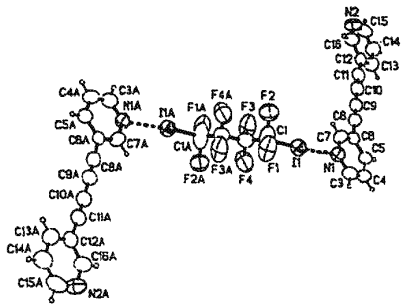


Figure 16. Crystal packing of $3_2{\cdot}F_8$DIBut, viewed down the *b*-axis.

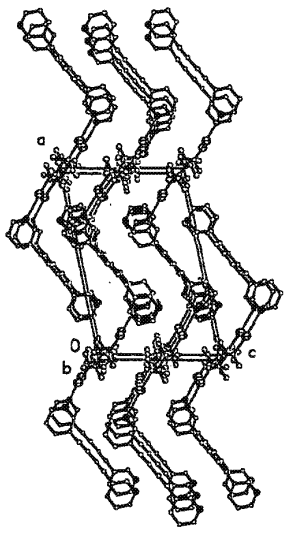


Figure 17. Thermal ellipsoid plot (50% probability) of $3_2{\cdot}F_8$DIBut (symmetry related atoms are generated by operations listed in Table 2).

Conclusions

Halogen bonding between bis(*N*-heterocycle)DAs **1**–**3** and various organoiodide acceptors generally leads to extended chain structures ordered into stacks of donors and acceptors perpendicular to the chains. With one major and one minor exception, the general structural motifs observed here are closely related to previously reported structures of other halogen bonded complexes involving planar bis(heterocycle) donors. While the stacking of DA donors can be engineered using planar organoiodide acceptors, it is clear that this simple approach is not sufficient to reliably produce geometries suitable for the topopolymerization of the DAs. In future papers, we will discuss the use of other supramolecular synthons, particularly the use of flexible "BCMU" tail groups on unsymmetrical DAs, for fine-tuning the stacking geometry of halogen bonded DAs.

Acknowledgment. Financial support by ACS-PRF (Grant No. 35462-B5), and the National Science Foundation (Grant Nos. CHE-0203402, research; CHE-0138535, Furman University REU; ESR-9108772 and CHE-9207230, Clemson University X-ray instrumentation) are gratefully acknowledged.

Supporting Information Available: X-ray crystallographic information file (CIF) for all seven complexes. This material is available free of charge via the Internet at http://pubs.acs.org.

References

(1) Part 1: Walsh, R. B.; Padgett, C. W.; Metrangolo, P.; Resnati, G.; Hanks, T. W.; Pennington, W. P. *Cryst. Growth Des.* **2001**, *1*, 165. A portion of these results have been previously communicated: Phelps, D.; Crihfield, A.; Hartwell, J.; Hanks, T. W.; Pennington, W. T.; Bailey, R. D. *Mol. Cryst. Liq. Cryst.* **2000**, *354*, 523.

(2) (a) Baughman, R. H.; Yee, K. C. *J. Poly. Sci.: Macromol Rev.* **1978**, *13*, 248. (b) *Polydiacetylenes*; Bloor, D., Chance, R. R., Eds.; Martinus Nijhoff, Boston, 1985. (c) Likhatchev, D.; Alexandrova, L.; Salcedo, R.; Ogawa, T. *Polym. Bull.* **1995**, *34*, 149.

(3) Coates, G. W.; Dunn, A. R.; Henling, L. M.; Dougherty, D. A.; Grubbs, R. H. *Angew. Chem., Int. Ed. Engl.* **1997**, *36*, 248.

(4) 4(a) Blake, A. J.; Champness, N. R.; Khlobystov, A.; Lemenovskii, D. A.; Li, W.-S.; Schroder, M. *Chem Commun.* **1997**, 2027. (b) Lin, J. T.; Sun, S.-S.; Wu, J. J.; Lee, L.; Lin, K.-J.; Huang, Y. F. *Inorg. Chem.* **1995**, *34*, 2323. (c) Maaekawa, M.; Konaka, H.; Suenaga, Y.; Kuroda-Sowa, T.; Manakata, M. *J. Chem. Soc. Dalton Trans.* **2000**, 4160. (d) Zaman, M. B.; Udachin, K. A.; Ripmeester, J. A. *CrystEngComm* **2002**, *4*, 613. (e) Moliner, N.; Munoz, C.; Letard, S.; Solans, X.; Menendez, N.; Goujon, A.; Varret, F.; Real, J. A. *Inorg. Chem.* **2000**, *39*, 5390. (f) Blake, A. J.; Baum, G.; Champness, N. R.; Chung, S. S. M.; Li, W.-S.; Schroder, M *J. Chem. Soc. Dalton Trans.* **2000**, 4285.

(5) There has been one report of a DA extended-sheet structure that undergoes a photoinduced color change that the authors suggest may be due to DA polymerization. Given the geometry of the starting compound, however, topopolymerization by the mechanisms described here seem to be extremely unlikely. Abrahams, B. F; Hardie, M. J.; Hoskins, B. F.; Robson, R.; Sutherland, E. E. *Chem. Commun.* **1994**, 1049.

(6) (a) Das, K.; Sinha, U. C.; Talwar, S. S.; Kamath, M. B.; Bohra, R. *Acta Cryst.* **1990**, *C46*, 2126 (b) Sarkar, A.; Talwar, S. S. *J. Chem. Soc. Perkins 1* **1998**, 4141.

(7) (a) Zaworotko, M. J. In *Electrical and Optical Polymer Systems: Fundamental, Methods and Applications*; Wise, D. L., Wnek, G. E., Trantolo, D. J., Cooper, T. M., Gresser, J. D., Eds; Marcel Dekker, Inc., New York, 1998; Ch 25. (b) Hoskins, B. F.; Robson, R. *J. Am. Chem. Soc.* **1990**, *112*, 1546.

(8) (a) Toda, F. in *Comprehensive Supramolecular Chemistry*; MacNicol, D. D., Toda, F., Bishop, R., Eds.; Elsevier, Oxford, U.K., 1996; Vol 6, Ch 15. (b) Roy, B. C.; Mallik, S. *J. Org. Chem.* **1999**, *64*, 2969. (c) Shimada, S.; Masaki, A.; Hayamizu, K.; Matsuda, H.; Okada, S.; Nakanishi, H. *Chem. Lett.* **2000**, 1128.

(9) Rodriquez, J. G.; Martin-Villamil, R.; Cano, F. H.; Fonseca, I. *J. Chem Soc. Perkins 1* **1997**, 709.

(10) Subramanyam, S.; Blumstein, A. *Macromolecules* **1991**, *24*, 2668.

(11) (a) Jay, J. I.; Padgett, C. W.; Walsh, R. D. B.; Hanks, T. W.; Pennington, W. T. *Cryst. Growth Des.* **2001**, *1*, 501. (b) Bailey, R. D.; Hook, L. L.; Watson, R. P.; Hanks, T. W.; Pennington, W. T. *Cryst. Eng.* **2000**, *3*, 155. (c) Hanks, T. W.; Pennington; W. T.; Bailey, R. D. In *Anisotropic Organic Materials Approaches to Polar Order*, ACS Symp. Ser., Vol. 798; Glaser, R., Kaszynski, P., Eds; American Chemical Society: Washington, DC, 2001; p 83.

(12) (a) Guthrie, F. *J. Chem. Soc.* **1863**, *16*, 239. (b) Remses, I.; Norris, J. F. *Am. Chem. J* **1896**, *18*, 90.

(13) For recent reviews, see (a) Metrangolo, P.; Resnati, G. *Chem. Eur. J.* **2001**, *7*, 2511. (b) Cardillo, P.; Corradi, E.; Lunghi, A.; Meille, S. V.; Messina, M. T.; Metrangolo, P.; Resnati, G. *Tetrahedron* **2000**, *56*, 5535. (c) Romaniello, P.; Lelj, F. *J. Phys. Chem. A* **2002**, *106*, 9114.

(14) Jacobson, R. A. (1998). Empirical Absorption Correction, Version 1.1, Rigaku/Molecular Structure Corp., The Woodlands, TX.

UM00014192
NOVARTIS EXHIBIT 1517
Novartis v. Regents, IPR2023-01347
Page 2938 of 4460

(15) Sheldrick, G. M. SHELXTL, Version 6.10, Crystallographic Computing System (2000), Bruker: AXS, Madison, WI.
(16) International Tables for X-ray Crystallography, Vol. C; Wilson, A. J. C., Ed.; Kluwer Academic Publishers: Dordrecht, 1992; Table 6.1.1.4, pp 500–502, and Table 4.2.6.8, pp 219–222, .
(17) Sonogashira, K.; Tohda, Y.; Hagihara, N. *Tetrahedron Lett.* **1975**, *4467*.
(18) In fact, except for a difference in orientation (matrix to relate cell lengths of the TIE complex to those of the F_4DIB complex is: {0 1 0, 0 0 1, 1 0 0}) and choice of angles (angles of one are very nearly the complement of the other), the cells for 2·TIE and 2·F_4DIB are nearly isomorphous.
(19) Das, K.; Sinha, U. C. *Acta Crystallogr.* **1990**, *C46*, 2126.
(20) Rodriguez, J. G.; Martin-Villamil, R.; Cano, F. H.; Fonesca, I. J. *Chem. Soc., Perkin Trans. 1* **1997**, 709.
(21) Chaplot, S. L.; McIntyre, G. J.; Mierzejewski, A.; Pawley, G. S. *Acta. Crystallogr.* **1981**, *B37*, 2210–2214.

CG0340042

UM00014193
NOVARTIS EXHIBIT 1517
Novartis v. Regents, IPR2023-01347
Page 2939 of 4460

This Page is Inserted by IFW Indexing and Scanning Operations and is not part of the Official Record

BEST AVAILABLE IMAGES

Defective images within this document are accurate representations of the original documents submitted by the applicant.

Defects in the images include but are not limited to the items checked:

- ☐ BLACK BORDERS
- ☐ IMAGE CUT OFF AT TOP, BOTTOM OR SIDES
- ☐ FADED TEXT OR DRAWING
- ☐ BLURRED OR ILLEGIBLE TEXT OR DRAWING
- ☐ SKEWED/SLANTED IMAGES
- ☐ COLOR OR BLACK AND WHITE PHOTOGRAPHS
- ☐ GRAY SCALE DOCUMENTS
- ☐ LINES OR MARKS ON ORIGINAL DOCUMENT
- ☐ REFERENCE(S) OR EXHIBIT(S) SUBMITTED ARE POOR QUALITY
- ☐ OTHER: _____

IMAGES ARE BEST AVAILABLE COPY.
As rescanning these documents will not correct the image problems checked, please do not report these problems to the IFW Image Problem Mailbox.

ARTIFACT SHEET

Enter artifact number below. Artifact number is application number + artifact type code (see list below) + sequential letter (A, B, C …). The first artifact folder for an artifact type receives the letter A, the second B, etc.. Examples: 59123456PA, 59123456PB, 59123456ZA, 59123456ZB

10378956 X A

Indicate quantity of a single type of artifact received but not scanned. Create individual artifact folder/box and artifact number for each Artifact Type.

☐ CD(s) containing:
- computer program listing ☐ — Doc Code: Computer — Artifact Type Code: P
- pages of specification and/or sequence listing and/or table ☐ — Doc Code: Artifact — Artifact Type Code: S
- content unspecified or combined ☐ — Doc Code: Artifact — Artifact Type Code: U

☐ Stapled Set(s) Color Documents or B/W Photographs
Doc Code: Artifact Artifact Type Code: C

☐ Microfilm(s)
Doc Code: Artifact Artifact Type Code: F

☐ Video tape(s)
Doc Code: Artifact Artifact Type Code: V

☐ Model(s)
Doc Code: Artifact Artifact Type Code: M

☐ Bound Document(s)
Doc Code: Artifact Artifact Type Code: B

☒ Confidential Information Disclosure Statement or Other Documents marked Proprietary, Trade Secrets, Subject to Protective Order, Material Submitted under MPEP 724.02, etc.
Doc Code: Artifact Artifact Type Code X

☐ Other, description: _____
Doc Code: Artifact Artifact Type Code: Z

March 8, 2004

PATENT APPLICATION FEE DETERMINATION RECORD
Effective January 1, 2003

Application or Docket Number: 10378986

CLAIMS AS FILED - PART I

	(Column 1)	(Column 2)
TOTAL CLAIMS	36	
FOR	NUMBER FILED	NUMBER EXTRA
TOTAL CHARGEABLE CLAIMS	36 minus 20=	* 16
INDEPENDENT CLAIMS	9 minus 3 =	* 6
MULTIPLE DEPENDENT CLAIM PRESENT	☐	

* If the difference in column 1 is less than zero, enter "0" in column 2

SMALL ENTITY TYPE ☐		OR	OTHER THAN SMALL ENTITY	
RATE	FEE		RATE	FEE
BASIC FEE	$375	OR	BASIC FEE	$750
X$ 9=	144	OR	X$18=	234
X42=	252	OR	X84=	504
+140=		OR	+280=	
TOTAL	771	OR	TOTAL	

7-27-06

CLAIMS AS AMENDED - PART II

AMENDMENT A

	(Column 1) CLAIMS REMAINING AFTER AMENDMENT		(Column 2) HIGHEST NUMBER PREVIOUSLY PAID FOR	(Column 3) PRESENT EXTRA
Total	* 35	Minus	** 36	=
Independent	* 9	Minus	*** 6	=
FIRST PRESENTATION OF MULTIPLE DEPENDENT CLAIM	☐			

SMALL ENTITY		OR	OTHER THAN SMALL ENTITY	
RATE	ADDITIONAL FEE		RATE	ADDITIONAL FEE
X$ 9=		OR	X$18=	
X42=		OR	X84=	
+140=		OR	+280=	
TOTAL ADDIT. FEE		OR	TOTAL ADDIT. FEE	

11111

AMENDMENT B

	(Column 1) CLAIMS REMAINING AFTER AMENDMENT		(Column 2) HIGHEST NUMBER PREVIOUSLY PAID FOR	(Column 3) PRESENT EXTRA
Total	*	Minus	**	=
Independent	*	Minus	***	=
FIRST PRESENTATION OF MULTIPLE DEPENDENT CLAIM	☐			

SMALL ENTITY		OR	OTHER THAN SMALL ENTITY	
RATE	ADDITIONAL FEE		RATE	ADDITIONAL FEE
X$ 9=		OR	X$18=	
X42=		OR	X84=	
+140=		OR	+280=	
TOTAL ADDIT. FEE		OR	TOTAL ADDIT. FEE	

0 20 21 25 29 33

22 23 24

AMENDMENT C

	(Column 1) CLAIMS REMAINING AFTER AMENDMENT		(Column 2) HIGHEST NUMBER PREVIOUSLY PAID FOR	(Column 3) PRESENT EXTRA
Total	*	Minus	**	=
Independent	*	Minus	***	=
FIRST PRESENTATION OF MULTIPLE DEPENDENT CLAIM	☐			

SMALL ENTITY		OR	OTHER THAN SMALL ENTITY	
RATE	ADDITIONAL FEE		RATE	ADDITIONAL FEE
X$ 9=		OR	X$18=	
X42=		OR	X84=	
+140=		OR	+280=	
TOTAL ADDIT. FEE		OR	TOTAL ADDIT. FEE	

* If the entry in column 1 is less than the entry in column 2, write "0" in column 3.
** If the "Highest Number Previously Paid For" IN THIS SPACE is less than 20, enter "20."
*** If the "Highest Number Previously Paid For" IN THIS SPACE is less than 3, enter "3."
The "Highest Number Previously Paid For" (Total or Independent) is the highest number found in the appropriate box in column 1.

UM00014196
NOVARTIS EXHIBIT 1517
Novartis v. Regents, IPR2023-01347
Page 2942 of 4460

OTPE IAP62
AUG 31 2006
PAT & TRADEMARK OFFICE

IEW 1617

I hereby certify that this correspondence is being deposited with the United States Postal Service as first class mail in an envelope addressed to: Commissioner for Patents, P.O. Box 1450 Alexandria, VA 22313 on August 28, 2006

Frank C. Eisenschenk, Ph.D., Patent Attorney

SUPPLEMENTAL INFORMATION DISCLOSURE STATEMENT
Examining Group 1617
Patent Application
Docket No. USF-106XC1
Serial No. 10/378,956

IN THE UNITED STATES PATENT AND TRADEMARK OFFICE

Examiner	:	Leonard M. Williams
Art Unit	:	1617
Applicants	:	Michael J. Zaworotko, Brian Moulton, Nair Rodriguez-Hornedo
Serial No.	:	10/378,956
Filed	:	March 3, 2003
Conf. No.	:	4742
For	:	Multiple-Component Solid Phases Containing at Least One Active Pharmaceutical Ingredient

Mail Stop Amendment
Commissioner for Patents
P.O. Box 1450
Alexandria, VA 22313

SUPPLEMENTAL INFORMATION DISCLOSURE STATEMENT
UNDER 37 CFR §§1.97 AND 1.98

Sir:

In accordance with 37 CFR §1.56, the references listed on the attached form PTO/SB/08 are being brought to the attention of the Examiner for consideration in connection with the examination of the above-identified patent application. A copy of each cited reference is enclosed. However, Applicants have not submitted copies of the U.S. patents or published U.S. Patent Applications cited on attached Form PTO/SB/08 pursuant to 37 CFR 1.98(a)(2)(ii).

This information is being submitted subsequent to the later of three months after the filing date of the present application or the mailing of the first Office Action on the merits, but before the mailing of a final action or the notice of allowance. Please charge the fee of $180.00 to Deposit Account No. 19-0065.

J:\USF\106XC1\PTO\IDS.doc/DNB/sl

09/01/2006 LWONDIM1 00000007 190065 10378956
01 FC:1806 180.00 DA

Applicants respectfully assert that the substantive provisions of 37 C.F.R. §§ 1.97 and 1.98 are met by the foregoing statement.

Respectfully submitted,

Frank C. Eisenschenk, Ph.D.
Patent Attorney
Registration No. 45,332
Phone No.: 352-375-8100
Fax No.: 352-372-5800
Address: P.O. Box 142950
Gainesville, FL 32614-2950

FCE/gyl
Attachments: Form PTO/SB/08; copy of reference cited therein.

J:\USF\106XC1\PTO\IDS.supp2.doc/DNB/gyl

OIPE TAP62 AUG 31 2006 PATENT & TRADEMARK OFFICE

PTO/SB/08A (08-03)
Approved for use through 07/31/2006. OMB 0651-0031
U.S. Patent and Trademark Office: U.S. DEPARTMENT OF COMMERCE
Under the Paperwork Reduction Act of 1995, no persons are required to respond to a collection of information unless it contains a valid OMB control number.

Substitute for form 1449A/PTO

INFORMATION DISCLOSURE STATEMENT BY APPLICANT

(use as many sheets as necessary)

Sheet	1	of	1

Complete if Known	
Application Number	10/378,956
Filing Date	March 3, 2003
First Named Inventor	Michael J. Zaworotko
Art Unit	1617
Examiner Name	Leonard M. Williams
Attorney Docket Number	USF-106XC1

U.S. PATENT DOCUMENTS

Examiner Initials*	Cite No. [1]	Document Number Number - Kind Code[2] (if known)	Publication Date MM-DD-YYYY	Name of Patentee or Applicant of Cited Document	Pages, Columns, Lines, Where Relevant Passages or Relevant Figures Appear
	U1	US-			
	U2	US-			
	U3	US-			
	U4	US-			
	U5	US-			
	U6	US-			
	U7	US-			
	U8	US-			
	U9	US-			

FOREIGN PATENT DOCUMENTS

Examiner Initials*	Cite No. [1]	Foreign Patent Document Country Code [3] - Number [4] - Kind Code[5] (if known)	Publication Date MM-DD-YYYY	Name of Patentee or Applicant of Cited Document	Pages, Columns, Lines, Where Relevant Passages or Relevant Figures Appear	T[6]
	F1	IN 182620	10-24-1994	Bajaj *et al.*	All	
	F2					
	F3					
	F4					
	F5					
	F6					
	F7					

Examiner Signature		Date Considered	

*EXAMINER: Initial if reference considered, whether or not citation is in conformance with MPEP 609. Draw line through citation if not in conformance and not considered. Include copy of this form with next communication to applicant. [1] Applicant's unique citation designation number (optional). [2] See Kind Codes of USPTO Patent Documents at www.uspto.gov or MPEP901.04. [3] Enter Office that issued the document, by the two-letter code (WIPO Standard T.3). [4] For Japanese patent documents, the indication of the year of the reign of the Emperor must precede the serial number of the patent document. [5] Kind of document by the appropriate symbols as indicated on the document under WIPO Standard ST. 16 if possible. [6] Applicant is to place a check mark here if English language Translation is attached.

This collection of information is required by 37 CFR 1.97 and 1.98. The information is required to obtain or retain a benefit by the public which is to file (and by the USPTO to process) an application. Confidentiality is governed by 35 U.S.C. 122 and 37 CFR 1.14. This collection is estimated to take 2 hours to complete, including gathering, preparing, and submitting the completed application form to the USPTO. Time will vary depending upon the individual case. Any comments on the amount of time you require to complete this form and/or suggestions for reducing this burden, should be sent to the Chief Information Officer, U.S. Patent and Trademark Office, P.O. Box 1450, Alexandria, VA 22313-1450. DO NOT SEND FEES OR COMPLETED FORMS TO THIS ADDRESS. **SEND TO: Commissioner for Patents, P.O. Box 1450, Alexandria, VA 22313-1450.**

If you need assistance in completing the form, call 1-800-PTO-9199 (1-800-786-9199) and select option 2.

RECEIVED
CENTRAL FAX CENTER

SEP 21 2006

I hereby certify that this correspondence is being facsimile transmitted to the United States Patent and Trademark Office on September 21, 2006.

Frank C. Eisenschenk

Frank C. Eisenschenk, Ph.D., Patent Attorney

SUPPLEMENTAL INFORMATION
DISCLOSURE STATEMENT
Examining Group 1617
Patent Application
Docket No. USF-106XC1
Serial No. 10/378,956

IN THE UNITED STATES PATENT AND TRADEMARK OFFICE

Examiner	:	Leonard M. Williams
Art Unit	:	1617
Applicants	:	Michael J. Zaworotko, Brian Moulton, Nair Rodriguez-Hornedo
Serial No.	:	10/378,956
Filed	:	March 3, 2003
Conf. No.	:	4742
For	:	Multiple-Component Solid Phases Containing at Least One Active Pharmaceutical Ingredient

Mail Stop Amendment
Commissioner for Patents
P.O. Box 1450
Alexandria, VA 22313

SUPPLEMENTAL INFORMATION DISCLOSURE STATEMENT
UNDER 37 C.F.R. §§ 1.97 AND 1.98

Sir:

In accordance with 37 C.F.R. § 1.56, the references listed on the attached form PTO/SB/08 are being brought to the attention of the Examiner for consideration in connection with the examination of the above-identified patent application. However, Applicants have not submitted copies of the U.S. patents cited on attached Form PTO/SB/08 pursuant to 37 C.F.R. 1.98(a)(2)(ii).

This information is being submitted subsequent to the later of three months after the filing date of the present application or the mailing of the first Office Action on the merits, but before the mailing of a final action or the notice of allowance. Please charge the fee of $180.00 to Deposit Account No. 19-0065.

J:\USF\106XC1\PTOIDS.supp3.doc/DNH/gyl

UM00014207

NOVARTIS EXHIBIT 1517
Novartis v. Regents, IPR2023-01347
Page 2946 of 4460

It is respectfully requested that the references cited on the attached form PTO/SB/08 be considered in the examination of the subject application and that their consideration be made of record.

Applicants respectfully assert that the substantive provisions of 37 C.F.R. §§ 1.97 and 1.98 are met by the foregoing statement.

Respectfully submitted,

Frank C. Eisenschenk, Ph.D.
Patent Attorney
Registration No. 45,332
Phone No.: 352-375-8100
Fax No.: 352-372-5800
Address: P.O. Box 142950
Gainesville, FL 32614-2950

FCE/gyl
Attachment: Form PTO/SB/08

J:\USF\106XC\PTO\IDS supp3 do\DNB/gyl

NOVARTIS EXHIBIT 1517
Novartis v. Regents, IPR2023-01347
Page 2947 of 4460

RECEIVED
CENTRAL FAX CENTER
SEP 21 2006

FACSIMILE COVER SHEET

SALIWANCHIK, LLOYD & SALIWANCHIK
A Professional Association
P.O. Box 142950
Gainesville, FL 32614-2950

Telephone (352) 375-8100
Facsimile (352) 372-5800

TO:	Examiner Leonard Williams	**FROM:**	Christopher Eisenschenk, Ph.D.
COMPANY:	U.S. Patent Office	**DATE:**	September 21, 2006
FAX NO.:	(571)273-8300	**NO. OF PAGES (INCLUDING COVER SHEET):**	4

SUBJECT/MESSAGE:

Re: U.S. Patent Application Docket No. USF-106XC1
MULTIPLE-COMPONENT SOLID PHASES CONTAINING AT LEAST ONE ACTIVE PHARMACEUTICAL INGREDIENT
(Zaworotko, Moulton, Rodriguez-Hornedo)
Serial No. 10/378,956; filed March 3, 2003

Attachment: Information Disclosure Statement and Form PTO/SB/08 (3 pages)

THIS IS AN OFFICIAL DOCUMENT.

PLEASE DELIVER IMMEDIATELY.

The information contained in this facsimile message is intended only for the personal and confidential use of the designated recipients named above. This message may be an attorney-client communication, and as such is privileged and confidential. If the reader of this message is not the intended recipient or an agent responsible for delivering it to the intended recipient, you are hereby notified that you have received this document in error, and that any review, dissemination, distribution, or copying of this message is strictly prohibited. If you have received this communication in error, please notify us immediately by telephone and return the original message by mail. Thank you.

If you do not receive all pages or if any transmission is not legible, call the sender at (352) 375-8100.

J:\USF\106XC1\Fax2Examiner.doc/DNB/sl

NOVARTIS EXHIBIT 1517
Novartis v. Regents, IPR2023-01347
Page 2948 of 4460

PTO/SB/08A (08-03)
Approved for use through 07/31/2006. OMB 0651-0031
U.S. Patent and Trademark Office. U.S. DEPARTMENT OF COMMERCE

Under the Paperwork Reduction Act of 1995, no persons are required to respond to a collection of information unless it contains a valid OMB control number.

Substitute for form 1449A/PTO

INFORMATION DISCLOSURE STATEMENT BY APPLICANT

(use as many sheets as necessary)

Sheet 1 of 1

Complete if Known	
Application Number	10/378,956
Filing Date	March 3, 2003
First Named Inventor	Michael J. Zaworotko
Art Unit	1617
Examiner Name	Leonard M. Williams
Attorney Docket Number	USF-106XC1

U.S. PATENT DOCUMENTS

Examiner Initials*	Cite No.[1]	Document Number: Number - Kind Code[2] (if known)	Publication Date MM-DD-YYYY	Name of Patentee or Applicant of Cited Document	Pages, Columns, Lines, Where Relevant Passages or Relevant Figures Appear
	U1	US-3,028,420	04-03-1962	Petrow *et al.*	All
	U2	US-5,521,207	05-28-1996	Graneto	All
	U3	US-			
	U4	US-			
	U5	US-			
	U6	US-			
	U7	US-			
	U8	US-			
	U9	US-			

FOREIGN PATENT DOCUMENTS

Examiner Initials*	Cite No.[1]	Foreign Patent Document: Country Code[3] - Number[4] - Kind Code[5] (if known)	Publication Date MM-DD-YYYY	Name of Patentee or Applicant of Cited Document	Pages, Columns, Lines, Where Relevant Passages or Relevant Figures Appear	T[6]
	F1					
	F2					
	F3					
	F4					
	F5					
	F6					
	F7					

Examiner Signature		Date Considered	

*EXAMINER: Initial if reference considered, whether or not citation is in conformance with MPEP 609. Draw line through citation if not in conformance and not considered. Include copy of this form with next communication to applicant. [1] Applicant's unique citation designation number (optional). [2] See Kind Codes of USPTO Patent Documents at www.uspto.gov or MPEP 901.04. [3] Enter Office that issued the document, by the two-letter code (WIPO Standard ST.3). [4] For Japanese patent documents, the indication of the year of the reign of the Emperor must precede the serial number of the patent document. [5] Kind of document by the appropriate symbols as indicated on the document under WIPO Standard ST. 16 if possible. [6] Applicant is to place a check mark here if English language Translation is attached.

This collection of information is required by 37 CFR 1.97 and 1.98. The information is required to obtain or retain a benefit by the public which is to file (and by the USPTO to process) an application. Confidentiality is governed by 35 U.S.C. 122 and 37 CFR 1.14. This collection is estimated to take 2 hours to complete, including gathering, preparing, and submitting the completed application form to the USPTO. Time will vary depending upon the individual case. Any comments on the amount of time you require to complete this form and/or suggestions for reducing this burden, should be sent to the Chief Information Officer, U.S. Patent and Trademark Office, P.O. Box 1450, Alexandria, VA 22313-1450. DO NOT SEND FEES OR COMPLETED FORMS TO THIS ADDRESS. SEND TO: Commissioner for Patents, P.O. Box 1450, Alexandria, VA 22313-1450.

If you need assistance in completing the form, call 1-800-PTO-9199 (1-800-786-9199) and select option 2.

NOVARTIS EXHIBIT 1517
Novartis v. Regents, IPR2023-01347
Page 2949 of 4460

UNITED STATES PATENT AND TRADEMARK OFFICE

UNITED STATES DEPARTMENT OF COMMERCE
United States Patent and Trademark Office
Address: COMMISSIONER FOR PATENTS
P.O. Box 1450
Alexandria, Virginia 22313-1450
www.uspto.gov

APPLICATION NO.	FILING DATE	FIRST NAMED INVENTOR	ATTORNEY DOCKET NO.	CONFIRMATION NO.
10/378,956	03/03/2003	Michael J. Zaworotko	USF-106XC1	4742

23557 7590 11/15/2006

SALIWANCHIK LLOYD & SALIWANCHIK
A PROFESSIONAL ASSOCIATION
PO BOX 142950
GAINESVILLE, FL 32614-2950

EXAMINER	
WILLIAMS, LEONARD M	
ART UNIT	**PAPER NUMBER**
1617	

DATE MAILED: 11/15/2006

Please find below and/or attached an Office communication concerning this application or proceeding.

PTO-90C (Rev. 10/03)

Office Action Summary	Application No.	Applicant(s)	
	10/378,956	ZAWOROTKO ET AL.	
	Examiner	Art Unit	
	Leonard M. Williams	1617	

-- The MAILING DATE of this communication appears on the cover sheet with the correspondence address --

Period for Reply

A SHORTENED STATUTORY PERIOD FOR REPLY IS SET TO EXPIRE 3 MONTH(S) OR THIRTY (30) DAYS, WHICHEVER IS LONGER, FROM THE MAILING DATE OF THIS COMMUNICATION.

- Extensions of time may be available under the provisions of 37 CFR 1.136(a). In no event, however, may a reply be timely filed after SIX (6) MONTHS from the mailing date of this communication.
- If NO period for reply is specified above, the maximum statutory period will apply and will expire SIX (6) MONTHS from the mailing date of this communication.
- Failure to reply within the set or extended period for reply will, by statute, cause the application to become ABANDONED (35 U.S.C. § 133). Any reply received by the Office later than three months after the mailing date of this communication, even if timely filed, may reduce any earned patent term adjustment. See 37 CFR 1.704(b).

Status

1)☐ Responsive to communication(s) filed on _____.

2a)☒ This action is **FINAL**. 2b)☐ This action is non-final.

3)☐ Since this application is in condition for allowance except for formal matters, prosecution as to the merits is closed in accordance with the practice under *Ex parte Quayle*, 1935 C.D. 11, 453 O.G. 213.

Disposition of Claims

4)☒ Claim(s) *25,27 and 28* is/are pending in the application.

4a) Of the above claim(s) _____ is/are withdrawn from consideration.

5)☐ Claim(s) _____ is/are allowed.

6)☒ Claim(s) *25, 27 and 28* is/are rejected.

7)☐ Claim(s) _____ is/are objected to.

8)☐ Claim(s) _____ are subject to restriction and/or election requirement.

Application Papers

9)☐ The specification is objected to by the Examiner.

10)☐ The drawing(s) filed on _____ is/are: a)☐ accepted or b)☐ objected to by the Examiner.

Applicant may not request that any objection to the drawing(s) be held in abeyance. See 37 CFR 1.85(a).

Replacement drawing sheet(s) including the correction is required if the drawing(s) is objected to. See 37 CFR 1.121(d).

11)☐ The oath or declaration is objected to by the Examiner. Note the attached Office Action or form PTO-152.

Priority under 35 U.S.C. § 119

12)☐ Acknowledgment is made of a claim for foreign priority under 35 U.S.C. § 119(a)-(d) or (f).

a)☐ All b)☐ Some * c)☐ None of:

1.☐ Certified copies of the priority documents have been received.

2.☐ Certified copies of the priority documents have been received in Application No. _____.

3.☐ Copies of the certified copies of the priority documents have been received in this National Stage application from the International Bureau (PCT Rule 17.2(a)).

* See the attached detailed Office action for a list of the certified copies not received.

Attachment(s)

1) ☐ Notice of References Cited (PTO-892)
2) ☐ Notice of Draftsperson's Patent Drawing Review (PTO-948)
3) ☒ Information Disclosure Statement(s) (PTO/SB/08) Paper No(s)/Mail Date 2/5/06; 9/21/06; 7/27/06
4) ☐ Interview Summary (PTO-413) Paper No(s)/Mail Date. _____.
5) ☐ Notice of Informal Patent Application
6) ☐ Other: _____.

UM00014212
NOVARTIS EXHIBIT 1517
Novartis v. Regents, IPR2023-01347
Page 2951 of 4460

Detailed Action

Response to Amendment

Applicant's arguments with respect to claims 25-28 have been considered but are moot in view of the new rejections necessitated by applicant's amendment.

Applicant's have amended claims 25, 27 and 28 and canceled claim 26 in the amendment received 7/27/2006.

The amendment of claims 25, 27 and 28 are sufficient to overcome the 112-2 rejection of the prior action and thus the 112-2 rejection of claims 25-28 is withdrawn.

The applicant's have argued that the '293 patent is not prior art under 102(e) as the evidence set forth in the rejection is drawn from a provisional application later than applicant's. The examiner without agreeing to applicant's assertion, respectfully points out the following from pages 14-15 of provisional application No. 60/356764: "A further embodiment of the invention encompasses a method for treating or preventing cluster headache in a patient which comprises administering to a patient in need of such treatment or prevention a therapeutically or prophylactically effective amount of a pharmaceutically acceptable salt of topiramate, or a polymorph, solvate, hydrate, dehydrate, anhydrous, or amorphous form thereof. Preferably, the pharmaceutically acceptable salt of topiramate is selected from the group consisting of topiramate sodium, topiramate lithium, and topiramate potassium, or a polymorph, solvate, hydrate, dehydrate, anhydrous, or amorphous form thereof.

Topiramate can be made using various methods known to those skilled in the art. For example, methods for the chemical synthesis of topiramate are described in U.S. Pat. No. 4,513,006, which is incorporated by reference herein in its entirety. Other methods well known in the art for preparing topiramate may also be used, including, for example, those disclosed in U.S. Pat. Nos. 6,319,903, 5,387,700; 5,258,402, 5,384,327, 5,242,942, 4,792,569, 2,554,816 and 2,980,679, all of which are incorporated by reference in their entirety.

The present invention involves the unexpected discovery that the sulfamate (-OSO2NH2) group of topiramate is slightly acidic and thus may be a handle for generation of salts. Salts are often associated with improved chemical stability and increased solubility of drugs leading to better delivery of drug to the body, by reducing unwanted degradation product exposure and increasing levels of drug in the body. Salt forms of drugs therefore constitute a useful set of options for development of drug formulations.

Pharmaceutically acceptable salts of topiramate can be prepared by treating topiramate with appropriate bases, such as organic or inorganic bases. Bases that can be used to prepare pharmaceutically acceptable salts of topiramate are those that form non-toxic base addition salts, i.e., salts containing pharmacologically acceptable cations, including, but not limited to, sodium, potassium, lithium, magnesium, calcium, aluminum, zinc, procaine, benzathine, chloroprocaine, choline, diethylamine, ethylenediamine, N-methylglucamine, benethamine, clemizole, diethylamine, piperazine, tromethamine, triethylamine, ethanolamine, triethanolamine, arginine, lysine,

histidine, tributylamine, 2-amino-2-pentylpropanol, 2-amino-2-methyl-1,3-propanediol, tris(hydroxymethyl)aminomethane, benzylamine, 2-(dimethylamino)ethanol, barium or bismuth counter ions. Particularly preferred cations are sodium, lithium, and potassium. The most preferred cation is sodium.

Crystallization of pharmaceutically acceptable salts of topiramate can be accomplished by several means, as would be apparent to one skilled in the art. For instance, saturation of an aqueous solution of the salt can be increased by cooling, and the cooling curve can be a determinant of the particle properties (e.g,. size, habit) that result from a crystallization process.

Alternatively, addition of an anti-solvent (or non-solvent), such as an alcohol or other water miscible solvent, can be used to increase saturation of the salt form in the medium and hence effect nucleation and growth of crystals. Examples of anti-solvents include, but are not limited to, iso-propanol, THF, and ethanol. Preferably, ethanol would be used, due to its azeotrope with water, anti-solvent quality with many salt forms and pharmaceutical acceptance."

The examiner respectfully points out that even in this provisional it is indicated that topiramate can be reacted with an organic or inorganic base to make a salt and that such a salt can be made via crystallization of the topiramate and the base. Included bases that can be crystallized with topiramate include compounds such as procaine, arginine, lysine, benzathine, etc... (all compounds that can generate their own crystal forms). Thus the basic requirements of the current claims are met even as their exist a active pharmaceutical agent (topiramate), chemical functionalities capable of forming

supramolecular synthons with itself (topiramate crystals), other functionalities that can react with a second synthon via non-covalent bonding (topiramate's weak acidic properties and salt formation), and the formation of a multiple-component solid phase composition (recrystalized topiramate and the selected salt). The examiner asserts that this provisional disclosure provides basis for the 102(e) rejection as written and as this provisional has a date that is good for a 102(e) rejection, this patent constitutes appropriate prior art over the claims as presented.

The applicant's amendment to the claims necessitates the withdrawal of the 102(e) rejection from the prior office action. A new 102(e) rejection is detailed below commensurate in scope with the amended claims. No new art has been applied.

Claim Rejections - 35 USC § 102

The following is a quotation of the appropriate paragraphs of 35 U.S.C. 102 that form the basis for the rejections under this section made in this Office action:

> A person shall be entitled to a patent unless –
>
> (e) the invention was described in (1) an application for patent, published under section 122(b), by another filed in the United States before the invention by the applicant for patent or (2) a patent granted on an application for patent by another filed in the United States before the invention by the applicant for patent, except that an international application filed under the treaty defined in section 351(a) shall have the effects for purposes of this subsection of an application filed in the United States only if the international application designated the United States and was published under Article 21(2) of such treaty in the English language.

Claims 25-28 are rejected under 35 U.S.C. 102(e) as being anticipated by Almarsson et al. (US Patent No. 6559293).

Almarsson et al., in the abstract, teach novel salts of topiramate, along with pharmaceutically acceptable polymorphs, solvates, hydrates, dehydrates, and co-crystals thereof as well as pharmaceutical compositions containing the same. The invention further encompasses novel co-crystals or complexes of topiramate and pharmaceutical compositions comprising them.

In col. 1 lines 15-65, Almarsson et al. teach that topiramate is a sulfamate-substituted monosaccharide which is a white crystalline powder. In col. 6 lines 1-12, Almarsson et al. teaches that specific co-crystals are complexes with caffeine. Almarsson et al. teach in col. 14 line 14 to col. 15 line 20 and example 7, methods of making a topiramate-caffeine co-crystal compositions. Almarrson et al. states:

"The present invention involves the unexpected discovery that the sulfamate (--OSO.sub.2 NH.sub.2) group of topiramate is slightly acidic and thus may be a handle for generation of salts, co-crystals, and complexes with basic compounds such as, but not limited to, caffeine, N-methyl pyrrolidine, nicotine, nicotinamide, and ethers such as PEGs (examples include but are not limited to PEG 200 and PEG 300). Salts are often associated with improved chemical stability and increased solubility of drugs leading to better delivery of drug to the body, by reducing unwanted degradation product exposure and increasing levels of drug in the body. Salt forms of drugs therefore constitute a useful set of options for development of drug formulations."

Additional salts useful in the invention can be prepared by reaction of topiramate with organic and inorganic bases such as procaine, benzanthine, chloroprocaine etc...

Further in col. 14 Almarrson et al. state:

"Co-crystals and complexes of topiramate and other compounds can be prepared using conventional crystallization techniques, e.g., from solutions comprising topiramate and the other compounds. Without being limited by theory, it is believed that the compounds within co-crystals and complexes can interact via hydrogen bonding, ionic, or other interactions. Crystallization from melts of topiramate and other compounds may also be used to prepare co-crystals or complexes of topiramate. For example, a co-crystal or complex of topiramate and caffeine can be prepared by melting and recrystallizing caffeine, allowing such to cool, then contacting topiramate melt with the recrystallized caffeine, and allowing this to cool. In a particular method, caffeine is melted and recrystallized between a glass slide and glass cover slip on a hot-stage microscope (such as a Mettler-Toledo FP950tstage mounted on a Zeiss Axioplan II polarized light microscope). The hot-stage is allowed to cool to about 30.degree. C. Topiramate is then placed on a glass slide in contact with the edge of the glass cover slip. The solid topiramate is melted and the melt is allowed to come into contact with the recrystallized caffeine. The temperature of the hotstage is lowered (e.g., to about 70.degree. C.) and held there overnight. During that time the melted topiramate recrystallizes and a co-crystalline phase crystallizes between the caffeine and topiramate regions. The slide can then be heated to determined the melting point of the caffeine:topiramate co-crystal."

Thus Almarsson et al. teach that topiramate has an acidic proton, the acidity can be exploited to make salts and/or co-crystals (such as when complexed with caffeine) and that such salts and/or co-crystals can be used to alter the structural and

pharmaceutical properties of the salts and/or co-crystals. In example 7 the synthesis and characterization of the topiramate-caffeine co-crystal is detailed wherein caffeine was melted, recrystallized between a glass slide and a cover slip, allowed to cool and then topiramate was placed on the glass slide in contact with the cover slip and melted wherein the melt came into contact with the recrystallized caffeine. The melted topiramate was then recrystalized overnight and the interfacial region of the topiramate and caffeine was determined to be crystalline and showed a different morphology than the pure caffeine and pure topiramate phases. The absence of multiple melt regions (eutectics) between the topiramate and caffeine indicated only one pure topiramate-caffeine co-crystalline phase anticipating the "...method for identifying complementary chemical functionalities in order to form a desired supramolecular synthon, said method comprising: (a) evaluating the structure of an active pharmaceutical ingredient; (b) determining whether the active pharmaceutical ingredient contains chemical functionalities capable of forming supramolecular synthons with itself; (c) identifying from a plurality of chemical functionalities that are known to form a supramolecular synthon at least one functionality that will form a further supramolecular synthon to the supramolecular synthon formed by the active pharmaceutical ingredient, wherein the identified chemical functionality is not capable of disrupting non-covalent bonding within the supramolecular synthon formed by the supramolecular synthon formed by the active pharmaceutical ingredient, and wherein the selected chemical functionality is capable of forming a noncovalent bond to the supramolecular synthon formed by the active pharmaceutical ingredient; (d) identifying co-crystal formers having chemical

functionalities that are complementary with the active pharmaceutical ingredient and (e) preparing a multiple-component solid phase composition, wherein the multiple-component solid phase composition comprises the active pharmaceutical ingredient and at least one of the identified co-crystal formers" of claim 25, the "...method...wherein the at least one co-crystal former is selected from the group consisting of a different active pharmaceutical ingredient, a GRAS compound, a food additive, a low toxicity organic, and a metal-organic complex" of claim 27, and the "....method...wherein the multiple-component solid phase composition is formed by one or more methods selected from the group consisting of crystallization from solution, cooling the melt, sublimation, and grinding" of claim 28.

Conclusion

Applicant's amendment necessitated the new ground(s) of rejection presented in this Office action. Accordingly, **THIS ACTION IS MADE FINAL**. See MPEP § 706.07(a). Applicant is reminded of the extension of time policy as set forth in 37 CFR 1.136(a).

A shortened statutory period for reply to this final action is set to expire THREE MONTHS from the mailing date of this action. In the event a first reply is filed within TWO MONTHS of the mailing date of this final action and the advisory action is not mailed until after the end of the THREE-MONTH shortened statutory period, then the shortened statutory period will expire on the date the advisory action is mailed, and any extension fee pursuant to 37 CFR 1.136(a) will be calculated from the mailing date of

the advisory action. In no event, however, will the statutory period for reply expire later than SIX MONTHS from the date of this final action.

Any inquiry concerning this communication or earlier communications from the examiner should be directed to Leonard M. Williams whose telephone number is 571-272-0685. The examiner can normally be reached on MF 9-5:30.

If attempts to reach the examiner by telephone are unsuccessful, the examiner's supervisor, Sreeni Padmanabhan can be reached on 571-272-0629. The fax phone number for the organization where this application or proceeding is assigned is 571-273-8300.

Information regarding the status of an application may be obtained from the Patent Application Information Retrieval (PAIR) system. Status information for published applications may be obtained from either Private PAIR or Public PAIR. Status information for unpublished applications is available through Private PAIR only. For more information about the PAIR system, see http://pair-direct.uspto.gov. Should you have questions on access to the Private PAIR system, contact the Electronic Business Center (EBC) at 866-217-9197 (toll-free). If you would like assistance from a USPTO Customer Service Representative or access to the automated information system, call 800-786-9199 (IN USA OR CANADA) or 571-272-1000.

LMW

SREENI PADMANABHAN
SUPERVISORY PATENT EXAMINER

OIPE TAPE
AUG 31 2006
PATENT & TRADEMARK OFFICE

PTO/SB/08A (08-03)
Approved for use through 07/31/2006. OMB 0651-0031
U.S. Patent and Trademark Office: U.S. DEPARTMENT OF COMMERCE
Under the Paperwork Reduction Act of 1995, no persons are required to respond to a collection of information unless it contains a valid OMB control number.

Substitute for form 1449A/PTO

INFORMATION DISCLOSURE STATEMENT BY APPLICANT

(use as many sheets as necessary)

Sheet 1 of 1

Complete if Known	
Application Number	10/378,956
Filing Date	March 3, 2003
First Named Inventor	Michael J. Zaworotko
Art Unit	1617
Examiner Name	Leonard M. Williams
Attorney Docket Number	USF-106XC1

U.S. PATENT DOCUMENTS

Examiner Initials*	Cite No.[1]	Document Number Number - Kind Code[2] (if known)	Publication Date MM-DD-YYYY	Name of Patentee or Applicant of Cited Document	Pages, Columns, Lines, Where Relevant Passages or Relevant Figures Appear
	U1	US-			
	U2	US-			
	U3	US-			
	U4	US-			
	U5	US-			
	U6	US-			
	U7	US-			
	U8	US-			
	U9	US-			

FOREIGN PATENT DOCUMENTS

Examiner Initials*	Cite No.[1]	Foreign Patent Document Country Code[3] - Number[4] - Kind Code[5] (if known)	Publication Date MM-DD-YYYY	Name of Patentee or Applicant of Cited Document	Pages, Columns, Lines, Where Relevant Passages or Relevant Figures Appear	T[6]
LW	F1	IN 182620	10-24-1994	Bajaj *et al.*	All	
	F2					
	F3					
	F4					
	F5					
	F6					
	F7					

Examiner Signature	/Leonard Williams/ (11/12/2006)	Date Considered	

*EXAMINER: Initial if reference considered, whether or not citation is in conformance with MPEP 609. Draw line through citation if not in conformance and not considered. Include copy of this form with next communication to applicant. [1] Applicant's unique citation designation number (optional). [2] See Kind Codes of USPTO Patent Documents at www.uspto.gov or MPEP901.04. [3] Enter Office that issued the document, by the two-letter code (WIPO Standard T.3). [4] For Japanese patent documents, the indication of the year of the reign of the Emperor must precede the serial number of the patent document. [5] Kind of document by the appropriate symbols as indicated on the document under WIPO Standard ST. 16 if possible. [6] Applicant is to place a check mark here if English language Translation is attached.

This collection of information is required by 37 CFR 1.97 and 1.98. The information is required to obtain or retain a benefit by the public which is to file (and by the USPTO to process) an application. Confidentiality is governed by 35 U.S.C. 122 and 37 CFR 1.14. This collection is estimated to take 2 hours to complete, including gathering, preparing, and submitting the completed application form to the USPTO. Time will vary depending upon the individual case. Any comments on the amount of time you require to complete this form and/or suggestions for reducing this burden, should be sent to the Chief Information Officer, U.S. Patent and Trademark Office, P.O. Box 1450, Alexandria, VA 22313-1450. DO NOT SEND FEES OR COMPLETED FORMS TO THIS ADDRESS. **SEND TO: Commissioner for Patents, P.O. Box 1450, Alexandria, VA 22313-1450.**

If you need assistance in completing the form, call 1-800-PTO-9199 (1-800-786-9199) and select option 2.

J:\USF\106XC1\PTO\IDS.supp2.form.doc/DNB/gyl

PTO/SB/08A (08-03)
Approved for use through 07/31/2006. OMB 0651-0031
U.S. Patent and Trademark Office. U.S DEPARTMENT OF COMMERCE
Under the Paperwork Reduction Act of 1995, no persons are required to respond to a collection of information unless it contains a valid OMB control number.

Substitute for form 1449/PTO

INFORMATION DISCLOSURE STATEMENT BY APPLICANT

(use as many sheets as necessary)

Sheet 1 of 1

Complete if Known	
Application Number	10/378,956
Filing Date	March 3, 2003
First Named Inventor	Michael J. Zaworotko
Art Unit	1617
Examiner Name	Leonard M. Williams
Attorney Docket Number	USF-106XC1

U.S. PATENT DOCUMENTS

Examiner Initials*	Cite No.[1]	Document Number Number - Kind Code[2] (if known)	Publication Date MM-DD-YYYY	Name of Patentee or Applicant of Cited Document	Pages, Columns, Lines, Where Relevant Passages or Relevant Figures Appear
LW	U1	US-3,028,420	04-03-1962	Petrow *et al.*	All
LW	U2	US-5,521,207	05-28-1996	Graneto	All
	U3	US-			
	U4	US-			
	U5	US-			
	U6	US-			
	U7	US-			
	U8	US-			
	U9	US-			

FOREIGN PATENT DOCUMENTS

Examiner Initials*	Cite No.[1]	Foreign Patent Document Country Code[3] - Number[4] - Kind Code[5] (if known)	Publication Date MM-DD-YYYY	Name of Patentee or Applicant of Cited Document	Pages, Columns, Lines, Where Relevant Passages or Relevant Figures Appear	T[6]
	F1					
	F2					
	F3					
	F4					
	F5					
	F6					
	F7					

Examiner Signature	/Leonard Williams/ (11/12/2006)	Date Considered	

*EXAMINER: Initial if reference considered, whether or not citation is in conformance with MPEP 609. Draw line through citation if not in conformance and not considered. Include copy of this form with next communication to applicant. [1] Applicant's unique citation designation number (optional). [2] See Kind Codes of USPTO Patent Documents at www.uspto.gov or MPEP 901.04. [3] Enter Office that issued the document, by the two-letter code (WIPO Standard ST.3). [4] For Japanese patent documents, the indication of the year of the reign of the Emperor must precede the serial number of the patent document. [5] Kind of document by the appropriate symbols as indicated on the document under WIPO Standard ST. 16 if possible. [6] Applicant is to place a check mark here if English language Translation is attached.

This collection of information is required by 37 CFR 1.97 and 1.98. The information is required to obtain or retain a benefit by the public which is to file (and by the USPTO to process) an application. Confidentiality is governed by 35 U.S.C. 122 and 37 CFR 1.14. This collection is estimated to take 2 hours to complete, including gathering, preparing, and submitting the completed application form to the USPTO. Time will vary depending upon the individual case. Any comments on the amount of time you require to complete this form and/or suggestions for reducing this burden, should be sent to the Chief Information Officer, U.S. Patent and Trademark Office, P.O. Box 1450, Alexandria, VA 22313-1450. DO NOT SEND FEES OR COMPLETED FORMS TO THIS ADDRESS. SEND TO: Commissioner for Patents, P.O. Box 1450, Alexandria, VA 22313-1450.

If you need assistance in completing the form, call 1-800-PTO-9199 (1-800-786-9199) and select option 2.

UM00014223

NOVARTIS EXHIBIT 1517
Novartis v. Regents, IPR2023-01347
Page 2962 of 4460

OIPE IAP60 JUL 27 2006 PATENT & TRADEMARK OFFICE

PTO/SB/08A (08-03)
Approved for use through 07/31/2006. OMB 0651-0031
U.S. Patent and Trademark Office: U.S. DEPARTMENT OF COMMERCE
Under the Paperwork Reduction Act of 1995, no persons are required to respond to a collection of information unless it contains a valid OMB control number.

Substitute for form 1449A/PTO

INFORMATION DISCLOSURE STATEMENT BY APPLICANT

(use as many sheets as necessary)

Sheet 1 of 33

Complete if Known	
Application Number	10/378,956
Filing Date	March 3, 2003
First Named Inventor	Michael J. Zaworotko
Art Unit	1617
Examiner Name	Leonard Williams
Attorney Docket Number	USF-106XC1

U.S. PATENT DOCUMENTS

Examiner Initials*	Cite No.[1]	Document Number Number - Kind Code[2] (if known)	Publication Date MM-DD-YYYY	Name of Patentee or Applicant of Cited Document	Pages, Columns, Lines, Where Relevant Passages or Relevant Figures Appear
LW	U1	US-2,711,411	06-21-1955	Holbert, *et al.*	All
	U2	US-4,198,507	04-15-1980	Barry, *et al.*	All
	U3	US-4,368,197	01-11-1983	Shefter, *et al.*	All
	U4	US-4,994,604	02-19-1991	Tung, *et al.*	All
	U5	US-5,177,262	01-15-1993	Taylor, *et al.*	All
	U6	US-5,332,834	07-26-1994	Bhattacharya, *et al.*	All
	U7	US-5,338,644	08-16-1994	Taylor, *et al.*	All
	U8	US-5,380,867	01-10-1995	Bhattacharya, *et al.*	All
	U9	US-5,412,094	05-02-1995	Amos, *et al.*	All
	U10	US-5,523,090	06-04-1996	Znaiden, *et al.*	All
	U11	US-5,614,342	03-25-1997	Molaire, *et al.*	All
	U12	US-5,998,413	12-07-1999	Heeres, *et al.*	All
	U13	US-6,001,996	12-14-1999	Amos, *et al.*	All
	U14	US-6,268,385	07-31-2001	Whittle, *et al.*	All
	U15	US-6,570,036	05-27-2003	Reuter	All
	U16	US-2003/0162226	08-28-2003	Cima, *et al.*	All
	U17	US-2003/0166581	09-04-2003	Almarsson, *et al.*	All
	U18	US-2003/0224006	12-04-2003	Zaworotko, *et al.*	All
	U19	US-2004/0019211	01-29-2004	Remenar, *et al.*	All
LW	U20	US-2004/0106052	06-03-2004	Molaire	All

Examiner Signature	/Leonard Williams/ (11/12/2006)	Date Considered	

*EXAMINER: Initial if reference considered, whether or not citation is in conformance with MPEP 609. Draw line through citation if not in conformance and not considered. Include copy of this form with next communication to applicant. [1] Applicant's unique citation designation number (optional). [2] See Kind Codes of USPTO Patent Documents at www.uspto.gov or MPEP901.04. [3] Enter Office that issued the document, by the two-letter code (WIPO Standard T.3). [4] For Japanese patent documents, the indication of the year of the reign of the Emperor must precede the serial number of the patent document. [5] Kind of document by the appropriate symbols as indicated on the document under WIPO Standard ST. 16 if possible. [6] Applicant is to place a check mark here if English language Translation is attached.

This collection of information is required by 37 CFR 1.97 and 1.98. The information is required to obtain or retain a benefit by the public which is to file (and by the USPTO to process) an application. Confidentiality is governed by 35 U.S.C. 122 and 37 CFR 1.14. This collection is estimated to take 2 hours to complete, including gathering, preparing, and submitting the completed application form to the USPTO. Time will vary depending upon the individual case. Any comments on the amount of time you require to complete this form and/or suggestions for reducing this burden, should be sent to the Chief Information Officer, U.S. Patent and Trademark Office, P.O. Box 1450, Alexandria, VA 22313-1450. DO NOT SEND FEES OR COMPLETED FORMS TO THIS ADDRESS. SEND TO: Commissioner for Patents, P.O. Box 1450, Alexandria, VA 22313-1450.

If you need assistance in completing the form, call 1-800-PTO-9199 (1-800-786-9199) and select option 2.

PTO/SB/08A (08-03)
Approved for use through 07/31/2006. OMB 0651-0031
U.S. Patent and Trademark Office: U.S. DEPARTMENT OF COMMERCE
Under the Paperwork Reduction Act of 1995, no persons are required to respond to a collection of information unless it contains a valid OMB control number.

Substitute for form 1449A/PTO

INFORMATION DISCLOSURE STATEMENT BY APPLICANT

(use as many sheets as necessary)

Sheet 2 of 33

Complete if Known	
Application Number	10/378,956
Filing Date	March 3, 2003
First Named Inventor	Michael J. Zaworotko
Art Unit	1617
Examiner Name	Leonard Williams
Attorney Docket Number	USF-106XC1

U.S. PATENT DOCUMENTS

Examiner Initials*	Cite No.[1]	Document Number Number - Kind Code[2] (if known)	Publication Date MM-DD-YYYY	Name of Patentee or Applicant of Cited Document	Pages, Columns, Lines, Where Relevant Passages or Relevant Figures Appear
LW	U21	US-2004/0106053	06-03-2004	Molaire, *et al.*	All
	U22	US-2004/0106055	06-03-2004	Molaire, *et al.*	All
	U23	US-2004/0171062	09-02-2004	Hirth, *et al.*	All
	U24	US-2004/0176335	09-09-2004	Childs	All
	U25	US-2005/0070551	03-31-1995	Remenar, *et al.*	All
	U26	US-2005/0181041	08-18-2005	Goldman	All
	U27	US-2005/0169982	08-04-2005	Almarsson, *et al.*	All
	U28	US-2005/0252649	11-17-2005	Chiu, *et al.*	All
	U29	US-2005/0256127	11-17-2005	Ku, *et al.*	All
	U30	US-6,559,293	05-06-2003	Almarsson, *et al.*	All
	U31	US-6,699,840	03-02-2004	Almarsson, *et al.*	All
	U32	US-2004-0053853	03-18-2004	Almarsson, *et al.*	All
	U33	US-2005/0070551 A1	03-31-2005	Remenar, *et al.*	All
	U34	US-2003/00224006	12-04-2003	Zaworotko *et al.*	All
	U35	US-3,536,809	04-09-1991	Schaller *et al.*	All
	U36	US-3,598,123	08-10-1971	Zaffaroni	All
	U37	US-3,845,770	11-05-1974	Theeuwes *et al.*	All
	U38	US-3,916,899	11-04-1975	Theeuwes *et al.*	All
	U39	US-4,008,719	02-22-1977	Theeuwes *et al.*	All
	U40	US-4,267,179	05-12-1981	Heeres *et al.*	All
LW	U41	US-4,764,604	08-16-1988	Muller	All

Examiner Signature	/Leonard Williams/ (11/12/2006)	Date Considered	

*EXAMINER: Initial if reference considered, whether or not citation is in conformance with MPEP 609. Draw line through citation if not in conformance and not considered. Include copy of this form with next communication to applicant. [1] Applicant's unique citation designation number (optional). [2] See Kind Codes of USPTO Patent Documents at www.uspto.gov or MPEP901.04. [3] Enter Office that issued the document, by the two-letter code (WIPO Standard T.3). [4] For Japanese patent documents, the indication of the year of the reign of the Emperor must precede the serial number of the patent document. [5] Kind of document by the appropriate symbols as indicated on the document under WIPO Standard ST. 16 if possible. [6] Applicant is to place a check mark here if English language Translation is attached.

This collection of information is required by 37 CFR 1.97 and 1.98. The information is required to obtain or retain a benefit by the public which is to file (and by the USPTO to process) an application. Confidentiality is governed by 35 U.S.C. 122 and 37 CFR 1.14. This collection is estimated to take 2 hours to complete, including gathering, preparing, and submitting the completed application form to the USPTO. Time will vary depending upon the individual case. Any comments on the amount of time you require to complete this form and/or suggestions for reducing this burden, should be sent to the Chief Information Officer, U.S. Patent and Trademark Office, P.O. Box 1450, Alexandria, VA 22313-1450. DO NOT SEND FEES OR COMPLETED FORMS TO THIS ADDRESS. **SEND TO: Commissioner for Patents, P.O. Box 1450, Alexandria, VA 22313-1450.**

If you need assistance in completing the form, call 1-800-PTO-9199 (1-800-786-9199) and select option 2.

J:\USF\106XC1\PTO\IDS.supp.form.doc/DNB/esc

PTO/SB/08A (08-03)
Approved for use through 07/31/2006. OMB 0651-0031
U.S. Patent and Trademark Office: U.S. DEPARTMENT OF COMMERCE
Under the Paperwork Reduction Act of 1995, no persons are required to respond to a collection of information unless it contains a valid OMB control number.

Substitute for form 1449A/PTO

INFORMATION DISCLOSURE STATEMENT BY APPLICANT

(use as many sheets as necessary)

Sheet 3 of 33

Complete if Known	
Application Number	10/378,956
Filing Date	March 3, 2003
First Named Inventor	Michael J. Zaworotko
Art Unit	1617
Examiner Name	Leonard Williams
Attorney Docket Number	USF-106XC1

U.S. PATENT DOCUMENTS

Examiner Initials*	Cite No. [1]	Document Number Number - Kind Code [2] (if known)	Publication Date MM-DD-YYYY	Name of Patentee or Applicant of Cited Document	Pages, Columns, Lines, Where Relevant Passages or Relevant Figures Appear
LW	U42	US-4,916,134	04-10-1990	Heeres *et al.*	All
	U43	US-5,006,513	04-09-1991	Hector *et al.*	All
	U44	US-5,059,595	10-22-1991	Le Grazie	All
	U45	US-5,073,543	12-17-1991	Marshall *et al.*	All
	U46	US-5,120,548	06-09-1992	McClelland *et al.*	All
	U47	US-5,354,556	10-11-1994	Sparks *et al.*	All
	U48	US-5,414,997	05-16-1995	Tailer	All
	U49	US-5,474,997	12-12-1995	Gray *et al.*	All
	U50	US-5,591,767	01-07-1997	Mohr *et al.*	All
	U51	US-5,633,015	05-27-1997	Gilis *et al.*	All
	U52	US-5,639,476	06-17-1997	Oshlack *et al.*	All
	U53	US-5,661,151	08-26-1997	Saksena *et al.*	All
	U54	US-5,674,533	10-07-1997	Santus *et al.*	All
	U55	US-5,707,975	01-13-1998	Francois *et al.*	All
	U56	US-5,733,566	03-31-1998	Lewis	All
LW	U57	US-2003/0096014	05-22-2003	Sherman	All
	U58				
	U59				
	U60				
	U61				

Examiner Signature	/Leonard Williams/ (11/12/2006)	Date Considered	

*EXAMINER: Initial if reference considered, whether or not citation is in conformance with MPEP 609. Draw line through citation if not in conformance and not considered. Include copy of this form with next communication to applicant. [1] Applicant's unique citation designation number (optional). [2] See Kind Codes of USPTO Patent Documents at www.uspto.gov or MPEP901.04. [3] Enter Office that issued the document, by the two-letter code (WIPO Standard T.3). [4] For Japanese patent documents, the indication of the year of the reign of the Emperor must precede the serial number of the patent document. [5] Kind of document by the appropriate symbols as indicated on the document under WIPO Standard ST. 16 if possible. [6] Applicant is to place a check mark here if English language Translation is attached.

This collection of information is required by 37 CFR 1.97 and 1.98. The information is required to obtain or retain a benefit by the public which is to file (and by the USPTO to process) an application. Confidentiality is governed by 35 U.S.C. 122 and 37 CFR 1.14. This collection is estimated to take 2 hours to complete, including gathering, preparing, and submitting the completed application form to the USPTO. Time will vary depending upon the individual case. Any comments on the amount of time you require to complete this form and/or suggestions for reducing this burden, should be sent to the Chief Information Officer, U.S. Patent and Trademark Office, P.O. Box 1450, Alexandria, VA 22313-1450. DO NOT SEND FEES OR COMPLETED FORMS TO THIS ADDRESS. **SEND TO: Commissioner for Patents, P.O. Box 1450, Alexandria, VA 22313-1450.**

If you need assistance in completing the form, call 1-800-PTO-9199 (1-800-786-9199) and select option 2.

PTO/SB/08A (08-03)
Approved for use through 07/31/2006. OMB 0651-0031
U.S. Patent and Trademark Office: U.S. DEPARTMENT OF COMMERCE
Under the Paperwork Reduction Act of 1995, no persons are required to respond to a collection of information unless it contains a valid OMB control number.

Substitute for form 1449A/PTO

INFORMATION DISCLOSURE STATEMENT BY APPLICANT

(use as many sheets as necessary)

Sheet	4	of	33

Complete if Known	
Application Number	10/378,956
Filing Date	March 3, 2003
First Named Inventor	Michael J. Zaworotko
Art Unit	1617
Examiner Name	Leonard Williams
Attorney Docket Number	USF-106XC1

FOREIGN PATENT DOCUMENTS

Examiner Initials*	Cite No. [1]	Foreign Patent Document: Country Code [3] - Number [4] - Kind Code [5] (if known)	Publication Date MM-DD-YYYY	Name of Patentee or Applicant of Cited Document	Pages, Columns, Lines, Where Relevant Passages or Relevant Figures Appear	T [6]
LW	F1	EP 413528	11-15-1995	Yu, R. *et al.*	All	
	F2	EP 1364649	11-26-2003	Cilag AG	All	
	F3	WO 94/16733	08-04-1994	Chiesi Farmaceutici S.P.A.	All	
	F4	WO 96/07331	03-14-1996	Xyrofin Oy	All	
	F5	WO 98/57967	12-23-1998	Dong-A Pharmaceutical Co., Ltd.	All	
	F6	WO 2000/53283	09-14-2000	Reuter Chemische Apparatebau KG	All	
	F7	WO 2001/13904	03-01-2001	Ortho-McNeil Pharmaceutical, Inc.	All	
	F8	JP 54-16494	02-07-1979	Yamanouchi Pharmaceutical Co., Ltd.	All	X
	F9	WO 2001/42221	06-14-2001	Pharmacia Corporation	All	
	F10	FR 769,586	06-11-1934	Chemische Fabrik von Heyden	All	X.
	F11	IT 01303251	11-06-2000	Industriale Chimica, S.R.L.	All	X
	F12	WO 2001/97853	12-27-2001	Biochemie Gesellschaft MBH	All	
	F13	EP 0310122	04-05-1989	Kaken Pharma	All	
	F14	WO 2002/062318	08-15-2002	DSM N.V.	All	
	F15	EP 0283992	09-16-1992	Janssen Pharma	All	
	F16	WO 2003/101392	12-11-2003	Transform Pharmaceuticals, Inc.	All	
	F17	WO 2004/054571	07-01-2004	Cilag AG	All	
	F18	WO 2004/078161 (CD-ROM)	09-16-2004	Transform Pharmaceuticals, Inc.	All	
LW	F19	WO 2004/078163 (CD-ROM)	09-16-2004	Transform Pharmaceuticals, Inc.	All	

Examiner Signature	/Leonard Williams/ (11/12/2006)	Date Considered	

*EXAMINER: Initial if reference considered, whether or not citation is in conformance with MPEP 609. Draw line through citation if not in conformance and not considered. Include copy of this form with next communication to applicant. [1] Applicant's unique citation designation number (optional). [2] See Kind Codes of USPTO Patent Documents at www.uspto.gov or MPEP901.04. [3] Enter Office that issued the document, by the two-letter code (WIPO Standard T.3). [4] For Japanese patent documents, the indication of the year of the reign of the Emperor must precede the serial number of the patent document. [5] Kind of document by the appropriate symbols as indicated on the document under WIPO Standard ST. 16 if possible. [6] Applicant is to place a check mark here if English language Translation is attached.

This collection of information is required by 37 CFR 1.97 and 1.98. The information is required to obtain or retain a benefit by the public which is to file (and by the USPTO to process) an application. Confidentiality is governed by 35 U.S.C. 122 and 37 CFR 1.14. This collection is estimated to take 2 hours to complete, including gathering, preparing, and submitting the completed application form to the USPTO. Time will vary depending upon the individual case. Any comments on the amount of time you require to complete this form and/or suggestions for reducing this burden, should be sent to the Chief Information Officer, U.S. Patent and Trademark Office, P.O. Box 1450, Alexandria, VA 22313-1450. DO NOT SEND FEES OR COMPLETED FORMS TO THIS ADDRESS. **SEND TO: Commissioner for Patents, P.O. Box 1450, Alexandria, VA 22313-1450.**

If you need assistance in completing the form, call 1-800-PTO-9199 (1-800-786-9199) and select option 2.

J:\USF\106XC1\PTO\IDS.supp.form.doc/DNB/esc

PTO/SB/08B (08-03)
Approved for use through 07/31/2006. OMB 0651-0031
U.S. Patent and Trademark Office: U.S. DEPARTMENT OF COMMERCE
Under the Paperwork Reduction Act of 1995, no persons are required to respond to a collection of information unless it contains a valid OMB control number.

Substitute for form 1449B/PTO

INFORMATION DISCLOSURE STATEMENT BY APPLICANT

(use as many sheets as necessary)

Sheet 5 of 33

Complete if Known	
Application Number	10/378,956
Filing Date	March 3, 2003
First Named Inventor	Michael J. Zaworotko
Group Art Unit	1617
Examiner Name	Leonard Williams
Attorney Docket Number	USF-106XC1

FOREIGN PATENT DOCUMENTS

Examiner Initials*	Cite No.[1]	Foreign Patent Document: Country Code[3] - Number[4] - Kind Code[5] (if known)	Publication Date MM-DD-YYYY	Name of Patentee or Applicant of Cited Document	Pages, Columns, Lines, Where Relevant Passages or Relevant Figures Appear	T[6]
LW	F20	WO 2004/089313	10-21-2004	Transform Pharmaceuticals, Inc.	All	
	F21	WO 2005/023198 (CD-ROM)	03-17-2005	Transform Pharmaceuticals, Inc.	All	
	F22	WO 2005/037424	04-28-2005	Salvias AG	All	
	F23	WO 2005/055983	06-23-2005	Medcrystalforms, LCC	All	
	F24	WO 2005/060968 (CD-ROM)	07-07-2005	Sepracor, Inc.	All	
	F25	WO 2005/089375 (CD-ROM)	09-29-2005	S.S.C.I., Inc.	All	
	F26	WO 2005/094804	10-13-2005	The Regents of the University of Michigan	All	
	F27	WO 2006/024930	03-09-2006	Pharmacia and Upjohn Co., LCC	All	
	F28	WO 03/070738	08-28-2003	Transform Pharmaceuticals, Inc.	All	
	F29	WO 03/074474	09-12-2003	Univ. South Fl	All	
LW	F30	WO 95/17407	06-29-1995	Schering Corp	All	
	F31					
	F32					
	F33					
	F34					
	F35					
	F36					
	F37					
	F38					
	F39					
	F40					
	F41					
	F42					

Examiner Signature	/Leonard Williams/ (11/12/2006)	Date Considered	

*EXAMINER: Initial if reference considered, whether or not citation is in conformance with MPEP 609. Draw line through citation if not in conformance and not considered. Include copy of this form with next communication to applicant. [1] Applicant's unique citation designation number (optional). [2] See Kind Codes of USPTO Patent Documents at www.uspto.gov or MPEP901.04. [3] Enter Office that issued the document, by the two-letter code (WIPO Standard T.3). [4] For Japanese patent documents, the indication of the year of the reign of the Emperor must precede the serial number of the patent document. [5] Kind of document by the appropriate symbols as indicated on the document under WIPO Standard ST. 16 if possible. [6] Applicant is to place a check mark here if English language Translation is attached.

This collection of information is required by 37 CFR 1.97 and 1.98. The information is required to obtain or retain a benefit by the public which is to file (and by the USPTO to process) an application. Confidentiality is governed by 35 U.S.C. 122 and 37 CFR 1.14. This collection is estimated to take 2 hours to complete, including gathering, preparing, and submitting the completed application form to the USPTO. Time will vary depending upon the individual case. Any comments on the amount of time you require to complete this form and/or suggestions for reducing this burden, should be sent to the Chief Information Officer, U.S. Patent and Trademark Office, P.O. Box 1450, Alexandria, VA 22313-1450. DO NOT SEND FEES OR COMPLETED FORMS TO THIS ADDRESS. SEND TO: **Commissioner for Patents, P.O. Box 1450, Alexandria, VA 22313-1450.**

If you need assistance in completing the form, call 1-800-PTO-9199 (1-800-786-9199) and select option 2.

PTO/SB/08B (08-03)
Approved for use through 07/31/2006. OMB 0651-0031
U.S. Patent and Trademark Office: U.S. DEPARTMENT OF COMMERCE
Under the Paperwork Reduction Act of 1995, no persons are required to respond to a collection of information unless it contains a valid OMB control number.

Substitute for form 1449B/PTO

INFORMATION DISCLOSURE STATEMENT BY APPLICANT

(use as many sheets as necessary)

Sheet 6 of 33

Complete if Known	
Application Number	10/378,956
Filing Date	March 3, 2003
First Named Inventor	Michael J. Zaworotko
Group Art Unit	1617
Examiner Name	Leonard Williams
Attorney Docket Number	USF-106XC1

NON PATENT LITERATURE DOCUMENTS			
Examiner Initials*	Cite No. [1]	Include name of the author (in CAPITAL LETTERS), title of the article, (when appropriate), title of the item (book, magazine, journal, serial, symposium, catalog, etc.), date, page(s), volume-issue number(s), publisher, city and/or country where published.	T[2]
LW	R1	AAKERÖY, C. *et al.* "Crystal engineering of hydrogen-bonded assemblies- a progress report" *Aust. J. Chem.*, 2001, pp. 409-421, Vol. 54.	
LW	R2	BINGHAM, A. *et al.* "Over one hundred solvates of sulfathiazole" *Chem. Commun.*, 2001, pp. 603-604.	
LW	R3	BYRIEL, K., *et al.* "Molecular cocrystals of carboxylic acids. IX Carboxylic acid interactions with organic heterocyclic bases. The crystal structures of the adducts of (2,4-dichlorophenoxy) acetic acid with 3-hydroxypyridine, 2,4,6,-trinitrobenzoic acid with 2-aminopyrimidine, and 4-nitrobenzoic acid with 3-amino-1,2,4-triazole" *Aust. J. Chem.*, 1992, pp. 969-981, Vol. 45, No. 6.	
LW	R4	SALMON, J. *et al.* "Supramolecular chemistry of boronic acids (Abstract)" 38th Midwest Regional Meeting of the American Chemical Society in Columbia, MO., November 5-7, 2003, published by the American Chemical Society, Washington, D.C.	
LW	R5	URBINA, J. *et al.* "Supramolecular design of inorganic/organic networks using flexible ligands with self-complementary hydrogen bonds (Abstract)" 38th Midwest Regional Meeting of the American Chemical Society in Columbia, MO., November 5-7, 2003, published by the American Chemical Society, Washington, D.C.	

Examiner Signature	/Leonard Williams/ (11/12/2006)	Date Considered	

*EXAMINER: Initial if reference considered, whether or not citation is in conformance with MPEP 609. Draw line through citation if not in conformance and not considered. Include copy of this form with next communication to applicant. [1] Applicant's unique citation designation number (optional). [2] See Kind Codes of USPTO Patent Documents at www.uspto.gov or MPEP901.04. [3] Enter Office that issued the document, by the two-letter code (WIPO Standard T.3). [4] For Japanese patent documents, the indication of the year of the reign of the Emperor must precede the serial number of the patent document. [5] Kind of document by the appropriate symbols as indicated on the document under WIPO Standard ST. 16 if possible. [6] Applicant is to place a check mark here if English language Translation is attached.

This collection of information is required by 37 CFR 1.97 and 1.98. The information is required to obtain or retain a benefit by the public which is to file (and by the USPTO to process) an application. Confidentiality is governed by 35 U.S.C. 122 and 37 CFR 1.14. This collection is estimated to take 2 hours to complete, including gathering, preparing, and submitting the completed application form to the USPTO. Time will vary depending upon the individual case. Any comments on the amount of time you require to complete this form and/or suggestions for reducing this burden, should be sent to the Chief Information Officer, U.S. Patent and Trademark Office, P.O. Box 1450, Alexandria, VA 22313-1450. DO NOT SEND FEES OR COMPLETED FORMS TO THIS ADDRESS. **SEND TO: Commissioner for Patents, P.O. Box 1450, Alexandria, VA 22313-1450.**

If you need assistance in completing the form, call 1-800-PTO-9199 (1-800-786-9199) and select option 2.

PTO/SB/08B (08-03)
Approved for use through 07/31/2006. OMB 0651-0031
U.S. Patent and Trademark Office: U.S. DEPARTMENT OF COMMERCE
Under the Paperwork Reduction Act of 1995, no persons are required to respond to a collection of information unless it contains a valid OMB control number.

Substitute for form 1449B/PTO

INFORMATION DISCLOSURE STATEMENT BY APPLICANT

(use as many sheets as necessary)

Sheet 7 of 33

Complete if Known	
Application Number	10/378,956
Filing Date	March 3, 2003
First Named Inventor	Michael J. Zaworotko
Group Art Unit	1617
Examiner Name	Leonard Williams
Attorney Docket Number	USF-106XC1

NON PATENT LITERATURE DOCUMENTS

Examiner Initials*	Cite No.[1]	Include name of the author (in CAPITAL LETTERS), title of the article, (when appropriate), title of the item (book, magazine, journal, serial, symposium, catalog, etc.), date, page(s), volume-issue number(s), publisher, city and/or country where published.	T[2]
LW	R6	SMITH, D. *et al.* "Structure confirmation by single crystal X-ray diffraction of a series of new schiff bases and theoretical computations on 3-(N-2-α, α, α-triflourotoluylidene amino) tetrahydrothiophene-1, 1-dioxide (Abstract)" 216th ACS National Meeting in Boston, MA., August 23-27, 1998, published by the American Chemical Society, Washington, D.C.	
LW	R7	DESIRAJU, G. "Supramolecular synthons in crystal engineering- A new organic synthesis" *Angew. Chem. Int. Ed. Engl.*, 1995, pp. 2311-2327, Vol. 34.	
LW	R8	FRITCHIE, C. *et al.* "The configuration of phenothiazine in various molecular complexes" *Chem. Commun.*, 1968, pp. 833-834.	
LW	R9	HUANG, C.-M. *et al.* "Molecular packing modes. Part XI. Crystal structures of the 2:1 complexes of benzamide with succinic acid and furamide with oxalic acid" *J. Chem. Soc. Perkins Trans. 2: Physical Organic Chemistry*, 1973, pp. 503-508, Vol. 5.	
LW	R10	JACKISCH, M. *et al.* "Structures of three related biphenyl compounds: 4,4'-biphenyldiol, 3, 3',5,5'-tetra-*tert*-butyl-4,4'-biphenyldiol, and 3,3',5,5'- tetra-*tert*-butyl-1,1'-bicyclohexa-2,5-dienylidene-4,4'-dione" *Acta Cryst.*, 1990, pp. 919-922, Vol. C46.	
LW	R11	KIM, S. *et al.* "The structure of a crystalline complex containing one phenobarbital molecule and two adenine derivatives" *Proc. Natl. Acad. Sci. USA*, 1968, pp. 402-408, Vol. 60.	
LW	R12	KOBAYASHI, H. *et al.* "Sinusoidal structure of the 1:1 complex of phenothiazine and 7,7,8,8-tetracyanoquinodimethane, PTZ-TCNQ" *Acta Cryst.*, 1974, pp. 1010-1017, Vol. B30.	
LW	R13	ERMER, O. *et al.* "Molecular recognition among alcohols and amines: super-tetrahedral crystal architectures of linear diphenol-diamine complexes and aminophenols" *J. Chem. Soc. Perkins Trans. 2*, 1994, pp. 925-944.	
LW	R14	MARTIN, R. *et al.* "Polyphenal-caffeine complexation" *J. Chem. Soc., Chem. Commun.*, 1986, pp. 105-106.	
LW	R15	LEHN, J.-M. *et al.* "Molecular recognition directed self-assembly of ordered supramolecular strands by cocrystallization of complementary molecular components" *Chem. Soc., Chem. Commun.*, 1990, pp. 479-481.	

Examiner Signature	/Leonard Williams/ (11/12/2006)	Date Considered	

*EXAMINER: Initial if reference considered, whether or not citation is in conformance with MPEP 609. Draw line through citation if not in conformance and not considered. Include copy of this form with next communication to applicant. [1] Applicant's unique citation designation number (optional). [2] See Kind Codes of USPTO Patent Documents at www.uspto.gov or MPEP901.04. [3] Enter Office that issued the document, by the two-letter code (WIPO Standard T.3). [4] For Japanese patent documents, the indication of the year of the reign of the Emperor must precede the serial number of the patent document. [5] Kind of document by the appropriate symbols as indicated on the document under WIPO Standard ST. 16 if possible. [6] Applicant is to place a check mark here if English language Translation is attached.

This collection of information is required by 37 CFR 1.97 and 1.98. The information is required to obtain or retain a benefit by the public which is to file (and by the USPTO to process) an application. Confidentiality is governed by 35 U.S.C. 122 and 37 CFR 1.14. This collection is estimated to take 2 hours to complete, including gathering, preparing, and submitting the completed application form to the USPTO. Time will vary depending upon the individual case. Any comments on the amount of time you require to complete this form and/or suggestions for reducing this burden, should be sent to the Chief Information Officer, U.S. Patent and Trademark Office, P.O. Box 1450, Alexandria, VA 22313-1450. DO NOT SEND FEES OR COMPLETED FORMS TO THIS ADDRESS. SEND TO: Commissioner for Patents, P.O. Box 1450, Alexandria, VA 22313-1450.

If you need assistance in completing the form, call 1-800-PTO-9199 (1-800-786-9199) and select option 2.

PTO/SB/08B (08-03)
Approved for use through 07/31/2006. OMB 0651-0031
U.S. Patent and Trademark Office: U.S. DEPARTMENT OF COMMERCE
Under the Paperwork Reduction Act of 1995, no persons are required to respond to a collection of information unless it contains a valid OMB control number.

Substitute for form 1449B/PTO

INFORMATION DISCLOSURE STATEMENT BY APPLICANT

(use as many sheets as necessary)

Sheet 8 of 33

Complete if Known	
Application Number	10/378,956
Filing Date	March 3, 2003
First Named Inventor	Michael J. Zaworotko
Group Art Unit	1617
Examiner Name	Leonard Williams
Attorney Docket Number	USF-106XC1

NON PATENT LITERATURE DOCUMENTS

Examiner Initials*	Cite No. [1]	Include name of the author (in CAPITAL LETTERS), title of the article, (when appropriate), title of the item (book, magazine, journal, serial, symposium, catalog, etc.), date, page(s), volume-issue number(s), publisher, city and/or country where published.	T[2]
LW	R16	LYNCH, D. *et al.* "Molecular cocrystals of carboxylic acids. XV Preparation and characterization of heterocyclic base adducts with a series of carboxylic acids, and the crystal structures of the adducts of 2-aminopyrimidine with 2,6-dihydroxybenzoic acid, 4-aminobenzoic acid, phenoxyacetic acid, (2,4-dichlorophenoxy) acetic acid, (3,4-dichlorophenoxy)- acetic acid and salicylic acid, and 2-aminopyridmine with 2,6-dihydroxybenzoic acid" *Aust. J. Chem.*, 1994, pp. 1097-1115, Vol. 47.	
LW	R17	MCINTOSH, J. *et al.* "Chemotherapeutic drugs in anaerobic infections of wounds" *The Lancet*, June 26, 1943, pp. 793-795.	
LW	R18	MCINTOSH, J. *et al.* "Zinc peroxide, proflavine and penicillin in experimental *cl. welchii* infections" *The Lancet*, December 26, 1942, pp. 750-752.	
LW	R19	SMITH, G. *et al.* "Molecular cocrystals of carboxylic acids. XXI The role of secondary group interactions in adduct formation between 2-aminopyramidine and substituted benzoic acids: the crystal structures of the adducts with *o*-phthalic acid, *o*-nitrobenzoic acid, *o*-aminobenzoic acid and *m*-aminobenzoic acid" *Aust. J. Chem.*, 1995, pp. 1151-1166, Vol. 48.	
LW	R20	WEISSBUCH, I. *et al.* "Crystal morphology control with tailor-made additives; a stereochemical approach" *Advances in Crystal Growth Research*, 2001, pp. 381-400.	
LW	R21	MCMAHON, J. *et al.* "Crystal engineering of the composition of pharmaceutical phases. 3'. Primary amide supramolecular heterosynthons and their role in the design of pharmaceutical co-crystals" *Z. Kristallogr.*, 2005, pp. 340-350, Vol. 220.	
LW	R22	MEEJOO, S. *et al.* "The interplay of aryl-perfluoroaryl stacking interactions and interstack hydrogen bonding in controlling the structure of a molecular cocrystal" *Chemphyschem*, 2003, pp. 766-769, Vol. 4.	
LW	R23	MIRMEHRABI, M. *et al.* "Improving the filterability and solid density of ranitidine hydrochloride form 1" *Journal of Pharmaceutical Sciences*, July 2004, pp. 1692-1700, Vol. 93, No. 7.	
LW	R24	MORRIS, K. *et al.* "Theoretical approaches to physical transformations of active pharmaceutical ingredients during manufacturing processes" *Advanced Drug Delivery Reviews*, 2001, pp. 91-114, Vol. 48.	

Examiner Signature	/Leonard Williams/ (11/12/2006)	Date Considered	

*EXAMINER: Initial if reference considered, whether or not citation is in conformance with MPEP 609. Draw line through citation if not in conformance and not considered. Include copy of this form with next communication to applicant. [1] Applicant's unique citation designation number (optional). [2] See Kind Codes of USPTO Patent Documents at www.uspto.gov or MPEP901.04. [3] Enter Office that Issued the document, by the two-letter code (WIPO Standard T.3). [4] For Japanese patent documents, the indication of the year of the reign of the Emperor must precede the serial number of the patent document. [5] Kind of document by the appropriate symbols as indicated on the document under WIPO Standard ST. 16 if possible. [6] Applicant is to place a check mark here if English language Translation is attached.

This collection of information is required by 37 CFR 1.97 and 1.98. The information is required to obtain or retain a benefit by the public which is to file (and by the USPTO to process) an application. Confidentiality is governed by 35 U.S.C. 122 and 37 CFR 1.14. This collection is estimated to take 2 hours to complete, including gathering, preparing, and submitting the completed application form to the USPTO. Time will vary depending upon the individual case. Any comments on the amount of time you require to complete this form and/or suggestions for reducing this burden, should be sent to the Chief Information Officer, U.S. Patent and Trademark Office, P.O. Box 1450, Alexandria, VA 22313-1450. DO NOT SEND FEES OR COMPLETED FORMS TO THIS ADDRESS. **SEND TO: Commissioner for Patents, P.O. Box 1450, Alexandria, VA 22313-1450.**

If you need assistance in completing the form, call 1-800-PTO-9199 (1-800-786-9199) and select option 2.

PTO/SB/08B (08-03)
Approved for use through 07/31/2006. OMB 0651-0031
U.S. Patent and Trademark Office: U.S. DEPARTMENT OF COMMERCE
Under the Paperwork Reduction Act of 1995, no persons are required to respond to a collection of information unless it contains a valid OMB control number.

Substitute for form 1449B/PTO

INFORMATION DISCLOSURE STATEMENT BY APPLICANT

(use as many sheets as necessary)

Sheet	9	of	33

Complete if Known	
Application Number	10/378,956
Filing Date	March 3, 2003
First Named Inventor	Michael J. Zaworotko
Group Art Unit	1617
Examiner Name	Leonard Williams
Attorney Docket Number	USF-106XC1

NON PATENT LITERATURE DOCUMENTS

Examiner Initials*	Cite No.[1]	Include name of the author (in CAPITAL LETTERS), title of the article, (when appropriate), title of the item (book, magazine, journal, serial, symposium, catalog, etc.), date, page(s), volume-issue number(s), publisher, city and/or country where published.	T[2]
LW	R25	NAKANISHI, I. *et al.* "X-ray structural studies on two forms of β-cyclodextrin barbital complexes" *Journal of Inclusion Phenomena*, 1984, pp. 689-699, Vol. 2.	
LW	R26	NAKAO, S. *et al.* "The crystal and molecular structure of the 2:1 molecular complex of theophylline with phenobarbital" *Acta Cryst.*, 1977, pp. 1373-1378, Vol. B33.	
LW	R27	NATARAJAN, S. *et al.* "Reinvestigation of the crystal structure of diglycine hydrochloride" *Zeitschrift für Kristallographic*, 1992, pp. 265-270, Vol. 198.	
LW	R28	OLENIK, B. *et al.* "Cooperative and anticooperative effects in the cocrystals of mono- and diazanaphthalenes with *meso*-1, 2-diphenyl-1,2-ethanediol" *Crystal Growth & Design*, 2003, pp. 175-181, Vol. 3, No. 2.	
LW	R29	OLENIK, B. *et al.* "Supramolecular synthesis by cocrystallization of oxalic and fumaric acid with diazanaphthalenes" *Crystal Growth & Design*, 2003, pp. 183-188, Vol. 3, No. 2.	
LW	R30	GROTH, P. "*d*-Glucose-sodium chloride-monohydrate (glucose-sodium chloride) = $2C_6H_{12}O_6.NaCl.H_2O$" *Chemische Krystallographie*, 1910, pp. 438-439.	X
LW	R31	OSWALD, I. *et al.* "Rationalisation of co-crystal formation through knowledge-mining" *Crystallography Reviews*, 2004, pp. 57-66, Vol. 10, No. 1.	
LW	R32	OUYANG, X. *et al.* "Single-crystal-to-single-crystal topochemical polymerizations of a terminal diacetylene: two remarkable transformations give the same conjugated polymer" *J. Am. Chem. Soc.*, 2003, pp. 12400-12401, Vol. 125.	
LW	R33	PATEL, U. *et al.* "Structure of the 1:1 complex between 4-amino-*N*-(4,6-dimethyl-2-pyrimidinyl)- benzenesulfonamide (sulfadimidine) and 2-hydroxybenzoic acid (salicylic acid)" *Acta Cryst.*, 1988, pp. 1264-1267, Vol. C44.	
LW	R34	REDDY, L. *et al.* "Phenyl-perfluorophenyl synthon mediated cocrystallization of carboxylic acids and amides" *Crystal Growth & Design*, 2004, pp. 89-94, Vol. 4., No. 1.	
LW	R35	REMENAR, J. *et al.* "Crystal engineering of novel cocrystals of a triazole drug with 1,4-dicarboxylic acids" *J. Am. Chem. Soc.*, 2003, pp. 8456-8457, Vol. 125.	

Examiner Signature	/Leonard Williams/ (11/12/2006)	Date Considered	

*EXAMINER: Initial if reference considered, whether or not citation is in conformance with MPEP 609. Draw line through citation if not in conformance and not considered. Include copy of this form with next communication to applicant. [1] Applicant's unique citation designation number (optional). [2] See Kind Codes of USPTO Patent Documents at www.uspto.gov or MPEP901.04. [3] Enter Office that issued the document, by the two-letter code (WIPO Standard T.3). [4] For Japanese patent documents, the indication of the year of the reign of the Emperor must precede the serial number of the patent document. [5] Kind of document by the appropriate symbols as indicated on the document under WIPO Standard ST. 16 if possible. [6] Applicant is to place a check mark here if English language Translation is attached.

This collection of information is required by 37 CFR 1.97 and 1.98. The information is required to obtain or retain a benefit by the public which is to file (and by the USPTO to process) an application. Confidentiality is governed by 35 U.S.C. 122 and 37 CFR 1.14. This collection is estimated to take 2 hours to complete, including gathering, preparing, and submitting the completed application form to the USPTO. Time will vary depending upon the individual case. Any comments on the amount of time you require to complete this form and/or suggestions for reducing this burden, should be sent to the Chief Information Officer, U.S. Patent and Trademark Office, P.O. Box 1450, Alexandria, VA 22313-1450. DO NOT SEND FEES OR COMPLETED FORMS TO THIS ADDRESS. SEND TO: **Commissioner for Patents, P.O. Box 1450, Alexandria, VA 22313-1450.**

If you need assistance in completing the form, call 1-800-PTO-9199 (1-800-786-9199) and select option 2.

PTO/SB/08B (08-03)
Approved for use through 07/31/2008. OMB 0651-0031
U.S. Patent and Trademark Office: U.S. DEPARTMENT OF COMMERCE
Under the Paperwork Reduction Act of 1995, no persons are required to respond to a collection of information unless it contains a valid OMB control number.

Substitute for form 1449B/PTO

INFORMATION DISCLOSURE STATEMENT BY APPLICANT

(use as many sheets as necessary)

Sheet 10 of 33

Complete if Known	
Application Number	10/378,956
Filing Date	March 3, 2003
First Named Inventor	Michael J. Zaworotko
Group Art Unit	1617
Examiner Name	Leonard Williams
Attorney Docket Number	USF-106XC1

NON PATENT LITERATURE DOCUMENTS

Examiner Initials*	Cite No.[1]	Include name of the author (in CAPITAL LETTERS), title of the article, (when appropriate), title of the item (book, magazine, journal, serial, symposium, catalog, etc.), date, page(s), volume-issue number(s), publisher, city and/or country where published.	T[2]
LW	R36	SCHMIDT, G. "Photodimerization in the solid state" *Pure Appl. Chem.*, 1971, pp. 647-678, Vol. 27.	
LW	R37	SHAN, N. *et al.* "Co-crystal of 4,7-phenanthroline and carboxylic acids: synthon competition and prediction" *Tetrahedron Letters*, 2002, pp. 8721-8725, Vol. 43.	
LW	R38	SHAN, N. *et al.* "Crystal engineering using 4,4'-bipyridyl with di- and tricarboxylic acids" *Crystal Engineering*, 2002, pp. 9-24, Vol. 5.	
LW	R39	SHAN, N. *et al* "Supramolecular synthons in the co-crystal structures of 2-aminopyrimdine with diols and carboxylic acids" *Tetrahedron Letters*, 2002, pp. 3101-3104, Vol. 43.	
LW	R40	MCINTOSH, J. *et al.* "Further observations on the chemotherapy of experimental gas gangrene: flavazole, marfanil, V187 and V335" *British Journal of Experimental Pathology*, 1946, pp. 46-54, Vol. 27.	
LW	R41	SHAVIV, R. *et al.* "Magnetochemistry of the tetrahaloferrate (III) ions 6. Crystal structure and magnetic ordering in $[(pyH)_3Cl]$ $[FeCl_4]_2$" *Inorganica Chimica Acta*, 1992, pp. 613-621, Vol. 198-200.	
LW	R42	SHEFTER, E. "Structural studies on complexes IV: Crystal structure of a 1:1 5-chlorosalicylic acid and theophylline complex" *Journal of Pharmaceutical Sciences*, 1969, pp. 710-714, Vol. 58.	
LW	R43	SHIMIZU, N. *et al.* "Structure of 2,4-diamino-5-(3,4,5-trimethoxybenzyl) pyrimidine-5,5-diethylbarbituric acid (1:1)" *Acta Cryst.*, 1982, pp. 2309- 2311, Vol. B38.	
LW	R44	SINGH, N. B. *et al.* "Solid state reaction between 8-hydroxyquinoline and *p*-nitrobenzoic acid" *Indian Journal of Chemistry*, May 1988, pp. 429-432, Vol. 37B.	
LW	R45	SMITH, G. *et al.* "The 1:1 adduct of 4-aminobenzoic acid with 4-aminobenzonitrile" *Acta Cryst.*, 2000, pp. 1155-1156, Vol. C56.	

Examiner Signature	/Leonard Williams/ (11/12/2006)	Date Considered	

*EXAMINER: Initial if reference considered, whether or not citation is in conformance with MPEP 609. Draw line through citation if not in conformance and not considered. Include copy of this form with next communication to applicant. [1] Applicant's unique citation designation number (optional). [2] See Kind Codes of USPTO Patent Documents at www.uspto.gov or MPEP901.04. [3] Enter Office that issued the document, by the two-letter code (WIPO Standard T.3). [4] For Japanese patent documents, the indication of the year of the reign of the Emperor must precede the serial number of the patent document. [5] Kind of document by the appropriate symbols as indicated on the document under WIPO Standard ST. 16 if possible. [6] Applicant is to place a check mark here if English language Translation is attached.

This collection of information is required by 37 CFR 1.97 and 1.98. The information is required to obtain or retain a benefit by the public which is to file (and by the USPTO to process) an application. Confidentiality is governed by 35 U.S.C. 122 and 37 CFR 1.14. This collection is estimated to take 2 hours to complete, including gathering, preparing, and submitting the completed application form to the USPTO. Time will vary depending upon the individual case. Any comments on the amount of time you require to complete this form and/or suggestions for reducing this burden, should be sent to the Chief Information Officer, U.S. Patent and Trademark Office, P.O. Box 1450, Alexandria, VA 22313-1450. DO NOT SEND FEES OR COMPLETED FORMS TO THIS ADDRESS. **SEND TO: Commissioner for Patents, P.O. Box 1450, Alexandria, VA 22313-1450.**

If you need assistance in completing the form, call 1-800-PTO-9199 (1-800-786-9199) and select option 2.

PTO/SB/08B (08-03)
Approved for use through 07/31/2006. OMB 0651-0031
U.S. Patent and Trademark Office: U.S. DEPARTMENT OF COMMERCE
Under the Paperwork Reduction Act of 1995, no persons are required to respond to a collection of information unless it contains a valid OMB control number.

Substitute for form 1449B/PTO

INFORMATION DISCLOSURE STATEMENT BY APPLICANT

(use as many sheets as necessary)

Sheet 11 of 33

Complete if Known	
Application Number	10/378,956
Filing Date	March 3, 2003
First Named Inventor	Michael J. Zaworotko
Group Art Unit	1617
Examiner Name	Leonard Williams
Attorney Docket Number	USF-106XC1

NON PATENT LITERATURE DOCUMENTS

Examiner Initials*	Cite No. [1]	Include name of the author (in CAPITAL LETTERS), title of the article, (when appropriate), title of the item (book, magazine, journal, serial, symposium, catalog, etc.), date, page(s), volume-issue number(s), publisher, city and/or country where published.	T[2]
LW	R46	STEINER, T. "Donor and acceptor strengths in C-H•••O hydrogen bonds quantified from crystallographic data of small solvent molecules" *New. J. Chem.*, 1998, pp. 1099-1103.	
LW	R47	STOREY, R. et al. "Automation of solid form screening procedures in the pharmaceutical industry- how to avoid the bottlenecks" *Crystallography Reviews*, 2004, pp. 45-56, Vol. 10, No. 1.	
LW	R48	SZAFRAN, M. *et al.* "Molecular structures and hydrogen bonding in the 1:1 and 1:2 complexes of pyridine betaine with 2,6-dichloro-4-nitrophenol; an example of strongly coupled hydrogen bonds, O-H•••O=C-O-H•••O-" *Journal of Molecular Structure*, 1997, pp. 145-160, Vol. 416.	
LW	R49	TAKEUCHI, M. *et al.* "Synchrotron radiation SAXS/WAXS study of polymorph-dependent phase behavior of binary mixtures of saturated monoacid triacylglycerols" *Crystal Growth & Design*, 2003, pp. 369-374, Vol. 3, No. 3.	
LW	R50	TANG, C. P. *et al.* "Reaction pathways in crystalline host-guest inclusion complexes: rotation by a net 180° of the acetyl group on photoaddition of guest- acetophenone and *–m-*Chloroacetophenone to the atom C5 of host deoxycholic acid" *J. Am. Chem. Soc.*, 1985, pp. 4058-4070, Vol. 107.	
LW	R51	TAYLOR, R. *et al.* "Rules governing the crystal packing of mono- and dialcohols" *Acta Crystallographica Section B, Structural Science*, 2001, pp. 815-827, Vol. B57.	
LW	R52	THALLAPALLY, P. *et al.* "Polymorphism of 1,3,5-trinitrobenzene induced by a trisindane additive" *Angew. Chem. Int. Ed.*, 2004, pp. 1149-1155, Vol. 43.	
LW	R53	TIMMERMAN, P. *et al.* "Noncovalent Assembly of functional groups on calix[4]arene molecular boxes" *Chem. Eur. J.*, 1997, pp. 1823-1832, Vol. 3., No. 11.	
LW	R54	SHAN, N. *et al.* "Mechanochemistry and co-crystal formation: effect of solvent on reaction kinetics" *Chem. Commun.*, 2002, pp. 2372-2373.	
LW	R55	CAIRA, M. *et al.* "X-ray structure and thermal analysis of a 1:1 complex between (S)-naproxen and heptakis (2,3,6-tri-O-methyl)-β-cyclodextrin" *Journal of Inclusion Phenomena and Molecular Recognition in Chemistry*, 1995, pp. 277-290, Vol. 20.	

Examiner Signature	/Leonard Williams/ (11/12/2006)	Date Considered	

*EXAMINER: Initial if reference considered, whether or not citation is in conformance with MPEP 609. Draw line through citation if not in conformance and not considered. Include copy of this form with next communication to applicant. [1] Applicant's unique citation designation number (optional). [2] See Kind Codes of USPTO Patent Documents at www.uspto.gov or MPEP901.04. [3] Enter Office that issued the document, by the two-letter code (WIPO Standard T.3). [4] For Japanese patent documents, the indication of the year of the reign of the Emperor must precede the serial number of the patent document. [5] Kind of document by the appropriate symbols as indicated on the document under WIPO Standard ST. 16 if possible. [6] Applicant is to place a check mark here if English language Translation is attached.

This collection of information is required by 37 CFR 1.97 and 1.98. The information is required to obtain or retain a benefit by the public which is to file (and by the USPTO to process) an application. Confidentiality is governed by 35 U.S.C. 122 and 37 CFR 1.14. This collection is estimated to take 2 hours to complete, including gathering, preparing, and submitting the completed application form to the USPTO. Time will vary depending upon the individual case. Any comments on the amount of time you require to complete this form and/or suggestions for reducing this burden, should be sent to the Chief Information Officer, U.S. Patent and Trademark Office, P.O. Box 1450, Alexandria, VA 22313-1450. DO NOT SEND FEES OR COMPLETED FORMS TO THIS ADDRESS. SEND TO: **Commissioner for Patents, P.O. Box 1450, Alexandria, VA 22313-1450.**

If you need assistance in completing the form, call 1-800-PTO-9199 (1-800-786-9199) and select option 2

PTO/SB/08B (08-03)
Approved for use through 07/31/2006. OMB 0651-0031
U.S. Patent and Trademark Office: U.S. DEPARTMENT OF COMMERCE
Under the Paperwork Reduction Act of 1995, no persons are required to respond to a collection of information unless it contains a valid OMB control number.

Substitute for form 1449B/PTO

INFORMATION DISCLOSURE STATEMENT BY APPLICANT

(use as many sheets as necessary)

Sheet 12 of 33

Complete if Known	
Application Number	10/378,956
Filing Date	March 3, 2003
First Named Inventor	Michael J. Zaworotko
Group Art Unit	1617
Examiner Name	Leonard Williams
Attorney Docket Number	USF-106XC1

NON PATENT LITERATURE DOCUMENTS

Examiner Initials*	Cite No. [1]	Include name of the author (in CAPITAL LETTERS), title of the article, (when appropriate), title of the item (book, magazine, journal, serial, symposium, catalog, etc.), date, page(s), volume-issue number(s), publisher, city and/or country where published.	T[2]
LW	R56	TRASK, A. *et al.* "Crystal engineering of organic cocrystals by the solid-state grinding approach" *Top Curr. Chem.*, 2005, pp. 41-70, Vol. 254.	
LW	R57	TRASK, A. *et al.* "Pharmaceutical cocrystallization: engineering a remedy for caffeine hydration" *Crystal Growth & Design*, 2005, pp. 1013-1021, Vol. 5, No. 3.	
LW	R58	TRASK, A. *et al.* "Solvent-drop grinding: green polymorph control of cocrystallisation" *Chem. Commun.*, 2004, pp. 890-891 in addition to supplemental materials.	
LW	R59	TROWBRIDGE, L. *et al.* "Composites for nonlinear optics: Crystal growth and polymorphism" *University of Sussex, Falmer Brighton UK, School of Chemistry and Molecular Sciences*, pp. 272.	
LW	R60	UNO, T. *et al.* "Structure of 5,5-diphenylhydantoin-1- (4-bromophenyl)-4-dimethylamino-2,3-dimethyl-3-pyrazolin-5-one (1:1)" *Acta Cryst.*, 1980, pp. 2794-2796, Vol. B36.	
LW	R61	VAN ROEY, P. *et al.* "Structure-activity studies of non-steroidal aromatase inhibitors: the crystal and molecular structures of CGS 16949A and CGS 18320B" *J. Enzyme Inhibition*, 1991, pp. 119-132, Vol. 5.	
LW	R62	VAN ROEY, P. *et al.* "Structure of *cis*-1-{[4-(1-imidazolylmethyl) cyclohexyl] methyl} imidazole- succinic acid complex" *Acta Cryst.*, 1991, pp. 1015-1018, Vol. C47.	
LW	R63	VISHWESHWAR, P. *et al.* "Crystal engineering of pharmaceutical co-crystals from polymorphic active pharmaceutical ingredients" *Chem. Commun.*, 2005, pp. 4601-4603.	
LW	R64	VISHWESHWAR, P. *et al.* "Recurrence of carboxylic acid- pyridine supramolecular synthon in the crystal structures of some pyrazinecarboxylic acids" *J. Org. Chem.*, 2002, pp. 556-565, Vol. 67.	
LW	R65	VISHWESHWAR, P. *et al.* "Supramolecular synthons based on N-H•••N and C-H•••O hydrogen bonds. Crystal engineering of a helical structure with 5,5-diethylbarbituric acid" *Chem. Commun.*, 2002, pp. 1830-1831.	
LW	R66	VISHWESHWAR, P. *et al.* "Supramolecular synthons in phenol-isonicotinamide adducts" *Cryst. Eng. Comm.* 2003, pp. 164-168, Vol. 5, No. 31.	

Examiner Signature	/Leonard Williams/ (11/12/2006)	Date Considered	

*EXAMINER: Initial if reference considered, whether or not citation is in conformance with MPEP 609. Draw line through citation if not in conformance and not considered. Include copy of this form with next communication to applicant. [1] Applicant's unique citation designation number (optional). [2] See Kind Codes of USPTO Patent Documents at www.uspto.gov or MPEP901.04. [3] Enter Office that issued the document, by the two-letter code (WIPO Standard T.3). [4] For Japanese patent documents, the indication of the year of the reign of the Emperor must precede the serial number of the patent document. [5] Kind of document by the appropriate symbols as indicated on the document under WIPO Standard ST. 16 if possible. [6] Applicant is to place a check mark here if English language Translation is attached.

This collection of information is required by 37 CFR 1.97 and 1.98. The information is required to obtain or retain a benefit by the public which is to file (and by the USPTO to process) an application. Confidentiality is governed by 35 U.S.C. 122 and 37 CFR 1.14. This collection is estimated to take 2 hours to complete, including gathering, preparing, and submitting the completed application form to the USPTO. Time will vary depending upon the individual case. Any comments on the amount of time you require to complete this form and/or suggestions for reducing this burden, should be sent to the Chief Information Officer, U.S. Patent and Trademark Office, P.O. Box 1450, Alexandria, VA 22313-1450. DO NOT SEND FEES OR COMPLETED FORMS TO THIS ADDRESS. SEND TO: Commissioner for Patents, P.O. Box 1450, Alexandria, VA 22313-1450.

If you need assistance in completing the form, call 1-800-PTO-9199 (1-800-786-9199) and select option 2.

PTO/SB/08B (08-03)
Approved for use through 07/31/2006. OMB 0651-0031
U.S. Patent and Trademark Office: U.S. DEPARTMENT OF COMMERCE
Under the Paperwork Reduction Act of 1995, no persons are required to respond to a collection of information unless it contains a valid OMB control number.

Substitute for form 1449B/PTO

INFORMATION DISCLOSURE STATEMENT BY APPLICANT

(use as many sheets as necessary)

Sheet 13 of 33

Complete if Known	
Application Number	10/378,956
Filing Date	March 3, 2003
First Named Inventor	Michael J. Zaworotko
Group Art Unit	1617
Examiner Name	Leonard Williams
Attorney Docket Number	USF-106XC1

NON PATENT LITERATURE DOCUMENTS

Examiner Initials*	Cite No. [1]	Include name of the author (in CAPITAL LETTERS), title of the article, (when appropriate), title of the item (book, magazine, journal, serial, symposium, catalog, etc.), date, page(s), volume-issue number(s), publisher, city and/or country where published.	T[2]
LW	R67	VOET, D. *et al.* "The crystal and molecular structure of the intermolecular complex 9-ethyladenine-5, 5-diethylbarbituric acid" *Journal of the American Chemical Society*, November 15, 1972, pp. 8213-8222, Vol. 94, No. 23.	
	R68	VOET, D. *et al.* "The structure of an intermolecular complex between cytosine and 5-fluorouracil" *Journal of the American Chemical Society*, May 21, 1969, pp. 3069-3075, Vol. 91, No. 11.	
	R69	STEZOWSKI, J. J. *et al.* "Characterization of a 1:1 complex of an unusual structure in the phenothiazine/phenazine binary phase diagram" *Zeitschrift fur Kristallographie* in International Journal for Structural, Physical, Chemical Aspects of Crystalline Materials, 1983, pp. 213-215, Vol. 162, No. 1-4.	X
	R70	WANG, A. *et al.* "Crystal structure of 1:1 complex of barbital with 1-methylimidazole" *Journal of Pharmaceutical Sciences*, March 1979, pp. 361-363, Vol. 68, No. 3.	
	R71	ALBEROLA, S. *et al.* "Crystalline and Molecular Structure of Sulfanilimide-Antipyrine" *Acta Cryst.*, 1977, pp. 3337-3341, Vol. B33.	X
	R72	WOOD, R. A. *et al.* "2,5-O-methylene-D-mannitol sodium-chloride, $C_7 H_{14} O_6$. NaCl" *Cryst. Struct. Comm.*, 1976, 207-210, Vol. 5.	
	R73	XU, J. *et al.* "Effect of composition distribution on miscibility and co-crystallization phenomena in the blends of low density polyethylene with conventional and metallocene-based ethylene-butene copolymers" *Polymer*, 2001, pp. 3867-3874, Vol. 42.	
	R74	YOO, J. *et al.* "Cocrystallization of a dinuclear platinum complex as a monomer and a one-dimensional polymer" *Polyhedron*, 2002, pp. 715-719, Vol. 21.	
	R75	ZAITU, S. *et al.* "A 2:1 molecular complex of theophylline and 5-fluorouracil as the monohydrate" *Acta Cryst.*, 1995, pp. 1857-1859, Vol. C51.	
	R76	ZAMAN, M. B. *et al.* "Linear hydrogen-bonded molecular tapes in the cocrystals of squaric acid with 4,4'-dipyridylacetylene and 1,2-bis(4-pyridyl) ethylene" *Acta Cryst.*, 2001, pp. 621-624, Vol. C57.	
LW	R77	ZERKOWSKI, J. *et al.* "Design of organic structures in the solid state: hydrogen-bonded molecular "tapes"[1n] *J. Am. Chem. Soc.*, 1990, pp. 9025-9026, Vol. 112.	

Examiner Signature	/Leonard Williams/ (11/12/2006)	Date Considered	

*EXAMINER: Initial if reference considered, whether or not citation is in conformance with MPEP 609. Draw line through citation if not in conformance and not considered. Include copy of this form with next communication to applicant. [1] Applicant's unique citation designation number (optional). [2] See Kind Codes of USPTO Patent Documents at www.uspto.gov or MPEP901.04. [3] Enter Office that issued the document, by the two-letter code (WIPO Standard T.3). [4] For Japanese patent documents, the indication of the year of the reign of the Emperor must precede the serial number of the patent document. [5] Kind of document by the appropriate symbols as indicated on the document under WIPO Standard ST. 16 if possible. [6] Applicant is to place a check mark here if English language Translation is attached.

This collection of information is required by 37 CFR 1.97 and 1.98. The information is required to obtain or retain a benefit by the public which is to file (and by the USPTO to process) an application. Confidentiality is governed by 35 U.S.C. 122 and 37 CFR 1.14. This collection is estimated to take 2 hours to complete, including gathering, preparing, and submitting the completed application form to the USPTO. Time will vary depending upon the individual case. Any comments on the amount of time you require to complete this form and/or suggestions for reducing this burden, should be sent to the Chief Information Officer, U.S. Patent and Trademark Office, P.O. Box 1450, Alexandria, VA 22313-1450. DO NOT SEND FEES OR COMPLETED FORMS TO THIS ADDRESS. SEND TO: Commissioner for Patents, P.O. Box 1450, Alexandria, VA 22313-1450.

If you need assistance in completing the form, call 1-800-PTO-9199 (1-800-786-9199) and select option 2.

PTO/SB/08B (08-03)
Approved for use through 07/31/2006. OMB 0651-0031
U.S. Patent and Trademark Office: U.S. DEPARTMENT OF COMMERCE
Under the Paperwork Reduction Act of 1995, no persons are required to respond to a collection of information unless it contains a valid OMB control number.

Substitute for form 1449B/PTO

INFORMATION DISCLOSURE STATEMENT BY APPLICANT

(use as many sheets as necessary)

Sheet 14 of 33

Complete if Known	
Application Number	10/378,956
Filing Date	March 3, 2003
First Named Inventor	Michael J. Zaworotko
Group Art Unit	1617
Examiner Name	Leonard Williams
Attorney Docket Number	USF-106XC1

NON PATENT LITERATURE DOCUMENTS

Examiner Initials*	Cite No. [1]	Include name of the author (in CAPITAL LETTERS), title of the article, (when appropriate), title of the item (book, magazine, journal, serial, symposium, catalog, etc.), date, page(s), volume-issue number(s), publisher, city and/or country where published.	T[2]
LW	R78	ZERKOWSKI, J. *et al.* "Investigations into the robustness of secondary and tertiary architecture of hydrogen-bonded crystalline tapes" *Chem. Mater.*, 1994, pp. 1250-1257, Vol. 6.	
	R79	ZERKOWSKI, J. *et al.* "New varieties of crystalline architecture produced by small changes in molecular structure in tape complexes of melamines and barbiturates" *J. Am. Chem. Soc.*, 1994, pp. 4305-4315, Vol. 116.	
	R80	ZERKOWSKI, J. *et al.* "Polymorphic packing arrangements in a class of engineered organic crystals" *Chem. Mater.*, 1997, pp. 1933-1941, Vol. 9.	
	R81	ZERKOWSKI, J. *et al.* "Solid-state structures of "Rosette" and "Crinkled Tape" motifs derived from the cyanuric acid-melamine lattice" *J. Am. Chem. Soc.*, 1992, pp. 5473-5475, Vol. 114.	
	R82	ZHANG, R. *et al.* "Atmospheric new particle formation enhanced by organic acids" *Science*, June 4, 2004, pp. 1487-1490 with additional supporting online material, Vol. 304.	
	R83	ZHU, H. *et al.* "Influence of water activity in organic solvent + water mixtures on the nature of the crystallizing drug phase. 1. theophylline" *International Journal of Pharmaceutics*, 1996, pp. 151-160, Vol. 135.	
	R84	AAKERÖY, C. *et al.* "Aromatic dicarboxylic acids as building blocks of extended hydrogen-bonded architectures" *Supramolecular Chemistry*, 1998, pp. 127-135, Vol. 9.	
	R85	AAKERÖY, C. *et al.* "Assembly of 2-D inorganic/organic lamellar structures through a combination of copper (I) coordination polymers and self-complimentary hydrogen bonds" *J. Chem. Soc., Dalton Trans.*, 2000, pp. 3869-3872.	
	R86	AAKERÖY, C. *et al.* "Building organic assemblies with 2-pyridone and dicarboxylic acids: relating molecular conformation and synthon stability to crystal structure" *Crystal Engineering*, 1998, pp. 225-241, Vol. 1, No. 3-4.	
	R87	AAKERÖY, C. *et al.* "The C-H•••C1 hydrogen bond: does it exist?" *New J. Chem.*, 1999, pp. 145-152.	
LW	R88	AAKERÖY, C. *et al.* "Crystal engineering of ionic solids" Modular Chemistry (ed. by Michl, J.), 1997, pp. 153-162, Kluwer Academic Publishers, The Netherlands.	

Examiner Signature	/Leonard Williams/ (11/12/2006)	Date Considered	

*EXAMINER: Initial if reference considered, whether or not citation is in conformance with MPEP 609. Draw line through citation if not in conformance and not considered. Include copy of this form with next communication to applicant. [1] Applicant's unique citation designation number (optional). [2] See Kind Codes of USPTO Patent Documents at www.uspto.gov or MPEP901.04. [3] Enter Office that issued the document, by the two-letter code (WIPO Standard T.3). [4] For Japanese patent documents, the indication of the year of the reign of the Emperor must precede the serial number of the patent document. [5] Kind of document by the appropriate symbols as indicated on the document under WIPO Standard ST. 16 if possible. [6] Applicant is to place a check mark here if English language Translation is attached.

This collection of information is required by 37 CFR 1.97 and 1.98. The information is required to obtain or retain a benefit by the public which is to file (and by the USPTO to process) an application. Confidentiality is governed by 35 U.S.C. 122 and 37 CFR 1.14. This collection is estimated to take 2 hours to complete, including gathering, preparing, and submitting the completed application form to the USPTO. Time will vary depending upon the individual case. Any comments on the amount of time you require to complete this form and/or suggestions for reducing this burden, should be sent to the Chief Information Officer, U.S. Patent and Trademark Office, P.O. Box 1450, Alexandria, VA 22313-1450. DO NOT SEND FEES OR COMPLETED FORMS TO THIS ADDRESS. **SEND TO: Commissioner for Patents, P.O. Box 1450, Alexandria, VA 22313-1450.**

If you need assistance in completing the form, call 1-800-PTO-9199 (1-800-786-9199) and select option 2.

PTO/SB/08B (08-03)
Approved for use through 07/31/2006. OMB 0651-0031
U.S. Patent and Trademark Office: U.S. DEPARTMENT OF COMMERCE
Under the Paperwork Reduction Act of 1995, no persons are required to respond to a collection of information unless it contains a valid OMB control number.

Substitute for form 1449B/PTO

INFORMATION DISCLOSURE STATEMENT BY APPLICANT

(use as many sheets as necessary)

Sheet 15 of 33

Complete if Known	
Application Number	10/378,956
Filing Date	March 3, 2003
First Named Inventor	Michael J. Zaworotko
Group Art Unit	1617
Examiner Name	Leonard Williams
Attorney Docket Number	USF-106XC1

NON PATENT LITERATURE DOCUMENTS

Examiner Initials*	Cite No.[1]	Include name of the author (in CAPITAL LETTERS), title of the article, (when appropriate), title of the item (book, magazine, journal, serial, symposium, catalog, etc.), date, page(s), volume-issue number(s), publisher, city and/or country where published.	T[2]
LW	R89	AAKERÖY, C. *et al.* "Crystal engineering: strategies and architectures" *Acta Cryst.*, 1997, pp. 569-586, Vol. B53.	
	R90	AAKERÖY, C. *et al.* "Crystal engineering using intermolecular hydrogen-bonded connectors and classic coordination chemistry" *Transactions ACA*, 1998, pp. 97-103, Vol. 33.	
	R91	AAKERÖY, C. *et al.* "The crystal structure of the molecular cocrystal *L*-malic acid *L*-tartaric acid (1/1)" *Supramolecular Chemistry*, 1996, pp. 153-156, Vol. 7.	
	R92	AAKERÖY, C. *et al.* "Deliberate combination of coordination polymers and hydrogen bonds in a supramolecular design strategy for inorganic/organic hybrid networks" *Chem. Commun.*, 2000, pp. 935-936.	
	R93	AAKERÖY, C. *et al.* "Di-hydroxy malonic acid as a building block of hydrogen-bonded 3-dimensional architectures" *Journal of Chemical Crystallography*, 1998, pp. 111-117, Vol. 28, No. 2.	
	R94	AAKERÖY, C. *et al.* "Do polymorphic compounds make good cocrystallizing agents? A structural case study that demonstrates the importance of synthon flexibility" *Crystal Growth & Design*, 2003, 159-165, Vol. 3, No. 2.	
	R95	AAKERÖY, C. *et al.* "Heteromeric intermolecular interactions as synthetic tools for the formation of binary co-crystals" *Cryst. Eng. Comm.*, 2004, pp. 19-24, Vol. 6, No. 5.	
	R96	AAKERÖY, C. *et al.* "A high-yielding supramolecular reaction" *J. Am. Chem. Soc.*, 2002, 14425-14432, Vol. 124.	
	R97	AAKERÖY, C. *et al.* "The hydrogen bond and crystal engineering" *Chemical Society Reviews*, 1993, pp. 397-407.	
	R98	AAKERÖY, C. *et al.* "Hydrogen-bond assisted assembly of organic and organic-inorganic solids" Crystal Engineering: From Molecules and Crystals to Materials, 1999, pp. 89-106, Kluwer Academic Publishers, The Netherlands.	
LW	R99	AAKERÖY, C. *et al.* "Hydrogen-bonding in solids" Crystal Engineering (ed. by Seddon, K. R. *et al.*), 1999, pp. 303-324, Kluwer Academic Publishers, The Netherlands.	

Examiner Signature	/Leonard Williams/ (11/12/2006)	Date Considered	

*EXAMINER: Initial if reference considered, whether or not citation is in conformance with MPEP 609. Draw line through citation if not in conformance and not considered. Include copy of this form with next communication to applicant. [1] Applicant's unique citation designation number (optional). [2] See Kind Codes of USPTO Patent Documents at www.uspto.gov or MPEP901.04. [3] Enter Office that issued the document, by the two-letter code (WIPO Standard T.3). [4] For Japanese patent documents, the indication of the year of the reign of the Emperor must precede the serial number of the patent document. [5] Kind of document by the appropriate symbols as indicated on the document under WIPO Standard ST. 16 if possible. [6] Applicant is to place a check mark here if English language Translation is attached.

This collection of information is required by 37 CFR 1.97 and 1.98. The information is required to obtain or retain a benefit by the public which is to file (and by the USPTO to process) an application. Confidentiality is governed by 35 U.S.C. 122 and 37 CFR 1.14. This collection is estimated to take 2 hours to complete, including gathering, preparing, and submitting the completed application form to the USPTO. Time will vary depending upon the individual case. Any comments on the amount of time you require to complete this form and/or suggestions for reducing this burden, should be sent to the Chief Information Officer, U.S. Patent and Trademark Office, P.O. Box 1450, Alexandria, VA 22313-1450. DO NOT SEND FEES OR COMPLETED FORMS TO THIS ADDRESS. SEND TO: Commissioner for Patents, P.O. Box 1450, Alexandria, VA 22313-1450.

If you need assistance in completing the form, call 1-600-PTO-9199 (1-800-786-9199) and select option 2.

PTO/SB/08B (08-03)
Approved for use through 07/31/2006. OMB 0651-0031
U.S. Patent and Trademark Office: U.S. DEPARTMENT OF COMMERCE
Under the Paperwork Reduction Act of 1995, no persons are required to respond to a collection of information unless it contains a valid OMB control number.

Substitute for form 1449B/PTO

INFORMATION DISCLOSURE STATEMENT BY APPLICANT

(use as many sheets as necessary)

Sheet 16 of 33

Complete if Known	
Application Number	10/378,956
Filing Date	March 3, 2003
First Named Inventor	Michael J. Zaworotko
Group Art Unit	1617
Examiner Name	Leonard Williams
Attorney Docket Number	USF-106XC1

NON PATENT LITERATURE DOCUMENTS

Examiner Initials*	Cite No. [1]	Include name of the author (in CAPITAL LETTERS), title of the article, (when appropriate), title of the item (book, magazine, journal, serial, symposium, catalog, etc.), date, page(s), volume-issue number(s), publisher, city and/or country where published.	T[2]
LW	R100	AAKERÖY, C. *et al.* "Low-dimensional architectures of silver coordination compounds assembled *via* amide-amide hydrogen bonds" *Crystal Engineering*, 1998, pp. 39-49, Vol. 1, No. 1.	
	R101	AAKERÖY, C. *et al.* "Molecular mechanics and crystal engineering" " Crystal Engineering (ed. by Seddon, K. R. *et al.*), 1999, pp. 69-82, Kluwer Academic Publishers, The Netherlands.	
	R102	AAKERÖY, C. *et al.* "New building blocks for crystal engineering. Syntheses and crystal structures of oxime-substituted pyridines" *Cryst. Eng. Comm.*, 2000, pp. 1-6, Vol. 27.	
	R103	AAKERÖY, C. *et al.* "Novel colorless composite materials for nonlinear optics" *Adv. Mater.*, 1993, pp. 364-367, Vol. 5, No. 5.	
	R104	AAKERÖY, C. *et al.* "Organic assemblies of 2-pyridones with dicarboxylic acids" *Tetrahedron*, 2000, pp. 6693-6699, Vol. 56.	
	R105	AAKERÖY, C. *et al.* "Pitfalls in the supramolecular assembly of silver(I) coordination compounds" *Journal of Molecular Structure*, 1999, pp. 91-101, Vol. 474.	
	R106	AAKERÖY, C. *et al.* "A structural study of 2-amino-5-nitropyridine and 2-amino-3-nitropyridine: intermolecular forces and polymorphism" *J. Mater. Chem.*, 1998, pp. 1385-1389, Vol. 8, No. 6.	
	R107	AAKERÖY, C. *et al.* "Supramolecular assembly of low-dimensional silver (I) architectures *via* amide-amide hydrogen bonds" *Chem. Commun.*, 1998, pp. 1067-1068.	
	R108	AAKERÖY, C. *et al.* "'Total synthesis' supramolecular style: design and hydrogen-bond-directed assembly of ternary supermolecules" *Angew. Chem. Int. Ed.*, 2001, pp. 3240-3242, Vol. 40, No. 17.	
	R109	AAKERÖY, C. *et al.* "Two-fold interpenetration of 3-D nets assembled via three-co-ordinate silver(I) ions and amide-amide hydrogen bonds" *J. Chem. Soc., Dalton Trans.*, 1998, pp. 1943-1945.	
LW	R110	AHN, S. *et al.* "Polymorphs of a 1:1 cocrystal with tunnel and layer structures: *p,p'*-biphenol/dimethyl sulfoxide" *Crystal Growth & Design*, 2001, pp. 107-111, Vol. 1, No. 2.	

Examiner Signature	/Leonard Williams/ (11/12/2006)	Date Considered	

*EXAMINER: Initial if reference considered, whether or not citation is in conformance with MPEP 609. Draw line through citation if not in conformance and not considered. Include copy of this form with next communication to applicant. [1] Applicant's unique citation designation number (optional). [2] See Kind Codes of USPTO Patent Documents at www.uspto.gov or MPEP901.04. [3] Enter Office that issued the document, by the two-letter code (WIPO Standard T.3). [4] For Japanese patent documents, the indication of the year of the reign of the Emperor must precede the serial number of the patent document. [5] Kind of document by the appropriate symbols as indicated on the document under WIPO Standard ST. 16 if possible. [6] Applicant is to place a check mark here if English language Translation is attached.

This collection of information is required by 37 CFR 1.97 and 1.98. The information is required to obtain or retain a benefit by the public which is to file (and by the USPTO to process) an application. Confidentiality is governed by 35 U.S.C. 122 and 37 CFR 1.14. This collection is estimated to take 2 hours to complete, including gathering, preparing, and submitting the completed application form to the USPTO. Time will vary depending upon the individual case. Any comments on the amount of time you require to complete this form and/or suggestions for reducing this burden, should be sent to the Chief Information Officer, U.S. Patent and Trademark Office, P.O. Box 1450, Alexandria, VA 22313-1450. DO NOT SEND FEES OR COMPLETED FORMS TO THIS ADDRESS. SEND TO: Commissioner for Patents, P.O. Box 1450, Alexandria, VA 22313-1450.

If you need assistance in completing the form, call 1-800-PTO-9199 (1-800-786-9199) and select option 2.

PTO/SB/08B (08-03)
Approved for use through 07/31/2006. OMB 0651-0031
U.S. Patent and Trademark Office: U.S. DEPARTMENT OF COMMERCE
Under the Paperwork Reduction Act of 1995, no persons are required to respond to a collection of information unless it contains a valid OMB control number.

Substitute for form 1449B/PTO

INFORMATION DISCLOSURE STATEMENT BY APPLICANT

(use as many sheets as necessary)

Sheet 17 of 33

Complete if Known	
Application Number	10/378,956
Filing Date	March 3, 2003
First Named Inventor	Michael J. Zaworotko
Group Art Unit	1617
Examiner Name	Leonard Williams
Attorney Docket Number	USF-106XC1

NON PATENT LITERATURE DOCUMENTS

Examiner Initials*	Cite No. [1]	Include name of the author (in CAPITAL LETTERS), title of the article, (when appropriate), title of the item (book, magazine, journal, serial, symposium, catalog, etc.), date, page(s), volume-issue number(s), publisher, city and/or country where published.	T[2]
LW	R111	AKAZOME, M. *et al.* "Enantioselective inclusion of methyl phenyl sulfoxides and benzyl methyl sulfoxides by (*R*)-phenylglycyl-(*R*)-phenylglycine and the crystal structures of the inclusion cavities" *J. Org. Chem.*, 2000, pp. 68-76, Vol. 65.	
	R112	AKHTARUZZAMAN, M.D. *et al.* "One-dimensional hydrogen-bonded molecular tapes in 1, 4-bis[(4-pyridinio) ethynyl]benzene chloranilate" *Acta. Cryst.*, 2001, pp. o353-o355, Vol. E57.	
	R113	ALLEN, F. *et al.* "Systematic analysis of structural data as a research technique in organic chemistry" *Acc. Chem. Res.*, 1983, pp. 146-153, Vol. 16.	
	R114	ALMARSSON, Ö. *et al.* "Crystal engineering of the composition of pharmaceutical phases. Do pharmaceutical co-crystals represent a new path to improved medicines?" *Chem. Commun.*, 2004, pp. 1889-1896.	
	R115	AMAI, M. *et al.* "1:1 complex of octadecanoic acid and 3-pyridinecarboxamide" *Acta Cryst.*, 1998, pp. 1367-1369, Vol. C54.	
	R116	ANDERSON, N. *et al.* "Sulfonation with inversion by mitsunobu reaction: an improvement on the original conditions" *J. Org. Chem.*, 1996, pp. 7955-7958, Vol. 61.	
	R117	AOKI, K. *et al.* "A 1:1 complex of theophylline and *p*-nitrophenol" *Acta Cryst.*, 1978, pp. 2333-2336, Vol. B34.	
	R118	ASHTON, P. *et al.* "Combining different hydrogen-bonding motifs to self-assemble interwoven superstructures" *Chem. Eur. J.*, 1998, pp. 577-589, Vol. 4, No. 4.	
	R119	BARKER, P. A. *et al.* "Effect of crystallization temperature on the cocrystallization temperature on the cocrystallization of hydroxybutyrate/ hydroxyvalerate copolymers" *Polymer*, pp. 913-919, Vol. 38, No. 4.	
	R120	BERKOVITCH-YELLIN, Z. *et al.* "Electron density distribution in cumulenes: an x-ray study of the complex allenedicarboxylic acid- acetamide (1:1) at -150°C" *Acta Cryst.*, 1977, pp. 3670-3677, Vol. B33.	
	R121	BERKOVITCH-YELLIN, Z. *et al.* "The role played by C-H•••O and C-H•••N interactions in determining molecular packing and conformation" *Acta Cryst.*, 1984, pp. 159-165, Vol. B40.	
LW	R122	BERL, V. *et al.* "Induced fit selection of a barbiturate receptor from a dynamic structural and conformational/configurational library" *Eur. J. Org. Chem.*, 1999, pp. 3089-3094.	

Examiner Signature	/Leonard Williams/ (11/12/2006)	Date Considered	

*EXAMINER: Initial if reference considered, whether or not citation is in conformance with MPEP 609. Draw line through citation if not in conformance and not considered. Include copy of this form with next communication to applicant. [1] Applicant's unique citation designation number (optional). [2] See Kind Codes of USPTO Patent Documents at www.uspto.gov or MPEP901.04. [3] Enter Office that issued the document, by the two-letter code (WIPO Standard T.3). [4] For Japanese patent documents, the indication of the year of the reign of the Emperor must precede the serial number of the patent document. [5] Kind of document by the appropriate symbols as indicated on the document under WIPO Standard ST. 16 if possible. [6] Applicant is to place a check mark here if English language Translation is attached.

This collection of information is required by 37 CFR 1.97 and 1.98. The information is required to obtain or retain a benefit by the public which is to file (and by the USPTO to process) an application. Confidentiality is governed by 35 U.S.C. 122 and 37 CFR 1.14. This collection is estimated to take 2 hours to complete, including gathering, preparing, and submitting the completed application form to the USPTO. Time will vary depending upon the individual case. Any comments on the amount of time you require to complete this form and/or suggestions for reducing this burden, should be sent to the Chief Information Officer, U.S. Patent and Trademark Office, P.O. Box 1450, Alexandria, VA 22313-1450. DO NOT SEND FEES OR COMPLETED FORMS TO THIS ADDRESS. SEND TO: Commissioner for Patents, P.O. Box 1450, Alexandria, VA 22313-1450.

PTO/SB/08B (08-03)
Approved for use through 07/31/2006. OMB 0651-0031
U.S. Patent and Trademark Office: U.S. DEPARTMENT OF COMMERCE
Under the Paperwork Reduction Act of 1995, no persons are required to respond to a collection of information unless it contains a valid OMB control number.

Substitute for form 1449B/PTO

INFORMATION DISCLOSURE STATEMENT BY APPLICANT

(use as many sheets as necessary)

Sheet 18 of 33

Complete if Known	
Application Number	10/378,956
Filing Date	March 3, 2003
First Named Inventor	Michael J. Zaworotko
Group Art Unit	1617
Examiner Name	Leonard Williams
Attorney Docket Number	USF-106XC1

NON PATENT LITERATURE DOCUMENTS

Examiner Initials*	Cite No.[1]	Include name of the author (in CAPITAL LETTERS), title of the article, (when appropriate), title of the item (book, magazine, journal, serial, symposium, catalog, etc.), date, page(s), volume-issue number(s), publisher, city and/or country where published.	T[2]
LW	R123	BERTOLASI, V. *et al.* "Competition between hydrogen bonding and donor-acceptor interactions in co-crystals of 1,3-dimethylbarbituric acid with aromatic amines" *New J. Chem.*, 2001, pp. 408-415, Vol. 25.	
	R124	BERTOLASI, V. *et al.* "General rules for the packing of hydrogen-bonded crystals as derived from the analysis of squaric acid anions: aminoaromatic nitrogen base co-crystals" *Acta Cryst.*, 2001, pp. 591-598, Vol. B57.	
	R125	BETTINETTI, G. *et al.* "Structure and solid-state chemistry of anhydrous and hydrated crystal forms of the trimethoprim-sulfamethoxypyridazine 1:1 molecular complex" *Journal of Pharmaceutical Sciences*, April 2000, pp. 478-489, Vol. 89, No. 4.	
	R126	BETTINETTI, G. *et al.* "Thermal analysis of binary systems of the pharmaceuticals trimethoprim and benzoic acid" *Journal of Thermal Analysis*, 1983, pp. 285-294, Vol. 28.	
	R127	BETTIS, J. *et al.* "Biopharmaceutics and dosage form design" *Amer. J. Hosp. Pharm.*, March 1973, pp. 240-243, Vol. 30.	
	R128	BOLTON, S. *et al.* "Complexes formed in solution by homologs of caffeine" *Journal of the American Pharmaceutical Association*, January 1957, pp. 38-41, Vol. XLVI, No. 1.	
	R129	BOND, A. "*In situ* co-crystallisation as a tool for low-temperature crystal engineering" *Chem. Commun.*, 2003, pp. 250-251, Vol. 2.	
	R130	BONIN, M. *et al.* "Urotropin azelate: a rather unwilling co-crystal" *Acta Cryst.*, 2003, pp. 72-86, Vol. B59.	
	R131	BOSSHARD, C. *et al.* "Microscopic nonlinearities of two-component organic crystals" *J. Opt. Soc. Am. B*, November 2001, pp. 1620-1626, Vol. 18, No. 11.	
	R132	GLUZMAN, M. Kh. *et al.* "Investigation of Eutectic Melting in Systems Composed of Organic Salts and Acids" *Journal of Physical Chemistry*, 1960, pp. 2742-2747, Vol. 34.	
	R133	BRAGA, D. *et al.* "Hydrogen bonding interactions between ions: a powerful tool in molecular crystal engineering" *Structure and Bonding*, 2004, pp. 1-32, Vol. 111.	
LW	R134	BRIERLEY, C. *et al.* "Preparation and structure of the 1:2 π-molecular complex of phenothiazine with pyromellitic dianhydride" *J. Chem. Phys.*, February 1, 1985, pp. 1522-1528, Vol. 82, No. 1.	

Examiner Signature	/Leonard Williams/ (11/12/2006)	Date Considered	

*EXAMINER: Initial if reference considered, whether or not citation is in conformance with MPEP 609. Draw line through citation if not in conformance and not considered. Include copy of this form with next communication to applicant. [1] Applicant's unique citation designation number (optional). [2] See Kind Codes of USPTO Patent Documents at www.uspto.gov or MPEP901.04. [3] Enter Office that issued the document, by the two-letter code (WIPO Standard T.3). [4] For Japanese patent documents, the indication of the year of the reign of the Emperor must precede the serial number of the patent document. [5] Kind of document by the appropriate symbols as indicated on the document under WIPO Standard ST. 16 if possible. [6] Applicant is to place a check mark here if English language Translation is attached.

This collection of information is required by 37 CFR 1.97 and 1.98. The information is required to obtain or retain a benefit by the public which is to file (and by the USPTO to process) an application. Confidentiality is governed by 35 U.S.C. 122 and 37 CFR 1.14. This collection is estimated to take 2 hours to complete, including gathering, preparing, and submitting the completed application form to the USPTO. Time will vary depending upon the individual case. Any comments on the amount of time you require to complete this form and/or suggestions for reducing this burden, should be sent to the Chief Information Officer, U.S. Patent and Trademark Office, P.O. Box 1450, Alexandria, VA 22313-1450. DO NOT SEND FEES OR COMPLETED FORMS TO THIS ADDRESS. SEND TO: Commissioner for Patents, P.O. Box 1450, Alexandria, VA 22313-1450.

If you need assistance in completing the form, call 1-800-PTO-9199 (1-800-786-9199) and select option 2.

PTO/SB/08B (08-03)
Approved for use through 07/31/2006. OMB 0651-0031
U.S. Patent and Trademark Office: U.S. DEPARTMENT OF COMMERCE
Under the Paperwork Reduction Act of 1995, no persons are required to respond to a collection of information unless it contains a valid OMB control number.

Substitute for form 1449B/PTO

INFORMATION DISCLOSURE STATEMENT BY APPLICANT

(use as many sheets as necessary)

Sheet 19 of 33

Complete if Known	
Application Number	10/378,956
Filing Date	March 3, 2003
First Named Inventor	Michael J. Zaworotko
Group Art Unit	1617
Examiner Name	Leonard Williams
Attorney Docket Number	USF-106XC1

NON PATENT LITERATURE DOCUMENTS

Examiner Initials*	Cite No.[1]	Include name of the author (in CAPITAL LETTERS), title of the article, (when appropriate), title of the item (book, magazine, journal, serial, symposium, catalog, etc.), date, page(s), volume-issue number(s), publisher, city and/or country where published.	T[2]
LW	R135	BURGI, H. *et al.* "Crystallisation of supramolecular materials" *Current Opinion in Solid State & Materials Science*, 1998, pp. 425-430, Vol. 3.	
	R136	BYRN, S. R. *et al.* "Solid-state pharmaceutical chemistry" *Chem. Mater.*, 1994, pp. 1148-1158, Vol. 6.	
	R137	CAIRA, M. "Molecular complexes of sulfonamides. Part 1. 1:1 complexes between sulfadimidine [4-amino-N-(4,6-dimethyl-2-pyrimidinyl) benzenesulfonamide] and 2- and 4-aminobenzoic acids" *Journal of Crystallographic and Spectroscopic Research*, 1991, pp. 641-648, Vol. 21, No. 5.	
	R138	CAIRA, M. "Molecular complexes of sulfonamides. Part 2. 1:1 complexes between drug molecules: sulfadimidine –acetylsalicylic acid and sulfadimidine-4-aminosalicylic acid" *Journal of Crystallographic and Spectroscopic Research*, 1992, pp. 193-200, Vol. 22, No. 2.	
	R139	CAIRA, M. "Molecular complexes of sulfonamides. 3. Structure of 5-methoxysulfadiazine (Form II) and its 1:1 complex with acetylsalicylic acid" *Journal of Chemical Crystallography*, 1994, pp. 695-701, Vol. 24, No. 10.	
	R140	CAIRA, M. *et al.* "Order-disorder enantiotropy, monotropy, and isostructurality in a tetroxoprim-sulfametrole 1:1 molecular complex: crystallographic and thermal studies" *Journal of Pharmaceutical Sciences*, November 2003, pp. 2164-2176, Vol. 92, No. 11.	
	R141	CAIRA, M. *et al.* "Selective formation of hydrogen bonded cocrystals between a sulfonamide and aromatic carboxylic acids in the solid state" *J. Chem. Soc. Perkin Trans.* 2, 1995, pp. 2213-2216.	
	R142	CAIRA, M. *et al.* "Structure of a 1:1 complex between the anthelmintic drug mebendazole and propionic acid" *Journal of Chemical Crystallography*, 1998, Vol. 28, No. 1.	
	R143	CAMERMAN, A. *et al.* "Hydrogen bonding interaction of diphenylbarbituric acid and 9-ethyladenine. Crystal structure of a 1:1 complex" *Can. J. Chem.*, 2000, pp. 1045-1051, Vol. 78.	
	R144	CAMERMAN, A. *et al.* "Molecular structure of acetylacetone. A crystallographic determination" *J. Am. Chem. Soc.*, 1983, pp. 1584-1586, Vol. 105, No. 6.	
LW	R145	CANNON, A. *et al.* "Noncovalent derivatization: green chemistry applications of crystal engineering" *Crystal Growth & Design*, 2002, pp. 255-257, Vol. 2. No. 4.	

Examiner Signature	/Leonard Williams/ (11/12/2006)	Date Considered	

*EXAMINER: Initial if reference considered, whether or not citation is in conformance with MPEP 609. Draw line through citation if not in conformance and not considered. Include copy of this form with next communication to applicant. [1] Applicant's unique citation designation number (optional). [2] See Kind Codes of USPTO Patent Documents at www.uspto.gov or MPEP901.04. [3] Enter Office that issued the document, by the two-letter code (WIPO Standard T.3). [4] For Japanese patent documents, the indication of the year of the reign of the Emperor must precede the serial number of the patent document. [5] Kind of document by the appropriate symbols as indicated on the document under WIPO Standard ST. 16 if possible. [6] Applicant is to place a check mark here if English language Translation is attached.

This collection of information is required by 37 CFR 1.97 and 1.98. The information is required to obtain or retain a benefit by the public which is to file (and by the USPTO to process) an application. Confidentiality is governed by 35 U.S.C. 122 and 37 CFR 1.14. This collection is estimated to take 2 hours to complete, including gathering, preparing, and submitting the completed application form to the USPTO. Time will vary depending upon the individual case. Any comments on the amount of time you require to complete this form and/or suggestions for reducing this burden, should be sent to the Chief Information Officer, U.S. Patent and Trademark Office, P.O. Box 1450, Alexandria, VA 22313-1450. DO NOT SEND FEES OR COMPLETED FORMS TO THIS ADDRESS. **SEND TO: Commissioner for Patents, P.O. Box 1450, Alexandria, VA 22313-1450.**

If you need assistance in completing the form, call 1-800-PTO-9199 (1-800-786-9199) and select option 2.

PTO/SB/08B (08-03)
Approved for use through 07/31/2006. OMB 0651-0031
U.S. Patent and Trademark Office: U.S. DEPARTMENT OF COMMERCE
Under the Paperwork Reduction Act of 1995, no persons are required to respond to a collection of information unless it contains a valid OMB control number.

Substitute for form 1449B/PTO

INFORMATION DISCLOSURE STATEMENT BY APPLICANT

(use as many sheets as necessary)

Sheet 20 of 33

Complete if Known	
Application Number	10/378,956
Filing Date	March 3, 2003
First Named Inventor	Michael J. Zaworotko
Group Art Unit	1617
Examiner Name	Leonard Williams
Attorney Docket Number	USF-106XC1

NON PATENT LITERATURE DOCUMENTS

Examiner Initials*	Cite No. [1]	Include name of the author (in CAPITAL LETTERS), title of the article, (when appropriate), title of the item (book, magazine, journal, serial, symposium, catalog, etc.), date, page(s), volume-issue number(s), publisher, city and/or country where published.	T[2]
LW	R146	CHINNAKALI, K. *et al.* "2-aminopyrimidine and *p*-phenylene-diacetic acid (1:1) co-crystal" *Acta Cryst.*, 1999, pp. 399-401, Vol. C55.	
	R147	CHOI, C. *et al.* "Cocrystallization of melaminium levulinate monohydrate" *Acta Cryst.*, 2004, pp. o295-o296, Vol. C60.	
	R148	CHOW, Y. P. *et al.* "Complexation of acetaminophen with methyl xanthines" *Journal of Pharmaceutical Sciences*, 1972, pp. 1454-1458, Vol. 61.	
	R149	CHRISTIAN, S. *et al.* "Activity coefficient effects in spectral and solubility studies of molecular complex equilibria" *Journal of the American Chemical Society*, September 20, 1972, pp. 6861-6862, Vol. 94, No. 19, Communications to the editor.	
	R150	COLL, M. *et al.* "Molecular structure of the complex formed between the anticancer drug cisplatin and d(pGpG): $C222_1$ crystal form" *Journal of Biomolecular Structure & Dynamics*, 1990, pp. 315-330, Vol. 8, No. 2.	
	R151	COPP, S. *et al.* "Supramolecular chemistry of $[Mn(CO)_3(\mu_3\text{-}OH)]_4$: Assembly of a cubic hydrogen-bonded diamondoid network with 1,2-diamineothane" *J. Am. Chem. Soc.*, 1992, pp. 8719-8720, Vol. 114.	
	R152	CORDI, A. *et al.* "(*S*)-Spiro [(1, 3-diazacyclopent-1-ene)-5, 2' –(7'-methyl-1',2',3',4'-tetrahydronaphthalene)]: resolution, stereospecific synthesis, and preliminary pharmacological characterization as a partial α-adrenergic agonist" *J. Med. Chem.*, 1997, pp. 2931-2935, Vol. 40.	
	R153	CRAVEN, M. *et al.* "The 2:1 crystal complex of 5, 5-diethylbarbituric acid (barbital) and caffeine" *Acta Cryst.*, 1974, pp. 1191-1195, Vol. B30.	
	R154	CRAVEN, M. *et al.* "The crystal structures of two polymorphs of 5,5'-diethylbarbituric acid (barbital)" *Acta Cryst.*, 1969, pp. 1978-1993, Vol. B25.	
LW	R155	CUDNEY, B. *et al.* "Screening and optimization strategies for macromolecular crystal growth" *Acta Cryst.*, 1994, pp. 414-423, Vol. D50.	

Examiner Signature	/Leonard Williams/ (11/12/2006)	Date Considered	

*EXAMINER: Initial if reference considered, whether or not citation is in conformance with MPEP 609. Draw line through citation if not in conformance and not considered. Include copy of this form with next communication to applicant. [1] Applicant's unique citation designation number (optional). [2] See Kind Codes of USPTO Patent Documents at www.uspto.gov or MPEP901.04. [3] Enter Office that issued the document, by the two-letter code (WIPO Standard T.3). [4] For Japanese patent documents, the indication of the year of the reign of the Emperor must precede the serial number of the patent document. [5] Kind of document by the appropriate symbols as indicated on the document under WIPO Standard ST. 16 if possible. [6] Applicant is to place a check mark here if English language Translation is attached.

This collection of information is required by 37 CFR 1.97 and 1.98. The information is required to obtain or retain a benefit by the public which is to file (and by the USPTO to process) an application. Confidentiality is governed by 35 U.S.C. 122 and 37 CFR 1.14. This collection is estimated to take 2 hours to complete, including gathering, preparing, and submitting the completed application form to the USPTO. Time will vary depending upon the individual case. Any comments on the amount of time you require to complete this form and/or suggestions for reducing this burden, should be sent to the Chief Information Officer, U.S. Patent and Trademark Office, P.O. Box 1450, Alexandria, VA 22313-1450. DO NOT SEND FEES OR COMPLETED FORMS TO THIS ADDRESS. **SEND TO: Commissioner for Patents, P.O. Box 1450, Alexandria, VA 22313-1450.**

If you need assistance in completing the form, call 1-800-PTO-9199 (1-800-786-9199) and select option 2.

PTO/SB/08B (08-03)
Approved for use through 07/31/2006. OMB 0651-0031
U.S. Patent and Trademark Office: U.S. DEPARTMENT OF COMMERCE
Under the Paperwork Reduction Act of 1995, no persons are required to respond to a collection of information unless it contains a valid OMB control number.

Substitute for form 1449B/PTO

INFORMATION DISCLOSURE STATEMENT BY APPLICANT

(use as many sheets as necessary)

Sheet 21 of 33

Complete if Known	
Application Number	10/378,956
Filing Date	March 3, 2003
First Named Inventor	Michael J. Zaworotko
Group Art Unit	1617
Examiner Name	Leonard Williams
Attorney Docket Number	USF-106XC1

NON PATENT LITERATURE DOCUMENTS

Examiner Initials*	Cite No.[1]	Include name of the author (in CAPITAL LETTERS), title of the article, (when appropriate), title of the item (book, magazine, journal, serial, symposium, catalog, etc.), date, page(s), volume-issue number(s), publisher, city and/or country where published.	T[2]
LW	R156	DATTA, S. *et al.* "Molecular complex formation between riboflavin and salicylate in an aqueous medium" *Bull. Chem. Soc. Jpn.*, 2003, pp. 1729-1734, Vol. 76.	
	R157	DAVEY, R. J. *et al.* "Crystal engineering- nucleation, the key step" *Cryst. Eng. Comm.*, 2002, pp. 257-264, Vol. 4, No. 47.	
	R158	DAVEY, R. J. *et al.* "Crystallisation in polymer films: control of morphology and kinetics of an organic dye in a polysilicone matrix" *J. Mater. Chem.*, 1997, pp. 237-241, Vol. 7, No. 2.	
	R159	DEBERNARDIS, J. *et al.* "Conformationally defined adrenergic agents. 5. Resolution, absolute configuration, and pharmacological characterization of the enantiomers of 2-(5,6-dihydroxy-1,2,3,4-tetrahydro-1-naphthyl) imidazoline: a potent agonist at α-adrenoceptors" *J. Med. Chem.*, 1987, pp. 1011-1017, Vol. 30.	
	R160	DESIRAJU, G. *et al.* "Crystal and co-crystal" *Cryst. Eng. Comm.*, 2003, pp. 466-467, Vol. 5, No. 82.	
	R161	DESIRAJU, G. *et al.* "Crystal engineering: outlook and prospects" *Current Science*, October 25, 2001, pp. 1038-1042, Vol. 81, No. 8.	
	R162	DUAX, W. *et al.* "The structure of the crystalline complex estradiol. Urea (1:1)" *Acta Cryst.*, 1972, pp. 1864-1871, Vol. B28.	
	R163	DUNITZ, J. "Crystal and co-crystal: a second opinion" *Cryst. Eng. Comm.*, 2003, pp. 506, Vol. 5, No. 91.	
	R164	DUNITZ, J. "New light on an old story: the solid-state transformation on ammonium cyanate into urea" *J. Am. Chem. Soc.*, 1998, pp. 13274-13275, Vol. 120.	
	R165	ENRIGHT, G. *et al.* "Thermally programmable gas storage and release in single crystals of an organic van der Waals host" *J. Am. Chem. Soc.*, 2003, pp. 9896-9897, Vol. 125.	
LW	R166	EPSTEIN, R. *et al.* "The x-ray crystal structure of the molecular complex 8-bromo-9-ethyladenine-5-allyl-5-isobutylbarbituric acid" *Acta Cryst.*, 1976, pp. 2180-2188, Vol. B32.	

Examiner Signature	/Leonard Williams/ (11/12/2006)	Date Considered	

*EXAMINER: Initial if reference considered, whether or not citation is in conformance with MPEP 609. Draw line through citation if not in conformance and not considered. Include copy of this form with next communication to applicant. [1] Applicant's unique citation designation number (optional). [2] See Kind Codes of USPTO Patent Documents at www.uspto.gov or MPEP901.04. [3] Enter Office that issued the document, by the two-letter code (WIPO Standard T.3). [4] For Japanese patent documents, the indication of the year of the reign of the Emperor must precede the serial number of the patent document. [5] Kind of document by the appropriate symbols as indicated on the document under WIPO Standard ST. 16 if possible. [6] Applicant is to place a check mark here if English language Translation is attached.

This collection of information is required by 37 CFR 1.97 and 1.98. The information is required to obtain or retain a benefit by the public which is to file (and by the USPTO to process) an application. Confidentiality is governed by 35 U.S.C. 122 and 37 CFR 1.14. This collection is estimated to take 2 hours to complete, including gathering, preparing, and submitting the completed application form to the USPTO. Time will vary depending upon the individual case. Any comments on the amount of time you require to complete this form and/or suggestions for reducing this burden, should be sent to the Chief Information Officer, U.S. Patent and Trademark Office, P.O. Box 1450, Alexandria, VA 22313-1450. DO NOT SEND FEES OR COMPLETED FORMS TO THIS ADDRESS. **SEND TO: Commissioner for Patents, P.O. Box 1450, Alexandria, VA 22313-1450.**

If you need assistance in completing the form, call 1-800-PTO-9199 (1-800-786-9199) and select option 2.

PTO/SB/08B (08-03)
Approved for use through 07/31/2006. OMB 0651-0031
U.S. Patent and Trademark Office: U.S. DEPARTMENT OF COMMERCE
Under the Paperwork Reduction Act of 1995, no persons are required to respond to a collection of information unless it contains a valid OMB control number.

Substitute for form 1449B/PTO

INFORMATION DISCLOSURE STATEMENT BY APPLICANT

(use as many sheets as necessary)

Sheet 22 of 33

Complete if Known	
Application Number	10/378,956
Filing Date	March 3, 2003
First Named Inventor	Michael J. Zaworotko
Group Art Unit	1617
Examiner Name	Leonard Williams
Attorney Docket Number	USF-106XC1

NON PATENT LITERATURE DOCUMENTS

Examiner Initials*	Cite No.[1]	Include name of the author (in CAPITAL LETTERS), title of the article, (when appropriate), title of the item (book, magazine, journal, serial, symposium, catalog, etc.), date, page(s), volume-issue number(s), publisher, city and/or country where published.	T[2]
LW	R167	ETTER, M. "Encoding and decoding hydrogen-bond patterns of organic compounds" *Acc. Chem. Res.*, 1990, pp. 120-126, Vol. 23.	
	R168	ETTER, M. *et al.* "Graph-set analysis of hydrogen-bond patterns in organic crystals" *Acta Cryst.*, 1990, pp. 256-262, Vol. B46.	
	R169	ETTER, M. *et al.* "Hydrogen bond directed cocrystallization and molecular recognition properties of acyclic imides" *J. Am. Chem. Soc.*, 1991, pp. 2586-2598, Vol. 113.	
	R170	ETTER, M. "Hydrogen bonds as design elements in organic chemistry" *J. Phys. Chem.*, 1991, pp. 4601-4610, Vol. 95.	
	R171	FABIAN, L. *et al.* "Volumetric measure of isostructurality" *Acta Cryst.*, 1999, pp. 1099-1108, Vol. B55.	
	R172	FALLON III, L. "The crystal and molecular structure of 5-fluorouracil" *Acta Cryst.*, pp. 2549-2556, Vol. B29.	
	R173	FEIBUSH, B. *et al.* "Chiral separation of heterocyclic drugs by HPLC: solute-stationary phase base-pair interactions" *J. Am. Chem. Soc.*, 1986, pp. 3310-3318, Vol. 108.	
	R174	FIFER, E. *et al.* "Fentanyl analogues 3. 2-(1,2,3,4-tetrahydro)-naphthyl substituted 4-anilidopiperidines" *Eur. J. Med. Chem.- Chim. Ther.*, 1984, pp. 519-524, Vol. 19, No. 6.	
	R175	RECK, G. *et al.* "Crystal structures of the carbamazepine/ammonium chloride and carbamazepine/ammonium bromide adducts and their transformation into carbamazepine dihydrate" *Pharmazie*, 1991, pp. 509-512, Vol. 46, No. 7.	X
	R176	FOXMAN, B. M. *et al.* "Environmentally benign synthesis using crystal engineering: steric accommodation in non-covalent derivatives of hydroquinones" *Crystal Engineering*, 1998, pp. 109-118, Vol. 1, No. 1.	
	R177	FOXMAN, B. M. *et al.* "Noncovalent derivatives of hydroquinone: *BIS*- (*N,N*-dialkyl) bicyclo[2.2.2]octane-1,4-dicarboxamide complexes" *Crystal Engineering*, 1999, pp. 55-64, Vol. 2. No. 1.	
LW	R178	FUJII, S. *et al.* "Crystal and molecular structure of a 1:1 molecular complex of adenine and riboflavin" *Archives of Biochemistry and Biophysics*, 1977, pp. 363-370, Vol. 181.	

Examiner Signature	/Leonard Williams/ (11/12/2006)	Date Considered	

*EXAMINER: Initial if reference considered, whether or not citation is in conformance with MPEP 609. Draw line through citation if not in conformance and not considered. Include copy of this form with next communication to applicant. [1] Applicant's unique citation designation number (optional). [2] See Kind Codes of USPTO Patent Documents at www.uspto.gov or MPEP901.04. [3] Enter Office that issued the document, by the two-letter code (WIPO Standard T.3). [4] For Japanese patent documents, the indication of the year of the reign of the Emperor must precede the serial number of the patent document. [5] Kind of document by the appropriate symbols as indicated on the document under WIPO Standard ST. 16 if possible. [6] Applicant is to place a check mark here if English language Translation is attached.

This collection of information is required by 37 CFR 1.97 and 1.98. The information is required to obtain or retain a benefit by the public which is to file (and by the USPTO to process) an application. Confidentiality is governed by 35 U.S.C. 122 and 37 CFR 1.14. This collection is estimated to take 2 hours to complete, including gathering, preparing, and submitting the completed application form to the USPTO. Time will vary depending upon the individual case. Any comments on the amount of time you require to complete this form and/or suggestions for reducing this burden, should be sent to the Chief Information Officer, U.S. Patent and Trademark Office, P.O. Box 1450, Alexandria, VA 22313-1450. DO NOT SEND FEES OR COMPLETED FORMS TO THIS ADDRESS. **SEND TO: Commissioner for Patents, P.O. Box 1450, Alexandria, VA 22313-1450.**

If you need assistance in completing the form, call 1-800-PTO-9199 (1-800-786-9199) and select option 2.

J:\USF\106XC1\PTO\IDS.supp.form.doc/DNB/esc

PTO/SB/08B (08-03)
Approved for use through 07/31/2006. OMB 0651-0031
U.S. Patent and Trademark Office: U.S. DEPARTMENT OF COMMERCE
Under the Paperwork Reduction Act of 1995, no persons are required to respond to a collection of information unless it contains a valid OMB control number.

Substitute for form 1449B/PTO

INFORMATION DISCLOSURE STATEMENT BY APPLICANT

(use as many sheets as necessary)

Sheet 23 of 33

Complete if Known	
Application Number	10/378,956
Filing Date	March 3, 2003
First Named Inventor	Michael J. Zaworotko
Group Art Unit	1617
Examiner Name	Leonard Williams
Attorney Docket Number	USF-106XC1

NON PATENT LITERATURE DOCUMENTS

Examiner Initials*	Cite No. [1]	Include name of the author (in CAPITAL LETTERS), title of the article, (when appropriate), title of the item (book, magazine, journal, serial, symposium, catalog, etc.), date, page(s), volume-issue number(s), publisher, city and/or country where published.	T[2]
LW	R179	GAO, X. *et al.* "Supramolecular construction of molecular ladders in the solid state" *Angew. Chem. Int. Ed.*, 2004, pp. 232-236, Vol. 43.	
	R180	GARTLAND, G. L. *et al.* "Hydrogen bonding NH•••O=C of barbiturates: the (1:1) crystal complex of urea and 5,5-diethylbarbituric acid (barbital)" *Acta Cryst.*, 1974, pp. 980-987, Vol. B30.	
	R181	GHOSH, M. "Structure and conformation of the 1:1 molecular complex sulfaproxyline-caffeine" *Acta Cryst.*, 1991, pp. 577-580, Vol. C47.	
	R182	GIUSEPPETTI, G. P. *et al.* "The crystal structure of a sulfamethoxazole-trimethoprim 1:1 molecular compound" *Il Farmaco- Ed. Sc.*, pp. 138-151, Vol. 35.	
	R183	GOSWAMI, S. *et al.* "2-aminopyrimidine-fumaric acid cocrystal" *Acta Cryst.*, 1999, pp. 583-585, Vol. C55.	
	R184	HAYNES, D. "Supramolecular synthon competition in organic sulfonates: A CSD survey" *Cryst. Eng. Comm.*, 2004, pp. 584-588, Vol. 6, No. 95.	
	R185	GOSWAMI, S. *et al.* "1:1 Hetero-assembly of 2-amino-pyramidine and (+)-camphoric acid" *Acta Cryst.*, 2000, pp. 477-478, Vol. C56.	
	R186	GOSWAMI, S. *et al.* "Molecular recognition induced supramolecular array of 2-aminopyrimidine with terephthalic acid, 1,4-phenylenediacetic acid and furmaric acid in solid state *via* H-bonding and π-stacking interactions" *Supramolecular Chemistry*, 1999, pp. 25-33, Vol. 11.	
	R187	GRAJA, A. *et al.* "Interplay of acceptor molecule shape, crystal structure and physical properties of a new molecular complex C_{70} • 2[(Ph_3P) AuCl]" *Chemical Physics Letters*, November 19, 1999, pp. 725-732. Vol. 313.	
LW	R188	HAIXIN, L. *et al.* "Structure of the 1:1 complex of 6,6'-diquinolyl ether with 5,5-diethylbarbituric acid" *Acta Cryst.*, 1992, pp. 2096-2098, Vol. C48.	

Examiner Signature	/Leonard Williams/ (11/12/2006)	Date Considered	

*EXAMINER: Initial if reference considered, whether or not citation is in conformance with MPEP 609. Draw line through citation if not in conformance and not considered. Include copy of this form with next communication to applicant. [1] Applicant's unique citation designation number (optional). [2] See Kind Codes of USPTO Patent Documents at www.uspto.gov or MPEP901.04. [3] Enter Office that issued the document, by the two-letter code (WIPO Standard T.3). [4] For Japanese patent documents, the indication of the year of the reign of the Emperor must precede the serial number of the patent document. [5] Kind of document by the appropriate symbols as indicated on the document under WIPO Standard ST. 16 if possible. [6] Applicant is to place a check mark here if English language Translation is attached.

This collection of information is required by 37 CFR 1.97 and 1.98. The information is required to obtain or retain a benefit by the public which is to file (and by the USPTO to process) an application. Confidentiality is governed by 35 U.S.C. 122 and 37 CFR 1.14. This collection is estimated to take 2 hours to complete, including gathering, preparing, and submitting the completed application form to the USPTO. Time will vary depending upon the individual case. Any comments on the amount of time you require to complete this form and/or suggestions for reducing this burden, should be sent to the Chief Information Officer, U.S. Patent and Trademark Office, P.O. Box 1450, Alexandria, VA 22313-1450. DO NOT SEND FEES OR COMPLETED FORMS TO THIS ADDRESS. SEND TO: Commissioner for Patents, P.O. Box 1450, Alexandria, VA 22313-1450.

If you need assistance in completing the form, call 1-800-PTO-9199 (1-800-786-9199) and select option 2.

PTO/SB/08B (08-03)
Approved for use through 07/31/2006. OMB 0651-0031
U.S. Patent and Trademark Office: U.S. DEPARTMENT OF COMMERCE
Under the Paperwork Reduction Act of 1995, no persons are required to respond to a collection of information unless it contains a valid OMB control number.

Substitute for form 1449B/PTO

INFORMATION DISCLOSURE STATEMENT BY APPLICANT

(use as many sheets as necessary)

Sheet 24 of 33

Complete if Known	
Application Number	10/378,956
Filing Date	March 3, 2003
First Named Inventor	Michael J. Zaworotko
Group Art Unit	1617
Examiner Name	Leonard Williams
Attorney Docket Number	USF-106XC1

NON PATENT LITERATURE DOCUMENTS

Examiner Initials*	Cite No. [1]	Include name of the author (in CAPITAL LETTERS), title of the article, (when appropriate), title of the item (book, magazine, journal, serial, symposium, catalog, etc.), date, page(s), volume-issue number(s), publisher, city and/or country where published.	T[2]
LW	R189	HENCK, J. *et al.* "Disappearing and reappearing polymorphs. The benzocaine:picric acid system" *J. Am. Chem. Soc.*, 2001, pp. 1834-1841, Vol. 123.	
	R190	HIGUCHI, T. *et al.* "Complexation of organic substances in aqueous solution by hydroxyaromatic acids and their salts" *J. Pharm. Sci.*, 1961, pp. 905-909, Vol. 50.	
	R191	HINO, T. *et al.* "Assessment of nicotinamide polymorphs by differential scanning calorimetry" *Thermochimica Acta*, 2001, pp. 85-92, Vol. 374.	
	R192	HÖGBERG, T. *et al.* "Crystallographic, theoretical and molecular modelling studies on the conformations of the salicylamide, raclopride, a selective dopamine-D_2 antagonist" *J. Pharm. Pharmacol.*, 1987, pp. 787-796, Vol. 39.	
	R193	HSU, I. *et al.* "The 2:1 crystal complex of 2-aminopyridine and 5,5-diethylbarbituric acid (barbital)" *Acta Cryst.*, 1974, pp. 994-997, Vol. B30.	
	R194	HSU, I. *et al.* "The 1:1 crystal complex of *N*-methyl-2-pyridone and 5,5-diethylbarbituric acid (barbital)" *Acta Cryst.*, 1974, pp. 998-1001, Vol. B30.	
	R195	HSU, I. *et al.* "The crystalline complex (1:1) of salicylamide and 5-ethyl-5-isoamylbarbituric acid (amobarbital)" *Acta Cryst.*, 1974, pp. 843-846, Vol. B30.	
	R196	HSU, I. *et al.* "The crystal structure of the 1:1 complex of acetamide with 5,5-diethylbarbituric acid (barbital)" *Acta Cryst.*, 1974, pp. 974-979, Vol. B30.	
	R197	HSU, I. *et al.* "The crystal structure of the triclinic 1:2 complex of hexamethylphosphoramide with 5,5-diethylbarbituric acid (barbital)" *Acta Cryst.*, 1974, pp. 1299-1304, Vol. B30.	
	R198	HSU, I. *et al.* "Hydrogen bonding NH...N of barbiturates: The 1:1 crystal complex of imidazole and 5,5-diethylbarbituric acid (barbital)" *Acta Cryst.*, 1974, pp. 988-993, Vol. B30.	
LW	R199	IBRAGIMOV, B. "A simple correlation between the structures of different crystal modifications of a given host-guest complex and their crystallization temperatures" *Journal of Inclusion of Phenomena and Macrocyclic Chemistry*, 1999, pp. 345-353, Vol. 34.	

Examiner Signature	/Leonard Williams/ (11/12/2006)	Date Considered	

*EXAMINER: Initial if reference considered, whether or not citation is in conformance with MPEP 609. Draw line through citation if not in conformance and not considered. Include copy of this form with next communication to applicant. [1] Applicant's unique citation designation number (optional). [2] See Kind Codes of USPTO Patent Documents at www.uspto.gov or MPEP901.04. [3] Enter Office that issued the document, by the two-letter code (WIPO Standard T.3). [4] For Japanese patent documents, the indication of the year of the reign of the Emperor must precede the serial number of the patent document. [5] Kind of document by the appropriate symbols as indicated on the document under WIPO Standard ST. 16 if possible. [6] Applicant is to place a check mark here if English language Translation is attached.

This collection of information is required by 37 CFR 1.97 and 1.98. The information is required to obtain or retain a benefit by the public which is to file (and by the USPTO to process) an application. Confidentiality is governed by 35 U.S.C. 122 and 37 CFR 1.14. This collection is estimated to take 2 hours to complete, including gathering, preparing, and submitting the completed application form to the USPTO. Time will vary depending upon the individual case. Any comments on the amount of time you require to complete this form and/or suggestions for reducing this burden, should be sent to the Chief Information Officer, U.S. Patent and Trademark Office, P.O. Box 1450, Alexandria, VA 22313-1450. DO NOT SEND FEES OR COMPLETED FORMS TO THIS ADDRESS. SEND TO: Commissioner for Patents, P.O. Box 1450, Alexandria, VA 22313-1450.

If you need assistance in completing the form, call 1-800-PTO-9199 (1-800-786-9199) and select option 2.
If you need assistance in completing the form, call 1-800-PTO-9199 (1-800-786-9199) and select option 2.

PTO/SB/08B (08-03)
Approved for use through 07/31/2006. OMB 0651-0031
U.S. Patent and Trademark Office: U.S. DEPARTMENT OF COMMERCE
Under the Paperwork Reduction Act of 1995, no persons are required to respond to a collection of information unless it contains a valid OMB control number.

Substitute for form 1449B/PTO

INFORMATION DISCLOSURE STATEMENT BY APPLICANT

(use as many sheets as necessary)

Sheet 25 of 33

Complete if Known	
Application Number	10/378,956
Filing Date	March 3, 2003
First Named Inventor	Michael J. Zaworotko
Group Art Unit	1617
Examiner Name	Leonard Williams
Attorney Docket Number	USF-106XC1

NON PATENT LITERATURE DOCUMENTS

Examiner Initials*	Cite No. [1]	Include name of the author (in CAPITAL LETTERS), title of the article, (when appropriate), title of the item (book, magazine, journal, serial, symposium, catalog, etc.), date, page(s), volume-issue number(s), publisher, city and/or country where published.	T [2]
LW	R200	ISHIDA, T. *et al.* "Structural study of histamine H_2-receptor antagonists. Five 3-[2-(diamino-methyleneamino)-4-thiazolymethylthio] propionamidine and –amide derivatives" *Acta Cryst.*, 1989, pp. 505-512, Vol. B45.	
	R201	KATAKAI, R. *et al.* "Stepwise synthesis of oligopeptides with *N*-carboxy-α-amino acid anhydrides. IV. Glycine NCA" *J. Org. Chem.*, 1972, pp. 327-329, Vol. 37, No. 2.	
	R202	KAWAKAMI, Y. *et al.* "The rationale for E2020 as a potent acetylcholinesterase inhibitor" *Bioorganic & Medicinal Chemistry*, 1996, pp. 1429-1446, Vol. 4, No. 9.	
	R203	KELDERS, H. *et al.* "Automated protein crystallization and a new crystal form of a subtilisin: eglin complex" *Protein Engineering*, 1987, pp. 301-303, Vol. 1, No. 4.	
	R204	KHALIL, R. M. "Complexation of paracetamol with xanthine derivatives" *Egypt. J. Pharm. Sci.*, 1992, pp. 757-769, Vol. 33, No. 5-6.	
	R205	KIM, S. "Crystal structure of the 1:1 complex of 5-fluorouracil and 9-ethylhypoxanthine" *Science*, November 24, 1967, pp. 1046-1048, Vol. 158, No. 3804.	
	R206	KIRYU, S. *et al.* "Crystal structure of a 1:1 aminopyrine-barbital complex" *Journal of Pharmaceutical Sciences*, May 1971, pp. 699-703, Vol. 60, No. 5.	
	R207	KIRYU, S. *et al.* "Crystal structure of a 1:1 aminopyrine-cyclobarbital complex" *Chem. Pham. Bull.*, 1974, pp. 1588-1592, Vol. 22.	
	R208	KLEIN, C. *et al.* "Molecular structure of two conformationally restrained fentanyl analogues: cis- and trans-isomers of *N*-(3-methyl-1-[1,2,3,4-tetrahydro) naphthyl]-4-piperidinyl}-*N*-phenylpropanamide" *Journal of Pharmaceutical Sciences*, November 1985, pp. 1147-1151, Vol. 74, No. 11.	
	R209	KOSHIMA, H. *et al.* "Photoreactivities of two kinds of bimolecular crystals formed from acridine and phenothiazine" *J. Chem. Soc., Perkins Trans. 2*, 1997, pp. 2033-2038.	
LW	R210	KOSHIMA, H. *et al.* "Polymorphs of a cocrystal with achiral and chiral structures prepared by pseudoseeding: tryptamine/hydrocinnamic acid" *Crystal Growth & Design*, 2001, pp. 355-357, Vol. 1, No. 5.	

Examiner Signature	/Leonard Williams/ (11/12/2006)	Date Considered	

*EXAMINER: Initial if reference considered, whether or not citation is in conformance with MPEP 609. Draw line through citation if not in conformance and not considered. Include copy of this form with next communication to applicant. [1] Applicant's unique citation designation number (optional). [2] See Kind Codes of USPTO Patent Documents at www.uspto.gov or MPEP901.04. [3] Enter Office that issued the document, by the two-letter code (WIPO Standard T.3). [4] For Japanese patent documents, the indication of the year of the reign of the Emperor must precede the serial number of the patent document. [5] Kind of document by the appropriate symbols as indicated on the document under WIPO Standard ST. 16 if possible. [6] Applicant is to place a check mark here if English language Translation is attached.

This collection of information is required by 37 CFR 1.97 and 1.98. The information is required to obtain or retain a benefit by the public which is to file (and by the USPTO to process) an application. Confidentiality is governed by 35 U.S.C. 122 and 37 CFR 1.14. This collection is estimated to take 2 hours to complete, including gathering, preparing, and submitting the completed application form to the USPTO. Time will vary depending upon the individual case. Any comments on the amount of time you require to complete this form and/or suggestions for reducing this burden, should be sent to the Chief Information Officer, U.S. Patent and Trademark Office, P.O. Box 1450, Alexandria, VA 22313-1450. DO NOT SEND FEES OR COMPLETED FORMS TO THIS ADDRESS. SEND TO: Commissioner for Patents, P.O. Box 1450, Alexandria, VA 22313-1450.

If you need assistance in completing the form, call 1-800-PTO-9199 (1-800-786-9199) and select option 2.

PTO/SB/08B (08-03)
Approved for use through 07/31/2008. OMB 0651-0031
U.S. Patent and Trademark Office: U.S. DEPARTMENT OF COMMERCE
Under the Paperwork Reduction Act of 1995, no persons are required to respond to a collection of information unless it contains a valid OMB control number.

Substitute for form 1449B/PTO

INFORMATION DISCLOSURE STATEMENT BY APPLICANT

(use as many sheets as necessary)

Sheet 26 of 33

Complete if Known	
Application Number	10/378,956
Filing Date	March 3, 2003
First Named Inventor	Michael J. Zaworotko
Group Art Unit	1617
Examiner Name	Leonard Williams
Attorney Docket Number	USF-106XC1

NON PATENT LITERATURE DOCUMENTS

Examiner Initials*	Cite No.[1]	Include name of the author (in CAPITAL LETTERS), title of the article, (when appropriate), title of the item (book, magazine, journal, serial, symposium, catalog, etc.), date, page(s), volume-issue number(s), publisher, city and/or country where published.	T[2]
LW	R211	KRISHNAMOHAN SHARMA, C. V. *et al.* "X-ray crystal structure of $C_6H_3(CO_2H)_3$-1,3,5•1.5(4,4'-bipy): a 'super trimesic acid' chicken-wire grid" *Chem. Commun.*, 1996, pp. 2655-2656.	
	R212	KURODA, R. *et al.* "Generation of a co-crystal phase with coloristic properties *via* solid state grinding procedures" *Chem. Commun.*, 2002, pp. 2848-2849.	
	R213	LEISEROWITZ, L. *et al.* "The molecular packing modes and hydrogen-bonding properties of amide: dicarboxylic acid complexes" *Acta Cryst.*, 1977, pp. 2719-2733, Vol. B33.	
	R214	LEISEROWITZ, L. "Molecular packing modes. Carboxylic acids" *Acta Cryst.*, 1976, pp. 775-802, Vol. B32.	
	R215	LYNCH, D. *et al.* "Molecular cocrystals of carboxylic acids. XXXI adducts of 2-aminopyrimidine and 3-amino-1,2,4-triazole with heterocyclic carboxylic acids" *Aust. J. Chem.*, 1998, pp. 403-408, Vol. 51.	
	R216	MACGILLIVRAY, L. *et al.* "Supramolecular control of reactivity in the solid state using linear molecular templates" *J. Am. Chem. Soc.*, 2000, pp. 7817-7818, Vol. 122.	
	R217	MATHIAS, J. *et al.* "Structural preferences of hydrogen-bonded networks in organic solution- the cyclic $CA_3 \cdot M_3$ 'rosette'" *J. Am. Chem. Soc.*, 1994, pp. 4316-4325, Vol. 116.	
	R218	MASTROPAOLO, D. *et al.* "Hydrogen bonding interaction of diphenylhydantoin and 9-ethyladenine" *Molecular Pharmacology*, 1983, pp. 273-277, Vol. 23.	
	R219	MARYANOFF, B. "Stereochemistry in a medium-sized ring. Highly diastereoselective N-oxidation of a substituted 3-benzazonine. X-ray crystal structure of an unusual complex between an amine *N*-oxide and saccharin" *J. Org. Chem.*, 1990, pp. 760-764, Vol. 55.	
	R220	MARTIN, R. *et al.* "The caffeine-potassium chlorogenate molecular complex" *Phytochemistry*, 1987, pp. 273-279, Vol. 26, No. 1.	
LW	R221	ANDERSON, J. "Constitution of aurous compounds: Gold mirrors" *Nature*, October 2, 1937, pp. 583-584, Letters to the Editor.	

Examiner Signature	/Leonard Williams/ (11/12/2006)	Date Considered	

*EXAMINER: Initial if reference considered, whether or not citation is in conformance with MPEP 609. Draw line through citation if not in conformance and not considered. Include copy of this form with next communication to applicant. [1] Applicant's unique citation designation number (optional). [2] See Kind Codes of USPTO Patent Documents at www.uspto.gov or MPEP901.04. [3] Enter Office that issued the document, by the two-letter code (WIPO Standard T.3). [4] For Japanese patent documents, the indication of the year of the reign of the Emperor must precede the serial number of the patent document. [5] Kind of document by the appropriate symbols as indicated on the document under WIPO Standard ST. 16 if possible. [6] Applicant is to place a check mark here if English language Translation is attached.

This collection of information is required by 37 CFR 1.97 and 1.98. The information is required to obtain or retain a benefit by the public which is to file (and by the USPTO to process) an application. Confidentiality is governed by 35 U.S.C. 122 and 37 CFR 1.14. This collection is estimated to take 2 hours to complete, including gathering, preparing, and submitting the completed application form to the USPTO. Time will vary depending upon the individual case. Any comments on the amount of time you require to complete this form and/or suggestions for reducing this burden, should be sent to the Chief Information Officer, U.S. Patent and Trademark Office, P.O. Box 1450, Alexandria, VA 22313-1450. DO NOT SEND FEES OR COMPLETED FORMS TO THIS ADDRESS. SEND TO: Commissioner for Patents, P.O. Box 1450, Alexandria, VA 22313-1450.

If you need assistance in completing the form, call 1-800-PTO-9199 (1-800-786-9199) and select option 2.

PTO/SB/08B (08-03)
Approved for use through 07/31/2006. OMB 0651-0031
U.S. Patent and Trademark Office: U.S. DEPARTMENT OF COMMERCE
Under the Paperwork Reduction Act of 1995, no persons are required to respond to a collection of information unless it contains a valid OMB control number.

Substitute for form 1449B/PTO

INFORMATION DISCLOSURE STATEMENT BY APPLICANT

(use as many sheets as necessary)

Sheet 27 of 33

Complete if Known	
Application Number	10/378,956
Filing Date	March 3, 2003
First Named Inventor	Michael J. Zaworotko
Group Art Unit	1617
Examiner Name	Leonard Williams
Attorney Docket Number	USF-106XC1

NON PATENT LITERATURE DOCUMENTS

Examiner Initials*	Cite No.[1]	Include name of the author (in CAPITAL LETTERS), title of the article, (when appropriate), title of the item (book, magazine, journal, serial, symposium, catalog, etc.), date, page(s), volume-issue number(s), publisher, city and/or country where published.	T[2]
LW	R222	ROBBINS, A. H. *et al.* "The crystal structure of the 1:2 adduct of potassium triiodide and 5,5-diethylbarbituric acid (barbital)" *American Crystallographic Association- Series 2, Papers and Abstracts*, 1973, p. 87.	
	R223	BEERGES, P. *et al.* "Phenothiazine tetracyanoethylene" *Private Communication*, 1994.	
	R224	MADARASZ, J. *et al.* "Thermal, ftir and xrd study on some 1:1 molecular compounds of theophylline" *Journal of Thermal Analysis and Calorimetry*, 2002, pp. 281-290, Vol. 69.	
	R225	CARONNA, T. *et al.* "Halogen bonding and π•••π stacking control reactivity in the solid state" *J. Am. Chem. Soc.*, 2004, pp. 4500-4501, Vol. 126.	
	R226	ZERKOWSKI, J. *et al.* "Steric control of secondary, solid-state architecture in 1:1 complexes of melamines and barbiturates that crystallize as crinkled tapes" *J. Am. Chem. Soc.*, 1994, pp. 4298-4304, Vol. 116.	
	R227	ZAITU, S. *et al.* "1:1 Molecular complex of theophylline and *p*-nitroaniline" *Acta Cryst.*, 1995, pp. 2390-2392, Vol. C51.	
	R228	KOFLER, L. *et al.*, Thermal micromethods for the study of organic compounds and their mixtures, pp. 1-145, 148-351, 354-386, Innsbruck, Austria, 1980.	
	R229	QUEHENBERGER, H. "Concerning organic molecular compounds and their polymorphism" *Monatshefte für Chemie*, 1949, pp. 595-606, Vol. 80, No. 5.	X
	R230	WIEDENFELD, H. *et al.* "The crystal structure of the theophylline-urea complex" *Arch. Pharm.*, 1986, pp. 654-659, Vol. 319.	X
	R231	BUNICK, G. *et al.* "The crystal and molecular structure of the complex 2,6-diamino-9-ethylpurine 5,5-diethylbarbituric acid" *American Crystallographic Association, Abstract Papers*" Winter 1976, p. 30.	
LW	R232	BUCZAK, G. *et al.* "Crystal structure and vibrational spectra of the 1:1 and 1:2 complexes of pyridine betaine with pentachlorophenol" *Journal of Molecular Structure*, 1997, pp. 143-151, Vol. 436-437.	

Examiner Signature	/Leonard Williams/ (11/12/2006)	Date Considered	

*EXAMINER: Initial if reference considered, whether or not citation is in conformance with MPEP 609. Draw line through citation if not in conformance and not considered. Include copy of this form with next communication to applicant. [1] Applicant's unique citation designation number (optional). [2] See Kind Codes of USPTO Patent Documents at www.uspto.gov or MPEP901.04. [3] Enter Office that issued the document, by the two-letter code (WIPO Standard T.3). [4] For Japanese patent documents, the indication of the year of the reign of the Emperor must precede the serial number of the patent document. [5] Kind of document by the appropriate symbols as indicated on the document under WIPO Standard ST. 16 if possible. [6] Applicant is to place a check mark here if English language Translation is attached.

This collection of information is required by 37 CFR 1.97 and 1.98. The information is required to obtain or retain a benefit by the public which is to file (and by the USPTO to process) an application. Confidentiality is governed by 35 U.S.C. 122 and 37 CFR 1.14. This collection is estimated to take 2 hours to complete, including gathering, preparing, and submitting the completed application form to the USPTO. Time will vary depending upon the individual case. Any comments on the amount of time you require to complete this form and/or suggestions for reducing this burden, should be sent to the Chief Information Officer, U.S. Patent and Trademark Office, P.O. Box 1450, Alexandria, VA 22313-1450. DO NOT SEND FEES OR COMPLETED FORMS TO THIS ADDRESS. SEND TO: **Commissioner for Patents, P.O. Box 1450, Alexandria, VA 22313-1450.**

If you need assistance in completing the form, call 1-800-PTO-9199 (1-800-786-9199) and select option 2.

PTO/SB/08B (08-03)
Approved for use through 07/31/2006. OMB 0651-0031
U.S. Patent and Trademark Office: U.S. DEPARTMENT OF COMMERCE
Under the Paperwork Reduction Act of 1995, no persons are required to respond to a collection of information unless it contains a valid OMB control number.

Substitute for form 1449B/PTO

INFORMATION DISCLOSURE STATEMENT BY APPLICANT

(use as many sheets as necessary)

Sheet 28 of 33

Complete if Known	
Application Number	10/378,956
Filing Date	March 3, 2003
First Named Inventor	Michael J. Zaworotko
Group Art Unit	1617
Examiner Name	Leonard Williams
Attorney Docket Number	USF-106XC1

NON PATENT LITERATURE DOCUMENTS

Examiner Initials*	Cite No. [1]	Include name of the author (in CAPITAL LETTERS), title of the article, (when appropriate), title of the item (book, magazine, journal, serial, symposium, catalog, etc.), date, page(s), volume-issue number(s), publisher, city and/or country where published.	T[2]
LW	R233	TOMURA, M. *et al.* "One-dimensional zigzag chain structures with intermolecular C-H••• π and C-H•••O interactions consisted of phthalic acid and pyridine derivatives" *Chemistry Letters*, 2001, pp. 532-533.	
	R234	ZERKOWSKI, J. *et al.* "Design of organic structures in the solid state: molecular tapes based on the network of hydrogen bonds present in the cyanuric acid•melamine complex" *J. Am. Chem. Soc.*, 1994, pp. 2382-2391, Vol. 116.	
	R235	HARKEMA, S. *et al.* "The crystal structure of urea oxalic acid (2:1)" *Acta Cryst.*, 1972, pp. 1646-1648, Vol. B28.	
	R236	KRANTZ, J. *et al.* "Sodium theophylline glycinate" *Journal of the American Pharmaceutical Association*, 1946, pp. 248-250.	
	R237	DATTA, S. *et al.* "Crystal structures of drugs: advances in determination, prediction and engineering" *Nature*, January 2004, pp. 42-57, Vol. 3.	
	R238	AAKERÖY, C. *et al.* "Charge-assisted hydrogen bonds and halogen-halogen interactions in organic salts: benzylammonium benzoates and pentaflourobenzoates" *Structural Chemistry*, 1999, pp. 229-242, Vol. 10, No. 3.	
	R239	CHILDS, S. *et al.* "Crystal engineering approach to forming cocrystals of amine hydrochlorides with organic acids. Molecular complexes of fluoxetine hydrochloride with benzoic, succinic, and fumaric acids" *J. Am. Chem. Soc.*, 2004, pp. 13335-13342, Vol. 126.	
	R240	AAKEROY, C. *et al.* "Modular supramolecular synthesis based on a dominance hierarchy of intermolecular interactions (Abstract)" 223rd ACS National Meeting in Orlando, FL., April 7-11, 2002, published by the American Chemical Society, Washington, D.C.	
	R241	HELFRICH, B. *et al.* "Polymorphism as an indication of structural versatility (Abstract)" 223rd ACS National Meeting in Orlando, FL., April 7-11, 2002, published by the American Chemical Society, Washington, D.C.	
LW	R242	WEBER, E. *et al.* "Synthesis of new Schiff bases: reaction of monofluorobenzaldehydes with 3-aminosulfolane hydrochloride (Abstract)" 216th ACS National Meeting in Boston, MA., August 23-27, 1998, published by the American Chemical Society, Washington, D.C.	

Examiner Signature	/Leonard Williams/ (11/12/2006)	Date Considered	

*EXAMINER: Initial if reference considered, whether or not citation is in conformance with MPEP 609. Draw line through citation if not in conformance and not considered. Include copy of this form with next communication to applicant. [1] Applicant's unique citation designation number (optional). [2] See Kind Codes of USPTO Patent Documents at www.uspto.gov or MPEP901.04. [3] Enter Office that issued the document, by the two-letter code (WIPO Standard T.3). [4] For Japanese patent documents, the indication of the year of the reign of the Emperor must precede the serial number of the patent document. [5] Kind of document by the appropriate symbols as indicated on the document under WIPO Standard ST. 16 if possible. [6] Applicant is to place a check mark here if English language Translation is attached.

This collection of information is required by 37 CFR 1.97 and 1.98. The information is required to obtain or retain a benefit by the public which is to file (and by the USPTO to process) an application. Confidentiality is governed by 35 U.S.C. 122 and 37 CFR 1.14. This collection is estimated to take 2 hours to complete, including gathering, preparing, and submitting the completed application form to the USPTO. Time will vary depending upon the individual case. Any comments on the amount of time you require to complete this form and/or suggestions for reducing this burden, should be sent to the Chief Information Officer, U.S. Patent and Trademark Office, P.O. Box 1450, Alexandria, VA 22313-1450. DO NOT SEND FEES OR COMPLETED FORMS TO THIS ADDRESS. SEND TO: Commissioner for Patents, P.O. Box 1450, Alexandria, VA 22313-1450.

If you need assistance in completing the form, call 1-800-PTO-9199 (1-800-786-9199) and select option 2.

PTO/SB/08B (08-03)
Approved for use through 07/31/2006. OMB 0651-0031
U.S. Patent and Trademark Office: U.S. DEPARTMENT OF COMMERCE
Under the Paperwork Reduction Act of 1995, no persons are required to respond to a collection of information unless it contains a valid OMB control number.

Substitute for form 1449B/PTO

INFORMATION DISCLOSURE STATEMENT BY APPLICANT

(use as many sheets as necessary)

Sheet 29 of 33

Complete if Known	
Application Number	10/378,956
Filing Date	March 3, 2003
First Named Inventor	Michael J. Zaworotko
Group Art Unit	1617
Examiner Name	Leonard Williams
Attorney Docket Number	USF-106XC1

NON PATENT LITERATURE DOCUMENTS

Examiner Initials*	Cite No.[1]	Include name of the author (in CAPITAL LETTERS), title of the article, (when appropriate), title of the item (book, magazine, journal, serial, symposium, catalog, etc.), date, page(s), volume-issue number(s), publisher, city and/or country where published.	T[2]
LW	R243	SCARBROUGH, F. *et al.* "Crystal structure of a complex between lumiflavin and 2,6-diamino-9-ethylpurine: a flavin adenine dinucleotide model exhibiting charge-transfer interactions" *Proc. Natl. Acad. Sci. USA*, November 1976, pp. 3807-3811, Vol. 73, No. 11.	
	R244	MUNN, R. *et al.* "A Model for resonance-assisted hydrogen bonding in crystals and its graph set analysis" *J. Phys. Chem. A*, 2001, pp. 6938-6942, Vol. 105.	
	R245	LYNCH, D. et al. "1:1 Molecular complexes of 4-amino-N-(4,6-dimethylpyrimidin-2-yl) benzene-sulfonamide (sulfamethazine) with indole-2-carboxylic acid and 2,4-dinitrobenzoic acid" Aust. J. Chem., 2000, pp. 383-387, Vol. 53.	
	R246	AAKEROY, C. *et al.* "Solid state, crystal engineering and hydrogen bonds" Comprehensive Coordination Chemistry II (ed. by McCleverty, J. *et al.*), pp. 679-688, Elsevier Ltd., Oxford, UK.	
	R247	LEVIN, B. *et al.* "The not-so-trivial synthesis and characterization of heterocyclic boronic acids (Abstract)" 38th Midwest Regional Meeting of the American Chemical Society in Columbia, MO., November 5-7, 2003, published by the American Chemical Society, Washington, D.C.	
	R248	SMITH, G. *et al.* "Interactions of aromatic carboxylic acids with quinolin-8-ol (oxine): Synthesis and the crystal structures of the proton-transfer compounds with the nitro-substituted benzoic acids" *Aust. J. Chem.*, 2001, pp. 171-175, Vol. 54.	
	R249	STALKER, R. *et al.* "Asymmetric synthesis of two new conformationally constrained lysine derivatives" *Tetrahedron*, 2002, pp. 4837-4849, Vol. 58.	
	R250	VOET, D. *et al.* "Barbiturates and adenine derivatives. Molecular structure of a hydrogen-bonded complex" *Journal of the American Chemical Society*, August 9, 1972, pp. 5888-5891, Vol. 94, No. 16.	
	R251	VISHWESHWAR, P. *et al.* "Molecular complexes of homologous alkanedicarboxylic acids with isonicotinamide: X-ray crystal structures, hydrogen bond synthons, and melting point alternation" *Crystal Growth & Design*, 2003, pp. 783-790, Vol. 3, No. 5.	
	R252	LE JEUNNE, C. *et al.* "Comparative efficacy and safety of calcium carbasalate plus metoclopramide versus ergotamine tartrate plus caffeine in the treatment of acute migraine attacks" *Eur. Neurol.*, 1999, pp. 37-43, Vol. 41.	
LW	R253	AAKERÖY, C. *et al.* "Hydrogen-bonded layers of hydrogentartrate anions: two-dimensional building blocks for crystal engineering" *J. Mater. Chem.*, 1993, 1129-1135, Vol. 3, No. 11.	

Examiner Signature	/Leonard Williams/ (11/12/2006)	Date Considered	

*EXAMINER: Initial if reference considered, whether or not citation is in conformance with MPEP 609. Draw line through citation if not in conformance and not considered. Include copy of this form with next communication to applicant.

[1] Applicant's unique citation designation number (optional). [2] Applicant is to place a check mark here if English language Translation is attached.

This collection of information is required by 37 CFR 1.98. The information is required to obtain or retain a benefit by the public which is to file (and by the USPTO to process) an application. Confidentiality is governed by 35 U.S.C. 122 and 37 CFR 1.14. This collection is estimated to take 2 hours to complete, including gathering, preparing, and submitting the completed application form to the USPTO. Time will vary depending upon the individual case. Any comments on the amount of time you require to complete this form and/or suggestions for reducing this burden, should be sent to the Chief Information Officer, U.S. Patent and Trademark Office, P.O. Box 1450, Alexandria, VA 22313-1450. DO NOT SEND FEES OR COMPLETED FORMS TO THIS ADDRESS. SEND TO: Commissioner for Patents, P.O. Box 1450, Alexandria, VA 22313-1450.

If you need assistance in completing the form, call 1-800-PTO-9199 (1-800-786-9199) and select option 2.

PTO/SB/08B (08-03)
Approved for use through 07/31/2006. OMB 0651-0031
U.S. Patent and Trademark Office: U.S. DEPARTMENT OF COMMERCE
Under the Paperwork Reduction Act of 1995, no persons are required to respond to a collection of information unless it contains a valid OMB control number.

Substitute for form 1449B/PTO

INFORMATION DISCLOSURE STATEMENT BY APPLICANT

(use as many sheets as necessary)

Sheet 30 of 33

Complete if Known	
Application Number	10/378,956
Filing Date	March 3, 2003
First Named Inventor	Michael J. Zaworotko
Group Art Unit	1617
Examiner Name	Leonard Williams
Attorney Docket Number	USF-106XC1

NON PATENT LITERATURE DOCUMENTS

Examiner Initials*	Cite No. [1]	Include name of the author (in CAPITAL LETTERS), title of the article, (when appropriate), title of the item (book, magazine, journal, serial, symposium, catalog, etc.), date, page(s), volume-issue number(s), publisher, city and/or country where published.	T[2]
LW	R254	HU, Z. *et al.* "Separation of 4-aminobenzoic acid by cocrystallization: Crystal structure of the complex of 4-aminobenzoic acid with (2*R*,3*R*)-tartaric acid" *Journal of Chemical Crystallography*, December 2002, pp. 525-529, Vol. 32, No. 12.	
	R255	GUARRERA, D. *et al.* "Molecular self-assembly in the solid state. The combined use of solid state NMR and differential scanning calorimetry for the determination of phase constitution" *Chem. Mater.*, 1994, pp. 1293-1296, Vol. 6.	
	R256	DOI, M. *et al.* "Conformational study of a potent human renin inhibitor: x-ray crystal structure of isopropyl (2*R*, 3*S*) -4-cyclohexyl-2-hydroxy-3-{*N*-[(2*R*)-2-morpholinocarbonylmethyl-3-(1-naphthyl) propionyl] –L-histidylamino}butyrate (KRI-1314), a pentapeptide analogue with amino acid sequence corresponding to the cleavage site of angiotensinogen" *J. Chem. Soc. Perkin Trans. 1*, 1991, pp. 1153-1158.	
	R257	CRIHFIELD, A. *et al.* "Crystal engineering through halogen bonding. 2. Complexes of diacetylene-linked heterocycles with organic iodides" *Crystal Growth & Design*, 2003, pp. 313-320, Vol. 3, No. 3.	
	R258	AAKERÖY, C. *et al.* "A versatile route to porous solids: organic-inorganic hybrid materials assembled through hydrogen bonds" *Angew. Chem. Int. Ed.*, 1999, pp. 1815-1819, Vol. 38, No. 12.	
	R259	SHEFTER, E. *et al.*, ACS, Abstr. Papers (Summer), 1970, 35, compound name: sulfathiazole-theophylline complex.	
	R260	SHEFTER, E. *et al.*, ACS, Abstr. Papers (Summer), 1970, 35, compound name: sulfathiazole-sulfanilamide complex.	
	R261	WIEDENFELD, H. *et al.* "Solubilization of aminophenazone" *Arch. Pharm.*, 1982, pp. 633-641, Vol. 315.	X
	R262	CACCIAPUOTI, A. *et al.* "In vitro and in vivo activities of SCH 56592 (Posaconazole), a new triazole antifungal agent, against *Aspergillus* and *Candida*" *Antimicrobial Agents and Chemotherapy*, August 2000, pp. 2017-2022, Vol. 44, No. 8.	
	R263	CALLAHAN, J.C. *et al.* "Equilibrium moisture content of pharmaceutical excipients" *Drug Development and Industrial Pharmacy*, 1982, pp. 355-369, Vol. 8, No. 3.	
LW	R264	DANNAOUI, E. *et al.* "Acquired itraconazole resistance in *Aspergillus fumigatus*" *Journal of Antimicrobial Chemotherapy*, 2001, pp. 333-340, Vol. 47.	

Examiner Signature	/Leonard Williams/ (11/12/2006)	Date Considered	

*EXAMINER: Initial if reference considered, whether or not citation is in conformance with MPEP 609. Draw line through citation if not in conformance and not considered. Include copy of this form with next communication to applicant.

[1] Applicant's unique citation designation number (optional). [2] Applicant is to place a check mark here if English language Translation is attached.

This collection of information is required by 37 CFR 1.98. The information is required to obtain or retain a benefit by the public which is to file (and by the USPTO to process) an application. Confidentiality is governed by 35 U.S.C. 122 and 37 CFR 1.14. This collection is estimated to take 2 hours to complete, including gathering, preparing, and submitting the completed application form to the USPTO. Time will vary depending upon the individual case. Any comments on the amount of time you require to complete this form and/or suggestions for reducing this burden, should be sent to the Chief Information Officer, U.S. Patent and Trademark Office, P.O. Box 1450, Alexandria, VA 22313-1450. DO NOT SEND FEES OR COMPLETED FORMS TO THIS ADDRESS. SEND TO: Commissioner for Patents, P.O. Box 1450, Alexandria, VA 22313-1450.

If you need assistance in completing the form, call 1-800-PTO-9199 (1-800-786-9199) and select option 2.

PTO/SB/08B (08-03)
Approved for use through 07/31/2006. OMB 0651-0031
U.S. Patent and Trademark Office: U.S. DEPARTMENT OF COMMERCE
Under the Paperwork Reduction Act of 1995, no persons are required to respond to a collection of information unless it contains a valid OMB control number.

Substitute for form 1449B/PTO

INFORMATION DISCLOSURE STATEMENT BY APPLICANT

(use as many sheets as necessary)

Sheet 31 of 33

Complete if Known	
Application Number	10/378,956
Filing Date	March 3, 2003
First Named Inventor	Michael J. Zaworotko
Group Art Unit	1617
Examiner Name	Leonard Williams
Attorney Docket Number	USF-106XC1

NON PATENT LITERATURE DOCUMENTS

Examiner Initials*	Cite No.[1]	Include name of the author (in CAPITAL LETTERS), title of the article, (when appropriate), title of the item (book, magazine, journal, serial, symposium, catalog, etc.), date, page(s), volume-issue number(s), publisher, city and/or country where published.	T[2]
LW	R265	DENNING, D. W. *et al.* "In vitro activity of Saperconazole (R66 905) compared with Amphotericin B and Itraconazole against *Aspergillus* species" *Eur. J. Clin. Microbial. Infect. Dis.*, 1990, pp. 693-697, Vol. 9.	
	R267	DRESSMAN, J. B. *et al.* "Dissolution testing as a prognostic tool for oral drug absorption: immediate release dosage forms" *Pharmaceutical Research*, 1998, pp. 11-22, Vol. 15, No. 1.	
	R268	EBERT, W. R. "Soft elastic gelatin capsules: a unique dosage form" *Pharmaceutical Technology*, October 1977, pp. 44-50, Vol. 1, No. 5.	
	R269	GASCON, M. –P. *et al.* "In vitro forecasting of drugs which may interfere with the biotransformation of midazolam" *Eur. J. Clin. Pharmacol.*, 1991, pp. 573-578, Vol. 41.	
	R270	HEERES, J. *et al.* "Antimycotic azoles. 7. Synthesis and antifungal properties of a series of novel triazol-3-ones" *J. Med. Chem.*, 1984, pp. 894-900, Vol. 27.	
	R271	HONIG, P. K. *et al.* "Itraconazole affects single-dose Terfenadine pharmacokinetics and cardiac repolarization pharmacodynamics" *J. Clin. Pharmacol.*, 1993, pp. 1201-1206, Vol. 33.	
	R272	IMAI, T. *et al.* "Successful treatment of cerebral Aspergillosis with a high oral dose of Itraconazole after excisional surgery" *Internal Medicine*, October 1999, pp. 829-832, Vol. 38, No. 10.	
	R273	KOVACS, J. *et al.* "New type of bridged monoamino-β-cyclodextrins" *Journal of Inclusion Phenomena and Molecular Recognition in Chemistry*, 1996, pp. 53-56, Vol. 25.	
	R274	LAVRIJSEN, A. P. M. *et al.* "Hepatic injury associated with itraconazole" *The Lancet*, July 25, 1992, pp. 251-252, Vol. 340.	
	R275	NEUVONEN, P. J. *et al.* "Itraconazole drastically increases plasma concentrations of lovastatin and lovastatin acid" *Clinical Pharmacology & Therapeutics*, 1996, pp. 54-61, Vol. 60, No. 1	
LW	R276	NOMEIR, A. A. *et al.* "Pharmacokinetics of SCH 56592, a new azole broad-spectrum antifungal agent, in mice, rats, rabbits, dogs, and cynomolgus monkeys" *Antimicrobial Agents and Chemotherapy*, March 2000, pp. 727-731, Vol. 44, No. 3.	

Examiner Signature	/Leonard Williams/ (11/12/2006)	Date Considered	

*EXAMINER: Initial if reference considered, whether or not citation is in conformance with MPEP 609. Draw line through citation if not in conformance and not considered. Include copy of this form with next communication to applicant.
[1] Applicant's unique citation designation number (optional). [2] Applicant is to place a check mark here if English language Translation is attached.

This collection of information is required by 37 CFR 1.98. The information is required to obtain or retain a benefit by the public which is to file (and by the USPTO to process) an application. Confidentiality is governed by 35 U.S.C. 122 and 37 CFR 1.14. This collection is estimated to take 2 hours to complete, including gathering, preparing, and submitting the completed application form to the USPTO. Time will vary depending upon the individual case. Any comments on the amount of time you require to complete this form and/or suggestions for reducing this burden, should be sent to the Chief Information Officer, U.S. Patent and Trademark Office, P.O. Box 1450, Alexandria, VA 22313-1450. DO NOT SEND FEES OR COMPLETED FORMS TO THIS ADDRESS. SEND TO: Commissioner for Patents, P.O. Box 1450, Alexandria, VA 22313-1450.
If you need assistance in completing the form, call 1-800-PTO-9199 (1-800-786-9199) and select option 2.

PTO/SB/08B (08-03)
Approved for use through 07/31/2006. OMB 0651-0031
U.S. Patent and Trademark Office: U.S. DEPARTMENT OF COMMERCE
Under the Paperwork Reduction Act of 1995, no persons are required to respond to a collection of information unless it contains a valid OMB control number.

Substitute for form 1449B/PTO

INFORMATION DISCLOSURE STATEMENT BY APPLICANT

(use as many sheets as necessary)

Sheet 32 of 33

Complete if Known	
Application Number	10/378,956
Filing Date	March 3, 2003
First Named Inventor	Michael J. Zaworotko
Group Art Unit	1617
Examiner Name	Leonard Williams
Attorney Docket Number	USF-106XC1

NON PATENT LITERATURE DOCUMENTS

Examiner Initials*	Cite No. [1]	Include name of the author (in CAPITAL LETTERS), title of the article, (when appropriate), title of the item (book, magazine, journal, serial, symposium, catalog, etc.), date, page(s), volume-issue number(s), publisher, city and/or country where published.	T[2]
LW	R277	ODDS, F. C. "Antifungal activity of saperconazole (R 66 905) *in vitro*" *Journal of Antimicrobial Chemotherapy*, 1989, pp. 533-537, Vol. 24.	
	R278	REMENAR, J. F. *et al.* "Crystal engineering of novel cocrystals of a triazole drug with 1,4-dicarboxylic acids" *J. Am. Chem. Soc.*, 2003, pp. 8456-8457, Vol. 125.	
	R279	SAKSENA, A. K. *et al.* "Advances in the chemistry of novel broad-spectrum orally active azole antifungals: recent studies leading to the discovery of SCH 56592" in Advances in the Chemistry of Novel Broad-Spectrum Orally Active Azole Antifungals (Royal Soc. Chem., Cambridge), 1997, pp. 180-199.	
	R280	SAKSENA, A. K. *et al.* "Concise asymmetric routes to 2,2,4-trisubstituted tetrahydrofurans via chiral titanium imide enolates: key intermediates towards synthesis of highly active azole antifungals SCH 51048 and SCH 56592" *Tetrahedron Letters*, 1996, pp. 5657-5660, Vol. 37, No. 32.	
	R281	HEPPERLE, M. *et al.* "Mono *N*-arylation of piperazine(III): metal-catalyzed *N*-arylation and its application to the novel preparations of the antifungal posaconazole and its advanced intermediate" *Tetrahedron Letters*, 2002, pp. 3359-3363, Vol. 43.	
	R282	CUTSEM, J. V. *et al.* "Oral and parenteral therapy with saperconazole (R 66905) of invasive aspergillosis in normal and immunocompromised animals" *Antimicrobial Agents and Chemotheraphy*, December 1989, pp. 2063-2068, Vol. 33, No. 12.	
	R283	VILLA, L. A. *et al.* "Central nervous system paracoccidioidomycosis. Report of a case successfully treated with itraconazol" *Rev. Inst. Med. Trop. S. Paulo*, July-August, 2000, pp. 231-234, Vol. 42, No. 4.	
	R284	WEST, A. R., "Solid Solutions" In: Solid State Chemistry and its Applications, 1988, p. 358, p. 365, Wiley, NY.	
	R285	ARONHIME, J. *et al.* "Crystalline forms of pharmaceuticals and characterization thereof", Oral Presentation, March 8, 2005, USPTO, Alexandria, VA.	
	R286	DESIRAJU, G. R. "Chemistry beyond the molecule" *Nature*, July 26, 2001, pp. 397-400, Vol. 412.	
LW	R287	GAVEZZOTTI, A. "Are crystal structures predictable?" *Acc. Chem. Res.*, 1994, pp. 309-314, Vol. 27.	

Examiner Signature	/Leonard Williams/ (11/12/2006)	Date Considered	

*EXAMINER: Initial if reference considered, whether or not citation is in conformance with MPEP 609. Draw line through citation if not in conformance and not considered. Include copy of this form with next communication to applicant.

[1] Applicant's unique citation designation number (optional). [2] Applicant is to place a check mark here if English language Translation is attached.

This collection of information is required by 37 CFR 1.98. The information is required to obtain or retain a benefit by the public which is to file (and by the USPTO to process) an application. Confidentiality is governed by 35 U.S.C. 122 and 37 CFR 1.14. This collection is estimated to take 2 hours to complete, including gathering, preparing, and submitting the completed application form to the USPTO. Time will vary depending upon the individual case. Any comments on the amount of time you require to complete this form and/or suggestions for reducing this burden, should be sent to the Chief Information Officer, U.S. Patent and Trademark Office, P.O. Box 1450, Alexandria, VA 22313-1450. DO NOT SEND FEES OR COMPLETED FORMS TO THIS ADDRESS. SEND TO: **Commissioner for Patents, P.O. Box 1450, Alexandria, VA 22313-1450.**

If you need assistance in completing the form, call 1-800-PTO-9199 (1-800-786-9199) and select option 2.

PTO/SB/08B (08-03)
Approved for use through 07/31/2006. OMB 0651-0031
U.S. Patent and Trademark Office: U.S. DEPARTMENT OF COMMERCE
Under the Paperwork Reduction Act of 1995, no persons are required to respond to a collection of information unless it contains a valid OMB control number.

Substitute for form 1449B/PTO

INFORMATION DISCLOSURE STATEMENT BY APPLICANT

(use as many sheets as necessary)

Sheet 33 of 33

Complete if Known	
Application Number	10/378,956
Filing Date	March 3, 2003
First Named Inventor	Michael J. Zaworotko
Group Art Unit	1617
Examiner Name	Leonard Williams
Attorney Docket Number	USF-106XC1

NON PATENT LITERATURE DOCUMENTS

Examiner Initials*	Cite No. [1]	Include name of the author (in CAPITAL LETTERS), title of the article, (when appropriate), title of the item (book, magazine, journal, serial, symposium, catalog, etc.), date, page(s), volume-issue number(s), publisher, city and/or country where published.	T[2]
LW	R288	Physician's Desk Reference, 56th Ed., pp. 1800-1804, 2002.	
LW	R289	KIM, H. *et al.* "High-performance liquid chromatographic analysis of the anti-fungal agent SCH 56592 in dog serum" *Journal of Chromatography B*, 2000, pp. 93-98, Vol. 738.	
LW	R290	VIPPAGUNTA, S. R. *et al.* "Crystalline solids" *Advanced Drug Delivery Reviews*, 2001, pp. 3-26, Vol. 48.	
LW	R291	MCCRONE, W. C. "Polymorphism", In: The Physics and Chemistry of the Organic Solid State, Vol. II, FOX, D. *et al.* (eds.), 1965, pp. 725-767, Interscience, New York.	
LW	R292	LEGER, J.M. *et al.* "Crystal Structure of the 1:1 Sulfacetamide-Caffeine Complex" *Acta Cryst.*, 1977, pp. 1455-1459, Vol. B33.	X
LW	R293	SIMONOV, Y. *et al.* "Structure of the caffeine-copper(II) acetate additional compound", *Izvestiya Akademii Nauk Moldavskoi SSR, Seriya Fiziko-Tekhnicheskikh i Matematicheskikh Nauk*, 1972, Vol. 3, pp. 83-84, abstract only.	
	R294		
	R295		
	R296		
	R297		
	R298		

Examiner Signature	/Leonard Williams/ (11/12/2006)	Date Considered	

*EXAMINER: Initial if reference considered, whether or not citation is in conformance with MPEP 609. Draw line through citation if not in conformance and not considered. Include copy of this form with next communication to applicant.

[1] Applicant's unique citation designation number (optional). [2] Applicant is to place a check mark here if English language Translation is attached.

This collection of information is required by 37 CFR 1.98. The information is required to obtain or retain a benefit by the public which is to file (and by the USPTO to process) an application. Confidentiality is governed by 35 U.S.C. 122 and 37 CFR 1.14. This collection is estimated to take 2 hours to complete, including gathering, preparing, and submitting the completed application form to the USPTO. Time will vary depending upon the individual case. Any comments on the amount of time you require to complete this form and/or suggestions for reducing this burden, should be sent to the Chief Information Officer, U.S. Patent and Trademark Office, P.O. Box 1450, Alexandria, VA 22313-1450. DO NOT SEND FEES OR COMPLETED FORMS TO THIS ADDRESS. SEND TO: Commissioner for Patents, P.O. Box 1450, Alexandria, VA 22313-1450.

If you need assistance in completing the form, call 1-800-PTO-9199 (1-800-786-9199) and select option 2.

Index of Claims

Application/Control No.	Applicant(s)/Patent under Reexamination
10/378,956	ZAWOROTKO ET AL.
Examiner	**Art Unit**
Leonard M. Williams	1617

R	Rejected	–	(Through numeral) Cancelled	N	Non-Elected	A	Appeal
=	Allowed	+	Restricted	I	Interference	O	Objected

Claim		Date
Final	Original	11/12/06
	1	
	2	
	3	
	4	
	5	
	6	
	7	
	8	
	9	
	10	
	11	
	12	
	13	
	14	
	15	
	16	
	17	
	18	
	19	
	20	
	21	
	22	
	23	
	24	
	25	R
	26	
	27	R
	28	R
	29	
	30	
	31	
	32	
	33	
	34	
	35	
	36	
	37	
	38	
	39	
	40	
	41	
	42	
	43	
	44	
	45	
	46	
	47	
	48	
	49	
	50	

Claim		Date
Final	Original	
	51	
	52	
	53	
	54	
	55	
	56	
	57	
	58	
	59	
	60	
	61	
	62	
	63	
	64	
	65	
	66	
	67	
	68	
	69	
	70	
	71	
	72	
	73	
	74	
	75	
	76	
	77	
	78	
	79	
	80	
	81	
	82	
	83	
	84	
	85	
	86	
	87	
	88	
	89	
	90	
	91	
	92	
	93	
	94	
	95	
	96	
	97	
	98	
	99	
	100	

Claim		Date
Final	Original	
	101	
	102	
	103	
	104	
	105	
	106	
	107	
	108	
	109	
	110	
	111	
	112	
	113	
	114	
	115	
	116	
	117	
	118	
	119	
	120	
	121	
	122	
	123	
	124	
	125	
	126	
	127	
	128	
	129	
	130	
	131	
	132	
	133	
	134	
	135	
	136	
	137	
	138	
	139	
	140	
	141	
	142	
	143	
	144	
	145	
	146	
	147	
	148	
	149	
	150	

UM00014257
NOVARTIS EXHIBIT 1517
Novartis v. Regents, IPR2023-01347
Page 2996 of 4460

Search Notes	Application/Control No.	Applicant(s)/Patent under Reexamination	
	10/378,956	ZAWOROTKO ET AL.	
	Examiner	Art Unit	
	Leonard M. Williams	1617	

SEARCHED			
Class	Subclass	Date	Examiner
424	401	3/9/2006	LMW
Updates		11/12/06	

INTERFERENCE SEARCHED			
Class	Subclass	Date	Examiner

SEARCH NOTES (INCLUDING SEARCH STRATEGY)		
	DATE	EXMR
PALM MICHAEL J. ZAWOROTKO BRIAN MOULTON NAIR RODRIGUEZ-HORNEDO	3/9/2006	LMW
Updates 11/12/06		
EAST MICHAEL J. ZAWOROTKO BRIAN MOULTON NAIR RODRIGUEZ-HORNEDO	3/9/2006	LMW
Updated 11/12/06		

UM00014258

NOVARTIS EXHIBIT 1517
Novartis v. Regents, IPR2023-01347
Page 2997 of 4460